PhD Thesis

Arylation with Bismuthonium Salts

Author
Lorenzo Maggi

Supervisor
Dr Liam T. Ball

Thesis submitted to the University of Nottingham for the degree of
Doctor of Philosophy, November 2020

Mens agitat molem
Virgil, Aeneid, VI, 727

Table of Contents

Abstract

Organobismuth reagents have been employed as electrophilic arylating agents since the 1980s, but both their synthesis and use in arylation reactions suffer from poor atom economy. Improvements in the economy of Bi-mediated arylation would render this potentially powerful methodology both general and convenient. This Thesis discusses two approaches towards this goal: arylation catalysed by bismuthonium complexes and synthesis and reactivity of heteroleptic complexes. In particular, the feasibility of a catalytic approach for the arylation of phenols was extensively explored. The investigation separated the overall transformation in three key steps: oxidation, transmetalation and arylation. Direct access to tetraarylbismuthonium salts from readily available triarylbismuth species was provided by a new oxidation-transmetalation sequence. Attempts to merge the arylation step with the previous two proved challenging. Intrinsic incompatibilities of some components of the system were identified. Time separation of the oxidation-transmetalation steps from the arylation phase allowed the overall transformation to be performed in one-pot, however, at the expense of the catalytic approach.

The formation of heteroleptic bismuthonium salts by introduction of a unique group in the transmetalation step was explored for more than eighty different groups. A library of bismuthonium salts was obtained, which allowed mechanistic studies to be carried out, focusing in particular on the ability to transfer the unique group to the substrate during the arylation phase. This chemoselectivity was modelled and the influence of both steric and electronic effects was identified. Attempts to enable the fully selective transfer of the unique group were made by linking together three of the four aryl groups of the bismuthonium salt. A novel bismatriptycene complex was synthesised for this purpose and its capabilities in the arylation reaction were explored, showing promising results.

Acknowledgements

Foremost, I wish to thank the individual without whom this Thesis would not have existed, the mastermind behind it all, Liam. Thanks for the uncountable chats at every hour of day and night, for your immense availability, both in time and effort, and for your continuous scientific and moral support. What I learnt from you made me both a better scientist and a better person, which is both rare and precious.

For better or for worse, I would not be the same person if Mark had not crossed my path. So thanks for setting the bar very high, whilst leading the way through the frustrating land of bismuth chemistry. The group would not be where it is now, without the excellent standards which you instilled (this does not entail swamping NMR tubes with grease). Spending three years with you was not always easy, but ultimately you left a mark (no pun intended) and this is what matters in the end.

Such a joyful adventure could not have failed to attract more explorers, who now gather together under the name of Team Bismuth. To Aaron for assisting me in the annual sacrifice to the God Bismuth, for always keeping at bay my impulsive Italianness while at the same time sharing my love for coffee. You have been an amazing friend and this says it all. To Katie, the true boss here, for being an inspiring example of dedication. I haven't managed to convert you to proper food (or coffee!) so I hope our paths will cross again and will be given another chance. To Charlie, a living reminder of how good being optimistic and enthusiastic felt four years ago. Your positivity is contagious, and this is most certainly needed when bismuth is concerned. As an honorary member of Team Bismuth, my thanks also go to Sir Derek Barton, for being generous and leaving the posterity something to investigate. Also, for sprinkling copper all over his reactions like oregano on pizza, making the interpretation of his results so much more interesting.

A huge thanks to Val, my invaluable friend, for always offering a listening ear and providing precious advice. If the past two years have flown by, it is certainly also thanks to the amazing moments we have shared. To Tom, for the inestimable discussions on the most varied topics. I have learnt an uncountable number of random facts and this is only thanks to you. Give it a couple of years and I'm sure our minor conjugal fights will become a good memory to drink over.

To the other members of the Ball group, present and past, for having made my permanence so enjoyable. In particular, Gemma, for having redefined the concept of holidays, Desiree for her tingly presence and her prompt daily good mornings, and Ben, for assisting in the dodgy experiments and trying to educate my music taste. Also, a special thanks to all those who have proofread this document, making it possibly the most read Thesis of the year: without your help, sentences would have been at least three times longer.

Simon Woodward deserves a special place here, since he accompanied me in the entirety of this travel, always providing advice and guidance of the highest quality.

Most of the research behind this Thesis could have not been accomplished without the help of the Analytical team. In particular, I would like to thank Kev for always listening to my kinky NMR fantasies and often making them a reality, and Shaz for always crushing my 32k scans daytime dreams. To Ben, for his always prompt help with any kind of chromatography. Finally, I could have not learnt most of what (little) I know about crystallography without the patience of Stephen, who managed to give an unexpected inorganic twist to my PhD.

If three quarters of my PhD was spent in the lab, the remaining part was carried out at home. Thanks to Sarah, Letizia and Bianca for enduring the past year with me, I know it must have been pretty hard. Thank you all for keeping both the spirit and the flesh in good shape by providing invaluable material and immaterial joys.

Finally, to my parents, for the continuous effort of supporting me in this long trip. I promise this is my last degree.

Table of Abbreviations

Common abbreviations are used, as listed in the Journal of Organic Chemistry*, in addition to those below:

3c-4e	Three-centre four-electron
Ar^F	4-Fluorophenyl
BCF	Tris(pentafluorophenyl)borane
BPO	Benzoyl peroxide
Bs	Benzenesulfonyl
BTMG	2-*tert*-Butyl-1,1,3,3-tetramethylguanidine
CEBE	Core-Electron Binding Energy
CEPA	Coupled Electron Pair Approximation
CIPE	Complexation-Induced Proximity Effect
DCM	Dichloromethane
DMAN	*N*,*N*,*N*′,*N*′-Tetramethyl-1,8-naphthalenediamine (Proton Sponge®)
DoM	Directed *ortho*-Metalation
DTBMP	2,6-di-*tert*-butyl-4-methylpyridine

*http://pubs.acs.org/paragonplus/submission/joceah/joceah_abbreviations.pdf

ESR	Electron Spin Resonance
FPDE	Fluorine Plus Detachment Energy
HMDS	Hexamethyldisilazane
HMPT	Hexamethylphosphorous triamide
LA	Lewis acid
MTBD	7-Methyl-1,5,7-triazabicyclo[4.4.0]dec-5-ene
on	Overnight
ORTEP	Oak Ridge Thermal Ellipsoid Plot
Ox	Oxidant
Pn	Pnictogen, *i.e.* element of Group 15
SCE	Saturated Calomel Electrode
Tfa	Trifluroacetyl
X	(Pseudo)halide

1

Introduction to Organobismuth Chemistry

Bismuth is the 69th most abundant element in the Earth's crust, with an abundance comparable to that of silver and twice of that of gold. It can be found both in the native state and as an ore, with bismuthinite (Bi_2S_3) and bismite (Bi_2O_3) being the two most significative minerals.[1]

The name 'bismuth' appears to have originated from Georgius Agricola's latinisation *bisemutum* of the old German *wis mat*, 'white matter', where *wis* could be a miner's contraction from Old High German *hwiz*, 'white', referring to the crystals' white-silver hue when their surface is not passivated by its oxide.[2] Agricola himself was the first to assert (although without proving it) that bismuth was a specific metal, substantially different from the others.[3]

Bismuth is a post-transition metal belonging to the group of pnictogens (group 15), its electronic configuration being [Xe] $4f^{14}$ $5d^{10}$ $6s^2$ $6p^3$. It has one naturally occurring isotope, ^{209}Bi, which was considered the heaviest stable isotope, until de Marcillac *et al.* in 2003 demonstrated its radioactive decay to ^{205}Tl, upon emission of a low energy α particle.[4] The measured half-life is $(1.9 \pm 0.2) \times 10^{19}$ years, over 1 billion times longer than the current estimated age of the universe.[5] Such an enormous half-life means, *de facto*, that bismuth can be considered non-radioactive and stable for the majority of purposes. This stability goes hand in hand with a very low toxicity: compared to its notoriously toxic neighbours, such as lead, antimony or polonium, and regardless of its heavy-metal status, bismuth is considered to be non-toxic (even less toxic than sodium chloride),[6,7] a uniqueness possibly due to the poor water solubility of its salts.[8]

The pharmaceutical industry has always paid considerable attention to bismuth:[1] in the early 20th century 'milk of bismuth' was commercialised as a cure-all remedy for disorders of the gastrointestinal tract,[9] a field which has been bismuth's major pertinency for the last century. Bismuth subgallate, for example is used in the treatment of malodour caused by flatulence, while bismuth subnitrate can be used as a mild internal and external disinfectant. Bismuth subsalicylate (commercialised as Pepto-Bismol) is an antacid used to soothe temporary discomforts such as diarrhoea, indigestion, heartburn and nausea.[10]

Other fields of employment are cosmetics, where bismuth oxychloride is used as a pigment in eye shadow, hair spray and nail polish.[11] Bismuth is also used as a nontoxic alternative to lead in ammunitions,[12] radiopaque protheses,[13] water pipes, and soldering.[14]

1.1 Synthesis and structure of organobismuth compounds

Georg Wittig laid the foundations for organobismuth chemistry in the 1950s,[15] which was then developed primarily through the fundamental contribution of Sir Derek Barton and co-workers.[16]

Organobismuth compounds, whose structures and syntheses will be explored in this Section, exploit the two most common Bi oxidation states, *i.e.* Bi^{III} and Bi^{V}, employing, respectively, 6p and 6s and 6p orbitals in the formation of bonds. A substantial difference compared to lighter members of the 15th group is that bismuth does not efficiently hybridise its valence orbitals.[17] This has at least two notable consequences: firstly, the lone pair of tertiary bismuthines has a marked s-character, making them better Lewis acids than nitrogen or phosphorus analogues,[18] and secondly, Bi^{V} complexes have higher than expected oxidation potentials.[19]

The lanthanide contraction is responsible for both these behaviours: elements with an atomic number greater than 57 show smaller-than-expected atomic radii. This effect is caused by the poor shielding of the nuclear charge granted by core d and f electrons to valence electrons. In bismuth's case, due to the greater perceived charge, valence 6s electrons are thus closer to the nucleus, *i.e.* lower in energy, that is to say more Lewis acidic and less prone to hybridisation to sp^3 orbitals.

Relativistic effects must be considered as well. According to the special relativity, the relativistic mass of the electron $m_{\text{rel.}}$ is defined as per equation 1.1:

$$m_{\text{rel.}} = \frac{m_e}{\sqrt{1-(v_e/c)^2}} \tag{1.1}$$

where m_e is the mass of the electron at rest, v_e is the velocity of the electron and c the speed of light. In non-relativistic calculations, c is approximated to $c = \infty$ and no mass correction should be applied to the mass of the electron, thus $m_{\text{rel.}} = m_e$. In atoms with atomic number Z greater than 70, electrons spin at a tangential velocity that is no longer negligible compared to that of light.[20] Therefore it is necessary to apply a correction to the quantum chemical description of the wave function of these atoms. This results in a contraction of the orbital radii, as depicted in Fig. 1.1 for the 6s orbital. An additional measure of these effects is given by the variation of the ionisation energy of 6s orbitals, which for bismuth was estimated to increase by 23%.[21]

In the next pages, organobismuth compounds of both oxidation states will be examined, focusing on their syntheses as well as on their structures.

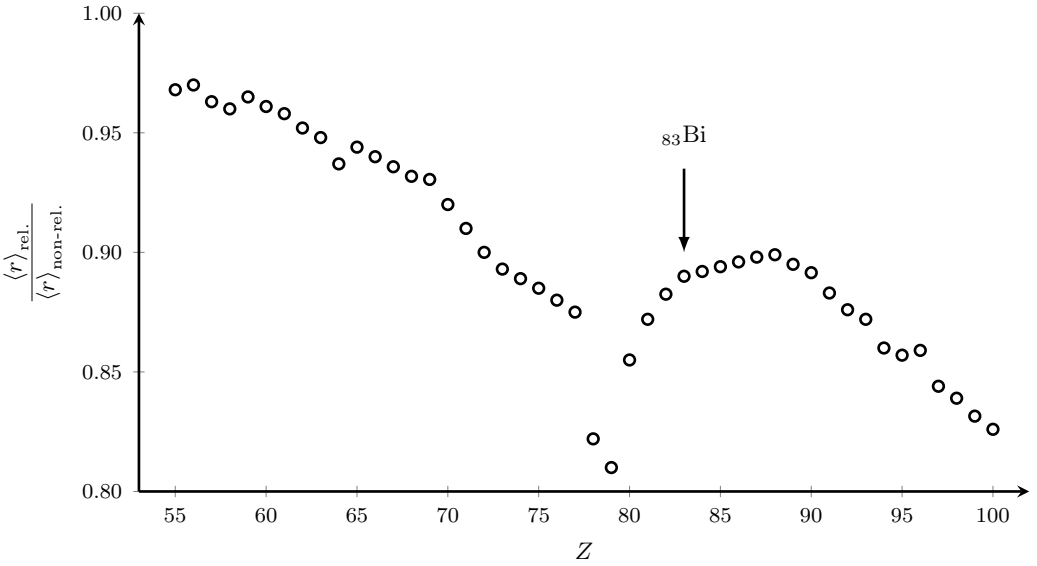

Figure 1.1: The relativistic contraction of the 6s orbital. The relativistic and non-relativistic orbital radii, $\langle r \rangle$, were determined computationally by Desclaux.[22] Bismuth is highlighted.

1.1.1 Bi^{III} compounds

Trivalent organobismuthines usually represent the starting material of many bismuth compounds, including those of higher valency. Simple trialkylbismuth species can be prepared *via* standard organometallic routes,[23] but are spontaneously ignited in air.[7] On the other hand, triaryl species are generally air- and moisture-stable. The most convenient synthetic route involves the reaction of inexpensive bismuth halides with carbanion equivalents, that is aryllithium species or arylmagnesium halides, in an ethereal solvent (Scheme 1.1).

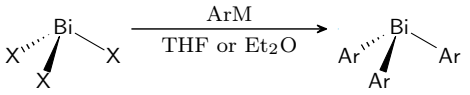

Scheme 1.1: The standard synthesis of triaryl bismuth compounds involves organolithium or -magnesium sources. M = Li, MgX.

These procedures have been successfully used in the preparation of variously substituted triarylbismuthines,[7,24–27] but are limited to groups that do not contain electrophilic functionalities. The tolerance can be increased by forming the organometallic reagent *via* Knochel's magnesium-iodine exchange,[28] as demonstrated for aryl groups decorated with CN, CO_2Et and CHO functionalities (the latter was protected throughout the process as an isopropylimine) in a seminal work by Murufuji and co-workers.[29]

Other procedures have been investigated using, for example, organozinc reagents (Scheme 1.2). These are less reactive than the aforementioned organolithium and -magnesium reagents, thus allowing the formation of bismuth compounds bearing esters, ketones, nitriles and even heterocyclic groups, all in excellent yields.[30] Reactions are performed at room temperature in MeCN in most cases, but a slight temperature increase was shown to be advantageous for electron-rich substrates.

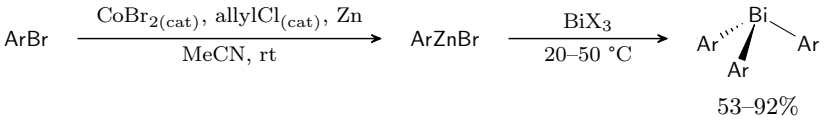

Scheme 1.2: Organozinc reagents expand the scope of aryl groups that can be installed on bismuth.[30]

Urano *et al.*, on the other hand, explored a solvent-free pathway, which allowed the formation of *ortho*-functionalised electron-poor arylbismuthines by milling together aryl iodides with bismuth shots, $CaCO_3$ (to modulate the milling rate of bismuth shots), copper powder and CuI.[31]

A recent result by Stavila *et al.* proposed the synthesis of triarylbismuthines by transmetalation of sodium tetraarylborate salts to bismuth(III) salicylates.[32] The reaction was carried out at room temperature in different solvents and good yields (see Scheme 1.3). Since those salicylates are prepared by protodebismutation of Ph_3Bi with salicylic acid, a different source of Bi was sought. Bismuth oxide was identified as a good candidate, due to its broad availability and low cost. Treatment with carboxylic acids, such as pivalic, acetic or trifluoroacetic acid, gives the corresponding bismuth carboxylate, which can then be used as the starting material for the transmetalation reaction. It is worth noting that the borate is used in a 3:1 ratio to Bi, with an actual 4:1 excess of aryl rings per each transferred group. Moreover, the scope explored in this work is limited to two different aryl groups, phenyl and tolyl.

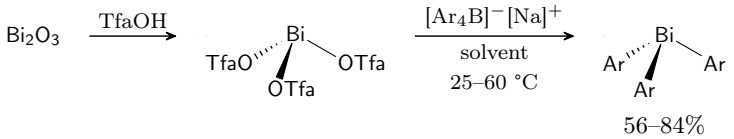

Scheme 1.3: A rare example of transmetalation from B to Bi.[32] Solvent: THF, alcohols or acetone. Tfa = trifluoroacetyl.

With regard to their structure, Ar_3Bi species are predicted to have a trigonal pyramidal geometry, thus with C-Bi-C bond angles slightly smaller than the 109.5° expected in a pure tetrahedral geometry, due to the presence of a lone pair in the valence shell. However, a more pronounced deviation from this prediction, with angles around 90°, is observed. This has been attributed to the fact that the 6s orbital does not mix favourably with 6p orbitals, due to a significant energy gap between the two types of orbitals.[33] This in turn is caused by the aforementioned lanthanide contraction, enhanced by relativistic effects. Specifically, the crystal structure of Ph_3Bi (Fig. 1.2) illustrates this. The notable length of bismuth–carbon bonds (2.260(14) Å)[34] translates into a general weakness: the mean Bi–C bond dissociation energy has been calculated to be 46.34(43) kcal/mol for Ph_3Bi.[35] As a comparison, this value is 89.3(10) kcal/mol for Ph_3N and 76(5) kcal/mol for Ph_3P.

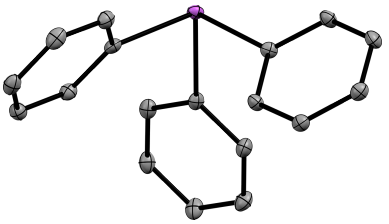

Figure 1.2: Molecular structure of triphenylbismuthine.[34] ORTEP drawing with 50% probability ellipsoid, H atoms omitted for clarity.

Differently from nitrogen compounds, which undergo rapid inversion around the central atom, triarylbismuthines are found to have a high inversion barrier (37 kcal/mol).[36] Trialkyl bismuthines inversion barrier is estimated to be even greater (69 kcal/mol). As a comparison, that of ammonia is just 5.8 kcal/mol. Such inertness with regard to the inversion can again be ascribed to bismuth's poor tendency to hybridise its orbitals. The process, in fact, passes through a trigonal planar transition state, where the metal centre is required to have an sp^2 geometry. The lack of hybridisation is thus likely to contribute significantly to the high inversion barrier.

1.1.2 Triaryl bismuth^{V} compounds

Bismuth(V) compounds can be easily accessed by oxidation of the corresponding Bi^{III} species. Traditionally, this was achieved by treatment with elemental halogens, in particular chlorine.[37] More recently this has been substituted with sulfuryl chloride,[38,39] making the whole process significantly more practical. Another possible pathway involves hypervalent iodine, such as phenyliodine dichloride ($PhICl_2$), as

reported by Ikegami *et al.*[40] The resulting triaryl bismuth dichloride is usually the entry point to other Bi^V species, although direct oxidations of Ar_3Bi to the corresponding difluoride[41] or diacetate,[42] with XeF_2 and sodium perborate in acetic acid, respectively, have been reported. Other counterions are introduced *via* metathesis with the corresponding silver salt.[43,44]

Amongst the possible higher oxidation state bismuth species, triarylbismuth oxide ($Ar_3Bi{=}O$) species have never really been investigated extensively, despite the thorough study of lighter pnictogens oxides.[45] One notable work is that of Suzuki *et al.*, in which the treatment of triarylbismuth with iodosylbenzene (PhI=O) afforded a polymeric bismuth oxide $(Ar_3Bi{-}O{-})_n$. This was successively broken down with a suitable acid, such as toluenesulfonic acid or $BF_3{\cdot}OEt_2$, yielding, respectively, triarylbismuth ditosylate and tetraarylbismuthonium tetrafluoroborate.[46,47]

As far as geometry is concerned, Bi^V dihalides are predicted to be trigonal bipyramidal,[37] which is confirmed by crystallographic analysis of different species (see Fig. 1.3).[48–50] Usually the aryl groups reside in the equatorial plane, while the halides preferentially lie in the axial position. This preference is common within pentacoordinate complexes of main group elements and was termed 'apicophilicity'. It describes the empirical observation that ligands that are sterically small and electron withdrawing prefer to sit in the apical positions.[51,52]

All pentacoordinate bismuth species formally host 10 electrons in the coordination sphere, therefore they are all considered hypervalent. In this case, the traditional 'octet expansion' argument is overcome by the more recent multi-centre bonding approach,[54] firstly used by Rundle in the description of bonding in Xe compounds[55] and presented below. This theory is to be preferred to the one suggesting that such 'octet expansion' occurs by delocalisation of the two extra electrons in the empty 6d orbitals, by analogy to transition metal complexation. In fact, even for phosphorus the energy gap between the 3p and the 3d orbitals is already too substantial to allow this to happen,[56] and for bismuth this gap is expected to be even more accentuated.

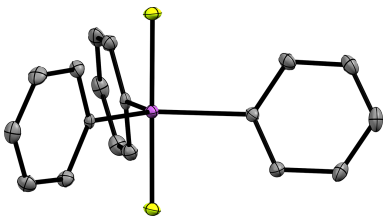

Figure 1.3: Molecular structure of Ph_3BiF_2.[53] ORTEP drawing with 20% probability ellipsoid, H atoms omitted for clarity.

Species described with multi-centre bonds are classified under the following notation: x-A-y, where 'x' represents the number of electrons around the centre A and 'y' the number of ligands. An Ar_3BiX_2 compound would be classified as a 10-Bi-5 species.

For any given trigonal bipyramidal complex of a group 15 element, in order to simplify the treatment of its bonding system, one could temporarily ignore the bonds with equatorial ligands, which are assumed to form with the contribution of the s, p_x and p_y orbitals of the central atom.[57] The remaining p_z orbital, on the other hand, takes part in a three-centre four-electron (3c-4e) bond with the axial ligands. Three molecular orbitals are generated by such interaction (see Fig. 1.4 for the molecular orbital diagram of BiH_5). Starting from the lower in energy, they have bonding, non-bonding and anti-bonding character and possess, respectively, one, two and three nodal planes. The non-bonding orbital is filled by an electron pair and represents the HOMO of the molecule. The fact that the latter contains two nodes suggests that it is delocalised on the outer atoms. Therefore, the there residing electrons do not formally contribute to the electron count of the central atom, thus allowing the preservation of its octet configuration.

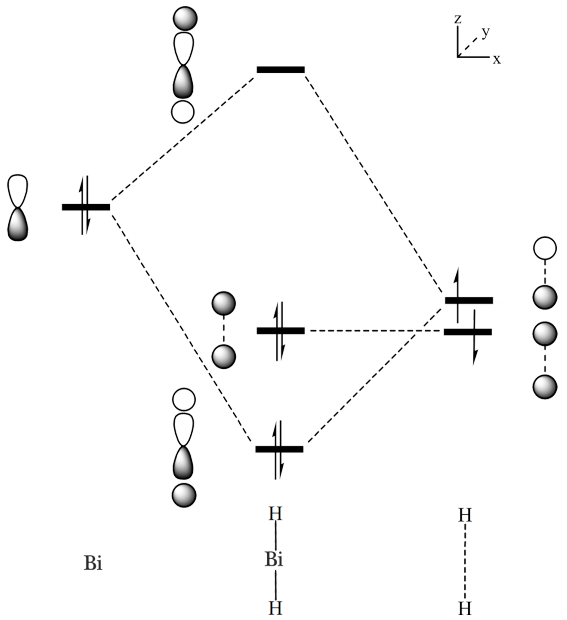

Figure 1.4: Simplified representation of the molecular orbitals involved in the hypervalent bonding in the yet to be synthesised BiH_5. Only axial bonds, resulting from the linear combination of the $6p_z$ orbital of a planar BiH_3 and two axial hydrogens, are considered. The two hydrogens are assumed to interact weakly with each other.[57] Adapted from Goodman.[58]

This only apparently counterintuitive delocalisation has at least two distinct consequences:[51] firstly, it rationalises the tendency of electron-withdrawing ligands to occupy the axial positions, since the presence of those groups there stabilises the high electron density; secondly, it accounts for the different bond lengths observed in crystal structures when comparing apical and equatorial ligands, since the axial bonds are more polarised and therefore longer.

Hypervalent compounds of group 15, when in solution, are subject to pseudorotation, a stereoisomerisation process that causes axial ligands to exchange position with equatorial ones. Figure 1.5 reports a graphical depiction of the most established mechanism for this process: Berry pseudorotation. According to this, the positional isomerisation occurs by a series of bending motions which pushes the trigonal bipyramidal structure through a square planar transition state.[59] The process has activation energies in the range of 2–3 kcal/mol,[60] implying that it is extremely difficult to freeze out, even at low temperatures. In this context, apicophilicity can be described as follows: the structure with electronegative and π-electron-withdrawing ligands occupying the axial positions represents a minimum in the energy curve of Berry pseudorotation.[57,60,61]

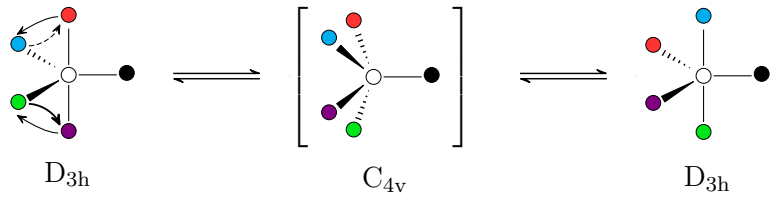

Figure 1.5: Berry pseudorotation causes axial ligand to exchange position with equatorial ones, through bending motions.[62] For simple ligands, the energetic barrier of the process is extremely low.[60]

1.1.3 Pentaaryl bismuth compounds

A specific class of Bi^{V} compounds is worth separate discussion: this is constituted by pentaaryl bismuth species, which were among the first organobismuth derivatives to be synthesised.[15] This traditionally occurs by reacting 2 equiv of ArLi with Ar_3BiCl_2, as shown in Scheme 1.4. Only twelve compounds of this kind have been isolated and characterised.[15,41,63–65] Most of the research effort, in fact, was devoted to understanding the curious properties of pentaphenylbismuth, such as the fact that its crystals are violet, in striking contrast to lighter pnictogens analogues, which are colourless.[66] Schmuck hypothesised that the colour originates from a ligand-to-metal charge transfer transition, a theory that is corroborated by the variation in colour

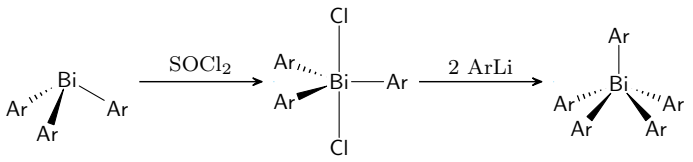

Scheme 1.4: Pentaaryl bismuths are obtained *via* ligand exchange with ArLi species and adopt square pyramidal geometries.

towards the yellow (bathochromic shift) that is observed when two of the aryl groups are rendered electron deficient.[64] Its crystal structure also revealed a square pyramidal geometry, which is similar to what is found for Ph_5Sb but different from all the other pnictogens, which are trigonal bipyramidal.[64] The introduction of substituents in different positions of the aromatic rings induces not always predictable changes in the geometry: for instance, (*p*-tolyl)$_3$(*o*-fluorophenyl)$_2$Bi is trigonal bipyramidal, the only pentaarylbismuth with such geometry.[65] The latter forms orange crystals, suggesting that the square pyramidal geometry is somehow necessary for the bathochromic shift.[67]

1.1.4 Tetraaryl bismuth compounds

Among bismuth(V) species, there is a specific class which will turn out to be of particular interest for this project: tetraaryl bismuth compounds. These species have been investigated since the early 1950s, when Wittig first synthesised tetraphenylbismuth chloride and bromide by reacting pentaphenylbismuth with HCl and elemental bromine, respectively (Scheme 1.5).[15] However, once isolated, these species were found to decompose in the solid state above −30 °C to triphenylbismuth and the corresponding halobenzene. In water, on the other hand, these species were found to be stable for several days.

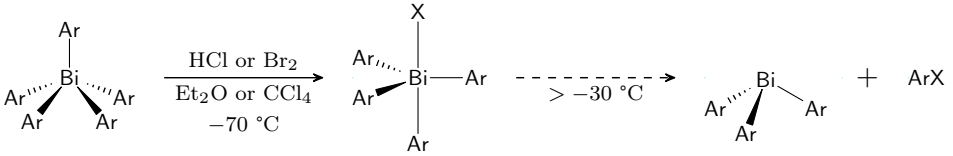

Scheme 1.5: Seminal attempts to synthesise tetraphenylbismuth complexes relied on the protodebismuthation of pentaphenylbismuth species, but were impaired by decomposition of products.[15]

Other attempts to synthesise these compounds were unsuccessfully carried out in the 1960s. Notably, Doak reported the unexpected formation of Ph_4BiClO_4, upon reaction of Ph_3BiCl_2 with $AgClO_4$.[68] However, upon repetition of the same

reaction, Beaumont *et al.* observed the formation of three different species, with the perchlorate salt isolated only in very poor yield.[69]

Although salt metathesis from aqueous solutions of Ph_4BiCl, obtained with Wittig's method, has been performed successfully to introduce different, more weakly coordinating counterions,[70] this method is invalidated by harsh conditions required both for the synthesis of the pentavalent species and its breakdown. According to Matano and Suzuki, there are two major pathways to access tetraaryl bismuth compounds, one being the electrophilic addition to triarylbismuths and the other the nucleophilic addition to bismuth(V) dihalides.[71] However, as pointed out before, Bi^{III} compounds are very weak nucleophiles, due to the strong s-character of the lone pair in the 6s orbital. Therefore, the first method was considered less auspicious and thus explored no further by these authors.

The second approach, on the other hand, has been taken in greater consideration, giving credit to the fact that the electrophilic bismuth(V) centre can easily form new Bi–C bonds under mild conditions by coupling with carbon nucleophiles.[72] Examples of such weak nucleophiles are silyl enol ethers or silyloxy cyclopropanes (see Scheme 1.6).[71] These were reacted with Ph_3BiF_2 in the presence of a Lewis acid, such as TMSOTf or $BF_3{\cdot}OEt_2$, yielding the corresponding triarylalkylbismuthonium salts. The importance of those Lewis acids must be stressed, insofar as they effectively coordinate the fluorides, increasing the acidity of the metal centre and making the addition of the weak nucleophile feasible.[73] The resulting tetrafluoroborate then acts as a new, less coordinating counterion, hence stabilising the complex.

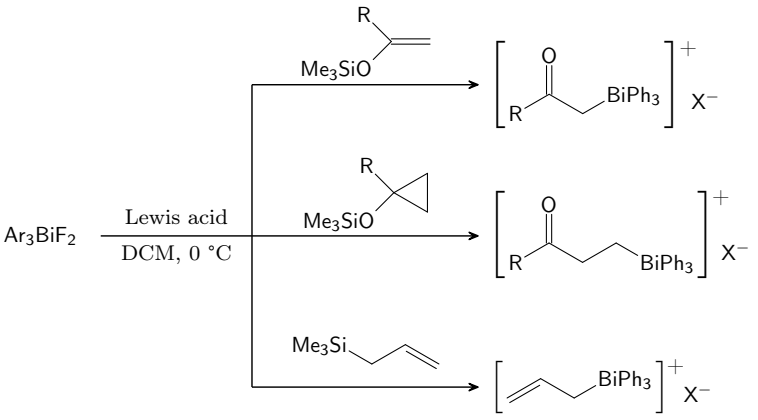

Scheme 1.6: Matano's approach to the synthesis of bismuthonium salts.[73,74] LA = $BF_3{\cdot}OEt_2$, TMSOTf; X = BF_4, TfO, respectively; R = alkyl, aryl.

A more recent paper from Matano and his co-workers suggested a new and appealing way to access tetraarylbismuthonium salts (see Scheme 1.7),[75] which does not involve the undesirable pentaarylbismuth pathway.[15] A boronic acid was instead used to transmetalate the fourth aryl group to a Ar_3BiF_2 species under Lewis acidic conditions, leading to a tetraaryl species in which the counterion was tetrafluoroborate. Notably, the latter originated from the reaction of the Lewis acid employed, $BF_3{\cdot}OEt_2$, and one of the two fluorides on the original bismuth complex. The reaction does not proceed without this Lewis acid, which is assumed to activate the metal centre and favour the aryl transfer from the boronic acid. The latter is said to form an intermediate in which a new B–F bond is being formed while the B–Ar bond is being broken, yielding the aforementioned product.

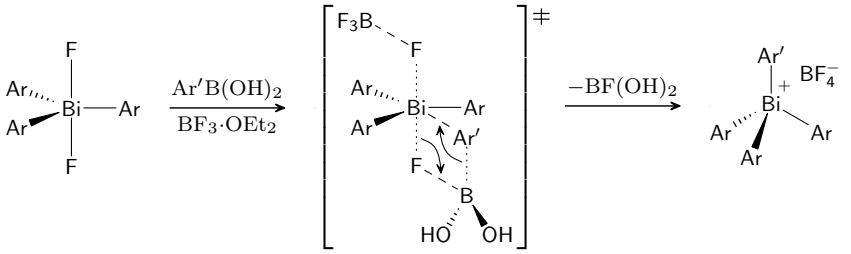

Scheme 1.7: Matano *et al.* demonstrated that transmetalation from boronic acids can be used to introduce a fourth aryl group to a triarylbismuth difluoride species. The reaction is thought to go through the transition state shown: dashed bonds are being formed, while dotted ones are being broken.[75]

The nucleophilicity of counterions determines the molecular geometry of these complexes. Accordingly, they adopt different names: when the counterion is ion-separated, the bismuth centre formally hosts a positive charge and the complex is an -onium species; on the other hand, when the anion is more nucleophilic the complex is covalent and does not get the -onium suffix.[76] Tetraarylismuth compounds with non-coordinating ligands generally adopt a distorted tetrahedral geometry. The interaction with the counterion is ionic, as a consequence of its limited nucleophilicity and as observed by the fact that the interatomic distance is greater than that with coordinating ligands.[69] For perchlorate, tetrafluoroborate and hexafluorophosphate, proof of the ionic nature of these bonds was given by detection *via* IR spectroscopy of the stretching relative to the free counterions, as well as by conductance measurements, which attested their behaviour as 1:1 electrolytes.[69] On the other hand, quite different case are tetraphenylbismuth tosylate and fluoride, among others, which are best described by a trigonal bipyramidal geometry.[77,78] The tosylate or the fluoride occupy one of the apical positions and formally maintain a

covalent interaction. For example, the fluoride-containing compound is characterised by a Bi–C_{ax} bond length of 2.260(6) Å, slightly longer than average Bi–C_{eq} bonds (2.205(12) Å).[78] Interestingly, the Bi–F length is 2.218(4) Å, 0.30 Å shorter than in Ph_3BiF_2.[78] These compounds, despite being tetraaryl complexes, are not considered -onium species and their metal centre does not formally possess a net positive charge.

The greater stability of bismuthonium salts of non-coordinating anions compared to salts of coordinating anions was empirically known since Wittig's time, when it was observed that the chloride, bromide, iodide and cyanide salts decomposed above −30 °C, whereas the perchlorate and tetraphenylborate did not.[15] Although some advances have been made since then, with Suzuki and co-workers being able to isolate several tetra-(*ortho*-alkoxyphenyl)-bismuthonium halides,[79] finding a clear explanation for the intrinsic instability of non-*ortho*-substituted phenylbismuthonium salts is not trivial.

A comparison between the molecular orbital energy levels of the two different geometries provides insight into the different stability and reactivity of those species:[80] when a coordinating counterion is employed, the bismuth centre has to accommodate its electrons and becomes involved in a highly energetic 3c-4e hypervalent bond. In a tetrahedral species, on the other hand, this is not required and compounds are more stable. On the other hand, as the hardness of the anion increases, the polarisation and the energy gap between the bonding and non-bonding (HOMO) orbitals increases, leading, in the extreme, to the formation of a positively charged bismuth species. The trigonal bipyramidal structure can be seen as the

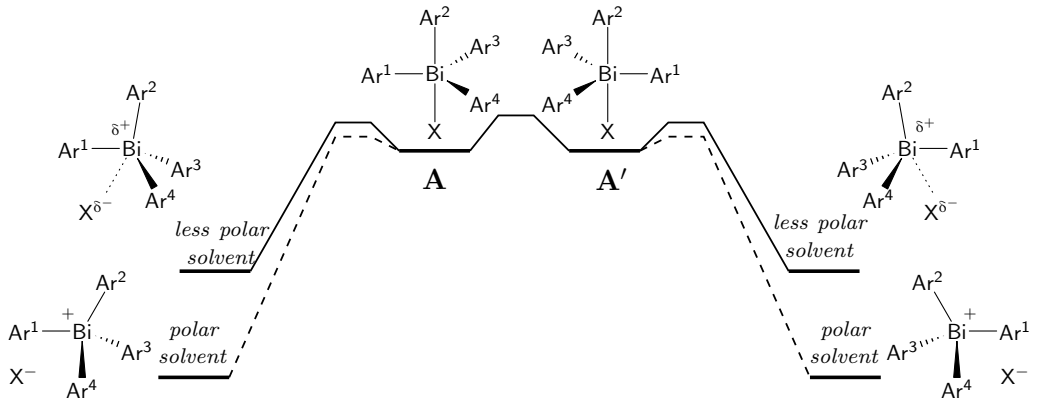

Figure 1.6: Inversion of tetraaryl bismuthonium species pass through a hypyervalent trigonal bipyramidal intermediate **A**, which is thought to interconvert *via* Berry pseudoratoation to **A′**. In apolar solvents the process is favoured by the poorer stabilisation of the naked charge.[76]

more energetic and thus less favoured intermediate between the tetrahedral structure and another tetrahedral structure generated by inversion at the bismuth centre (see Fig. 1.6).[76,77] This is in perfect analogy with the hypervalent transition state of an S_N2 reaction undergoing a Walden inversion.[81]

1.2 Reactions with organobismuth(V) species

Organobismuth(V) species have been used as oxidising agents since the 1930s, when Challenger reported the first oxidation of different alcohols using $Ph_3Bi(OH)_2$.[82] Arylbismuth reagents of the type Ar_3BiX_2 are mild and efficient oxidising agents toward a wide range of primary, secondary, allylic, and benzylic alcohols (Scheme 1.8).[83,84] Often good selectivity can be observed in the presence of different reactive functional groups, so that even rather complex molecules undergo selective oxidation of primary or secondary alcohols with good yields.[83] Usually a basic environment accelerates the reaction rate, as was observed for Ar_3BiCl_2, Ar_3BiBr_2 or $Ar_3Bi(OAc)_2$.[85] Also tetraaryl bismuth species act as oxidants for alcohols and thiols, again preferring basic conditions.[16]

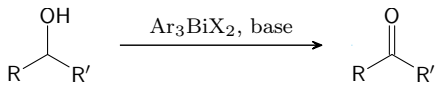

Scheme 1.8: Bismuth(V) species are powerful oxidants for primary, secondary, allylic and benzylic alcohols. Both organic and inorganic bases can be employed to accelerate the oxidation reactions.[83,84]

Significant interest has also grown around another kind of reaction, where bismuth can potentially be extremely valuable: the formation of a new C–C bond by arylation of different kinds of substrates. The first reported arylation performed using an organobismuth reagent involved the quinine molecule:[86,87] in 1980, Sir Derek Barton, who thereafter became the major pioneer in the field, was attempting to oxidise its secondary alcohol to the corresponding ketone, but observed that triphenylbismuth carbonate also induced the α-arylation of quininone (see Scheme 1.9). He postulated that the mechanism involved the formation of a bismuth enolate intermediate, prior to C–C forming 'reductive elimination'.[87]

Next, Barton turned his attention to the behaviour of pentaphenyl bismuth, a species he was extensively employing in the oxidation of alcohols,[85,88] in this kind of reaction and proved that also this pentavalent bismuth compound was capable of arylating several substrates.[89] Enols conceal two possible reactivities, leading either to the *C*- or *O*-arylated product. However, only the first type had been

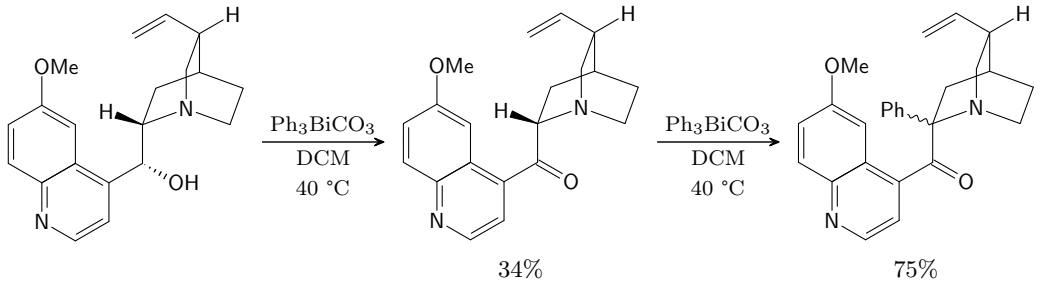

Scheme 1.9: Tandem oxidation-arylation of quinine. This was the first example of bismuth-mediated arylation. The yield reported for the second step is from isolated quininone.[86]

observed at that time. In order to understand if the second kind was possible as well, phenols were chosen as test substrates and exposed to different conditions. Eventually, Barton observed that treatment of 4-nitrophenol with Ph_5Bi yielded the *O*-phenyl ether,[89] demonstrating that this product was also achievable (although this transformation had already been reported by Sharutin in 1975).[90]

In order to understand what generated that different selectivity and how to influence it, Barton tested different conditions. First, he further explored the scope of bismuth, by employing a bismuthonium compound ($Ph_4BiOTfa$) for the first time, as reported in Scheme 1.10.[91] Quite surprisingly, complete selectivity for the diaryl ether was obtained. Other enolisable species, such as dimedone and a ketoester, were submitted to this protocol, highlighting the same chemoselectivity. With these substrates, the chemoselectivity was not complete and a small percentage of *C*-arylated product was detected. The role of the electron-withdrawing trifluoroacetoxy group was held responsible. In fact, when the ketoester was subjected to Ph_4BiOAc under the same conditions, it gave the *C*-arylated product exclusively.[92]

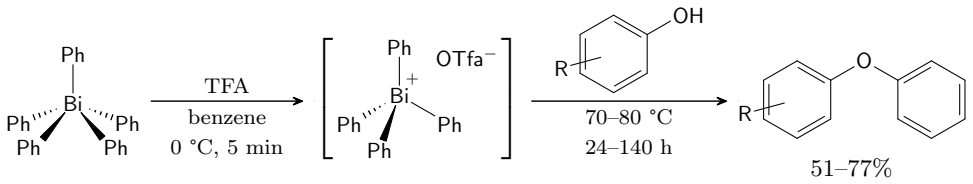

Scheme 1.10: The first example of use of a tetraaryl bismuth species in an arylation reaction.[91] The compound was obtained *in situ* by protodebismuthation from pentaphenylbismuth.

Varying the acidity of the counterion and the pH of the solution also generated instructive results: Table 1.1 reports the outcome of arylation of 2-naphthol in neutral, acidic and basic conditions.[92] Under neutral and acidic conditions, an

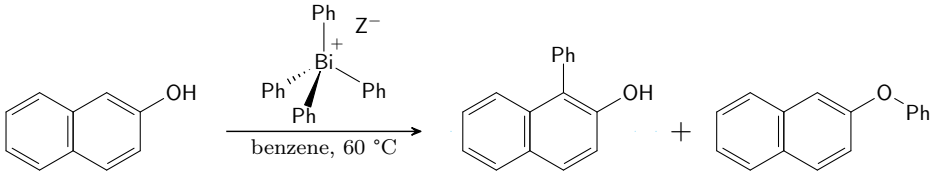

#	Z	Neutral	Acidic[a]	Basic[b]
1	**AcO**	19% SM 25% C 26% O	/	90% C
2	**TfaO**	75% O	90% O	90% C
3	**TsO**	58% SM 42% O	83% SM 11% O	90% C
4	**TfO**	95% SM	96% SM	86% C

Table 1.1: Barton's study on the effect of the pH on the chemoselectivity of phenylation of 2-naphthol with different tetraaryl bismuth species.[92] Isolated yields. [a]With 0.6 equiv of trichloroacetic acid; [b]Naphthoxide pre-formed by reaction with BTMG. SM = starting material, 2-naphthol; C = *C*-arylated product; O = *O*-arylated product.

increasing amount of unreacted substrate was recovered using different counterions ($AcO^- < TfaO^- < TsO^- < TfO^-$). The trend suggested that electron-withdrawing counterions disfavour the coordination of the substrate and hence the formation of any product. This counterintuitive behaviour may be explained by the fact that in a hypervalent species the metal centre is made more electrophilic by using more nucleophilic ligands,[81] since in a 3c-4e bond the electron density resides on the apical ligands. Moreover, when product formed, it was exclusively the diaryl ether in all cases except in neutral conditions with AcO^- as the counterion, where *C*-arylation was as effective as *O*-arylation. Trifluoroacetate performed better both in neutral and acidic conditions, showing high yields of *O*-arylated product, exclusively. On the other hand, under basic conditions, all four bismuthonium salts gave the *C*-arylated naphthol with excellent yields. These preliminary results encouraged further mechanistic studies which will be presented thoroughly in the next Section.

A few years after the discovery of his first bismuth-mediated arylation reaction, Barton reported that copper additives allow the selective *O*-arylation of phenols and enols (see Scheme 1.11).[93] Catalytic amounts of copper were shown to significantly improve the rate of such reaction, thus allowing it to be performed at room temper-

ature, instead of at reflux, and for 1 h, rather than for 23 h. Metallic copper powder gave slightly higher yields than copper acetate and was consequently employed as the copper source of choice. With base, a competition between the *O*- and *C*-arylation is observed, with the first being significantly predominant. Compared to the copper-free reaction, steric hindrance, normally one of bismuth's strong points, is less tolerated: *e.g.* 2,4-di-*t*-butylphenol is almost unreactive. Finally, an argon atmosphere is required.

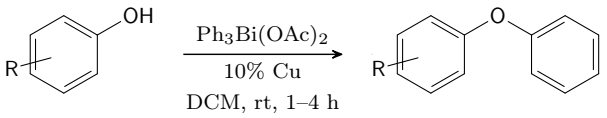

Scheme 1.11: Barton's copper-catalysed *O*-arylation of phenols.

Aliphatic alcohols undergo *O*-phenylation under similar conditions, in a reaction that is sometimes referred to as the David and Thieffry reaction.[94] An anomalous 2 h induction time was reported, as well as a strict preference for dichloromethane (DCM) and $Ph_3Bi(OAc)_2$. Later work by Coles showed that the rate can be accelerated by exposure to ambient light.[95] This reaction can be performed asymmetrically too, as envisaged by Brunner, who desymmetrised a *meso*-diol by using a chiral oxazoline ligand for copper, obtaining the mono *O*-arylation product in 43% yield and 30% *ee*.[96] These conditions can be applied to both aliphatic and aromatic amines.[16,97]

1.3 Mechanistic observations and considerations

Due to the considerable number of variables changed by Barton in his prolific early studies (bismuth species, acidity of the medium, substrate...), a unified model to explain the different results (*O*- vs *C*-arylation selectivity, formation of biphenyl, scarce reactivity toward some classes of substrates...) was desirable. The role of radicals in the transformation had to be clarified too.

The first mechanistic considerations were laid down in 1985 by Barton, by examining the reactions of pentaphenylbismuth and different tetraaryl bismuthonium salts with β-naphthol.[98] On the basis of the detected generation of benzene, he initially postulated the intermediate depicted in Table 1.2 (note that this possesses only three phenyl groups) and proposed that, when the X group was relatively electron withdrawing (such as $TfaO^-$), its breakdown under neutral conditions caused *O*-arylation. He also proposed that an electron-deficient substrate, such as

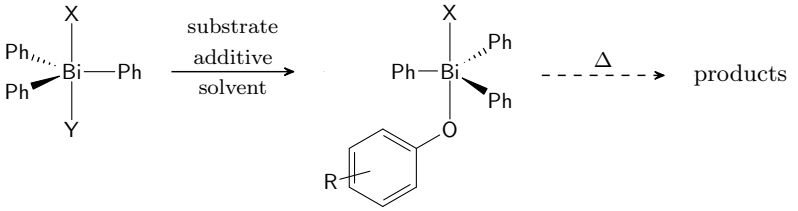

#	Substrate	[Bi]	Additive	Solvent	Ref.
1	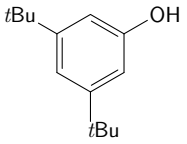	Ph_5Bi	/	THF	98
2		Ph_3BiCl_2	BTMG	THF	98
3	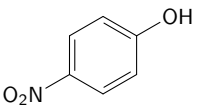	Ph_5Bi	/	Benzene	98
4		Ph_3BiCl_2	NaH	THF	98
5		$Ph_3Bi(OTfa)_2$	NaH	THF	98
6		$Ph_4Bi(OTs)_2$	NaH	Et_2O	98
7	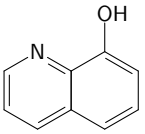	Ph_3BiCl_2	NaOMe	DCM/MeOH	77
8		$Ph_3Bi(OTfa)_2$	NaH	THF	98

Table 1.2: The intermediate first hypothesised by Barton for the reaction between β-naphthol and Ph_3BiXY species (X = Ph, OTfa, Y = Ph) in acidic and neutral media has never been isolated.[98] Isolation of Nu–Bi intermediates was achieved reliably and with different substrates and bismuth species when basic conditions were used. Pentaphenylbismuth did not require base. For entry 7 the crystal structure of the resulting intermediate could be determined crystallographically, confirming the substrate's apical preference.[77] The thermal breakdown of these intermediates gave the *C*-arylation products, with the exception of the adduct of nitrophenol, which gave the diarylether.[98]

p-nitrophenol, could induce the same effect and yield the *O*-arylated compound, even if reacted with a relatively electron-rich X ligand like Ph (*i.e.* in the case the bismuth species was Ph_5Bi). However, after running the series of experiments presented in Table 1.1, it became apparent that the discriminating factor for reaction outcomes was not the electron density of the intermediate but the acidity of the environment. Nitrophenol, at that point, had to be considered an exception.[98]

Barton thus depicted two different mechanisms, reported in Scheme 1.12, the first (**A**) in neutral/acidic environment, the second (**B**) for basic conditions. The former proceeds essentially *via* S_N2, with the phenol's oxygen directly attacking one of the phenyl ligands on the electron poor carbon *ipso* to bismuth. Ph_3BiX then acts as the nucleofuge and is reduced back to Bi^{III} by expelling the inorganic ligand.

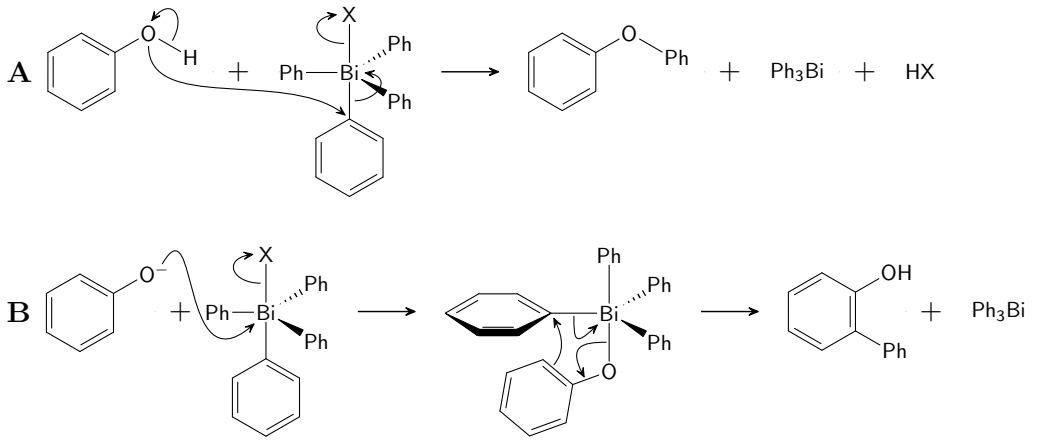

Scheme 1.12: Barton's proposed mechanisms for the arylation of phenol (X = Ph, $TfaO^-$):[39,98,99] the acid catalysed process (**A**) produces a phenyl ether, while the one in basic conditions (**B**) yields the *C*-arylation product.

Mechanism **A** does not proceed through a discrete Bi–Nu intermediate. On the other hand in basic conditions (mechanism **B**), the phenolate attacks Ph_4BiX, which expels X,[99] thus forming said intermediate,[39] whose collapse gives the *C*-arylated phenol and Ph_3Bi. Under these conditions, nitrophenol was said to break down this intermediate in a different and unexplained way, generating the *O*-phenylated product instead of the expected *C*-phenylated one.[98]

A possible radical mechanism was investigated: ESR (Electron Spin Resonance) and chemical trapping showed no free radicals, which was taken as evidence for a 2-electron pathway.[39] Despite this evidence, a measurement of the migratory aptitudes of different $Tol_2Ar'BiCO_2$ and $TolAr_2'BiCO_2$ species was taken* and, being similar to that of another process known to be radical (the decarbonylation of 6-arylisovaleraldehyde), did not initially allow the complete exclusion of a radical pathway.[39] However, Barton explained the observed migratory pattern by invoking a direct relation with the electron density of the carbon directly bound to bismuth. This concerted mechanism is, in fact, such that the π-electrons of the nucleophile attack the *ipso* carbon (Scheme 1.12B). The bond dissociation energy was suggested to become, at that point, the determining factor for the relative ratios.[39]

*A quantitative presentation of these data is intentionally avoided in this Thesis due to their questionable derivation. Qualitatively, a preference for the transfer of electron-deficient groups was observed.

1.3.1 Ligand coupling theory

A more systematic understanding of the aryl group transfer mechanism was sought later on. The ligand coupling theory, that had originally been developed for sulfur[100–103] was in time expanded to iodine,[104–107] group 14 elements[108–111] and pnictogens.[39,92,112–114] This theory describes the behaviour of hypervalent complexes, which, in certain conditions undergo extrusion of two ligands and are reduced to a lower oxidation state:[115]

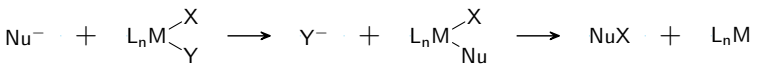

In organometallic chemistry the term 'reductive elimination' would be used to describe this process but, for main group elements, the term 'ligand coupling' is preferred to avoid ambiguity with other reactions characteristic of these elements (*e.g.* the synthesis of alkenes from 1,2-disubstituted alkanes) and because, differently from the former, it carries a mechanistic connotation.[116] Species in which the apical ligands are the same or have similar stereoelectronic properties are less prone to ligand coupling (*e.g.* Ph_3BiCl_2 is a crystalline solid of indefinite stability). Therefore, in the following discussion only pentavalent complexes that result from ligand exchange between a nucleophile (the substrate, in Bi arylation chemistry) and one of the ligands will be considered, as anticipated in the Scheme above.

Before delving into this, it is worth noting that ligand coupling is only one of the possible ways these hypervalent species can undergo reductive elimination. Ionic and radical pathways are theoretically possible too and their contribution needs to be taken into account, and eventually ruled out, for each individual case.

This theory, although some computational experiments had already been carried out (see below), was vastly developed to explain the stereochemical observation that, when sulfur species containing a chiral ligand were reacted with nucleophiles, the moiety of the product which originated from that ligand retained its configuration.[102,103,117] The same retention was observed for ligands notoriously prone to isomerisation, such as allyl and vinyl groups.[118] This suggested that the process must be concerted (since there was no epimerisation) *and* not follow a standard back-side S_N2 (otherwise complete inversion would have been observed).

The concertedness has been demonstrated by Barton for bismuth complexes too, by showing that the migratory aptitude of mixed Bi^V species does not follow the same trend of known ionic and radical processes and the process is not inhibited by radical traps.[39,99] However, with bismuth, a standard back-side S_N2 pathway

cannot be entirely ruled out, since there have not been experiments which studied the conformation of products of bismuth-mediated ligand coupling.

A priori, from a trigonal bipyramid, there are three possible concerted pathways, presented in Fig. 1.7: axial-equatorial (the least-motion pathway), equatorial-equatorial and axial-axial. From a theoretical point of view, the argument of which of them is favoured, or even possible, has been tackled in two different ways: with the orbital symmetry conservation approach and *via ab initio* calculations. Since both of them were developed or carried out in the late 1980s-early 1990s, drastic simplifications were required. Thus, most of the studies have been conducted on symmetric species, which usually bore Cl, F or even just H atoms as a ligand, so care will be required in the transposition of the results presented below to more complex systems.

The first concept is based on the Woodward-Hoffmann rules,[119] which predict the outcome of a reaction by studying the transformations that orbitals undergo. In the following case, the collapse of PH_5 to PH_3 and H_2 was taken as a model. In order to understand whether each of the three pathways is symmetry allowed or forbidden, the evolution of the molecular orbitals of the pentavalent D_{3h} species to those of the coupling product (H_2) and the reduced complex (PH_3), which eventually adopts a C_{3v} symmetry, is followed.[57]

For the axial-equatorial pathway, which is the least-motion mode, the trigonal bipyramidal structure is initially distorted to a C_S structure by pushing together the axial and equatorial ligands which would be extruded at the end of the process. Therefore, it is easier to directly compare the orbitals of this C_S structure with

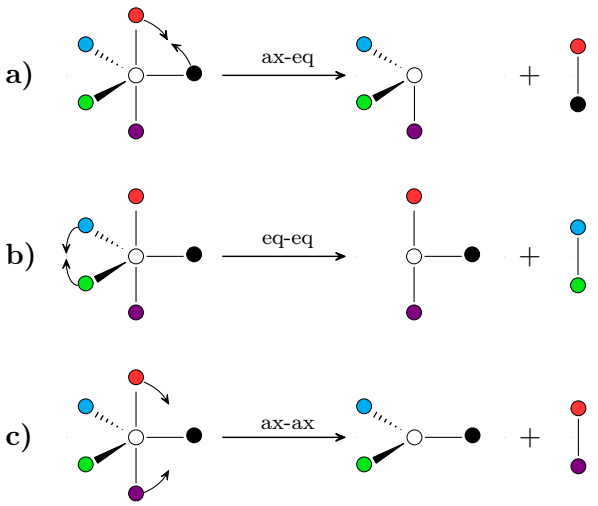

Figure 1.7: The three possible modes of ligand coupling.

those of the products, rather than using the initial D_{3h} set. Figure 1.8 helps keep track of the following transformation visually: orbitals 1a′, 2a′ and 1a″ have the proper shape to become the three P–H bonds in the product. Orbital 3a′ will host the lone pair, therefore 4a′ must originate the σ_g orbital of H_2. However, the presence of a node between the two ligands to be coupled renders the entire transformation symmetry forbidden: 'no continuous evolution of orbitals is possible in this mode such that the PH_5 orbitals yield a ground-state configuration of PH_3, and simultaneously one of H_2'.[57] 'Simultaneously' is the key term in Hoffmann's words: to paraphrase them, the *concerted* axial-equatorial ligand coupling is not symmetry allowed.

From similar correlation diagrams, equatorial-equatorial and axial-axial ligand couplings are both symmetry allowed. The former terminates with PH_3 in a T-shaped C_{2v} structure (see Fig. 1.7b), which immediately converts to the lower energy C_{3v} counterpart. The latter evolves into a trigonal planar D_{3h} structure, as in Fig. 1.7c, which eventually rearranges in the usual C_{3v}. The axial-axial process

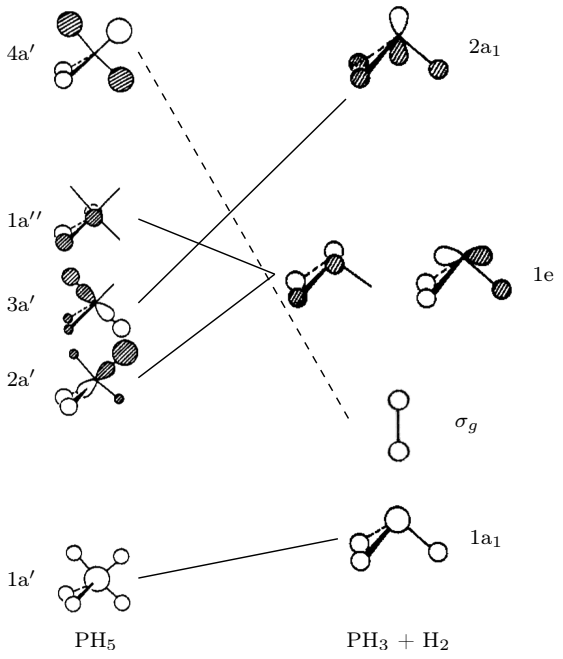

Figure 1.8: Correlation diagram for the departure of one equatorial and one axial hydrogen ligand from a C_S PH_5 to yield a C_{3v} PH_3 and H_2. Only occupied molecular orbitals are shown. In the 4a′ orbital of PH_5, the presence of a node between the two hydrogens that will be extruded makes the process symmetry forbidden, since the σ_g orbital of H_2 does not contain any node. The forbidden correlation is shown with a dashed line. Orbital energies for the products of the transformation are arbitrary. Adapted from Hoffmann.[57]

may intuitively seem unlikely, due to the 180° angle between the two ligands, but can be seen as a continuation of a Berry pseudorotation (see Fig. 1.5). Also, the fact that symmetry does not forbid the process does not necessarily imply that it will be energetically feasible.

In order to understand whether the extrusion of H_2 could occur from any of the square planar C_{4v} intermediates of the pseudorotation,[†] similar orbital evolution studies were performed on them. This led to the conclusion that only two modes are symmetry allowed. With the C_{4v} intermediate of Fig. 1.5 in mind, these are: the one between diagonally opposite, or *trans*-basal, (*e.g.* red and purple) ligands and the one between the pivotal and one of basal ligands. On the other hand, coupling between two neighbouring basal, or *cis*-basal, ligands (*e.g.* red and blue), which derive from the axial and equatorial ligand in a D_{3h} structure, is symmetry forbidden. In short, an axial and an equatorial ligand cannot be coupled in a concerted fashion, either directly or during Berry pseudorotation.

Ab initio calculations provide some more insight into the axial-equatorial mode. Firstly, the D_{3h} and C_{4v} structures of pnictogen pentahydrides in Berry pseudorotation were confirmed to be local minima and transition states, respectively.[60] The activation energy for the process was calculated to be around 2 kcal/mol for all the complexes, confirming their extreme conformational fluidity. Secondly, the ligand coupling process was modelled and the energetic profiles were calculated. These showed that, if for P, As and Sb compounds the energy of the collapse of the corresponding C_S structure to their respective products is comprised between 45 and 55 kcal/mol, the same quantity raises to around 75–79 kcal/mol for Bi.[60,121] The much higher energy released, together with the strong charge separation found in the TS for the Bi complex, was held responsible for a variation in the ligand coupling mechanism: in fact, according to Moc and Morokuma's calculations, a concerted equatorial-equatorial ligand coupling is the pathway of choice for light pnictogens, while bismuth prefers an ionic course, *via* axial-equatorial coupling.

In another computational investigation on the nature of the $PH_5 \rightarrow PH_3 + H_2$ reaction, depending on the method chosen, one or two saddle points were identified.[122] Using a intermediate level calculation (SCF with polarisation functions), there are two of them: the first, at 46 kcal/mol above PH_5, corresponds to the Woodward-Hoffmann allowed equatorial-equatorial coupling, the second, at 48 kcal/mol, only

[†]Turnstile rotation, first proposed by Ugi for his bridged systems,[120] is often mentioned in the literature of the time as a possible motion these species can undergo. However, a recent study demonstrated that the process is topologically equivalent to Berry pseudorotation,[62] so it will not be discussed any further in this Thesis.

slightly more energetic, coincides with the zwitterionic axial-equatorial process, which is therein referred to as non-least-motion. Interestingly, the region between the two saddle points was found to be extremely flat, which would suggest that there is no strong energetic preference for one process over the other, even though the structures of the two TSs are very different (for example their dipole moments measure 0.62 D and 4.53 D, respectively). Therefore, the nature of the real transformation might be the result of a non-deconvolutable contribution of the two. However, with a more sophisticated method (CEPA with polarisation functions), the second saddle point was found to have higher energy (8 kcal/mol more than the first, instead of only 2 kcal/mol), thus becoming less likely, although according to the authors, the region next to the ionic saddle point still needs to be considered when calculating potential trajectories.[122]

To summarise, there is a reasonable certainty that the collapse of bismuth(V) complexes upon reaction with a nucleophile occurs through ligand coupling. It would be possible to argue that radical trapping experiments performed by Barton did not completely rule out a radical mechanism, because perhaps the latter had a greater rate than the reaction with an intermolecular trap. An internal radical trap would provide a definitive answer and, in particular, the use of a calibrated 'radical clock'[123] would give a more precise idea about the rate constant of the process. This experiment was performed by Combes and Finet, almost ten years after Barton's studies, with tri(2-allyloxyphenyl)bismuth diacetate, similarly to what Pinhey had done for lead,[124] and failed to show the formation of cyclised products derived from aryl radicals.[125] Quite surprisingly, a radical intervention was ruled out for the copper catalysed transformation too.

Essentially all the most important reviews on ligand coupling theory questionably apply the theoretical predictions and calculations presented above to real systems, thus generating confusion.[51,115,126] For a start, despite the availability of a few *ab initio* studies for Bi, most of them focus on the prediction of bonding and geometry, with only the ones discussed earlier addressing the coupling reactions. This scarcity led to analogies being drawn to data calculated for lighter pnictogens, above all phosphorus. However, this cannot be done reliably. For instance, relativistic effects have not been taken into account and Pyykkö showed that these cause significant deviations in the energy levels,[65,80] so they can be reasonably expected to have an influence on the reactivity, too. Also, bismuth hydrides are an extremely simplified system, considering that any real bismuth-mediated transformation involves ligands which have p orbitals, to say the least.[127] So, although the conclusions of Moc

and Morokuma, *i.e.* that the axial-equatorial coupling is preferred for Bi, are in accordance with some of the experimental results, it would be naive to explain the latter exclusively with these theoretical arguments.

More importantly, only symmetric species have been considered in these theoretical studies. In reality, if for example one wanted to observe the relative relevance of the three possible ligand coupling modes (Fig. 1.7), non-symmetric species would be required. This would enable the detection of the different products arising from different pathways. Unfortunately, the effect of a mixed coordination sphere on ligand coupling has not been studied yet from a theoretical perspective. On the other hand, there are several reports of crystal structures (*e.g.* tetraphenylbismuth aryloxides)[128,129] that clearly show distortions from pure D_{3h} geometries.

While it is certain that ligands bearing electron-withdrawing groups are more likely to sit axial (see apicophilicity discussion in Section 1.1.2), with the tools provided so far, it is difficult to predict what effects they may have on ligand coupling or even just on Berry pseudorotation. It would not be surprising if a process that was classified as 'symmetry-forbidden' for BiH_5, such as the axial-equatorial coupling, would, upon symmetry lowering, be in reality symmetry-allowed.[122] Therefore, even though Woodward-Hoffmann rules predict that this mode of coupling would only be allowed *via* an ionic, and thus non-concerted, pathway, experimental evidence showed that this is indeed happening and the mechanism is concerted. However, the process is likely to be non-synchronous,[‡39] due to the polar nature of the transition state and the fact that multi-bond processes very rarely are synchronous,[130] especially when three bonds are involved in the transformation, as in this case (Scheme 1.12B).

All this considered and based on the literature, we propose the following 'cheat sheet' to interpret the chemistry of tetraarylbismuth-mediated arylation of phenols, well aware of its limitations:

- upon coordination of the nucleophile, bismuth forms a covalent bond with its oxygen atom and adopts a distorted trigonal bipyramidal structure, with the phenolate in one of the axial positions (this is consistent with the intermediate proposed by Barton and depicted in Table 1.2);

[‡]In a transformation that involves breaking a bond and forming a new one, the two steps are separated by one TS only, *i.e.* the process is identified by one kinetic transformation and is concerted. If the intermediate that forms after the first step can collapse to the product (but not to the starting material) without overcoming any further energetic barrier, then the process is non-synchronous. Its energy profile is characterised by the presence of a flat region between the TS and the reaction coordinate where the collapse starts. If the intermediate could collapse *both to the starting material and to the product* without overcoming any activation energy, the process would be concerted and synchronous and the intermediate would coincide with the TS.

- if already pentacoordinate, the complex expels one of the axial ligands to accommodate the nucleophile (as shown in Scheme 1.12B);
- given the electronegativity of the phenolate's oxygen, Berry pseudorotation equilibria are perturbed so that the probability of an axial phenolate is high, *i.e.* the activation energy is higher than for a symmetric pentavalent complex;
- for the sake of simplicity the phenolate ligand will be assumed always axial.
- once the Nu–Bi complex has formed, the rate of bimolecular ligand exchange is assumed negligible relative to unimolecular ligand coupling;[114]
- *C*-arylation occurs through axial-equatorial coupling, which is favoured both due to being the least-motion mode,[131] and the presence of a beneficial overlap of π electrons of the phenolate and one of the aryl groups. The latter has been suggested as an explanation for lead's good tolerance of steric hindrance,[132] and the concept is likely transferable to bismuth too;
- *O*-arylation can occur both through axial-axial coupling and *via* the S_N2 mechanism proposed by Barton when neutral or acidic conditions[§] are employed (Scheme 1.12A);[98,99,134]
- formation of biphenyl is also a possible, although rarer, outcome and can occur both *via* equatorial-equatorial and axial-equatorial coupling;
- all these ligand coupling modes are non-synchronous, concerted and effectively irreversible (since highly exergonic);
- in basic conditions, competition between the three modes becomes relevant when the normally favoured *C*-arylation becomes disfavoured, *e.g.* due to electron-withdrawing groups on the substrate,[99] which deplete electron density from the aromatic ring meant to attack the *ipso* carbon of one of the aryl ligands, as in Scheme 1.12B.

[§]Due to the irreproducibility in our group of any of Barton's results in neutral and acidic conditions, we are prone to believe that solvents used during his studies contained some source of copper as a stabiliser, as has been suggested in a private communication from Prof. Samir Zard. Copper has been shown by Barton himself to very effectively catalyse the *O*-arylation of phenols, both with Bi^{V} and, more recently, Bi^{III} reagents,[93,133] so these results could be ascribed to a different mechanism, which would explain why a Ph-O-$BiPh_4$ intermediate was not observed. The absence of an intermediate could also be ascribed to the nucleophilic attack being rate-determining.

1.4 The 2-hydroxybiphenyl moiety

Among the variety of substrates bismuth can arylate (see Section 1.2),[135] we decided to make phenols our testing ground for the development of an organobismuth catalysed arylation strategy. In particular, we decided to focus on the *C*-arylation process, since the products of *O*-arylation, *i.e.* diarylethers, are obtained *via* well established methods, such as the Chan-Lam[136] and the Ullmann[137] couplings. On the other hand, there is a lack of a universal protocol to build functionalised 2-hydroxyaryl biphenyls. Nonetheless, these represent an extremely common motif in biologically and synthetically important molecules, with more than 4000 examples among natural products.[138–140] The combined rigidity and hydrogen-bonding properties of this moiety are thought to be responsible for the bioactivity of several medications.[141,142] The latter can be modulated by the nature of the flanking aryl group[143] and by the stereo-electronic properties of the phenol.[144] This Section will present existing methods for making this important motif, highlighting pros and cons, especially in comparison to the bismuth-mediated reactions.

1.4.1 Cross-coupling

The most common way to access this core is *via* transition metal catalysed cross-coupling (Scheme 1.13),[145] be it Suzuki,[146–148] Stille,[149,150] Kumada[151] or Negishi.[152–155] This approach has certainly a few advantages: the transformation is well studied,[156–159] and thus predictable, and, for simple molecules, the two partners are likely to be commercially available. However, it is not free from drawbacks: in some contexts, such as medicinal chemistry, the metal content in the final product is strictly regulated,[160] and palladium and nickel, the metals normally employed, are known for their toxicity.[161,162] While this could be addressed,[163,164] a methodology that does not exploit toxic metals would be preferable.

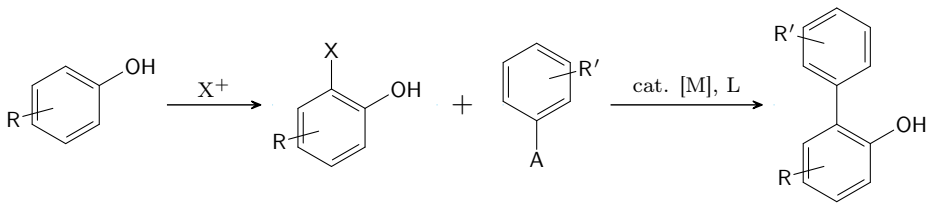

Scheme 1.13: Cross-coupling approach to 2-hydroxyphenyl biphenyls. A = $B(OR)_2$, SnR_3, MgX, ZnX; M = Pd, Ni.

Oxygen-free conditions are often necessary for all these transformations but the most limiting requirement is probably the fact that the phenol needs to be pre-functionalised to enable the cross-coupling, thus increasing the step count of the overall transformation. This pre-functionalisation can be done either *via* halogenation[165–167] or, less commonly, *via* metalation.[168,169] The first method (Scheme 1.13) is based on S_EAr, so it is subject to the same regioselectivity limitations, that is halogenation can occur in either the two *ortho* or the *para* positions.[170] Newer methods for the regioselective *ortho*-halogenation of phenols are emerging such as an ammonium catalysed example.[171] However, more traditional protocols are often employed. These encompass highly reactive species (*e.g.* X_2, *N*-X-succinimides, X^- ions with an oxidant...)[172] and it is not difficult to imagine that in late-stage functionalisation this could be problematic, due to incompatibility with other functionalities. On the other hand, if the halide is installed in early stages, the entire synthesis needs to be modelled to avoid undesired reactions with that group, which could mean excluding the totality of cross-couplings from the library of available methods. Finally, protection and subsequent deprotection of the hydroxy group can be required, thus increasing the number of steps.[146,154,173,174]

1.4.2 C–H activation

Attempts to limit these issues have pushed researchers towards the direct activation of the C–H bond *ortho* to the hydroxyl group. A recent study from Truong and Daugulis demonstrated the 'transition metal-free' arylation of that position *via* a benzyne species, generated from chloroarenes by using a strong base, as reported in Scheme 1.14.[175] This species subsequently performs a [2+2] cycloaddition with the phenol and the resulting cyclobutene intermediate collapses to the desired *ortho* *C*-arylated phenol, driven by the re-aromatisation energy gain. This protocol requires stoichiometric silver, which is supposed to favour *C*-arylation. The base used has an influence on the chemoselectivity, too: LiTMP gives *O*-arylation, while *t*BuONa yields the desired *C*-arylation products. This was ascribed to counterion effects.

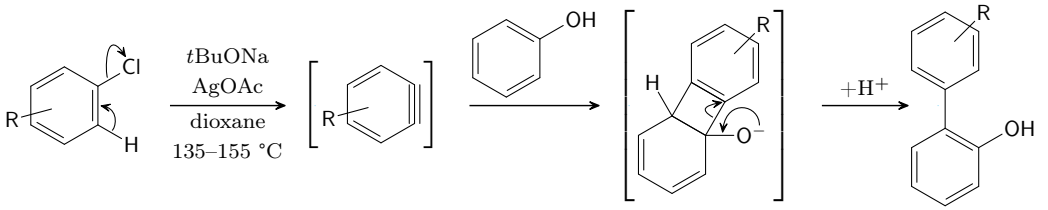

Scheme 1.14: Daugulis' benzyne-based *ortho*-arylation of phenol.[175]

The protocol is effective for electron-poor and -neutral aryl chlorides, however, the yields drop dramatically for electron-rich ones. This, together with the high temperature required, renders this system intrinsically not general.

When the electrophile is an aryl (pseudo)halide, this activation of the bond *ortho* to the hydroxyl group is best done with transition metals, with several examples employing Pd[176–178] and Rh[179–182] catalysts, as per Scheme 1.15. Compared to cross-coupling, the role of the partner coupling with phenol changes from being a carbanion equivalent (in the form of an organometallic reagent) to becoming a carbocation analogue (*i.e.* the aryl halide).

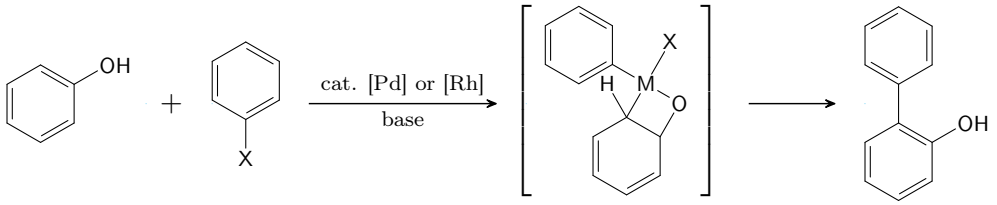

Scheme 1.15: C–H activation of the *ortho* position of phenols with transition metals is difficult, since it goes through an unfavourable four-membered metallacycle. M = Pd, Rh.

This approach has the substantial advantage that pre-functionalisation of the phenol, in theory, becomes unnecessary. Unfortunately, the transformation does not work with simple phenols, since it requires the formation of highly strained 4-membered metallacycles, as shown in Scheme 1.15.[183,184] Benzoic acids, for example, do not suffer of the same issue, since they form a much more stable five-membered metallacyle, and, in fact, their *ortho* C–H activation is more common.[185,186] The issue of the strain of the intermediate can be overcome in case of intramolecular transformations and, in fact, the majority of reported examples belong to this category.[187,188] A measure of the difficulty of the reaction is given by the catalyst loading, which remains exceptionally high in most cases, such as in the work of Hennings (Scheme 1.16), where palladium was used in 20 mol%.

A common strategy is to introduce directing groups, usually on the phenolic oxygen.[176,184,189–192] These enable the so-called complexation-induced proximity effect (CIPE):[193] the directing group, chosen to be a better Lewis base than the hydroxy group, coordinates to the metal, whose local concentration near the desired C–H bond consequently increases, thus enabling metalation of the latter. This was first exploited by Bedford in his Rh-catalysed *ortho*-arylation of phenols in which an aryl phosphite co-catalyst acts as a transient directing group, upon esterification with the hydroxy group (see Scheme 1.17).[179,183] 2,4-di-*tert*-Butylphenol was chosen

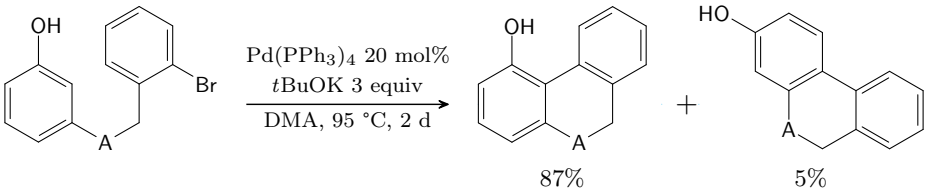

Scheme 1.16: Henning's methodology for the C–H activation of phenols: a tethered aryl bromide avoids the unfavourable four-membered metallacycle.[187] A mixture of *ortho*- and *para*-functionalised products is formed. A = O, CH_2, NCO_2Me.

as a test substrate, since C–H activation is enhanced by steric bulk and side reactions on the other *ortho* position could be thus avoided. The phosphite incorporates at least one 2,4-di-*tert*-butylphenyl group, which then undergoes C–H activation with rhodium. The latter had previously undergone oxidative addition with an aryl halide. Reductive elimination yields *ortho*-arylated arylphosphite, which is released as the corresponding phenol, while a new molecule of starting material undergoes transesterification with the free phosphite and the cycle turns over.

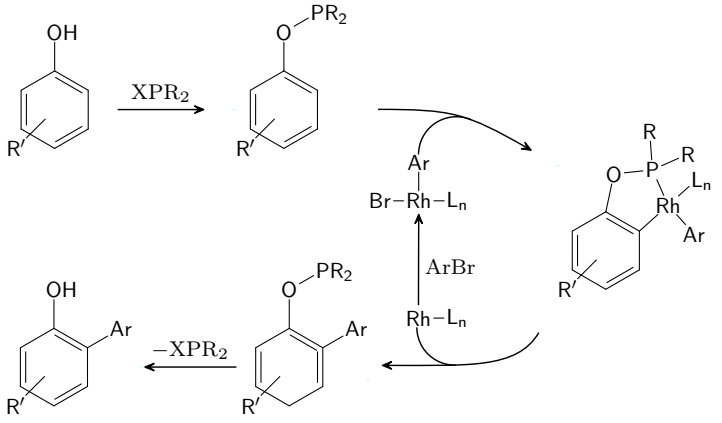

Scheme 1.17: Bedford's transient directing group approach: a removable phosphite group allows the Rh-catalysed regioselective C–H arylation of phenols. The transformation was initially developed with phosphites (X = R = OAr) and was then improved by using phosphinites (X = OAr, R = *i*Pr).[179] Eventually chlorophosphines (X = Cl, R = *i*Pr) proved superior.[181]

Optimal conditions employ Wilkinson's catalyst $(Ph_3P)_3RhCl$ in 5 mol% loading, diisopropylaryl phosphinite 15 mol%, an excess of the desired aryl bromide (1.5 equiv) and Cs_2CO_3 as a base to trigger the transesterification. The scope spans from electron-rich to electron-poor aryl bromides and tolerates some steric hindrance too. Yields are generally good (>80%) and aryl chlorides can be coupled as well,

although with much lower yields (<15%). Finally, the *tert*-butyl group in the 6-position in the product can be effectively removed by treatment of the phenol with $AlCl_3$ in $MeNO_2$.[181] The protocol was subsequently improved by the same group by replacing the phosphite with a more practical chlorophosphine, thus removing the biggest limitation the original protocol had, that is the phosphite had to be synthesised to incorporate the same phenol used as starting material, in order to avoid competition between two different groups.[180]

Oi and colleagues reported a similar methodology, in which the phosphite co-catalyst is replaced by hexamethylphosphorous triamide (HMPT), as presented in Scheme 1.18.[194] Under these conditions, the phenol forms an $ArOP(NMe_2)_2$ species *in situ*, which then undergoes *ortho*-metalation, similarly to Bedford's procedure. This approach has the advantage that the co-catalyst does not need to be prepared beforehand, but can be generated *in situ* from a bench stable and commercially available material, such as HMPT. Although this reactivity is certainly intriguing, the Rh catalyst is moderately expensive (£70/g) and requires strictly inert conditions and the phenol needs to be blocked in the other *ortho* position to avoid over-arylation, which narrows down the applicability of the process.

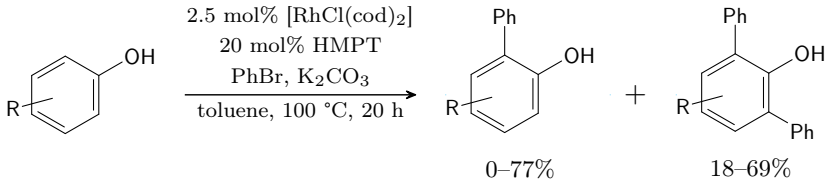

Scheme 1.18: Oi's Rh-catalysed process ameliorates Bedford's approach by employing commercially available reagents, thus overcoming the need to prepare the co-catalyst.[194]

By using carbamates as directing groups, the much cheaper $Pd(OAc)_2$ can be used instead of rhodium, as shown in Scheme 1.19.[176] Di-arylation remains an issue for non-functionalised phenols. Moreover, the reaction is carried out in TFA, a corrosive and toxic solvent,[195] and in the presence of superstoichiometric AgOAc. The selectivity toward mono-arylation can be improved by using di-aryliodonium salts as a source of Ar^+. In this case, the reaction mixture is heated at 100 °C in a microwave for 4 h and yields the free phenol directly, without an extra deprotection step. The authors explained this selectivity by invoking the fact that, at high temperatures, the rate of deprotection is competitive with that of double arylation.

In a similar transformation, the carbamate can be replaced with an ester, as showcased by Xiao and co-workers (see Scheme 1.20).[192] Conditions are milder than in the previous method (DCE, rt, 3 h) but still not optimal, since catalytic triflic

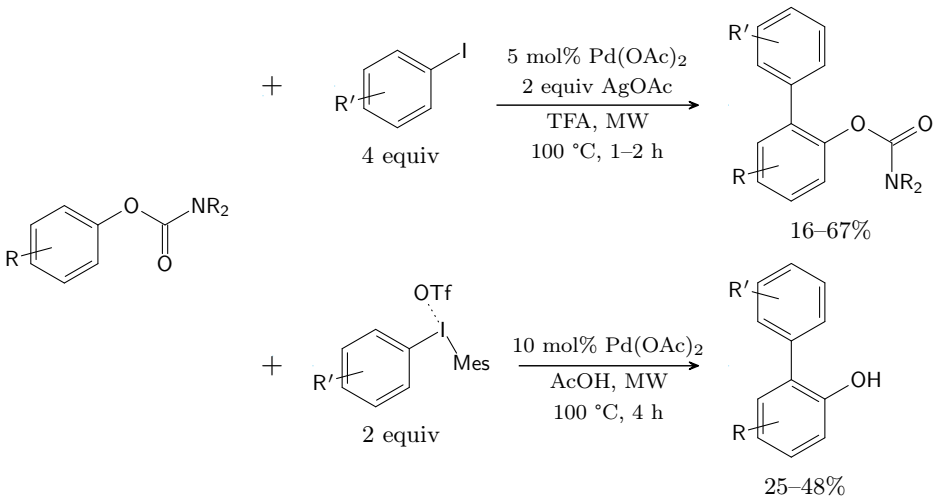

Scheme 1.19: Bedford's Pd-catalysed synthesis of phenols.[176] R = Me, Et, *i*Pr, Ph. Aryl iodides can be replaced with diaryliodonium triflates: mono-arylation is achieved without blocking the 6-position and the resulting carbamate is hydrolysed *in situ*, thus yielding the free phenol analogue.

acid and pivalic anhydride are necessary. A good selection of aryl iodonium salts are tolerated, allowing access to several differently substituted 2-arylphenols in good yields (generally >70%). Interestingly, 2-naphthol is phenylated in the 3-position.

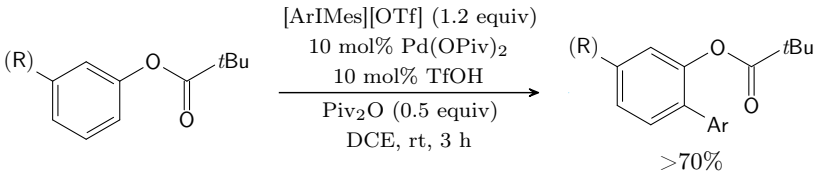

Scheme 1.20: Xiao employed esters of phenols to direct the C–H activation of the position *ortho* to them.[192] With pivalic esters, the reaction is easier and milder conditions can be used. Over-arylation is avoided by placing a substituent in the 5- or 6-position.

In the last example presented here, Ackermann employed ruthenium and a carboxylate co-catalyst to perform arylation of 2-phenoxypyridines (see Scheme 1.21).[184] The transition metal loading is acceptable (2.5 mol%) and, notably, the scope could be extended to aryl chlorides. However, removal of the directing group requires particularly harsh conditions, including treatment with metallic sodium, but yields for this step, as well as for the arylation, are generally very good. On the other hand, reaction times are long and over-arylation remains an issue. The latter is minimised by employing substoichiometric amounts of aryl halide.

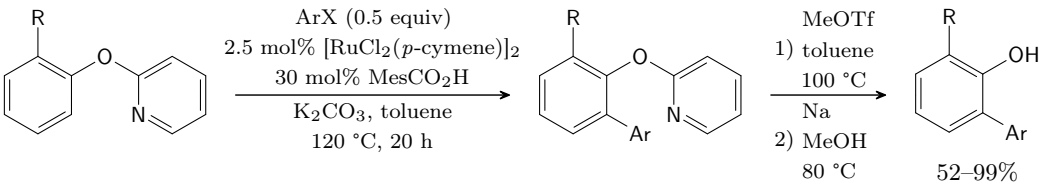

Scheme 1.21: Ackermann's ruthenium-catalysed arylation of phenols. An additional step is required to remove the pyridine directing group. R = Me, F; X = Br, Cl; Mes = mesityl; *p*-cymene = 4-isopropyltoluene.

Although the installation of a directing group on the hydroxyl moiety is critical to enabling rhodium, ruthenium or palladium catalysed *ortho* C–H functionalisation, the step economy is poor when these groups need to be installed and removed *ex situ*. Even though this drawback can be overcome by performing those steps *in situ*, *i.e.* by using transient Lewis-basic groups, the scope of these reactions remains generally limited. Moreover, since the existing methodologies for C–H activation rely on the oxidative insertion into a carbon–halogen bond, chemoselectivity issues arise in the presence of polyhalogenated substrates. Finally, regioselectivity is incredibly difficult to control and biased substrates are frequently employed, in which the second *ortho* position is either pre-substituted or deactivated.

1.4.3 Hypervalent iodine

Diaryliodonium salts (diaryl-λ^3-iodanes) can be used as arylating agents on their own.[196] Similar to the Bi^V species discussed previously, these compounds fulfil the requirements for hypervalency. The counterion, which can be more or less coordinating, is in fact found in one of the two axial positions of a pseudo trigonal bipyramidal structure, maintaining a 3c-4e bond with one of the two aryl groups. The second, on the other hand, sits equatorial together with the two lone pairs, which in this case are termed 'phantom ligands'.[104]

Diaryliodanes can be asymmetric, *i.e.* with two different aryl groups. These are easier to synthesise than symmetric ones, especially when the electronics of the two groups is biased towards one of the extremes.[197] The same applies to sterically hindered ligands, since the installation of two such groups in not facile. Asymmetric iodanes are made by oxidising a iodoarene in the presence of $BF_3{\cdot}OEt_2$, followed by transmetalation from a boronic acid to introduce the second aryl group, as shown in Scheme 1.22.[198] This yields the corresponding (tetrafluoroborate)-diaryl-λ^3-iodane.

Alternatively, upon oxidation of the aryl iodide in the presence of TFA or TfOH, the resulting species can react with an arene, so as to make the corresponding

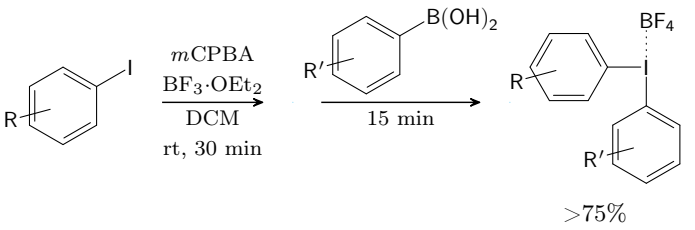

Scheme 1.22: A straightforward synthesis of aryliodonium salts.[198]

trifluoroacete or triflate salt, as in Scheme 1.23.[199,200] This second method poses issues of regioselectivity for complex arenes, which makes the first one more general and versatile. In general, the counterion modulates the solubility: halide salts are usually sparingly soluble in organic solvents, while triflates and tetrafluoroborates are less so. Other counterions can be accessed *via* salt metathesis.[201]

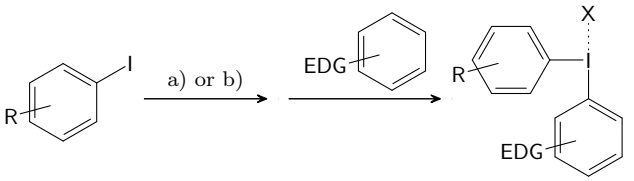

Scheme 1.23: a) NaH_2BO_4, AcOH[202] then TfOH, DCM, 0–25 °C, 1 h, X = TfO;[200] b) *m*CPBA (1.2 equiv), TFA, MeCN, 55 °C, 50 min, X = TfaO.[199]

When a phenol or phenolate is reacted with a diaryl iodane, the latter undergoes ligand exchange with expulsion of the counterion (usually the most labile ligand).[104] Then axial-equatorial ligand coupling occurs and a diaryl ether is formed (see Scheme 1.24).[105,203,204] With asymmetric iodanes and phenolates as nucleophiles, it has been observed that electron-rich and sterically demanding aryl groups are transferred preferentially.[205] Both are expected to sit equatorial, the first because of apicophilicity, the second because the equatorial position is less sterically hindered and can accommodate bigger groups. The unusual result for more sterically-

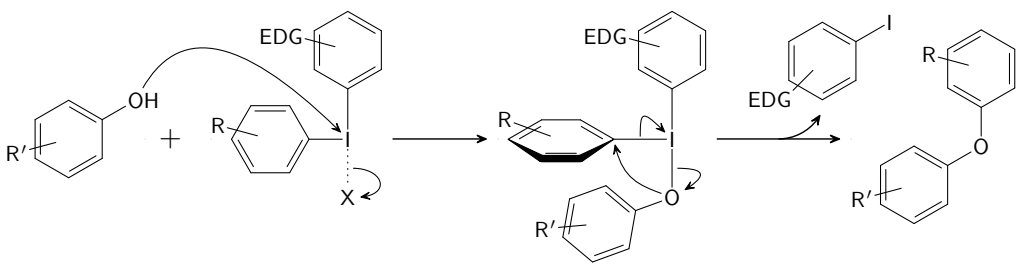

Scheme 1.24: Metal-free arylation of phenols with diaryl iodane gives the *O*-arylated product selectively.[105]

demanding ligand has been termed '*ortho* effect'[106] and ascribed to the steric relief iodine achieves by transferring that group. Different nucleophiles show different behaviours in this regard: for instance, malonates are arylated with the least sterically hindered group.[104,197]

In order to achieve *ortho* *C*-arylation a transition metal catalyst is required. At the moment of writing there are only two papers which report this kind of transformation with free phenol, using copper[206,207] and rhodium,[208] respectively. In this case, the selectivity of transfer from mixed species is inverted, with electron-poor and sterically hindered groups remaining bound to iodine, basically acting as dummy groups. This trend is general among different nucleophiles.[207,209,210]

Although diaryliodonium salts are excellent *O*-arylating agents, the paucity of examples for the *C*-arylation reaction renders this methodology non-competitive when compared to bismuth or lead.

1.4.4 Lead

Among the options available to achieve the *ortho*-arylation of phenols, organolead chemistry is certainly interesting. This was pioneered in the 1980s by Pinhey[211,212] and shows several similarities to Barton's organobismuth chemistry:[213] by reacting an aryl lead species, which carries three dummy groups, such as carboxylates, with a phenol, *ortho*-arylation of the latter is obtained. These reactions are carried out at room temperature or slightly above and, for electron-neutral and -rich phenols, are generally complete in minutes (see Scheme 1.25). Their regioselectivity can be controlled by varying the electronics of the phenol, since the preferred attack occurs on the most electron-rich position, similarly to the bismuth-mediated reaction. As far as the mechanism is concerned, the reaction is thought to abide by the ligand coupling concepts,[124,214] with a predilection for *C*-arylation *via* axial-equatorial coupling,[132] although *O*-arylation products are sometimes detected in traces.[212]

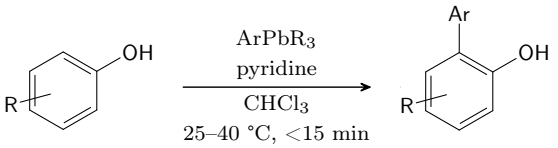

Scheme 1.25: Organolead reagents are capable arylating agents.[215]

The reaction performs better in basic media (in fact, protodeplumbylation was suspected to occur in strongly acidic conditions),[212] tolerates electron-rich and -poor substituents on the aryl group,[216] as well as sterically demanding ones.[217,218] On the other hand the reaction rate drops for electron-poor phenols, to the point the

reactivity is completely shut down with nitrophenol and polychlorinated phenols.[211] This could be addressed by using a Lewis-basic ligand, with phenanthroline showing a promising thousand-fold rate increment.[219] This is consistent with Pinhey's finding that pyridine increases the rate of these arylation reactions,[216] but with hindsight this should be ascribed to the heterocycle acting as a σ-donor for Pb, rather than as a base for the phenol.[220] Yamamoto *et al.* showed that, if the base employed is optically active, such as brucine, an asymmetric version of the arylation can be performed, thus obtaining, for example, axially chiral 2-arylphenols.[111] Similar results can be obtained by using chiral carboxylic acids instead of the more frequent acetate as ligands.[221,222] Both these approaches are unique to lead and analogues for bismuth have currently not been developed yet.

	Pros	**Cons**
Cross-coupling	• Well understood • Catalytic • No regioselectivity issues	• Substrate pre-functionalisation required • Toxic metals • Issues with poly-halogenated partners
C–H activation	• No substrate pre-functionalisation	• Directing groups necessary • High catalyst loading • Regioselectivity issues • Overarylation • Long reaction times
Diaryliod-onium salts	• Excellent for *O*-arylation • Mixed iodanes can be used • Synthesis is straightforward	• TMs required for *C*-arylation • Aryl iodides are expensive and less available than other halides
Lead	• No substrate pre-functionalisation • Tolerates steric hindrance • Asymmetric version described	• Toxic • Synthesised by trans-metalation from Sn or Hg • Phenols with EWGs do not react

Table 1.3: A comprehensive list of pros and cons of currently available methods for the *C*-arylation of phenols.

Unfortunately, the aryl lead compounds are synthesised *via* less-than-ideal routes, namely direct plumbation of the desired aromatic compound in acetic or haloacetic acid,[223] or transmetalation from mercurials[224] or stannanes.[225] Only more recently was transmetalation from boronic acids demonstrated.[226] Plumbation can only be employed with arenes that are not excessively electron poor and also, has obvious drawbacks for acid sensitive species. The transmetalation approach is definitely more versatile, however, the required organomercury and -tin species are generally not commercially available and need to be prepared beforehand, thus compromising the step economy of the process. For the boronic acid case, the reaction is carried out in the presence of catalytic $Hg(OAc)_2$, suggesting a potential transmetalation to mercury first, followed by a second one from mercury to lead. Also, even the authors of the paper claim to prefer the tin-mediated reaction, when isolation of the transmetalation product is required.[226]

To conclude, organolead reagents remain an extremely powerful tool in the hands of organic chemists, especially when an asymmetric synthesis is undertaken. However, due to their extreme toxicity,[227–229] they can hardly be regarded as sustainable and future-proof arylating agents. Luckily, most of their useful properties are shared with their bismuth analogues, which makes the latter even more appealing. Table 1.3 summarises the major advantages and disadvantages of the different approaches available to arylate phenols in the *ortho* position.

1.5 Research aims

Trivalent organobismuth compounds can be easily accessed from Grignard reagents and cheap, nontoxic inorganic bismuth salts, as illustrated in Section 1.1.1. The oxidation state of the metal centre modulates two different modes of reactivity: trivalent organobismuthines, despite the strong relativistic contraction, behave as (poor) nucleophiles, while bismuth(V) species are generally electrophilic.[71] The ability of bismuth to manoeuvre between the two oxidations states, a feature that granted transition metals their prominent position in the organic chemist's toolbox, is also what allows the metal to be employed in a variety of organic transformations, such as the oxidation of an assortment of alcohols[16,230] and the arylation of several enolisable species.[16,84,127] Despite this behaviour, which closely mimics that of d-block metals, the redox chemistry of bismuth is impaired by its use as a stoichiometric reagent. Only in 2020 has the metal been shown to support

catalytic manifolds,[231,232] however these have not been extended to the arylation of carbon nucleophiles, which remains an unresolved challenge, both with catalytic and traditional, stoichiometric methodologies.

We reasoned that we could contribute to solving both issues and envisaged a bismuth-catalysed process for the *ortho*-arylation of phenols. This would ideally exploit all the bismuth's strengths demonstrated by Barton and Suzuki, such as tolerance for non-inert atmospheres, quick conversion to product even at room temperature, excellent regioselectivity and tunable chemoselectivity. At the same time some of its weaknesses, such as the inherent wastage of two to four aryl groups or the poor step economy of the synthesis of any high-valent bismuth species, would be addressed. Phenols would be suitable substrates, as their bismuth-catalysed arylation would represent a breakthrough *per se*, in a field populated by stoichiometric, expensive or toxic processes. The resulting 2-hydroxybiaryl system would also be highly valuable.

With these premises a process based on the Bi^{III}-Bi^{V} redox couple was envisaged. This would provide the required robustness and ability to withstand atmospheric conditions, while at the same time allowing the use of classic stoichiometric processes as a benchmark. In particular the bismuth(III) component was set to be a triarylbismuth species, for ease of access and stability.

Two possible reaction pathways can be conceived: in the first, the metal centre of triarylbismuth is oxidised to bismuth(V) and coordinates the nucleophile; the arylated product is then formed by ligand coupling, while a new ligand is transferred to the resulting Ar_2BiX species to regenerate Ar_3Bi. The second cycle, depicted in Scheme 1.26, differs from the first in the order of these steps and, consequently, in the minimum number of ligands bismuth bears in the process: a fourth ligand is introduced after the initial oxidation to form a tetraarylated complex, which then coordinates the nucleophile and reductively eliminates the arylated product, thus re-forming triarylbismuth. The first possibility involves potentially unstable Ar_2BiX species and for this reason was considered more challenging. The individual steps of the second manifold (oxidation of Ar_3Bi species, transmetalation at the Bi^{V} centre and bismuth-mediated ligand coupling of phenols), on the other hand, are know and reliable processes. Therefore the second pathway was embraced and we will henceforth exclusively be referring to this.

It was reasoned that, if it were possible to oxidise a triarylbismuthine to a suitable Bi^{V} counterpart, we would then be in the condition to introduce the fourth aryl group by transmetalation, ideally from a boronic acid, as it had already been demonstrated

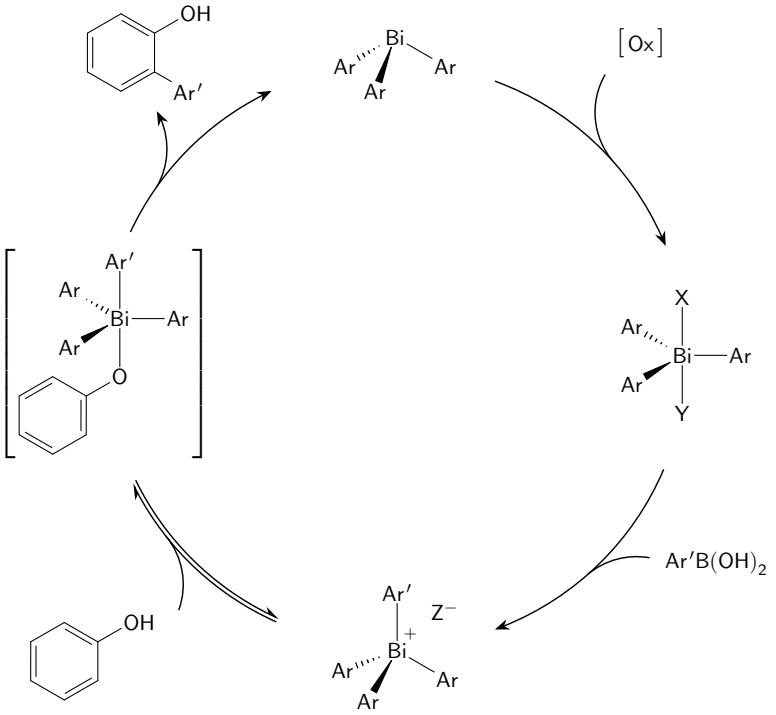

Scheme 1.26: Envisaged mechanism for the catalytic arylation of phenol-like substrates mediated by tetraarylbismuthonium salts. Ox = oxidant.

by Matano for triarylbismuth difluoride.[75] At that point, if our hypothesis were sound, the reaction of a nucleophile with the obtained tetraarylbismuthonium would lead to the formation of the desired arylated product, re-forming a Bi^{III} species, ready for the next oxidation and subsequent cycle. A judicious choice of reagents would make this outcome possible.

The research presented in this Thesis will, at first, address the attempts to develop a catalytic system for the oxidative arylation of C–H bonds through tetravalent bismuthonium species. Once a working system is established, the challenging idea of forming catalytic heteroleptic bismuthonium species, comprising three spectator ligands and a unique group, and chemoselective transfer the latter to the substrate will then be tackled. Mechanistic investigations will be employed to understand the individual steps of the transformation and will provide the necessary insight in the determination and optimisation of such processes.

2

Studies towards bismuth catalysed arylation

The investigation into a catalytic bismuth manifold commenced from the synthesis and isolation of a stable tetraarylbismuth species, which could be employed in early tests. This allowed us to have a better grasp of the robustness and reproducibility of the different approaches available from the literature. We foresaw that, from a methodological point of view, NMR spectroscopy would be the most effective and least invasive method for reaction monitoring. In particular, to further simplify the interpretation of reaction outcomes, the labelling of the majority of the components with fluorine atoms was decided, so as to enable the use of ^{19}F NMR spectroscopy. Maximum sensitivity to chemical environment with minimal electrostatic perturbation (the Hammett σ_{p} value for F is 0.06) would be achieved by the introduction of a fluorine atom in the *para* position of the aromatic rings of each of the components of the system, *i.e.* bismuth reagents, organometallic species and substrates.

2.1 Synthesis of organobismuth species and early tests

According to what has been discussed in Section 1.1.1, triarylbismuth species are the precursors of essentially all the higher valent species, so we started off by synthesising the fluorine-labelled analogue **2** (hereafter 'Ar^F' will represent the 4-fluorophenyl group). This was achieved in excellent yields *via* the addition of the corresponding aryl Grignard reagent to a bismuth trihalide salt, as shown in Scheme 2.1. The electrophile can be either $BiCl_3$, which is commercially available and relatively cheap (£ 55/100 g*), but was often found to be wet and impure, or $BiBr_3$ (**1**), which can be easily synthesised by dissolving Bi_2O_3 in hot HBr and then removing the resulting water *in vacuo*. The latter was preferred over the course of a few reiterations of this reaction, due to both its higher solubility and purity.

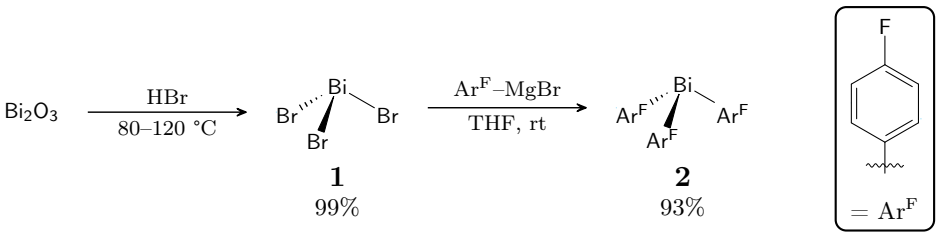

Scheme 2.1: The precursor **2** can be easily synthesised by treating a bismuth halide (here the bromide) with the desired Grignard reagent.

The bismuthine crystallised from EtOH, which is the preferred isolation method, especially when the reaction is performed on a 50 g scale. The product was

*From Fluorochem Ltd., URL consulted on the 13/04/2020.

successively oxidised to the corresponding triarylbismuth dichloride **3** by treatment with sulfuryl chloride,[44] with excellent yields. Finally, anion metathesis was carried out to convert the dichloride **3** to the corresponding difluoride **4**, as per Scheme 2.2.[48] The latter was the fundamental starting material to submit to Matano's protocol:[75] attempts to carry out the transmetalation of the fourth aryl group directly on the dichloride **3** were unsuccessful, due to the absence of the driving force embodied by the formation of strong B–F bonds (see Scheme 1.7 for the proposed mechanism of this reaction).

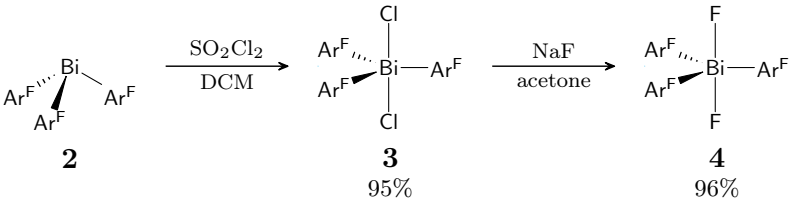

Scheme 2.2: Synthesis of $Ar^F_3BiCl_2$ and $Ar^F_3BiF_2$ according to literature procedures.[44,48] Both compounds were obtained in excellent yields upon recrystallisation from cyclohexane/DCM.

Initially, the synthesis of Ar^F_4BiF was attempted (see Scheme 2.3), following the work by Ooi *et al.*:[78] the compound had been obtained by the authors in 80% yield, by simple anion exchange, *i.e.* by stirring the BF_4 complex **5a** in MeCN with a five-fold excess of a soluble[233] source of fluoride ions, such as CsF. This seemed promising in view of the possibility of having a stable and easily accessible tetrarylbismuth source. The process was attempted several times and only worked once. The caesium salt seems to be fundamental, since KF did not afford the desired product, probably due to its limited solubility. Even when the metathesis worked, the isolation was problematic and the final product contained traces of fluorobenzene, triarylbismuth and $[Ar^F_4Bi][BF_4]$. In fact, simply stirring the impure compound in MeCN for a week resulted in an increased amount of decomposition

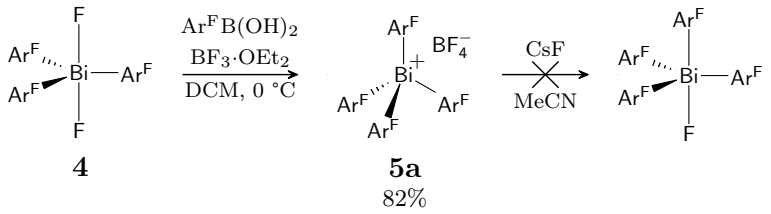

Scheme 2.3: The synthesis of tetraarylbismuth fluoride is hindered by the difficult crystallisation and was not pursued. On the other hand, the tetrafluoroborate salt **5a** is easily isolated.

products. For these reasons, the Ar^F_4BiF route was abandoned and a step back was taken: isolation of tetraarylbismuthonium tetrafluoroborate **5a** was decided, since the species had previously been detected as the intermediate product before the metathesis. Gratifyingly, needle-shaped crystals of **5a** were obtained in good yields.

In order to have the full overview of possible methods from which to draw, we briefly explored the classical synthesis widely employed first by Wittig then by Barton.[15,91] This occurs *via* the cleavage of one of the five aryl groups of pentaaryl bismuth complexes by protodebismuthation, *i.e.* by treatment with a strong acid, as discussed in Scheme 1.5. Unfortunately, the formation of the pentavalent species proved challenging. After a careful review of the literature, a brief mention of the inexplicable instability in solution, even at low temperatures, of the 4-fluorophenyl analogue of pentaphenylbismuth was found.[41] Therefore this pathway was abandoned, too, and Matano's approach to make $[Ar^F_4Bi][BF_4]$ **5a** was in conclusion considered more versatile and worth further investigation.

The isolated organobismuth compound **5a** was promptly tested in the arylation of 4-fluorophenol under the conditions that were found to be optimal in related investigations in the group, *i.e.* in THF at 60 °C. The reaction was performed with and without DBU as a base (see Scheme 2.4). The latter was chosen since it is a relatively strong, non-nucleophilic base with a pK_a of 24.3 in acetonitrile[234] (as a comparison phenol's pK_a in acetonitrile was measured to be 29.1[†]).[235–238] No reaction was observed over 24 h in the absence of base. In the presence of base, complete consumption of the Bi^V species occurred in 2 h, producing the complex mixture of arylation products reported in Scheme 2.4. The *O*-arylated phenol **6c** accounts for just 10% of the products, while the *C*-arylated species **6a** and **6b** combined represent 28% of the total (38%, if the number of C–C bonds formed is considered), showing a certain predilection towards this kind of transformation. Around 60% of the starting material 4-fluorophenol was found

[†]According to Coetzee, such a high pK_a value for phenol in acetonitrile must be attributed to the three different factors: first, the proton-acceptor power of this solvent is smaller than that of water by 10^5, so the dissociation of Brønsted acids is less complete, since usually this occurs through the protonation of the solvent; second, the dielectric constant of acetonitrile is significantly smaller than that of water (36.0 vs 78.5, respectively), hence, even just from an electrostatic point of view, ions are less stabilised by this solvent than they are by water; third, the limited capacity of acetonitrile to stabilise anions by hydrogen bonding causes certain anions, including specifically phenolates but also carboxylates, to resort to hydrogen bond with the undissociated acid, in the so-called 'homoconjugation' reaction.[235] In this case that would be:

$$2\ \mathrm{PhOH} + \mathrm{MeCN} \rightleftharpoons [\mathrm{MeCN{-}H}]^+[\mathrm{PhOH{-}PhO}]^-$$

Hence, the formation of homoconjugation complexes decreases the acidity of phenols in MeCN.

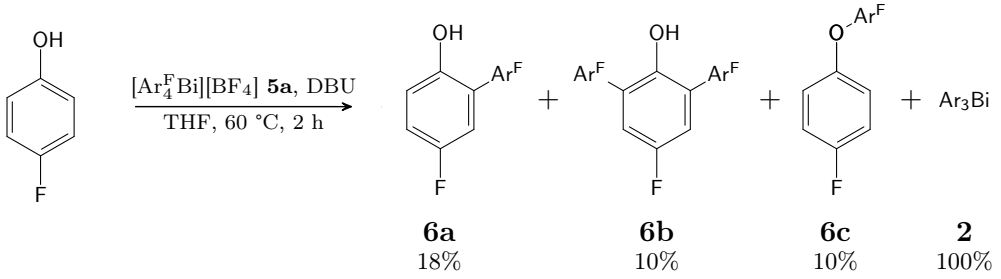

Scheme 2.4: Early tests were run to ascertain [Ar$_4^F$Bi][BF$_4$] capabilities in the arylation reactions. No reaction is observed without added base. Conditions: 1 equiv of phenol, 1 equiv of [Ar$_4^F$Bi][BF$_4$], 1.2 equiv of DBU. Percentages correspond to conversions determined by ^{19}F NMR spectroscopy. Approximately 60% of fluorophenol was left unreacted, whereas the bismuthonium was completely consumed. The reaction behaved similarly in deuterated acetonitrile.

unreacted. Interestingly, formation of fluorobenzene was not detected, even though the bismuthonium was fully consumed. On the other hand, several unidentified peaks were detected (ca. 20%). It is not unreasonable to assume that at least some of them are oxidation and over-arylation products, since both of them were detected and characterised by Barton.[89,98] These results, despite the highlighted flaws, were considered promising since they showed that bismuthonium **5a** is able to mediate the arylation of phenols.

In order to simplify subsequent analyses, a more appropriate substrate was sought. Prior work demonstrated that 2-naphthol could fulfil this role.[239] Compared to phenol, it is significantly more reactive and shows complete chemoselectivity towards *C*-arylation.[92] Moreover, since the two *ortho* positions are not electronically equivalent,[240] due to a better ability of the 1-position to delocalise the negative charge resulting from deprotonation,[241] over-arylation was envisaged to be less likely, in accordance to what observed by Barton in basic conditions.[92]

Labelling of 2-naphthol with a fluorine atom was required and 6-fluoro-2-naphthol was targeted because the 6-position can be considered (pseudo-)*para* to the hydroxy group, therefore the reasoning used before for *para*-fluorophenyl groups still holds. Synthesis of 6-fluoro-2-naphthol **7** was initially achieved as per Table 2.1. This exploits an intermolecular Friedel-Crafts acylation of trimethylsilyl acetylene, followed by an intramolecular Friedel-Crafts alkylation.[242,243] Unfortunately, the overall yield proved very poor,[239] ranging from 10 to 25%. Polymerisation of the acetylene was thought to be responsible for the poor outcome, so catalytic amounts of Lewis acid and lower temperatures were considered as potential improvements. Unfortunately none of the attempted modifications resulted in improved yield.

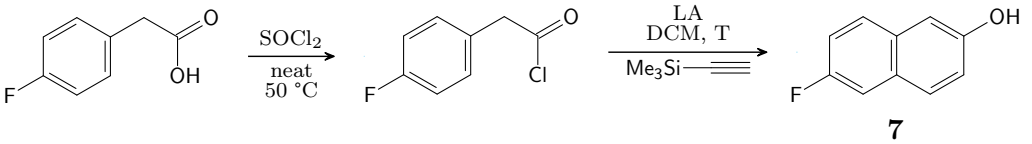

7

99% 19%

#	LA	mol%	T	Yield
1	$AlCl_3$	100	rt	19%
2	$AlCl_3$	100	−20 °C	0%
3	$AlCl_3$	10	rt	3%
4	$InCl_3$	10	rt	0%
5	$BF_3{\cdot}OEt_2$	10	rt	0%
6	$ZnCl_2$	10	rt	0%

Table 2.1: A tandem Friedel-Crafts acylation-alkylation process was initially employed to make 6-fluoro-2-naphthol. Optimisation did not provide the expected improvements. Reactions 2–6 were performed in a sealed MW tube under inert atmosphere and analysed by ^{19}F NMR spectroscopy.

Currently, the preferred method to synthesise this starting material encompasses the use of commercially available 2-bromo-6-fluoronaphthalene and is shown in Scheme 2.5. The halide is subjected to lithium-bromine exchange and the resulting lithiated species is then quenched with trimethyl borate to form the corresponding boronic ester, which is finally oxidised with hydrogen peroxide in acetic acid. With this method, the desired product was obtained in 76% yield.

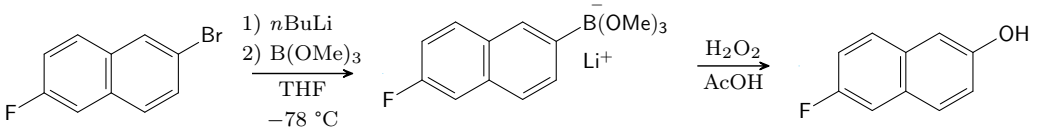

7

76%

Scheme 2.5: Improved synthesis of 6-fluoro-2-naphthol.

Fluoronaphthol **7** was then reacted under the same conditions used for fluorophenol (Scheme 2.4) and gratifyingly afforded the expected 1-arylated naphthol **8** selectively (Table 2.2, entry 2). Once again, DBU was fundamental: in its absence no reaction was observed even over a prolonged time (entry 1). Compared to the previously tested substrate, naphthol proved to react much faster, with quantitative conversion to product observed in 5 min. For all these reasons, naphthol was elected as the substrate of choice and henceforth used in all further investigations.

Different bases were tested in the reaction between $[Ar^F_4Bi][BF_4]$ **5a** and naphthol **7**: results are reported in Table 2.2. Tetrahydrofuran was replaced with

acetonitrile, due to a greater availability of pK_a data in the second solvent. The pK_aH$^+$ values in acetonitrile or water for the bases employed in this screening are reported for reference. A visual indication of reaction progress was provided by formation of a bright orange colour. This is in accordance with Barton's findings, who proposed that this derived from the formation of a substrate-bismuth complex.[134] The only exception is the reaction with NaOH (entry 10), in which the colour was light blue.

First, organic bases were assessed (entries 3–9): only DBU and BTMG allowed full conversion to the arylated product **8** within 5 min. On the other hand, pyridines (entries 8 and 9) proved extremely slow, with only a low percent conversion after several hours. Running the arylation in pyridine did not improve the outcome. Amine bases DABCO and DMAN (1,8-bis(dimethylamino)naphthalene, the parent

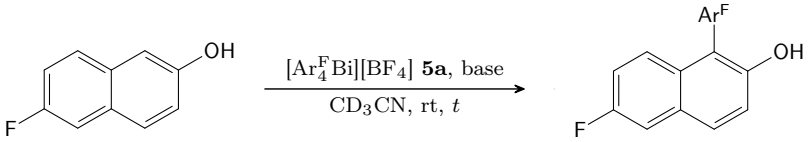

7 **8**

#	**Base**	p$\boldsymbol{K}_a$**H**$^+$$_{water}$	p$\boldsymbol{K}_a$**H**$^+$$_{MeCN}$	**Yield**	$\boldsymbol{t}$
1	none[a]	/	/	no reaction	
2	DBU[a]	11.5[244]	24.34[234]	100%	<5 min
3	DBU	11.5[244]	24.34[234]	100%	<5 min
4	DBU[b]	11.5[244]	24.34[234]	100%	<5 min
5	BTMG	14[245]	26.5[246]	100%	<5 min
6	DABCO	8.82[247]	18.29[247,248]	77%	2 h
7	DMAN	12.1[249]	18.62[234]	72%	3 h
8	collidine	7.45[250]	14.98[234]	2%	3 h
9	pyridine[c]	5.25[247]	12.33[251]	5%	1 d
10	NaOH[d]	14.0[252]	n.a.	100%	<5 min
11	K_3PO_4	12.3[253]	n.a.	100%	<1 h
12	K_2CO_3	10.3[244]	n.a.	100%	<1 h
13	$KHCO_3$	6.36	n.a.	9%	1 h
14	$KHCO_3$[e]	6.36	n.a.	54%	1 h

Table 2.2: 6-Fluoro-2-naphthol was identified as a better substrate than phenol, since it reacts faster and regioselectively. Over-arylation is also precluded. Conditions: 1 equiv of naphthol **7** and bismuthonium **5a**, 1.5 equiv of base. Yields determined by ^{19}F NMR spectroscopy. For entries 11–14, the suspensions were stirred at 1000 rpm. The pK_a values of the conjugate acid in water or acetonitrile are reported. For reference those of 6-fluoro-2-naphthol are 9.46 in water[254] and ca. 26 in acetonitrile.[236,255] [a] In THF at 60 °C; [b] in 5% water/CD_3CN; [c] in pyridine; [d] in 25% water/CD_3CN; [e] at 80 °C.

'proton sponge')[256] exhibited an intermediate behaviour, reaching around 70% completion in 2–3 h (entries 6 and 7). Interestingly, 5% water was shown not to hinder the arylation (entry 4), which occurred in the same amount of time required in the absence of water.

Inorganic bases were tested as well (entries 10–14). The reaction with NaOH (entry 10) was performed in an NMR tube in a 1:4 mixture of H_2O and MeCN, which was biphasic and had to be shaken to trigger the transformation. Despite this phase separation, naphthol **7** was fully arylated in less than 5 min. To avoid this complication, the remaining experiments (entries 11–14) were run in pure CD_3CN. The suspensions were stirred, since all the bases were insoluble. K_3PO_4 and K_2CO_3 yielded the arylated naphthol in less than 1 h, while $KHCO_3$ converted just 9% of the original substrate in the same amount of time. Conversion in the presence of $KHCO_3$ was improved to 54% in 1 h by heating the reaction to 80 °C (entry 14).

To summarise, a clear trend between reaction rate and pK_aH^+ value of these bases is evident, with DABCO possibly being an outlier. Moreover, it was pleasing to find that inorganic bases could be employed, too. Their advantage would be low toxicity, low cost and high availability. On the other hand, a biphasic (both liquid-liquid as in the water-acetonitrile mixture and solid-liquid) system introduces complications in the determination of reaction outcomes so their use was deemed inappropriate for optimisation studies.

2.2 The oxidation-transmetalation sequence

Having confirmed that all the individual steps of our ideal transformation (oxidation, transmetalation and ligand coupling) work and having identified a suitable substrate for testing, we focused on the goal of performing those steps in the same pot, without isolation of any of the intermediates. We reasoned that, if this stoichiometric approach were successful elevation to a catalytic regime would then be within reach.

The presence of fluoride counterions in the bismuth(V) species subjected to transmetalation with boronic acid was demonstrated to be essential for this reaction to occur.[257] For this reason the possibility of introducing such counterion directly during the oxidation of triarylbismuth was considered. This would by-pass the oxidation-metathesis sequence presented in Scheme 2.3. We questioned if electrophilic fluorinating agents were capable of oxidising Bi^{III} to Bi^{V}, while at the same time introducing the desired fluoride counterion.

These reagents allow the exploitation of a reactivity similar to that of elemental fluorine, minus the serious drawbacks that usually accompany this gas. Such

reagents typically comprise O–F- and, more recently, N–F-containing species. The first category was dominated by trifluoromethyl hypofluorite (CF_3OF), an extremely toxic gas (bp −95 °C), which used to be commercially available until the 1980s and was employed as a milder and more selective F^+ source than F_2 itself. In time, N–F species have entirely replaced O–F ones.[258] In fact, most of these newer reagents are air-stable solids, which makes them more practical reagents for synthesis.[259]

In the upcoming Schemes and Figures, these compounds will collectively be referred to as 'F^+' reagents, however it must be noted that this is a non-formal notation. There is, in fact, controversy regarding the mode of cleavage of the N–F bond and the two prevailing mechanisms of electrophilic fluorination (see Scheme 2.6). It is hypothesised that homolytic cleavage and S_N2-like displacement can both be operating, depending on substrate and conditions.[258,260]

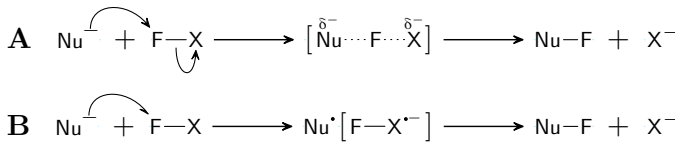

Scheme 2.6: The two possible mechanisms for the cleavage of N–F bond: **A** S_N2 substitution and **B** homolytic scission, the former initiated by a nucleophilic attack at the fluorine, the second by a single-electron transfer.

The most common N–F reagents are bench stable solids that are commercially available at reasonable prices. These include Selectfluor, NFSI and 1-fluoro-2,4,6-trimethylpyridinium tetrafluoroborate (hereafter referred to as collidinium salt), whose structures are shown in Fig. 2.1. Each of them represent the parent or most prominent example of three classes of these reagents, which are based on, respectively, tertiary amines, sulfonimides or pyridines and were first discovered by Banks,[261,262] Barnette[263] and Umemoto.[264,265]

The strength of these oxidants can be estimated by cyclic voltammetry (CV):[266] irreversible reductions occur at −0.04 V for Selectfluor, −0.78 V for NFSI and −0.73 V for the collidinium salt (MeCN, $[Bu_4N][BF_4]$ vs SCE). Interestingly, the same trend observed for their reduction potential is found in their ^{19}F chemical shifts in CD_3CN: +48.02 ppm, −15.89 ppm and −38.89 ppm, for Selectfluor, the collidinium salt and NFSI respectively. A more practical, although less quantitative, measure of their strength is given by their chemical behaviour: Selectfluor was shown to oxidise iodide and bromide (but not chloride) salts to the corresponding elements. This allows its standard reduction potential to be comprised between 2.16

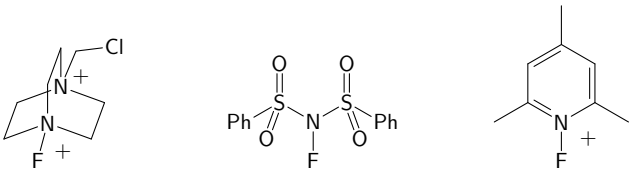

Banks Barnette Umemoto

Figure 2.1: A selection of commercially available electrophilic fluorinating agents. From left to right: Selectfluor, NFSI and 1-fluoro-2,4,6-trimethylpyridinium tetrafluoroborate. BF_4^- counterions omitted for the first and the last compounds.

and 2.72 V, double[‡] the standard reduction potentials for Br_2 and Cl_2, respectively. Triphenylbismuth has been reported to have an oxidation peak potential of 1.60 V (MeCN, $[Et_4N][OTs]$ vs SCE),[267] corresponding to the reaction: $Ph_3Bi^{III} + 2e^- \rightarrow [Ph_3Bi^V]^{2+}$. Cyclic voltammetry studies performed within the group showed a similar value (1.50 V, $[Bu_4][PF_6]$ vs ferrocene).[239] The measured oxidation potential for tri(*p*-fluorophenyl)bismuth is 1.66 V ($[Bu_4][PF_6]$ vs ferrocene), suggesting that Selectfluor had to be expected to be able to oxidise this species.

Having established the thermodynamical feasibility of the oxidation, we set out to test the three commercially available fluorinating agents in the oxidation of **2**. Due to its ionic nature, Selectfluor is poorly soluble in most organic solvents, but readily soluble in water and MeCN.[268,269] The collidinium salt is soluble is MeCN, DCM, Et_2O and THF,[270] while NFSI is soluble in an wider variety of solvents.[271] Acetonitrile thus represents the least common denominator among the three species and was therefore adopted as the solvent of choice for consistency. This was considered a reasonable choice, since also the arylation step was demonstrated to work well in acetonitrile (Table 2.2). Moreover, the availability of a deuterated version of the solvent at reasonable prices allowed most of the following reactions to be performed in NMR tubes. This enabled an efficient screening of different conditions and combinations of reagents: from now on it should be assumed all the reactions discussed in this Chapter were performed in NMR tubes in CD_3CN, unless specified otherwise.

Submitting triarylbismuthine **2** to these oxidants resulted in the formation of the corresponding Bi^V species (see Scheme 2.7), detected as a substantial downfield change in the chemical shift in ^{19}F NMR spectra (as shown in Fig. 2.2). The nature of the oxidised species depends on the oxidant, since the moiety (X in Scheme 2.7)

[‡]to take into account the fact that 2 electrons are required to reduce one molecule of halogen to the halide according to the following half cell reaction: $X_2 + 2e^- \rightarrow 2X^-$.

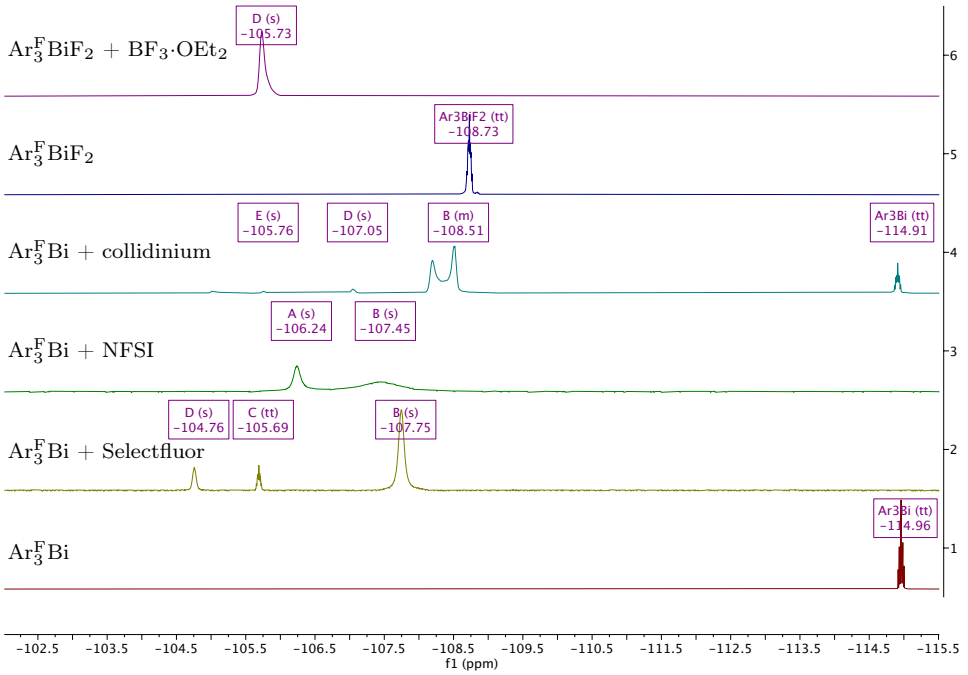

Figure 2.2: Stacked ^{19}F NMR spectra of the products of the oxidation of Ar_3^FBi **2** after 24 h. Only the region where *p*-fluorophenyl groups usually resonate is shown. From the bottom: 1) triarylbismuth **2** starting material; 2) oxidation with Selectfluor; 3) oxidation with NFSI; 4) (incomplete) oxidation with the collidinium salt; 5) isolated $Ar_3^FBiF_2$ **4**; 6) $Ar_3^FBiF_2$ with BF_3·OEt_2.

resulting from the detachment of the 'fluoronium' is expected to maintain some kind of coordination with the oxidised Bi species. To confirm the successful oxidation, a few crystals of LiCl were added so as to convert the different Ar_3^FBiFX species to $Ar_3^FBiCl_2$. Gratifyingly in all three cases, all the peaks which had formed upon oxidation of Ar_3^FBi converged to the peak corresponding to $Ar_3^FBiCl_2$, at the same time confirming the successful oxidation and the fact that the several species present at the end of the oxidation were species with different counterions equilibrating.

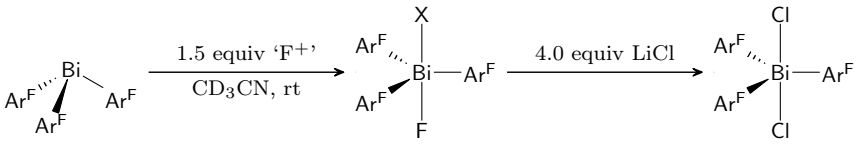

Scheme 2.7: Oxidation of triarylbismuthine and its *in situ* trapping with an excess of LiCl. X = the reduced oxidant.

Despite its reduction potential being higher than that of NFSI, the collidinium derivative was observed to be significantly slower than both Selectfluor and NFSI,

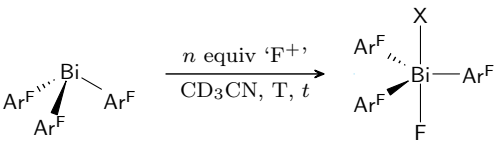

#	Oxidant	*n*	T	*t* for completion
1	Selectfluor	1.5	rt	<5 min
2	NFSI	1.5	rt	<5 min
3	Collidinium	1.5	rt	>1 d
4	Collidinium	2.0	rt	18 h
5	Collidinium	3.0	rt	6 h
6	Collidinium	2.0	40 °C	<2 h

Table 2.3: Selectfluor and NFSI were very effective in the oxidation of Ar^F_3Bi, whereas *N*-fluorocollidinium tetrafluoroborate required further optimisation. Reactions were performed in CD_3CN in NMR tubes and conversion was determined by ^{19}F NMR spectroscopy. For entry 3, monitoring was stopped at 24 h. At that point the yield had reached 91%.

with the latter oxidants completely consuming Ar^F_3Bi within a few minutes (see entries 1 and 2 of Table 2.3), while the former required more than 24 h (entry 3). This behaviour is consistent with the findings of Rozatian and co-workers, who observed that the pyridine-based fluorinating agent is 100 times slower than NFSI and 1 million times slower than Selectfluor in the fluorination of a malonate derivative.[272] In order to improve the performance of the oxidation with this oxidant, some reaction parameters were briefly optimised and results are reported in Table 2.3. Doubling the equivalents of oxidant shortened the reaction time from more than 1 d to just 6 h (entries 3 and 5, respectively). The oxidation is also very sensitive to temperature, since a 15 °C increment caused the reaction to reach completion in less than 2 h, versus 18 h at rt (entries 6 and 4, respectively).

Having confirmed that fluorinating agents are capable oxidants for Ar^F_3Bi, the competence of the resulting Bi^V species in the transmetalation was tested. We were pleased to see that simply combining the Bi^{III} starting material, one of the three oxidants discussed above and *p*-fluorophenylboronic acid in the presence of $BF_3{\cdot}OEt_2$ at rt afforded the desired tetraarylbismuthonium, as shown in Table 2.4.

When Selectfluor and NFSI were used, *i.e.* when the oxidation was complete within minutes rather than hours, the formation of $Ar^F_4Bi^+$ reached completion after 3 h in the first case and got to 79% yield after 24 h in the second case (entries 2 and 4, respectively). When $BF_3{\cdot}OEt_2$ was omitted, the yields at 24 h dropped to 38% and 13%, respectively (entries 1 and 3), thus showing that the

Lewis acid significantly enhances the rates of the transmetalation. It must be noted that *p*-fluorophenylboronic acid is only partially soluble in MeCN: saturation is reached at $[Ar^FB(OH)_2] = 5.0$ mM, as measured by ^{19}F NMR spectroscopy before adding the oxidants (this is approximately one sixth of the Ar^F_3Bi concentration in this set of reactions). If the rate of the mass transfer is lower than the rate of the transformation itself (*i.e.* it is the limiting factor), stirring the suspension is expected to improve the overall rate.

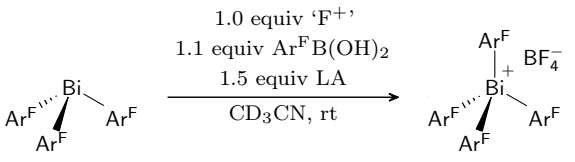

2 **5a**

#	**'F$^+$'**	**LA**	**Yield at 24 h**
1	Selectfluor		38%
2	Selectfluor	$BF_3{\cdot}OEt_2$	98%
3	NFSI		13%
4	NFSI	$BF_3{\cdot}OEt_2$	79%
5	NFSI[a]		23%
6	[F-TEDA][$(PhSO_2)_2N$]$_2$		13%

Table 2.4: *In situ* oxidation of triarylbismuthine and transmetalation of the fourth aryl group to form bismuthonium **5a**. The transmetalation is twice as fast when Selectfluor is employed instead of NFSI, possibly due to the presence of preformed tetrafluoroborate ions. Yields determined by ^{19}F NMR spectroscopy using 4,4′-bis(trifluoromethyl)-1,1′-biphenyl **9** as an internal standard. [a] With 2 equiv of $NaBF_4$.

The transmetalation is significantly faster if the oxidation is performed with Selectfluor (entries 2 vs 4 and 1 vs 3). The reason for this possibly lies in the nature of the species that occupies the vacant coordination position of the oxidised Bi species: when NFSI is employed, the sulfonimide derived from the oxidant (Fig. 2.3, left) can act as a moderately coordinating ligand for the Bi oxidised species. When the reaction is performed with Selectfluor, on the other hand, there are two potential ligands available in solution (Fig. 2.3, centre and right): the tertiary amine derived from Selectfluor and tetrafluoroborate. Among the two, tetrafluoroborate is expected to be the ligand of the oxidised Bi species. Differently from the sulfonimide, tetrafluoroborate is less coordinating, *i.e.* it donates less electron density into the bismuth centre, and this presumably makes the transmetalation more facile, by making the bismuth more electrophilic.

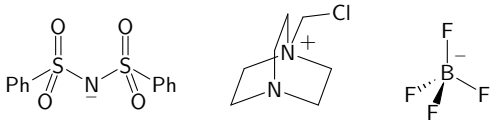

Figure 2.3: The sulfonimide resulting from the reduction of NFSI (left), the DABCO derivative resulting from the reduction of Selectfluor (centre) and tetrafluoroborate (right), the counterion of Selectfluor. Each of them can occupy the fifth coordinative position of $Ar^F_3BiF^+$. It is postulated that the transmetalation rate depends on the nature of the fifth ligand of bismuth.

It was interesting to notice that, despite the fact that tetrafluoroborate is not immediately available when NFSI is employed, it was observed to form over the course of the transmetalation reaction, both by ^{19}F and ^{11}B NMR spectroscopy. Tetrafluoroborate is thought to form as a consequence of the following equilibrium:

$$3\ FB(OH)_2 \rightleftharpoons BF_3 + 2\ B(OH)_3$$

Fluoroboronic acid, $FB(OH)_2$, is the by-product of the transmetalation: it forms upon coordination of the boron atom of the boronic acid to the bismuth-bound fluoride, as discussed in Scheme 1.7. The BF_3 that forms through this equilibrium is then able to sequester another fluoride from bismuth. Finally, boric acid, which is insoluble in most organic solvents, is detected as a white precipitate. From the stoichiometry of this reaction, four successful transmetalations are required to provide one tetrafluoroborate ion. This may explain why using Selectfluor as the oxidant improves the rate of the transmetalation, since it provides a pre-made counterion for the oxidised Bi species. The same effect is achieved by using $BF_3{\cdot}OEt_2$, which is thought to interact with the bismuth-bound fluoride, making tetrafluoroborate *in situ*.

In order to confirm the influence of the counterion of the oxidised species on the rate of the transmetalation, oxidation of Ar^F_3Bi with NFSI was performed in the presence of $NaBF_4$ and $ArB(OH)_2$, but in the absence of $BF_3{\cdot}OEt_2$ (see entry 5 of Table 2.4). A significant improvement was observed, compared to the reaction without the salt (entry 3), with the yield at 24 h rising from 13% to 23%. This figure is still not quite as good as in the case of Selectfluor being used as the oxidant (38%, entry 1). This is presumably because the counterion exchange is not fully effective, due both to the partial solubility of $NaBF_4$ in MeCN, as detected by ^{19}F NMR spectroscopy, and to the fact that the sulfonimide anion is coordinating and, hence, difficult to replace. Overall there is no strong preference for tetrafluoroborate, that is to say, an equilibrium between the two is in action.

An additional experiment was performed to confirm the previous hypothesis. It was reasoned that since the transmetalation shows an improved rate when BF_4^- is present (entries 4 vs 6), then the opposite effect may be achieved by removing such counterion. The most informative experiment would employ an F-TEDA-based oxidant, in order to rule out any influence from the nature of the oxidant, but with a different counterion. Such a derivative was synthesised by Wu and colleagues by replacing the two tetrafluoroborate ions with two bisphenylsulfonylimides (the counterion derived from NFSI),[273] according to Scheme 2.8. The procedure could be easily reproduced in our laboratory and, interestingly, shows a unique example of a stronger oxidant being prepared from a milder one.

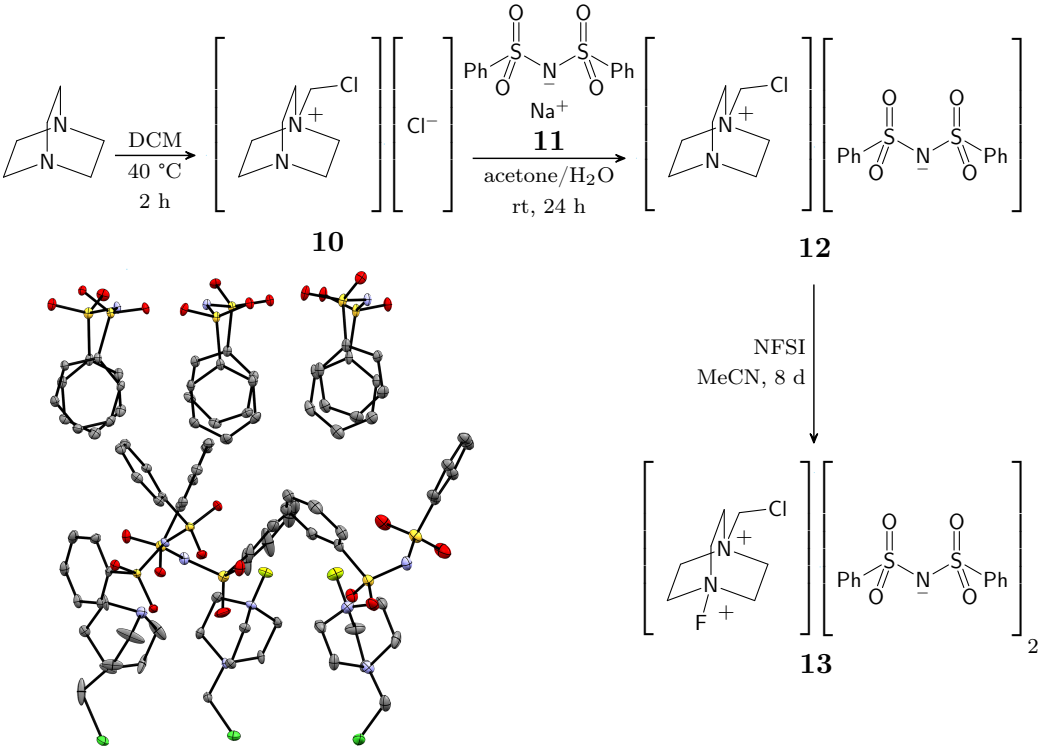

Scheme 2.8: Synthesis of the F-TEDA oxidant **13** was achieved *via* Wu's procedure.[273] Differently from Selectfluor, this compound does not contain tetrafluoroborate ions, as can be seen in the crystal structure (more details can be found in Section 6.8).

When the transmetalation was performed after oxidation with this newly synthesised oxidant, the yield measured at 24 h resulted to be comparable to that of the reaction performed with NFSI (entries 6 and 3 of Table 2.4), with a noticeable drop compared to the one performed with Selectfluor (13% vs 38%, entries 6 and 1, respectively), thus corroborating the theory that BF_4^- has a positive influence on the overall oxidation and transmetalation process.

Similarly to the NFSI case, tetrafluoroborate was observed to form over the course of the reaction. When its ^{19}F NMR integral was plotted against time (Figure 2.4), a sigmoid curve could be seen, which suggests there is an induction period at the beginning of the reaction, during which fluoroboronic acid accumulates. The stoichiometry of BF_4^- formation is confirmed by the fact that its concentration superimposes with the normalised concentration of $Ar^F_4Bi^+$ after 48 h (Fig. 2.4). Moreover, the induction period discussed above can also be seen clearly.

Attempts to extrapolate other quantitative data failed, due to the complexity of the reaction: although the transmetalation in itself can be expected to exhibit second order kinetics, resulting from the interaction of one molecule of oxidised Ar^F_3Bi and one molecule of boronic acid, the overall process is, in reality, the result of several other background processes that are hard to deconvolute. First of all, two separate mechanisms for the transmetalation are expected to be active: the one resulting only from the interaction of Bi and the boronic acid, and the BF_3-mediated one. However, BF_3 is initially only produced through the first mechanism, causing the second one to start later. Since the products of both mechanisms are the same, there is no way to quantify the independent contribution of each of them.

The speciation of $Ar^F_3BiF^+$, which is already complex when only an oxidant is used, as shown in Fig. 2.2, is now also directly intertwined with the transmetalation. In fact, the speciation varies with the availability of different counterions, namely dibenzene sulfonimide and tetrafluoroborate. An additional complication is that the latter is produced as a co-product of transmetalation. According to the results presented so far, $[Ar^F_3BiF][BF_4]$ should be more active in the transmetalation than the other species, since it is presumably more electrophilic. However, there is currently no data available on the rate constants or the equilibria involved in the formation of these two species.

Finally, because of this extremely dynamic behaviour, NMR peaks are often broad and the presence of extra underlying peaks can often be hinted at, thus making a full, accurate, quantitative analysis almost impossible. The evolution of $Ar^F_4Bi^+$ over time therefore cannot be easily linearised by first or second order analyses. Despite the fact that addition of BF_4^- can improve the overall rate, the reaction performs significantly better with $BF_3{\cdot}OEt_2$, so its use for the one-pot oxidation and transmetalation of Ar^F_3Bi was taken forward and the following step, the *in situ* arylation of 6-fluoro-2-naphthol, was investigated in order to complete the desired one-pot arylation sequence.

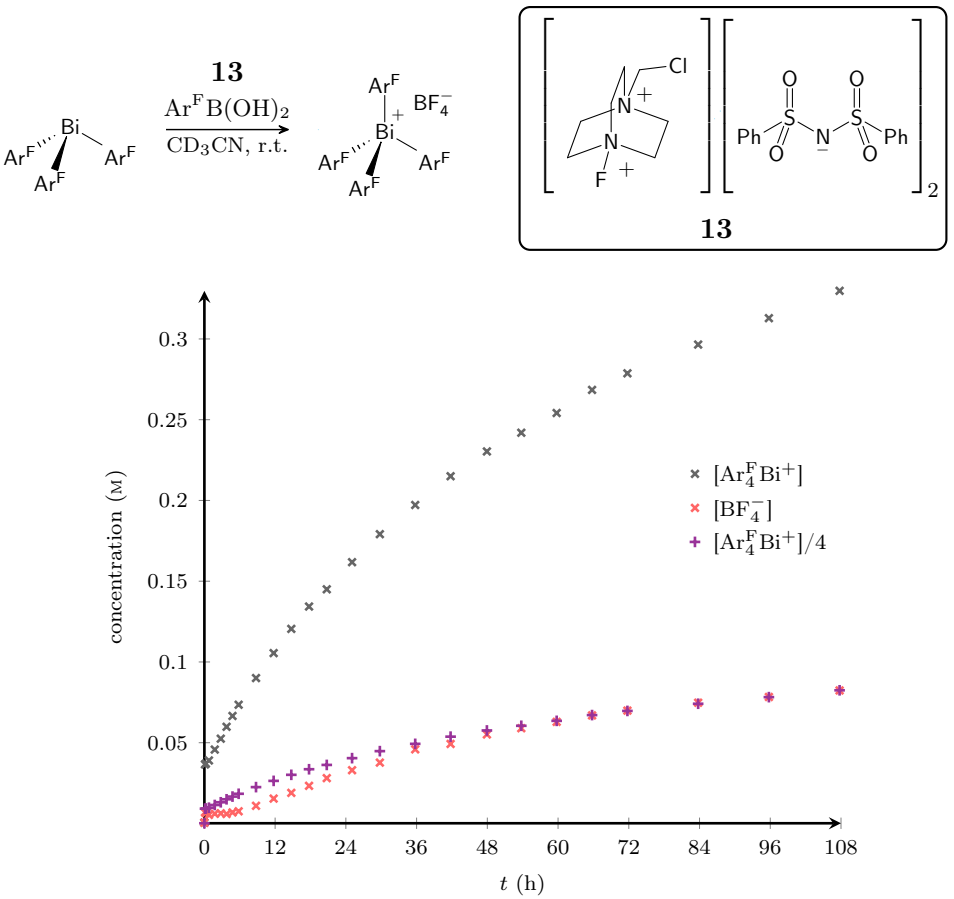

Figure 2.4: The Selectfluor-like oxidant **13** was used in the one-pot oxidation-arylation procedure to demonstrate the positive influence of tetrafluoroborate ions in the second step of that sequence. In this case, the overall transformation is affected by the absence of BF_4^- ions, that, however are generated *in situ*. If $[Ar^F_4Bi^+]$ is divided by 4, the resulting data points (violet) are shown to superimpose after 48 h to $[BF_4^-]$, while in early times an induction period can be spotted. This also confirms the stoichiometry of the formation of tetrafluoroborate ions: every 4 successively made bismuthonium salts, one BF_4^- is made. Concentrations determined by ^{19}F NMR spectroscopy by integration against an internal standard.

In order to test the feasibility of the arylation under the optimal oxidation-transmetalation conditions, 6-fluoro-2-naphthol and DBU were added to a solution of Ar^F_3Bi and boronic acid. An oxidant (either Selectfluor or NFSI) and $BF_3{\cdot}OEt_2$ were then added (Scheme 2.9). In both these experiments, the solutions turned rapidly black and the interpretation of the resulting ^{19}F NMR spectra proved non-trivial, due to the presence of 15–20 peaks, most of them unknown and evolving over time. Notably, considerable amounts of Ar^F_3Bi were detected, suggesting either a partial oxidation or a fast successive reduction. Interestingly, a partial conversion to $Ar^F_4Bi^+$ could be observed as well, demonstrating that at least oxidation and transmetalation are effective under these conditions. Because of the complex ^{19}F NMR spectrum, the reaction mixtures were analysed also by HRMS, showing no formation of the arylation product.

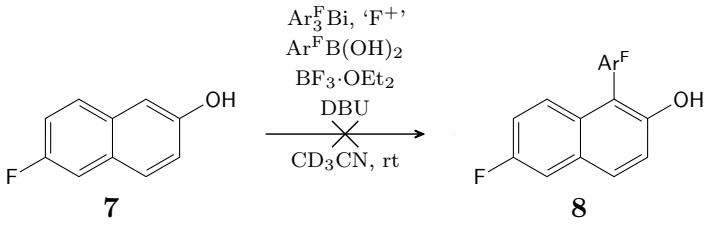

7 **8**

Scheme 2.9: The one-pot oxidation-transmetalation-arylation sequence did not yield product **8**, seemingly stopping at the transmetalation step.

Attempts to split the transformation in two parts, by adding naphthol and base in a second step, *i.e.* once bismuthonium was formed, also proved unsuccessful. Considering the reaction with $[Ar^F_4Bi][BF_4]$ and naphthol in the presence of a base was clean and straightforward when performed using the isolated bismuth species (see Table 2.2), a more thorough understanding of the reaction outcome was sought.

2.3 Understanding potential side-reactions

In order to deconvolute the complex series of reactions taking place when all the components were mixed together, the independent interactions between a selected number of these reagents were investigated.

2.3.1 $Ar^FB(OH)_2$ with oxidants

According to different reports, boronic acids are susceptible to fluorodeboronation when mixed with the fluorinating agents employed in this work.[274–276] The broadest

scope is obtained by using stoichiometric silver as a catalyst,[274] while the non-catalysed process is only effective for moderately electron-rich boronic acids (*p*-*t*Bu, *p*-OR...), with a significant amount of protodeboronation observed (up to 1:1 with the desired product in certain cases).[276] With this precedent in mind we tested for potential side-reactions between 4-fluorophenylboronic acid and either Selectfluor or NFSI, as described in Table 2.5.

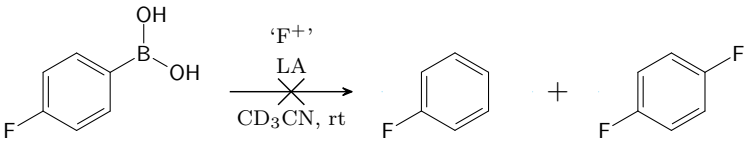

#	**Oxidant**	**LA**	**Decomposition**
1	NFSI		No
2	Selectfluor		No
3	NFSI	$BF_3{\cdot}OEt_2$	No
4	Selectfluor	$BF_3{\cdot}OEt_2$	Yes, only Ar^FH identified

Table 2.5: 4-Fluorophenylboronic acid does not react with Selectfluor and NFSI at rt. Addition of $BF_3{\cdot}OEt_2$ causes decomposition when used in conjunction with Selectfluor. The reaction products could not be identified. All reactions were performed in NMR tubes using 1.5 equiv of oxidant and 1.5 equiv of Lewis acid and were monitored by ^{19}F NMR spectroscopy.

These transformations are affected by the scarce solubility of the boronic acid in acetonitrile, so quantification was not possible. No decomposition was detected with either oxidants in the absence of $BF_3{\cdot}OEt_2$ (entries 1 and 2), nor in the reaction with NFSI and $BF_3{\cdot}OEt_2$ (entry 3). However, when Selectfluor was used in conjunction with $BF_3{\cdot}OEt_2$ (entry 4) several species could be seen forming over time by ^{19}F NMR spectroscopy. Of these, only one could be identified with certainty, fluorobenzene, but no traces of 1,4-difluorobenzene (expected to resonate at -121 ppm, as determined by ^{19}F NMR analysis on an authentic sample) could be detected. Attempts to gain further insight into this decomposition pathway thus failed. However, comparison between the reactions performed in the presence of $BF_3{\cdot}OEt_2$ and those in its absence highlighted that $BF_3{\cdot}OEt_2$ indirectly affects the speciation of the boronic acid, presumably by reacting with trace water:[277]

$$4\ BF_3 \ + \ 3\ H_2O \ \rightleftharpoons \ 3\ HBF_3 \ + \ B(OH)_3$$

This sequesters water and thus shifts the equilibrium between the boronic acid (-112.0 ppm) and the corresponding boroxine (-108.3 ppm). Figure 2.5 shows the

shift towards the boroxine (spectra 1 and 3). However, this happens consistently in the reactions with both oxidants, so none of the other peaks observed in the reaction with Selectfluor and $BF_3{\cdot}OEt_2$ can be ascribed to the boroxine.

Despite this undesirable reactivity of Selectfluor, the effects on the transmetalation of boronic acid to bismuth are negligible in the one-pot procedure. In fact, when $BF_3{\cdot}OEt_2$ is employed, the transmetalation is significantly faster than its decomposition. However this reaction may become relevant in a catalytic approach, since the concentrations of boronic acid and oxidant would be significantly higher than that of bismuth and thus their decomposition may become competitive.

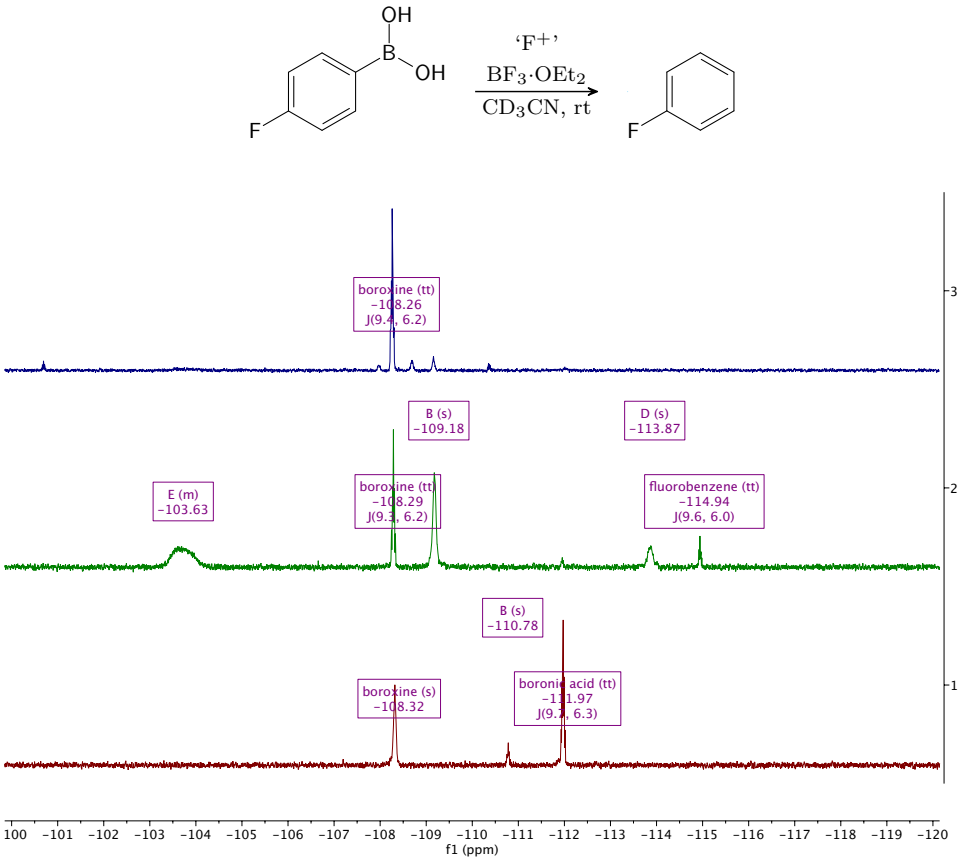

Figure 2.5: Stacked ^{19}F NMR spectra of the decomposition products of the reaction between *p*-fluorophenylboronic acid and Selectfluor or NFSI measured after 24 h. The reactions were performed in NMR tubes. Only the region where *p*-fluorophenyl groups usually resonate is shown. From the bottom: 1) *p*-fluorophenylboronic acid speciation in CD_3CN: both the boronic acid and the corresponding boroxine are visible; 2) reaction with Selectfluor: traces of fluorobenzene detected around −115 ppm; 3) reaction with NFSI: similarly to the Selectfluor case all the boronic acid in solution is converted to the boroxine but here decomposition is negligible.

2.3.2 Ar^F_3Bi with $BF_3{\cdot}OEt_2$

Addition complexes of BF_3 to amines,[278] phosphines,[279] arsines,[280] and even stibines[281] are known, while, on the other hand, this is not the case for the bismuth analogues. Such adducts are expected to be significantly less stable than those of lighter pnictogens, due to a poorer overlap of the diffuse 6s orbital of bismuth with the $2p_z$ of boron. In order to assess the effects of this foreseen instability, Ar^F_3Bi and $BF_3{\cdot}OEt_2$ were reacted together in CD_3CN and the reaction outcome was monitored over time. Complete consumption of Ar^F_3Bi was observed within 24 h.

Four different species were tracked in the reaction course (Fig. 2.6): Ar^F_3Bi (−114.95 ppm), fluorobenzene (−114.86 ppm), two new species (−111.41 ppm, tt, $J = 9.6$, 5.9 Hz and −108.90 ppm, br, respectively); the mass balance was maintained throughout the reaction. The unidentified species undergo decomposition when isolation is attempted, therefore *in situ* characterisation was performed. Formation

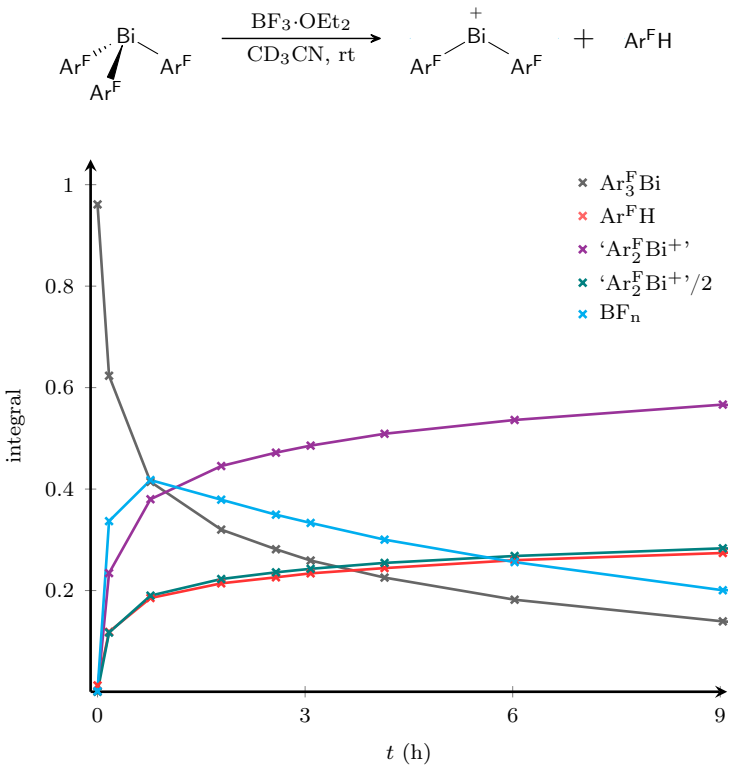

Figure 2.6: Plot of the integrals (normalised against the internal standard) of the species involved in the decomposition of Ar^F_3Bi by $BF_3{\cdot}OEt_2$ vs time. The exact nature of the diarylbismuthinium species drawn in the Scheme above is not certain. Conversion measured by ^{19}F NMR spectroscopy.

of the species at −111.41 ppm (teal blue curve, Fig. 2.6) occurred at the same rate as formation of fluorobenzene (red curve), assuming that the former consist of two Ar^F groups. GC-MS (EI) analysis of the reaction mixture revealed a peak with a fragmentation pattern of a Ar^F_2BiX species (Bi^{3+}, 209.0 m/z; Ar^FBi^{2+}, 304.0 m/z; $Ar^F_2Bi^+$, 399.0 m/z).

Analysis by ESI HRMS was even more informative. In addition to the three peaks detected by EI, the following ones were found: $[(Ar^F_2BiF_2)(MeCN)]^+$ (477.0528 m/z) and $[(Ar^F_2Bi)_2–F]^+$ (817.0769 m/z). It is worth noting that, despite the absence of any oxidant in the reaction mixture, the former is a Bi^V species: its origin is currently unclear. Nonetheless, these findings pointed towards the existence of a bismuth-bound fluoride (Scheme 2.10). No further data on the nature of this compound could be gathered, since attempted isolation destroyed the species. A careful look in the shielded region of the ^{19}F NMR spectrum revealed the presence of a peak at −148.95 ppm (cyan curve in Fig. 2.6), which could be tentatively assigned to a tetragonal BF_n species and integrated approximately 1:2 with the peak of the species at −111.41 ppm. The tetrahedral nature of this species and the NMR integration would both be consistent with the $Ar^F_2BiBF_4$ species depicted on the right hand side of Scheme 2.10.

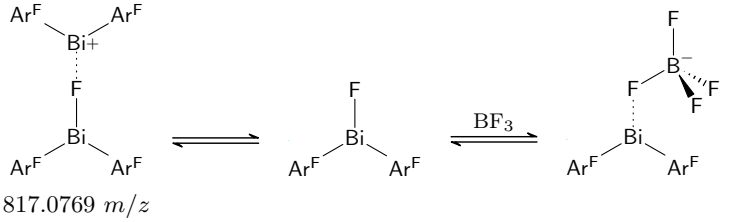

Scheme 2.10: Possible products of the decomposition of Ar^F_3Bi when exposed to $BF_3{\cdot}OEt_2$. The right hand side species is consistent with NMR observations, whereas the first species on the left with the HRMS result.

The decomposition pathway just described is negligible when the oxidation of Ar^F_3Bi is fast but becomes relevant when a milder oxidant, such as 1-fluoro-2,4,6-pyridinium tetrafluoroborate, is used in conjunction with $BF_3{\cdot}OEt_2$, for example during the one-pot oxidation-transmetalation reaction. In this case, after 18 h at rt all Ar^F_3Bi was consumed and the integral ratio for $Ar^F_4Bi^+$:$Ar^F_2Bi^+$ (corrected for the number of fluorine atoms in each molecule) was 2:1.

2.3.3 Oxidants with substrates

The 2-isomer of naphthol is known to be easily oxidised in basic conditions,[282] or, when fluorinating agents are employed, to undergo mono- or difluorination in the 1-position.[283–285] Therefore a series of experiments was undertaken to understand the degree of reactivity between these reagents under different conditions. The investigation started with Selectfluor. Simply mixing the two reagents in a 1:1 ratio caused the formation of two new species which could be identified as 1,6-difluoronaphthalen-2-ol and 1,1,6-trifluoronaphthalen-2-one **14** (Scheme 2.11).

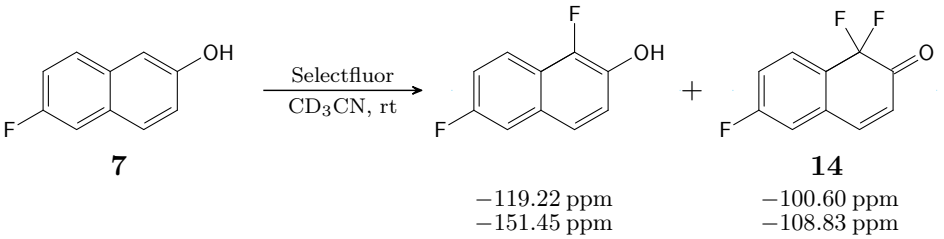

Scheme 2.11: Oxidation of 6-fluoro-2-naphthol by Selectfluor and NFSI in CD_3CN at room temperature.

Under these conditions, Selectfluor was completely consumed within a few minutes and the ratio of 6-fluoro-2-naphthol : 1,6-difluoronaphthalen-2-ol : 1,1,6-trifluoronaphthalen-2-one was 36:51:13 (entry 1 of Table 2.6). Compound **14** could be isolated performing reaction of **7** with 4 equiv of Selectfluor at 80 °C overnight. Isolation of the other product, on the other hand, proved challenging, due to the tendency towards overfluorination, even in the initial phases and with no excess of oxidant. The latter could be separated from **14** with a basic work-up, but could not be separated from the naphthol starting material. Isolation was not further attempted, since this kind of reactivity is known[283–285] and 1-fluoro-2-naphthol (the non-6-substituted analogue) is reported in the literature.[286] Finally, the reaction occurred both in the presence of just Selectfluor and $BF_3{\cdot}OEt_2$, and with additional DBU (entries 2 and 3 of Table 2.6), in the first case maintaining the same ratio of products, while in the second giving rise to the formation of various peaks, among which the identified fluorination products. These results led to a reconsideration of Selectfluor as the oxidant of choice in the envisaged catalytic system, given evidence of substantial incompatibility with the substrate.

NFSI showed a significantly lower reactivity compared to Selectfluor: with no additives (entry 3), 93% of naphthol was found intact after 3 d at rt, the remaining mass being 1,6-difluoronaphthalen-2-ol (6%) and 1,1,6-trifluoronaphthalen-2-one **14** (1%). Interestingly, in the presence of $BF_3{\cdot}OEt_2$ (entry 5), two extra species were detected and the conversion of 6-fluoronaphthol **7** after 3 d increased to 20%.

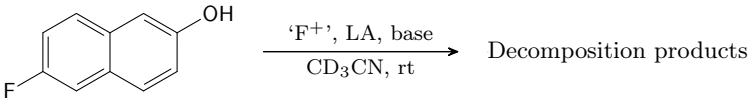

7

#	'F$^+$'	LA	Base	SM	Mono-F	Di-F	BsNHF	ArOBs
1	Selectfluor			36%	51%	13%	/	/
2	Selectfluor	BF_3		35%	52%	13%	/	/
3	Selectfluor	BF_3	DBU	30%	53%	17%	/	/
4	NFSI			93%	6%	1%	n.d.	n.d.
5	NFSI	BF_3		80%	7%	0%	7%	6%
6	NFSI	BF_3	DBU	0%	n.d.	n.d.	50%	50%

Table 2.6: Distribution of the indicated decomposition products of naphthol under different conditions. All reagents used in stoichiometric amounts compared to 6-fluoronaphth-2-ol **7**, with the exception of $BF_3{\cdot}OEt_2$, which was used in a 1.5 fold excess. In entry 3 several additional species were observed, too. In entries 1–3 and 6 the oxidant was consumed within minutes. For entries 4–5 the data point was taken at 3 d. SM = starting material = 6-fluoronapht-2-ol; Mono-F = 1,6-difluoronaphthalen-2-ol; Di-F = 1,1,6-trifluoronaphthalen-2-one; Bs = benzenesulfonyl; Ar = 6-fluoronaphth-2-yl.

Finally, when DBU was employed in conjunction with $BF_3{\cdot}OEt_2$ (entry 6), the naphthol starting material was immediately consumed, forming exclusively the two new species detected in the previous experiment, in a 1:1 ratio.

NFSI is reported to decompose in the presence of different nucleophiles following two different pathways:[287,288] soft nucleophiles react at fluorine, while harder ones at sulfur. The preference for the first type of reactivity was attributed by Antelo and co-workers to the ease with which single electrons can be transferred from soft nucleophiles compared to harder ones.[287] In the latter case, a 2-electron nucleophilic attack is presumed to occur instead. The presence of a full negative charge localised on a small, electronegative element such as oxygen, makes naphtholate a hard nucleophile, which therefore reacts at sulfur making *N*-fluorobenzenesulfonamide and 6-fluoronaphthalen-2-yl benzenesulfonate, as reported in Scheme 2.12.[287] This clearly put under consideration the use of NFSI in the one-pot arylation procedure.

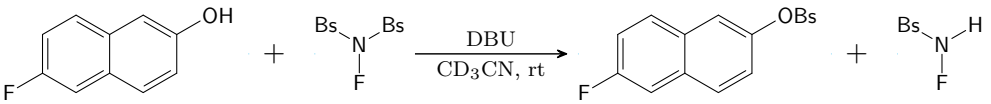

Scheme 2.12: NFSI was found to suffer a nucleophilic attack at the sulfur by the naphtholate, yielding the two products depicted. Antelo reported analogous products when 2-naphthol was employed.[287] Bs = benzenesulfonyl.

2.3.4 Oxidants with bases

Due to the essential role of a base in the ligand coupling reaction (Scheme 2.4 and Table 2.2), its influence on the stability of oxidants and bismuth(V) species was investigated. The latter kind of reactivity will be tackled in Section 2.3.5. Selectfluor and NFSI were reacted with DBU in CD_3CN. A plethora of new fluorinated species formed, essentially destroying both the oxidants upon mixing with the base. These results, together with those presented in Section 2.3.3, led to a reconsideration of the F-collidinium derivative as a potential alternative to Selectfluor and NFSI, despite it being significantly slower than these in the oxidation of triarylbismuth, as discussed in Table 2.3.

The F-collidinium salt was found to be inert towards naphthol, even over a three-day period, and even in the presence of $BF_3{\cdot}OEt_2$. However, as soon as DBU was added to the system (Scheme 2.13), the oxidant was completely and immediately consumed, while 6-fluoro-2-naphthol **7** remained untouched. Formation of 3-fluoro-2,4,6-trimethylpyridine and 2-(fluoromethyl)-3,4,6-trimethylpyridine in a 1.2:1 ratio was detected. Their chemical shifts were, respectively, −138.01 and −217.54 ppm, in accordance with Umemoto.[265,289] As reported by this author, both the reactions involve an ion pair intermediate, resulting from the base-induced detachment of the fluorine atom, similarly to what is observed for rearrangements of 2- and 4-methylpyridine *N*-oxides.[265] Unfortunately, *N*-fluorocollidinium undergoes the same decomposition reactions with other bases as well, such as DABCO, collidine, sodium naphtholate and even K_2CO_3. These results are consistent with the literature.[290]

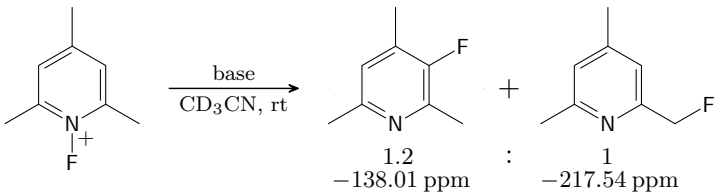

Scheme 2.13: Decomposition products of 1-fluoro-2,4,6-trimethylpyridinium tetrafluoroborate (counterion omitted for clarity) upon exposure to various bases, including DBU, DABCO, collidine and K_2CO_3. All the reactions were performed in CD_3CN, monitored by ^{19}F NMR spectroscopy and showed complete consumption of the oxidant within minutes.

2.3.5 Bismuthonium with DBU

The reaction of $[Ar^F_4Bi][BF_4]$ **5a** with DBU was monitored by ^{19}F NMR spectroscopy and was shown to form Ar^F_3Bi and fluorobenzene. The reaction exhibited net

second-order kinetics, showing first-order dependance on both $[Ar^F_4Bi][BF_4]$ and DBU ($k = 3.65 \pm 0.10 \times 10^{-4}$ $M^{-1}s^{-1}$). Deviation from linearity was observed in the kinetic analysis at early times. In fact, the reaction appeared to be more complex than suggested by its net kinetic profile: for example, the bismuthonium peak, that in the isolated material resonates at −107.07 ppm, in the presence of DBU shifted over time almost to −110 ppm. The origin of this behaviour is unclear. The top plot in Fig. 2.9 shows the variation of chemical shift for the aforementioned species over time. It is evident that such variation is not linear at all, nor follows a similar behaviour with different excesses of base. However, looking at the spectra reported in Figs. 2.7 and 2.8, the most striking observation is that there appears to be at least two species, which are likely to have very similar structures (due to the small difference in chemical shift), and that are presumably involved in some sort of interconversion process. Interestingly, the two species eventually converge into one (t = 2.8 h for 1.5 equiv DBU, t = 4.6 h for 1.75 equiv DBU), which proceeds as such until the end of the reaction. The merge points can be clearly seen both in Figs. 2.7 and 2.8 and in the chemical shift plot in Fig. 2.9, where they are shown to form cusps.

The mass balance of the reaction is quite informative, too. In this case, this was defined as the sum of the integrals of $Ar^F_4Bi^+$, Ar^F_3Bi and Ar^FH and normalised by dividing this value by the mass balance at t_0, so that it could be compared between two different reactions. This is then plotted against time in the top graph in Fig. 2.10. Although the mass balance is expected to remain constant and equal to 1 throughout the reaction, a deviation from ideality can be seen for both the reactions with different excesses of base. This is consistent with the fact that several minor peaks, that do not match any previously encountered species, were observed in the ^{19}F NMR spectra. On the other hand, no precipitate was detected. This indicates that the decomposition of the bismuthonium involves processes more complex than just the cleavage of one Bi–C bond.

If the latter occurs, it is suspected to be a homolytic process triggered by a SET event from DBU to Bi, which is reduced to an unstable Bi^{IV} species (see Scheme 2.14). This then breaks one of the four labile Bi–C bonds, getting reduced to Ar^F_3Bi and forming a 4-fluorophenyl radical, which presumably picks up a hydrogen atom from the environment, finally forming the detected fluorobenzene. Analyses of the final mixtures of both reactions by GC-MS did not show any trace of 1-deutero-4-fluorobenzene, the expected product in case the deuterated solvent were the source of the quenching radical. This is in accordance with ^1H NMR spectroscopy results.

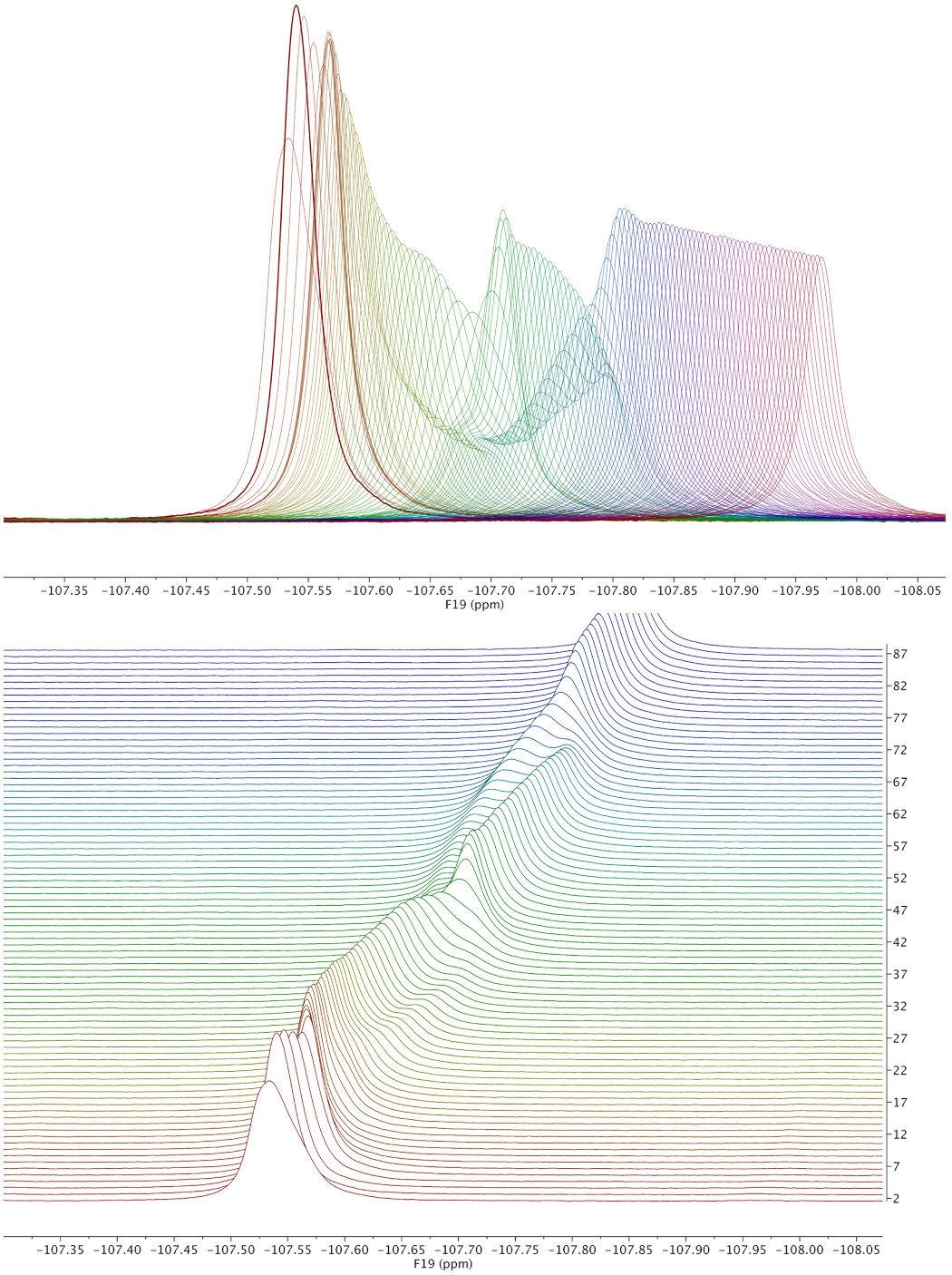

Figure 2.7: Reaction monitoring by $^{19}F\{^{1}H\}$ NMR spectroscopy of the decomposition of $[Ar^{F}_{4}Bi][BF_4]$ with 1.50 equiv of DBU. Superimposed (above) and stacked (below) spectra for the first 2.5 h. Only the region with the bismuthonium peak is shown as an example of the complexity of the reaction.

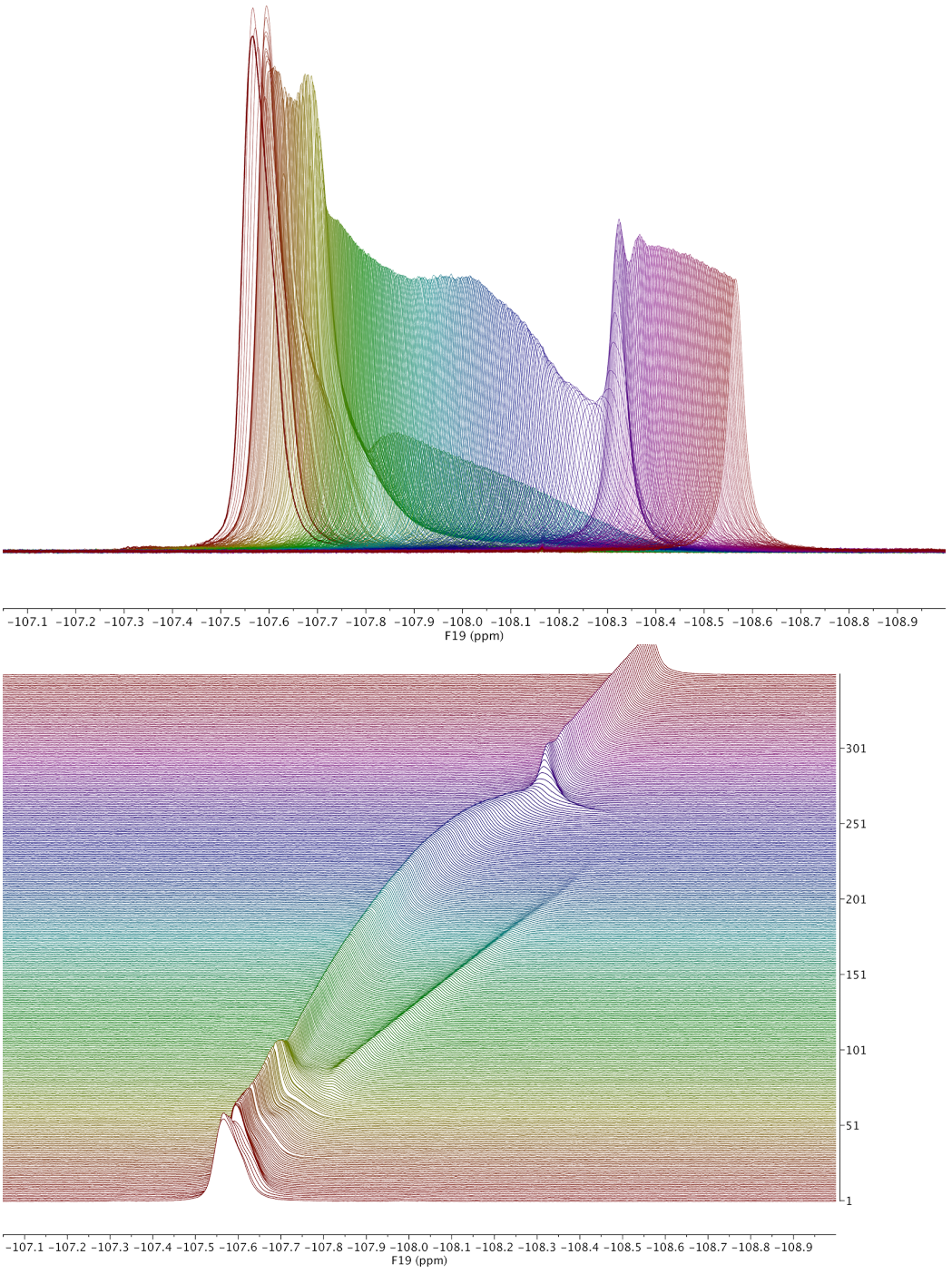

Figure 2.8: Reaction monitoring by $^{19}F\{^{1}H\}$ NMR spectroscopy of the decomposition of $[Ar^{F}_{4}Bi][BF_4]$ with 1.75 equiv of DBU. Superimposed (above) and stacked (below) spectra for the first 6 h. Only the region with the bismuthonium peak is shown as an example of the complexity of the reaction.

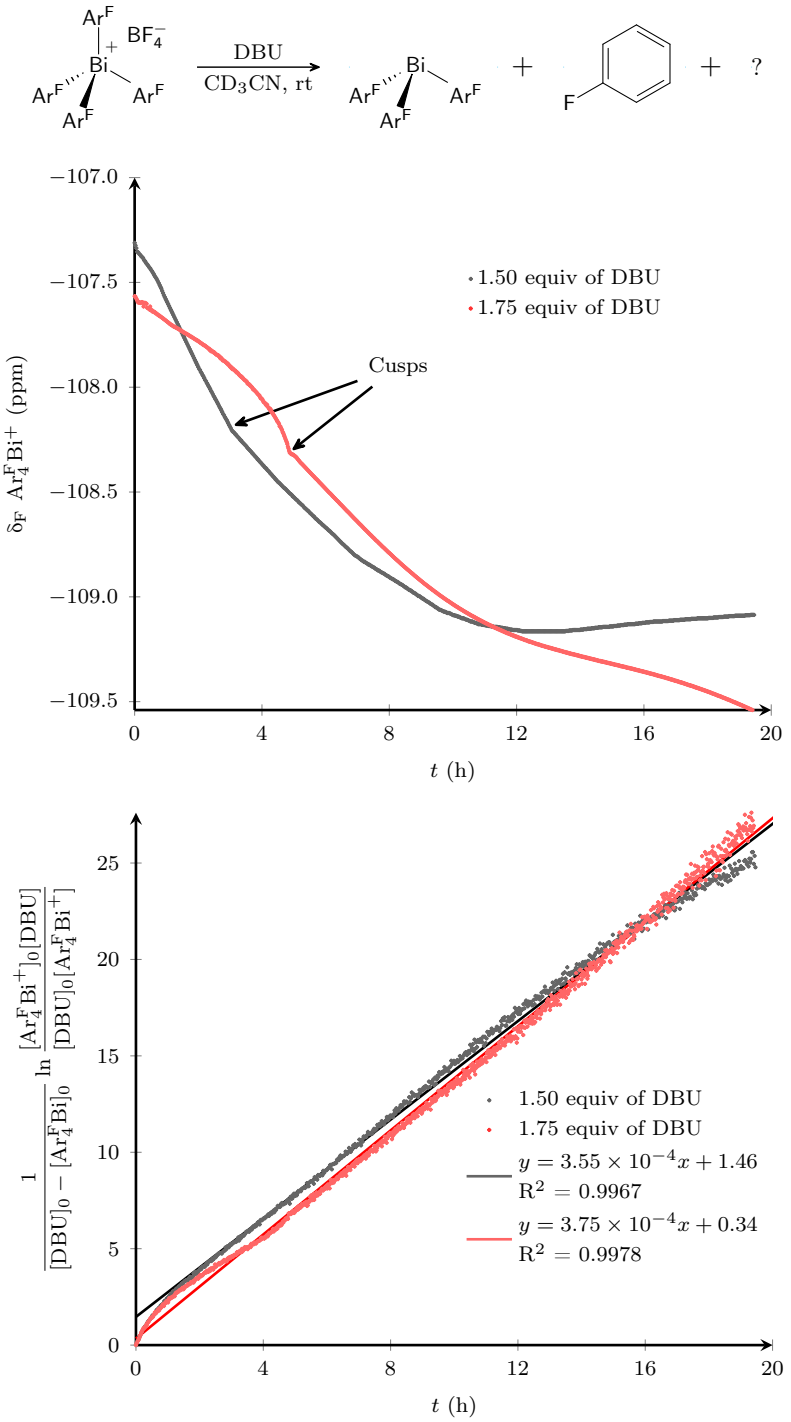

Figure 2.9: The variation over time of the chemical shift of the bismuthonium peak when exposed to DBU (top). The process follows second-order kinetics (bottom). Reactions monitored by ^{19}F NMR spectroscopy.

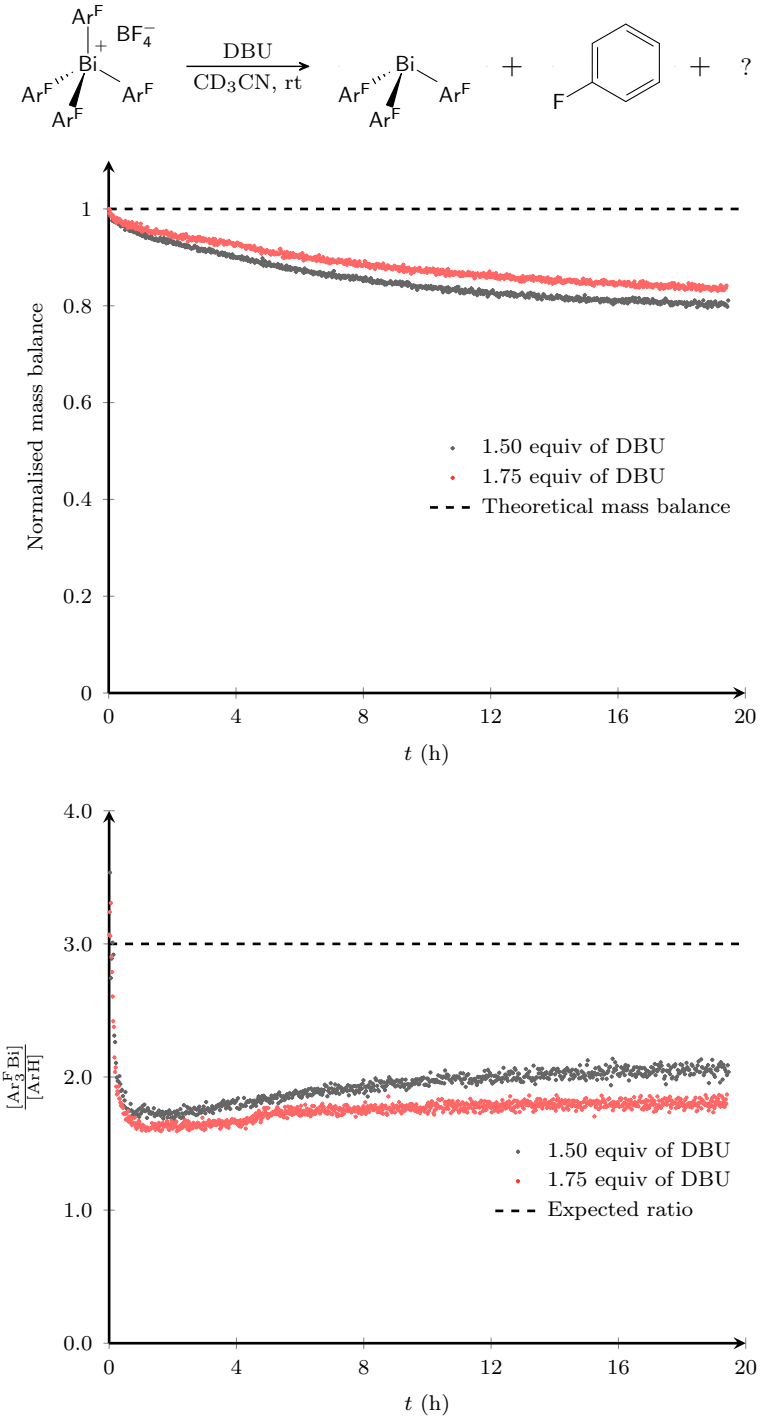

Figure 2.10: The mass balance of the reaction is not fully conserved (top). The ratio of the by-products of the decomposition does not remain constant through the process (bottom), suggesting the existence of side-reactions.

Similarly, there is no indication that the fluorophenyl radical was transferred to the radical cation of DBU. Unfortunately, none of the DBU-derived decomposition products could be identified.

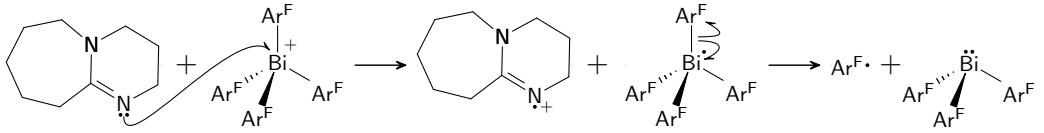

Scheme 2.14: Hypothesised mechanism for the decomposition of $[Ar^F_4Bi][BF_4]$ with DBU. This would explain the formation of fluorobenzene and the reduction to Ar^F_3Bi, however there is no definitive evidence confirming this.

In order to confirm that the decomposition reaction follows a radical mechanism, a selection of known radical scavengers was added to a solution of the bismuthonium salt in CD_3CN and the reactions were started by adding 1.5 equiv of DBU (Table 2.7). Diphenylethylene is the most frequently used radical inhibitor in combination with bismuth.[99,125,231] It found application in important work with diaryliodanes too.[104,105,107] Notably, it was used by McEwen and colleagues to study the alkoxide-induced decomposition of diaryliodanes.[291–293] The authors found that, when this inhibitor was used, one of the two possible decomposition pathways could be discounted. In the case of the decomposition of bismuthonium, no such marked effect could be detected and several unidentified peaks could still be observed. However, the consumption of bismuth compound after 18 h was considerably lower than in the reaction without scavenger (47 vs 84%, entries 1 and 5 of Table 2.7). The same positive effect was shared by TEMPO (entry 2), while the same could not be said for 1,3-dinitrobenzene and 1,4-benzoquinone. The former did not seem to have any effect at all, while the quinone induced instantaneous reduction of $Ar^F_4Bi^+$ to Ar^F_3Bi, with no traces of fluorobenzene detected.

This last result seemed at first surprising, given that quinones are often employed as oxidants.[294] However, arylation of quinone can be held responsible for the rapid consumption of the bismuth(V) species. This is expected to occur through a Morita-Baylis-Hillman-type intermediate, which forms upon 1,4-conjugate addition of DBU to the quinone. Despite DBU is usually considered a non-nucleophilic base, it was found by the Aggarwal group to be extremely effective in this type of reaction, ten time more than DABCO, a classic example of non-hindered nucleophilic amine.[295] Moreover, bismuth(V) is know to efficiently arylate enones under Morita-Baylis-Hillman conditions.[296] The occurrence of this reaction was demonstrated by HRMS analysis, which confirmed the presence in solution of both the benzosemiquinone

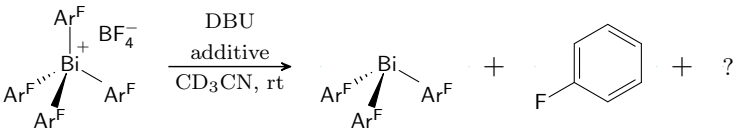

#	Additive	Conversion of $Ar^F_4Bi^+$
1	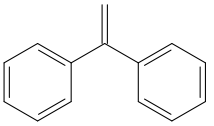	47%
2	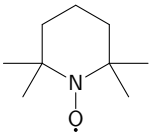	42%
3	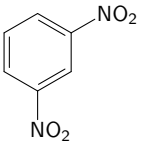	91%
4	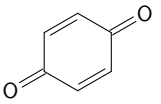	100%
5	None	84%

Table 2.7: The effect of radical scavengers on decomposition of the bismuthonium with DBU was assessed. All the reactions were performed in CD_3CN, using 1.5 equiv of DBU and monitored by ^{19}F NMR spectroscopy. Conversions measured at 18 h.

intermediate depicted in Scheme 2.15 (261.1594 m/z) and its mono-, di- and triarylation products (355.1813, 449.2033 and 543.2252 m/z, respectively).

Regarding the beneficial effects of 1,1-diphenylethylene and TEMPO, a clear explanation is currently not available, since no derivative of the two inhibitors could be detected, nor the decomposition completely prevented. If decomposition was prevented, one could have argued that these scavengers interacted with a potential propagation chain. However, since the decomposition was only slowed down, it could be suggested that the reactions occur through at least two different pathways: one in which the radical source is DBU itself, the second where the source is different, for example a 4-fluorophenyl radical. The inhibitor in that case could interact with that source. This would explain why the decomposition was not fully inhibited,

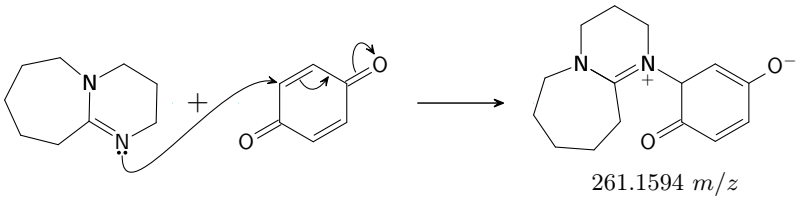

Scheme 2.15: Plausible mechanism for the formation of a potential substrate for the bismuth-mediated arylation of the quinone radical inhibitor through 1,4-conjugate addition, corresponding to the first phases of a Morita-Baylis-Hillman reaction.

since the first pathway would remain active. However, this is just a hypothesis and further research would be needed to understand the reaction mechanism properly.

2.4 Synthesis of an *ad hoc* oxidant

The previous Section explored the incompatibilities between different components of the system. The most detrimental interaction is that of the oxidant with both the base and the nucleophile, since in a catalytic system these reagents would be in excess compared to the bismuth species and therefore would be likely to react with each other in side reactions. In order to minimise this possibility, a milder oxidant was sought. Fluorocollidinium tetrafluoroborate would have been a good candidate, since it is commercially available and was shown not to react with naphthol. At the same time it is able to oxidise Ar^F_3Bi, although over a longer time than the stronger Selectfluor and NFSI. Table 2.3 showed that the rate of the oxidation could be improved significantly just by using a larger excess of collidinium, a condition similar to a catalytic set up. Unfortunately, the oxidant undergoes decomposition in the presence of any base, as discussed in Scheme 2.13.

Other oxidants were then considered, keeping in mind that most of their syntheses involved gaseous fluorine and that an alternative approach had to be taken. According to the experiments outlined in the previous Section, the ideal oxidant must possess the following characteristics:

1. it should be strong enough to oxidise Ar^F_3Bi;
2. it should be inert towards both the base employed to activate the naphthol and the naphthol itself;
3. it must be a fluorinating agent so that the resulting Ar^F_3BiFX species can be activated by the favourable formation of B–F bonds either with the boronic acid or with both the boronic acid and the Lewis acid.

An extensive examination by Cheng and co-workers reported two computational scales of more than 130 different N–F species, in which their behaviour as F^+,[259] or $F^{\cdot}$[297] was calculated. These data have been employed as a starting point to understand the strength of a potential oxidant. Fluorinating species with calculated Fluorine Plus Detachment Energy (FPDE), defined as the ΔH° associated to the detachment of an F^+ from a fluorine-containing species,[298] substantially higher than that calculated for Selectfluor were excluded from the pool of potential oxidants, because they would likely not respect point 2 of the previous list.

A series of moderately mild oxidants that should adhere to these principles was then envisaged. These are a modified version of NFSI in which one of the two benzenesulfonyl groups is substituted with an aryl ring. A comprehensive overview is given in Table 2.8. By substituting a sulfonyl group with an alkyl or aryl group, it was thought that the S_N2 mechanism that brought about the decomposition of the NFSI scaffold (see Scheme 2.12) could be prevented, due to the poor leaving group behaviour of the aryl group. These compounds had to be synthesised by fluorination of the corresponding sulfonamides **15a**–**f**, in turn obtained by condensation of an amine with benzenesulfonyl chloride (see Scheme 2.16). The newly introduced aromatic ring can be functionalised so as to modulate the strength of the oxidant. According to different studies, electron-donating groups depress the fluorinating reactivity, whereas electron-withdrawing moieties enhance it.[300]

The introduction of the 'F^+' functionality was carried out using Taylor's procedure,[299] *i.e.* deprotonating the sulfonamide with KH and then reacting this species with a strong fluorinating agent, such as NFSI. The use of such a strong and reactive base was justified by the fact that with other analogues formation of several side products was observed. Moreover, despite Selectfluor being generally considered stronger than NFSI,[259,297] only the latter was able to deliver product.

Although there are no reports of *N*-fluorosulfonamides in which the R group is an aromatic ring, it was decided to follow Taylor's method for the preparation of those compounds too, as discussed in Table 2.8. Entry 1 represents the only example where R is an aliphatic chain, the idea being to use it as a standard for comparison.

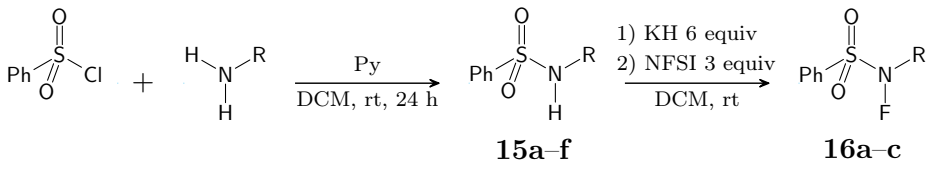

15a–f **16a–c**

Scheme 2.16: Synthesis of *N*-fluorosulfonamides.[299]

The synthesis of **16a** was achieved in acceptable yield after purification by flash column chromatography to remove the excess NFSI. The ^{19}F NMR chemical shift of the compound is upfield (−75 ppm), which suggests the species is decidedly more electron rich and therefore milder than the parent NFSI (−40 ppm). Its synthesis could be achieved with NaH instead of KH, with no drop in yield. However, attempts to switch to Selectfluor in order to simplify the purification (the oxidant could be removed with an aqueous work-up) failed, confirming Taylor's results.

Unfortunately, not all the syntheses were successful: referring to Table 2.8, *p*-fluoro- (entry 2), *p*-*tert*-butyl- (entry 4) and *p*-methoxy-substituted examples (entry 7) could not be obtained. Fluorine NMR spectra of crude materials reported a large number of species. A closer inspection of the spectra revealed complete consumption of NFSI, even though a three-fold excess compared to the sulfonamide was used. Moreover, the majority of the new peaks appeared in the aryl fluoride region, suggesting fluorination of the aromatic ring R. This hypothesis is corroborated by the chemical shift and multiplicity of one of the two major impurities in the crude for entry 2 (the second is an unresolved multiplet): −109.14 (ddd, J = 27.6, 9.2, 5.2 Hz). The largest coupling constant is indicative of a second fluorine atom *ortho* to the first one. This also explains the two other coupling constants, which show the presence of at least two other protons on the aromatic ring, one *ortho* to this new fluorine, the second *meta*. Admittedly, the number of peaks for entries 4 and 7 is significantly greater, so a clear identification of all the species formed is unfeasible.

Electron poor analogues (entries 3, 5 and 6) did not suffer from the same issues and could be synthesised without forming side-products. However, their stability was sometimes found to be poor. The synthesis of the bis-trifluoromethyl derivative **16b**, was studied in greater detail and identified a series of issues. The compound was suspected to be unstable to silica, so subjection of the crude mixture to different conditions was then studied: surprisingly, the compound was found to be stable towards filtration over silica and celite, as well as to dilution in deuterated chloroform (that is, exposure to trace water and oxygen). However, both a basic and a neutral aqueous work-up caused the partial decomposition of the product, yielding a mixture of starting material **15b** and product **16b**: in the first case the amount of starting material corresponded to 36%, whereas in the second case the amount of decomposition was more limited (13%). To avoid the need for column chromatography, two contaminants had to be avoided: mineral oil in which KH is dispersed and the excess NFSI. The first was removed by washing the dispersion with dry Et_2O under inert conditions, the second was simply avoided by using the

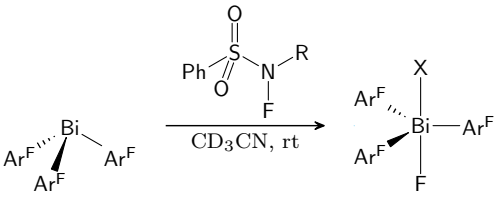

#	Oxidant	Cpd.	δ_F/ppm	Yield
1	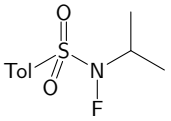	**16a**	−75.32	7% in 3 d
2	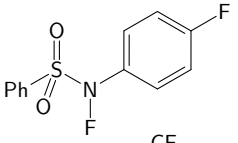	synthesis failed		
3	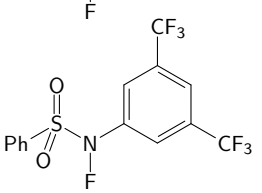	**16b**	−39.18	n.a.*
4	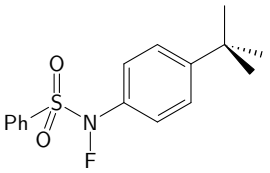	synthesis failed		
5	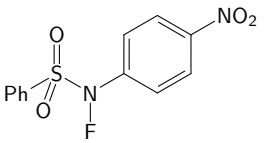	**16c**	−41.07	100% in 15 min
6	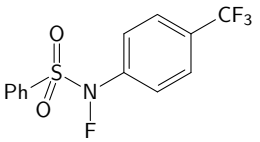	not isolated		
7	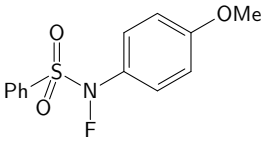	synthesis failed		

Table 2.8: *N*-Fluorosulfonamides whose synthesis has been attempted. Fluorine NMR chemical shifts of the N–F fluorine in CD_3CN are reported only for those species which were successfully isolated. *Oxidation of Ar^F_3Bi was observed, but could not be quantified due to decomposition products.

compound in slight deficit (0.95 equiv). This optimised procedure provided the desired product in good yield.

The isolated F–sulfonamides **16a**–**c** were tested in the oxidation of Ar^F_3Bi. The isopropyl derivative **16a** resulted to be a very poor oxidant for Ar^F_3Bi, converting just 7% of the bismuth(III) to its higher oxidation counterpart over a three-day period at room temperature. On the other hand, it proved completely inert towards naphthol in the same conditions. The scarce reactivity has been ascribed to the steric hindrance supplied by the isopropyl group.[301] Despite the fact that the rate of the oxidation with this compound could probably be improved by a slight increase of temperature, it was set aside, preferring to concentrate our investigations on the aryl derivatives, whose reactivity, differently from the alkyl species, can be tuned with the insertion of the appropriate substituent.

The bis-CF_3 derivative **16b** was only tested in the one-pot oxidation and transmetalation procedure in the presence of $BF_3{\cdot}OEt_2$ and was initially thought to have performed better than the isopropyl analogue, consuming Ar^F_3Bi in less than 1 h. With the benefit of hindsight however, the consumption of Ar^F_3Bi can now be attributed only partially to the oxidation by **16b**, since signs of the decomposition caused by $BF_3{\cdot}OEt_2$ and discussed in Section 2.3.2 were detected. Unfortunately the ratio $Ar^F_4Bi^+/Ar^F_2Bi^+$ was only 1:4, as determined by ^{19}F NMR spectroscopy, suggesting that the decomposition of Ar^F_3Bi is significantly faster than its oxidation by the *N*-fluorosulfonamide. It is worth noting that such decomposition required a few hours when only Ar^F_3Bi and $BF_3{\cdot}OEt_2$ were reacted together, whereas in this case all the Ar^F_3Bi that had not been oxidised already underwent decomposition within minutes.

To our dismay, when isolated **16b** was exposed to $BF_3{\cdot}OEt_2$ in $CDCl_3$, even more decomposition products were detected. The major one was identified as the product of the reaction in Scheme 2.17. The assignment was confirmed both by ^{19}F NMR spectroscopy and HRMS. The first technique showed two peaks: -61.69 ppm (d, $^4J_{F-F} = 13.4$ Hz) and -119.98 ppm (heptt, $^4J_{F-F} = 13.4$ Hz, $^4J_{H-F} = 5.5$ Hz). The second displayed a peak in negative mode at 386.0101 m/z, which is consistent with the deprotonated sulfonamide. This instability is a major drawback, considering that the presence of BF_3 is unavoidable, since it is produced as a side product of the transmetalation of boronic acid to bismuth (Section 2.2).

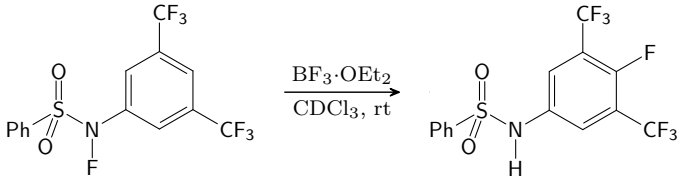

16b

Scheme 2.17: *N*-fluorosulfonamide **16b** underwent rapid decomposition when exposed to $BF_3{\cdot}OEt_2$.

On a positive note, further experiments assessed the behaviour of **16b** with bases and confirmed its stability at room temperature. In particular it was tested both with organic bases and with potassium naphtholate, proving that, differently from NFSI, no elimination was observable. Moreover, addition of naphthol and base to the bismuthonium obtained *via in situ* oxidation and transmetalation showed formation of traces of product (as confirmed by HRMS). The same result could not be achieved with either Selectfluor or NFSI (Scheme 2.9).

The *p*-nitro derivative **16c** was put to the test, as well. The compound resulted to be significantly more efficient than the isopropyl analogue **16a**, fully oxidising Ar^F_3Bi within 15 min. Unfortunately, the oxidant was found to decompose on standing: storing the solid in a vial for three months caused the consumption of 66% of the species and generated one major product, tentatively assigned to the *ortho*-fluorination product depicted in the Scheme 2.18, on the basis of ^{19}F NMR spectroscopy alone (−124.87 ppm, dddd, J = 10.2, 7.8, 2.3, 1.2 Hz).

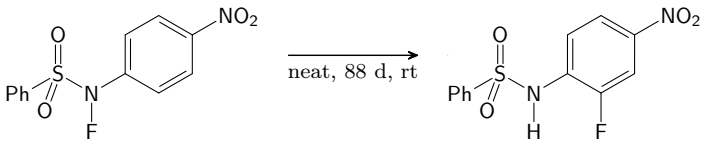

16c

Scheme 2.18: *N*-fluorosulfonamide **16c** underwent decomposition upon standing at rt. The possible decomposition product is reported.

The mechanism for the formation of products of both Schemes 2.17 and 2.18 is currently unknown. In addition to the fluorination of the aromatic ring, appearance of BF_n species was detected around −150 ppm by ^{19}F NMR spectroscopy. With the only source of boron being the glass of the vial in which the oxidant was stored, this suggests potential etching of glass. Due to this instability and suspecting an excessive oxidation potential for compound **16c** further tests were not performed.

2.5 Reassessing the innocence of $BF_3{\cdot}OEt_2$

Despite the considerable effort put into minimising side-reactions with oxidants, a clear-cut solution was not found. Moreover, a reconsideration of previous results led us to identify an issue that had been overlooked to this point. Section 2.2 mentioned that arylation of naphthol could not be achieved either when substrate and base were added before oxidation and transmetalation, or if their addition was done later on. The latter was performed by adding the naphthol to a solution containing the bismuthonium obtained *in situ* by oxidation and transmetalation in the presence of stoichiometric $BF_3{\cdot}OEt_2$, as per Scheme 2.19. Crucially, both the bismuthonium and the substrate remained unreacted, essentially ruling out the occurrence of the following reactions: 1) decomposition of Ar^F_3Bi by $BF_3{\cdot}OEt_2$, 2) fluorination of naphthol or base by the oxidant, 3) base-triggered reduction of the bismuthonium.

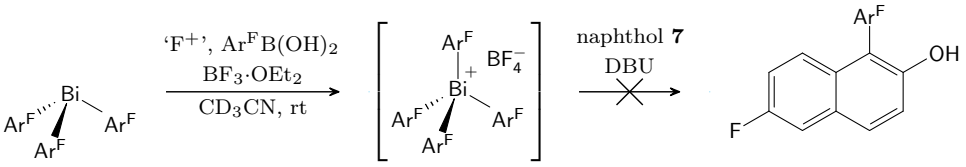

Scheme 2.19: The *in situ* arylation of naphthol does not occur even if the bismuthonium is pre-formed.

The absence of decomposition pathways 1) and 2) could be rationalised by assuming that oxidation of Ar^F_3Bi is fast. This would avoid prolonged contact of both Ar^F_3Bi with $BF_3{\cdot}OEt_2$, and oxidant with naphthol, outcompeting both reactions. However, fast formation of bismuthonium would lead to extended exposure to DBU, which is expected to result in base-induced decomposition (see Section 2.3.5). Yet, no such decomposition occurred.

It was reasoned that, in comparison to the arylation performed with isolated bismuthonium (which delivered product, see Table 2.2, entry 3), other species were present after the one-pot oxidation and transmetalation steps, including: excesses of $BF_3{\cdot}OEt_2$ and boronic acid, the reduced oxidant and boric acid. In order to test if the presence of any of them was actually impeding the arylation, each of them was added individually to solutions of isolated bismuthonium and naphthol, finally DBU was added and the reactions were monitored by ^{19}F NMR spectroscopy. Results are reported in Table 2.9.

At this point, the Lewis acid was suspected to be the most likely culprit, so the fact that arylation could be achieved in its presence (entry 1) was quite surprising.

When $BF_3{\cdot}OEt_2$ was added, the tetrafluoroborate peak disappeared and was replaced by a single broad peak, presumably corresponding to a fluoride-bridged $B_2F_7^-$ species.[302] Both the bismuthonium salt and the naphthol were stable over at least a few hours in the presence of the Lewis acid and no tetrahedral adduct of BF_3 could be detected. Addition of DBU caused the immediate consumption of ca. 70% of the bismuthonium and correspondingly the arylation of the substrate. After 3 h the reaction had stalled at ca. 85% conversion. Curiously, the bismuthonium peak, which usually moves upfield during the arylation, was found to move in the opposite direction after the initial phase of the arylation. At this stage, it was not clear why the reaction only worked partially, with a significant rate reduction observed after the first few minutes.

With this result in hand, other potential Lewis acids were considered for the same role of inhibitor. However, neither the addition of boronic acid nor boric acid (entries 2 and 3) prevented the arylation, although it must be noted that the former is only partially soluble in acetonitrile, while the latter is completely insoluble, as far as could be determined by ^{11}B NMR spectroscopy.

Finally, complexation of the bismuthonium salt by the reduced oxidant was considered as a potential cause for the interrupted arylation. The test reaction (entry 4) was performed as follows: 2 equiv of dibenzenesulfonimide were dissolved in CD_3CN, then DBU (3 equiv) was added; naphthol (1 equiv) was added as well and was immediately deprotonated by the excess of base, as detected by the variation in

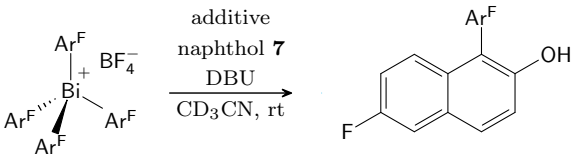

#	Additive	Yield at 10 min	Notes
1	$BF_3{\cdot}OEt_2$	70%	85% at 3 h
2	$Ar^FB(OH)_2$	100%	
3	$B(OH)_3$	100%	
4	Bs_2NH*	100%	
5	none	100%	
6	$BF_3{\cdot}OEt_2$ + $Ar^FB(OH)_2$	0%	no reaction

Table 2.9: Additives (1.5 equiv) were added to isolated bismuthonium **5a** (1 equiv) to understand if any of them was hindering the arylation of naphthol (1 equiv). DBU: 1.5 equiv. *2 equiv, with 3 equiv of DBU. Yields determined by ^{19}F NMR spectroscopy.

^{19}F NMR chemical shift from −120.70 to −123.60 ppm; finally the bismuthonium was added and instantaneous reduction to Ar^F_3Bi and complete arylation of naphthol were detected. An analogous experiment, in which dibenzenesulfonimide was deprotonated with NaH in THF, before the bismuthonium and the naphthol were added to the same solution, gave the same result.

These experiments are biased by the fact that coordination of the dibenzenesulfonimide anion to the bismuthonium salt could not be proven, hence the influence of reduced NFSI could not be assessed reliably. Moreover, there was no certainty that this condition was fully comparable with oxidising Ar^F_3Bi with NFSI, since in that case the sulfonimide presumably gains access to the inner coordination sphere of the bismuth(V) species. Therefore, a way to corroborate these results was sought, but taking the opposite approach. It has been shown that the arylation does not work when the bismuthonium is prepared *in situ* from Ar^F_3Bi using NFSI as the oxidant (Scheme 2.19). On the other hand, if the arylation had worked in a situation as close as possible to the one-pot procedure, but in the absence of the oxidant-derived sulfonimide, this would have proven the existence of a negative influence of the latter. In order to avoid the presence in solution of sulfonimide, it was necessary to start from a pre-oxidised Bi species. $Ar^F_3BiF_2$ was identified as the candidate of choice, since the transmetalation of boronic acids to this species had been demonstrated both by Matano[75] and ourselves (see first step of Scheme 2.3).

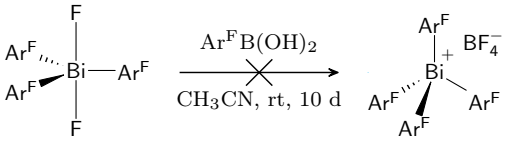

4 **5a**

Scheme 2.20: The transmetalation of 4-fluorophenylboronic acid to $Ar^F_3BiF_2$ did not proceed in the absence of $BF_3{\cdot}OEt_2$, showing only 10% conversion after 10 d, as measured by ^{19}F NMR spectroscopy. Conditions: 1.5 equiv of boronic acid, NMR tube.

Given the mixed results obtained when using $BF_3{\cdot}OEt_2$ as the additive and still suspecting a negative influence of the Lewis acid, transmetalation to $Ar^F_3BiF_2$ without $BF_3{\cdot}OEt_2$ was attempted first (see Scheme 2.20). In order to maximise the conversion rate, the solution was stirred at rt, rather than performing the reaction in an NMR tube. However, consistent with Matano's results,[75] the reaction performed poorly, forming less than 10% of the bismuthonium after 10 d. For a comparison, the same reaction carried out with $BF_3{\cdot}OEt_2$ reaches completion in ca. 12 h. The transmetalation was, therefore, performed with $BF_3{\cdot}OEt_2$ to test if

the arylation occurred in the absence of the reduced oxidant (Scheme 2.21). The absence of any arylation products suggested that either reagents or side-products of the transmetalation reaction were to be blamed.

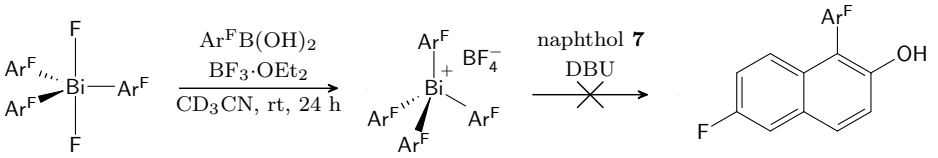

4 **5a** **8**

Scheme 2.21: The arylation did not occur when the bismuthonium was obtained *via* transmetalation to the isolated $Ar^F_3BiF_2$, which requires $BF_3{\cdot}OEt_2$, thus ruling out a negative influence of the reduced oxidant.

Taking into account the results displayed in entries 1–3 of Table 2.9, an additional experiment was performed, in which both $BF_3{\cdot}OEt_2$ and the boronic acid were employed as additives (entry 6). In this case, no sign of arylation could be detected: neither formation of Ar^F_3Bi, nor product, nor upfield shift of the bismuthonium peak. However, addition of an extra 1.5 equiv of DBU triggered instantaneous and full conversion to product.

A titration was performed to determine the exact amount of base necessary to trigger the arylation under these conditions. First, full conversion to the bismuthonium was obtained, then 6-fluoro-2-naphthol was added. Finally, DBU was added as a stock solution in increasing amounts up to 5 equiv. A ^{19}F NMR spectrum was measured 10 min after each addition, thus allowing time for the reaction to proceed before analysis. The results are reported in Fig. 2.11. Similarly to the first iteration of this experiment (Scheme 2.9), the consumption of $Ar^F_4Bi^+$ and the variation in chemical shift were minimal until the first equivalent of DBU had been added. Both values began to change around 1.2 equiv and the variation became significant after 1.4 equiv. Interestingly, the reaction did not reach full consumption of the bismuthonium, instead reaching a plateau around 5% of $Ar^F_4Bi^+$ left. This behaviour is consistent with the following phenomenon: the first equivalent of DBU was consumed by a side-reaction, then the excess base triggered deprotonation of the substrate, enabling the arylation. Differently from the situation where the bismuthonium reacted exclusively with naphthol and base, in this case the arylation is not instantaneous and complete, even when a five-fold excess of DBU is used.

With a precise culprit in mind, it was reasoned that, since the transmetalation would always give fluoroboronic and, eventually, boric acid as side-products, these species would always be present in solution at the end of the process. On the

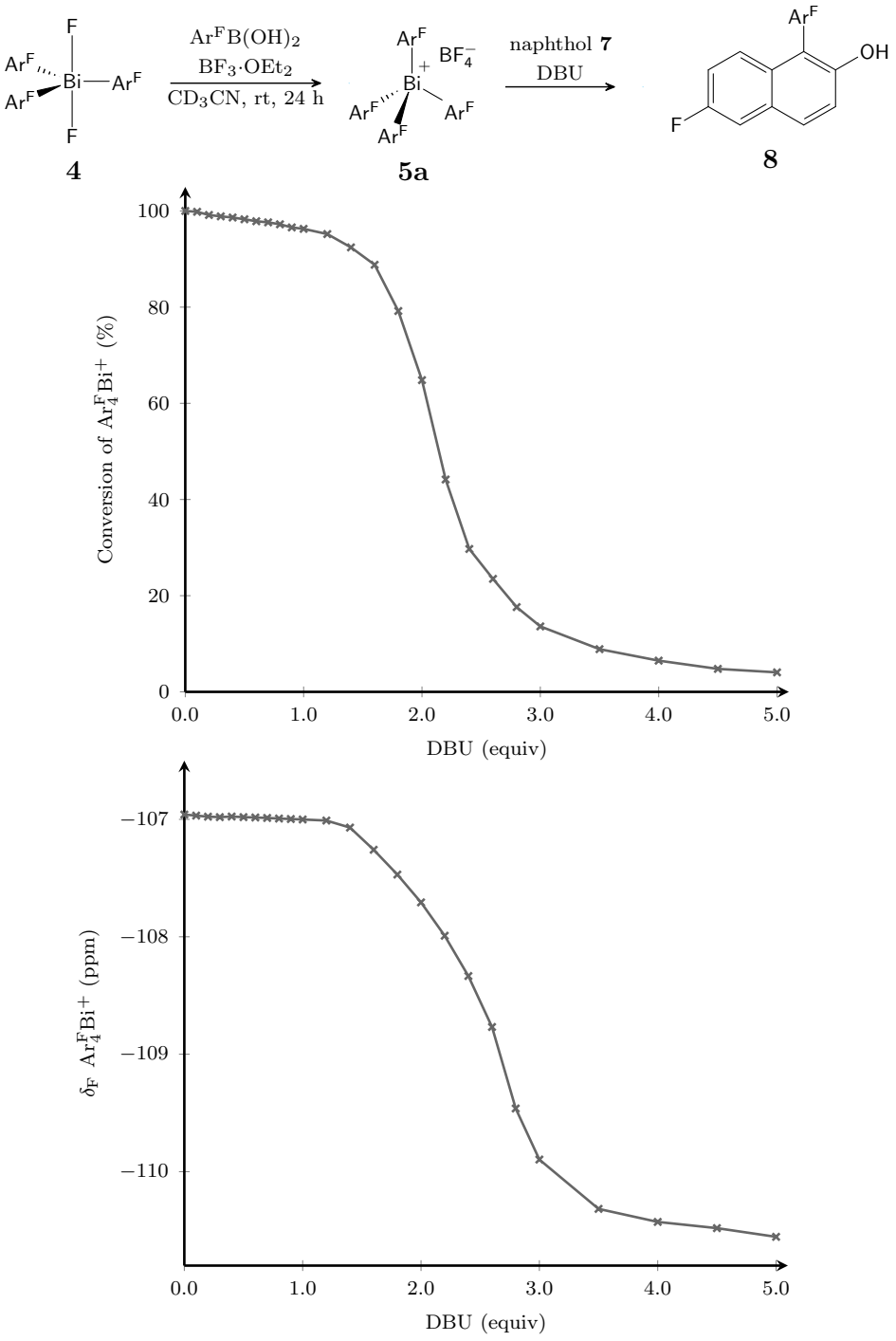

Figure 2.11: Titration with DBU of a solution of bismuthonium **5a** made by transmetalation to $Ar^F_3BiF_2$ in the presence of $BF_3{\cdot}OEt_2$. The consumption of $Ar^F_4Bi^+$ was monitored by ^{19}F spectroscopy and normalised against 4,4′-bis(trifluoromethyl)-1,1′-biphenyl (internal standard, **9**). The base was added as a stock solution in CD_3CN and each spectrum was acquired after letting the solution equilibrate for 10 min. The bottom plot suggests a potential (non-linear) correlation between the conversion and the ^{19}F chemical shift of the bismuthonium.

other hand, if the transmetalation could be achieved without the help of $BF_3{\cdot}OEt_2$, this would at least remove a potentially non-innocent species from the equation. Unfortunately, as discussed in Table 2.4 and Scheme 2.20, the transmetalation was significantly slower. Performing the transmetalation at 80 °C in the absence of $BF_3{\cdot}OEt_2$ did improve the conversion to the bismuthonium (48% at 24 h versus 10% after 10 d). Formation of the desired species was, however, accompanied by detection of several side-products, including fluorobenzene, Ar^F_3Bi, 4-fluorophenol,[§] and 4,4′-difluorobiphenyl.[¶] The same conditions (*i.e.* 80 °C and no $BF_3{\cdot}OEt_2$, as in Scheme 2.22) were then applied to the one-pot oxidation-transmetalation procedure, gratifyingly providing the bismuthonium salt quantitatively in 24 h, without any noticeable side-product. Moreover, rapid and quantitative arylation was observed upon addition of naphthol and DBU to the crude reaction mixture.

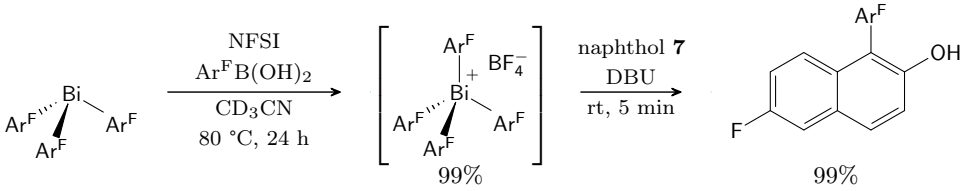

Scheme 2.22: By performing the oxidation-transmetalation sequence at 80 °C, the use of $BF_3{\cdot}OEt_2$ can be avoided. This allows the arylation step to occur successfully. Yields determined by ^{19}F NMR spectroscopy.

This result was incredibly important for at least two reasons: first of all, the fact that the one-pot oxidation-transmetalation method outperformed Matano's stepwise procedure gives a tangible demonstration that the procedure herein discussed not only is more convenient from a practical perspective but also activates the system towards the transmetalation in an unprecedented way. Secondly, and arguably more importantly, $BF_3{\cdot}OEt_2$ was finally found to be the reason why the arylation had not occurred previously.

A definitive explanation for the greater activity of our Ar^F_3BiFX species in comparison to Matano's $Ar^F_3BiF_2$ cannot currently be provided. However, a plausible argument would be that in $Ar^F_3BiF_2$ a strong intervention is required to perturb the hypervalent and symmetrical F–Bi–F bond. This is achieved with $BF_3{\cdot}OEt_2$, which, as we discussed several times, forms a strong B–F bond with one of the two apical fluorines, thus weakening the corresponding Bi–F bond. The removal of one of the two fluorides by the Lewis acid enables the boronic acid interaction with

[§]From the oxidation of the boronic acid.

[¶]This is a rarely observed, although theoretically possible, product of the ligand coupling from a hypervalent bismuth species, as discussed in Section 1.3.1. This reaction also forms Ar^F_3Bi.

bismuth, successively delivering the transmetalation product. On the other hand, by introducing a single fluoride counterion in the oxidation step, the initial activation is not required. In fact, the other component of the hypervalent bond is (presumably) a BF_4^- anion, which is likely to form a much weaker bond with bismuth than fluoride. The positive influence of tetrafluoroborate on the transmetalation in comparison to other ligands was discussed in Table 2.4 and now a possible explanation for that is also available: when BF_4^- coordinates to the oxidised species, it is essentially mimicking the product of the interaction of $BF_3{\cdot}OEt_2$ to $Ar^F_3BiF_2$, that is to say the activated species in Matano's protocol.

Finally, a rationalisation of the role of DBU in the titration reaction presented in Fig. 2.11 is as follows: an equilibrium, such as the one in the Scheme below, would bring about the formation of an adduct between the Lewis acid and the base. When this occurs, the adduct is not basic anymore and deprotonation of the substrate is prevented.

$$\text{DBU} + BF_3{\cdot}OEt_2 \rightleftharpoons \text{DBU–}BF_3$$

Three lines of research were born from this important result: first, hindered bases were investigated with the aim of disfavouring the formation of the adduct; second, different Lewis acids were tested with the same purpose; third, conditions for the one-pot oxidation and transmetalation were reinvestigated and re-optimised to take into account the detrimental influence of $BF_3{\cdot}OEt_2$ on the arylation step.

Hindered bases were explored at first, starting from 2,6-di-*t*-butyl-4-methylpyridine (DTBMP). The base has been reported in a few instances not to form adducts with Lewis acids, including BF_3.[303–305] However, when it was employed as the replacement for DBU in the arylation with the bismuthonium made *in situ*, no noticeable transformation occurred (entry 1 of Table 2.10). When the same reaction was executed with the isolated bismuthonium, formation of product was extremely slow, with full consumption of the substrate only happening after 2 months at 80 °C. When exclusively the bismuthonium was exposed to DTBMP, this inertness was matched with only 12% of decomposition observed after the same amount of time at the same temperature. This is consistent with DTBMP's very low pK_aH^+ values both in water and acetonitrile (see Table 2.10).[‖]

[‖]DTBMP is only slightly more basic than pyridine ($pK_aH^+ = 12.8$[306] vs 12.33[251]) and less basic than collidine, whose pK_aH^+ is 14.98 in MeCN.[234] These figures seem in first instance counterintuitive if the classic hyperconjugation argument is applied, that is to say that the replacement of two methyl groups in the 2- and 6-positions with two *tert*-butyl groups is expected to increase the basicity of DTBMP. However, it has been argued that the lower pK_aH^+ must be attributed to steric inhibition of the solvation, rather than a low proton affinity.[307]

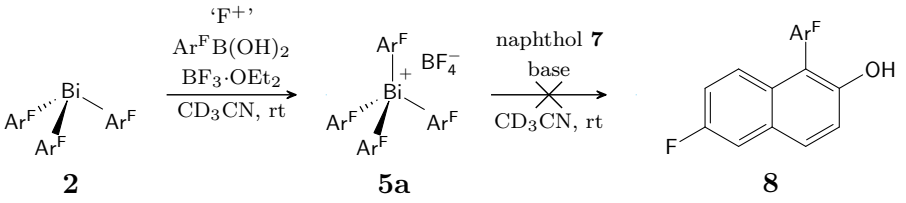

2 **5a** **8**

#	Base	Acronym	pK_aH$^+_{water}$	pK_aH$^+_{MeCN}$	Yield
1	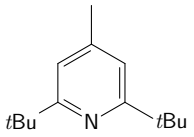	DTBMP	4.95[308]	12.8[306]	0%*
2	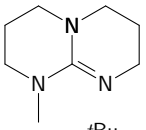	MTBD	n.a.	25.4[234]	0%
3	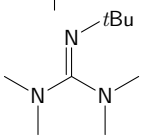	BTMG	14[245]	26.5[246]	0%
4	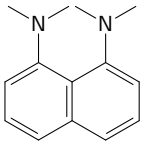	DMAN	12[309]	24.1[310]	0%

Table 2.10: Sterically hindered bases (1.5 equiv) were tested in the arylation of naphthol **7** with bismuthonium **5a** (made *in situ*). The pK_a values of 6-fluoro-2-naphthol are 9.46 in water[254] and ca. 26 in acetonitrile.[236,255] *100% after 2 months at 80 °C when performed from isolated bismuthonium **5a**. See Table 2.2 for additional results with the isolated bismuthonium salt.

The three other bases tried (entries 2–4), MTBD, BTMG and DMAN (Proton Sponge®), were all significantly stronger than DTBMP, with their pK_aH$^+$s being above 24. This, in fact, allowed the arylation reactions when the isolated bismuthonium was employed. However, when the bismuth compound was made *in situ*, no arylation occurred with any of these bases. Similarly to what happened with DBU, addition of an extra equivalent of base triggered the arylation, indirectly suggesting the issue remained the same with these bases too.

Since a good alternative for DBU was not found, it was decided to move on to explore the effect of other Lewis acids on both the transmetalation and the arylation. The outcome of these tests is presented in Table 2.11. In order to isolate the effects on the transmetalation, these reactions were performed with $Ar^F_3BiF_2$ rather than in

the one-pot procedure. This also carried the advantage that the influence of Lewis acids would be more evident, since the transmetalation to isolated Bi^V necessitates further activation compared to our methodology. Specifically, Lewis acids that form a strong bond with fluoride were investigated, so as to be able to break one of the Bi–F bonds and trigger the transmetalation. However, the selection was narrowed down by the requirement of a substantial inertness towards the other components of our one-pot system, including the non-water-free conditions. Therefore, extremely strong Lewis acids that have been employed, for example, to make $Ar^F_3Bi^{2+}$ by extraction of two fluorides from $Ar^F_3BiF_2$ were ruled out.[311]

On the other hand, tris(pentafluorophenyl)borane (BCF) is often considered the 'ideal Lewis acid', since it is moisture- and temperature-stable, while at the same time maintaining a Lewis acidity slightly higher than that of BF_3,[312] thus matching our requirements. In this case the feature of interest was a greater steric hindrance around the boron centre compared to BF_3, so as to disfavour the formation of adducts with Lewis bases. Different triflate salts were explored (TMS, Na and Li), with the idea that they would form either a volatile or insoluble fluoride species, while at the same time introducing in solution a non-coordinating anion. The same principles applied to lithium triflimidate, while for HMDS the formation of a strong Si–F bond was envisaged as the driving force for the activation of the Bi–F bond.

When no Lewis acid was employed (entry 1), only ca. 10% of the desired bismuthonium was obtained after 10 d, as discussed previously. Among the Lewis acids tested, $BF_3{\cdot}OEt_2$ was the most efficient, achieving a quantitative conversion within 12 h to the bismuthonium **5a**. BCF (entry 3) followed closely, reaching 82% in the same amount of time. Full conversion was achieved in approximately 36 h. With TMSOTf (entry 4), despite a promising initial rate of conversion, the transmetalation did not go past 60% conversion even after several days. Sodium and lithium triflates (entries 5 and 6), possibly showed an improvement in comparison to the non-Lewis-acid-mediated transformation (entry 1), however this was minimal and the reactions were not followed to completion. Finally, $LiNTf_2$ (entry 7) definitely improved the conversion compared to the reaction without Lewis acid, however not enough to allow the transmetalation to reach full conversion in a reasonable time. Finally, hexamethyldisilazane (HMDS, entry 8) did manage to extract the fluoride ion (TMS–F detected at −157 ppm by ^{19}F NMR spectroscopy as a resolved multiplet with J = 7.5 Hz) but caused the immediate reduction of $Ar^F_3BiF^+$ to Ar^F_3Bi, as observed with other amines, preventing any further transformation.

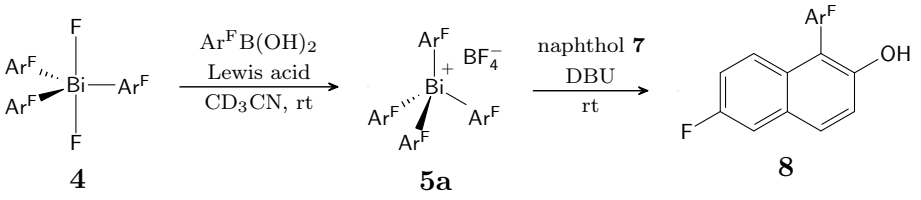

4 **5a** **8**

#	Lewis acid	5a	8
1	none	10% at 10 d	/
2	$BF_3{\cdot}OEt_2$	99% at 12 h	0% at 3 h
3	BCF	82% at 12 h	65% at 3 h
4	TMSOTf	57% at 12 h	76% at 3 h
5	NaOTf	11% at 1 d	/
6	LiOTf	9% at 1 d	/
7	$LiNTf_2$	26% at 1 d 59% at 10 d	/
8	HMDS	reduction	/

Table 2.11: Different Lewis acids were tested to activate $Ar^F_3BiF_2$ towards the transmetalation with 4-fluorophenylboronic acid. HMDS caused the complete reduction of the Bi^V species to Ar^F_3Bi. Only when the bismuthonium had completely formed (entries 2–4), this was subjected to arylation conditions (1.0 equiv of naphthol **7**, 1.5 equiv of DBU). All reactions were performed in NMR tubes. Yields measured by ^{19}F NMR spectroscopy.

Finally, the arylation of 6-fluoro-2-naphthol was tested for entries 2–4, when the bismuthonium could eventually be obtained quantitatively. As discussed in Scheme 2.21 the arylation did not occur at all when $BF_3{\cdot}OEt_2$ and 1.5 equiv of DBU were used. The reactions with BCF and TMSOTf showed an improvement in this regard, reaching between 65 and 75% conversion. However, this threshold could not be overcome in both cases and the conversion plateaued at these values. In the case of TMSOTf these findings are quite difficult to explain, considering that neither TMS–F nor the triflate ion were expected to have any influence on the acid-base equilibrium required for the arylation. However, it can be argued that triflate may have reacted with boron-containing side-products of the transmetalation, forming for example TfO–$B(OH)_2$. Upon hydrolysis this would yield triflic acid, which would protonate DBU. Addition of 5 equiv extra base brought the arylation to completion in all three cases. This similarity in behaviour demonstrated that, although some of these Lewis acids were capable of extracting fluorides from bismuth, none of them outperformed $BF_3{\cdot}OEt_2$. At the same time, the arylation reactions with the three Lewis acids tested showed only a partial improvement compared to $BF_3{\cdot}OEt_2$, thus still preventing the elevation to a catalytic regime for our one-pot procedure.

This Chapter demonstrated that tetraarylbismuthonium salts can be obtained in a very convenient and practical way from commercially available starting materials. This was achieved through the use of fluorinating agents as oxidants, thus allowing an unprecedented one-pot oxidation-transmetalation sequence. Given the excellent reactivity of the isolated bismuthonium towards the arylation of the chosen test substrate, 6-fluoro-2-naphthol, several attempts to combine the formation of the active bismuthonium and the arylation step in a one-pot approach were performed. Different side-reactions have been explored and their influence on the overall transformation has been discussed. Specifically, two major issues have been highlighted: first, the three commercially available fluorinating agents all showed a certain incompatibility with either the nucleophilic substrate or the base; second, the Lewis acid employed to mediate the formation of the bismuthonium interacts with the base, which is strictly necessary for the arylation step. In an attempt to address these issues, different fluorinating agents have been synthesised in order to modulate their strength, however, all of them proved either too weak to oxidise Ar_3^FBi or unstable under the reaction conditions or during storage. Secondly, although no strong evidence of the nature of this interaction could be found, numerous indirect hints at the existence of an adduct between the base and the Lewis acid have been provided. This was followed by attempts to disfavour the formation of such adduct, by increasing the steric hindrance of either the base or the Lewis acid. Although some promising results were obtained with BCF and TMSOTf, it was deemed that they were not sufficient to allow the arylation to be performed quantitatively in the same pot where oxidation and transmetalation had occurred.

As a consequence of these significant challenges, a new approach was adopted: the oxidation-transmetalation step would be separated from the arylation process. This would allow investigation of bismuthonium capabilities of selectively transferring a unique group, installed *via* transmetalation from a boronic acid. The next Chapter will build on the fact that the transmetalation can be achieved quantitatively without Lewis acid at higher temperatures. A re-optimisation of the reaction conditions will be discussed at first, which will take into account this result. Then, the isolation and characterisation of heteroleptic bismuthonium salts will be tackled. Finally, their behaviour in the arylation of selected substrates will be put to the test.

3

Synthesis and reactivity of heteroleptic bismuthonium salts

The previous Chapter discussed the synthesis of tetraarylbismuthonium salts *via* a one-pot oxidation-arylation sequence. In particular, one of the latest discoveries highlighted that this process can avoid the mediation of $BF_3{\cdot}OEt_2$, with a moderate adjustment of the reaction temperature. Herein we will build on that result and expand the scope, with the ultimate aim of exploiting the possibility of transferring a unique aryl group, installed on the bismuth compound *via* transmetalation from the corresponding boronic acid, to selected substrates.

The vast majority of the reactions discussed so far was performed in NMR tubes, in order to maximise throughput. However, since it was observed that boronic acids sometimes suffered from poor solubility in organic solvents, it was decided to re-optimise the oxidation-arylation procedure under stirring, so as to minimise mass transfer issues. All the reactions that will be discussed in the next two Sections were therefore performed under ambient atmosphere in 10 mL microwave tubes, sealed with appropriate microwave caps and stirred at 1000 rpm with cross-shaped magnetic stirrers. Tri(*p*-fluorophenyl)bismuth **2** was employed as the bismuth(III) starting material of choice, due to the utility of the *p*-fluoro substituent for NMR spectroscopy analysis and its relatively small electronic effect compared to the non-substituted counterpart.[313] The NMR yields of its transformation into different bismuthonium salts were measured against an internal standard: 4,4′-bis(trifluoromethyl)-1,1′-biphenyl **9**. The latter was identified as a good candidate, given its low volatility, inertness to the reaction conditions and ^{19}F NMR chemical shift in a relatively uncongested region of the spectrum. To quantify the T_1 for compounds **2**, **5a** and **9** ^{19}F NMR inversion recovery experiments were run. These determined that the relaxation delay* should be set to 30 s to achieve complete relaxation of all species and therefore quantitative integration.

3.1 Synthesis of bismuthonium salts: optimisation

The optimisation was started from a solvent screen. Previously, only acetonitrile had been used due to Selectfluor's poor solubility in other organic media.[268] Common organic solvents were tested in both oxidation and transmetalation, with NFSI used as the oxidant so as to avoid solubility issues. Results are reported in Table 3.1.

*D_1, sometimes referred to as 'recycle delay', is formally defined as $TT = PW + AQ + D_1$, where TT is the total time required for one scan, PW is the pulse width and AQ is the acquisition time. Since PW is in the microsecond range this can be ignored. Given a longitudinal relation time T_1 and a pulse angle of 90°, the magnetisation vector M relaxes *via* exponential decay: $M = e^{-\frac{TT}{T_1}}$. When $TT = 5T_1$, $M = 0.006$, that is to say it relaxed 99.33%. Given an AQ of 1.53 s and the greatest T_1 of 4.17 s, D_1 should be set to ≥ 20 s.

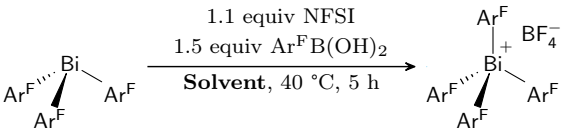

#	Solvent	Ratio Ar^F_4Bi :	Ar^F_3BiFX :	Ar^F_3Bi
1	EtOAc	0.52	1	0.01
2	THF	0.38	1	0.04
3	dioxane	n.d.	n.d.	1
4	EtOH	0.03	1	0.09
5	*i*PrOH	0.05	1	0.25
6	acetone	2.69	1	21.0
7	toluene	0.20	1	0.02
8	MeCN/H_2O	0.04	1	n.d.
9	DCM	1.35	1	n.d.
10	**MeCN**	**3.60**	1	n.d.

Table 3.1: Investigation of different solvents for the one-pot arylation and transmetalation. Conditions: 0.05 mmol of Ar^F_3Bi, 1.1 equiv of NFSI, 1.5 equiv of *p*-fluorophenylboronic acid, 1 mL of solvent. Reactions sampled after 5 h: 0.1 mL of each reaction mixtures was transferred into a vial, 1.5 mL of water and the same amount of DCM were added; the vials were shaken and the organic phases transferred into another set of vials, from which the solvent was removed; the resulting residues were redissolved in $CDCl_3$ and analyzed by ^{19}F NMR spectroscopy.

It must be noted that these preliminary tests were performed without internal standard, thus integral ratios vs the oxidised species (when available) are reported instead of yields.

In dioxane and acetone (entries 3 and 6 of Table 3.1) the oxidant presumably reacted with the solvents, thus Ar^F_3Bi was recovered quantitatively or almost quantitatively, respectively. In alcohols (entries 4 and 5) the oxidation was partially effective, but only minimal traces of bismuthonium could be detected. The situation was similar with toluene and the acetonitrile/water mixture (entries 7 and 8): in those cases the oxidation of Ar^F_3Bi reached completion but the transmetalation product proved negligible. Interestingly, tetrahydrofuran, ethyl acetate and dichloromethane allowed a reasonable conversion to the bismuthonium, however, all were substantially worse than acetonitrile. The latter was identified as the best performing solvent and was employed in all further studies.

Having established acetonitrile could not only still be used but was also the best solvent, the use of Selectfluor was reconsidered and the oxidant was put to the test against NFSI at different temperatures. From now on and for the rest of the

optimisation, sampling was performed by taking 0.1 mL of the reaction mixture and diluting this with CD_3CN. In order to discriminate between the different conditions the reactions were stopped after 1 h (Table 3.2), before achieving full conversion.

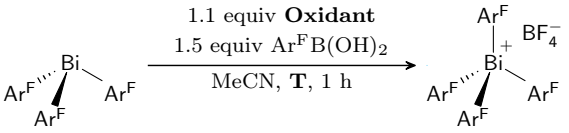

#	**Oxidant**	**T/°C**	**Yield/%**
1	Selectfluor	80	76
2	NFSI	80	74
3	**Selectfluor**	**60**	**57**
4	NFSI	60	51
5	Selectfluor	40	32
6	NFSI	40	24
7	Selectfluor	r.t.	16
8	NFSI	r.t.	6

Table 3.2: Screening of the two best commercially available oxidants at different temperatures. Conditions: 0.05 mmol of Ar^F_3Bi, 1.1 equiv of oxidant, 1.5 equiv of *p*-fluorophenylboronic acid, 1 mL of MeCN.

Similarly to what was observed in Section 2.2, Selectfluor exhibited slightly better reactivity throughout this screening, with such effect being accentuated at lower temperatures (*e.g.* compare entries 1 and 2 with 7 and 8). In general, yields at 1 h are acceptable for both oxidants even at low temperatures. Despite the reactions being faster at 80 °C than at 60 °C, it was decided to proceed with the lower temperature, since the transformation at 60 °C reached completion within 6 h, which was considered a good trade off between time and temperature.

Once the oxidant and the reaction temperature were identified, the number of equivalents of boronic acid was assessed. It is worth noting that in our methodology, especially if applied to late-stage functionalisation, the boronic acid represents the precious component of the system, since both the bismuth(III) starting material and the oxidant are commercially available at a limited cost, hence the need to identify a reasonable stoichiometry. Results reported in Table 3.3 showed that the optimum was reached with ca. 2 equiv of the boronic acid, whereas further increasing the equivalents did not improve the yield at all, an effect that may be ascribed to the saturation of the reaction solution. On the balance of economy and reaction time 1.5 equiv of boronic acid was selected for further studies.

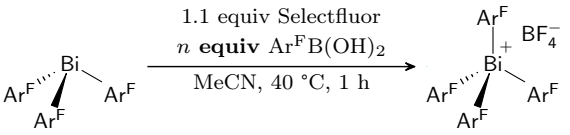

#	**Equiv**	**Yield/%**
1	1.1	23
2	1.3	27
3	**1.5**	**31**
4	1.9	35
5	2.9	35

Table 3.3: Screening of different equivalents of *p*-fluorophenylboronic acid. Conditions: 0.05 mmol of Ar^F_3Bi, 1.1 equiv of oxidant, 1 mL of MeCN. Yields measured by ^{19}F NMR spectroscopy.

Interestingly, the reaction rate was shown to be rather insensitive to the variation of the concentration of reagents, as evident from Table 3.4.

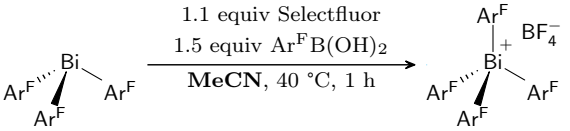

#	$[Ar^F_3Bi]_0$/M	**Yield/%**
1	0.050	28
2	0.100	31
3	0.200	31

Table 3.4: Screening of different equivalents of *p*-fluorophenylboronic acid. Conditions: 0.10 mmol of Ar^F_3Bi, 1.1 equiv of oxidant, 1.5 equiv of $Ar^FB(OH)_2$, 0.5–2.0 mL of MeCN. Yields measured by ^{19}F NMR spectroscopy.

This screening concluded the first phase of the optimisation, which resulted in the following conditions:

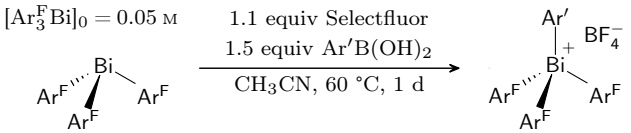

The attention was then turned to the bismuth(III) species: although a fluorine substituent is useful from a reaction analysis point of view, we did not want to incur the risk of over-optimising the reaction for a very specific triarylbismuth species. The fluorinated boronic acid was maintained, so that yields could still be calculated by ^{19}F NMR spectroscopy. Table 3.5 displays these investigations.

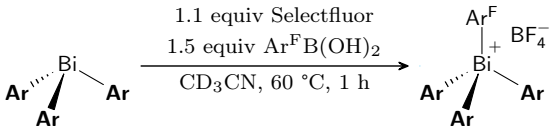

#	Ar	Yield/%
1	*p*-F-C_6H_4	57
2	Phenyl	62
3	*p*-MeO-C_6H_4	61
4	*p*-CF_3-C_6H_4	0
5	*p*-Cl-C_6H_4	50
6	*p*-*t*Bu-C_6H_4	61
7	*o*-Tolyl	3

Table 3.5: Screening of different triarylbismuth starting materials. Conditions: 0.05 mmol of Ar_3Bi, 1.1 equiv of Selectfluor, 1.5 equiv of $Ar^FB(OH)_2$, 1.0 mL of MeCN. Yields measured by ^{19}F NMR spectroscopy.

Gratifyingly, when subjected to the optimised conditions, both the non-substituted triphenylbismuth (entry 2) and a selection of electron-rich and electron-poor analogues afforded the corresponding bismuthonium salts. Specifically, *p*-MeO-, *p*-Cl- and *p*-*t*-Bu-substituted species (entries 3, 5 and 6, respectively) all performed similarly to the *p*-F-substituted case (entry 1). On the other hand, both the trifluorotolyl and the *o*-tolyl derivatives (entries 4 and 7) did not provide the desired product in appreciable yields. In the first case this can be ascribed to the incredibly high oxidation potential (2.2 V)[239] of the Bi^{III} species. For a comparison, the oxidation potential for the second most electron-poor ring in this series, *p*-Cl-C_4H_4-, was found to be 1.7 V,[239] *i.e.* very close to the *p*-F-substituted species (1.66 V).[239] This could suggest that, under the test conditions, Selectfluor was not able to oxidise the trifluorotolyl bismuth(III) species. The poor performance of the *o*-tolyl derivative also stems from its resistance to oxidation, in this case presumably due to sterics at the bismuth centre.

Having confirmed that the results obtained for the oxidation-transmetalation sequence were not limited to tri(4-fluorophenyl)bismuth, we then briefly explored a selection of boronic acids. In the majority of cases the optimised conditions proved to

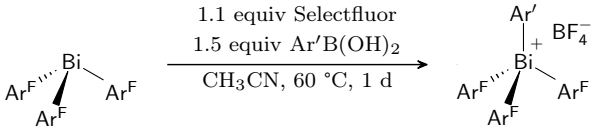

#	$\mathbf{Ar'B(OH)_2}$	**Yield at 1 h/%**	**Yield at 1 d/%**
1	*p*-F-C_6H_4	57	99
2	*p*-Cl-C_6H_4	27	69
3	*p*-CF_3-C_6H_4	3	12
4	*p*-CN-C_6H_4	2	4
5	*p*-MeO-C_6H_4	99	99
6	*m*-Br-C_6H_4	7	41
7	*m*-MeO-C_6H_4	57	75
8	*o*-Me-C_6H_4	77	99

Table 3.6: Screening of different boronic acids. Conditions: 0.05 mmol of Ar^F_3Bi, 1 mL of MeCN. Yields measured by ^{19}F NMR spectroscopy.

be effective for other boronic acids: electron-rich examples, such as *p*-methoxyphenyl and *o*-tolyl derivatives (entries 5 and 13 of Table 3.6) performed better than the parent *p*-fluorophenyl analogue (entry 1), regardless of the steric hindrance, whereas electron-poor boronic acids, such as *p*-chloro-, *p*-trifluoromethyl-, *p*-cyano- and *m*-bromo- and *m*-methoxy-phenyl boronic acids, gave mixed results. In particular, entries 3 (*p*-trifluorotolyl) and 4 (*p*-cyanophenyl) showed a significantly lower yield at 1 h, reaching only 3% and 2%, respectively. A further distinction can be made by taking into account the corresponding yields at 24 h: the *p*-chloro-, *m*-bromo- and *m*-methoxy-substituted species, although slower than the 4-fluorophenyl compound, were shown to be progressing towards completion. On the other hand, the yield with extremely electron-poor boronic acids (*e.g.* *p*-CF_3- and *p*-CN-subtituted ones) did not improve over time.

This last set of experiments satisfactorily concludes the optimisation, which allowed the identification of conditions for the one-pot oxidation and transmetalation. The next Section will extensively explore the scope of boronic acids.

3.2 Synthesis of bismuthonium salts: scope

As discussed previously, the use of boronic acids containing groups different from the three already present on the bismuth(III) starting material allows the synthesis of heteroleptic bismuthonium salts. The overall methodology would become powerful

if the unique group could then be selectively transferred to a substrate. En route to this ultimate aim, we have investigated the first part of the transformation for more than 80 different boronic acids. Isolation and characterisation of a good portion of these was also performed, even though in an optimal experiment this would usually not be necessary and the bismuthonium salts could be immediately exposed to the arylation substrate.

Matano already showcased the transmetalation of carbon nucleophiles from boronic acids to triarylbismuth difluoride species, however, the scope is somewhat limited to simply substituted phenyl groups, with only two heteroaromatic examples.[75,76] More importantly, the migratory aptitude of heteroleptic bismuthonium salts in arylation reactions was only studied for three of them (Ar′ = phenyl, *p*-tolyl and *p*-anisyl).[314] The migratory aptitude is the tendency of one group to transfer over another group.[315] In this case, when heteroleptic bismuthonium salts undergo ligand coupling upon reaction with an appropriate substrate, the migratory aptitude of the unique group can be measured as the ratio of product containing the unique group and product containing the non-unique group. This value can be normalised to take into account the number of non-unique groups. By building a library of heteroleptic bismuthonium salts it was hoped to expand the scope and identify potential limitations of the transmetalation. In addition, these studies would also afford a significantly larger data base for migratory aptitude studies.

3.2.1 *Para*- and *meta*-substituted boronic acids

First, electronic effects were investigated. Figure 3.1 reports the *para*- and *meta*-substituted boronic acids tested with the associated conversions (for the oxidation-transmetalation sequence, in brackets) and yields of the isolated bismuthonium salts, where appropriate.[†] Optimised conditions were employed at first: Fig. 3.2 shows a Hammett plot in which conversions were plotted against the appropriate Hammett constants. A progressive drop in conversion can be see for groups with $\sigma > 0.15$, particularly for extremely electron-poor aromatic rings, such as those containing cyano and trifluoromethyl substituents. This prompted a re-evaluation of the reaction conditions for cases that did not achieve full conversion under the

[†]In Figs. 3.1, 3.3, 3.6 and 3.8, the reported NMR conversions are those for the set of conditions that gave the highest conversion. In case the same conversion were achieved under different conditions, the mildest condition was preferred, which usually corresponded to the optimised conditions. Moreover, isolation yields are sometimes significantly lower than conversions. Since isolation was achieved by crystallisation, occasionally the crystal growth did not allow full recovery of the desired bismuthonium salts. However, this was not deemed an issue, since, as mentioned before, isolation of the bismuthonium intermediate would not be necessary.

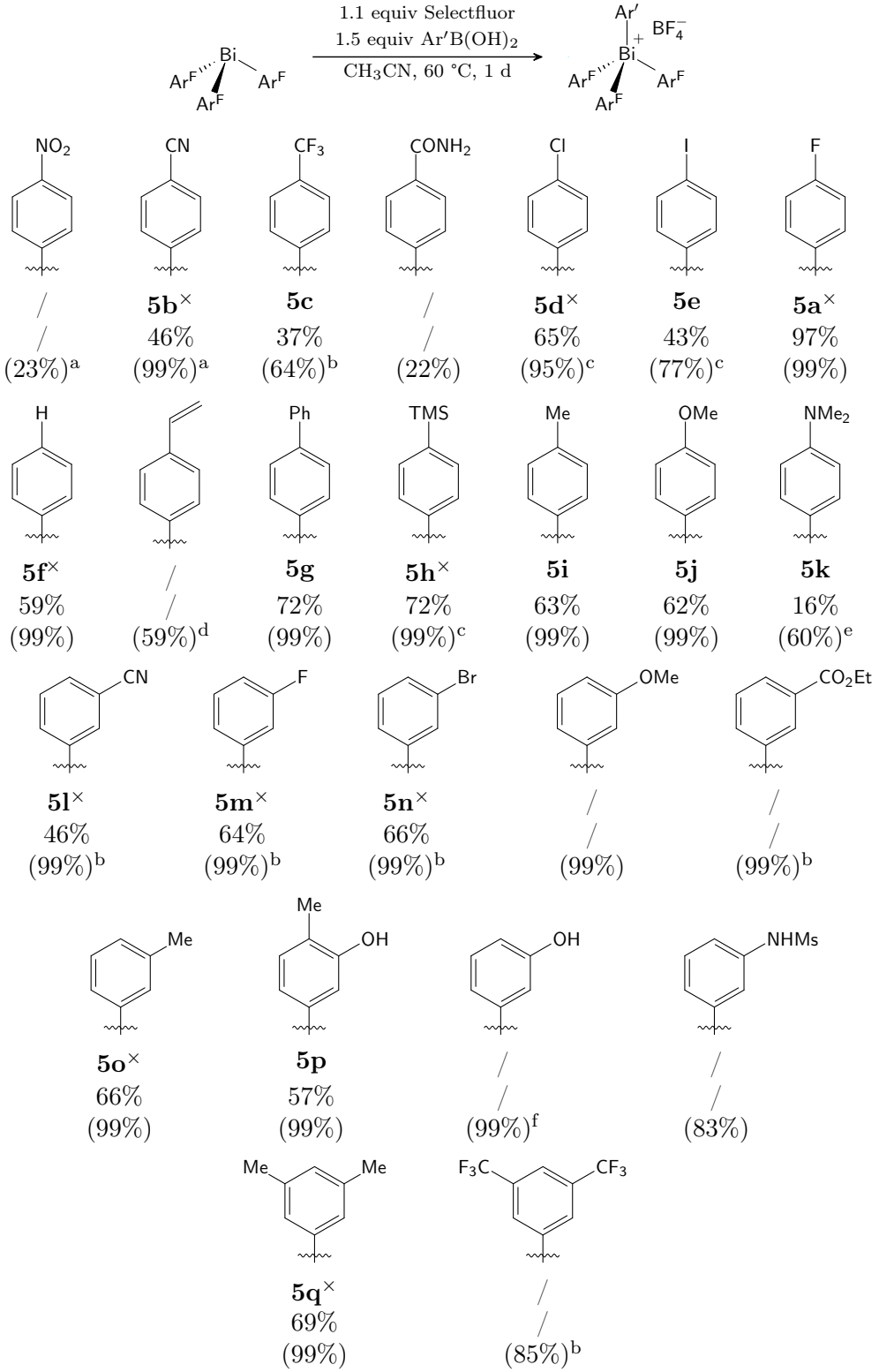

Figure 3.1: Scope of *para*- and *meta*-substituted boronic acids. NMR conversions are reported in parentheses, yields of isolated product and compound numbers are reported when available. Variations from standard conditions: [a]microwave, 150 °C, 1 h; [b]$BF_3{\cdot}OEt_2$, 80 °C, 3 d; [c]80 °C; [d]25 °C; [e]0 °C; [f]$BF_3{\cdot}OEt_2$, 5 h. [×] crystal structure was determined.

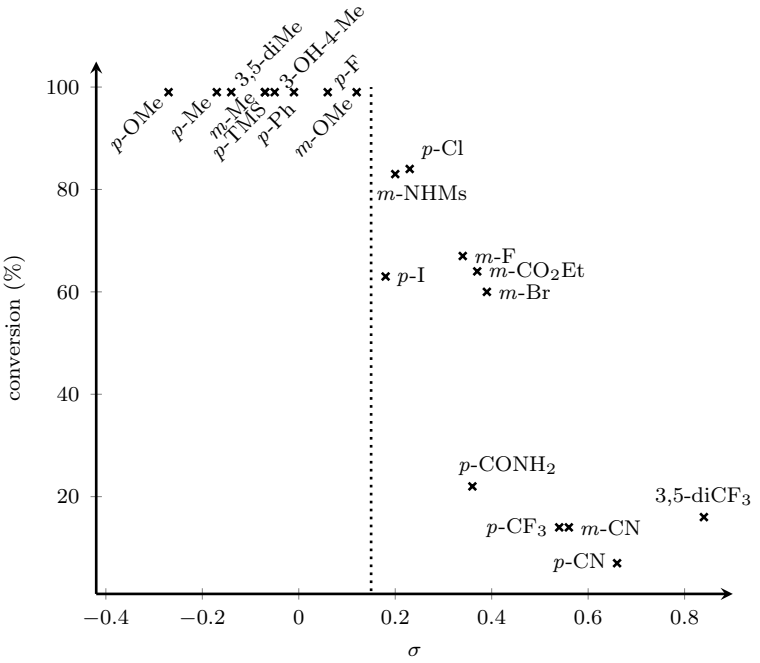

Figure 3.2: Hammett plot of the ^{19}F NMR conversions at 1 d for the transmetalation from boronic acids of Fig. 3.1 vs σ constant. For disubstituted groups, the corresponding constants were calculated by addition of those of mono-substituted groups.[316] p-NO_2 and m-OH were excluded from this plot since the corresponding reactions have not been performed under the standard conditions. p-vinyl and p-NMe_2 were excluded because the corresponding boronic acids underwent side-reactions, preventing full conversion (for reasons unrelated to the transmetalation itself).

standard conditions: an increase of temperature from 60 °C to 80 °C was sufficient to bring the reaction with p-chlorophenylboronic acid to completion, whereas this increased reaction temperature, together with $BF_3{\cdot}OEt_2$, were required to achieve the same result with more challenging substrates.

A few examples merit further discussion: the p-styrenyl species showed no conversion under the standard conditions. This was initially attributed to heat-induced polymerisation, however, $BF_3{\cdot}OEt_2$ is reported to catalyse the reaction, too.[317] Therefore it was decided to perform the reaction at room temperature and without $BF_3{\cdot}OEt_2$. This only gave 59% conversion, suggesting that the impact of this side-reaction was reduced but not fully mitigated. It was not possible to tell if polymerisation occurred on the boronic acid or on the bismuthonium. This result contrasts with Matano's, which showed full conversion to the heteroleptic bismuthonium even under Lewis acidic catalysis.[75] Curiously, this boronic acid

was able to deliver the styrenyl group to the bismuth(III) sulfone employed in our recently published paper,[318] even though the reaction was performed at 60 °C, suggesting a prominent role of $BF_3{\cdot}OEt_2$ or potentially any of the electrophilic Bi(V) species in the polymerisation of the vinyl moiety. Different explanations may be: formation of fluorohydrines upon reaction between the styrenyl moiety, Selectfluor and trace water,[319] or formation of fluoroamides, by reaction with Selectfluor and acetonitrile.[320] However, none of the possible by-products could be detected.

The *p*-NMe_2-substituted boronic acid incurred different issues. Under the standard conditions no conversion was observed. Interestingly, in this case full reduction to Ar^F_3Bi was detected. In order to test the innocence of the amino group, two additional reactions were performed: in the first, isolated $[Ar^F_4Bi][BF_4]$ was exposed to *N*,*N*-dimethylaniline in acetonitrile at 60 °C and no decomposition could be detected after 1 d; in the second, Ar^F_3Bi was oxidised with Selectfluor under the same conditions and then exposed to the aniline. In this case, immediate reduction of the oxidised intermediate was observed, thus suggesting that the boronic acid in question acted as a reductant for the oxidised bismuth species, before transmetalation could occur. In order to minimise this circumstance and exploiting the increased activity of the electron-rich boronic acid,[75] the transmetalation to bismuth was performed at 0 °C with exactly 1 equiv of boronic acid. Under these conditions 60% conversion was achieved, with the remaining 40% being Ar^F_3Bi.

The two boronic acids containing trifluoromethyl groups highlighted a different issue altogether. When such a group is in the *para* position, only 64% conversion could be reached, even when the reaction was performed at 80 °C with $BF_3{\cdot}OEt_2$ for 3 d. In this case unreacted Ar^F_3BiFX accounted for the remaining mass balance. On the other hand, with two $-CF_3$ groups in the 3- and 5-positions and contrary to all expectations, the product of the oxidation of Ar^F_3Bi was fully consumed, but two products formed, the desired heteroleptic bismuthonium and $Ar^F_4Bi^+$, which accounted for the missing 15% conversion. Traces ($< 5\%$) of homoleptic bismuthonium could also be found in the reaction with *p*-cyanophenylboronic acid. The formation of the homoleptic bismuthonium must be the outcome of a ligand exchange between two Bi^V species, since no bismuth(III) species could be detected by ^{19}F NMR spectroscopy.

This ligand exchange is not a completely unknown phenomenon in bismuth chemistry and there are at least three notable examples: Wittig observed a Bi-to-B ligand exchange when he exposed Ph_5Bi to Ph_3B, to yield $[Ph_4Bi][Ph_4B]$;[15] Suzuki observed a similar exchange when $ArTol_2Bi$ (Ar = 2-(*tert*-butylsulfonyl)phenyl)

was treated with $BF_3{\cdot}OEt_2$, yielding ArTolBiF and $TolBF_2$;[321] Matano, on the other hand, reported the formation of an amount comprised between 5% and 10% of Ph_4Bi^+ when using methylboronic acid in his transmetalation procedure, as well as the ligand exchange between isolated Ph_3MeBi^+ and Tol_3MeBi^+ to give mixed $Ph_{3-n}Tol_nMeBi^+$.[257] It is worth noticing that in Suzuki's work, the most electron-rich group is transferred. In our case, the ligand exchange was observed only when the transmetalation had to be carried out under harsh conditions ($BF_3{\cdot}OEt_2$, high temperature, prolonged reaction time), and when the boronic acid contained electron-poor substituents. On these bases, it would not be unreasonable to suggest the following mechanism:

$$Ar^F_3Ar'Bi^+ \;+\; BF_3{\cdot}OEt_2 \;\rightleftharpoons\; Ar^F_2Ar'BiF^+ \;+\; Ar^FBF_2$$

$$Ar^F_3Bi \;+\; [F^+] \longrightarrow Ar^F_3BiFX \;+\; Ar^FBF_2 \longrightarrow Ar^F_4Bi^+$$

The desired product of the reaction undergoes Bi-to-B transmetalation to BF_3 to form Ar^FBF_2, which then transfers the *p*-fluorophenyl group back to the product of oxidation of Ar^F_3Bi, in this instance replacing the role of $Ar'B(OH)_2$. The fate of $Ar^F_2Ar'BiF^+$ remains uncertain, since this species or any of its derivatives (*e.g.* $Ar^F_2Ar'_2Bi^+$) have never been observed. Prolonged reactions times and the presence of $BF_3{\cdot}OEt_2$ seem to be key for this process to occur. In fact, the *p*-cyanophenyl group could be transmetalated to bismuth quantitatively when the reaction was performed at 150 °C for 10 min without $BF_3{\cdot}OEt_2$ under microwave irradiation.

Overall, both electron-rich and electron-poor aryl groups can be installed onto bismuth *via* transmetalation from boronic acids. For groups whose $\sigma > 0.15$ it was shown that the reactions must be pushed to completion by increasing the reaction temperature or by employing a Lewis acid. With these adjustments only groups with $\sigma > 0.5$ exhibited non-ideal behaviour. Ligand exchange was identified as a potential side reaction in the presence of $BF_3{\cdot}OEt_2$. Pleasingly, among the aromatic groups transmetalated, several of them allow further functionalisation (–CN, $–CONH_2$, $–NMe_2$...) or would represent an issue in transition metal-catalysed cross-coupling (–Cl, –Br, –I...). Interestingly, even hydroxy groups are tolerated and their corresponding boronic acids are actually among the ones which performed better. This may at first seem surprising, considering phenols are classic substrates for bismuth-mediated arylation chemistry, but it should be kept in mind that bismuthonium salts do not undergo ligand coupling with phenols in neutral or acidic conditions, such as those of the transmetalation step.

3.2.2 *Ortho*-substituted boronic acids

The scope of *ortho*-substituted boronic acids was then explored (see Fig. 3.3). As in the previous case, at first mono-substituted groups were considered, then poly-substituted. Once again, an excellent tolerance was shown, however $BF_3{\cdot}OEt_2$ was required more often than with *para*- and *meta*-substituted boronic acids. With the Lewis acid almost any kind of mono-substituted aryl group could be installed, from very electron-poor, such as 2-trifluorotolyl, to strongly electron-rich, such as the several examples of 2-alkoxy-substituted groups. Among the groups containing a 2-alkoxy substituent which could be transferred, the trifluoromethoxy-substituted example is regarded with interest in medicinal chemistry, since this moiety can be used as a replacement for methoxy groups to mitigate *O*-demethylation or increase lipophilicity and membrane permeability.[322]

Similarly to what was observed before, prolonged heating in the presence of $BF_3{\cdot}OEt_2$ caused the formation of small amounts of homoleptic $Ar^F_4Bi^+$. This was detected with groups with the following substituents: *o*-CN (12%), *o*-CF_3 (5%), 2,4,6-triisopropyl (TRIP, 26%), 2,6-di-CF_3 (16%) and 2,6-dibromo (22%). Once again, these are groups that were expected to be more difficult to install on bismuth, either for being electron poor or for bearing sterically demanding substituents.

Notably, unprotected hydroxy and formyl substituents did not prevent the transmetalation. The only boronic acid that did not provide the corresponding bismuthonium to any extent is the 2-bromobenzyl-substituted: this reaction was repeated with or without $BF_3{\cdot}OEt_2$, with no difference. In fact, the characteristic ^{19}F NMR signal for bismuthonium species was not detected at any point and HRMS analysis of the reaction mixture could not identify the outcome of the reaction.

Di-*ortho*-substitution of the boronic acid does not *per se* prevent the transmetalation to bismuth: a mesityl group could be installed under the standard conditions, whereas the 2,6-xylyl analogue required $BF_3{\cdot}OEt_2$ to reach full completion. This implies that the electron-donating effect of the extra methyl present in the mesityl group, which enhances the nucleophilic character of this boronic acid, slightly favours the transmetalation. Excellent conversion was achieved with the 2,6-dimethoxy species, presumably for similar reasons. On the other hand an increase in the electron-withdrawing character of the two *ortho* substituents (R) has a negative and marked impact on the outcome of the transformation: the conversion decreased from 99% for R = Me, MeO to 95% for R = Cl to 26% when R = CF_3.

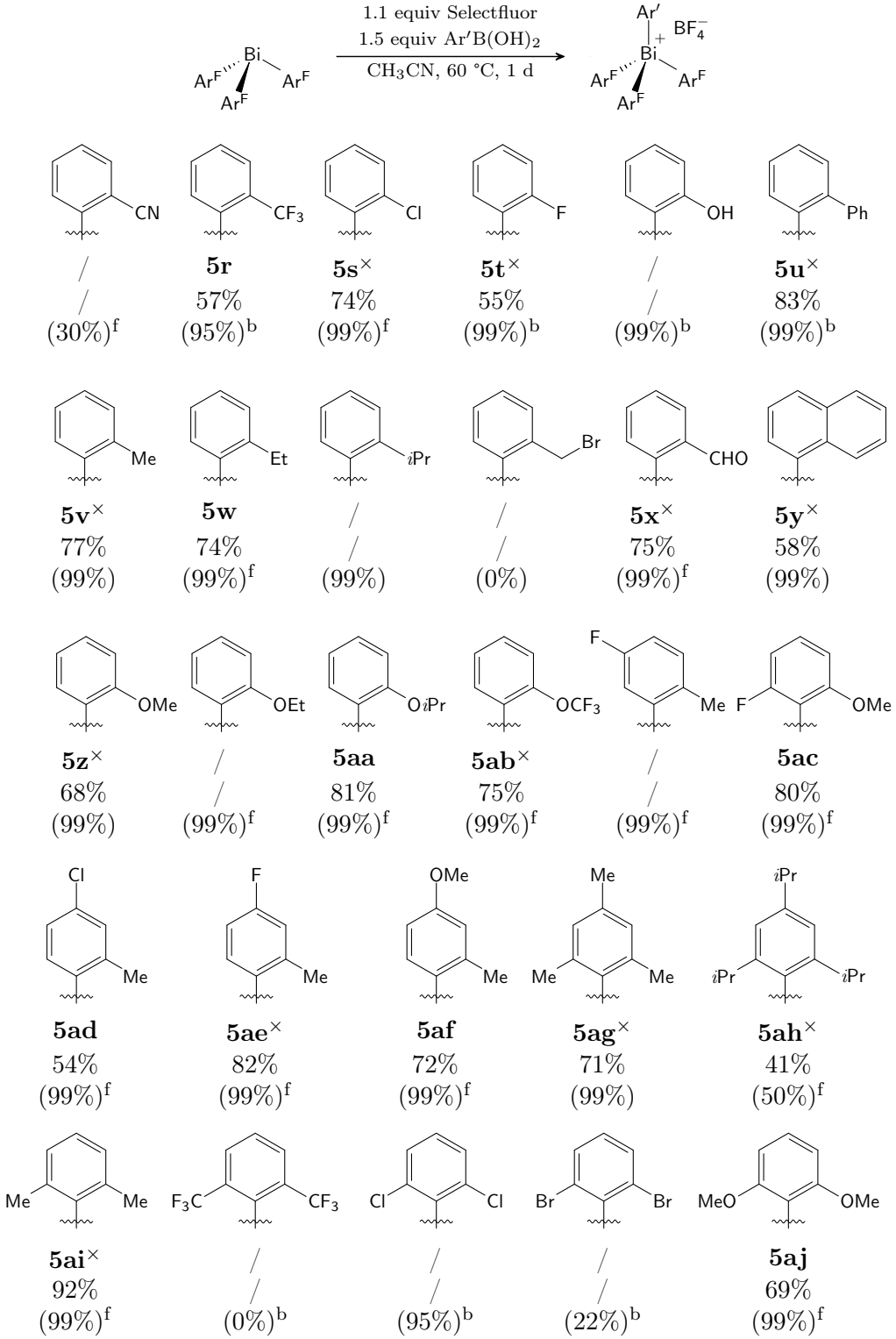

Figure 3.3: Scope of *ortho*-substituted boronic acids. NMR conversions are reported in parentheses, yields of isolated product and compound numbers are reported when available. Variations from standard conditions: $^{b}BF_3{\cdot}OEt_2$, 80 °C, 3 d; $^{f}BF_3{\cdot}OEt_2$, 5 h. $^{\times}$ crystal structure was determined.

Analysis of the performance of the transmetalation with *ortho*-substituted aryl boronic acids must include both electronic and steric effects. Conversions were measured under different conditions so a direct quantitative comparison would not be possible. Nonetheless some qualitative trends were observed, *e.g.* electron-rich but sterically hindered groups worked well, whereas electron-poor but moderately hindering groups were harder to transmetalate, so it would be desirable to identify the contribution of each factor to the difficulty of the transmetalation.

The separation of steric effects from electronic effects to obtain 'pure electronic' or 'pure steric' descriptors has always been challenging: in the paper from 1937 where the Hammett equation is first described, the author observed that, if good linear relationships were obtained by plotting the logarithm of ionisation constants of *para*- and *meta*-substituted benzoic acids against σ constants therein defined, the same equations only provided scattered results when applied to *ortho*-substituted benzoic acids. The conclusion was that *ortho* substituents exert effects that vary from one reaction to another, because of the presence of variable steric effects that can be neglected for distal *meta* and *para* substituents.[323]

Similarly, Taft developed steric descriptors (E_S and E_S^o) based on the rates of hydrolysis of aliphatic esters and *ortho*-substituted benzoates, respectively, after having observed a decrease in rates with the increase of the relative size of the substituents.[324] However, there was a substantial debate in the 1960s and 1970s regarding the concept that E_S was a purely steric descriptor and Charton demonstrated that only E_S correlated with the Van der Waals radii of the substituent, whereas E_S^o contained also an electronic contribution.[325]

Nowadays, σ_o constants can be computationally derived, for example by correlation with the core-electron binding energy (CEBE) of the *ipso* carbon atom.[326,327] Nonetheless, the same limitations discussed by Hammett still stand, that is to say the transferability of these calculated constants may not necessarily be presumed. Moreover, recently it has been pointed out that through-space (field) effects, as opposed to through-bonds (induction and resonance) effects, may make a significant contribution to the electron-donating/withdrawing capabilities of substituents, especially when in the *ortho* position.[328]

Given the complexity of factors involved, Sigman and Doyle showed independently that a more appropriate approach may be to let an algorithm pick the best combination of computationally-derived descriptors, either through stepwise regression in the first case or *via* a random forest algorithm applied to machine learning in the second.[329,330] For each molecule involved in the study, Doyle derived 120

descriptors, *e.g.* the electrostatic charge and the NMR chemical shift of every atom, the molecular volume, the dipole moment, the energies of HOMO and LUMO, and employed them to find a correlation with, and then predict, the yield of a Buchwald-Hartwig reaction across a dataset of 4608 individual reactions.

Inspired by these works, a similar approach was attempted. Due to the dearth of calculated σ_o constants, a different descriptor for electronics was sought. The ^{19}F NMR chemical shift of the *p*-fluorophenyl groups of each heteroleptic bismuthonium (δ_F^{scaff}) was initially identified for this role, due to its availability for all the compounds tested. Moreover, compared to σ constants, which are related to substituents and whose additivity in case of poly-substitution is uncertain, it was thought this could give a more comprehensive representation of the electronics of the unique group.

As far as steric descriptors are concerned, Sterimol parameters were initially considered. These were defined by Verloop to overcome the limitations of more traditional parameters (A-values,[333] interference values,[334] Taft-Charton parameters[324,325]), especially for non-spherical/anisotropic substituents.[335] Instead of aggregating all the spatial information in one parameter, Verloop defined five sub-parameters. The model eventually simplified to employ only three parameters.[331] With the primary axis defined as the direction in which the substituent is attached to the parent molecule, these are (see Fig. 3.4 for a graphical depiction): L, the length of the substituent along the primary axis; B_1, the minimum width of the projection of the substituent on the tangent plane perpendicular to the primary axis; B_5, the maximum width of the same projection.[331] Robert Paton modernised the way these parameters are calculated by introducing quantum mechanical optimisation of the structures and Boltzmann-weighting of the different conformations a flexible substituent may adopt.[336]

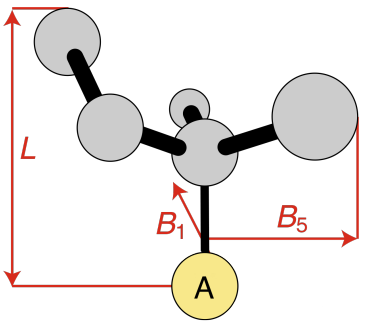

Figure 3.4: The Sterimol parameters L, B_1 and B_5 for a generic substituent as defined by Verloop.[331] A represents the atom to which the substituent is connected. Adapted from Falivene.[332]

The most important limitation in classic Sterimol parameters is that they are substituent-related, so if they are applied in the modelling of the steric hindrance of substituted arenes, as it is the intention here, it would not be possible to take into account poly-substitution. One may be tempted to calculate the Sterimol parameters for the entire Ar′ group but, if, for example, this bears two equal substituents in the 2- and 6-positions, the calculated parameters would be exactly the same as those for the mono-substituted analogue,[337] since Sterimol parameters only measure the minimum and maximum distances from the main axis. For these reasons, the percent buried volume (% V_{bur}) was deemed more appropriate, since it could take into account poly-substitution. This is defined as 'the fraction of the first coordination sphere around a metal centre that is occupied by the organic ligand' and, due to this broad definition, can be applied to the parametrisation of any class of catalyst and ligand.[332] Often the % V_{bur} is calculated from crystal structures but any structure file can be used as the input. The latter had to be the case in this work, due to the fact that crystal structures were not available for all the bismuthonium salts discussed.

Thus, even though the Sterimol approach had been abandoned, it was decided to take advantage of the software written by the Paton group to calculate weighted Sterimol parameters (wSterimol)[‡] to generate a series of Boltzmann-weighted conformers for each Ar′ group, optimised at the PM6-D3H4 level of theory. These were then subjected in batch to a locally run version of SambVca 2.1,[§] which calculated the % V_{bur} for each of the conformers of every group. For every Ar′ group, each of these % V_{bur} parameters was weighted with the weights extrapolated from the initial wSterimol calculation, thus giving the weighted % V_{bur}: wV_{bur}. All this otherwise tedious series of operations has been automated by a bash script, which can be found in Section 6.10. The parameters for all the aromatic groups mentioned in this Chapter are reported in Table 6.2 for reference, together with the wSterimol parameters calculated en route to wV_{bur} parameters.

With both the descriptors in hand, a plot of wV_{bur} vs δ_F^{scaff} was generated and is reported at the top of Fig. 3.5. The plot must be interpreted in a qualitative way and correlates the 'ease' of transmetalation against these two parameters. Three regions may be identified: in the first, depicted with a green background, the reaction occurred or is likely to occur under the optimised conditions; in the second, in yellow, the reaction gave good conversions but harsher conditions

[‡]https://github.com/bobbypaton/wSterimol

[§]https://www.molnac.unisa.it/OMtools/sambvca2.1/index.html

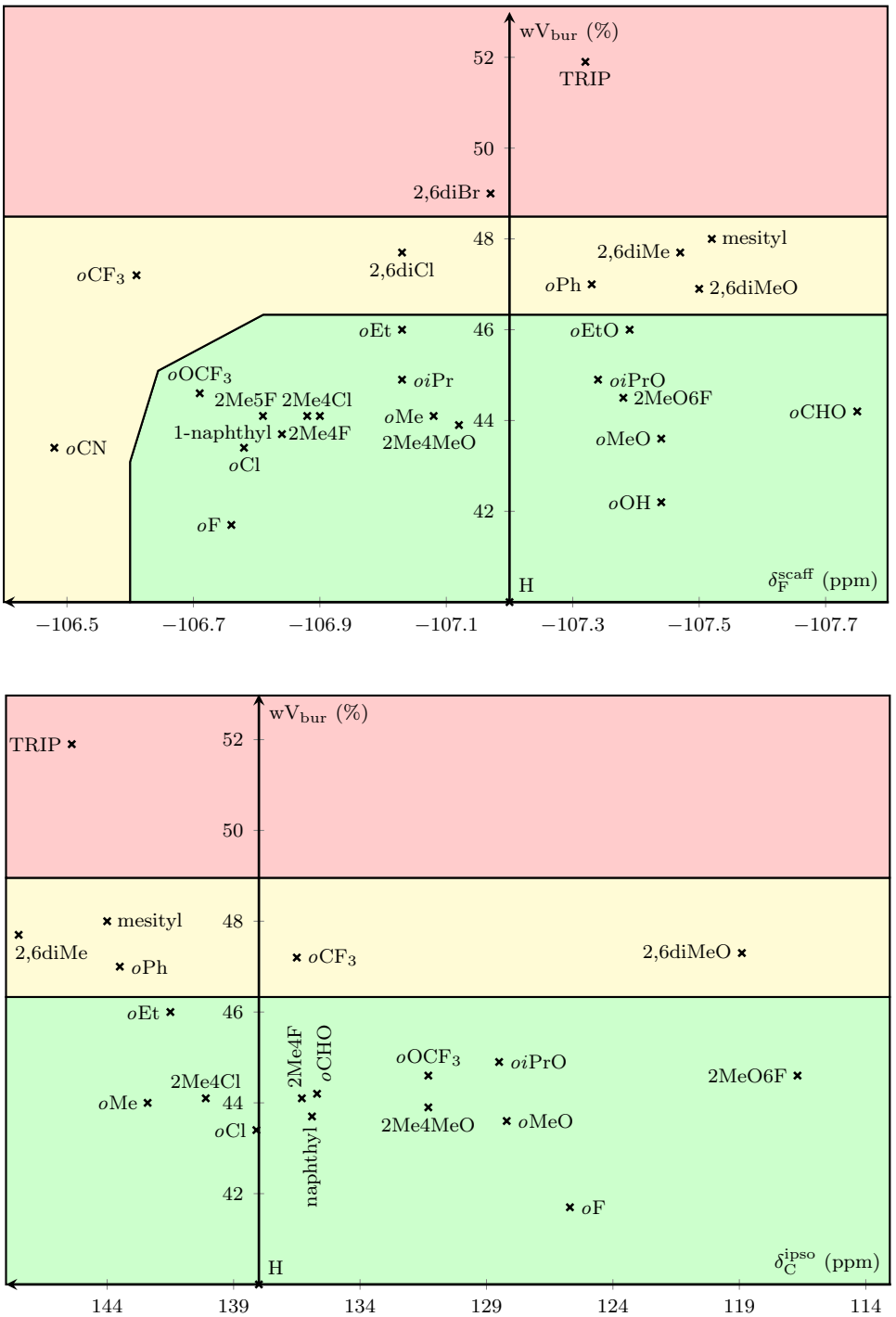

Figure 3.5: By plotting wV$_{bur}$ against δ_F^{scaff} (top plot) or δ_C^{ipso} it is possible to explain and predict which boronic acids did or will perform well in the transmetalation to bismuth. Ideally conversions or yields should be plotted on the z axis so as to generate a 3D scatter and obtain a fully quantitative tool. This was not possible as these reactions were not all performed under the same conditions (see Fig. 3.3).

were required ($BF_3{\cdot}OEt_2$, higher temperature...); finally, the remaining area, in red, is populated with groups whose conversion have been mediocre under all the conditions tested. The green region is characterised by small wV_{bur} (≤ 46) and spans across almost all the observed chemical shifts. The only group which has a small wV_{bur} (43.7) but does not belong to this region is *o*-cyanophenyl, which is likely to be very electron poor ($\delta_F^{scaff} = -106.49$ ppm). The use of $BF_3{\cdot}OEt_2$ or hotter temperatures allowed the transmetalation of some 2,6-disubstituted groups and mono-substituted but electron-poor groups: the yellow region is comprised roughly between $46 \leq wV_{bur} \leq 49$. With $wV_{bur} \geq 49$ the process becomes particularly hard (conversions for 2,4,6-triisopropylphenyl and 2,6-dibromophenyl reached only 50% and 22%, respectively). It did not come as a surprise that 2,6-di(trifluoromethyl)phenyl did not transmetalate at all, since its calculated wV_{bur} is 54.9 and the predicted δ_F^{scaff} is around -106.0 ppm, based on the mono-substituted analogue. This would place the group in the far top left region of the plot, marking the unlikeliness of its transmetalation.

Some caveats should be considered when using this plot. First of all δ_F^{scaff} may not be able to fully reflect the electronics of the Ar′ group, as the effect is measured at the fluorine atom, after propagating through the Ar′ group, the bismuth atom and the Ar^F group. This explains the observed small dynamic range of the descriptor and suggests a considerable error may be associated with the measure of the electronics of the Ar′ group by the ^{19}F NMR shift. Secondly, additional effects may influence the chemical shift: an example is given by the *o*-CHO-substituted group, which is *per se* electron-deficient,[313] but, due to the coordination of the oxygen atom into bismuth (see crystal structure in Section 6.8), the measured δ_F^{scaff} would suggest the group is electron rich. The wV_{bur} descriptor has overall a greater predicting power.

These issues prompted the search for an alternative descriptor for electronics. The ^{13}C NMR chemical shift of the carbon atom of the unique group that is *ipso* to bismuth (δ_C^{ipso}) was thus tested. The resulting scatter is reported in the bottom plot of Fig. 3.5. This approach is more limited as it relies on the isolation of the bismuthonium salts, which has not or could not be carried out for some. For this reason the following groups had to be excluded from the bottom plot: 2,6-dibromo-, *o*-EtO-, *o*-*i*Pr-, *o*-CN-, *o*-OH- and 2-Me-5F-substituted. This prevents a direct comparison of the two plots, even though the overall idea remains the same. However, the dynamic range of δ_C^{ipso} is significantly greater and is measured for an atom that is in the same aromatic ring of the substituent, thus preventing potential distortions due to the propagation through the bismuth atom.

3.2.3 Heteroaromatic boronic acids

The scope of heteroaromatic boronic acid was explored next: results are presented in Fig. 3.6. Furyl and thienyl derivatives are well tolerated, providing excellent conversions under the standard conditions. The presence of an acyl substituent in the 2-position of 3-thienylboronic acid significantly impacts the conversion, which dropped to 50%. Moreover, formation of 13% of $Ar^F_4Bi^+$ and 35% of Ar^F_3Bi should be noted. The origin of the latter is unclear. The pyrrole derivative did not yield the desired product, instead instantaneous reduction of Bi to Ar^F_3Bi was detected, accompanied by a peach black colouring of the reaction mixture, suggesting possible oxidation of the electron-rich aromatic system. This poor behaviour is in contrast to that observed with the sulfone bismacycle previously reported by our group.[318] Gratifyingly, the benzofused analogue 5-methoxy-2-indolylboronic acid fully converted to the corresponding bismuthonium. The two pyrazole derivatives did not yield the transmetalation products quantitatively and could not be isolated. No other species were detected that could suggest any decomposition pathway. Boron trifluoride did not help either. On the other hand, the isoxazolyl species reached a similar degree of conversion, but could be crystallised and was obtained pure nonetheless. All four examples of indolyl- and indazolylboronic acids worked well in the transmetalation. Notably three of them bore unprotected nitrogen atoms.

Finally, six-membered heterocyclic boronic acids were put to the test. Differently from the other examples in Fig. 3.6, conversions were in general poor. Both 4- and 3-pyridylboronic acids, as well as the 8-quinolyl analogue gave 0% conversion to the corresponding bismuthonium salts. Even heating the reactions at 150 °C under microwave irradiation did not convert any of the products of the oxidation of Ar^F_3Bi, which was recovered untouched. Interestingly, the presence of a methoxy group in the *para* position allowed a partial conversion (32%). The same fate was shared by the aminopyrimidine and dimethoxypyrimidine derivatives, which showed 64% and 38% conversions, respectively. The aminopyrimidine example is remarkable for two reasons: firstly, the amino group in the *para* position was shown to behave similarly to the methoxy group and increase the electron richness of the pyrimidine ring and allow the transformation, secondly, the very same amino group does not cause the reduction of the products of the oxidation of Ar^F_3Bi, which, on the other hand, was the case when a dimethylamino group was installed on a simple phenyl ring (see Fig. 3.1 and discussion earlier in this Section). In short, this aminopyrimidine moiety is electron rich enough to be transmetalated and electron poor enough not to cause

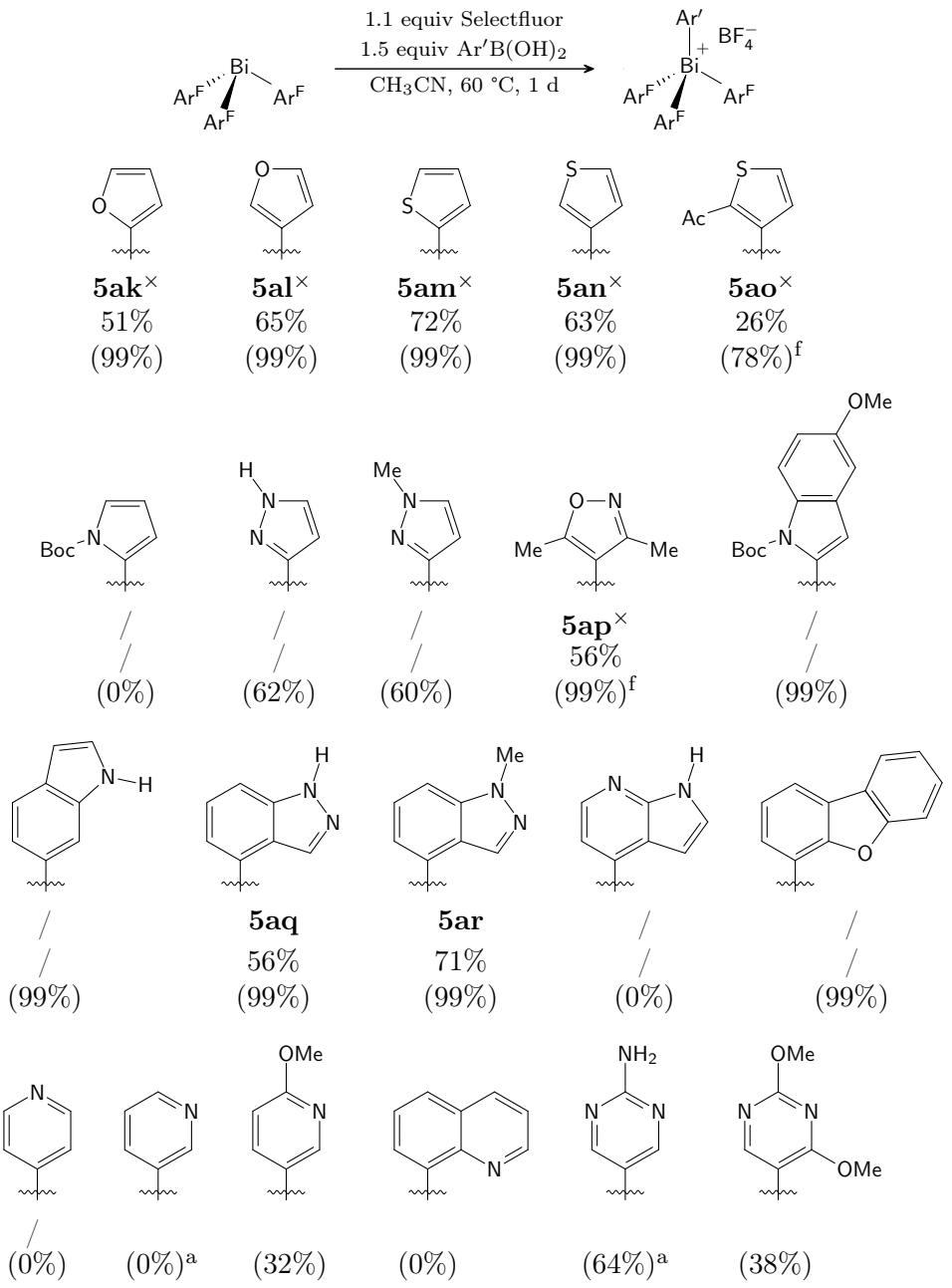

Figure 3.6: Scope of heteroaromatic boronic acids. NMR conversions are reported in parentheses, yields of isolated product and compound numbers are reported when available. Variations from standard conditions: [a]microwave, 150 °C, 1 h; [f]$BF_3{\cdot}OEt_2$, 5 h. [×] crystal structure was determined.

the reduction of Ar^F_3BiFX. Similar results were observed with the sulfone-bridged bismacycle, for which the methoxy-substituted pyridine was the only pyridinyl group that could be installed.[318]

The reason for the poor behaviour of pyridyl boronic acids remains unclear. The primary explanation would involve the electron-deficient nature of these groups. This is expected to hinder transmetalation, as discussed in Fig. 3.2. The performance improves with the presence of electron-donating substituents (MeO–) on the pyridyl rings, which would be consistent with this argument. An alternative explanation is provided by a closer look to the ^{19}F NMR spectra measured for aliquots taken during transmetalation: peaks with higher-order multiplicity were found in the spectra of the reactions with all the 6-membered ring heterocyclic boronic acids. Representative spectra are reported in Fig. 3.7. Their chemical shifts vary within the −137 and −147 ppm region and, when they are at least partially resolved, their coupling constants could be measured to be around 40–45 and 84–97 Hz. Not dissimilarly to what was observed in Section 2.5, boron trifluoride was initially proposed to form adducts with the basic nitrogen of these pyridine derivatives, further increasing their electron-poor character, to the point that transmetalation becomes unfeasible. Electron-releasing substituents would have the same role in this second theory, *i.e.* to increase the electron density of the aromatic ring, thus compensating for the formation of the electron-depleting adduct. These adducts are known in the literature: for instance the pyridine–BF_3 adduct is reported to resonate around −150 ppm in ^{19}F NMR spectroscopy and its shape strongly resembles the quartet-like shape of some of the peaks reported in Fig. 3.7.[338]

In favour of the pyridine-BF_3 adduct argument there is the fact that the chemical shift of the peaks reported in Fig. 3.7 varies for each of the boronic acids employed, suggesting that the observed peaks arise from the interaction between the boronic acid, the only variable in these reactions, and a fluorine-containing species. Against this argument is the fact that none of the reactions whose spectra are reported in Fig. 3.7 employed $BF_3{\cdot}OEt_2$. If BF_3 were present, then it must have originated from a different route. One would be the transmetalation itself, as discussed in Section 2.2. However, these ^{19}F NMR peaks were observed also for reactions in which the product of transmetalation, *i.e.* the bismuthonium salt, was not observed even in trace amount, such as with 3- and 4-pyridyl- and quinolylboronic acids (see Fig. 3.6). Therefore, in these reactions BF_3 did not form as a by-product of the transmetalation, since the latter did not work. Another pathway may involve reaction of the Selectfluor-derived BF_4^- with glass. This would cause F^- extraction and formation of BF_3, which could in turn form the adduct with pyridine nitrogens.

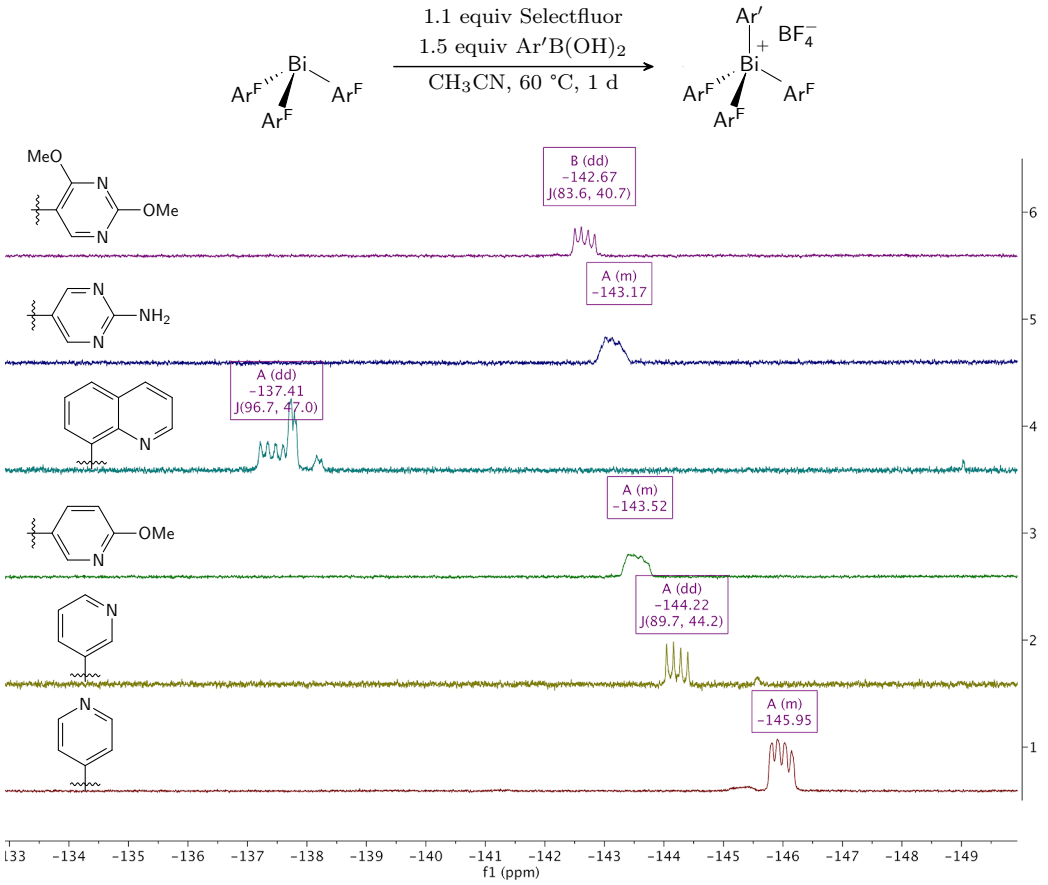

Figure 3.7: When transmetalation of the Ar′ groups depicted here was attempted, formation of different ^{19}F peaks was observed for each of the boronic acids employed. All reactions were performed in MeCN and diluted in CD_3CN for sampling and subsequent analysis by ^{19}F NMR spectroscopy.

An additional possibility was considered, that the Selectfluor-derived BF_4^- can undergo hydrolysis in wet acetonitrile, thus forming BF_3OH^- and fluoride.[339,340] The latter can react with borosilicate glass and form SiF_6^{2-}. The literature ^{19}F NMR chemical shifts for these three species are −143, −163 and −130 ppm, respectively. Interesting, the reported multiplet shape for BF_3OH^- strongly resembles those in Fig. 3.7 (quartet-like structure and similar coupling constants).[340] However, no trace of hexafluorosilicate or fluoride/HF could be observed in any of our reactions. Moreover, if the observed peaks corresponded to BF_3OH^-, the observed BF_3OH^-:BF_4^- ratio (not shown in Fig. 3.7) in the spectra reported in Fig. 3.7 would be comprised between 1:1.3 and 1:5, which, at least in certain cases, would suggest an important degree of decomposition of BF_4^- *via* this pathway. However, this decomposition has not been observed for any other reaction discussed in this Chapter, suggesting

it occurs specifically with these boronic acids. Finally, the hydrolysis of BF_4^- is likely to occur even in the absence of boronic acid. This, however, would not be consistent with the observed formation of peaks with varying chemical shift when different boronic acids are employed. All these reasons corroborate the initial idea that BF_3 forms adducts with pyridyl boronic acids, preventing further reactions.

3.2.4 Additional boronic acids

Figure 3.8 concludes the boronic acid scope and contains alkyl and alkenyl boronic acids and an example of a 'bidentate' boronic acid. None of the three aliphatic boronic acids gave any hint of conversion, instead they all caused complete reduction of the oxidised bismuth species to Ar^F_3Bi and fluorobenzene within 24 h. Significant amounts of $Ar^F_4Bi^+$ were detected in all cases, too, as well as methanol for the first boronic acid of this series. These outcomes are consistent with Matano's findings:[257] the author was able to obtain full conversion of $[Ph_3MeBi][BF_4]$ by reacting $Ar^F_3BiF_2$ with $MeB(OH)_2$ in the presence of $BF_3{\cdot}OEt_2$ but noted that strict anhydrous conditions are required to prevent hydrolysis of the bismuthonium, which would decompose to MeOH, Me_2O and Ph_3Bi. He also observed formation of the homoleptic species with yields up to 10% and noted that the reaction could not be performed with butylboronic acid. Considering that the acetonitrile employed in our experiments was not subjected to any process of water removal, it is likely that the transmetalation of $MeB(OH)_2$ worked and the product underwent decomposition. It would be interesting to repeat these reactions under dry conditions.

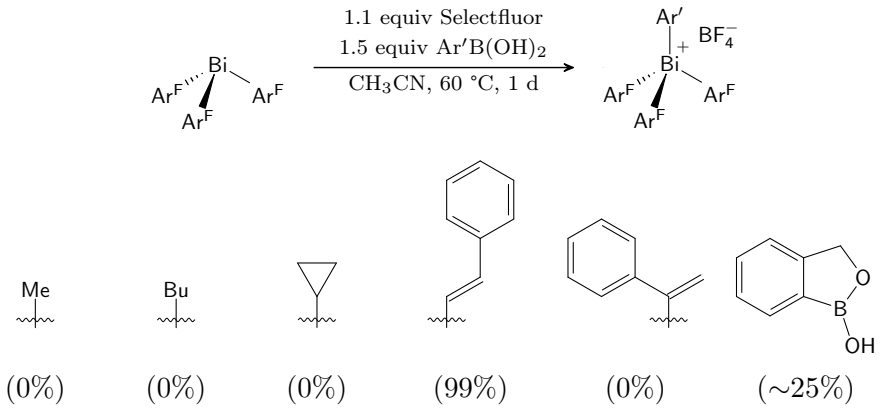

Figure 3.8: Additional boronic acids assessed. Fluorine NMR conversions are reported in brackets. Isolation of the corresponding bismuthonium salts was not achieved in any of these examples.

Among the two isomers of styrenyl boronic acid only the 2-substituted worked well, whereas the 1-substituted caused instantaneous reduction to Ar^F_3Bi. Finally, the outcome of the transmetalation of the benzoxaborol, which contains a masked benzyl alcohol functionality, was uncertain, since the desired product could be detected as the most intense ion by HRMS, whereas by ^{19}F NMR spectroscopy the only well resolved peak resonated at the exact chemical shift of one the oxidation products of Ar^F_3Bi, making quantification impossible. Moreover, its chemical shift (-108.32 ppm) would make it by far the most shielded bismuthonium in the series, considering that the observed chemical shift range for the bismuthonium salts in this Section is comprised between -106.8 and -107.8 ppm. This would usually suggest the peak corresponds to a Ar^F_3BiFX species, rather than a bismuthonium salt. Interestingly the second most shielded species would be the 2-formyl bismuthonium **5x**, with a measured chemical shift of -107.76 ppm. At first sight, this does not correlate well with the electron-withdrawing nature of the 2-formyl substituent.[327] However, a coordination of the benzyl oxygen to the bismuth centre may be postulated in both cases and is indeed detected in the crystal structure of the formyl derivative. This coordination is suggested to enhance the electron density on the Ar^F groups connected to the bismuth and explain the upfield chemical shift. Finally, the effect would be more marked in the case of a –CH_2OH group than with a –CHO group, due to the greater amount of localised charge in that oxygen atom.

3.2.5 Crystallographic analysis

Under the optimised conditions employed in this Section, the isolation of bismuthonium salts can be achieved by crystallisation. This in many cases provided single crystals that were suitable for X-ray crystallographic analysis. The solid-state structures of 29 bismuthonium salts were thus determined crystallographically. Selected bond lengths are reported in Table 3.7: more details can be found in Section 6.8. Two points are worth of discussion: the geometry of these complexes (trigonal bipyramidal or tetrahedral) and, in case of a D_{3h} symmetry, the position of the unique group Ar′ (axial or equatorial).

As discussed in Section 1.1.4, the Lewis basicity of the counterion determines the molecular geometry of tetraarylbismuth complexes: with basic anions, these adopt distorted trigonal biypramidal geometries; otherwise tetrahedral geometries are preferred. Among the tetraphenylbismuth structures deposited in the CCDC, the tosylate and the fluoride belong to the first category,[77,78], whereas the perchlorate is tetrahedral.[341] This can be determined quantitatively by measuring the Z–Bi

#	Ar′	Eq.	C1–Bi	C7–Bi	C13–Bi	C19–Bi	Bi–BF_4
1	*p*-F **5a**	n.d.	2.185(5)	2.191(5)	2.177(5)	2.189(6)	3.162(3)
2	*p*-CN **5b**	n.d.	2.192(9)	2.176(9)	2.180(9)	2.190(8)	**5.236(6)**
3	*p*-Cl* **5d**	n.d.	2.205(5)	2.194(4)	2.196(4)	2.204(4)	2.889(4)
4	*p*-H* **5f**	n.d.	2.197(4)	2.186(4)	2.185(3)	2.188(3)	3.001(2)
5	*p*-TMS **5h**	N	2.21(10)	2.20(10)	2.18(10)	2.16(10)	2.895(7)
6	*m*-CN **5l**	n.d.	2.196(3)	2.209(3)	2.190(3)	2.192(3)	**5.515(2)**
7	*m*-Br **5n**	Y	2.18(20)	2.20(20)	2.16(20)	2.20(20)	3.02(20)
8	*m*-F* **5m**	n.d.	2.189(4)	2.197(4)	2.196(4)	2.209(5)	2.83(3)
9	*m*-Me* **5o**	n.d.	2.20(20)	2.23(20)	2.14(20)	2.19(30)	3.20(10)
10	3,5-di-Me **5q**	Y	2.19(20)	2.20(10)	2.20(20)	2.20(20)	3.949(7)
11	*o*-Cl* **5s**	n.d	2.191(5)	2.187(5)	2.189(5)	2.205(5)	**4.181(3)**
12	*o*-F **5t**	Y	2.209(7)	2.194(6)	2.202(7)	2.182(8)	3.061(4)
13	*o*-Ph **5u**	Y	2.206(4)	2.219(3)	2.199(3)	2.202(3)	2.971(3)
14	*o*-Me **5v**	n.d.	2.190(8)	2.183(9)	2.195(9)	2.20(10)	**7.052(6)**
15	*o*-CHO **5x**	n.d.	2.224(6)	2.202(5)	2.193(6)	2.214(7)	**4.493(5)**
16	1-naphthyl **5y**	Y	2.20(30)	2.19(30)	2.18(30)	2.23(30)	3.16(20)
17	*o*-*i*PrO **5aa**	n.d.	2.22(3)	2.17(4)	2.20(3)	2.20(3)	**5.08(3)**
18	*o*-OCF_3 **5ab**	N	2.182(6)	2.191(5)	2.187(5)	2.224(7)	2.850(4)
19	2-Me-4-F* **5ae**	n.d.	2.19(1)	2.17(1)	2.21(1)	2.26(2)	3.05(8)
20	Mesityl **5ag**	Y	2.209(3)	2.199(3)	2.209(3)	2.216(2)	2.774(1)
21	TRIP **5ah**	Y	2.206(3)	2.203(3)	2.210(2)	2.227(3)	2.832(2)
22	2,6-di-Me **5ai**	n.d.	2.187(4)	2.202(4)	2.208(4)	2.212(4)	**4.757(3)**
23	2-furyl **5ak**	N	2.184(3)	2.198(3)	2.199(3)	2.188(4)	2.784(2)
24	3-furyl **5al**	N	2.189(4)	2.194(4)	2.192(4)	2.181(5)	2.797(3)
25	2-thienyl **5am**	N	2.19(3)	2.189(3)	2.191(3)	2.195(3)	2.805(2)
26	3-thienyl **5an**	N	2.188(7)	2.173(7)	2.178(9)	2.18(2)	2.871(5)
27	3thien2Ac **5ao**	N	2.15(30)	2.19(30)	2.22(30)	2.17(30)	2.93(20)
28	isoxazolyl **5ap**	Y	2.187(2)	2.171(2)	2.190(2)	2.158(2)	2.964(1)
29	Ph_3BiAr* **5as**	n.d.	2.195(7)	2.205(6)	2.184(8)	2.191(9)	3.288(7)
	Average		2.20(2)	2.19(2)	2.19(2)	2.20(2)	

Table 3.7: The 'Eq.' column indicates if the Ar′ group sits equatorial. This cannot be determined if the structure is disordered or tetrahedral. *Disordered aryl groups. Bold values for the BF_4–Bi length signify that the distance is greater than the sum of Bi and F Van der Waals radii: therefore the tetrafluoroborate is fully dissociated and the bismuthonium is tetrahedral. For all entries, C19 is the carbon atom *ipso* to Bi which belong to the Ar′ group, whereas C1, C7 and C13 are the carbon atoms *ipso* to Bi of the Ar^F groups. For entries 1–15, 17–19 and 22 'phenyl' is implied in the Ar′ name.

distance, where Z is the counterion: if this length is greater than the sum of the Van der Waals radii of Bi and the atom of the counterion pointing towards the pnictogen, then the counterion is ion-separated and the bismuth complex geometry is expected to have a considerable tetrahedral character. This is true for tetraphenylbismuthonium perchlorate: the Bi–Cl-OCl_3 is 5.266 Å, greater than the sum of Bi and O radii (4.47 Å) and all Bi–C bonds have the same length (2.163 Å).

The same concept was applied to the crystal structures determined in this Thesis: in Table 3.7 the Bi–BF_4 distances that were found to be larger than the sum of Bi and F Van der Waals radii are highlighted in bold. These complexes, here indicated by the nature of the Ar′ groups, are: *p*-cyanophenyl (entry 2), *m*-cyanophenyl (entry 6), *o*-chlorophenyl (entry 11), *o*-tolyl (entry 14), *o*-formylphenyl (entry 15), *o*-isopropoxyphenyl (entry 17) and 2,6-xylyl (entry 22). It is noticed that complexes with Ar′ groups bearing electron-withdrawing or sterically hindered substituents are more prone to maintain an ion-separated interaction with tetrafluoroborate. Entries 15 and 17 are likely to represent exceptions to this observation, since an interaction between their oxygen atoms and bismuth is present. Oxygen occupies bismuth's fifth coordinative position, possibly disfavouring tetrafluoroborate's contact.

The Ar′ group's preference for the equatorial position was then explored. The following complexes, once again identified for brevity by the unique group, were found to crystallise with said group in the equatorial position of a trigonal bipyramidal structure: *m*-bromophenyl (entry 7), *m*-xylyl (entry 10), *o*-fluorophenyl (entry 12), *o*-biphenyl (entry 13), 1-naphthyl (entry 16), mesityl (entry 20), TRIP (entry 21) and isoxazolyl (entry 28). This behaviour reflects the fact that the equatorial position accommodates bulkier groups, due to a wider angle between equatorial groups (120°) compared to that between axial groups and the equatorial plane (90°).

The next Section will investigate the behaviour of these complexes when exposed to the arylating conditions, and in particular will address the selective transfer of the unique group to the substrate. In this perspective, it will be interesting to determine if a correlation between the tetrahedral nature and/or the position of the Ar′ group in the trigonal bipyramid, and the selectivity exists.

3.3 Arylation with bismuthonium salts: chemoselectivity

One of the principal aims of this Thesis was to optimise a bismuth-based methodology to enable investigation of the selectivity for transfer of the unique group. Two works represent the primary sources of migratory aptitudes of heteroleptic bismuth complexes: the oldest is a paper by Barton in which he studied the behaviour of unsymmetrical bismuth carbonates ($Ar_2Ar'BiCO_3$) in the arylation of 2-naphthol and dimedone;[39] the second is by Matano and Suzuki and only briefly investigated the arylation of 2-naphthol with heteroleptic bismuthonium salts.[314] With both types of bismuth complexes and both nucleophiles the migratory aptitude was found to decrease with increased electron richness, that is to say electron-rich groups are retained on the bismuth more than electron-poor ones.

In Section 1.4.3, hypervalent diaryl-λ^3-iodanes were listed as an alternative to organobismuth complexes for the arylation of phenols. In particular it was highlighted that, in metal-free conditions, enol-like species undergo *O*-arylation with these complexes and the same migratory aptitude of bismuth is followed. Additionally, sterically hindered ligands were shown to have a greater tendency to transfer compared to non-hindered ones, even overriding the selectivity dictated by electronic factors (the so-called *ortho* effect). The tendency varies dramatically with the arylation substrate: differently from phenols, anilines do not show any *ortho* effect and only electronics dominates the chemoselectivity, whereas malonates show an anti-*ortho* effect, that is electron-poor and non-sterically hindered groups are transferred preferably.[197] In the presence of a transition-metal catalyst, opposite chemoselectivities were observed, with the most electron-rich and least sterically demanding group usually being transferred. A comparison with bismuth literature data could not be performed, since studies involving sterically demanding groups have not been published for complexes of the heavier element.

With such a vast library of heteroleptic bismuthonium salts in hand, we were able to fill in this gap in the knowledge of bismuth chemistry. Due to the discrepancies observed with hypervalent iodine chemistry between different substrates, we decided to test the chemoselectivity of the arylation with bismuthonium salts with two different nucleophiles: 6-fluoro-2-naphthol, as a prototype for phenol-like compounds, and dimethyl-2-fluoromalonate. The presence of a fluorine atom in the latter has a two-fold purpose: to prevent diarylation of the activated position and to enable reaction monitoring by ^{19}F NMR spectroscopy. With both substrates the chemoselectivity s was determined as the non-normalised ^{19}F NMR ratio of the arylation product with the unique group and that with the *p*-fluorophenyl group.

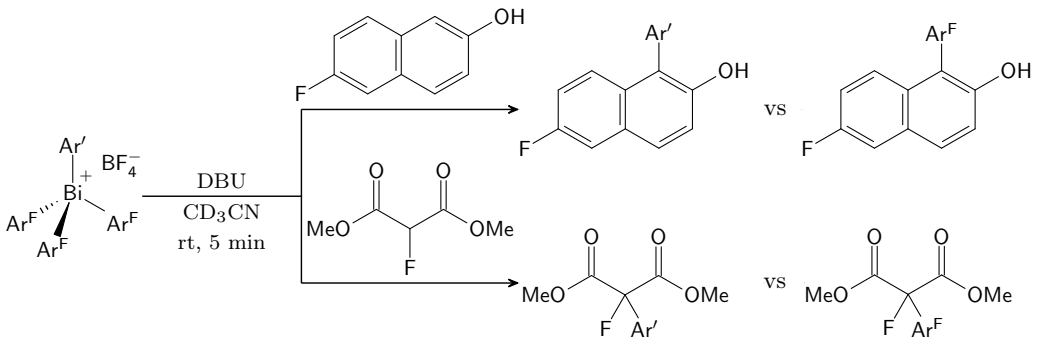

#	Ar′	Cmpd	Ar′:Ar^F Selectivity (s) Naphthol	Malonate
1	p-F	**5a**	1.00	1.00
2	p-CN	**5b**	8.35	3.03
3	p-Cl	**5d**	1.24	0.85
4	p-I	**5e**	1.05	1.03
5	p-H	**5f**	1.35	1.78
6	p-Ph	**5g**	1.17	1.64
7	p-TMS	**5h**	2.10	3.27
8	p-Me	**5i**	0.56	1.06
9	p-OMe	**5j**	0.19	n.t.
10	m-CN	**5l**	1.61	0.95
11	m-F	**5m**	1.63	1.13
12	m-Br	**5n**	1.86	1.43
13	m-OMe	/	2.69	n.t.
14	m-Me	**5o**	1.85	2.16
15	m-OH	/	2.39	n.t.
16	m-NMs	/	2.46	n.t.
17	3,5-diMe	**5q**	1.57	2.27
18	o-CF_3	**5r**	3.91	1.81
19	o-Cl	**5s**	7.47	0.63
20	o-F	**5t**	1.07	0.39
21	o-Ph	**5u**	0.09	n.d.
22	o-Me	**5v**	7.00	1.74
23	o-Et	**5w**	6.12	1.28
24	o-CHO	**5x**	n.t.	0.84
25	1-naphthyl	**5y**	24.4	2.88

#	**Ar′**	**Cmpd**	**Naphthol**	**Malonate**
26	*o*-MeO	**5z**	4.67	1.00
27	*o*-EtO	/	6.23	n.t.
28	*o*-*i*PrO	**5aa**	5.79	0.56
29	*o*-OCF_3	**5ab**	1.48	0.38
30	2-MeO-6-F	**5ac**	3.68	0.39
31	2-Me-4-Cl	**5ad**	8.58	0.31
32	2-Me-4-F	**5ae**	11.2	n.t.
33	2-Me-4-MeO	**5af**	1.81	n.t.
34	2-Me-5-F	/	10.4	n.t.
35	mesityl	**5ag**	27.5	0.92
36	TRIP	**5ah**	7.11	0.87
37	2,6-diMe	**5ai**	35.4	1.66
38	2,6-diMeO	**5aj**	11.2	n.t.
39	2-furyl	**5ak**	0.12	n.t.
40	3-furyl	**5al**	0.01	n.t.
41	2-thienyl	**5am**	0.01	n.t.
42	3-thienyl	**5an**	0.12	n.t.
43	*N*-Me-pyrazolyl	/	0.25	n.t.
44	isoxazolyl	**5ap**	0.01	n.t.
45	1-Me-4-indazole	**5ar**	1.86	n.t.
46	Ph_3Ar^FBi	**5as**	0.10	n.t.

Table 3.8: Selectivity study: 0.05 mmol of 6-fluoro-2-naphthol **7** or dimethyl-2-fluoromalonate were reacted with 1.0 equiv of bismuthonium **5** and 1.5 equiv of DBU in a NMR tube in CD_3CN at rt for 5 min. At reaction completion (the combined NMR yield was > 99% for all entries), the ^{19}F or $^{19}F\{^1H\}$ NMR peaks corresponding to the two arylation products were integrated yielding the reported selectivities. Spectra acquired with relaxation delay $D_1 > 30$ s to ensure full relaxation. n.t. = not tested. For entries 1–24, 26–34 and 37–38 'phenyl' is implied in the Ar′ name. TRIP = 2,4,6-tri-isopropylphenyl.

First, since not all the bismuthonium salts had been isolated, it was necessary to test if the chemoselectivity determined from isolated compounds was the same as that from compounds made *in situ*. This was confirmed to be the case and allowed all the results to be presented in a single data set (Table 3.8). For bismuthonium salts made *in situ*, only the compounds that showed full conversion to the tetravalent bismuth complexes were included in the selectivity determination study. This was crucial to avoid competition between the $Ar^F_3Ar'Bi^+$ salt and Ar^F_3BiFX in the

arylation reaction, since both complexes are competent in the reaction under basic conditions, which would bias the selectivity towards the product containing the *p*-fluorophenyl group.

3.3.1 Arylation of 6-fluoro-2-naphthol

We will initially discuss the chemoselectivity (s) of the arylation of the 2-naphthol. Instead of discussing the individual entries we will make use of linear free energy relationship (LFER) plots when possible. *Para*-substituted groups were analysed at first: the Hammett plot of $\log(s)$ versus σ_p is presented in Fig. 3.9. Unfortunately, the correlation is poor with the *p*-cyanophenyl group showing a comparatively high selectivity and thus being an outlier.

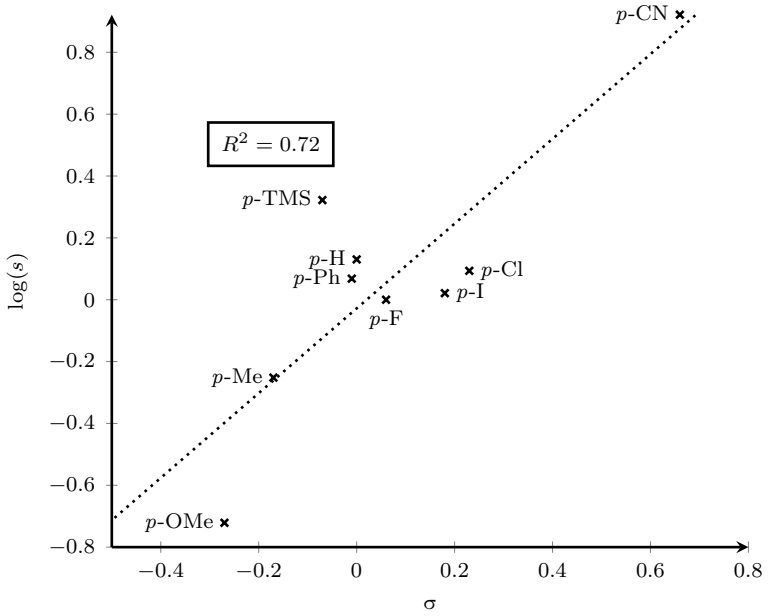

Figure 3.9: Hammett plots of $\log(s)$ against σ. The fit is mediocre, suggesting a more complex model is required.

Strongly conjugated substituents, such as $-NO_2$ or –CN, are known to have a greater than expected impact on the stabilisation of the incipient charge when the reactive site is conjugated with the aromatic ring.[323] This led to the definition of σ^+ and σ^- constants for reactions where the incipient conjugated charge is positive or negative, respectively.[342,343] Both these constants provided a better correlation than σ (entries 2 and 3 of Table 3.9), with the first one giving an R^2 of 0.90 and high significance. In order to improve the fit even more, the approach of Swain and Lupton was followed: these authors derived two new constants, $\mathcal{F}$, describing

the field/inductive effect, and $\mathcal{R}$, for the resonance effect, a linear combination of which is able to give any σ constants. The principle is that the relative influence of induction and resonance may vary from reaction to reaction, therefore this can be calculated for each data set as follows:

$$\sigma_{new} = f\mathcal{F} + r\mathcal{R} + i \tag{3.1}$$

where f and r are the weights for the two factors and i is the intercept. This approach enables the determination of the best combination of induction and resonance, without having to use pre-defined σ constants. Since the original definition of $\mathcal{F}$ and $\mathcal{R}$ constants, Hansch and other authors praised the concept of determining the weight of induction and resonance *via* a least-squares regression, however they argued that a single resonance constant would not suffice to describe all reactions, especially those where the reaction site is conjugated with the substituent, and defined $\mathcal{R}^+$ and $\mathcal{R}^-$ from σ^+ and σ^-.[313]

Linear least-squares regression analysis was performed on $\log(s)$ against $\mathcal{F}$ and each of the three $\mathcal{R}$ constants individually. The coefficient of determination (R^2) of each combination is reported in Table 3.9 (entries 4–6), from which it appears that the combination of $\mathcal{F}$ and $\mathcal{R}^+$ is the one that fits $\log(s)$ best, in this resembling the good fit obtained with σ^+ (entry 2). The new parameter results defined as follows:

$$\sigma_{\mathcal{F}+\mathcal{R}^+} = 0.81\,\mathcal{F} + 1.15\,\mathcal{R}^+ + 0.20 \tag{3.2}$$

The plot of $\log(s)$ against $\sigma_{\mathcal{F}+\mathcal{R}^+}$ is reported in Fig. 3.10. This result, together with that obtained with σ^+, suggests that the transition state of the selectivity-determining step involves a negative charge conjugated with the *para* substituent of the group that is being transferred. In this case the greater the amount of negative charge that is stabilised by the substituent, the higher the tendency to transfer, *i.e.* electron-poor groups tend to transfer more easily, which is in agreement with what was observed by Barton.[39] Before pushing this reasoning too far, it is worth noting that the goodness of this linear regression may depend on the two data points at the opposite extremes, that is –MeO and –CN, so additional data points near the two far ends of the plot may be necessary increase the robustness of this analysis.

Linear regression analysis was then performed for *meta*-substituted examples (see Table 3.9, entries 8–10). However, the correlation was poor, with an $R^2 = 0.44$ for $\mathcal{F}$ and $\mathcal{R}$. In fact, looking at the selectivities in Table 3.8 (entries 9–14), all the *meta*-substituted groups appear to transfer slightly better than the *p*-fluorophenyl group, regardless of their electronic properties.

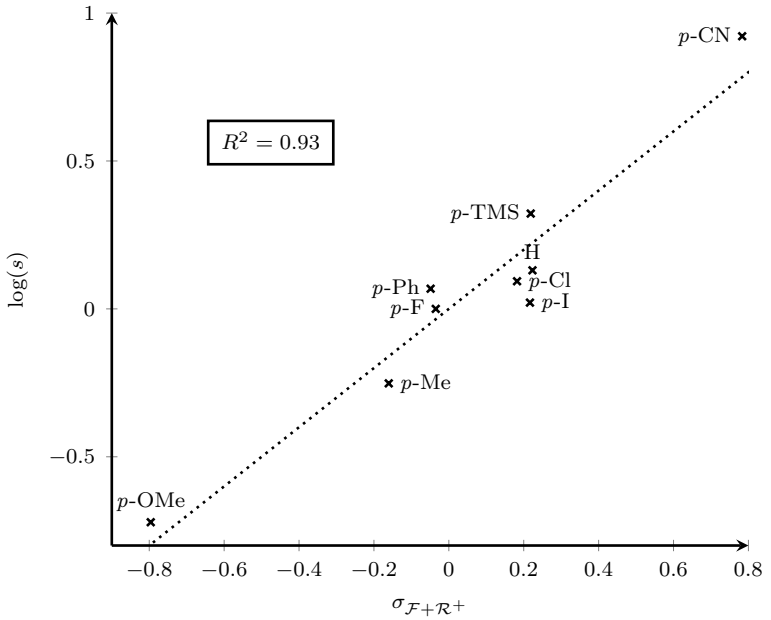

Figure 3.10: In order to improve the fit in Fig. 3.9 a new parameter $\sigma_{\mathcal{F}+\mathcal{R}^+}$ has been defined *via* linear least-square regression between $\mathcal{F}$ and $\mathcal{R}^+$ as per Eq. 3.2. This shows a more prominent contribution of resonance to the measured electronic effect on selectivity.

Next, the arylation with *ortho*-substituted groups was analysed. Since all the descriptors employed, with the exception of wV_{bur}, are substituent-specific and poly-substitution could not be taken into account, it was decided to discuss mono-substituted examples separately from poly-substituted, so that a larger pool of descriptors could be used in that case. As before, a correlation with σ_o was sought at first (entry 11 of Table 3.9). However, only six constants were available for the ten examples constituting the dataset.[327] Correlation was also extremely poor ($R^2 = 0.22$), so this descriptor was excluded from successive analyses.

Two different sets of Sterimol parameters were calculated with the wSterimol plugin developed by the Paton group:[336] the first follows the more conventional approach by being relative to the substituent and in Table 3.9 is indicated by a 'sub' superscript; the second, instead, was calculated for the entire Ar′ group and is indicated by a 'grp' superscript. The latter corresponds to those obtained as a by-product of the calculation of wV_{bur}. The calculated values of both descriptor for every Ar′ group discussed in this Chapter can be found in Tables 6.1 and 6.2, respectively. Table 3.10 lists all the descriptors used in this Section and their respective definitions. Theoretically, the two sets of descriptors should have the

Dataset (size)	#	Descriptors	R^2	F
para (9)	1	$1.37\,\sigma$	0.72	4.0×10^{-3}
	2	$1.07\,\sigma^{+}$	0.90	8.5×10^{-5}
	3	$1.07\,\sigma^{-}$	0.83	1.5×10^{-3}
	4	$0.81\mathcal{F} + 1.96\mathcal{R}$	0.91	8.3×10^{-4}
	5	$0.81\mathcal{F} + 1.15\mathcal{R}^{+}$	**0.93**	4.1×10^{-4}
	6	$0.70\mathcal{F} + 1.23\mathcal{R}^{-}$	0.88	5.0×10^{-3}
meta (7)	7	$-0.27\,\sigma$	0.31	0.19
	8	$-0.17\,\mathcal{F} - 0.20\mathcal{R}$	0.44	0.31
	9	$-0.11\,\mathcal{F} - 0.15\mathcal{R}^{+}$	0.45	0.41
	10	$-0.14\,\mathcal{F} - 0.089\mathcal{R}^{-}$	0.28	0.72
mono *ortho* (9)	11	$-0.63\,\sigma$	0.22	0.34
	12	$0.04\,\mathrm{w}B_5^{\mathrm{sub}}$	0.01	0.81
	13	$-0.26\,\mathrm{w}L^{\mathrm{sub}} + 2.04\,\mathrm{w}B_1^{\mathrm{sub}} + 0.49\,\mathrm{w}B_5^{\mathrm{sub}}$	0.47	0.24
	14	$-0.28\,\mathrm{w}B_5^{\mathrm{grp}}$	0.21	0.19
	15	$-0.05\,\mathrm{wV_{bur}}$	0.02	0.69
	16	$-0.01\,\delta_{\mathrm{C}}^{\mathrm{ipso}}$	0.02	0.73
	17	$0.002\,\delta_{\mathrm{F}}^{\mathrm{scaff}}$	0.06	0.49
	18	$-0.05\,\mathrm{wV_{bur}} - 0.006\,\delta_{\mathrm{C}}^{\mathrm{ipso}}$	0.04	0.88
	19	$-0.02\,\mathrm{wV_{bur}} + 0.02\,\delta_{\mathrm{F}}^{\mathrm{scaff}}$	0.07	0.78
	20	$-0.32\,\mathrm{w}B_5^{\mathrm{grp}} - 0.004\,\delta_{\mathrm{C}}^{\mathrm{ipso}}$	0.28	0.38
	21	$-0.26\,\mathrm{w}B_5^{\mathrm{grp}} + 0.001\,\delta_{\mathrm{F}}^{\mathrm{scaff}}$	0.22	0.42
	22	$5.25\,\mathrm{wV_{bur}} + 1.79\,\delta_{\mathrm{C}}^{\mathrm{ipso}} - 0.04\,\mathrm{wV_{bur}} \cdot \delta_{\mathrm{C}}^{\mathrm{ipso}}$	0.62	0.15
	23	$22.7\,\mathrm{wV_{bur}} - 9.27\,\delta_{\mathrm{F}}^{\mathrm{scaff}} + 0.21\,\mathrm{wV_{bur}} \cdot \delta_{\mathrm{F}}^{\mathrm{scaff}}$	0.15	0.80
	24	$9.50\,\mathrm{w}B_5^{\mathrm{sub}} + 0.19\,\delta_{\mathrm{C}}^{\mathrm{ipso}} - 0.07\,\mathrm{w}B_5^{\mathrm{sub}} \cdot \delta_{\mathrm{C}}^{\mathrm{ipso}}$	0.48	0.32
	25	$8.48\,\mathrm{w}B_5^{\mathrm{grp}} + 0.33\,\delta_{\mathrm{C}}^{\mathrm{ipso}} - 0.06\,\mathrm{w}B_5^{\mathrm{grp}} \cdot \delta_{\mathrm{C}}^{\mathrm{ipso}}$	**0.93**	2.5×10^{-3}
	26	$-11.9\,\mathrm{w}B_5^{\mathrm{grp}} - 0.37\,\delta_{\mathrm{C}}^{\mathrm{sub}} + 0.08\,\mathrm{w}B_5^{\mathrm{grp}} \cdot \delta_{\mathrm{C}}^{\mathrm{sub}}$	**0.91**	4.6×10^{-3}
all *ortho* (17)	27	$-0.34\,\mathrm{w}B_5^{\mathrm{grp}} + 0.01\,\delta_{\mathrm{C}}^{\mathrm{ipso}}$	0.23	0.18
	28	$7.29\,\mathrm{w}B_5^{\mathrm{grp}} + 0.29\,\delta_{\mathrm{C}}^{\mathrm{ipso}} - 0.06\,\mathrm{w}B_5^{\mathrm{grp}} \cdot \delta_{\mathrm{C}}^{\mathrm{ipso}}$	0.65	4.4×10^{-3}
	29	$-0.31\,\mathrm{w}B_5^{\mathrm{grp}} - 0.0004\,\delta_{\mathrm{F}}^{\mathrm{scaff}}$	0.18	0.25
	30	$40.4\,\mathrm{w}B_5^{\mathrm{grp}} - 1.69\,\delta_{\mathrm{F}}^{\mathrm{scaff}} + 0.38\,\mathrm{w}B_5^{\mathrm{grp}} \cdot \delta_{\mathrm{F}}^{\mathrm{scaff}}$	0.21	0.37
	31	$0.03\,\mathrm{wV_{bur}} + 0.06\,\delta_{\mathrm{C}}^{\mathrm{ipso}}$	0.03	0.83
	32	$0.77\,\mathrm{wV_{bur}} + 0.25\,\delta_{\mathrm{C}}^{\mathrm{ipso}} - 0.005\,\mathrm{wV_{bur}} \cdot \delta_{\mathrm{C}}^{\mathrm{ipso}}$	0.06	0.86
	33	$0.04\,\mathrm{wV_{bur}} + 0.001\,\delta_{\mathrm{F}}^{\mathrm{scaff}}$	0.03	0.79
	34	$-12.2\,\mathrm{wV_{bur}} + 5.00\,\delta_{\mathrm{F}}^{\mathrm{scaff}} - 0.11\,\mathrm{wV_{bur}} \cdot \delta_{\mathrm{F}}^{\mathrm{scaff}}$	0.06	0.85

Table 3.9: Results of the linear regression of $\log(s)$ on the descriptors discussed in the text (intercept coefficients omitted for clarity). Coefficients of determination (R^2) and significance F are reported for each analysis and give an indication of the goodness-of-fit. Regressions performed with MATLAB. Table 3.10 reports a summary of the newly defined descriptors.

Descriptor	Meaning
$\mathrm{w}L^{\mathrm{sub}}$	Substituent weighted Sterimol parameter: maximum length along the main axis
$\mathrm{w}B_1^{\mathrm{sub}}$	Substituent weighted Sterimol parameter: minimum width along the axis perpendicular to main axis
$\mathrm{w}B_5^{\mathrm{sub}}$	Substituent weighted Sterimol parameter: maximum width along the axis perpendicular to main axis
$\mathrm{w}B_5^{\mathrm{grp}}$	Weighted Sterimol parameter for the whole Ar′ group: maximum width along the axis perpendicular to main axis
$\mathrm{wV_{bur}}$	Weighted percent buried volume
$\delta_{\mathrm{C}}^{\mathrm{ipso}}$	^{13}C NMR chemical shift of the carbon atom, within the Ar′ group, which is *ipso* to Bi
$\delta_{\mathrm{C}}^{\mathrm{sub}}$	^{13}C NMR chemical shift of the carbon atom, within the Ar′ group, which is *ipso* to the *ortho* substituent.
$\delta_{\mathrm{F}}^{\mathrm{scaff}}$	^{19}F NMR chemical shift of the $\mathrm{Ar^F}$ groups

Table 3.10: A summary of the descriptors defined in this Section.

same meaning for mono-substituted aromatic rings, however the second set allows parametrisation of any ligand of bismuth and thus inclusion in the treatment also of heterocyclic rings with variable ring sizes and aliphatic ligands.

This approach has some limitations: a significant variation across the dataset is observable only for $\mathrm{w}B_5^{\mathrm{grp}}$, which represents the maximum width of the aromatic ring along the axis perpendicular to the primary axis, *i.e.* the Bi–C bond; $\mathrm{w}B_1^{\mathrm{grp}}$ describes the minimum width along the same axis which in this case corresponds to half the thickness of the aromatic ring, *i.e.* half the atomic radius of the biggest atom laying in the aromatic plane; finally $\mathrm{w}L^{\mathrm{grp}}$ is in this case the length of the aromatic ring along the primary bond, which realistically does not have any influence on the description of the steric effect of an *ortho* substituent. Therefore only $\mathrm{w}B_5^{\mathrm{grp}}$ will be taken into account.

Neither $\mathrm{w}B_5^{\mathrm{sub}}$ or $\mathrm{w}B_5^{\mathrm{grp}}$ on their own gave any good correlation with the observed selectivities (entries 12 and 14, respectively). The weighted percent buried volume ($\mathrm{wV_{bur}}$), calculated as discussed in Section 3.2.2, did not provide any good correlation either (entry 15). This suggested that the observed selectivities are not a simple function of steric hindrance. When the three substituent-related Sterimol parameters were considered at the same time (entry 13), an improvement in the correlation was observed, with an $R^2 = 0.47$, however this is probably due to overfitting, *i.e.* the inclusion in the regression analysis of too many variables (3) given the size of the dataset (10).

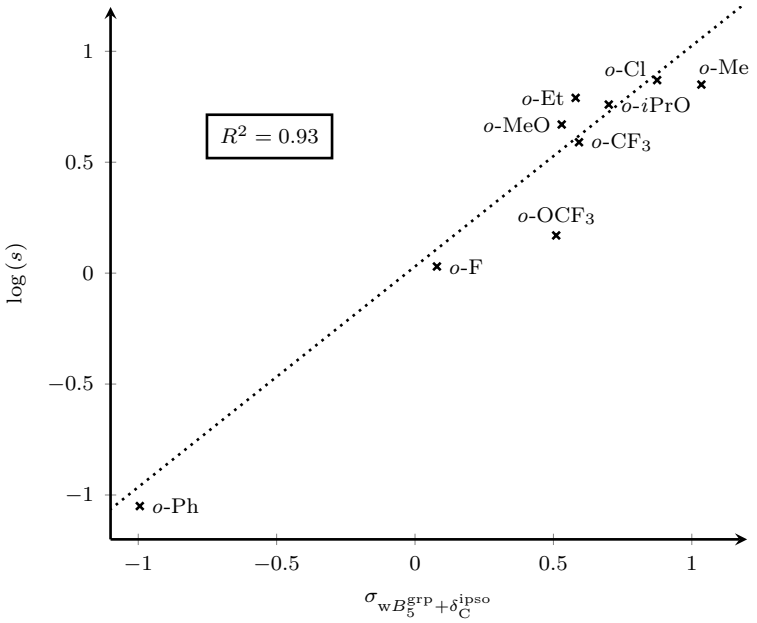

Figure 3.11: In order to account for electronics and sterics at the same time a new parameter was calculated, $\sigma_{\mathrm{w}B_5^{\mathrm{grp}}+\delta_{\mathrm{C}}^{\mathrm{ipso}}}$, which is defined as per Equation 3.3.

Due to to the lack of better descriptors for electronics, the ^{13}C chemical shift of the carbon atom of the Ar′ group connected to bismuth ($\delta_{\mathrm{C}}^{\mathrm{ipso}}$) and the ^{19}F chemical shift of the three *p*-fluorophenyl groups ($\delta_{\mathrm{F}}^{\mathrm{scaff}}$) were employed (entries 16 and 17, respectively). Neither of them individually was able to model the selectivity, so they were combined with the descriptors for sterics discussed above (entries 18–21). Unfortunately, no combination of $\mathrm{wV_{bur}}$ and $\mathrm{w}B_5^{\mathrm{grp}}$ with the two sets of chemical shifts gave any correlation.

Considering the limited size of the dataset, inclusion of too many degrees of freedom was undesirable, with an empirical threshold set to 2. However, cross-factors derived by the multiplication of the first variable by the second would not exceed this threshold. A first positive hit was obtained by including the $\mathrm{wV_{bur}} \cdot \delta_{\mathrm{C}}^{\mathrm{ipso}}$ factor (entry 22, $R^2 = 0.62$). A similar regression with the fluorine chemical shift instead of the carbon did not show the same promising result (entry 23). The best fit was obtained with $\mathrm{w}B_5^{\mathrm{grp}}$, $\delta_{\mathrm{C}}^{\mathrm{ipso}}$ and the relative cross-term (entry 25, $R^2 = 0.93$, significance $F = 0.0025$). The newly derived parameter results defined as follows:

$$\sigma_{\mathrm{w}B_5^{\mathrm{grp}}+\delta_{\mathrm{C}}^{\mathrm{ipso}}} = 8.48\,\mathrm{w}B_5^{\mathrm{grp}} + 0.33\,\delta_{\mathrm{C}}^{\mathrm{ipso}} - 0.06\,\mathrm{w}B_5^{\mathrm{grp}} \cdot \delta_{\mathrm{C}}^{\mathrm{ipso}} - 43.42 \qquad (3.3)$$

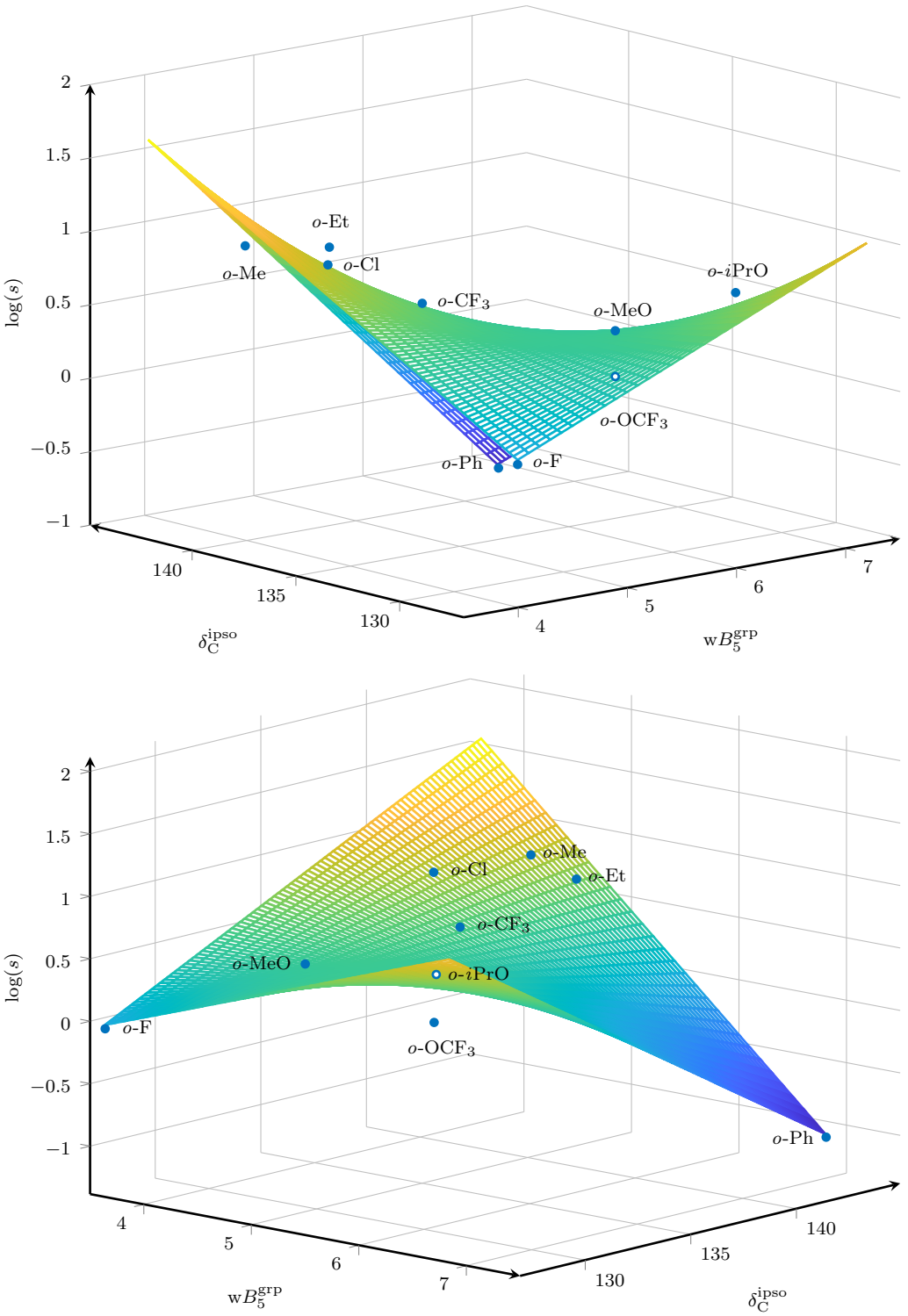

Figure 3.12: Two different views of the curve fitting the 3D scatter resulting by plotting $\log(s)$ against both $\mathrm{w}B_5^{\mathrm{grp}}$ and the ^{13}C NMR chemical shift of the carbon atom of the unique group connected to bismuth ($\delta_{\mathrm{C}}^{\mathrm{ipso}}$): $\log(s) = 8.48\,\mathrm{w}B_5^{\mathrm{grp}} + 0.33\,\delta_{\mathrm{C}}^{\mathrm{ipso}} - 0.06\,\mathrm{w}B_5^{\mathrm{grp}} \cdot \delta_{\mathrm{C}}^{\mathrm{ipso}}$. A saddle shape may be noticed.

It is worth noting that both the coefficients of $\delta_{\mathrm{C}}^{\mathrm{ipso}}$ and for the cross factor are one and two orders of magnitude smaller than the coefficient of $\mathrm{w}B_5^{\mathrm{grp}}$, respectively. However, this is offset by the large chemical shifts values (133.7–163.3 ppm). The plot of $\log(s)$ against $\sigma_{\mathrm{w}B_5^{\mathrm{grp}}+\delta_{\mathrm{C}}^{\mathrm{ipso}}}$ is reported in Fig. 3.11 and allows us to assess the goodness-of-fit: once again, the outlier (corresponding to the *o*-Ph group) is expected to have a significant impact of the high value of R^2, so interpretation of this result must be done carefully. Two different views of the 3D scatter of the logarithm of the selectivity against both $\mathrm{w}B_5^{\mathrm{grp}}$ and $\delta_{\mathrm{C}}^{\mathrm{ipso}}$ are presented in Fig. 3.12. The calculated model is plotted as a surface and helps the interpretation.

Electronics dominates this model: optimal selectivity is achieved with electron-neutral and -positive groups, regardless of their steric hindrance; alkoxy groups, that are electron donating as far as the carbon *ipso* to bismuth is concerned, are at least as sterically hindered as the ethyl group, which increases their selectivity by compensating for the unfavourable electronics; the *o*-fluorophenyl group, which has the smallest $\mathrm{w}B_5^{\mathrm{grp}}$ value across this dataset also shows the second poorest selectivity; finally the *o*-biphenyl group, the one with the highest calculated steric hindrance, almost did not transfer. Overall, the 'high selectivity area' of the plot is delimited by *o*-Cl and *o*-*i*PrO groups, as far as sterics is concerned, and by the *o*-MeO group as the lower threshold for the chemical shift descriptor.

The chemical shift of the carbon *ipso* to the substituent was trialled as a descriptor, too (entry 26 of Table 3.9). In fact, a simpler correlation between the electron-withdrawing nature of the substituent and the chemical shift of the carbon to which it is connected is present, so the ^{13}C chemical shift can be used as a descriptor for electronics with more confidence. Gratifyingly, an excellent correlation ($R^2 = 0.91$, Fig. 3.14) was found when this descriptor was employed in conjunction with the previously used steric descriptor $\mathrm{w}B_5^{\mathrm{grp}}$. Moreover, the 3D scatter was fit with a surface that retained a very strong resemblance (Fig. 3.13) with the one which used the ^{13}C shift of the carbon *ipso* to bismuth (Fig. 3.12). Therefore, even though the goodnesses-of-fit is slightly worse than with the previous descriptor, this descriptor may overall be better.

Criticism of the nature of $\mathrm{w}B_5^{\mathrm{grp}}$ may be brought forward: in fact, this only describes the length of the substituent along the axis perpendicular to the main axis, however, the branching of that substituent is here neglected, so this descriptor alone should not be able to differentiate between the steric hindrance of an *ortho*-ethyl substituent and that of an *ortho*-isopropyl. Thus $\mathrm{w}B_1^{\mathrm{sub}}$ was included in all the relevant regressions to account for this but did not improve the fit in any case. Since this deficiency does not affect the fits, branching may actually be not relevant.

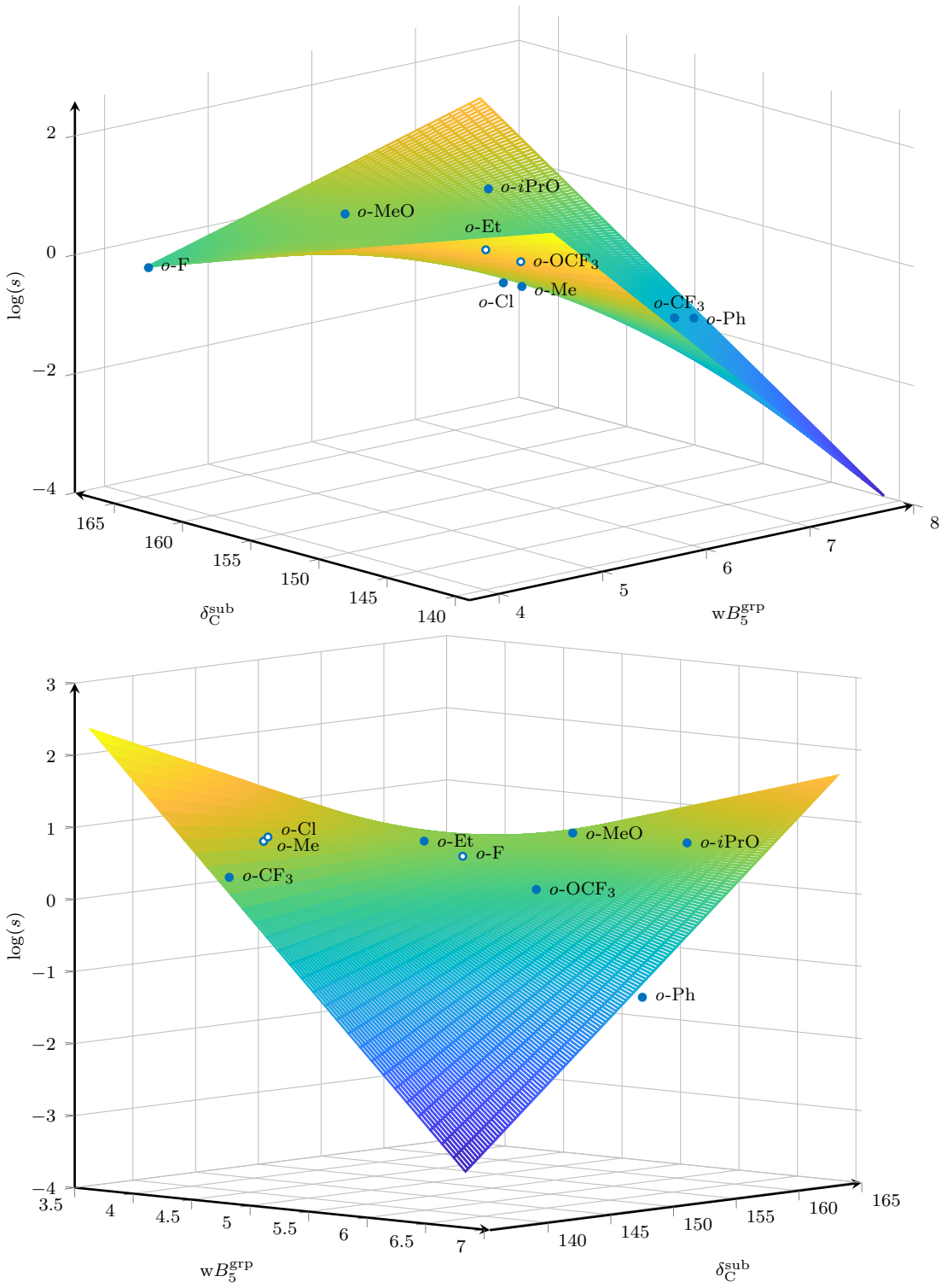

Figure 3.13: Two different views of the curve fitting the 3D scatter resulting by plotting $\log(s)$ against both $\mathrm{w}B_5^{\mathrm{grp}}$ and the ^{13}C NMR chemical shift of the carbon atom *ipso* to the substituent of the unique group connected to bismuth ($\delta_{\mathrm{C}}^{\mathrm{sub}}$): $\log(s) = -11.94\,\mathrm{w}B_5^{\mathrm{grp}} - 0.37\,\delta_{\mathrm{C}}^{\mathrm{sub}} + 0.08\,\mathrm{w}B_5^{\mathrm{grp}} \cdot \delta_{\mathrm{C}}^{\mathrm{sub}}$. The shape of the curve resembles that depicted in Fig. 3.12.

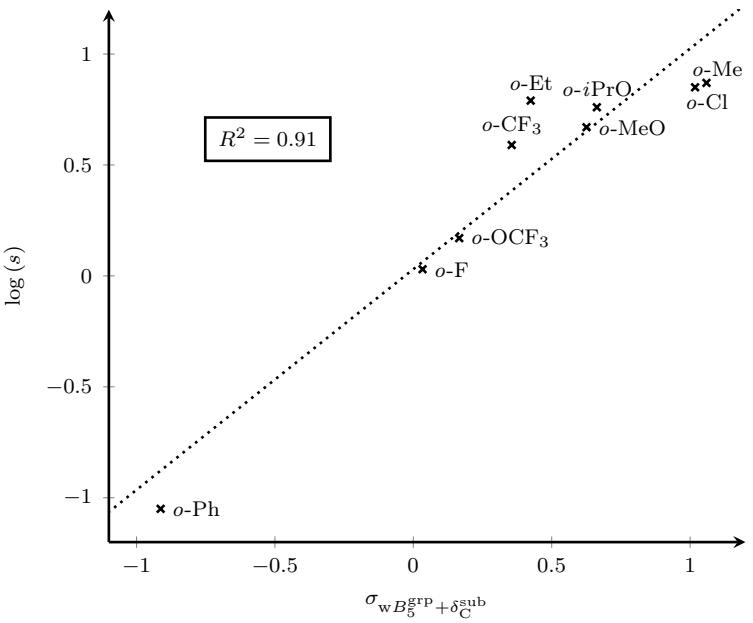

Figure 3.14: The NMR chemical shift of the carbon *ipso* to the substituent retains a predictive power similar to the chemical shift of the carbon *ipso* to bismuth, when used in combination with wB_5^{grp} as the steric descriptor.

Finally, an attempt was made to model the selectivity of poly-substituted Ar′ groups bearing at least one *ortho* substituent. In this case Sterimol parameters for the substituents had to be excluded from the pool of potential descriptors, due to their intrinsic non-additivity. Similarly, only the ^{13}C NMR chemical shift of the carbon connected to bismuth (δ_C^{ipso}) could be considered because otherwise one value for each substituent should have been employed. Although an average of the shifts of the carbon atoms in the 2- and 6-positions could have been employed, that would not have taken into account a third potential substituent. Therefore this would have not been a general approach and, for these reasons, was not pursued. Only wB_5^{grp}, wV_{bur}, δ_C^{ipso} and δ_F^{scaff} survived these considerations. Unfortunately, no good fit could be obtained with these descriptors (entries 27–34 of Table 3.9): similarly to mono-substituted cases, the best result was achieved with wB_5^{grp}, δ_C^{ipso} and their cross-term but in this case R^2 only reached 0.65. Once more, this highlights the need for a better descriptors, especially for electronics.

For mono-*ortho*-substituted groups, the combination of the wB_5^{grp} and δ_C^{ipso} constants discussed above afford a model that reliably interprets the reaction selectivity. The δ_C^{ipso} constant requires isolation of the bismuthonium salts and successive characterisation by ^{13}C NMR spectroscopy, both of which would not

be desirable in the one-pot arylation approach. Therefore, at the moment, this model allows an interpretation of the observed selectivity, rather than a prediction. To maximise this predictive power it would be extremely valuable if one of the carbon chemical shifts of the corresponding boronic acid could be used instead: this way one could predict the arylation selectivity before even synthesising the desired bismuthonium. A further achievement would be to use chemical shift predicted *via* commercial software such as ChemDraw or MestReNova.

3.3.2 Arylation of dimethyl-2-fluoromalonate

A strong substrate dependance has been observed in hypervalent iodine chemistry, so we wanted to explore the selectivity of the arylation of other substrates and compare them with that of naphthol. Dimethyl-2-fluoromalonate was chosen for the reasons discussed earlier. Similar analyses to those performed for the first substrate were performed, however, due to the poor results obtained and essentially to the lack of any significant correlation with the descriptors employed so far, only a qualitative discussion will be carried out, with reference again to Table 3.8.

The dynamic range of the selectivity values for the malonate is notably narrower across all the dataset. The highest value was achieved with the *p*-(trimethylsilyl)phenyl group (3.27). This is surprising, since the substituent is only slightly electron donating by resonance and does not cause any steric hindrance, since it is in the 4-position, and therefore would normally be considered rather innocent. While high selectivity was observed for the arylation of naphthol, the effect is enhanced for malonate. The *p*-cyanophenyl group does not share the same electronic properties but showed the second highest selectivity (3.03). The *m*-tolyl and *m*-xylenyl groups both gave rather high selectivities (2.16 and 2.27), which are higher than in the naphthol reaction (1.85 and 2.27, respectively).

As far as steric hindrance is concerned, *o*-tolyl was again a relatively good performer (1.74). Increase in the length of the aliphatic chain reduces the selectivity (Et = 1.28), similarly to what was observed for naphthol. The presence of a second methyl group in the 6-position does not have any effect, whereas with naphthol the di-substituted group had the highest selectivity ever observed (35.4). A clear cut anti-*ortho* effect[197] cannot be identified, although a decrease in selectivity seems to arise with increase steric hindrance: alkoxy substituents in the 2-position caused a drop in selectivity, which is always less than or equal to 1 and the effect is more marked for bulkier groups; alkyl substituents cause the same effect (Me $\simeq$ 2,6-diMe

$>$ Et $\gg$ Mes $\simeq$ TRIP), but the dynamic range of this subset is limited in any case ($0.87 < s < 1.74$). An explanation for the drop in selectivity from that observed for 2,6-dimethylphenyl to that of mesityl is forthcoming, especially given that phenyl is more selective than *p*-tolyl. Finally, the data collection would be concluded by considering also the reactions with heteroaromatic groups, which in this initial screening were excluded because of the poor behaviour showed with naphthol. In general it would be desirable to acquire more data points to allow more robust regression analyses.

3.4 Arylation of other substrates

Nucleophiles other than the naphthol and malonate derivatives discussed before were tested in order to identify substrates for future selectivity studies. Schemes 3.1–3.5 and Table 3.11 contain a selective list of examples investigated. It should be stressed that the focus was not to build a comprehensive scope table, so in most cases the bismuthonium compound employed was the homoleptic $[Ar^F_4Bi][BF_4]$ **5a**.

The arylation was demonstrated to be quite robust with regard to β-naphthol derivatives (Scheme 3.1), showing no particular change in reactivity when going from electron-rich to electron-poor examples: in all cases quantitative conversion to the desired product was observed, which could be isolated upon purification by preparative TLC. Among the naphthol series, the tolerance for a boronic acid functionality in the 6-position (**17g**) is particularly striking.

With 2-naphthols the observed product is always the 1-arylation isomer, so the reaction was attempted with derivatives with that position blocked (BINOL and 1-bromo-2-naphthol): in both cases no ligand coupling occurred. Instead, as determined by ^{19}F NMR spectroscopy, meta-stable intermediates formed as the result of the nucleophilic attack by the naphtholates on bismuth. These then decomposed forming Ar^F_3Bi and fluorobenzene, plus several additional unidentified species. With 1-naphthol the arylation afforded two products that proved inseparable by chromatography. Finally, umbelliferone was tested as a 2-naphthol analogue: one major product was detected by ^{19}F NMR spectroscopy but could not be isolated due to its low solubility, which prevented its recovery from silica.

Phenols were then explored (Table 3.11): differently from naphthols, electron-poor examples were not well tolerated, with *p*-bromo- and *p*-carbomethoxy- examples (entries 6 and 5, respectively) undergoing slow arylation over 9 d. Even more electron-poor phenols, such as those bearing *p*-cyano- and *p*-nitro- substituents (entries 4

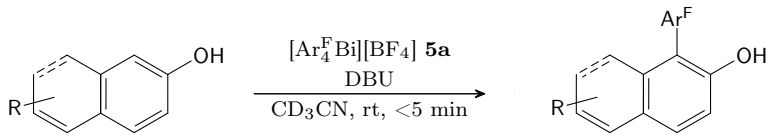

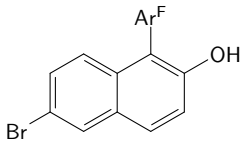

17a
91%

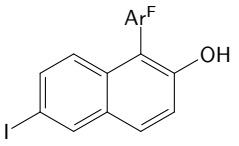

17b
88%

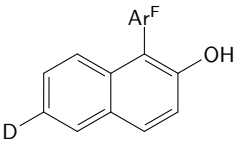

17c
89%

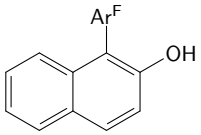

17d
96%

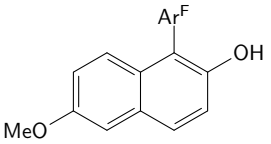

17e
95%

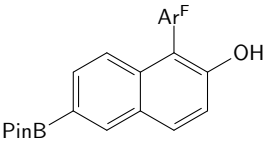

17f
82%

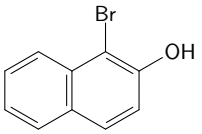

0%[a]

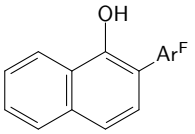

0%[b]

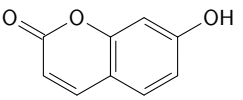

0%[c]

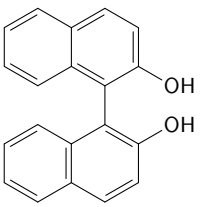

0%[a]

Scheme 3.1: Naphthols were tested in the bismuth-mediated arylation. 2-naphthols undergo arylation with full regioselectivity for the 1-position. [a]If that position is blocked, ligand coupling does not occur (no Ar$^F_3$Bi is formed) and decomposition of the Bi–OAr intermediate is observed only upon heating. [b]Two products formed, that could not be separated chromatographically. [c]One product detected by ^{19}F NMR spectroscopy but isolation could not be achieved. Conditions: 1.0 equiv of bismuthonium and substrate, 1.5 equiv of DBU; reactions performed in NMR tubes and monitored by ^{19}F NMR spectroscopy; yields are for isolated products.

and 3), did not react at all. The last two phenols, together with perfluorophenol (entry 2), were tested with the aim of isolating the nucleophilic attack intermediate observed by Barton.[98] This, however, was never achieved.

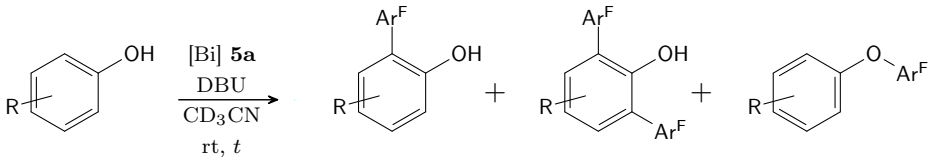

1	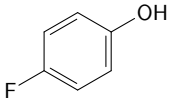	24 h	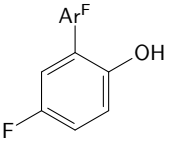 **6a** 15% (18%)	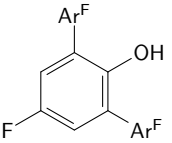 **6b** 7% (10%)	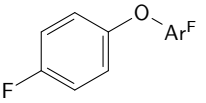 **18c** (10%)
2	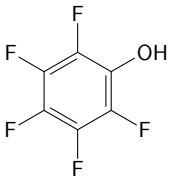	9 d	No reaction observed.		
3	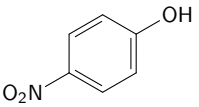	9 d	No reaction observed.[98]		
4	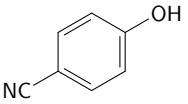	9 d	No reaction observed.		
5	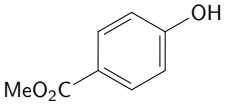 5 equiv	9 d	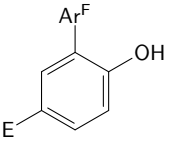 (18%)	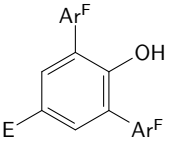 (2.7%)	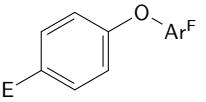 (2.3%)
6	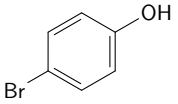 5 equiv	9 d	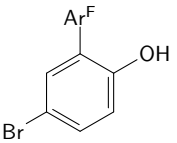 (38%)	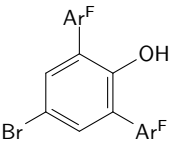 (4.5%)	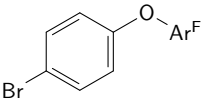 **18b** (9.4%)
7	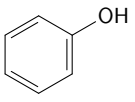 5 equiv	48 h	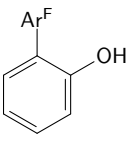 **19a** 37% (42%)	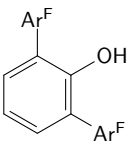 **19b** 7% (7.7%)	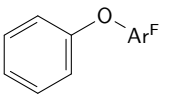 **18a** (4.2%)

8	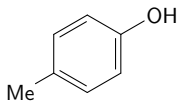 5 equiv	6 h	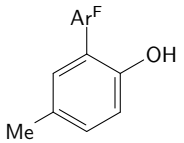 (49%)	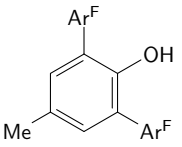 (11%)	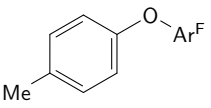 (2.8%)
9	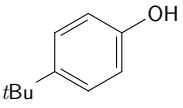 5 equiv	6 h	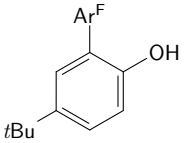 (49%)	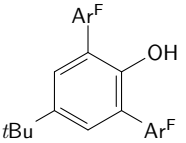 (13%)	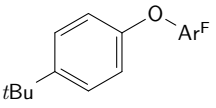 (1.0%)
10	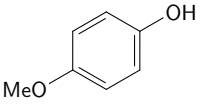 5 equiv	<1 h	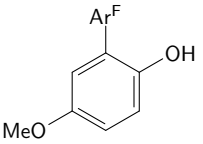 (44%)	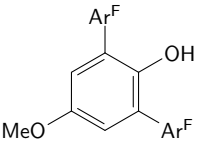 **20** 8% (16%)	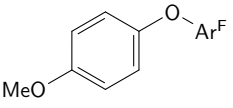 **18f** (0%)
11	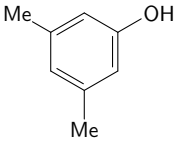	<1 h	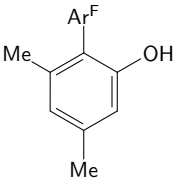 **21a** 10% (20%)	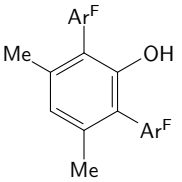 **21b** 33% (40%)	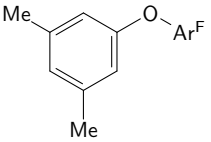 (0%)
12	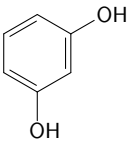	5 min	Di-, tri-, tetra-arylation detected by HRMS.		
13	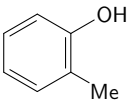	5 min	Ill-defined mixture of unidentified species.		

Table 3.11: Conditions: 1.0 equiv of $[Ar^F_4Bi][BF_4]$ **5a** and substrate, 1.5 equiv of DBU; reactions performed in NMR tubes and monitored by ^{19}F NMR spectroscopy; NMR conversions are reported in parentheses; yields are for isolated products; E = CO_2Me. Reported time is that required to fully consume the bismuthonium **5a**.

Due to the greater availability of phenols compared to naphthols, the former would be the ideal substrates of this methodology so it was deemed necessary to attempt an optimisation of their arylation reaction, since under the standard conditions a considerable amount of di- and *O*-arylation was observed (see for

example entries 6 and 11). Firstly, authentic samples of mixed diaryl ethers (Ar^F–O–Ar′, **18a**–**f**) were prepared, so as to facilitate the identification of those products during the arylation. Secondly, the arylation reaction was performed using a 5-fold excess of phenol and base relative to the bismuthonium, so as to disfavour di-arylation, which however could never be entirely suppressed. Similarly to the early tests presented in Scheme 2.4, the overall yield is mediocre but could be slightly improved from 38% to 50–60% for electron-neutral/rich examples. Moreover, differently from before, in all these cases the bismuth species was fully consumed. It is assumed that competing decomposition pathways, such as by reaction with DBU, or formation of undetectable amounts of several over-arylation products may be held responsible for the partial yields. Attempts to impede di-arylation were made also by blocking one of the two *ortho* positions (entry 13 of Table 3.11) but to no avail: over-arylation remained the major outcome. Moreover, the crude mixture resulted too complex to be successfully purified by chromatography.

Blockage of both *ortho* positions provided informative results (Scheme 3.2). With 2,6-dimethylphenol (R = Me, R′ = H) a single species formed quantitatively within minutes, as determined by ^{19}F NMR spectroscopy. The compound was isolated and identified as the *meta*-arylation product **22**. This is thought to form upon migration of the 4-fluorophenyl group to the *meta* position, followed by re-aromatisation of the resulting dienone. Gratifyingly, repetition of this reaction with mesitol (R = R′ = Me) as the substrate allowed the isolation of the hypothesised de-aromatised intermediate **23**. Similar de-aromatised species were reported by Barton,[134] however, the successive migration is unprecedented. This process is currently undergoing extensive investigation by another member of the Ball group, since it enables access to *meta*-arylated phenols *via* a unique C–H activation strategy.

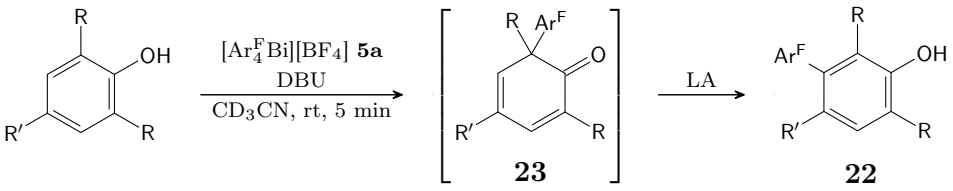

Scheme 3.2: Blocking both *ortho* positions of phenol provided the unexpected *meta*-arylated product **22** (R = Me, R′ = H, 69%). This is suggested to form through rearrangement of the de-aromatised intermediated shown, which was successfully isolated as compound **23** in 48% yield (R = R′ = Me). With R = Ph, R′ = H, a complex and inseparable mixture was obtained. Conditions: 1 equiv of every component. Reactions performed in NMR tubes and monitored by ^{19}F NMR spectroscopy.

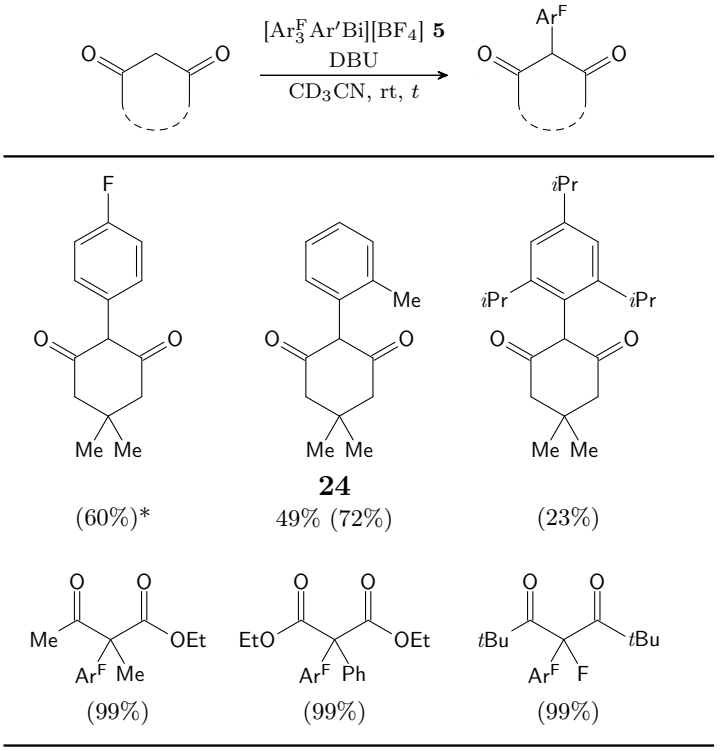

Scheme 3.3: Both cyclic and acyclic diketones are capable substrates for the bismuth-mediated arylation. Only the dimedone derivative **24** was isolated upon reaction with [Ar$_3^F$(*o*-tolyl)Bi][BF$_4$] **5v**. The other substrates were tested with [Ar$_4^F$Bi][BF$_4$] **5a**. NMR yields are reported in brackets, as measured by ^{19}F NMR spectroscopy. Conditions: 1 equiv of every component, t = 3–24 h for dimedone, $t < 5$ min for the other diketones. *Di-arylated product detected (20%).

Diketones were then explored (Scheme 3.3), starting from cyclic ones and in particular dimedone. As expected,[87] this gave mixtures of mono- and di-arylation products (3:1). Interestingly, over-arylation could be suppressed by employing a bismuthonium containing an *ortho*-substituted group. This group is transferred selectively and prevents a second arylation, presumably due to the increased steric congestion around the reactive site of the diketone. Selective transfer of the hindered group is a significant additional point, as this could not be achieved with naphthols and non-cyclic diketones. Moreover, this selectivity holds true also for extremely hindered groups such as 2,4,6-tri-isopropylphenyl, although the NMR yield dropped significantly (23%). Methods for the functionalisation of diketones with sterically hindered aromatic rings are particularly desirable, since numerous agrochemicals contain this moiety.[344] Another member of the Ball group is currently

exploring bismuth as an efficient arylating agent for cyclic diketones. Malonates and acetylacetone derivatives undergo arylation promptly and, if the activated position is occupied by a substituent, yield only one product, as described in the bottom three examples of Scheme 3.3. *O*-Arylation has not been observed for any diketones.

Nitrogen- and sulfur-based nucleophiles were briefly tested. Indole and indazole smoothly underwent arylation (Scheme 3.4) but two regioisomers were detected in both cases. For indazole separation and characterisation of the two species was achieved and showed a slight preference for 1-arylation over 2-arylation (compounds **25a** and **25b**, respectively). 4-Fluroaniline was tested as well (Scheme 3.5), but only decomposition products could be observed after 24 h. These are likely to derive from the interaction of DBU with the bismuthonium, as discussed in Section 2.3.5.

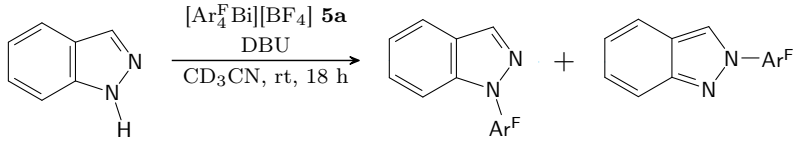

25a **25b**

Scheme 3.4: Arylation of indazole with bismuthonium **5a** gave a 63:37 mixture of 1- and 2-arylated products, **25a** and **25b**, as determined by ^{19}F NMR spectroscopy. Indole (not shown) gave a mixture of two isomers that could not be separated effectively.

Finally, thiol analogues of phenol were tested (Scheme 3.5) but none of them yielded arylation products, instead oxidation to the corresponding disulfides was suggested as a possible side-reaction with these substrates. This pathway may be enabled either by the aerobic conditions employed for this chemistry or by the oxidising nature of bismuth(V), as reported by Barton.[87]

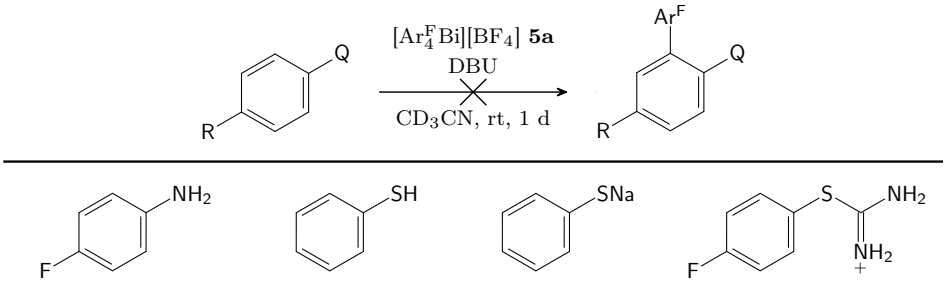

Scheme 3.5: Additional substrates tested in the arylation with bismuthonium **5a**. None of them provided any arylation products, as determined by ^{1}H and ^{19}F NMR spectroscopies and HRMS. Conditions: 1 equiv of **5a**, 1 equiv of DBU for the first two examples, 2 equiv of DBU for the isothiouronium (3,5-dinitrobenzoate counterion omitted for clarity).

3.5 Preliminary mechanistic investigations

Section 1.3.1 presented a list of summarised concepts extrapolated from the literature regarding bismuth-mediated arylation and in particular it was pointed out that the 'arylation reaction' may in reality be constituted of at least five elementary steps:

1. Enol deprotonation equilibrium;
2. Nucleophilic attack of the resulting enolate, which forms a Bi–O complex;
3. Berry pseudorotation;
4. Axial-equatorial ligand coupling;
5. Re-aromatisation.

Detailed mechanistic investigations are, however, absent in the literature, for example there is no indication regarding which one of these steps is rate-determining or what is the observed overall molecularity of the arylation process. In order to perform some mechanistic investigations, a suitable substrate had to be identified. The high rates at which naphthols and malonates undergo arylation makes studies of reaction kinetics by NMR spectroscopy impractical. We therefore focused on phenols, which were shown in Table 3.11 to undergo arylation in hours, rather than seconds.

Initially, the arylation of 4-fluorophenol with the homoleptic bismuthonium **5a** was studied by ^{19}F NMR spectroscopy. The previous Section discussed the use of a five-fold excess of phenol and base to prevent di-arylation. Those conditions were also used in the coming experiments. The following hypothesis was tested: that the rate-determining step of the arylation is the nucleophilic attack of the phenolate on bismuth and that, consequently, the reaction follows bimolecular kinetics.

A shown in Fig. 3.15, the reaction exhibits net second-order kinetics, with a first order dependence on both $[Ar^F_4Bi][BF_4]$ and phenol. This holds true even though the reaction was performed under pseudo-first order conditions in phenol: if the reaction were overall first order it could not have been modelled as a second order process. A dependance of the rate on the concentration of phenol and bismuthonium is consistent with the rate-determining step being the nucleophilic attack.

To investigate the effects of phenol electronics on the rate of the arylation, an absolute rates study was performed with different phenols and limiting $[Ar^F_4Bi][BF_4]$ **5a**. A Hammett plot of $\log\left(\frac{k^R_{eff}}{k^H_{eff}}\right)$, where k_{eff} are effective rate constants defined as $k^R_{eff} = k[R\text{-}C_6H_4\text{-}OH]$, against σ_p gives an excellent correlation (Fig. 3.16).

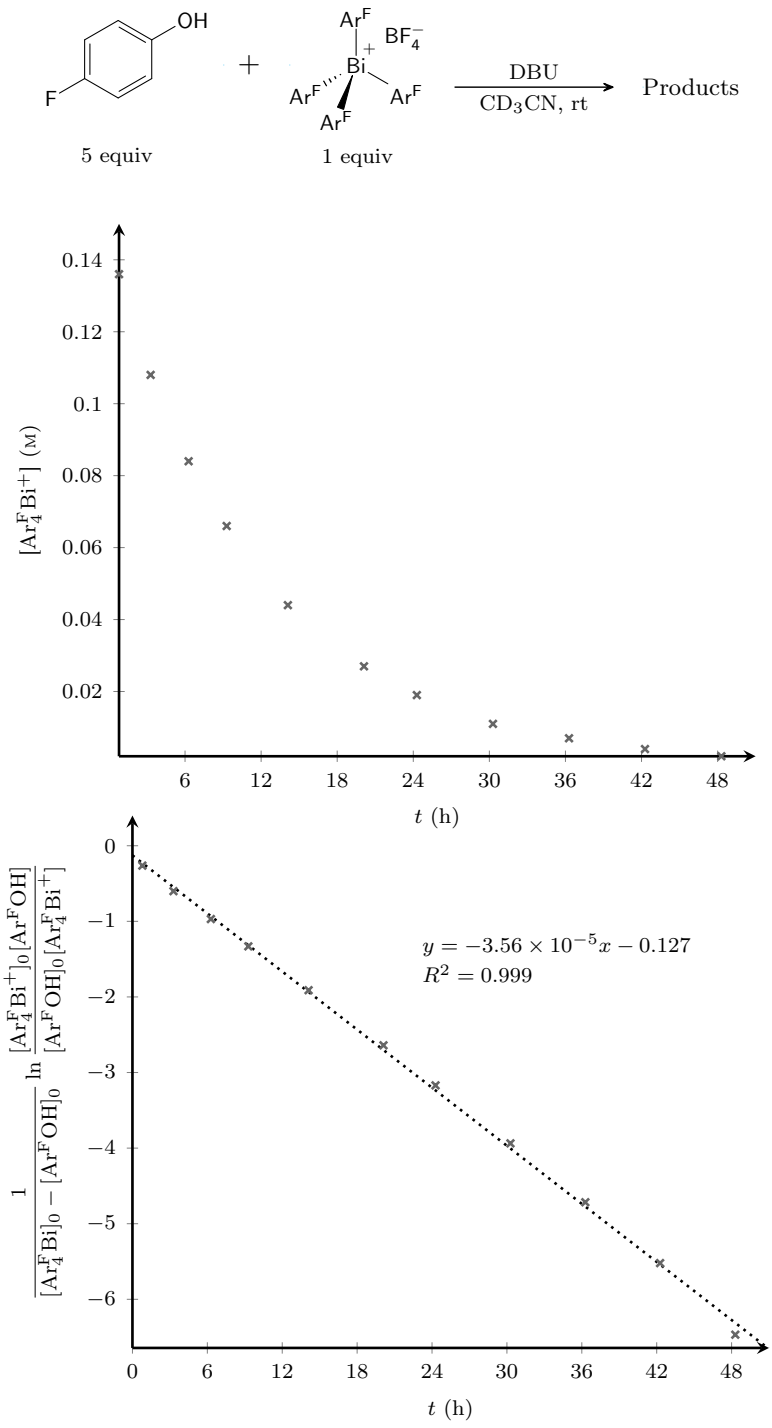

Figure 3.15: The arylation of 4-fluorophenol with $[Ar^F_4Bi][BF_4]$ is overall a second-order process ($k^F_{eff} = 3.56 \times 10^{-5}$ $M^{-1}s^{-1}$), with first-order dependance on the two components. Reaction performed in an NMR tube and monitored by ^{19}F NMR spectroscopy. Conditions: 0.500 mmol of 4-fluorophenol and DBU, 0.100 mmol of $[Ar^F_4Bi][BF_4]$ **5a** in 0.600 mL of CD_3CN.

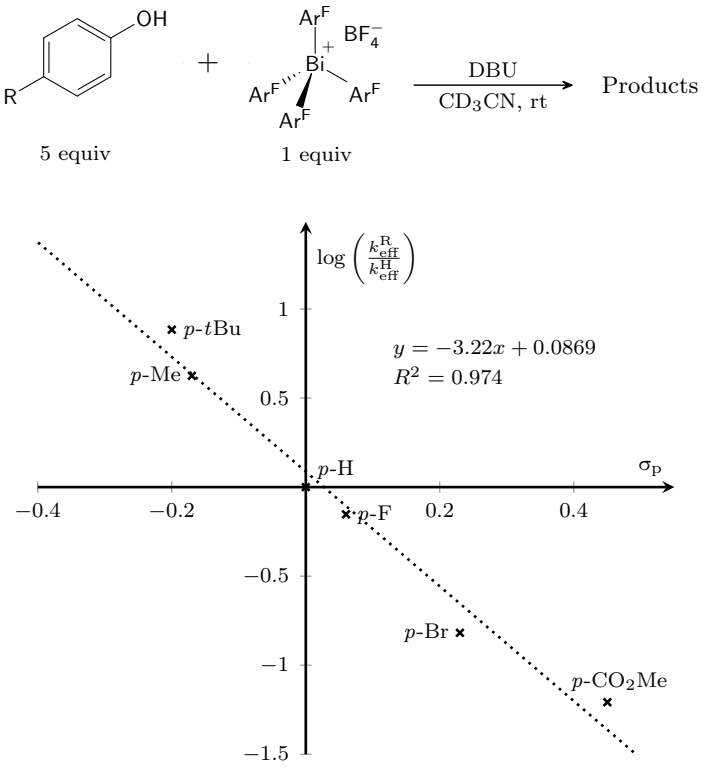

Figure 3.16: Hammett plot of the bismuth-mediated arylation of phenols. The existence of a correlation suggests the rate-determining step of the process involves the build-up of a positive charge. All reactions performed in NMR tubes and monitored by ^{19}F NMR spectroscopy by absolute rates. Conditions: 0.500 mmol of phenol and DBU, 0.100 mmol of $[Ar^F_4Bi][BF_4]$ **5a** in 0.600 mL of CD_3CN.

This further corroborates the hypothesis that phenol is involved in the rate-determining step. A strongly negative ρ (-3.22) indicates high degree of sensitivity towards the variation of the electronics of the phenol and the build-up of a positive charge in the transition state of the rate-determining step, which is consistent with the phenolate donating its electrons to establish a Bi–O bond.

The proposal that the nucleophilic attack is rate-determining is consistent with the fact that the complex resulting from the coordination of the substrate could not be detected by NMR spectroscopy. It has been noticed that the ^{19}F NMR bismuthonium peak moves from -107.0 ppm to -110.5 ppm as soon as a phenol and DBU are added (see also Fig. 2.11 for a similar phenomenon). When a considerable excess of those two reagents is used, as in the reactions just discussed, the peak intensity decreases over time and gives the plots above. Interestingly,

when the excess is small, the peak is observed to move back towards −107.0 ppm with the reaction progression. A similar but opposite behaviour has been described in Figs. 2.7–2.9 with regard to the decomposition of the bismuthonium when exposed to DBU, a process whose rate-determining step was demonstrated to involve a bimolecular transformation. The decomposition reaches completion in ca. 18 h. Moderately electron-poor phenols, such as *p*-bromophenol and methyl 4-hydroxybenzoate, underwent slow arylation over the course of 9 d, with the bismuthonium showing a significantly longer life span in comparison to the reaction in the absence of phenol.

A plausible explanation for these observations is presented in Scheme 3.6: DBU forms an adduct with the bismuthonium, whose chemical shift moves upfield to −110.5 ppm; the complexation of DBU is reversible but fast on the NMR scale, so the free bismuthonium and the adduct coalesce and one peak is detected; the $Ar^F_4Bi^+\cdots DBU$ adduct is then attacked by the phenolate in the rate-determining step, releasing the coordinated DBU; the effectively irreversible ligand coupling consumes phenolate, which is removed from the initial deprotonation equilibrium, which in turn irreversibly generates DBU–H^+; since the latter is less likely to form an adduct with the bismuthonium, at small excesses of DBU the concentration of such adduct decreases as the reaction proceeds; the position of the coalesced NMR peak moves with the variation of the relative concentrations of the components of the equilibrating reaction, *i.e.* the free bismuthonium and this adduct. Finally, the extended life span of the bismuthonium must depend on some kind of inactivation of DBU caused by the phenol. The most reasonable pathway is the deprotonation of the latter by the former and production of DBU–H^+, which would likely not form adducts with bismuth.

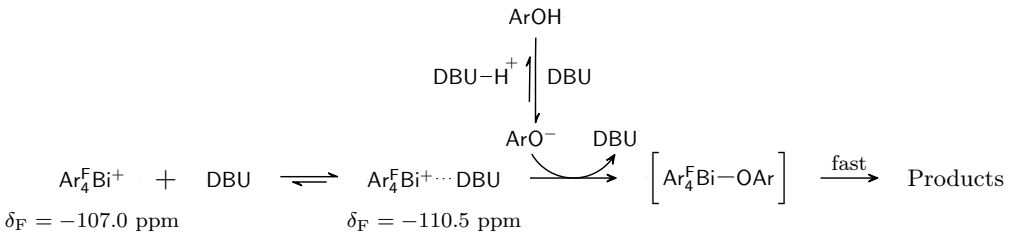

Scheme 3.6: DBU is suspected to form adducts with the bismuthonium, which causes the chemical shift of the bismuth species to move upfield. The adduct is proposed to break as a consequence of the nucleophilic attack of phenolate. With small excess of DBU the concentration of its adduct with Bi decreases over time, which is reflected by the drift of the bismuthonium chemical shift towards the initial value of −107.0 ppm.

The complex resulting from the nucleophilic attack then proceeds towards the ligand coupling step. The ligand coupling is the selectivity-determining step for both the regioselectivity (*O*- vs *C*-arylation) and the chemoselectivity (transfer of Ar′ vs Ar), since it is effectively irreversible due to the high kinetic barrier of the reverse reaction. The origin of the imperfect regioselectivity, in which *O*-arylation was observed for all phenols, is not yet clear. On the other hand naphthols and diketones were not observed to undergo *O*-arylation.

With reference to the chemoselectivity discussed in Section 3.3.1, it is clear that it is the consequence of several effects, whose separation and impact determination were not as straightforward as desired. From a synthetic perspective this methodology would be of limited use as it currently stands, since only five bismuthonium salts over the forty-four tested managed to transfer the unique group with a selectivity greater than 10. Separation of the two products by conventional chromatography is hard most of the times and has never been achieved in satisfactory purity for any of the examples discussed here. The last Chapter of this Thesis will discuss initial investigations into a true solution to the chemoselectivity challenges faced hitherto.

4

Tridentate ligands for bismuth

Given that heteroleptic tetra-arylbismuthonium salts undergo ligand coupling with little selectivity for transfer of the unique aryl group, and that this selectivity could not be reliably predicted, an alternative strategy was pursued. A brief survey of the literature showed that, for simpler triaryl bismuth species, similar issues have been addressed by linking together the 'spectator ligands', thus generating a bipodal structure. The nature of the linker varies, with essentially three classes of compounds (see Fig. 4.1):

- **I**, no bridging atom between the two spectator ligands, which are thus forming a biphenylene unit;[345,346]
- **II**, $CH_2N(alk)CH_2$ as a linker;[347]
- **III**, a single atom linker A, where A is CH_2, S, SO_2,[348] or $S(=O)NCF_3$.[349]

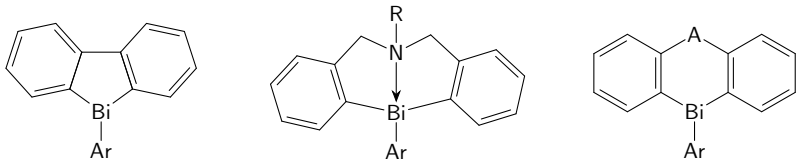

Figure 4.1: Bipodal complexes of bismuth known so far. Three different linkers are shown.

Fedorov and Finet studied the biphenylene system **I** in the arylation of phenols:[350] at first, a trigonal bipyramidal structure is formed from the coordination of the substrate (see Scheme 4.1). The authors suggested that the selective transfer of

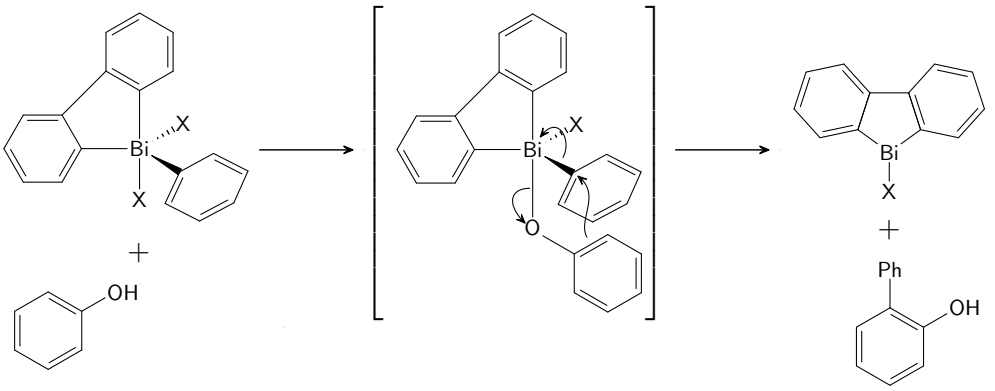

Scheme 4.1: During the arylation, the rigid biphenyl scaffold forces the exocyclic group to be equatorial thus favouring the coupling with the phenoxide ligand. Adapted from Fedorov and Finet.[350]

the exocyclic group is then achieved through an equatorial-axial ligand coupling between the phenoxide, which, due to its apicophilicity, lies in the axial plane, and the exocyclic group. In fact, the latter is now free to lie in the equatorial plane and rotate around its bond with Bi, while the biphenyl unit, the spectator ligand, is blocked in a rigid, and thus unfavourable, conformation across the equatorial and axial planes.[350] The same principle applies to the other classes of bismacycles.

These premises represented the basis of another project that was carried out and recently published by the Ball group, in which the authors established a convenient and modular methodology to transfer the exocyclic group to phenolic substrates, in a completely selective fashion (see Scheme 4.2).[318] This was achieved with the support of a sulfone-bridged bismacycle, onto which the exocyclic group was installed *via* transmetalation from a boronic acid. Both the transmetalation and the arylation steps were conducted under mild conditions, showing a broad tolerance to functional groups, both on the substrate and the transferred group.

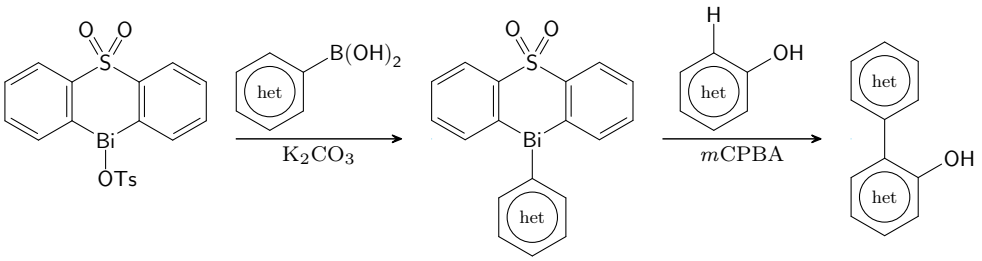

Scheme 4.2: The sulfone-linked scaffold allowed the construction of ca. 50 2-hydroxybiaryl compounds, *via* selective transfer of the exocyclic group. The latter can be introduced through a modular B-to-Bi transmetalation process.[318] het = heterocyclic.

Given the success of this concept when applied to the triaryl manifold, a transposition to the tetra-arylbismuthonium was planned. Bipodal ligands could be employed in the bismuthonium manifold and preliminary results within the group showed that they are capable of supporting the introduction of a fourth aryl group *via* the standard oxidation/transmetalation protocol discussed in the previous Chapter. However, despite the fact that they would represent an improvement over the non-linked system, this would not be a definitive solution to the selectivity problem, since there would still be competition between two groups. Therefore, we focused on their tridentate analogues.

Only four examples of tripodal complexes of bismuth are currently present in the literature,[351–356] with only one of them having been characterised crystallographically.[355] Due to this dearth of precedent, we looked into similar complexes of lighter main

group elements. We also reasoned that, given the unprecedented nature of our research, we were in the position to design a tripodal ligand from scratch, following a rational design approach. A few features were deemed vital:

1. both the ligand and the resulting Bi complex should be isolable and stable to air and moisture, so that this species could represent a convenient universal precursor for the bismuthonium manifold;

2. the synthesis of the complex should be as practical and high-yielding as possible, especially in view of scale-up;

3. the new species should be compatible with the oxidative conditions for bismuthonium synthesis;

4. although not strictly necessary, a high degree of symmetry would also be desirable, so as to simplify characterisation and reaction monitoring, especially *via* NMR spectroscopy.

To comply with our first point, we excluded from the list of potential candidates ligands which would form weak, non-covalent bonds with Bi, such as pincer ligands (Fig. 4.2), since these compounds normally require strictly inert conditions.[358,359] Moreover, the pendant arm, normally based on oxygen or nitrogen atoms, is easily oxidised,[360] and the Bi centre, due to the stabilising donation of electron density from these heteroatoms, is also more prone to be attacked by acids.[361] Although possibly limiting, an additional criterion to restrict the research to complexes containing three Bi–C bonds was set, on the basis that the only two reported tripodal complexes for bismuth in which the ligand is not bound to the pnictogen through C–Bi bonds, but rather *via* O–Bi bonds, were found to be either unstable in solution[356] or completely insoluble in any solvent.[362]

We envisaged that we could split the remaining candidates into two classes (see Fig. 4.3): linearly linked (in some cases, *macrocyclic* would be the term of choice in classic coordination chemistry) complexes and *bridged* complexes, in which the

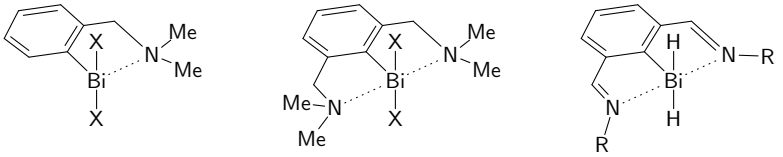

Figure 4.2: Some examples of pincer complexes of bismuth.[357–359] All of them require handling in strictly inert conditions.

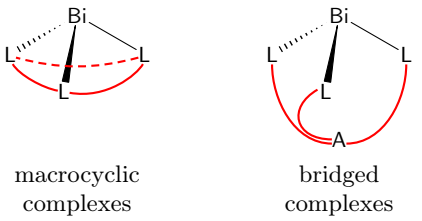

Figure 4.3: The two classes of potential tripodal complexes for bismuth, as envisaged in this Section: macrocyclic, or linearly linked, and bridged. L is a generic ligand, A is the atom in the second bridge-head position.

Bi atom sits in at least one of the two bridge-head positions. The following Sections will provide an overview of both systems.

4.1 Linearly linked ligands and their complexes

This class of compounds represents the first obvious approach when a constrained tripodal ligand is sought. A further distinction within this set can be drawn, whether all the three possible linkages are in place, or one of them is missing, thus forming a partially cyclic system. Examples of both the possibilities are found in Figs. 4.4 and 4.10, respectively.

The first sub-type is commonly referred to as '(hetero)triangulenes' and has been investigated since the early 1970s, when Hellwinkel and Melan synthesised the parent compound **IV** (see Scheme 4.3) by intramolecular Friedel-Crafts acylation of 2,2′,2′′-nitrilotribenzoic trimethyl ester.[363]

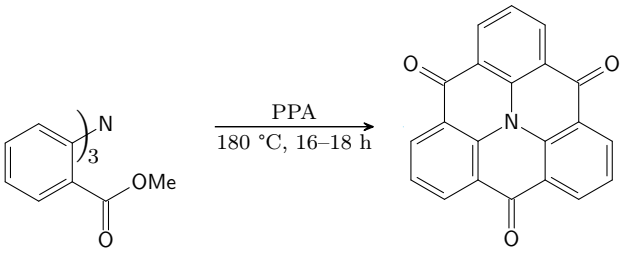

IV
46%

Scheme 4.3: The first synthesis of a heterotriangulene was achieved by Hellwinkel in 1971.[363]

The reaction was carried out in the presence of PPA at 180 °C for 16–20 h, forming insoluble crystals with a modest 46% yield, due to the formation of partially cyclised intermediates. An improved version of this process was published in 2002

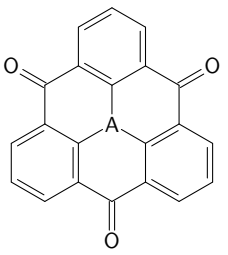

IV

A	D/Å	ϑ/°	Ref.
N	0	180	363,364

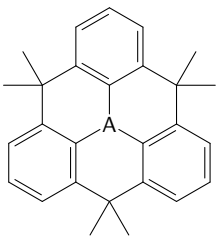

V

A	D/Å	ϑ/°	Ref.
B	0	180	365
N	0.59	166	366,367
P	2.27	121	368
As	/	/	368

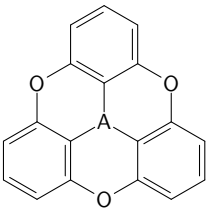

VI

A	D/Å	ϑ/°	Ref.
B	0	180	369
N	0.86	156	370
P	2.45	114	371

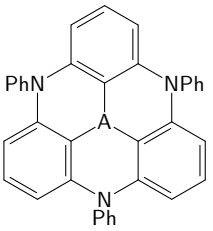

VIII

A	D/Å	ϑ/°	Ref.
B	0.13	177	372
SiMe	1.98	124	372
P	1.89	118	372
Sb	/	/	351
Bi	/	/	351

Figure 4.4: Summary of triangules currently reported in the literature. Excluded from this Figure are compounds that do not possess D_{3h}/C_{3v} symmetry (depending whether they are planar or concave, respectively), such as structures with different linking atoms. D is the bowl depth, defined as the distance in Å between the central atom A and the centroid, Q, of the mean plane passing through the three *para*-C_{sp^2} atoms. The cone angle, ϑ, is defined as the average of 2 $\cdot\measuredangle$ Q-C_{ipso}-A for the three C_{ipso}.

by Field and Venkataraman,[364] who formed the tri-acyl chloride analogue of the tri-ester used previously and subsequently cyclised it with catalytic $SnCl_4$, achieving an overall 80% yield. This *N*-triangulene is perfectly planar.

Three years after the first synthesis of a heterotriangulene, the same authors modified their original approach by reacting their precursor ester with MeLi, so as to form the corresponding tri-carbinol. This was later cyclised in the presence of phosphoric acid, affording **Va**, as per Scheme 4.4.[366] Interestingly, this compound possesses a shallow concavity, with a 0.59 Å bowl depth and 166° cone angle, as defined in Fig. 4.4.[367] Moreover, the dimethylmethylene linker prevents the tight facial packing observed for **IV** and, while still preserving a structural restraint, it allows a certain degree of flexibility. The combination of these two factors is thought to be responsible for its excellent solubility in common organic solvents.

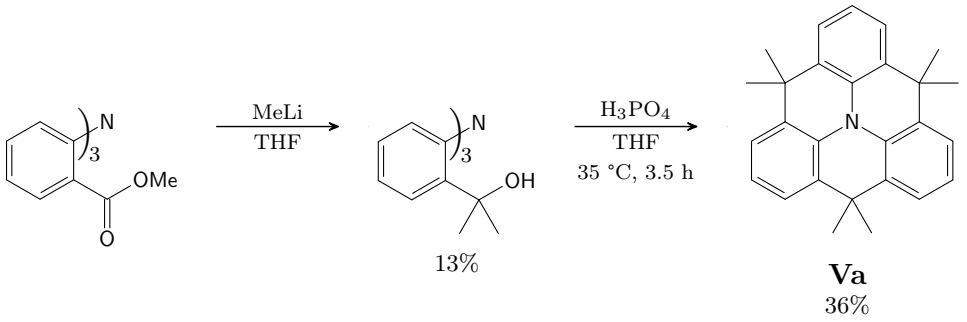

Scheme 4.4: Starting from a tricarbinol, rather than from a triester, grants access to a less polar, and thus more soluble, triangulene.[366]

The B, P and As counterparts **Vb–d** were obtained by similar transformations, *i.e.* a two-fold Brønsted or Lewis acid (LA) catalysed Friedel-Crafts alkylation on 5-(2,6-di-isopropenylphenyl)-10,10-dimethyl-5,10-dihydroacridophosphine, -arsine,

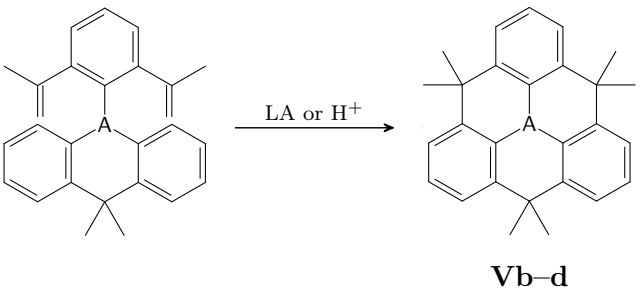

Scheme 4.5: A two-fold Friedel-Crafts reaction can be carried out on the compounds depicted for A = B (**Vb**), P (**Vc**) and As (**Vd**) to give the corresponding angulenes.[365,368] Yields were not reported by the authors.

or the boron analogues (see Scheme 4.5).[365,368] While the boron complex **Vb** is planar, **Vc** and **Vd** show a similar degree of concavity/pyramidalisation, which is significantly more pronounced than for **Va**, with a 2.27 Å bowl depth and a 29.5° cone angle in the case of the phosphangulene **Vc**. Although the heteroangulenes presented so far laid the foundations for a new field of macrocycles, their syntheses cannot be applied to bismuth, since the strongly acidic conditions employed in the cyclisation are not tolerated by complexes of the heavier pnictogen, which would undergo protodebismuthation.

In 1997, Krebs and co-workers optimised the synthesis for the first triangulene with a heteroatom acting as the linker between the three aryl moieties.[371] Specifically, they focused on phosphorus as the central atom and picked oxygen as the linker. Their elegant procedure started from 3-fluorophenol (see Scheme 4.6), which was protected with a THP group. A directed lithiation was then performed between the two substituents, the resulting organolithium was consequently quenched with PBr_3, so as to get to the triaryl phosphine. The protecting group was then hydrolysed and finally the structure was cyclised by a three-fold intramolecular S_NAr reaction. The resulting phosphangulene **VIa** has the deepest bowl depth and tightest cone angle (2.45 Å and 114°, respectively), among all the triangulenes ever reported (see Fig. 4.4 for a summary).

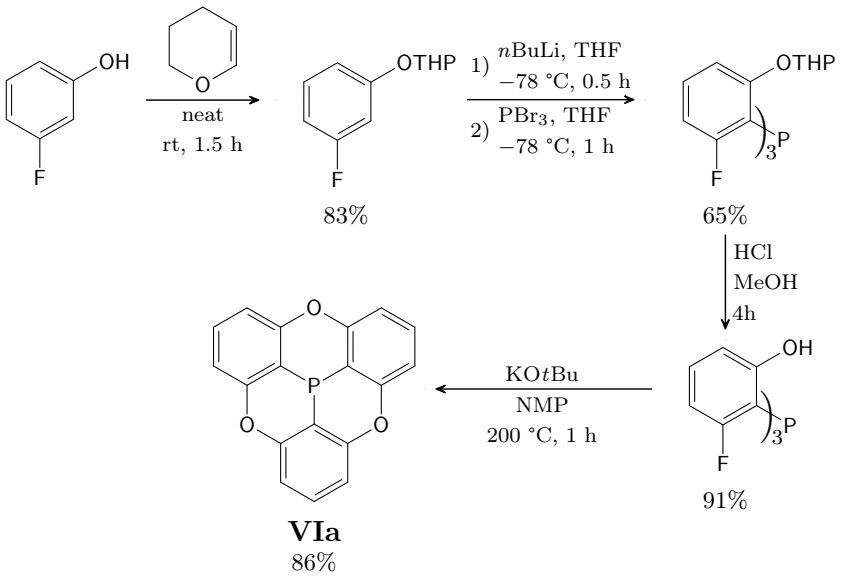

Scheme 4.6: Krebs's strategy for the synthesis of a phosphangulene encompasses the formation of three C–P bonds followed by macrocyclisation *via* three-fold S_NAr.[371]

Yamamura and co-workers were interested in understanding the effect of linking atoms on the geometry of phosphangulenes, so they prepared a series of complexes in which one oxygen at a time was replaced by sulfur.[373,374] As illustrated in Scheme 4.7 for the fully substituted example **VII**, this was achieved by selective functionalisation of the desired number of hydroxide groups of the same tri-*ortho*-hydroxyarylphosphine used by Krebs, with thiocarbamoylchloride. This was followed by Newman-Kwart rearrangement, deprotection of the sulfur and finally cyclisation in the usual S_NAr fashion. They observed that the increase in the number of sulfur atoms made the bowl shallow, with bowl depths varying progressively from 2.45 Å to 2.01 Å. A direct consequence of this could also be noticed in the ^{31}P NMR chemical shifts, which varied from −133 ppm for the fully oxygenated compound to −69 ppm for the one with three sulfur atoms. The authors suggested that such a marked difference is due to the hybridisation change of the phosphorus atom, with the oxygen phosphangulene having the most pronounced s character. The overall simplicity of this procedure makes it appealing for a transposition to bismuth, with only the deprotection in acid conditions requiring adjustment.

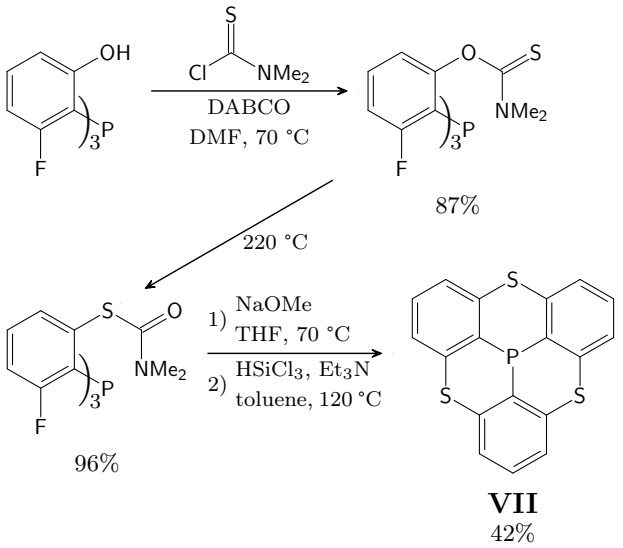

Scheme 4.7: Through a controlled introduction of 1 to 3 equiv of thiocarbamoyl chloride, Yamamura *et al.* were able to selectively substitute the linker atoms in phospangulene.[374] The fully substituted compound is shown.

Boron and nitrogen analogues of the parent phospangulene were obtained in 2016 and 2005, respectively.[369,370] Both the syntheses followed different approaches to that used by Krebs: instead of building the three linkers at the same time in the last step, both Oi and Okada assembled a linear precursor of the desired

ligand, then installed the central atom, and finally formed the remaining link by intramolecular S_NAr reaction. Scheme 4.8 reports the procedure followed to make boron triangulene **VIb**. The justification for this deviation from Krebs's protocol is found in the fact that the borylation of the tri-lithiated fluorinated intermediate proceeded with difficulty, due to elimination of LiF and benzyne formation, before the desired reaction could be accomplished.

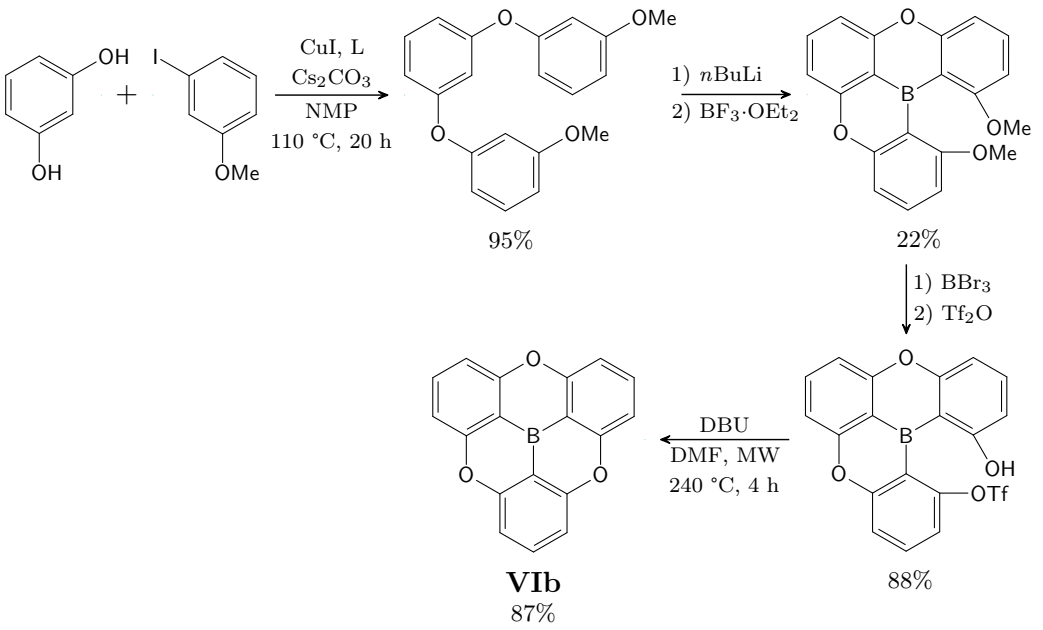

Scheme 4.8: An alternative to Krebs's method: the three linkers are formed in two separate operations to avoid benzyne-derived side-products. Ligand L in the first step is dipivaloylmethane.[369]

A completely different strategy was pursued by Nakatsuka *et al.* in order to overcome the fact that, in all the other methods presented so far, the central atom had to be inserted in early stages thus forcing the following steps to be atom-specific rather than of broad applicability.[372] The authors envisaged that a macrocyclic ligand, in which the linkers were based on nitrogen atoms, could be prepared beforehand, with the central atom being subsequently introduced. The procedure is presented in Scheme 4.9 and encompasses a series of Buchwald-Hartwig amination reactions, the last of which represents the final cyclisation. The latter was required to be conducted at very high dilution (0.007 M), slowly adding the substrate to the reaction mixture over the course of 17 h. The overall yield for the ligand synthesis was 24%. This was then subjected to *t*BuLi for a quite rare Li–Cl exchange* and the resulting intermediate was quenched with the electrophile

*Normally deprotonation of the position *ortho* to the chlorine is favoured over this, unless there

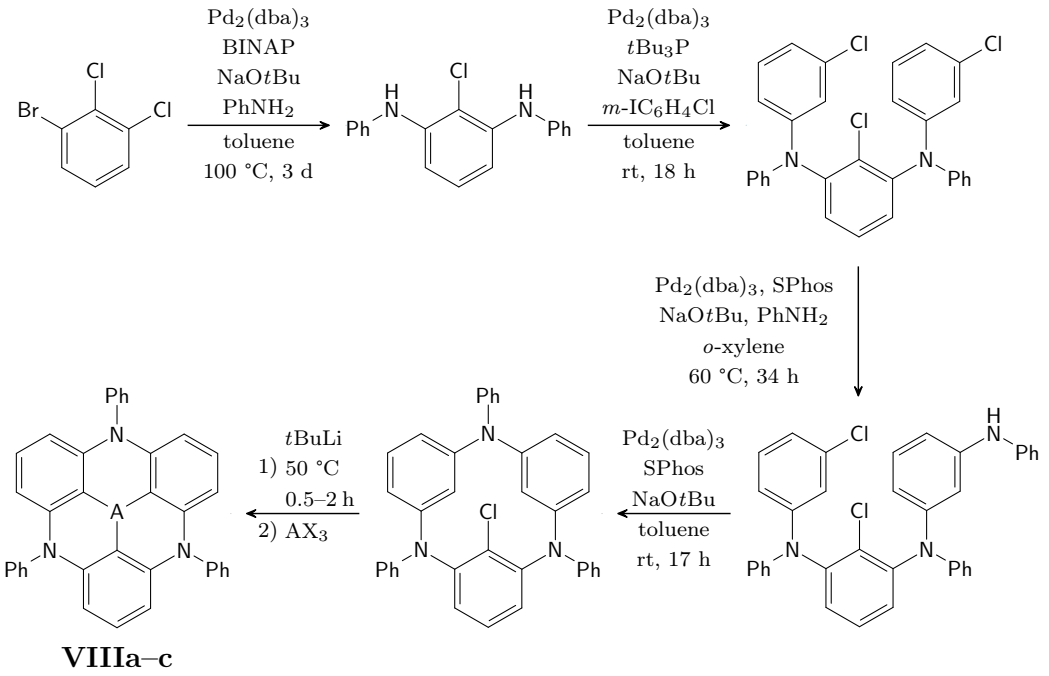

Scheme 4.9: Nakatsuka and co-workers pre-assembled the macrocyclic ligand, installing the central atom only in a later stage:[372] A = B (**VIIIa**), SiMe (**VIIIb**), P (**VIIIc**). Conditions for the last step: BBr_3, *tert*-butylbenzene, −45 °C, 1 h, followed by, in the same pot, $i Pr_2EtN$, 165 °C, 14 h gave **VIIIa** in 45% yield; $MeSiCl_3$, 150 °C, 18 h gave **VIIIb** in 52% yield; PCl_3, toluene, 50 °C, 2 h, the solvent was then exchanged for *o*-dichlorobenzene, then S_8, 110 °C, 12 h. This gave the phosphine sulfide which was reduced to the final product **VIIIc** with PEt_3, *o*-xylene, 120 °C, 2 d in 58% overall yield.

of choice: BBr_3, PCl_3 or $MeSiCl_3$. The final electrophilic aromatic substitution step was conducted in relatively harsh conditions, depending on the heteroatom that was incorporated. In a patent application from 2018 by the same research group the applicability of this procedure to the synthesis of Sb and Bi analogues is mentioned.[351] Interestingly, the boron compound **VIIIa** shows a slight deviation from planarity, which is not discussed by the authors. The phosphangulene **VIIIc**, on the other hand, assumes a bowl-shaped geometry, as expected from previous results, although with a shallower bowl depth (1.89 Å) compared to the oxygen-linked phosphangulene **VIa**. Despite the originality of this approach, the rather complex sequence of catalysts and conditions along with the poor overall yields (11–14%) were deemed detrimental to a practical use of this method.

---

are no protons there, as in this case. Also, given the peculiarity of the position of that chlorine, the formation of the incipient lithiated species might also be favoured by the strain release that takes place by replacing a big chlorine with a small lithium.[372]

4.1.1 Partially linked complexes

In order to avoid complex syntheses, such as that of Nakatsuka, partially linked ligands were also considered. Only five compounds of this kind have been described in the literature.[375–379] Scheme 4.10 shows the only phosphorus complex. The other four reported compounds contain either a different central atom (B or N) or a different atom in the linker (O or S). The nitrogen homologues were both obtained *via* twofold S_NAr reactions of appropriately functionalised triarylamines, similar to Krebs's method. On the other hand, the boron and phosphorus derivatives were all made by mono-directed lithiation of 1,3-diphenoxybenzene or 1,3-diphenylthiobenzene, followed by transmetalation either to BBr_3 or PCl_3 and finally electrophilic aromatic substitution to form the two linkers. Notably, for the boron compounds, the final borylation was conducted without a Lewis acid, in the presence of Hünig's base.

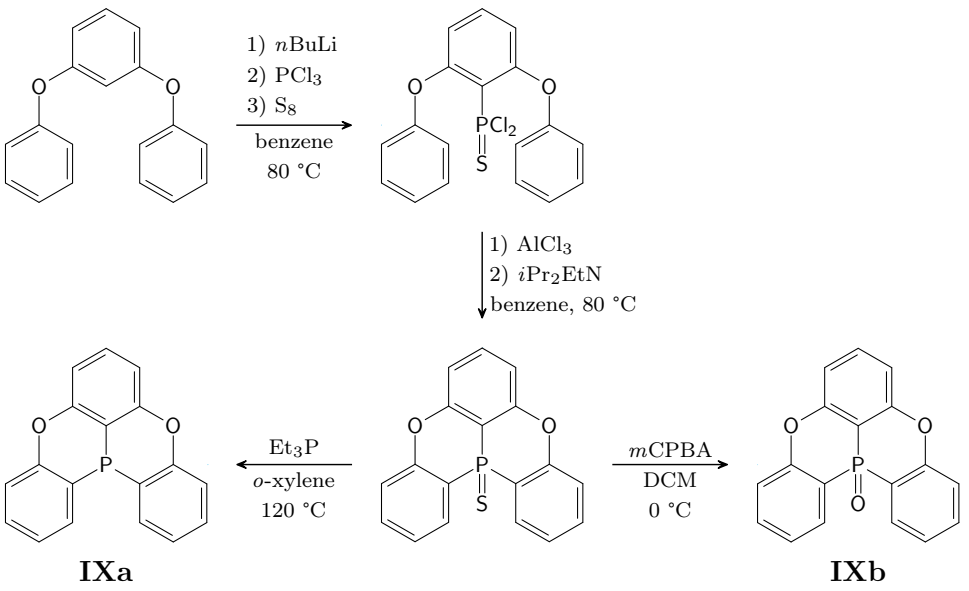

IXa **IXb**

Scheme 4.10: Partially linked complexes are restricted to boron,[375,378] nitrogen,[376,379] and phosphorus,[377] with no evidence in the literature for heavier atoms. Nakatsuka's synthesis of **IX** illustrates the necessity of separating the formation of the three P–C bonds in two different operations.[377]

Considering that, in order to form three C–A bonds in one step, a triple lithiation should be feasible, it is interesting to notice that none of the authors attempted this, deciding instead to separate the formation of the three bonds into two different operations (see Scheme 4.10 for a representative example). A possible explanation for pursuing this approach would be that, this way the risk of oligomerisation is reduced:

once the carbanion is quenched by the electrophile, intramolecular electrophilic aromatic substitution is favoured over intermolecular. The same argument would not be possible in case of tri-lithiation, where two different molecules of electrophile could quench two sites of the same lithiated ligand, thus initiating oligomerisation.

4.1.2 Different macrocycle size

Finally, bigger and smaller macrocycles were examined, since shortening or lengthening the linker(s) is likely to have the most significant impact on the geometry and strain of the resulting complex. We reasoned that additional strain would only be detrimental in the case of bismuth, since the atom is significantly bigger than its lighter counterparts, and Bi–C bonds are weak and prone to intermolecular exchange. Moreover, the only synthesis we could find for a complex with shorter linkers employed extremely harsh conditions (PPA, 180 °C) to form the linkers and was only optimised for nitrogen as the central atom, heavily relying on its nature for the complex synthesis.[380] For these reasons it was decided to exclude smaller macrocycles from the pool of potential ligands for bismuth.

On the other hand, considering that the bismuth atom in simple, non-linked or -bridged triarylbismuth complexes undergoes two structural changes, when going from Bi^{III} to bismuthonium(V) (from trigonal pyramidal, to trigonal bipyramidal, to tetrahedral), the flexibility granted to a tripodal ligand by longer linkers should be able to better accommodate these variations. Unfortunately, only one structure could be found that contained three longer linkers.[382] Its synthesis is reported in Scheme 4.11. This encompasses firstly, a double S_N2 reaction, initiated by deprotonation of the more acidic benzylic position *ortho* to the sulfonyl group.[381] This forms the core structure of the ligand, which then undergoes reductive desulfonylation using sodium amalgam. The resulting tri-bromide is then subjected to lithium-halogen exchange and borylation with $BF_3{\cdot}OEt_2$. Finally, bromodemethoxylation with BBr_3 enables the $Ni(COD)_2$ catalysed homocoupling to give the cyclised compound **X**.[382] The yields for some of the steps were not reported, but the borylation is said to be particularly challenging, with yields between 14 and 45%.[381,382]

As evidence of the higher flexibility and unlike triangulenes, the structure was found not to adopt a trigonal planar geometry, with both aryl rings and ethano-linkers laying out of the plane defined by the boron atom and the three carbon atoms attached to it. In fact, a C_{2v} axis that passes through atoms C1 and B could be identified (see inset of Scheme 4.11). Moreover, the energy required for an edge inversion is only 8 kcal/mol, as measured by VT-NMR experiments, since the process requires flipping of a single ethano linker.[382]

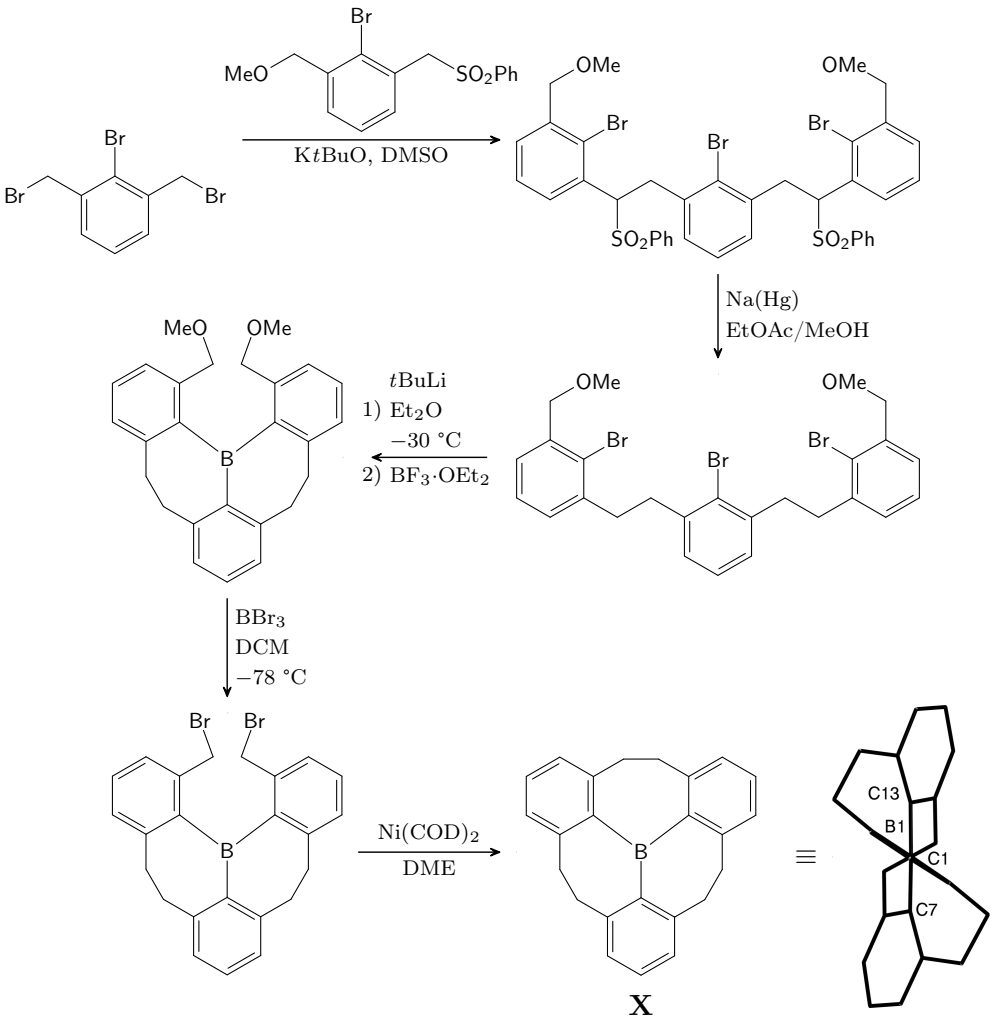

Scheme 4.11: The currently only reported synthesis of macrocycle containing a main group element in the central position and with linkers longer than one atom.[381,382] In the crystal structure, shown along the C1–B1 axis, C1, C7 and C13 are the sp^2 carbon atoms directly connected to boron B1. Thermal ellipsoids data for this structure are not available from the CCDC.

The next Section will cover bicyclic complexes in which at least one bismuth atom sits in one of the bridge-head positions. Bridged complexes for other elements of Groups 14 and 15 will be discussed as well.

4.2 Bridged complexes

Bicyclic systems have always piqued chemists' interest, due to the great strain that characterises them and the possibility of peculiar interactions between the two atoms in the bridge-head positions. Very few compounds without aryl ligands have been described. The three most significant examples are depicted in Scheme 4.12. The first one is the only bismatrane reported in the literature. It was made in 1940 by Miller by reacting triethanolamine with bismuth hydroxide in ethanol.[383] Despite the simplicity of its synthesis, this compound was soluble only in water and lower alcohols and was oxygen- and light-sensitive. Moreover, aqueous solutions of the compound underwent irreversible hydrolysis, which could not be prevented by the addition of triethanolamine.[383] One example of aromatic bismatrane, constituted of three 2-hydroxybenzylamine moieties, was prepared by Wilson *et al.* but was found to decompose in solution, so it will not be discussed any further.[356] The second example is the only barrelene-like compound ever reported in which bismuth sits in one of the bridge-head positions. It was obtained

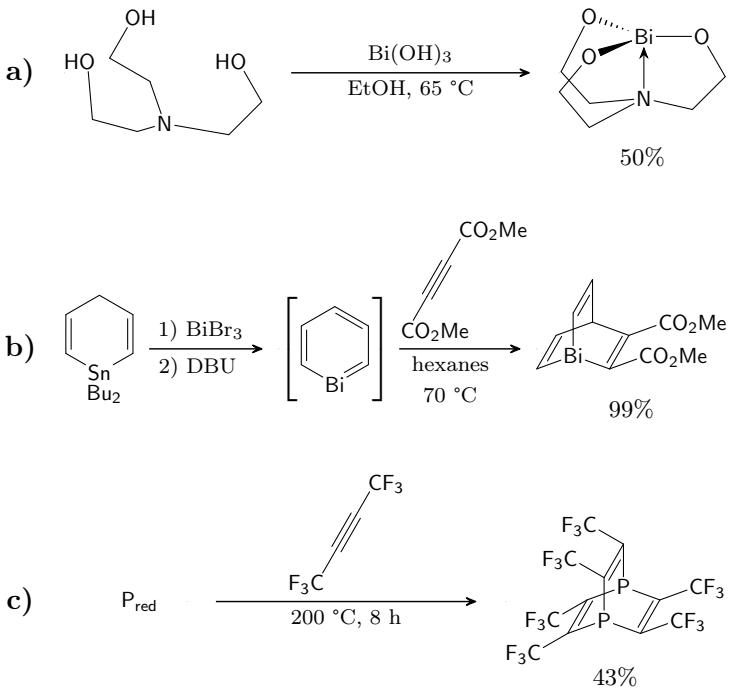

Scheme 4.12: Bismatrane (a) and two heterobarrelenes with Bi (b) and P atoms (c) in the bridge-head positions. The first is easy to synthesise but suffers from limited stability.[383] The synthesis of barrelenes is not trivial and suffers from limited scope.[352,384]

as the product of a Diels-Alder reaction between the extremely acid sensitive bismabenzene[352,385] and dimethylacetylenedicarboxylate. Bismabenzene, in turn, was prepared *in situ* by treating stannacyclohexa-1,4-diene with $BiBr_3$. Finally, the third example is a diphosphabarrelene obtained by treating red phosphorus with the same bistrifluoromethylacetylene.[384] Conditions for this required catalytic iodine and heating at 200 °C for 8 h in a sealed vessel under autogenous pressure. The diarsa-analogue was also obtained in a similar way. Both compounds are very insoluble and quite volatile, but relatively stable due to the strong electron-withdrawing effect of the six trifluoromethyl groups, which render the phosphorus or arsenic atoms less basic than usual. Due to the synthetic challenges and limitations, only aromatic barrelene-like structures will henceforth be considered.

In 1942, in a paper showcasing the synthesis of 9,10-*o*-benzenoanthracene, Paul Bartlett proposed to name such compounds 'triptycenes', after 'the triptych of antiquity, a book with three leaves hinged on a common axis'.[386] In the 1970s, several

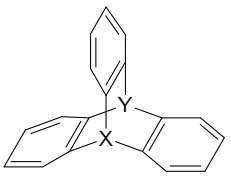

#	IX	Y	Ref.	CCDC	#	IX	Y	Ref.	CCDC
1	CH	CH	386	TRIPCN	13	N	P	400,401	MBPAZA§
2	BPh^-	CH	387	VOZJIG	14	N	As	402	/
3	N	CH	388	CEMPAL*	15	P	BPh^-	403	CEYRIK01
4	P	CH	389	ASTRPB	16	P	SiOH	404	OWOMAQ
5	As	CH	390	ASTRPA	17	P	SnPh	354	LOCLIB
6	Sb	CH	391	/	18	P	As	353,354	/
7	SiMe	SiMe	353,392	HAXSEE†	19	P	Sb	353,405	KUDCOC§
8	N	N	393	/	20	P	Bi	354	/
9	P	P	394,395	DPTRYP	21	As	Ge	406	WIZRIG
10	As	As	396	WIZROM	22	As	Sb	353,398	/
11	Sb	Sb	397,398	KATTIJ§	23	Bi	SiF	355	RANYIR
12	Bi	Bi	399	/					

Table 4.1: Most relevant triptycenes know in the literature and their corresponding reference of first report. For entries 7, 11, 18, 19 and 21 the first reference corresponds to the synthesis of the perfluoro analogue, which was chronologically antecedent. CCDC Database Identifier are reported too for ease of consultation. * Inclusion complex of C_{60} fullerene; † In the reported crystal structure Y = SiOH; § Crystal structure of the tris-3-methyl or tris-3,4-dimethyl analogues.

groups extended the scope to heterocyclic analogues of the parent compound. At first, bi-cycles with only one heteroatom were investigated,[388–391] then the same heteroatom was inserted in both the bridge-head positions,[353,394,396,399] and finally, more recently, two different heteroatoms were included in those positions.[354,355,400,402,405] A summary of the most relevant examples can be found in Table 4.1.

4.2.1 Mono-substituted heterotriptycenes

All the mono-substituted heterotriptycenes were originally made by installing the bicycle structure over a pre-assembled extended aryl system, *i.e.* by forming a second bond between a free aryl group and the base ring, as seen in Scheme 4.13. The third ring can be installed either in the benzylic position, as has been done for the aza- and arsatriptycenes,[388,390] or on the heteroatom, as for the phospha- and stiba- analogues.[389,391] The final bicyclisation occurs *via* intramolecular addition of either the heteroatom or the benzylic carbanion to the benzyne, formed by elimination of a conveniently placed chlorine atom beta to the bridge-head position. The two possibilities were exploited for the azatriptycene, in the former case,[388] and for phospha- and stiba- compounds, in the latter.[389,391] Arsatriptycene, on the other hand, was obtained by PPA-catalysed cyclisation to afford the arsine oxide, which was subsequently reduced to the final compound with SO_2/HCl.[390] However, the latter can also be obtained *via* the benzyne method.[391]

Jongsma, who pioneered the syntheses of the phospha- and stibatriptycenes, observed that the benzyne intermediate was not easily formed and that the benzylic carbanion tended to decompose before it could react with it.[391] This explains the mediocre yields obtained (<35%). Therefore, he envisaged that the use of lithium piperidide instead of LDA would facilitate benzyne formation, since the former had been shown to enable higher rate constants, thus making the competition more favourable.[407] Interestingly, he also pointed out that, due to the longer C–Sb bonds, the carbanion would have been farther from the benzyne, hence making the reaction less likely and more difficult. Nevertheless, in the end, the desired compound could be obtained. This argument remains valid for bismuth and could explain the lack of an analogue with this element. The immediate precursor could in fact be obtained *via* Suzuki's method (see Scheme 4.28), *i.e.* by quenching the Grignard generated from bis(2-bromophenyl)methane with $BiCl_3$ in the presence of KI, in order to generate the corresponding Bi–I (obtained by Suzuki only in 12% yield).[348] This could then be subjected to an appropriate ArMgBr species. It remains uncertain if the final cyclisation would be feasible.

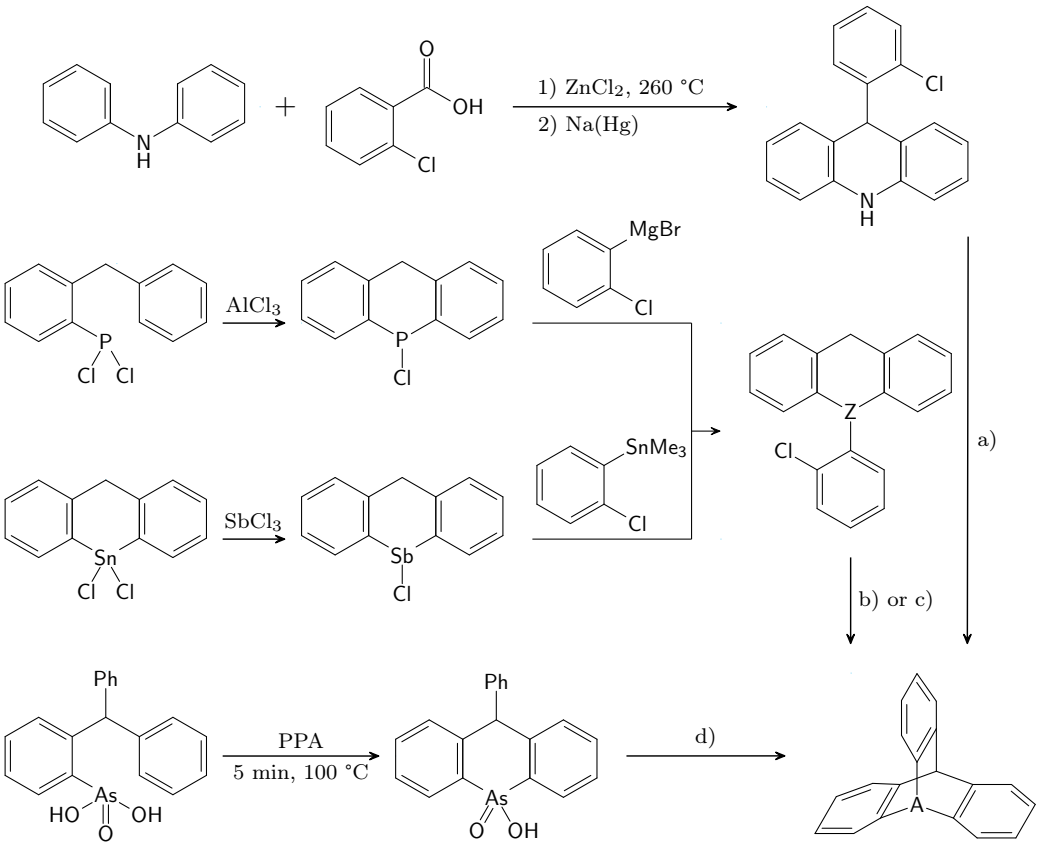

Scheme 4.13: Almost all the syntheses of mono-heterosubstituted triptycenes relied on the intramolecular addition of the heteroatom to a benzyne formed with different strong bases: a) KNH_2, NH_3, 17%;[388] b) LDA, 35%;[389] c) LTMP, 20%.[391] The arsatriptycene represents an exception, since it was obtained *via* electrophilic aromatic substitution, with the highest yield among these: d) PPA, 40 min, 110 °C, then SO_2, HCl, $CHCl_3$, 64%.[390] No viable route has been reported for the Bi analogue. Z = P, Sb. A = N, P, As, Sb.

Only recently was a novel route developed for the formation of phosphatriptycene. This is discussed in Scheme 4.14. The procedure exploits the directed mono-lithiation of tri-(3-methoxyphenyl)phosphine oxide. This is followed by quench with phenylchloroformate to install a phenoxycarbonyl functionality. Successively, this is attacked by the two carbanions generated by a second directed lithiation on the other two rings. This affords 1-phospha-6-hydroxymethyl-triptycene in 51% yield.[408] Deoxygenation could be achieved *via* the Barton-McCombie reaction, with a remarkable overall yield of 36%, as demonstrated a few months ago by Hu *et al.*[409] These authors also showed that it is possible to lithiate the starting material thrice first, then quench it with 1 equiv of the chloroformate, so as to make the triptycene *in situ*. If the chloroformate is replaced with triphenylphosphite, the process brings forth the corresponding 5,10-diphosphatriptycene oxide.[410]

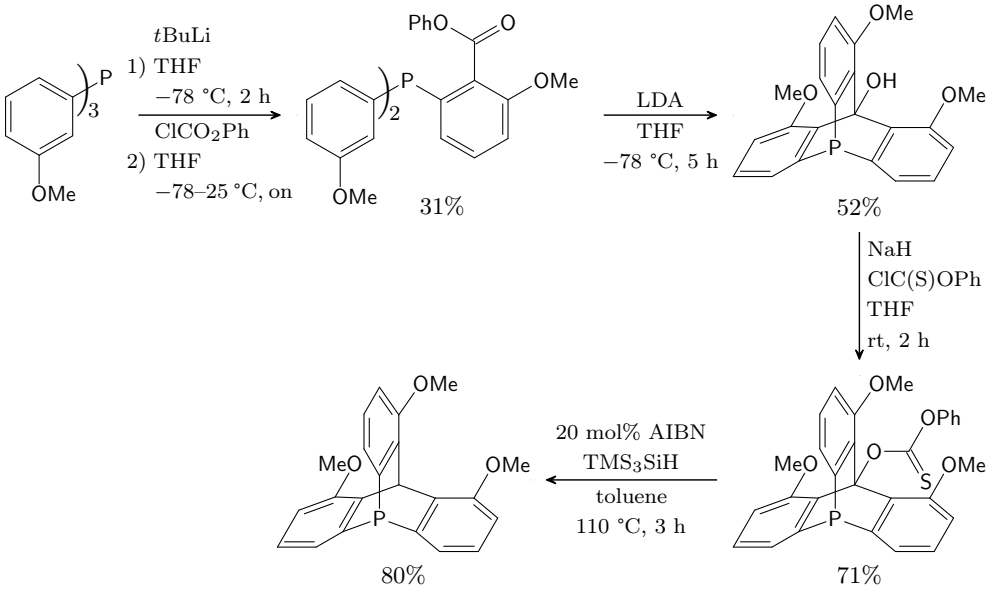

Scheme 4.14: Kobayashi's approach to the synthesis of phosphatriptycene: the atom that will be in the second bridge-head position in the product is installed by addition of phenyl chloroformate to a mono-lithiated triarylphosphine. Subsequently, the electrophilic groups undergoes a double attack by two carbanions, thus yielding an hydroxy derivative of phosphatriptycene.[408] Hu and co-workers recently showed that deoxygenation can occur *via* the Barton-McCombie protocol.[409]

4.2.2 5,10-disubstituted triptycenes

With regard to 5,10-disubstituted triptycenes, the landscape is more varied. Contrastingly from mono-substituted triptycenes, almost all the procedures build the desired bicyclic system from simple, appropriately functionalised benzene rings,

the only exception being azarsatriptycene. This makes such compounds potentially more interesting for our aims. The oldest synthesis dates back to 1927, when McCleland serendipitously obtained the diarsa compounds by distilling 1,2-bis(chloro(phenyl)arsaneyl)benzene at 340 °C (see Scheme 4.15).[396]

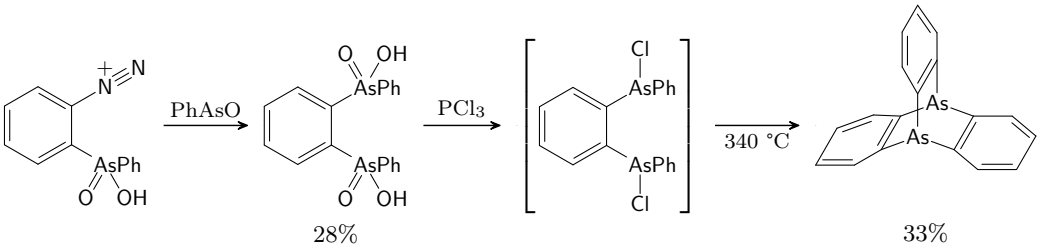

Scheme 4.15: The oldest synthesis for a diheterotriptycene dates back to 1927. Diarsatriptycene was isolated as one of the decomposition products of 1,2-bis(chloro(phenyl)arsaneyl)benzene, during attempts to purify the latter by distillation.[396]

When new explorations in the field started again in the 1970s, a distinction was drawn between 'direct' and 'indirect' syntheses.[411] The former type encompasses the reaction between 1,2-dihalobenzene with the desired metal in its elemental state. This also represents the oldest approach and was pursued predominantly by three authors (see Scheme 4.16): Weinberg in 1971,[394] Al-Jabar in 1984,[397] and Humphries in 1987.[398] Conditions are normally extremely harsh: Weinberg, for example, reacted 1,2-dichlorobenzene with 8 equiv of white phosphorus, in the presence of catalytic $FeCl_3$, at 280 °C (the boiling point of white phosphorus) to get diphosphatriptycene in a 20% yield (see Scheme 4.16a).[394] The latter could also be oxidised quantitatively to the dioxide by treatment with peracetic acid. Despite the modest yield, the process can be safely carried out on a decagram scale: the author performed the reaction on 0.5 mol scale, which required 0.6 Kg of white phosphorus. Al-Jabar and co-workers, on the other hand, focused on perhalogenotriptycenes, exploring their substitution with different heteroatoms. Under similar conditions (250 °C, 4 h) they obtained perfluoro-and perchlorodiarsatriptycene in 60% and 20% yield, respectively (see Scheme 4.16b).[397]

Finally, Humphries *et al.* replaced the dihalobenzene with *ortho*-phenylenemercury, a trimeric mercurial made by pyrolysis at 300 °C of mercuric-2,3,4,5-tetrafluorobenzoate.[412] Reacting this compound with fine metallic powders of As, Sb or Bi afforded the corresponding di-substituted triptycenes, as shown in Scheme 4.16c. Unfortunately the yields were so low that there was only enough material for IR and GC analyses. Using the perchloro mercurial as starting material increased

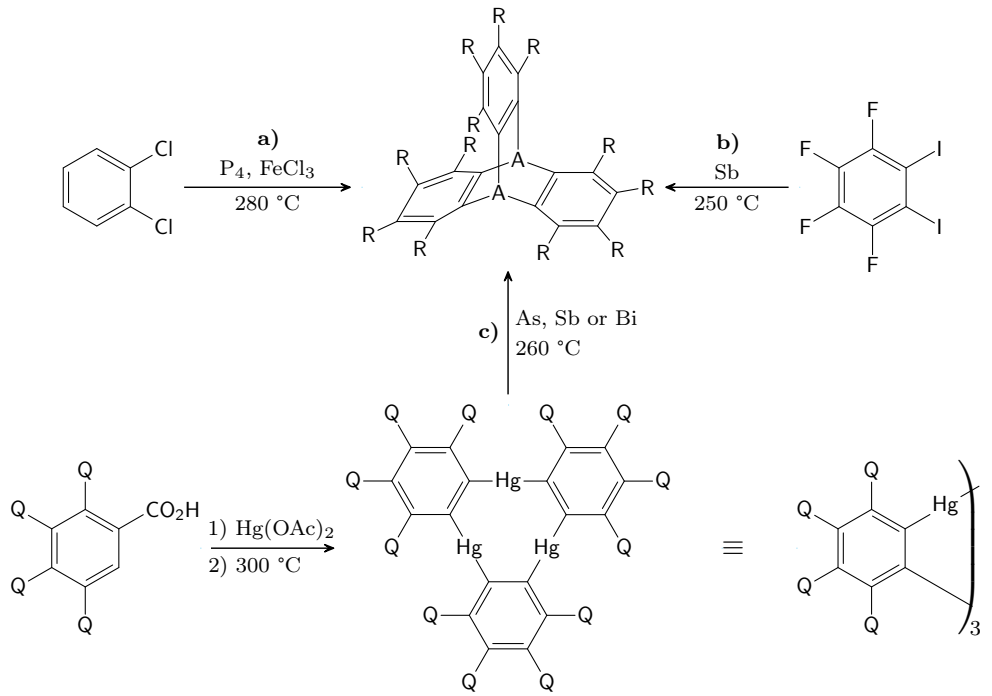

Scheme 4.16: 'Direct syntheses' of di-substituted triptycenenes: a) The strength of this method resides in the wide availability of all the components, however use of P_4 is required, A = P, R = H;[394] b) Perfluorotriptycenes were first synthesised by Al-Jabar, A = Sb, R = F;[397] c) The use of mercurials extended the scope to Bi compounds, although yields remain very poor for non-perchlorinated species, Q = R = H, Cl; A = As, Sb, Bi.[398]

the yields to a more acceptable 60–70% for both Sb and Bi. The reason for the discrepancies in yields between simple and perchloro compounds must be sought in the fact that these reactions do not occur below 250 °C but, at the same time, non-halogenated triptycene were shown to decompose above 100 °C. A workaround was found almost ten years later, when Rot *et al.* transmetalated the same organomercurial previously employed to zinc and reacted the resulting organozinc species with $AsCl_3$ at −196 °C, as shown in Scheme 4.18. This formed diarsatriptycene in the highest yield reported to date (49%).[406]

This last example sits at the cross-over between 'direct' and 'indirect' methods. In fact, the second equivalent of the electrophile $AsCl_3$ was added 36 h after the first, although in the same reaction vessel and without work-up in between the two additions.[406] Cullen and Al-Jabar had trialled this approach as well (see Scheme 4.17), in an attempt to gain a practical access to the so-called mixed triptycenes, substituted with two different heteroatoms in the bridge-head positions.[353,399] A single lithium-halogen exchange on 1,2-dibromoaryl species, followed by quench

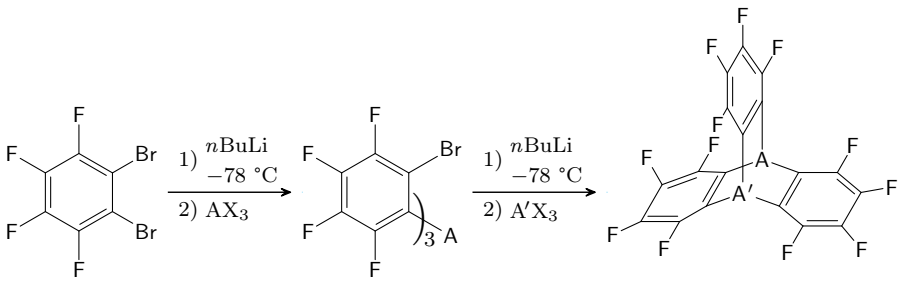

Scheme 4.17: Al-Jabar's attempts to perform two sequential Li–Br exchange and quench steps.[353] A = A′ = P, As, Sb, SiMe; A = P, A′ = As, Sb; A = As, A′ = Sb. For the bismuth compound, the intermediate was not isolated. Yields are extremely modest ($\leq$ 4%). See also Fig. 4.21 for an improved version of this method.

with a pnictogen trihalide formed the corresponding triaryl pnictogen, which could generally be isolated in good yields (with the only exception of the Bi species, which was carried over to the next step without isolation). This was then subjected to a second lithium-halogen exchange and quench with 1 equiv of the same or different PnX_3 species to give the desired triptycene.

Unfortunately, yields were particularly low, with the highest being 4% for the diarsa-compound. A reasonable explanation for this poor performance would be that, since all these reactions were performed on tetrafluorinated substrates, the carbanion formed in the second lithium-halogen exchange is too stabilised and, thus, not nucleophilic enough to react readily with the relatively mildly elecrophilic pnictogen trihalides. In fact, quenching the intermediate with water, yielded the protonated species quantitatively. The tridentate nature of the electrophile is also another aspect to take into account: the authors found evidence that, under their conditions, the lithiated intermediate reacts with different molecules of PnX_3, instead of the single molecule required if triple ring closure was to occur.

The nature of the organometallic intermediate appears to be relevant to the success of the reaction, as mentioned above for the synthesis of diarsatriptycene by Rot and colleagues.[406] In the same publication, the authors also managed to obtain arsa- and stibagermatriptycenes by reaction of tri-(2-chloromagnesiumphenyl)germanium in 75 and 68% isolated yields, respectively (see Scheme 4.18). These compounds represent some of the few examples of triptycenes containing group 14 atoms.[413] Once again, the *ortho*-phenylenemagnesium employed to make this intermediate was prepared by exposing the organomercury analogue to magnesium. Interestingly, the diarsa-compound could not be obtained at all *via* the Grignard route.

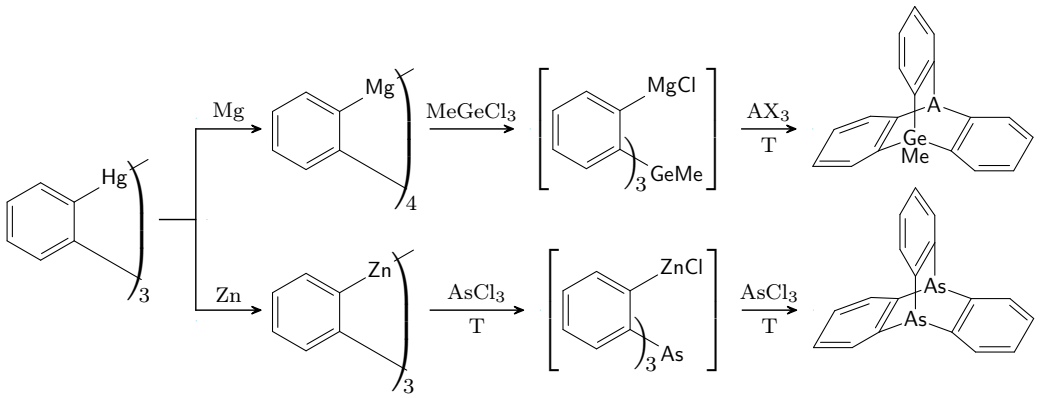

Scheme 4.18: Conditions for the final cyclisation of these triptycenes require careful temperature control: 24 h at −78 °C, then 4–24 h at −20 °C and finally 18–72 h at rt. Yields are good: A = P (50% conversion, not isolated), As (75%), Sb (68%). The diarsatriptycene was obtained in 49% yield by two sequential reactions with $AsCl_3$, starting from the organozinc species shown. The final cyclisation was performed at −196 °C.[406]

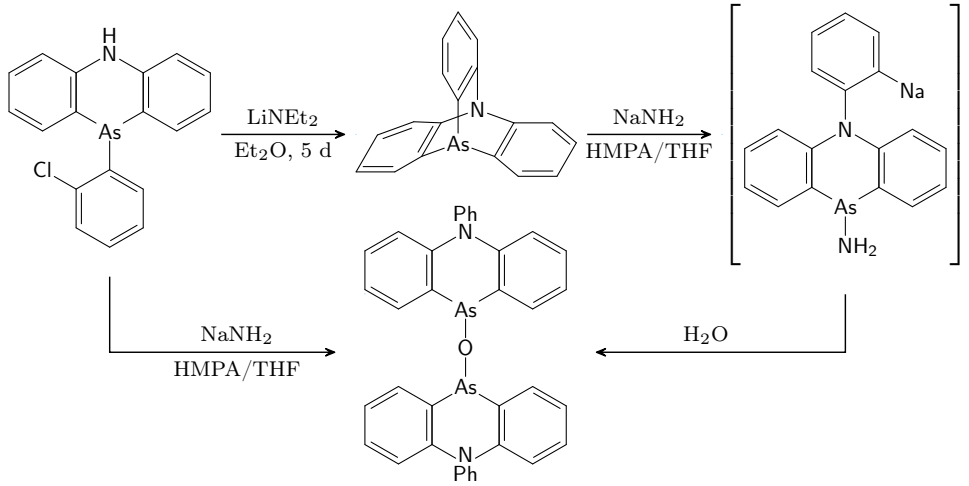

Scheme 4.19: Earley demonstrated that azaarsatriptycene can be obtained from a starting material similar to what Hellwinkel used for his azatriptycene synthesis (see Scheme 4.13a).[402] The base employed to generate the benzyne intermediate is crucial: while $LiNEt_2$ affords the desired product, $NaNH_2$ forms a dimer. The latter is formed also by reacting the triptycene with $NaNH_2$, followed by aqueous work-up, thus showing that the dimer is a decomposition product of the azaarsatriptycene.

Nitrogen-containing mixed triptycenes were developed in the early 1970s by Earley and Hellwinkel. The former essentially adapted Wittig's protocol, presented previously in Scheme 4.13a, to include an As atom in the desired position.[402] Bicyclisation was performed *via* the usual benzyne intermediate in Et_2O over the course of 5 d. The choice of base was vital (see Scheme 4.19): $LiNEt_2$ afforded the desired product in 48% yield; conversely, sodamide in a mixture of HMPA and THF gave a completely different compound. This could also be obtained in 85% yield by treating the desired triptycene with sodamide. The authors managed to identify this species as the dimeric product of decomposition of a metalation intermediate, in which the amide had attacked the As atom and cleaved the bicyclic ring. This triptycene skeleton is exceptionally stable: in Earley and Gallagher's own words 'the outstanding feature of the chemistry of azarsatriptycene is its lack of reactivity'.[402] It did not react with Raney nickel, nor with HCl or HBr; when treated with nitric acid it oxidised instead of being nitrated; MeI did not alkylate it, with or without $AgBF_4$; with Br_2 it formed a unidentified tribromo species, which decomposed back to the starting material. Similar experiments were performed with the pefluoro analogues by Al-Jabar, who showed that most of his compounds were similarly unreactive, with the exception of bismuth derivatives which were instantaneously cleaved both by concentrated acids and Cl_2 in CCl_4.[414]

Hellwinkel's synthesis of azaphosphatriptycene, depicted in Scheme 4.20, is very appealing in the fact that it is based on commercially available materials and uses conditions that would be perfectly feasible from a modern safety point of view. Bis(2-bromophenyl)amine was reacted with 1,2-dibromobenzene and copper bronze

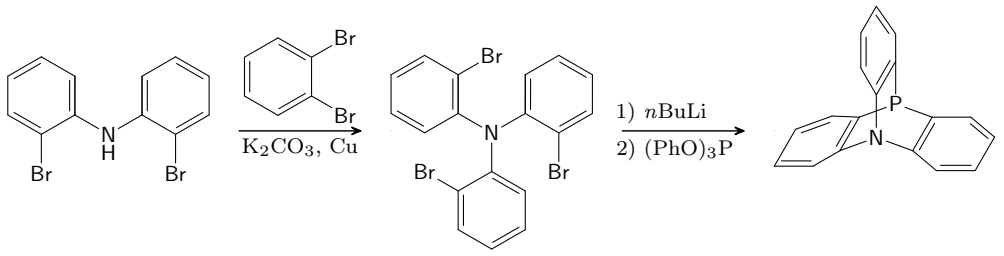

Scheme 4.20: Azaphosphatriptycene was obtained in 1969 by an appealing one-pot sequence of lithium-halogen exchange and addition of a trivalent phosphorus source (triphenylphosphite). Yields of the last step are also relatively good.[400]

in the presence of K_2CO_3, to give tri-(2-bromophenyl)amine, which was in turn subjected to lithium-halogen exchange. The tri-carbanion was finally quenched with triphenylphosphite, affording the desired bicyclic compound in 30% yield.[400] Given

Hellwinkel's presence in both the fields of linked and bridged tripodal ligands for phosphorus, interesting comparisons could be made. For example, in an attempt to make a turnstile P(V) complex, by treating his azaphosphatriptycene with *o*-chloranil, Hellwinkel noticed that the resulting complex surprisingly maintained a trigonal bipyramidal structure, suggesting that the bridged structure keeps some degree of flexibility.[415] The same could not be said for the dimethylmethylene bridged phosphangulene **Vc** (Scheme 4.5).[368]

The following two methods are the current state-of-the-art and represent a marked improvement compared to what has been presented so far. In fact, they show broader applicability, with higher yields and tolerance for several heteroatoms in the bridge-head positions. This is demonstrated, for example, by the variety of compounds made by Uchiyama and co-workers in the last ten years with these methods.[354,405,416] In both cases, the key step is a single metal-halogen exchange with 1,2-dihalobenzenes, which allows the insertion of the first heteroatom, supplied as the trihalide in 1/3 of an equivalent. The process is then repeated for the other halogen and the bicyclic structure is thus formed.

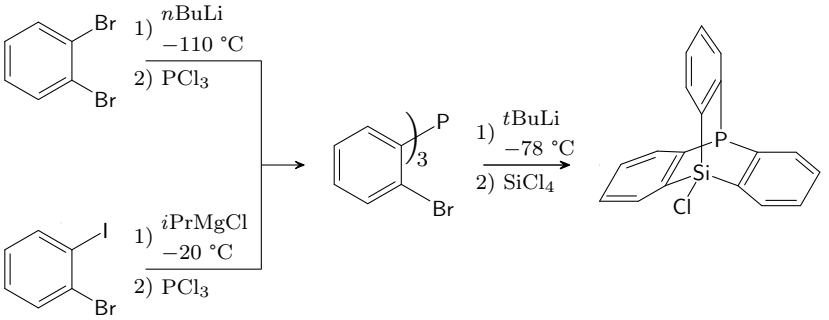

Scheme 4.21: A careful temperature control allows the synthesis of tri-2-bromophenylphosphine, either *via* a Li-X[405,417] or Mg-I[404] exchange (62% and 57% yield, respectively). This intermediate is then subjected to Li-Br exchange and the trilithiated species is quenched with an appropriate electrophile, to give the desired heterophosphatriptycene. Here phosphasilatriptycene is shown as an example.[417]

Notwithstanding the apparent similarities to Al-Jabar's method,[353] greater care is taken in the first metal-halogen exchange and this grants high reproducibility. Specifically, Tsuji carried out a lithium-halogen exchange between *n*BuLi and 1,2-dibromobenzene at −110 °C in 1:1 THF:Et_2O solution.[417] Temperature control is crucial: as pointed out by Chen *et al.* in 1980, the resulting lithiated species is only stable below −90 °C.[418] Above that temperature, benzyne starts to form and several oligomers form, so that the intermediate is completely consumed within 30 min. Notably, the second lithiation is performed with *t*BuLi. Tsuji showcased

this protocol for the synthesis of a phosphasilatriptycene, as represented in Scheme 4.21. Tomaschautzky further expanded it to make the bismasila-analogue, which at the time of writing is the only bismatriptycene whose crystal structure has been deposited to the CCDC.[355] On the other hand, Iwai *et al.* replaced the first lithiation with Knochel's magnesium-iodine exchange protocol.[404] Conditions are much milder than in the previous case, with the temperature kept at −20 °C for a few hours without any sign of decomposition. Lower temperatures are detrimental since they would prevent the transformation.[28] Appealingly, the procedure employs commercially available *i*PrMgCl as the metal source. The magnesiated intermediate then faces the same fate shown in Tsuji's procedure.

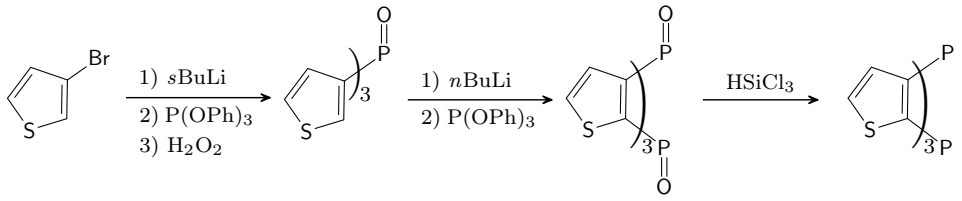

Scheme 4.22: An example of heterothiophenetriptycene.[419] The bicylisation step occurs in very poor yields if the first phosphine is not oxidised to the corresponding oxide beforehand. Even with these optimised conditions yields are comprised between 11 and 24%, depending on the substituents on the thiophene rings. Similar conditions were employed to make the phosphasila-[420] and monophospha- (both isomers)[421] analogues, with similarly mediocre yields (10% and 18%, respectively).

For the sake of completeness, it must be noted that there exist a very limited number of examples of heterotriptycenes which do not contain phenylene groups but instead 2,3- or 3,4-thiophenylene. The first mention of such compounds is in a work by Massey, who applied the chemistry discussed in Scheme 4.17 to make perfluorothiophenetriptycene,[422] however, these were investigated more thoroughly by Nakayama and colleagues in 1993:[419–421] a representative example from their studies is reported in Scheme 4.22. The process is marred by poor yields, especially as far as the bicyclisation is concerned and regardless of the alkyl lithium species employed. It is interesting to notice that all the thiophene rings are oriented in the same direction. Compared to standard phenylene triptycenes, these compounds are characterised by lower ^{31}P NMR chemical shifts, *e.g.* −93 and −87 ppm (for the P atom closer and farther to the sulfur, respectively) vs −43 ppm for diphosphatriptycene. The stronger electron-withdrawing nature of the 2-thienyl group and narrower C-P-C angles were invoked to explain this discrepancy.[420] These examples conclude this brief review. The next two Sections will address our attempts to synthesise tridentate complexes of bismuth.

4.3 Bismuth complexes bearing linear ligands

The search for a suitable tridentate ligand for bismuth started from linearly linked scaffolds and in particular not fully cyclised ones, similar to the examples discussed in Section 4.1.1. In fact, the literature review presented in the first two Sections of this Chapter highlighted several potential problems in the transposition of the synthetic approaches to fully closed macrocycles, *i.e.* angulenes, to the case when the central atom was bismuth. When acidic conditions could be avoided, such as in Krebs's,[371] Yamamura's[373] and Nakatskuka's[372] works, the requirement for highly optimised conditions was anticipated. Partially linked systems, on the other hand, were expected to be simpler to make and more tolerant to variations of the linkers, opening up possibilities to tune both their synthesis and behaviour.

The first compound that was targeted is the derivative of 1,3-diphenoxybenzene depicted in Scheme 4.23. This complex was particularly appealing since the starting material is commercially available. We envisaged that the installation of bismuth could occur *via* a sequence of a triple directed *ortho*-metalation and quenching of the metalated intermediate with $BiBr_3$.

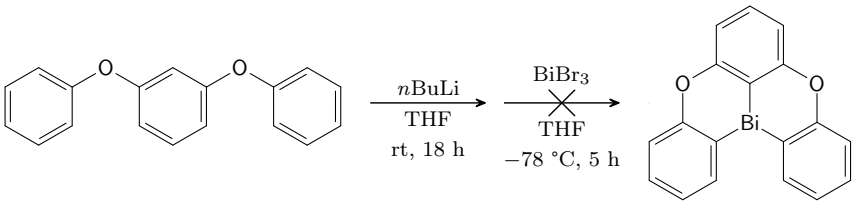

Scheme 4.23: The synthesis of the most simple tridentate complex of bismuth was envisaged to be based on commercially available diphenoxybenzene but its bismuthation step only gave oligomeric materials.

The first step was achieved quantitatively with *n*BuLi in THF at rt, as determined by a D_2O quench after 18 h. Addition of $BiBr_3$ to the lithiated intermediate failed in all the three iterations of this experiment: the proton NMR spectrum of the crude mixtures showed a contiguous unresolved peak spanning from 6 to 8 ppm. This suggested some sort of oligomerisation occurred.

At first, autometalation was considered as a potential side reaction involving the lithiated species.[423] This would involve one of the lithiated rings performing a directed lithiation *ortho* to a second phenoxy group. Further reaction with an electrophile would produce a variety of different products, depending on the position of the lithiated site at the moment of the quench. However, while this would provide a reasonable explanation, it is not consistent with experimental observations, since

the tri-deuterated species could be detected by NMR spectroscopy after 18 h at rt, thus suggesting the corresponding tri-lithiated species formed succesfully.

With hindsight, Nakatsuka's 'interrupted' synthesis of the phosphorus analogue of this compound (see Scheme 4.10) is quite enlightening.[377] That process entailed mono-lithiation, quench with PCl_3, *in situ* oxidation of the phosphorus atom with S_8 and finally formation of the two remaining P–C bonds under $AlCl_3$-mediated S_EAr conditions. A similar tri-lithiation could have been performed but presumably did not yield the desired product. Unfortunately, the procedure cannot be transplanted as it is to bismuth, due to the acidity of $AlCl_3$, which would cause protodebismuthation. The instability of the mono-arylated $ArBiX_2$ species should be taken into account too.

One final argument to explain the poor outcome of this reaction might be the acid-sensitivity of the product, which is rather electron rich, due to the presence of the *ortho*-phenoxy groups, and, once again, would be prone to protodebismuthation. However, if this occurred, 1,3-diphenoxybenzene should have been detected but this was not the case. Cleavage of one or two Bi–C bonds instead of all three remains a possibility. Moreover, triarylbismuth species containing two *ortho*-alkoxy groups have been synthesised and characterised crystallographically,[424,425] further downplaying this explanation. This also rules out a potential explanation attributing the lack of success to the narrow width between the alkoxy substituents and the consequent difficulty of the installation of a bismuth atom between them.

Given the tendency of heteroangulenes to maintain a rather flat structure, it was considered that this would constrain bismuth in a potentially unfavourable conformation in which its three ligands are far from the 90° angles that usually characterise triarylbismuth species. In order to minimise this risk, the linker length was extended by placing an additional CH_2 in the chain. Efforts to make the corresponding bismuth complexes are reported in Schemes 4.24 and 4.25.

In the first case the ligand **26** was synthesised from resorcinol and 2-bromobenzylbromide. Attempts to achieve halogenation of the central position of the middle ring failed. These encompassed lithiation with LDA, eventually followed by quenching with NBS (condition b) in Scheme 4.24) or, alternatively, iodination with I_2 and Ag_2SO_4.[426] In the first case metalation could not be detected when an aliquot of the reaction mixture was quenched with D_2O after 2 h. Due to the presence of several unidentified species already in this early phase, the reaction was stopped. Commercial LDA had been titrated beforehand, so the failure of the reaction was ascribed to issues with a contaminated batch of dry THF.

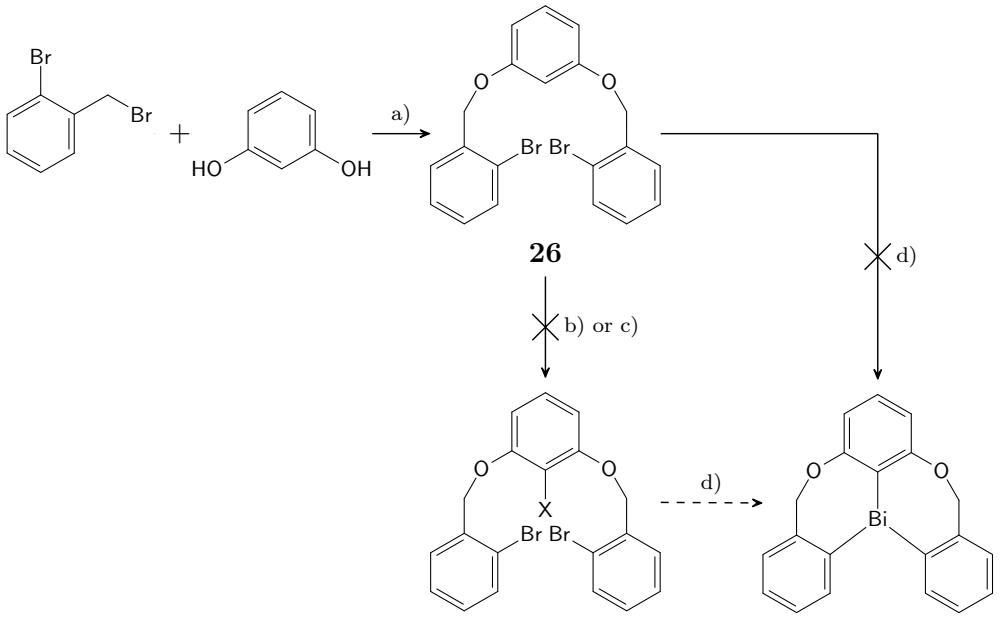

Scheme 4.24: The linker length was extended by introducing an extra methylene. Conditions: a) K_2CO_3, acetone, 60 °C, 84%; b) LDA, THF, 0 °C, then rt for 2 h (at this point NBS should have been added but lithiation did not work and the sequence was interrupted); c) I_2, Ag_2SO_4, MeOH, rt; d) *n*BuLi, THF, −78 °C for 15 min, then rt for 2.5 h, finally $BiBr_3$, THF, −78 °C for 15 min, then rt overnight.

The iodination with the silver salt was similarly unsuccessful (condition c) in Scheme 4.24): work-up of the reaction after 6 h revealed the presence of at least six different species, as determined by the diagnostic ^{1}H NMR benzylic signals. Only traces of the iodinated compound were detected by HRMS analysis, whereas starting material was not present at all, neither were any other species containing one or two bromines, due to the absence of the characteristic isotope distribution. Considering a scale-up of this method would be expensive due to the use of Ag_2SO_4, further understanding of the outcome of this reaction was not pursued. Instead, it was decided to by-pass the challenging halogenation by performing a one-pot tri-lithiatiation of the di-brominated species *via* two lithium-bromine exchanges and a directed lithiation (condition d) in Scheme 4.24). This method did not provide the desired product.

Our focus then briefly turned to the second bismuth complex with one methylene in the linker chain, as summarised in Scheme 4.25. Its synthesis was envisaged to entail an S_N2 reaction between 2-bromo-1,3-bis(bromomethyl)benzene **27** and 2-bromophenol. The former was prepared *via* radical bromination of the corresponding 2-bromo-*m*-xylene with NBS.

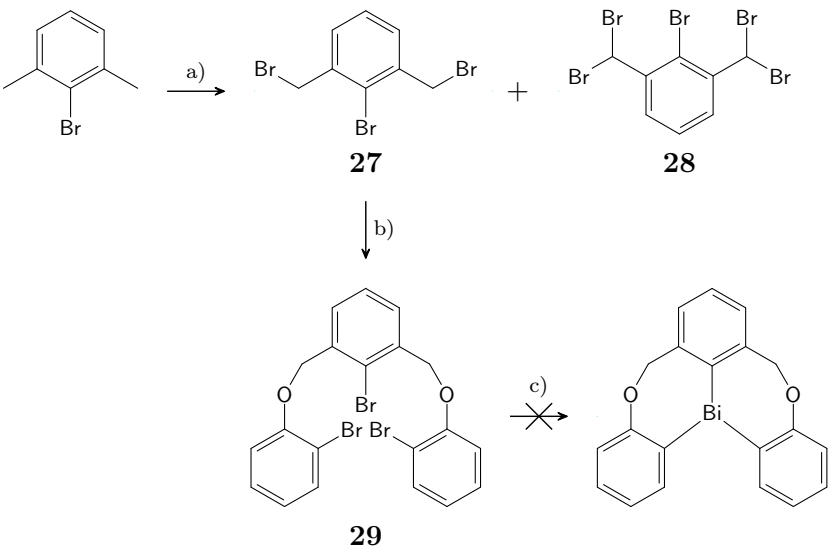

Scheme 4.25: Conditions: a) NBS, BPO (3.8%), CCl_4, 100 °C, 27 h, 22%; b) 2-bromophenol, K_2CO_3, acetone, 60 °C, 16 h, 68%; c) *n*BuLi, THF, −78 °C, then $BiBr_3$, THF, −78 °C.

Early tests performed the bromination reaction in DCM,[427] but rapid decomposition of the brominating reagent was observed. The solvent was therefore replaced with carbon tetrachloride, since the majority of the reported conditions employ this. Benzoyl peroxide (BPO) was also added in catalytic amount, following literature procedures.[428] Heating the reaction mixture in CCl_4 with a stoichiometric amount of NBS did not achieve completion. Additional NBS (1 equiv) was employed, which caused the complete consumption of the xylene starting material but, unfortunately, also formation of large amounts of over-brominated species. Purification of the crude mixture by chromatography was attempted but only allowed the isolation of the over-brominated species **28**, which was recrystallised from hot cyclohexane. A repetition of the reaction with 2.3 equiv of NBS and 3.8% BPO allowed the isolation of 22% of pure material by crystallisation.

Coupling of **27** with 2-bromophenol was then undertaken. The reaction was performed in acetone at reflux, in the presence of K_2CO_3 and gave the desired product **29** in 68% yield without further purification. Finally, lithiation was attempted but significant solubility issues were encountered: in THF (0.1 M) the compound was slightly insoluble at room temperature and heating was required to fully dissolve it; as soon as *n*BuLi was added and presumably lithiation occurred, the metalated species precipitated. Quench of an aliquot with D_2O after 2 h showed formation of several species, none of them being the desired tri-deuterated

compound. There remain doubts about the representativeness of the aliquot taken, since the desired intermediate may have not been in solution at the time of sampling. This reaction has not been explored further.

The synthesis of an analogue complex with two methylenes in the linkers instead of one was undertaken. This relies on the same starting material, 2-bromo-1,3-bis(bromomethyl)benzene **27**. The tridentate ligand **30** was obtained quantitatively and without further purification by nucleophilic substitution of the benzylic bromides by deprotonated (NaH/THF) 2-bromobenzyl alcohol. Bismuthation was then pursued. Differently form the bismuthation discussed in Scheme 4.25, no solubility issues were detected at concentrations around 0.5 M at rt. Nonetheless, further dilution was decided in order to disfavour oligomerisation arising from intermolecular quench of the lithiated species, therefore the reaction was carried out at $[\mathbf{30}]_0 = 0.05$ M. Another action taken with the same intent was to add diluted $BiBr_3$ (0.1 M) to the lithiated species instead of the other way around.

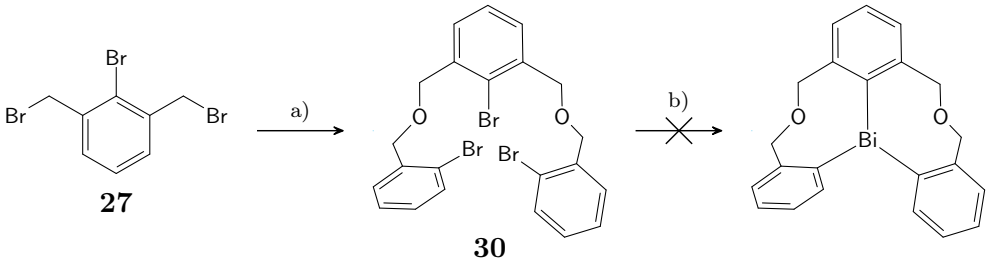

27 **30**

Scheme 4.26: Conditions: a) 2-bromobenzyl alcohol, NaH, THF, 0–25 °C, 18 h, 99%, b) *n*BuLi, THF, −78 °C, then $BiBr_3$, −78 °C, overnight.

Product formation was detected by HRMS, although not as the main species, during a sampling performed at 18 h. The corresponding NMR spectrum was not as rewarding. Once again, the benzylic region of the proton spectrum was quite diagnostic: two couples of diastereotopic protons, plus two additional non-diasterotopic ones were detected. Moreover, an unexpectedly densely populated aliphatic region was noticed. A more in depth look at the HRMS spectrum solved the conundrum: various butylations of the ligand had occurred during the reaction. In particular the following species were detected by HRMS: desired product with an extra butyl group (581.1875 m/z), fully debrominated mono-butylated starting material (392.2578 m/z, ammonium adduct) and fully debrominated di-butylated starting material (448.3203 m/z, ammonium adduct), fully debrominated starting material (336.1951 m/z).

These compounds are all products of the Wurtz-Fittig coupling, which consists in the reaction of a lithiated species with an alkyl halide to give the corresponding

alkylated compound. In this case the alkyl halide was butyl bromide, the side-product of lithium-bromine exchange. This is a well-recognised side-reaction of lithium-halogen exchange,[429] but was overlooked in this phase. It is reported to occur more readily in THF than in Et_2O and at temperatures higher than those at which lithium-halogen exchange reactions are performed, *e.g.* at room temperature.[430] The formation of this series of side products is thus explained by a slow reaction between the tri-lithiated species and $BiBr_3$. Upon warming to rt, the unreacted or partially unreacted lithiated species underwent Wurtz-like coupling with *n*-butylbromide, yielding the variety of products observed by HRMS.

The synthesis of one additional complex was attempted (see Scheme 4.27), which possessed nitrogen atoms instead of oxygens in a doubly benzylic linker similar to the one characterising the complex just discussed. Synthesis of ligand **33** was achieved quantitatively *via* S_N2 reaction between amine **31** and fluorinated of 2-bromo-1,3-bis(bromomethyl)benzene **32**. In turn, the amine was obtained quantitatively by reductive amination of 2-bromobenzaldehyde with isopropylamine. The dibrominated xylene represented again the weak point of the synthetic sequence, since the compound was synthesised only in 30% yield. This time, it was possible to isolate and characterise all the bromination products obtained.

Lithium-halogen exchange was performed as usual with *n*BuLi in tetrahydrofuran at −78 °C and a D_2O quench of an aliquot taken after 2 h showed full incorporation of deuterium and absence of any side-products. Addition of $BiBr_3$ caused the solution to turn dark within minutes. The reaction was allowed to warm up to rt over the course of 2 h. At that point it was sampled and the corresponding ^{19}F NMR spectrum showed a promising resolved peak (−113.7, t, J = 9.9 Hz) surrounded by several tiny peaks, some of which were broad. The reaction was then processed with an aqueous work up and the crude was purified by column chromatography in DCM/Et_3N 96:4. Triethylamine was added to minimise the risk of protodebismuthation on silica. Interestingly, the process yielded not the bismuth complex that was expected but its butylated counterpart **34** in 18% yield, as determined by NMR and HRMS analyses.

To negate the Wurtz-Fittig reaction *n*BuLi was replaced with *t*BuLi.[431,432] When treated with *t*BuLi, ligand **33** was fully lithiated, as determined by the usual D_2O quench after 2 h. A bismuth bromide solution in THF was consequently added dropwise and the reaction mixture was observed to turn dark after the first few drops. Addition was continued and no further change was detected. When the process was concluded, the reaction was left at −78 °C for an additional 1 h, then slowly

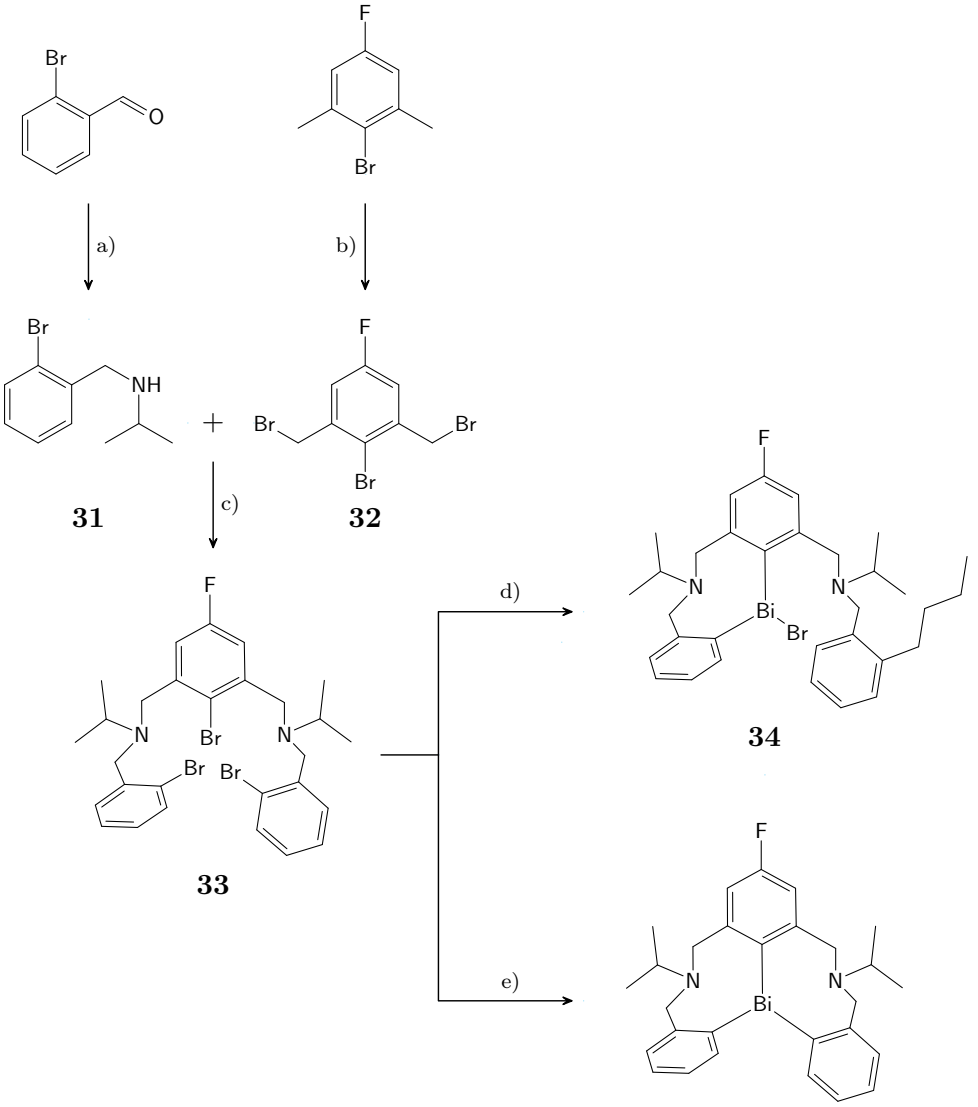

Scheme 4.27: Conditions: a) isopropylamine, EtOH, rt, 18 h, then $NaBH_4$, rt, 2 h, 98%; b) NBS, BPO (3.8 mol%), CCl_4, 100 °C, 18 h, 30%; c) K_2CO_3, acetone, 60 °C, 18 h, 99%; d) *n*BuLi, THF, −78 °C, 2 h, then $BiBr_3$, THF, −78 °C to rt, 2 h, 18%; e) *t*BuLi, THF, −78 °C, then $BiBr_3$, THF, −78 °C, 1 h, then rt, 15 h (compound not isolated due to purification issues).

allowed to warm up to rt. After 15 h an aliquot was taken, worked up and analysed by NMR spectroscopy. This revealed formation of 66% of the desired bismuth complex ($\delta_F = -118.31$ ppm, t, $J = 9.7$ Hz), together with the presence of 33% of debrominated starting material ($\delta_F = -115.20$ ppm, t, $J = 9.7$ Hz), whose assignment was corroborated by HRMS analysis. Unfortunately, purification could not be achieved and thus the compound has not been isolated. Recrystallisation was attempted and some oligomeric material was removed that way. Trituration with Et_2O further improved the purity, which however remained poor. Also, separation of the two species could not be achieved properly since the compound decomposed on silica. Moreover, additional species were detected by HRMS, such as the rather puzzling defluorinated product. The use of *t*BuLi, certainly improved the overall performance of the process, however this did not yield the single product that was hoped for and purification was problematic. Currently this line of research has been dropped, however, a reinvestigation and optimisation of some of the reactions presented in this Section may be valuable.

4.4 Bismatriptycenes

Having encountered serious synthetic challenges with the approach discussed in the previous Section, attention was then turned to bismatriptycene systems. In an effort to keep the synthesis simple and high-yielding, triptycenes with only one heteroatom (*i.e.* bismuth) in the bridge-head positions were excluded *a priori*. Their synthesis would potentially rely on procedures similar to those discussed in Scheme 4.13b–c. However, Suzuki encountered some difficulties in the synthesis of a compound similar to what would be the starting material for the envisaged bicyclisation reaction (see Scheme 4.28),[348] anticipating an even poorer outcome of the desired reaction.

Among 5,10-di-substituted complexes, mixed heterotriptycenes were preferred over homosubstituted examples, due to the fact that in the second case reported yields are always extremely poor for non-perhalogenated species, as discussed in Schemes 4.16 and 4.17.[353,398] Moreover, fully fluorinated or chlorinated species are likely very hard to oxidise,[239] undermining the possibility of successfully subjecting the corresponding bismatriptycene to the oxidation-transmetalation sequence.

The choice of the second atom in the bridge-head position was dictated by two factors: the availability or ease of access of the starting material and the predicted ability to withstand the oxidising conditions required for the oxidation-

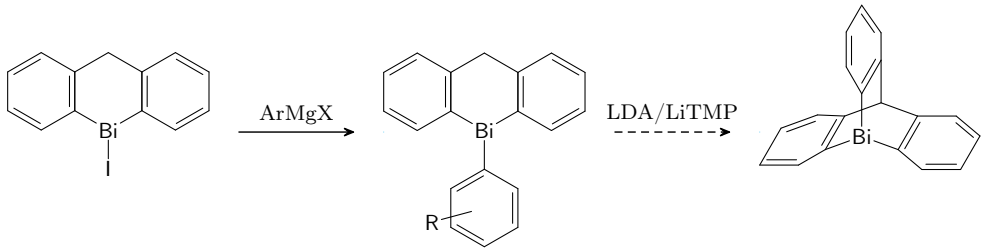

Scheme 4.28: Potential synthetic route for mono-substituted bismatriptycenes. For Ar = 4-tolyl the corresponding species was isolated in 12% yield.[348] If the bicyclisation step were to be performed similarly to that of the corresponding phospha- and arsatriptycene analogues, this would require prior installation of a 2-halosubstituted aryl group, so as to enable lithium-halogen exchange with LDA or LiTMP.[389,391]

transmetalation sequence. With reference to the second point, the safest way to ensure that was thought to be using an element in its highest oxidation state. Several phosphatriptycenes have been made and, in particular, the syntheses envisaged by Tsuji and Iwai and discussed in Scheme 4.21 were deemed particularly appealing.[404,417] The combination of these two considerations resulted in the identification of a phosphine oxide as the bridging unit of choice.

Initially, Tsuji's conditions were attempted,[417] modified to employ the desired phosphine oxide, according to the following sequence (see Scheme 4.29): lithium-halogen exchange of 1,2-dibromobenzene at −110 °C, followed by quenching with PCl_3 to provide tri-(*o*-bromophenyl)phosphine; oxidation of the latter to the corresponding phosphine oxide; triple lithium-halogen exchange of this species, followed by quenching with $BiBr_3$.

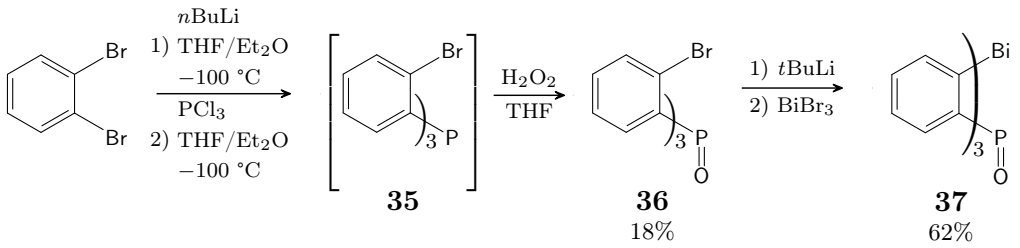

Scheme 4.29: Tsuji's conditions for the synthesis of **35** were employed at first,[417] but isolation of the phosphine resulted particularly complex. This step can be by-passed by oxidising the compound *in situ*.

Synthesis of phosphine **35** was carried out under strict temperature control, to prevent decomposition of the lithiated species.[418] This provided the desired product in 7% yield upon purification by flash column chromatography. More material could be recovered by subjecting some of the impure fractions to oxidation with H_2O_2,

followed by a second chromatographic purification. The pure phosphine **35** was oxidised as well and the two batches were combined to give **36** in 18% yield. A small portion of this material was then treated with *t*BuLi in a test-scale reaction and the resulting tri-lithiated species formed quantitatively, as confirmed by a D_2O quench of a small aliquot of the reaction mixture after 1 h. Quenching with $BiBr_3$ provided the desired bismatriptycene **37** in 62% yield (11% including previous steps).

Gratified by the good yield of the final step, alternative routes to the desired phosphine oxide **36** were briefly tested, in order to overcome the tedious and low-yielding synthesis of the phosphine **35**. In particular, the phosphine oxide moiety was employed as directing group in two different directed *ortho*-metalations (DoMs). However, it was reasoned that, due to the presence of only two lone pairs on the oxygen atom of the phosphine oxide, this group could only direct two lithiations, so an additional directing group on each aromatic ring was required. In the first case this was chosen to be a fluorine atom. An analogue strategy was employed by Kobayashi *et al.* but with a methoxy group instead and for only one of the three aryl rings, as discussed in Scheme 4.14.[408] The fluorine substituent, while providing a similar *ortho* direction for the metalation, was expected to be useful also from an NMR perspective and was preferred for this reason. The required phosphine oxide **38** is easily synthesised *via* a Grignard reaction on *m*-bromofluorobenzene followed by quenching with PCl_3 and oxidation with H_2O_2. Differently from the formation of tri-(*o*-bromophenyl)phosphine, in fact, there is no risk of decomposition *via* a benzyne intermediate in this phase.

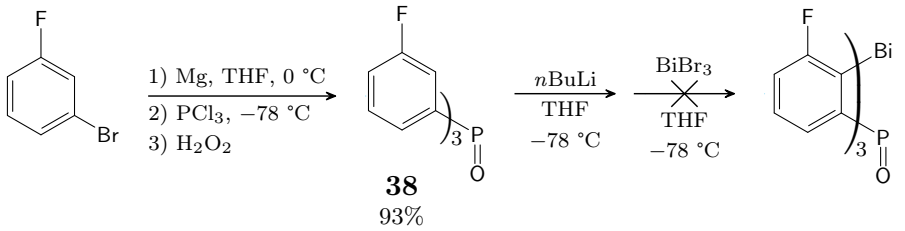

Scheme 4.30: In order to overcome the issues found in the synthesis of **36** a direct lithiation of a pre-formed phosphine oxide was envisaged. Addition to $BiBr_3$ did not fully provide the desired bismatriptycene.

Tri-lithiation of the fluorine-tagged phosphine oxide **38** occurred at −78 °C in the 2-position, as confirmed by NMR analysis of a D_2O quench performed on a small aliquot of the reaction mixture. Bismuth bromide was then added and the reaction was stirred overnight at room temperature. A second D_2O quench at that

point revealed a 7:3 mixture of triptycene and mono-deuterated starting material. This was interpreted as a sign of slow attack of the tri-lithiated species into bismuth bromide, which presumably quenched by an unidentified proton source (possibly butyl bromide *via* E_2)[429] when the reaction was left to warm up to room temperature overnight. The existence of a stabilising Li–F interaction in the lithiated species was held responsible for the slow attack into bismuth and different solutions were considered. The first one was making the bismuth source more electrophilic, *e.g.* by employing a $(PhO)_3Bi$-like species so that the addition of the lithiated species would be driven by the formation of an even stronger Li–O bond. However, differently from phosphorus, triphenylbismuthates are uncommon, with very limited examples in the literature.[362,433] Secondly, forming a harder organopotassium species by transmetalation from the organolithium to, for example, KO*t*Bu. Thirdly, avoiding the presence of the second directing group in the first place.

In order to avoid falling back to Tsuji's procedure, the third option had to be achieved in a different way. List demonstrated that, by performing the directed metalation with LiTMP in the presence of TMS–Cl, the metalated position is immediately quenched by a TMS group.[434] The two reagents do not react with each other due the steric hindrance of the piperidide, which, on the other hand, is absent in the aromatic ring. The silylated aromatic system can then be isolated and eventually reacted with an electrophilic halogen source, such as NBS, to replace the TMS groups with the corresponding halide. This could then undergo lithium-halogen exchange and provide the desired *ortho*-lithiated species, without the additional directing group. In order to make the lithium-halogen exchange even more favourable, it was decided to employ an iodinating species to displace the TMS group. Iodine monochloride (ICl) was chosen, due to its enhanced electrophilic character at the iodine, compared to molecular iodine or NIS.[435]

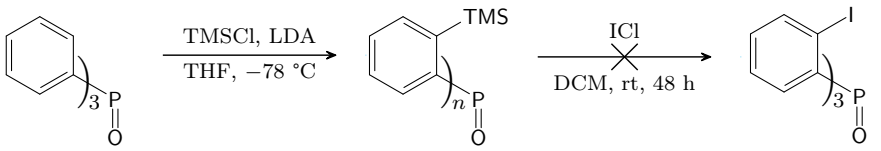

39

Scheme 4.31: An expansion of List's protocol for the *in situ* directed lithiation and TMS quench was explored.[434] This gave the desired tri-silylated species **39a** in 43% yield (plus an additional 26% of the di-silylated species **39b**). Halodesilylation with ICl only provided the di-iodinated species.

Compared to List's report, the transformation envisaged was more challenging, since it involved three sequential lithiation-silylation sequences instead of just one (Scheme 4.31). Importantly, however, still only one directing group, the phosphine oxide, was deemed necessary, since once each lithiation is done the directing ability of the oxide is restored by the TMS quench. Three species were detected in the crude mixture of the lithiation-silylation sequence, corresponding to desired product, di-silylated and mono-silylated species in 58:31:11 ratio and identified by three distinct ^{31}P NMR peaks: 40.6, 38.1, 35.2 ppm, respectively. The first two species, **39a** and **39b**, respectively, could be isolated and characterised. Unfortunately the iodination step was less successful and only di-iodination was achieved when the tri-silylated phosphine oxide was exposed to ICl in DCM at rt for 48 h. This approach was temporarily abandoned but would be interesting to test more extensively, possibly trying a more user-friendly halogen source, such as NBS. It should also be noted that in List's procedure the iodination is achieved with NCS and NaI in AcOH:DCM 6:1 at 80 °C, a fact that was overlooked at the time of the execution of this experiment.

Not satisfied by the less-than-straightforward processes tested so far, we re-considered the synthesis of the phosphine *via* metal-halogen exchange from a 1,2-dihalobenzene but with Iwai's modification.[404] This was presented in Scheme 4.21 and involves formation of a magnesiated species instead of a lithiated one. This allows use of milder cryogenic conditions and thus a better temperature control.

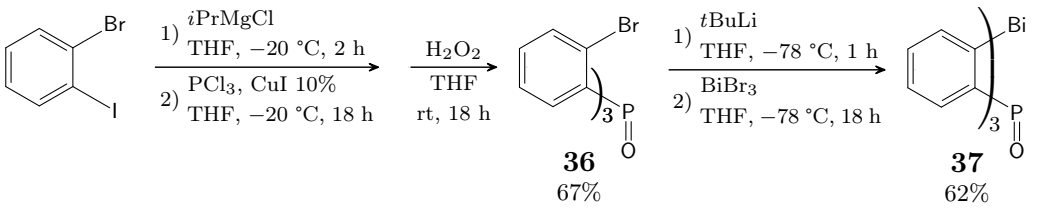

Scheme 4.32: Reinvestigation of Iwai's magnesium-iodine exchange protocol considerably improved the overall bismatriptycene synthesis (overall yield increased from 11% to 42%).

The approach was performed as follows (see Scheme 4.32): *i*PrMgBr was freshly prepared as a ∼0.8 M solution in THF, which was added to a cold (−20 °C) solution of 1,2-bromoiodobenzene and stirred for 2 h; freshly distilled PCl_3 was then added neat, instead of as a solution as done in all the previous experiments; finally catalytic CuI was added, as it was envisaged to form a softer organometallic species than magnesium, which in turn was expected to favour the reaction with PCl_3. The reaction was then allowed to warm up to room temperature overnight and

after aqueous work-up provided the desired phosphine, which was isolated as the oxide in 67% overall yield. The reaction was repeated four times, one of them using 1-bromo-2-iodo-4-fluorobenzene as the starting material, but was successful only when the Grignard reagent was prepared fresh, despite commercial ones had been titrated before use. Finally, it is noted that the commercial Grignard reagent was *i*PrMgCl, whereas the one prepared was *i*PrMgBr. The different reactivity could be attributed to different aggregation states.[436,437] It would be worth looking into this, since at least in one case no reactivity at all was observed with newly bought and titrated *i*PrMgCl. Formation of the bismatriptycene was achieved in 62% yield of isolated product, with an unoptimised 42% yield over two steps.

Single crystals could be grown that were suited for crystallographic analysis. The resulting crystal structure is shown in Fig. 4.5 in two orientations. A three-fold symmetry can be seen in the view from the top, along the Bi–P axis (henceforth the 'main axis'). The phenylene rings do not lie parallel to the main axis, with a larger average distance between this axis and the carbon atoms *ipso* to Bi than *ipso* to P (1.820 Å vs 1.651 Å), to accommodate the larger pnictogen. The bismuth atom adopts a trigonal pyramidal geometry, with C-Bi-C angles that are even narrower than in Ph_3Bi (88.51(10)° vs 93.9(5)°, respectively).[34] The Bi–C bond lengths reflect their weakness (2.259(3) Å). The difference with P–C bonds is remarkable (1.806(3) Å) but null in comparison with Ph_3Bi (2.260(14) Å).[34] A comparison with the only other bismatriptycene with a deposited crystal structure, which has a Si–F unit instead of a P=O, showed a close similarity with regard to the properties discussed (average distance main axis–$C_{ipso\ Bi}$ 1.859 Å, Bi–C bond length 2.273(9) Å, C-Bi-C angle 90.2(3)°).[355]

The compound was also characterised by NMR spectroscopy. Proton NMR spectroscopy revealed an extremely deshielded set of signals (8.66, 8.26, 7.44, 7.35 ppm), especially if compared to Ar^F_3Bi (7.64, 7.08 ppm), which may be an indication of the confined nature of the complex. A similar downfield shift is observed by ^{31}P NMR spectroscopy, where the phosphine oxide peak has a chemical shift of 64.7 ppm. As a comparison, tri-(*ortho*-bromophenyl)-phosphine oxide **36** has a ^{31}P NMR chemical shift of 31.6 ppm.

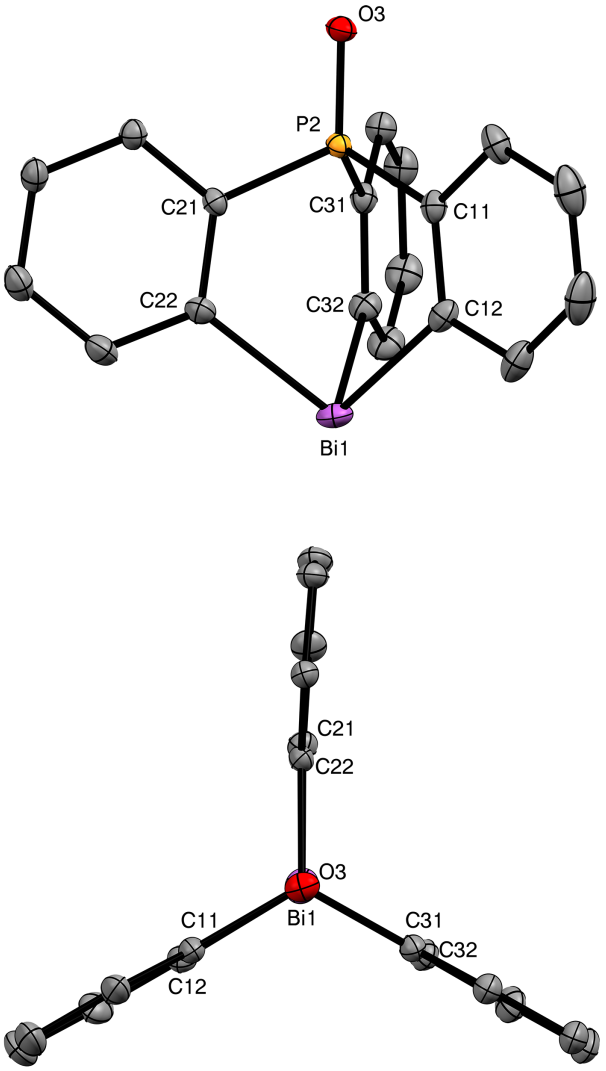

Figure 4.5: Two views of the crystal structure of the bismatriptycene **37**. A trifold axis is visible. Selected bond lengths and angles: average Bi–C_{ipso} = 2.259(3) Å; average P–C_{ipso} = 1.806(3) Å; P–O = 1.486(1); average ∡ C-Bi-C 88.51(10)°; ∡ C-P-C 104.75(12)°. See Section 6.8 for further crystallographic details. This is the second crystal structure ever reported for a bismatriptycene.

4.5 Preliminary tests of oxidation and transmetalation

With a satisfactory synthetic sequence in hand, we then proceeded to test the bismatriptycene under the conditions developed for simple triarylbismuth species. It is worth noting that, despite examples of triptycenes containing at least one bismuth atom,[353–355,398,438] these complexes have been employed as reagents for other reactions only once, to study Wittig reactions of non-stabilised ylides.[438,439] No transformation has ever been performed on the bismuth side of these complexes.

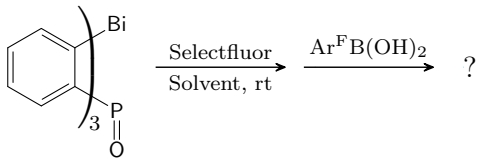

Scheme 4.33: The bismatriptycene was subjected to oxidation-transmetalation conditions. Conditions: CD_3CN or CD_3CN:D_2O 1:1; 1.2 equiv of Selectfluor, 1.5 equiv of $Ar^FB(OH)_2$. Reactions performed in NMR tubes and monitored by NMR spectroscopy.

Oxidation with Selectfluor in acetonitrile caused the complete precipitation of the resulting species. The bismatriptycene **37** was not very soluble to start with (the calculated solubility in acetonitrile is ∼25 mg/mL = 0.050 M) but the oxidation was performed anyway hoping that the reaction would have driven the compound into solution. This was not the case, so the transformation was attempted again in a 1:1 acetonitrile:water solution. Similar solubility issues were noticed before the addition of the oxidant, which worsened when this was added. Moreover, the solution turned vividly yellow. Partial oxidation (∼35%) occurred in both cases, since two sets of signals were detected by ^{1}H NMR spectroscopy for Selectfluor, the second of which corresponds to the reduced oxidant.

Having established that some of the triptycene may have been oxidised, 1.5 equiv of 4-fluorophenylboronic acid were added to the reaction mixture in acetonitrile. Interestingly, some unidentified triptycene species were then observed in solution and, at that point, different peaks were detected by ^{31}P NMR spectroscopy, the major one at 70.02 ppm (broad) and two additional ones at 83.68 and 98.47 ppm, in a 79:18:3 ratio, respectively (Figure 4.6). Interestingly, the peak at 83.68 was a quartet with $J = 7.2$ Hz. Fluorine NMR spectroscopy did not give any useful insight, as only one peak was detected, corresponding to the boronic acid. Leaving the reaction to stand for three weeks did not change the product distribution, suggesting that the species are rather stable. HRMS analysis performed at that point showed

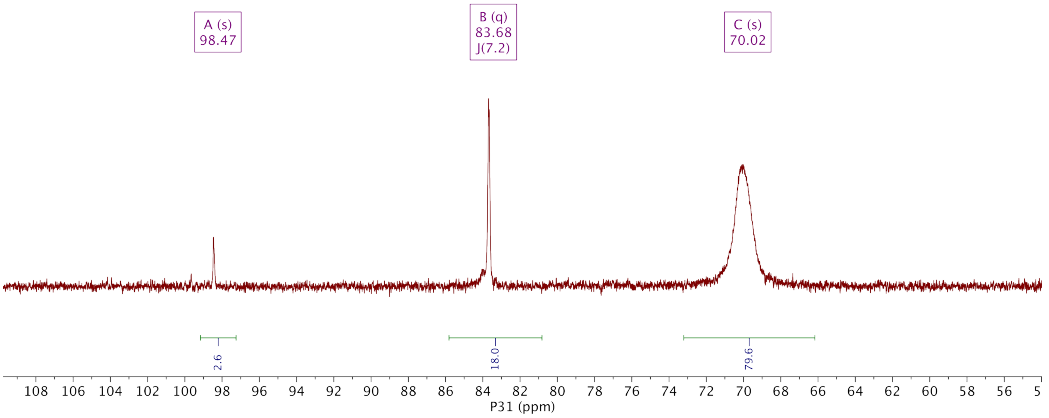

Figure 4.6: Phosphorus NMR peaks observed for the reaction discussed in Scheme 4.33, 30 min after the addition of boronic acid. None of them correspond to known species.

formation of the desired arylated bismuthonium (579.0707 m/z) plus an additional species tentatively assigned to the 4-fluorophenol adduct to the bismatriptycene (595.0659 m/z). The phenol could originate from oxidation of the boronic acid.

Attempts to increase the solubility of the oxidised triptycene were made by replacing Selectfluor with NFSI (Scheme 4.34), as this was expected to reduce the ionic strength of the solution and enable the use of different solvents. Reacting the triptycene with NFSI in acetonitrile did not result in any variation of the NMR spectra. Upon heating at 85 °C, partial consumption (70%) of NFSI was detected by ^{19}F NMR spectroscopy after 1 h and was complete after 2 h. As it can be seen in the first spectrum in Fig. 4.7, this corresponded to the formation of two new ^{31}P NMR peaks at 76.74 and 73.45 ppm (sharp), which are in a 72:6:22 ratio with the starting material **37** (65.7 ppm). At 2 h (Fig. 4.7, second spectrum) the peak at 76.7 ppm, which was the major species at 1 h, disappeared leaving only the other two in a 16:84 ratio. This suggests a considerable portion of material was reduced back to the starting material, which at that point was the major species.

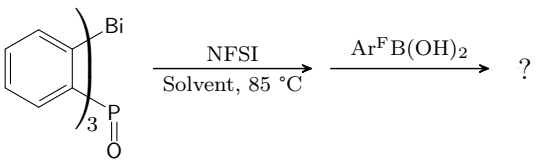

Scheme 4.34: Solvent: CD_3CN or $CDCl_3$. Conditions employed are the same as in Scheme 4.33. Reaction monitored by NMR spectroscopy.

Fluorophenylboronic acid was added and the solution was heated at 85 °C for 1.5 h. Formation of the characteristic peak of BF_4^- was detected in a 14% yield by ^{19}F NMR spectroscopy. The assignment was confirmed by ^{11}B NMR spectroscopy. As the anion can only derive from the transmetalation of the boronic acid to bismuth, as discussed in Section 2.2, this was taken as an indication of an at least partially working transmetalation.

Curiously, the ^{31}P NMR peak corresponding to starting material **37** had completely disappeared at that point. That peak was replaced by five different peaks (Fig. 4.7, third spectrum): 83.63 (encountered in the reaction with Selectfluor, here no multiplicity was evident), 81.58, 76.28 (major species after 1 h during the oxidation), 73.53 (the sharp peak detected during the oxidation) and 73.42 ppm. The ratio between these species was: 3:15:54:5:23. HRMS analysis confirmed the formation of arylated triptycene but it was not possible to determine which of the ^{31}P NMR peaks corresponded to that. Disappointingly, no peak corresponding to this species was detected by ^{19}F NMR spectroscopy either.

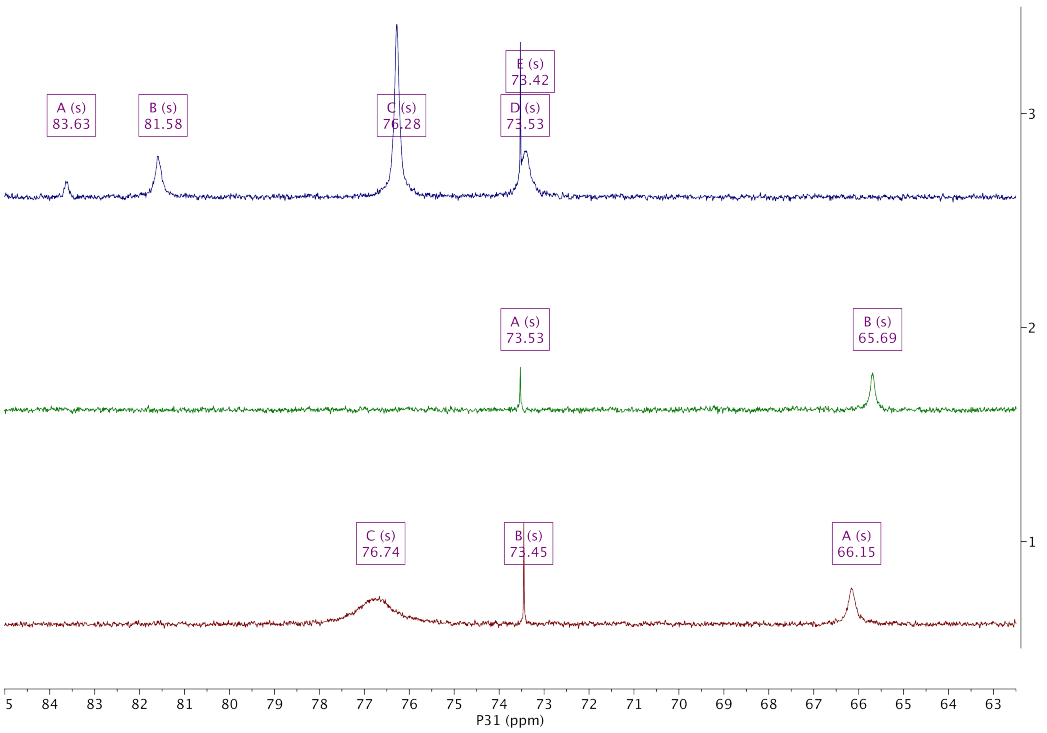

Figure 4.7: Phosphorus NMR peaks observed for the reaction in Scheme 4.34. 1) Spectrum measured 1 h after the addition of NFSI; 2) 2 h after the addition of NFSI; 3) 1.5 h after the addition of $Ar^FB(OH)_2$. The only known species is the bismatriptycene **37** which resonates around 66 ppm. This species is absent in the third spectrum.

The last experiment was repeated in $CDCl_3$ (Scheme 4.34). In this solvent the triptycene was fully soluble at the concentration employed (80 mM). While no reaction was observed at rt, NFSI was completely consumed upon heating at 85 °C for 2 h. At that point a new broad peak was visible by ^{31}P NMR spectroscopy, which integrated 88:12 against the starting material. At the same time NFSI had been fully consumed, so a side reaction may be occurring. A broad peak, possibly corresponding to a fluorine atom directly connected to bismuth could be seen by ^{19}F NMR spectroscopy at −100.9 ppm. The chemical shift would be consistent with a Bi–F signal of a bismuth species containing only one fluoride,[78] and the broadness would be explained by the quadrupolar nature of bismuth.

The boronic acid was added and the reaction was heated at 85 °C for 1.5 h. Only three species were observable by ^{31}P NMR spectroscopy at that point: 83.3 (q, $J = 7.1$ Hz), 80.5 and 75.5 ppm (very broad). The same coupling constant ($J = 7.1$ Hz) was measured for a ^{19}F NMR peak at −142.84 ppm. This peak also showed the usual tetrahedral boron pattern, as corroborated by a sharp peak observed by ^{11}B NMR spectroscopy, therefore the peaks observed by the three different NMR analyses was assigned to a BF_3 adduct of a phosphine oxide. It is unclear which triptycene formed the adduct: the starting material or any of the intermediates.

Independent experiments demonstrated the ease of formation of these adducts (Scheme 4.35). Phosphine oxide **38** was used for these tests, due to the similarity to the bismatriptycene and availability in large amounts. When 4-fluorophenylboronic acid was reacted with Selectfluor at 85 °C in the presence of the phosphine oxide, decomposition of the first species was observed over the course of 24 h and formation of traces of fluorobenzene, 1,4-difluorobenzene and, more importantly, the BF_3 adduct to the phosphine oxide, as confirmed by ^{31}P and ^{11}B NMR spectroscopies. The ^{31}P NMR peak resonated at 42.5 ppm, approximately 17 ppm more deshielded

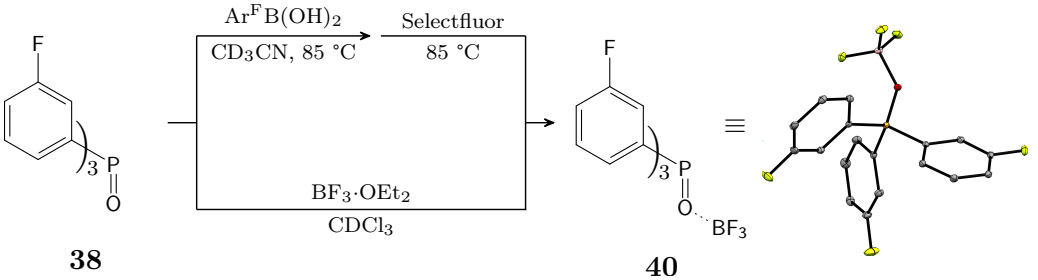

38 **40**

Scheme 4.35: In order to compare the effects of the formation of an adduct between BF_3 and the phosphine oxide moiety in the triptycene **37**, a similar authentic compound was made by adding $BF_3{\cdot}OEt_2$ to phosphine oxide **38**.

than phosphine oxide **38**. Curiously, the adduct did not form when the phosphine oxide was exposed only to Selectfluor, suggesting that BF_3 does not form favourably from BF_4^- and implying that the boron source is ultimately the boronic acid. Phosphine oxide **38** was finally reacted with $BF_3{\cdot}OEt_2$ and formed the BF_3 adduct **40** quantitatively (Scheme 4.35). The compound could also be crystallised and the structure determined by X-ray diffractometry (inset of Scheme 4.35). The analogue adduct **41** to bismatriptycene **37** was synthesised in the same way, *i.e.* by exposing a $CDCl_3$ solution of the latter to $BF_3{\cdot}OEt_2$. The desired species formed instantly and was shown to resonate at 82.4 ppm by $^{31}P\{^1H\}$ NMR spectroscopy as a quartet (J = 6.9 Hz). Correspondingly, a ^{19}F NMR peak resonating at −142.48 showed the same coupling constant (d, J = 6.9 Hz), corroborating the assignment. Upon standing for 10 d crystals formed that were suitable for SC-XRD analysis. A crystal structure of the adduct could be determined and is reported in Fig. 4.8. Compared to the free bismatriptycene **37** the following variations are noteworthy: the Bi–C bond length increases from 2.259(3) to 2.266(11) Å, conversely, the P–C bond length decreases from 1.806(3) to 1.787(11) Å, finally the coordination of BF_3 increases the P–O bond length from 1.486(1) to 1.527(5) Å. The increased Bi–C length, although minimal, may be suggestive of a greater weakness of those bonds.

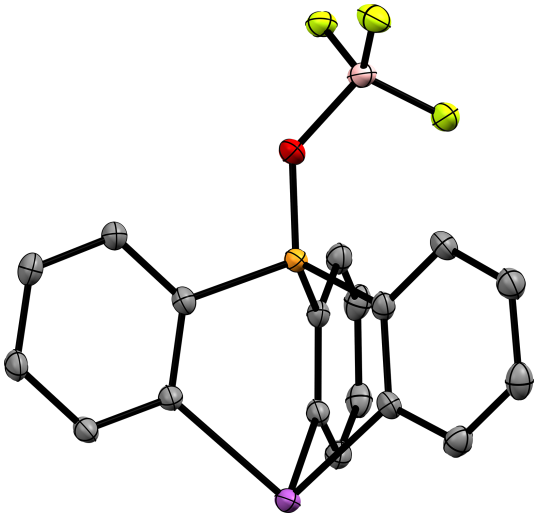

Figure 4.8: Crystal structure of the BF_3 adduct (**41**) to bismatriptycene **37**. The species was found to resonate at 82.4 ppm by ^{31}P NMR spectroscopy.

Slow evaporation of the reaction mixture corresponding to Scheme 4.34 over some weeks allowed the growth of two independent sets of single crystals that were suited for crystallographic analysis. One corresponded to the internal standard **9**

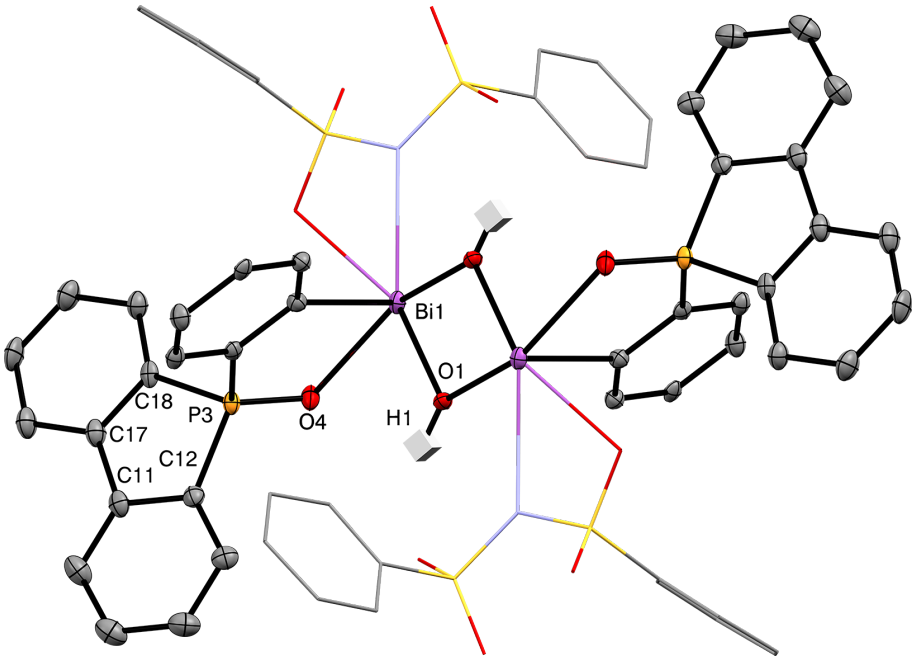

Figure 4.9: Crystal structure of dimer **42** obtained as a side product of the oxidation of bismatriptycene **37** with NFSI (here depicted with wireframes). The nature of the two bridging atoms, here depicted as oxygens, is uncertain, as solution of the structure with fluorides instead of oxygens gave similarly good results. Cubes indicate negative electron density.

and will not be discussed any further: more details can be found in Section 6.8. A preliminary solution of the second in depicted in Fig. 4.9. This shows a dimer, with two bismuth atoms bridged by two other atoms, whose exact identity remains at the moment unclear. In fact, both fluorine and oxygen gave reasonable solutions and are chemically meaningful, in the first case because of the use of a fluorinating agent as the oxidant, in the second because the reaction was performed in non-inert conditions, so water may have been included in the crystal.

The average Bi–A, where A is the bridging atom, bond length of 2.25(1) Å did not provide any further insight, since similar structures deposited in the CCDC have similar bond lengths with the two possible atoms (see for example CCDC entries EBOTOE,[440] QOWZEH[441] and IGETIA[318] for oxygen-bridged dimers and FUBKIZ[231] for the most relevant fluoride-bridged dimer). In the structure reported in Fig. 4.9 it was decided to assign the electron densities to two oxygen atoms, but there remain some unassigned electron density around those atoms, which seems too large for protons. If this was the case, a hydrogen bond with the oxygen of the sulfonimide may be in place.

A dibenzophospholene oxide moiety is well distinguishable, with a bismuth atom coordinating to the its oxygen atom (O4). The phosphorus atom also bears a 1,2-di-substituted phenylene ring, whose second substituent is the bismuth atom. The negative charge of the sulfonimide, the species resulting from the reduction of NFSI, is stabilised by an interaction with the bismuth(III) atom. The latter overall adopts a very distorted trigonal pyramidal geometry, with the three ligands being the phenyl ring, connected to bismuth through carbon C6, and the two oxygen atoms of the bridge. Secondary interactions are present with the oxygen atom of the oxaphosphetane O4, and with the nitrogen atom and one of the oxygen atoms of the sulfonimide.

The unexpected formation of this compound must occur through an unusual equatorial-equatorial coupling of two of the three aryl groups that constitute the triptycene structure, that consequently forms a new C–C bond between carbons C11 and C17 (Scheme 4.36). This is envisaged to occur before the transmetalation, potentially as a side effect of heating the reaction at 85 °C and certainly as a way to release some strain in the triptycene structure. The existence of a ligand coupling product requires prior oxidation of bismuth, therefore the bridging atoms in the crystal structure are expected to be fluorines. This of course does not exclude a ligand exchange before crystallisation occurs, replacing the fluorides with hydroxides.

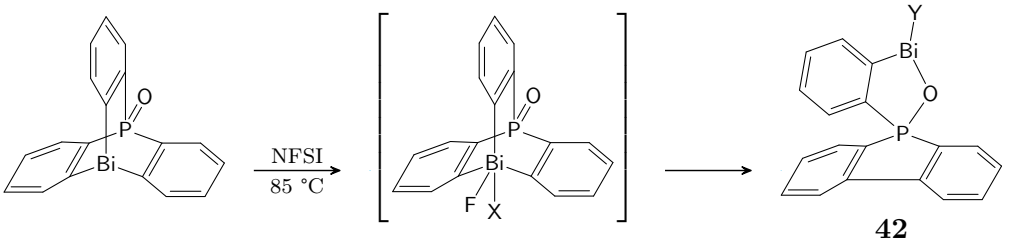

42

Scheme 4.36: The envisaged mechanism for the formation of the monomer of compound **42**. X is the sulfonimide resulting form the reduction of NFSI; Y can be either an OH unit or a fluoride.

Finally, the arylation of 6-fluoronaphthol was tested (Scheme 4.37) and this indeed occurred, even though only trace amounts (<5%) of product were detected, as confirmed both by ^{19}F NMR spectroscopy and HRMS. Despite the extremely modest yield, the result is of the utmost importance, since it demonstrated that the bismuthonium is capable, first of all, of undergoing nucleophilic attack from the naphtholate and, second, performing the desired ligand coupling to deliver the arylation product, both of which were not taken for granted, given the constrained structure of the triptycene.

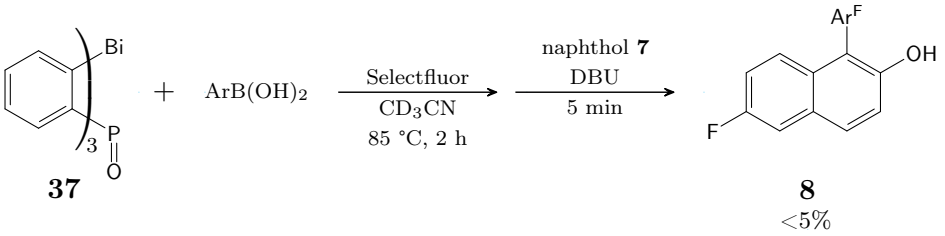

Scheme 4.37: The bismatriptycene **37**, upon oxidation and transmetalation, is capable of arylating naphthol **7**. Reaction performed in an NMR tube and monitored by NMR spectroscopy. Product formation was also confirmed by high-resolution mass spectrometry.

A possible reason for the low yield may be attributed, once again, to BF_3. The addition of DBU to trigger the arylation consumed the ^{31}P NMR quartet at 83.7 ppm (assigned to the BF_3 adduct **41** to the phosphine oxide moiety of the bismatriptycene, see Fig. 4.8), which reappeared at the chemical shift corresponding to the free bismatriptycene (65.6 ppm) This is consistent with DBU interacting with BF_3 and releasing the triptycene. It is suggested that a considerable amount of triptycene **37** is trapped as the adduct with BF_3 and does not undergo the oxidation-transmetalation sequence. This is the case at least when the boronic acid is added before the oxidant. If the oxidation is carried out beforehand this issue may be minimised. The 'inverted' order of addition had been tested in an attempt to prevent the formation of the dibenzophospholene oxide side product (Scheme 4.37). Therefore a good compromise might be to perform the sequence with the standard order of addition but employing a lower temperature. Alternatively a sacrificial phosphine oxide or any other Lewis base may be added before the oxidation, so that the triptycene remains free from BF_3 throughout the transformation.

Given the sparing solubility of the oxidation product of the reaction with Selectfluor, attempts have been made to isolate the oxidised triptycene, with the intent of employing that as a stable advanced precursor. These were not successful, since an aqueous work-up yielded the reduced starting material. Isolation could potentially be performed differently, so as to avoid water, for example by precipitation with an anti-solvent.

5

Conclusions and outlook

Tetraarylbismuthonium salts were explored as arylating agents for phenols and phenol-like compounds. Excellent performance was shown with a 2-naphthol test substrate. The requirement for base was highlighted. The synthesis of bismuthonium salts, traditionally achieved *via* multi-step protocols, was demonstrated to occur quantitatively in a one-pot methodology which employed bench-stable, commercially available triarylbismuth species. Key to this approach was the use of fluorinating agents as oxidants: these allowed the introduction of a fluoride moiety in the oxidised bismuth species, consequently enabling transmetalation. The fast and quantitative arylation showcased with isolated bismuthonium salts, together with the newly achieved facile access to the latter, were promising foundations for the investigation of a catalytic manifold for the arylation of phenols. For this to occur, the compatibility of all components of the system was crucial. Preliminary results showed that this was not the case, with the overall process seemingly stopping once transmetalation was completed. Possible side-reactions were extensively studied, indicating the interactions between the nucleophilic substrate, the required base and the fluorinating agent as potentially deleterious. Similarly, $BF_3{\cdot}OEt_2$, the Lewis acid hitherto employed to mediate the transmetalation, was shown to prevent arylation. Measures, such as the use of sterically hindered bases and Lewis acids, were taken to prevent this from occurring, to no avail. Finally, the discovery that the transmetalation could occur without Lewis acid, provided higher temperatures were maintained, led to a re-evaluation of the approach towards bismuthonium-mediated arylation. This resulted in the separation in time of the formation of the active bismuth species and the ligand coupling.

The formation of heteroleptic bismuthonium salts by the introduction of a unique group *via* transmetalation was explored for approximately eighty different boronic acids. The methodology was demonstrated to tolerate the vast majority of them, including several heteroaromatic examples. Excellent tolerance was demonstrated for moderately sterically hindered groups. The most significant limitations were found with extremely electron-poor or sterically demanding aryl groups, as well as with alkyl and pyridyl boronic acids. In the first two cases, $BF_3{\cdot}OEt_2$ was proposed as a solution to expand the boronic acid scope to more challenging groups. Semi-quantitative models were proposed to determine *a priori* the ease of these transmetalation reactions. This required the identification of suitable descriptors for electronics and sterics. The NMR chemical shift of appropriate nuclei was proposed in the first case, whereas Boltzmann-weighted buried volume (wV_{bur}) was defined and calculated through an original script in the second case. The migratory

aptitude of the unique group was then studied in the arylation of a 6-fluoro-2-naphthol and dimethyl-2-fluoromalonate. Interpretation of the results required the combination of steric and electronic effect, which was accomplished with linear regression analysis using different descriptors, including the two mentioned above. Two satisfactory models were identified for the interpretation of the chemoselectivity for the arylation of the naphthol. To explore the substrate-dependence of the chemoselectivity, other substrates were explored, including naphthols, phenols, diketones and *N*-nucleophiles. Phenols were also employed in some preliminary mechanistic investigations which suggested that with these substrates the rate-determining step of the ligand coupling is a bimolecular process involving both substrate and bismuthonium.

Chemoselectivity studies highlighted the difficulty in controlling the transfer of the desired group through variations of the electronic and/or steric properties of such group. A tridentate system was then envisaged to overcome these issues, by presenting the substrate with only one transferrable group. A literature review revealed dearth of precedent, thus a rational design approach was followed and two different classes of ligands were targeted. Different linearly-linked ligands were tried first, however, severe difficulties were encountered in either the synthesis or isolation of the corresponding bismuth complexes. Heterotriptycenes were explored next: an optimised synthetic procedure was presented that allowed isolation of a novel bismatriptycene, whose structure was determined by X-ray analysis. The bismatripycene was exposed to the oxidation-transmetalation and arylation conditions discussed in the first Chapters. Arylation of the substrate was achieved, although in poor yield, demonstrating the overall feasibility of the process. Solubility issues in the oxidation-transmetalation sequence were held responsible for the low yield.

Despite the chemoselectivity being less than satisfactory, the ligand coupling step is worth further consideration. In particular it would greatly benefit from computational investigations. In fact, there remains several unanswered questions regarding the mechanism. First of all the origin of the regioselectivity is still unclear: Barton proposed *O*-arylation to occur through an S_N2 mechanism, with the substrate attacking one of the aryl groups connected to bismuth. This could not be fully ruled out or corroborated by the brief mechanistic study presented in Chapter 3, since the process is kinetically identical to the one involving coordination of the substrate to bismuth prior to ligand coupling. Since *O*-arylation could also occur *via* axial-axial ligand coupling, it would be interesting to determine whether both mechanisms are active. This may also give some insights also on

the reasons behind the observed greater activity of naphthols compared to phenols. The role of base in the arylation should be modelled too, in particular whether deprotonation of the substrate occurs on the free species or upon coordination to bismuth. The intervention of the 3-component adduct between substrate, base and bismuthonium hypothesised in Section 3.5 should be ascertained. Regarding the regioselectivity of the arylation with heteroleptic bismuthonium salts, determination of computationally derived descriptors (especially for the electronic component) and creation of a model should be attempted. This should then be compared to the two models employed in Chapter 3. A greater understanding of the reasons governing the chemoselectivity would be highly enlightening.

The most considerable room for improvement lies within the bismatriptycene study. Initial efforts should focus on increasing the solubility of the species. This could be achieved by a solvent optimisation, although this may be limited by the fluorinating agent employed. A possibly more rewarding approach would be to modulate the lipophilic character of the triptycene by introducing non-polar substituents on the aromatic rings. The existence of a BF_3 adduct to the phosphine oxide moiety and its influence on solubility and reactivity of the bismatriptycene should then be assessed. In case of a detrimental effect, mitigation of the pathway resulting in this adduct should be considered. A sacrificial Lewis base was proposed for this. Establishment of a working system should, once again, trigger studies to elevate organobismuthonium chemistry to a catalytic regime, which remains the ultimate goal.

6

Experimental studies

Unless noted otherwise, all reagents were purchased from commercial suppliers and used as delivered. DCM, MeCN, Et_2O and THF were dried using an Inert PureSolv Grubbs-type system (alumina columns, argon atmosphere). Reactions requiring inert conditions were carried out in flame-dried glassware under an atmosphere of dinitrogen using standard Schlenk-techniques. Analytical thin-layer chromatography was performed on pre-coated aluminium-backed plates (Silica Gel 60 F254, Merck), and visualised either by UV light (254 nm) or aqueous acidic potassium permanganate stain. Preparative TLC was performed on pre-coated aluminium-backed analytical plates (Silica Gel 60 F254, Merck) or pre-coated glass-backed preparative plates (Silica Gel 15 F254, Analtech). Column chromatography was performed using Scharlab 60 silica gel (35–70 mesh).

NMR spectra were recorded at 298 K, unless otherwise specified, on the following spectrometers: Bruker Avance III-400 and Bruker Avance-III-500. Reaction monitoring by ^{19}F NMR spectroscopy was performed on the 400 MHz spectrometer: spectra were recorded at 298.0 K operating the spectrometer at 376.50 MHz. Fluorine NMR spectra were acquired using a recovery delay of 30 s followed by a 17.4 µs 90° pulse. Each spectrum consisted of 8 free induction decays (FIDs) collected into 24 K complex data points with a spectral width of 85227 Hz and an acquisition time of 1.538 s. FIDs were multiplied by an exponential window function (line broadening = 0.3 Hz) and zero-filled to 32 K before Fourier Transform. The resulting spectra were manually phased and baseline corrected using MestReNova (versions 11.0.4–14.2.0). Chemical shifts (δ) are given in ppm and coupling constants in Hz. All ^{13}C NMR spectra were measured with ^{1}H-decoupling ($^{13}C\{^{1}H\}$). ^{1}H and ^{13}C spectra are referenced to the deuterated solvent residual peaks, namely:

- $CDCl_3$ (7.260 ppm; 77.16 ppm),
- C_6D_6 (7.160 ppm; 128.06 ppm),
- CD_3CN (1.940 ppm; 1.32 ppm),
- CD_3OD (3.310 ppm; 49.00 ppm),
- $(CD_3)_2CO$ (2.050 ppm; 29.84 ppm),
- CD_3SO (2.500 ppm; 39.52 ppm).

Spectra of other nuclei were referenced *via* direct measurement of the absolute frequency of the lock signal, provided by the ^{2}H resonance of the deuterated solvent,

and consequent conversion with IUPAC 'unified scale'.[442] The following abbreviations were used for NMR spectra to indicate the signal multiplicity: s (singlet), br (broad signal), d (doublet), t (triplet), q (quartet), quint (quintet), hept (heptet) and m (multiplet) as well as combinations of them. When combinations of multiplicities are given, the first character noted refers to the biggest coupling constant. Coupling constants were extrapolated also from multiplets containing second order phenomena. These multiplets are indicated as following: $m^{IIord.}$. When the detected multiplicities were not in accordance with the expected ones (*e.g.* a triplet of triplets with the same coupling constants) the notation '$m_{app.}$' was used. For the assignments of ^{1}H, ^{13}C NMR and ^{19}F NMR spectra, DQF-COSY, HSQC-ME, HMBC, H2BC, NOESY, PSYCHE[443] and ^{19}F-HSQC experiments were also performed. The assignment are reported, for all nuclei, as an italicised number which refers to the numbered carbon atom to which they are connected in the drawn molecular structure. For the tetrafluoroborate ion, the reported ^{19}F NMR peak correspond to $^{11}BF_4^-$, which accounts for 79% of the total BF_4^- signal, the remaining 21% being $^{10}BF_4^-$.

High-resolution mass spectrometry (HRMS) analyses were performed on a Bruker micrOTOF II mass spectrometer, interfaced to an Agilent 1200 HPLC. A 1 µL aliquot of the sample was injected into the ion source of the instrument along with a flow of 0.2 mL/min of 70% methanol/water eluent. The mass spectrometer was operated in electrospray ionisation (ESI) mode. The ion peak is always given as that of lowest isotopic mass.

Infrared spectra of neat compounds were recorded over the range 4000–400 cm^{-1} on a Bruker Alpha FTIR spectrometer fitted with a Bruker Platinum ATR Quicksnap™ diamond cell. Melting points were measured using Stuart SMP20 melting point apparatus in open capillaries. IUPAC names of compounds were determined with the program ChemDraw Professional® (versions 16.0–19.1).

6.1 Compounds discussed in Chapter 2

Bismuth tribromide (1)

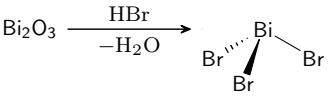

Hydrobromic acid (85 mL of a 48% w/w solution in water, 61 g, 750 mmol, 6.0 equiv) was added to a 500 mL round-bottom flask and heated at 70 °C. Bismuth oxide (58.2 g, 125 mmol, 1.0 equiv) was then added and the resulting suspension was stirred for 15 min. Additional HBr was added until all the material dissolved. The round-bottom flask was equipped with a distillation bridge, connected to a liquid nitrogen-cooled 250 mL Schlenk round-bottom flask. This was in turn connected to a Schlenk line and excess HBr and water were carefully distilled off. When the solids were dry, the bridge was disconnected and the flask was connected directely to the Schlenk line and put under vacuum for 18 h at 120 °C. The bright yellow solids (55.6 g, 124 mmol, 99%) were scraped off the flask and used without further purification. Bismuth bromide could be conserved in a desiccator under nitrogen for months without signs of decomposition. **m.p.** (°C): 217–219.[444]

Tri(4-fluorophenyl)bismuthine (2)

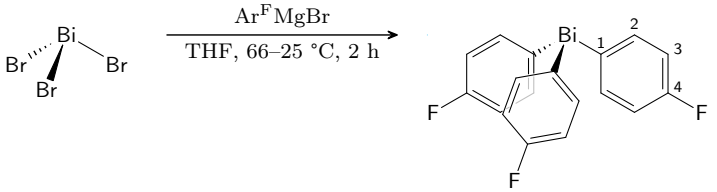

Magnesium turnings (1.60 g, 66.0 mmol, 3.3 equiv) were stirred in a 100 mL two-neck round-bottom flask, together with a couple of iodine crystals and gently heated until the development of purple vapours. Dry THF (30 mL) was then added, followed by drop-wise addition of 1-bromo-4-fluorobenzene (6.70 mL, 10.6 g, 62.0 mmol, 3.1 equiv): heat developed. This mixture was left to stir for 1 h, until it cooled down to rt again. In the meanwhile, another 100 mL round-bottom flask was charged with $BiBr_3$ **1** (8.97 g, 20.0 mmol, 1.0 equiv) and evacuated three times. Bismuth bromide was then suspended in THF (20 mL) and the Grignard reagent was finally added to this suspension* and left to stir for 2 h. The reaction was carefully quenched with H_2O (30 mL) and filtered through silica to remove magnesium

*Better reproducibility was found when the Grignard reagent is added to the bismuth halide, rather than the other way around.

residues. The organic component was extracted with Et_2O (3 × 20 mL) and the resulting organic phases were collected and washed with H_2O (3 × 20 mL), then dried over $MgSO_4$ and concentrated under reduced pressure. The resulting crude material was recrystallised from EtOH, yielding the desired product as a colourless solid (9.21 g, 18.6 mmol, 93%), whose characteristic data are in agreement with the literature.[445] The resulting crystals were suitable for X-ray diffraction analysis: details can be found in Section 6.8. **^{1}H NMR** (500.13 MHz, $CDCl_3$): δ 7.64 (dd$^{\text{II ord.}}$, J = 8.6, 6.2 Hz, 6H, *2*), 7.08 (t$^{\text{II ord.}}_{\text{app.}}$, J = 9.3 Hz, 6H, *3*).**^{13}C{^{1}H} NMR** (125.76 MHz, $CDCl_3$): δ 163.0 (d, J = 247.0 Hz, *4*), 149.6 (br, *1*), 139.3 (d, J = 7.2 Hz, *2*), 118.1 (d, J = 19.9 Hz, *3*). **^{19}F NMR** (470.59 MHz, $CDCl_3$): δ −112.76 (tt, J = 9.3, 6.1 Hz). **HRMS** (ESI$^-$, *m/z*) Calcd. for $C_{12}H_8BiF_2^-$ (M−C_6H_4F): 399.0403. Found: 399.0410. Error: 1.75 ppm.[†] ν_{max} (neat, cm^{-1}): 1572, 1481, 1382, 1209, 1156, 1015, 811, 504, 411. **m.p.** (°C): 92–93.

Dichlorotri(4-fluorophenyl)bismuth (3)

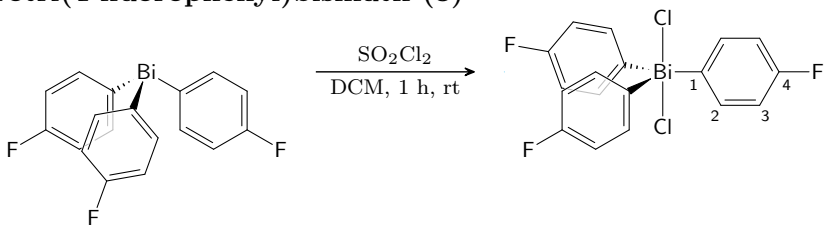

Tri(4-fluorophenyl)bismuthine **2** (4.94 g, 10.0 mmol, 1 equiv) was loaded into a 50 mL two-neck round-bottom flask and dissolved in 50 mL of dry DCM under nitrogen. Sulfuryl chloride (800 µL, 1.35 g, 10.0 mmol, 1 equiv) was then added drop-wise and the resulting mixture was stirred for 1 h. The solvent was then removed under vacuum and the crude thus obtained was recrystallised from cyclohexane, yielding the desired product (5.35 g, 9.47 mmol, 95%) as a colourless solid. **^{1}H NMR** (500.13 MHz, $CDCl_3$): δ 8.54 (dd$^{\text{II ord.}}$, J = 9.1, 5.1 Hz, 6H, *2*), 7.35 (7.08 (t$^{\text{II ord.}}_{\text{app.}}$, J = 8.7 Hz, 1H, *3*). **^{13}C{^{1}H} NMR** (125.76 MHz, $CDCl_3$): δ 164.6 (d, J = 254 Hz, *4*), 149.9 (d, J = 3 Hz, *1*), 136.8 (d, J = 8 Hz, *2*), 119.0 (d, J = 23 Hz, *3*). **^{19}F NMR** (470.59 MHz, $CDCl_3$): δ −106.37 (tt, J = 8.2, 5.1 Hz). **HRMS** (ESI$^-$, *m/z*) Calcd. for $C_{18}H_{12}BiClF_3^+$ (M−Cl): 529.0378. Found: 529.0418. Error: 7.56 ppm. ν_{max} (neat, cm^{-1}): 1567, 1471, 1388, 1223, 1155, 999, 821, 562, 493, 415. **m.p.** (°C): 136–137.

[†]The molecular peak is notoriously difficult to detect, probably due to the small Bi–C bond dissociation energy.[7]

Difluorotri(4-fluorophenyl)bismuth (4)

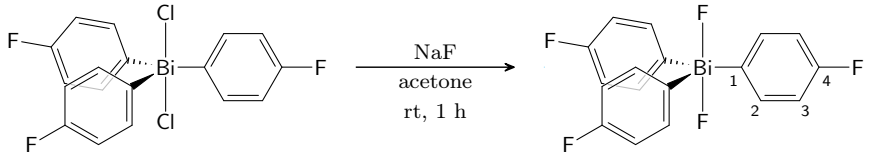

In a 50 mL round-bottom flask dichlorotri(4-fluorophenyl)bismuth **3** (1.13 g, 2 mmol) was dissolved in acetone (15 mL). In another 50 mL flask NaF (420 mg, 10 mmol, 5 equiv) was dissolved in 15 mL of water and this solution was added to the previous flask. The resulting mixture was let to stir 1 h, then acetone was removed by evaporation from the mixture and the aqueous phases were extracted with DCM (3 × 20 mL). The organic phases were collected and concentrated *in vacuo* and the resulting crude was recrystallised from cyclohexane to yield the desired product (1.02 g, 1.92 mmol, 96%) as a colourless solid. **^{1}H NMR** (500.13 MHz, $CDCl_3$): δ 8.22 ($dd^{II\ ord.}$, J = 9.1, 5.4 Hz, 6H, *2*), 7.36 ($t_{app.}$, J = 8.7 Hz, 6H, *3*). **^{13}C{^{1}H} NMR** (125.76 MHz, $CDCl_3$): δ 165.1 (d, J = 253.4 Hz, *4*), 147.7 (td, J = 10.3, 2.9 Hz, *1*), 136.3 (dt_{app}, J = 8.1, 4.0 Hz, *2*), 118.7 (d, J = 21.8 Hz, *3*). **^{19}F NMR** (470.59 MHz, $CDCl_3$): δ −106.13–−106.34 (m, 3F), −157.81 (s, 2F). **HRMS** (ESI^-, *m/z*) Calcd. for $C_{18}H_{12}BiF_4^+$ (M−F): 513.0674. Found: 513.0662. Error: 2.34 ppm. ν_{max} (neat, cm^{-1}): 1573, 1476, 1392, 1216, 1155, 1010, 828, 802, 572, 500. **m.p.** (°C): 111–112.

Tetra(4-fluorophenyl)bismuthonium tetrafluoroborate (5a)

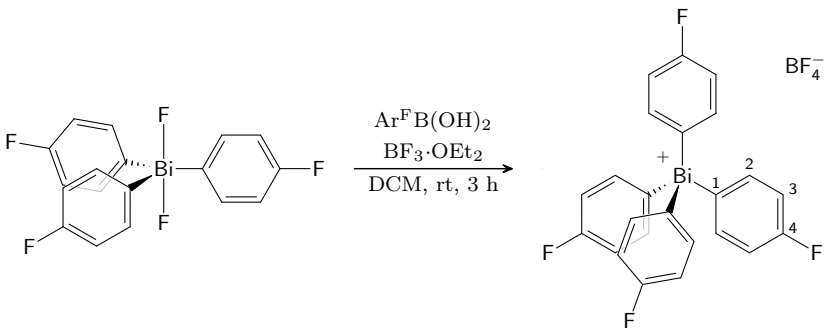

Difluorotri(4-fluorophenyl)bismuth **4** (1.06 g, 2.00 mmol, 1.0 equiv) and 4-fluorophenylboronic acid (308 mg, 2.20 mmol, 1.1 equiv) were dissolved in dry DCM (20 mL). This solution was cooled down to 0 °C, then $BF_3{\cdot}OEt_2$ (380 µL, 426 mg, 3.00 mmol, 1.5 equiv) was added. The reaction mixture was stirred at rt for 3 h, then sodium tetrafluoroborate (1.1 g, 10 mmol, 5.0 equiv) and water (20 mL) were added.

The organic phase was separated, dried over $MgSO_4$ and concentrated to dryness. The resulting crude material was recrystallised from a 10:1 Et_2O/DCM mixture, providing the named compound in 82% yield (1.11 g, 1.64 mmol). **^{1}H NMR** (500.13 MHz, $CDCl_3$): δ 7.79 (dd$^{\text{II ord.}}$, J = 8.7, 5.2 Hz, 8H, *2*), 7.38 (t$^{\text{II ord.}}_{\text{app.}}$, J = 8.5 Hz, 8H, *3*). **^{13}C{^{1}H} NMR** (125.76 MHz, $CDCl_3$): δ 165.2 (d, J = 255.6 Hz, *4*), 138.0 (d, J = 8.6 Hz, *2*), 133.2 (d, J = 3.6 Hz, *1*), 120.1 (d, J = 21.9 Hz, *3*). **^{19}F NMR** (470.59 MHz, $CDCl_3$): δ −103.87 (tt, J = 8.4, 5.2 Hz, 4F), −147.63 (s, 4F). **HRMS** (ESI$^-$, *m/z*) Calcd. for $C_{24}H_{16}BiF_4^+$ (M−BF_4): 589.0987. Found: 589.0986. Error: 0.17 ppm. ν_{max} (neat, cm^{-1}): 1589, 1574, 1483, 1392, 1303, 1230, 1160, 1056, 1002, 819, 570, 500, 413. **m.p.** (°C): 241–242.

4′,5-Difluoro-[1,1′-biphenyl]-2-ol (6a) and 4,4′′,5′-trifluoro-[1,1′:3′,1′′-terphenyl]-2′-ol (6b)

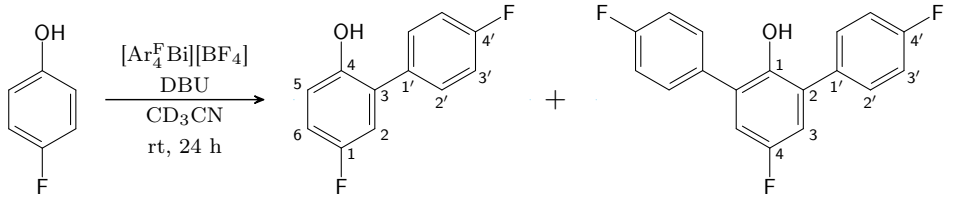

Tetra(4-fluorophenyl)bismuthonium tetrafluoroborate **5a** (306 mg, 0.453 mmol, 1 equiv) and 4-fluorophenol (50.8 mg, 0.453 mmol, 1 equiv) were added to an NMR tube and dissolved in CD_3CN (0.6 mL). DBU (100 µL, 103 mg, 0.675 mmol, 1.5 equiv) was then added and the solution turned bright orange. The reaction was monitored by NMR spectroscopy at 3 h intervals and after 24 h was quenched with a few drops of TFA[‡] until disappearance of the colour. The reaction mixture was diluted with DCM (2 mL) and transferred to a 10 mL round-bottom flask, then all the volatiles were evaporated under reduced pressure. The resulting crude was diluted with EtOAc (0.5 mL), loaded on a preparative TLC plate with a 100 µL micro-syringe and eluted with 250 mL of a 9:1 CyH:EtOAc mixture. Two different bands could be separated and each of them was isolated by scraping the silica off the TLC plate. The material thereon adsorbed was solubilised by stirring the silica in DCM for 1 h, then filtering off the solids and removing the solvent under reduced pressure. The first band (R_f = 0.14–0.30) contained the mono-arylated product **6a**, isolated as an off-white solid (14.0 mg, 68.0 µmol, 15%) whose characteristic data are reported below and are consistent with the literature (^{1}H NMR and mp).[446] **^{1}H NMR** (500.13 MHz, $CDCl_3$): δ 7.48–7.42 (m, 2H, *2′*), 7.21–7.14 (m,

[‡]This causes the decomposition of Ar_3^FBi, simplifying the separation of the different products.

2H, *3′*), 7.00–6.87 (m, 3H, *2, 5 and 6*), OH signal not detected. **^{13}C{^{1}H} NMR** (125.76 MHz, $CDCl_3$): δ 162.8 (d, J = 248.0 Hz, *4′*), 157.2 (d, J = 238.8 Hz, *1*), 148.6 (d, J = 2.7 Hz, *4*), 132.4 (d, J = 3.9 Hz, *1′*), 131.0 (d, J = 8.2 Hz, *2′*), 128.3 (d, J = 8.1 Hz, *3*), 117.0 (d, J = 8.1 Hz, *5*), 116.6 (d, J = 23.3 Hz, *2*), 116.4 (d, J = 21.1 Hz, *3′*), 115.6 (d, J = 22.7 Hz, *6*). **^{19}F NMR** (470.59 MHz, $CDCl_3$): δ −113.43 (tt, J = 8.5, 5.3 Hz, 1F, *4′*), −123.83–−124.10 (m, 1F, *1*). **^{19}F{^{1}H} NMR** (376.50 MHz, $CDCl_3$): δ −113.47 (s, 1F, *4′*), −123.95 (s, 1F, *1*). **HRMS** (ESI$^-$, *m/z*) Calcd. for $C_{12}H_7F_2O^-$ (M−H): 205.0470. Found: 205.0472. Error: 0.98 ppm. ν_{max} (neat, cm^{-1}): 2926, 1605, 1515, 1500, 1434, 1398, 1261, 1224, 1177, 839, 776, 589.

The second band (R_f = 0.41–0.51) contained the di-arylated product **6b**, which was isolated as a pale yellow oil (9.51 mg, 31.7 µmol, 7%) and whose characteristic data are reported below: **^{1}H NMR** (500.13 MHz, $CDCl_3$): δ 7.51 (dd$^{\text{II ord.}}$, J = 8.7, 5.3 Hz, 4H, *2′*), 7.18 (t$^{\text{II ord.}}_{\text{app.}}$, J = 8.6 Hz, 4H, *3′*), 6.97 (d, J = 8.7 Hz, 2H, *3*), 5.05 (s, 1H, *OH*). **^{13}C{^{1}H} NMR** (125.76 MHz, $CDCl_3$): δ 162.7 (d, J = 248.0 Hz, *4′*), 156.8 (d, J = 239.7 Hz, *4*), 145.5 (d, J = 2.3 Hz, *1*), 132.6 (br, *2*), 131.2 (d, J = 8.2 Hz, *2′*), 129.0 (d, J = 8.1 Hz, *1′*), 116.3 (d, J = 23.3 Hz, *3*), 116.1 (d, J = 21.2 Hz, *3′*). **^{19}F NMR** (470.59 MHz, $CDCl_3$): δ −113.51 (tt, J = 8.6, 5.3 Hz, *4′*), −123.76 (t, J = 8.7 Hz, *4*). **HRMS** (ESI$^-$, *m/z*) Calcd. for $C_{18}H_{10}F_3O^-$ (M−H): 299.0689. Found: 299.0694. Error: 1.67 ppm. ν_{max} (neat, cm^{-1}): 3551, 1606, 1510, 1445, 1442, 1396, 1228, 1160, 837, 784, 548.

6-Fluoronaphthalen-2-ol (7)

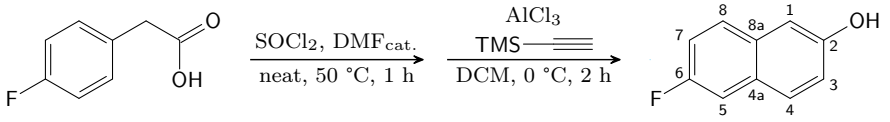

Under an atmosphere of nitrogen, thionyl chloride (7.1 mL, 12 g, 98 mmol, 1.5 equiv) and a drop of DMF were added to 4-fluorophenylacetic acid (10 g, 65 mmol, 1.0 equiv). The reaction mixture was stirred at 50 °C for 1 h, then excess thionyl chloride was removed *in vacuo*. The resulting acid chloride was then added to a stirred suspension of aluminium chloride (12 g, 98 mmol, 1.5 equiv) in dry DCM (25 mL) at 0 °C. Trimethylsilyl acetylene (9.7 mL, 7.7 g, 78 mmol, 1.2 equiv) was then added drop-wise to the resulting red solution over the course of 1 h. The resulting black solution was stirred at room temperature for an additional 1 h. The reaction mixture was then poured onto ice and the organic component was extracted with DCM (3 × 200 mL). The combined organic fractions were then

extracted with aqueous sodium hydroxide (2.0 M, 3 × 150 mL). The aqueous fractions were combined, acidified with concentrated hydrochloric acid until pH<1 and then extracted with DCM (3 × 200 mL). The combined organic fractions were then dried over $MgSO_4$, filtered and the solvent was removed *in vacuo*. The resulting crude residue was purified by silica gel column chromatography (5–10% EtOAc/CyH) to yield the title compound as a pale yellow[§] crystalline solid (2.05 g, 12.4 mmol, 19%).

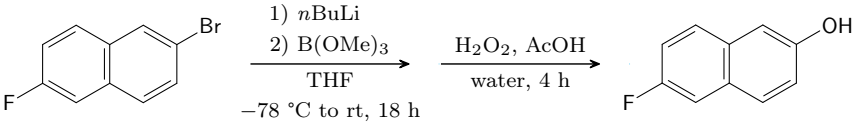

A more effective procedure to synthesise 6-fluoronaphthalen-2-ol is reported below. 2-Bromo-6-fluoronaphthalene (3.00 g, 13.3 mmol, 1.0 equiv) was loaded in a 100 mL Schlenk round-bottom flask and three cycles of vacuum/nitrogen were performed, then dry THF (50 mL) was added and this solution was cooled down to −78 °C, then *n*BuLi (7.0 mL of a 2.3 M solution in hexanes, 16 mmol, 1.2 equiv), was added drop-wise. The resulting solution was stirred for 15 min, then trimethylborate (2.25 mL, 2.08 g, 20.0 mmol, 1.5 equiv) was added over the course of 10 min and the solution went through the following colour changes: from yellow to green, to pale blue, to colourless. The reaction was let to slowly warm up to room temperature and was then stirred overnight. Water (5 mL), acetic acid (5 mL) and hydrogen peroxide (4.5 mL of a 30% solution in water, corresponding to 40 mmol, 3.0 equiv of pure reagent) were added. After 3 h the completion of the reaction was determined by NMR spectroscopy and thus the reaction mixture was diluted with Et_2O and water and extracted thrice. The organic phases were merged, dried over $MgSO_4$ and concentrated under reduced pressure, yielding a crude material that was purified by flash column chromatography (5–10% EtOAc/CyH). The desired product **7** was finally isolated in 76% yield (1.64 g, 10.1 mmol, R_f = 0.38 in 20% EtOAc/CyH). Its characteristic data are reported below and are consistent with the literature (^{1}H and ^{13}C NMR and HRMS).[447] **^{1}H NMR** (500.13 MHz, CD_3CN): δ 7.73 (dd_{app}, J = 8.9, 5.7 Hz, 2H, *4 and 8*), 7.46 (dd, J = 10.3, 2.5 Hz, 1H, *5*), 7.25 (td, J = 8.9, 2.6 Hz, 1H, *7*), 7.20 (d, J = 2.4 Hz, 1H, *1*), 7.17 (br, 1H, OH), 7.14 (dd, J = 8.7, 2.4 Hz, 1H, *3*). **^{13}C{^{1}H} NMR** (125.76 MHz, CD_3CN):

[§]This could be further purified by sublimation using a cold finger apparatus at a severe expense of the yield. In fact, the compound decomposes upon heating. Also, it was observed that the naphthol oxidises over time and darkens, however, even after two years under air, no impurity could be detected by ^{19}F NMR spectroscopy.

δ 158.9 (d, ^1J = 239.9 Hz, *6*), 154.3 (d, ^6J = 2.7 Hz, *2*), 131.9 (*8a*), 128.78 (d, ^4J = 5.4 Hz, *4*), 128.74 (d, ^3J = 9.0 Hz, *4a*), 128.6 (d, ^3J = 8.7 Hz, *8*), 119.3 (*3*), 116.3 (d, ^2J = 25.4 Hz, *7*), 110.5 (d, ^2J = 20.2 Hz, *5*), 109.1 (*1*). **^{19}F NMR** (470.59 MHz, CD_3CN): δ −120.70 ($td_{app.}$ 9.5, 5.6 Hz). **HRMS** (ESI^-, *m/z*) Calcd. for $C_{10}H_6FO^-$ (M − H): 161.0408. Found: 161.0410. Error: 1.24 ppm. ν_{max} (neat, cm^{-1}): 3241, 1602, 1511, 1453, 1394, 1378, 1360, 1278, 1224, 1140, 1107, 958, 940, 870, 806, 680, 652, 578, 525, 481, 471, 425. **m.p.** (°C): 114–115.

6-Fluoro-1-(4-fluorophenyl)naphthalen-2-ol (8)

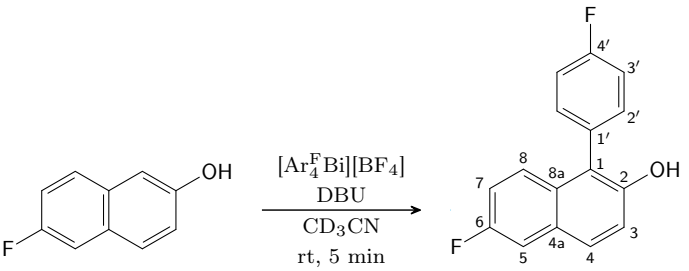

In an NMR tube, 6-Fluoronaphthalen-2-ol (**7**, 13.0 mg, 80.0 µmol, 1.0 equiv) and tetra(4-fluorophenyl)bismuthonium tetrafluoroborate (**5a**, 54.1 mg, 80.0 µmol, 1.0 equiv) were dissolved in CD_3CN, then DBU (18 µL, ca. 18 mg, 120 µmol, 1.5 equiv) was added. The solution turned immediately orange but the colour faded within 5 min, indicating reaction completion. The reaction mixture was worked-up as discussed for compound **6** and isolated by preparative TLC (5% EtOAc/CyH) as a colourless oil (17.0 mg, 66.4 µmol, 83%). **^{1}H NMR** (400.13 MHz, CD_3CN): δ 7.74 (d, J = 8.9 Hz, 1H, *4*), 7.48 (dd, J = 10.0, 2.8 Hz, 1H, *5*), 7.37–7.30 (m, 3H, *8, 2′*), 7.29–7.21 (m, 3H, *3, 3′*), 7.13 (ddd, J = 9.3, 8.6, 2.7 Hz, 1H, *7*). **^{13}C{^{1}H} NMR** (100.61 MHz, CD_3CN): δ 163.2 (d, J = 243.9 Hz, *4′*), 160.0 (d, J = 240.7 Hz, *6*), 152.0 (d, J = 2.8 Hz, *2*), 134.0 (d, J = 8.1 Hz, *2′*), 132.7 (d, J = 3.1 Hz, *1′*), 131.8, (s, *8a*), 130.0 (d, J = 9.2 Hz, *4a*), 129.4 (d, J = 5.1 Hz, *4*), 127.8 (d, J = 8.8 Hz, *8*), 121.9 (s, *1*), 120.4 (s, *3*), 117.1 (d, J = 25.0 Hz, *7*), 116.4 (d, J = 21.8 Hz, *3′*), 111.8 (d, J = 20.6 Hz, *5*). **^{19}F NMR** (376.50 MHz, CD_3CN): δ −116.7 (tt, J = 9.1, 5.6 Hz, *4′*), −121.4 ($td_{app.}$, J = 9.3, 5.6 Hz, *6*). **^{1}H NMR** (500.13 MHz, CD_3OD): δ 7.73 (d, J = 8.9 Hz, 1H, *4*), 7.46 (dd, J = 9.9, 2.7 Hz, 1H, *5*), 7.39 (dd, J = 9.4, 5.6 Hz, 1H, *8*), 7.37–7.32 (m, 2H, *2′*), 7.27–7.20 (m, 3H, *3, 3′*), 7.12 (ddd, J = 9.3, 8.4, 2.7 Hz, 1H, *7*), OH peak not detected. **^{1}H{^{1}H} NMR** (500.13 MHz, CD_3OD): δ 7.73 (s, *4*), 7.46 (d, $^3J_{F-H}$ = 9.8 Hz, *5*), 7.39 (d, $^4J_{F-H}$ = 5.6 Hz, *8*), 7.35 (d, $^4J_{F-H}$ = 5.5 Hz, *2′*), 7,244 (s, *3*), 7.236 (d, $^3J_{F-H}$ = 8.9 Hz, *3′*), 7.12

(d, $^3J_{F-H}$ = 8.5 Hz, *7*), OH peak not detected. **^{13}C{^{1}H} NMR** (125.76 MHz, CD_3OD): δ 163.6 (d, ^1J = 244.3 Hz, *4′*), 160.3 (d, ^1J = 241.6 Hz, *6*), 152.4 (d, ^6J = 2.7 Hz, *2*), 134.0 (d, ^3J = 8.1 Hz, *2′*), 133.7 (d, ^4J = 3.6 Hz, *1′*), 132.4 (s, *8a*), 130.5 (d, ^3J = 8.3 Hz, *4a*), 129.3 (d, ^4J = 5.3 Hz, *4*), 127.9 (d, ^3J = 8.3 Hz, *8*), 122.4 (s, *1*), 120.4 (s, *3*), 117.0 (d, ^2J = 25.4 Hz, *7*), 116.2 (d, ^2J = 21.7 Hz, *3′*), 111.7 (d, ^2J = 20.3 Hz, *5*). **^{19}F NMR** (470.59 MHz, CD_3OD): δ −117.67 (tt, J = 8.9, 5.5 Hz, *4′*), −122.32 (ddd, J = 9.9, 8.4, 5.5 Hz, *6*). **HRMS** (ESI$^+$, *m/z*) Calcd. for $C_{16}H_{11}F_2O^+$ (M+H): 257.0772. Found: 257.0773. Error: 0.39 ppm. ν_{max} (neat, cm^{-1}): 3544, 2924, 1608, 1520, 1507, 1375, 1230, 1169, 1106, 961, 867, 836, 816, 631, 580, 498.

4,4′-Bis(trifluoromethyl)-1,1′-biphenyl (9)

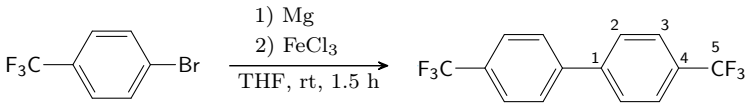

Following a procedure by Zhang,[448] magnesium turnings (4.00 g, 165 mmol, 6.6 equiv) were stirred in a 100 mL Schlenk tube overnight, then dry THF (30 mL) was added, followed by 1-bromo-4-(trifluoromethyl)benzene (7.0 mL, 11 g, 50 mmol, 2.0 equiv). Heat developed and and the solvent started to reflux. This solution was left to stir for 1.5 h, then transferred with a cannula into a THF (40 mL) solution of $FeCl_3$ (243 mg, 1.50 mmol, 3 mol%) and 1,2-dibromoethane (2.6 mL, 5.6 g, 30 mmol, 1.2 equiv). The resulting solution was left to stir overnight and then the reaction was quenched with 1 M HCl and diluted with DCM. The organic layer was separated, dried over $MgSO_4$ and concentrated to dryness. The crude mixture was purified by flash column chromatography on silica gel (CyH, R_f = 0.57), yielding the desired pure product as a white solid (4.27 g, 14.7 mmol, 59%). A crystal structure for this compound was determined from single crystals grown by slow evaporation of the solvent in a reaction where this compound was used as an internal standard (see Fig. 4.9). Crystallographic detail can be found in Section 6.8. **^{1}H NMR** (500.13 MHz, $CDCl_3$): δ 7.75 ($q_{app.}$, J = 8.3 Hz, 8H). **^{13}C{^{1}H} NMR** (125.76 MHz, $CDCl_3$): δ 143.4 (*1*), 130.5 (q, J = 32.7 Hz, *4*), 127.8 (*2*), 126.1 (q, J = 3.7 Hz, *3*), 124.3 (q, J = 272.1 Hz, *5*). **^{19}F NMR** (470.59 MHz, $CDCl_3$): δ −62.57. **HRMS** (EI$^+$, *m/z*) Calcd. for $C_{14}H_8F_6^{\cdot+}$ (M+): 290.0525. Found: 290.0538. Error: 4.48 ppm. ν_{max} (neat, cm^{-1}): 1593, 1580, 1548, 1374, 1215, 1147, 1117, 1080, 1028, 1011, 873. **m.p.** (°C): 85–87.

1-(Chloromethyl)-1,4-diazabicyclo[2.2.2]octan-1-ium chloride (10)

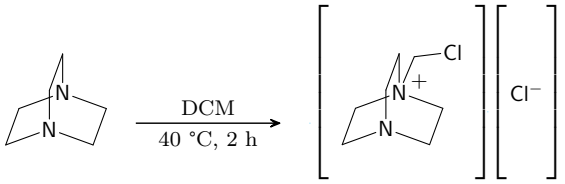

According to Wu's procedure,[273] in a 100 mL round-bottom flask, DABCO (2.50 g, 22.3 mmol) was dissolved in DCM (45 mL) and stirred for 2 h at reflux, then the reaction mixture was let to cool down to rt and solids were transferred on a Büchner filter and washed with additional DCM. The desired compound **10** was isolated as a colourless solid (3.10 g, 15.7 mmol, 71%) whose characteristic data correspond to those reported in literature.[273] **^{1}H NMR** (400.13 MHz, D_2O): δ 5.05 (s, 1H), 3.48 (t, J = 7.5 Hz, 3H), 3.19 (dd, J = 8.9, 6.2 Hz, 3H).

Sodium bis(phenylsulfonyl)amide (11)

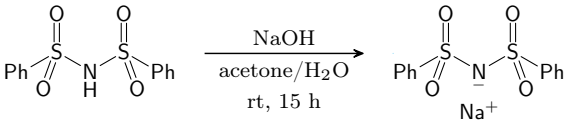

Dibenzenesulfonimide (1.00 g, 3.36 mmol, 1.0 equiv) was dissolved in a 1:1 acetone/water mixture, then NaOH (135 mg, 3.36 mmol, 1.0 equiv) was added and the reaction mixture was stirred for 15 h at rt. The solvent was then removed under reduced pressure and the product was isolate without further purification (1.01 g, 3.16 mmol, 94%) as a colourless solid. **^{1}H NMR** (400.13 MHz, D_2O): 7.59–7.50 (m, 2H), 7.50–7.40 (m, 1H), 7.32 (t, J = 7.9 Hz, 2H). **^{13}C{^{1}H} NMR** (100.61 MHz, D_2O): 141.0, 132.3, 128.9, 126.1.

1-(Chloromethyl)-1,4-diazabicyclo[2.2.2]octan-1-ium bis(phenylsulfonyl)amide (12)

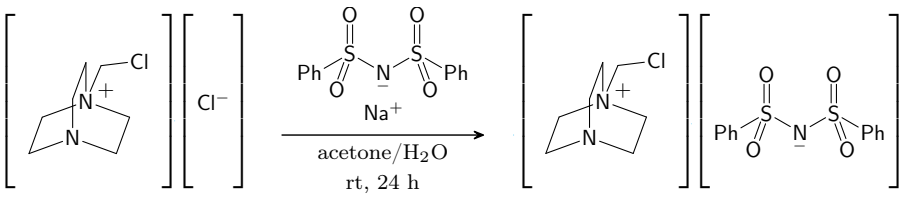

According to Wu's procedure,[273] compound **10** (493 mg, 2.50 mmol, 1.0 equiv) was stirred in MeCN (50 mL) until the solution got clear, then compound **11** (800 mg,

2.50 mmol, 1.0 equiv) was added and the resulting mixture was stirred overnight. The suspension was then passed through a filter to remove NaCl and the resulting solution was concentrated, causing the crystallisation of the desired product, which was isolated quantitatively (1.12 g, 2.45 mmol, 98%). **^{1}H NMR** (400.13 MHz, CD_3CN): 7.81–7.67 (m, 4H), 7.49–7.28 (m, 6H), 4.99 (d, J = 1.7 Hz, 2H), 3.37 (t, J = 7.4 Hz, 6H), 3.16 (t, J = 7.4 Hz, 6H).

1-(chloromethyl)-4-fluoro-1,4-diazabicyclo[2.2.2]octane-1,4-diium bis-(bis(phenylsulfonyl)amide) (13)

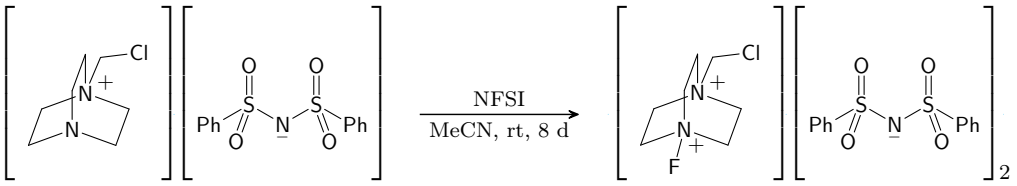

According to Wu's procedure,[273] compound **12** (1.09 g, 2.38 mmol, 1.0 equiv) and NFSI (7.52 g, 23.8 mmol, 10 equiv) were dissolved in MeCN (76.8 mL) and this solution was stirred for 8 d at rt. The solvent was then removed under reduced pressure and the crude solid was washed with EtOAc to recover the excess NFSI. Finally the product was obtained with 95% purity by recrystallisation from EtOAc/MeCN (1.72 g, 2.23 mmol, 94%). The resulting crystals were suitable for X-ray diffraction analysis: details can be found in Section 6.8. **^{1}H NMR** (500.13 MHz, CD_3CN): δ 7.81–7.68 (m, 8H), 7.47–7.39 (m, 4H), 7.39–7.31 (m, 8H), 5.60–5.45 (m, 2H), 5.04–4.83 (m, 6H), 4.67–4.47 (m, 6H). **^{13}C{^{1}H} NMR** (125.76 MHz, CD_3CN): δ 145.3, 130.6, 128.1, 126.4, 69.0, 57.4 (d, J = 15.1 Hz), 53.8. **^{19}F NMR** (470.59 MHz, CD_3CN): δ 48.82.

1,1,6-Trifluoronaphthalen-2(1*H*)-one (14)

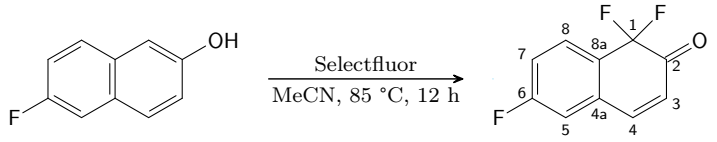

In an NMR tube, Selectfluor (283 mg, 800 µmol, 4 equiv) was added to a solution of 6-fluoronaphthalen-2-ol **7** (32.4 mg, 200 µmol, 1 equiv) in CD_3CN (0.6 mL), which was heated at 85 °C for 12 h. Formation of a 72:28 mixture of 1,1,6-trifluoronaphthalen-2(1*H*)-one and 1,6-difluoronaphthalen-2-ol was detected by ^{19}F NMR spectroscopy, as well as full consumption of the naphthol starting material. The reaction mixture was diluted with Et_2O (10 mL) and extracted with 1 M NaOH (3 × 10 mL) to

remove the mono-fluorinated species. Purification was achieved by preparatory TLC, eluting with 1:9 CyH:EtOAc ($R_f = 0.56$) and the desired product was isolated as a dark yellow oil (14.9 mg, 75.2 mmol, 38%). **^{1}H NMR** (500.13 MHz, $CDCl_3$): δ 7.83 (ddt, J = 8.5, 5.2, 1.6 Hz, 1H, *8*), 7.38 (d, J = 10.1 Hz, 1H, *4*), 7.22 (td, J = 8.3, 2.5 Hz, 1H, *7*), 7.09 (ddt, J = 8.3, 2.5, 1.2 Hz, 1H, *5*), 6.29 (dtd, J = 10.2, 2.7, 0.8 Hz, 1H, *3*). **^{1}H{^{1}H} NMR** (500.13 MHz, $CDCl_3$): δ 7.86–7.81 (m, *8*), 7.38 (s, *4*), 7.22 (d, ^3J = 8.4 Hz, *7*), 7.09 (d, ^3J = 7.8 Hz, *5*), 6.29 (s, *3*). **^{13}C{^{1}H} NMR** (125.76 MHz, $CDCl_3$): δ 187.16 (t, ^2J = 24.9 Hz, *2*), 164.76 (dt, $^{1,5}J$ = 253.4, 2.0 Hz, *6*), 144.17 (s, *4*), 132.84 (dt, $^{3,3}J$ = 8.3, 5.6 Hz, *4a*), 130.24 (dt, $^{3,3}J$ = 9.0, 3.2 Hz, *8*), 129.30 (td, $^{2,4}J$ = 23.8, 3.7 Hz, *8a*), 124.87 (t, ^3J = 2.2 Hz, *3*), 117.78 (dt, $^{2,4}J$ = 22.0, 1.7 Hz, *7*), 116.93 (d, ^2J = 22.8 Hz, *5*), 105.36 (t, ^1J = 244.8 Hz, *1*). **^{19}F NMR** (470.59 MHz, $CDCl_3$): δ −100.12–−100.30 (m, 2F, *1*), −106.77 (tq, J = 8.6, 4.2 Hz, 1F, *6*). **^{19}F{^{1}H} NMR** (376.50 MHz, $CDCl_3$): δ −100.21 (d, ^6J = 3.9 Hz, 2F, *1*), −106.77 (t, ^6J = 3.9 Hz, 1F, *6*). **HRMS** (ESI^+, *m/z*) Calcd. for $C_{10}H_5F_3NaO^+$ (M+ Na): 221.0185. Found: 221.0206. Error: 9.50 ppm. ν_{max} (neat, cm^{-1}): 3070, 2921, 2851, 1668, 1579, 1509, 1298, 1264, 1128, 1047, 887, 837.

6.2 Sulfonamides

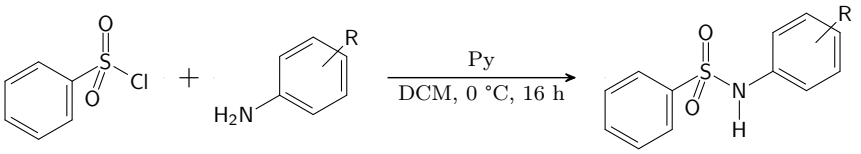

GP-1: benzenesulfonyl chloride (1.1 equiv) was added to a solution of aniline (1.0 equiv) and pyridine (3.0 equiv) in DCM (0.2 M) at 0 °C. The reaction was gradually warmed to room temperature and stirred for 16 h before quenching with water. This solution was then extracted with DCM (3 × 20 mL) and the resulting the organic phases were collected and washed with HCl (1 M), $NaHCO_{3\,(sat.)}$ and brine, dried over $MgSO_4$ and the solvent removed under reduced pressure.

N-(4-fluorophenyl)benzenesulfonamide (15a)

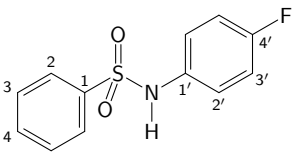

According to GP-1, 4-fluoroaniline (222 mg, 2.00 mmol, 1.0 equiv), pyridine (490 µL, 476 mg, 6 mmol, 3.0 equiv) and benzenesulfonyl chloride (280 µL, 389 mg, 2.2 mmol, 1.1 equiv) were reacted together, yielding the desired product (485 mg, 1.93 mmol, 97%) as a white solid. Its characteristic data are consistent with the literature.[449]

^{1}H NMR (500.13 MHz, $CDCl_3$): δ 7.80–7.67 (m, 2H, *2*), 7.55 ($tt^{IIord.}$, J = 7.5, 1.3 Hz, 1H, *4*), 7.50–7.41 (m, 2H, *3*), 7.10–6.99 (m, 2H, *2′*), 6.93 ($t^{II\,ord.}_{app.}$, J = 8.7, 8.3 Hz, 2H, *3′*), 6.75 (br, 1H, *NH*). **^{13}C{^{1}H} NMR** (125.76 MHz, $CDCl_3$): δ 160.9 (d, J = 245.7 Hz, *4′*), 138.7 (s, *1*), 133.1 (s, *4*), 132.1 (d, J = 3.0 Hz, *1′*), 129.1 (s, *3*), 127.2 (s, *2*), 124.9 (d, J = 8.1 Hz, *2′*), 116.2 (d, J = 22.9 Hz, *3′*). **^{19}F NMR** (470.59 MHz, $CDCl_3$): δ −115.9 (tt, J = 8.5, 4.7 Hz). **HRMS** (ESI^-, *m/z*) Calcd. for $C_{12}H_9FNO_2S^-$ (M− H): 250.0344. Found: 250.0348. Error: 1.60 ppm. ν_{max} (neat, cm^{-1}): 3246, 1505, 1469, 1444, 1392, 1324, 1284, 1225, 1147, 1089, 1019, 922, 848, 754, 717, 688, 572, 520. **m.p.** (°C): 106–108.

N-(3,5-Bis(trifluoromethyl)phenyl)benzenesulfonamide (15b)

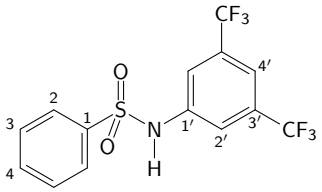

According to GP-1, 3,5-bis(trifluoromethyl)aniline (310 µL, 458 mg, 2.00 mmol, 1.0 equiv), pyridine (490 µL, 476 mg, 6.00 mmol, 3.0 equiv) and benzenesulfonyl chloride (280 µL, 389 mg, 2.20 mmol, 1.1 equiv) were reacted together, yielding the desired product (694 mg, 1.88 mmol, 94%) as a white solid. **^{1}H NMR** (500.13 MHz, $CDCl_3$): δ 7.89–7.81 (m, 2H, *2*), 7.65–7.57 (m, 2H, *2 and 16*), 7.56–7.48 (m, 4H, *3 and 2′*), 7.25 (s, 1H, *NH*). **^{13}C{^{1}H} NMR** (125.76 MHz, $CDCl_3$): δ 138.3 (*1*), 138.3 (*1′*), 134.1 (*4*), 133.1 (q, ^2J = 33.9 Hz, *3′*), 129.7 (*3*), 127.4 (*2*), 122.8 (q, ^1J = 273.1 Hz, *CF*$_3$), 120.3 (q, ^3J = 3.9 Hz, *2′*), 118.7 (p, J = 3.9 Hz, *4′*). **^{19}F NMR** (470.59 MHz, $CDCl_3$): δ −63.18. **HRMS** (ESI^-, *m/z*) Calcd. for $C_{14}H_8F_6NO_2S^-$ (M− H): 368.0185. Found: 368.0182. Error: 0.82 ppm. ν_{max} (neat, cm^{-1}): 3258, 1621,1509, 1469, 1421, 1375, 1333, 1276, 1124, 1088, 1001, 974, 877, 834, 752, 735, 717, 696, 682, 553. **m.p.** (°C): 107–108.

N-(4-(*tert*-Butyl)phenyl)benzenesulfonamide (15c)

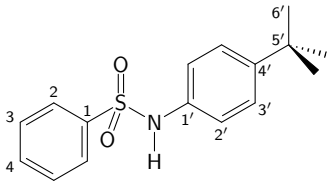

According to GP-1, 4-*tert*-butylaniline (800 µL, 746 mg, 5.00 mmol, 1.0 equiv), pyridine (1.20 mL, 396 mg, 15.0 mmol, 3.0 equiv) and benzenesulfonyl chloride (700 µL, 971 mg, 5.50 mmol, 1.1 equiv) were reacted together, yielding the desired product (1.31 g, 4.52 mmol, 90%) as a cream-white solid. Its characteristic data are consistent with the literature.[449] **^{1}H NMR** (500.13 MHz, $CDCl_3$): δ 7.81–7.74 (m, 2H, *1*), 7.54 ($tt_{app.}$, J = 7.5, 1.2 Hz, 1H, *4*), 7.45 ($t^{II\,ord.}_{app.}$, J = 8.0 Hz, 2H, *3*), 7.32–7.20 (m, 2H, *3′*), 7.03–6.92 (m, 2H, *2′*), 6.44 (s, 1H, *NH*), 1.28 (s, 9H,

6′). ^{13}**C{^{1}H} NMR** (125.76 MHz, $CDCl_3$): δ 149.0 (*4′*), 139.5 (*1*), 133.6 (*1′*), 133.0 (*4*), 129.1 (*3*), 127.4 (*2*), 126.4 (*3′*), 122.1 (*2′*), 34.5 (*5′*), 31.4 (*6′*). **HRMS** (ESI$^-$, *m/z*) Calcd. for $C_{16}H_{18}NO_2S^-$ (M− H): 288.1064. Found: 288.1069. Error: 1.74 ppm. ν_{max} (neat, cm^{-1}): 3200, 2962, 1510, 1448, 1395, 1363, 1328, 1266, 1227, 1153, 1090, 1019, 914, 820, 724, 686, 658, 574, 529. **m.p.** (°C): 154–155.

N-(4-nitrophenyl)benzenesulfonamide (15d)

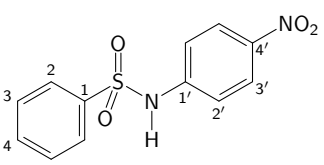

According to GP-1, 4-nitroaniline (700 mg, 5.00 mmol, 1.0 equiv), pyridine (1.20 mL, 396 mg, 15.0 mmol, 3.0 equiv) and benzenesulfonyl chloride (700 µL, 971 mg, 5.50 mmol, 1.1 equiv) were reacted together, yielding the desired product (1.26 g, 4.54 mmol, 91%) as a tanned solid. Its characteristic data are consistent with the literature.[450] ^{1}**H NMR** (500.13 MHz, $CDCl_3$): δ 8.13 (d$^{\text{II ord.}}$, J = 9.1 Hz, 2H, *3′*), 7.97–7.86 (m, 2H, *2*), 7.66 (s, 1H, *NH*), 7.61 (tt$_{\text{app.}}$, J = 7.6, 1.1 Hz, 1H, *4*), 7.52 (t$^{\text{II ord.}}_{\text{app.}}$, J = 8.2, 7.4 Hz, 2H, *3*), 7.29–7.19 (m, 2H, *2′*). ^{13}**C{^{1}H} NMR** (125.76 MHz, $CDCl_3$): δ 144.2 (*4′*), 142.7 (*1′*), 138.5 (*1*), 134.1 (*4*), 129.7 (*3*), 127.4 (*2*), 125.6 (*3′*), 118.9 (*2′*). **HRMS** (ESI$^-$, *m/z*) Calcd. for $C_{12}H_9N_2O_4S^-$ (M− H): 277.0289. Found: 277.0292. Error: 1.08 ppm. ν_{max} (neat, cm^{-1}): 3234, 1594, 1518, 1494, 1447, 1341, 1286, 1233, 1180, 1157, 1111, 1087, 898, 855, 821, 747, 719, 694, 681, 646, 625, 578, 562, 500, 452. **m.p.** (°C): 138–140.

N-(4-(trifluoromethyl)phenhyl)benzenesulfonamide (15e)

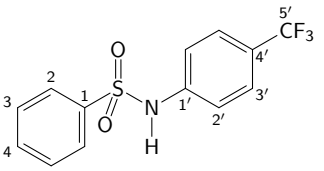

According to GP-1, 4-(trifluoromethyl)aniline (640 µL, 800 mg, 5.00 mmol, 1.0 equiv), pyridine (1.20 mL, 396 mg, 15.0 mmol, 3.0 equiv) and benzenesulfonyl chloride (700 µL, 971 mg, 5.50 mmol, 1.1 equiv) were reacted together, yielding the desired product (1.47 g, 4.89 mmol, 98%) as a white solid. Its characteristic data are consistent with the literature.[451] ^{1}**H NMR** (500.13 MHz, $CDCl_3$): δ 7.91–7.81 (m, 2H, *2*), 7.62–7.55 (m, 1H, *4*), 7.53–7.45 (m, 4H, *3 and 3′*), 7.19 (d, J = 8.4 Hz, 2H, *2′*), 7.13 (br, 1H, *NH*). ^{13}**C{^{1}H} NMR** (125.76 MHz, $CDCl_3$): δ 139.8 (*1′*), 138.9 (*1*), 133.7 (*4*), 129.5 (*3*), 127.3 (*2*), 127.1 (q, J = 32.6 Hz, *4′*), 126.8 (q, J = 3.7 Hz, *3′*), 124.0 (q, J = 271.8 Hz, *5′*), 120.1 (*2′*). ^{19}**F NMR** (470.59 MHz, $CDCl_3$): δ −62.31. **HRMS** (ESI$^-$, *m/z*) Calcd. for $C_{13}H_9F_3NO_2S^-$ (M− H): 300.0312. Found: 300.0316. Error: 1.33 ppm. ν_{max} (neat, cm^{-1}): 3277, 1617, 1517, 1466, 1401, 1320, 1287, 1226, 1157, 1108, 1089, 1067, 1012, 911, 845, 754, 718, 685, 658, 590, 556, 506, 437. **m.p.** (°C): 100–102.

N-(4-methoxyphenhyl)benzenesulfonamide (15f)

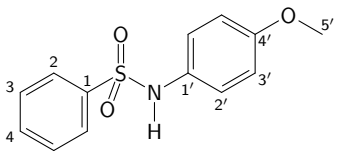

According to GP-1, 4-methoxyaniline (615 mg, 5.00 mmol, 1.0 equiv), pyridine (1.20 mL, 396 mg, 15.0 mmol, 3.0 equiv) and benzenesulfonyl chloride (700 µL, 971 mg, 5.50 mmol, 1.1 equiv) were reacted together, yielding the desired product (1.31 g, 4.97 mmol, 99.5%) as a black solid. Its characteristic data are consistent with the literature.[451] **^{1}H NMR** (500.13 MHz, $CDCl_3$): δ 7.76–7.66 (m, 2H, *2*), 7.54 (tt, J = 7.6, 1.1 Hz, 1H, *4*), 7.43 ($t^{IIord.}$, J = 8.1, 7.6 Hz, 2H, *3*), 7.01–6.92 (m, 2H, *2′*), 6.82–6.73 (m, 2H, *3′*), 6.39 (br, 1H, *NH*), 3.78 (s, 3H, *5′*). **^{13}C{^{1}H} NMR** (125.76 MHz, $CDCl_3$): δ 158.3 (*4′*), 139.1 (*1*), 133.0 (*4*), 129.1 (*3*), 128.7 (*1′*), 127.4 (*2*), 125.9 (*2′*), 114.6 (*3′*), 55.6 (*5′*). **HRMS** (ESI$^-$, *m/z*) Calcd. for $C_{13}H_{12}NO_3S^-$ (M − H): 262.0543. Found: 262.0540. Error: 1.14 ppm. ν_{max} (neat, cm^{-1}): 3253, 1505, 1465, 1445, 1399, 1332, 1287, 1248, 1148, 1086, 1036, 914, 823, 759, 720, 686, 630, 579, 540, 512. **m.p.** (°C): 93–95.

6.3 *N*-Fluorosulfonamides

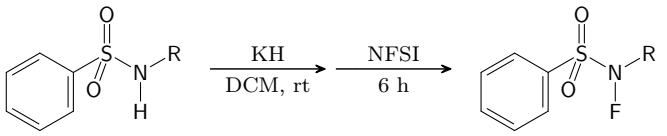

GP-2: Following Taylor's procedure,[299] in a two-neck round-bottom flask under argon KH was added, without removing the mineral oil in which it was dispersed, to a 0.1 M DCM solution of sulfonamide kept at rt. The resulting solution was stirred for 1 h. A 0.1 M solution of NFSI was then added to the first flask and the slurry was stirred for other 6 h. The reaction was then quenched with a NaOH-NH_4OH solution (6.5 g of NaOH and 7.2 mL of 35% NH_4OH solution, in 100 mL of distilled water), then extracted with Et_2O (3 × 20 mL). The resulting organic layers were collected and washed with the NaOH-NH_4OH solution (3 × 20 mL), 1 M saturated NaOH (3 × 20 mL) and 1 M HCl (3 × 20 mL). The organic phase was then dried over $MgSO_4$ and the solvent was removed under pressure. The resulting crude was purified by flash chromatography (20% EtOAc/CyH) affording the pure product.

N-fluoro-*N*-isopropyl-4-methylbenzenesulfonamide (16a)

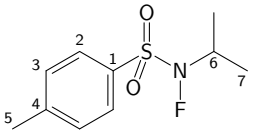

According to **GP-2**, *N*-isopropyl-4-methylbenzenesulfonamide (213 mg, 1.00 mmol, 1 equiv), KH (ca. 800 mg of 30% dispersion in mineral oil, 241 mg of KH, 6.00 mmol, 6 equiv) and NFSI (950 mg, 3.00 mmol, 3 equiv) were reacted together to yield the desired product (126 mg, 0.545 mmol, 55%) as a colourless oil, whose characteristic data are consistent with the literature.[299] **^{1}H NMR** (500.13 MHz, $CDCl_3$): δ 7.87 (d, J = 8.4 Hz, 2H, *2*), 7.40 (d, J = 8.1 Hz, 2H, *3*), 4.11 (dhept, J = 34.2, 6.8 Hz, 1H, *6*), 2.49 (s, 3H, *5*), 1.34 (dd, J = 6.6, 1.2 Hz, 6H, *7*). **^{19}F NMR** (470.59 MHz, $CDCl_3$): δ −75.49 (d, J = 34.2 Hz).

N-(3,5-bis(trifluoromethyl)phenyl)-*N*-fluorobenzenesulfonamide (16b)

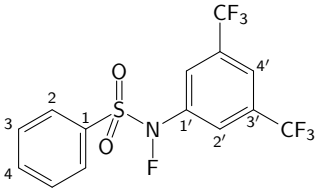

According to **GP-2**, compound **15b** (185 mg, 0.500 mmol, 1 equiv), KH (ca. 400 mg of 30% dispersion in mineral oil, 120 mg of KH, 3.00 mmol, 6 equiv) and NFSI (473 mg, 1.50 mmol, 3 equiv) were reacted together to yield the desired product (81.0 mg, 0.248 mmol, 50%) as a white solid. **^{1}H NMR** (500.13 MHz, C_6D_6): δ 7.49 (br, 1H, *4′*), 7.31 (br, 2H, *2′*), 7.30–7.24 (m, 2H, *2*), 6.89–6.75 (m, 1H, *4*), 6.70–6.56 (m, 2H, *2*). **^{13}C{^{1}H} NMR** (125.76 MHz, C_6D_6): δ 141.8 (d, J = 9.9 Hz, *1′*), 138.8 (*1*), 134.9 (*4*), 132.0 (q, J = 33.7 Hz, *3′*), 129.8 (*2*), 128.7 (*3*), 122.5 (q, J = 273.2 Hz, *CF*$_3$), 122.3 (dd$_{app.}$, J = 9.7, 3.3 Hz, *2′*), 122.1 (p, J = 3.8 Hz, *4′*). **^{19}F NMR** (470.59 MHz, C_6D_6): δ −38.18 (1F), −63.05 (6F). **HRMS** (ESI$^-$, *m/z*) Calcd. for $C_{14}H_7F_7NO_2S^-$ (M− H): 386.0091. Found: 386.0104. Error: 3.37 ppm. ν_{max} (neat, cm^{-1}): 1450, 1367, 1277, 1174, 1135, 1089, 970, 893, 750, 728, 682.

N-fluoro-*N*-(4-nitrophenyl)benzenesulfonamide (16c)

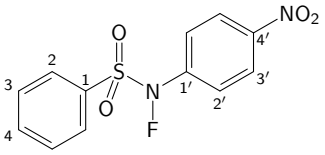

According to **GP-2**, compound **15d** (835 mg, 3.00 mmol, 1 equiv), KH (ca. 800 mg of 30% dispersion in mineral oil, 240 mg of KH, 3.00 mmol, 6 equiv) and NFSI (846 mg, 3.00 mmol, 3 equiv) were reacted together to yield the desired product (172 mg, 0.581 mmol, 58%) as an ivory solid. **^{1}H NMR** (500.13 MHz, $CDCl_3$): δ 8.27–8.19 (m, 2H, *3′*), 7.78 (tt$^{IIord.}$, J = 7.4, 1.3 Hz, 1H, *4*), 7.74–7.67 (m, 2H, *2*), 7.56 (dd$^{IIord.}$, J = 8.3, 7.4 Hz, 2H, *3*), 7.32 (d$^{II\ ord.}_{app.}$, J = 8.8 Hz, 2H, *2′*). **^{13}C{^{1}H} NMR** (125.76 MHz, $CDCl_3$): δ 147.3 (*4′*),

145.0 (d, J = 8.8 Hz, *1′*), 135.7 (*4*), 130.8 (*1*), 130.1 (*2*), 129.2 (*3*), 124.2 (d, J = 2.6 Hz, *3′*), 122.0 (d, J = 10.1 Hz, *2′*). **^{19}F NMR** (470.59 MHz, $CDCl_3$): δ −40.41. **HRMS** (ESI^+, *m/z*) Calcd. for $C_{12}H_9N_2O_4SNa^+$ (M+ Na − F): 300.0303. Found: 300.0309. Error: 2.00 ppm. ν_{max} (neat, cm^{-1}): 1609, 1589, 1517, 1485, 1445, 1381, 1347, 1311, 1185, 1168, 1109, 1084, 939, 872, 853, 753, 728, 691, 608, 568, 535.

6.4 Bismuthonium salts

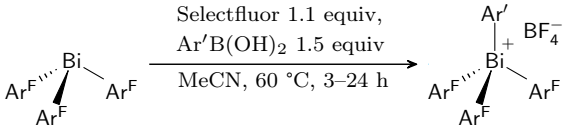

GP-3: tri(4-fluorophenyl)bismuthine **2**, Selectfluor (1.05 equiv) and the boronic acid of choice (1.25 equiv) were loaded in a 10 mL microwave tube and suspended in MeCN (0.1 M). This suspension was stirred with a cross-shaped stirrer bar at 400 rpm and heated at 60 °C for 3–24 h. The reaction was checked by ^{19}F NMR spectroscopy, by taking a small aliquot and diluting it in 0.5 mL of CD_3CN. At completion, the solvent was evaporated under reduced pressure and the residues dissolved in DCM and water and transferred into a separatory funnel, where the organic phase was extracted three times with water. The resulting organic phase was then dried over $MgSO_4$, filtered over filter paper and evaporated to dryness under vacuum. The crude was purified by crystallisation. Crystals were grown either by slow diffusion of an anti-solvent into a solvent carefully layered one over the other, or by adding the anti-solvent to a swirled solution of the crude in a solvent, until the resulting solution turned cloudy. The resulting crystals were filtered on a Büchner funnel, washed with the anti-solvent, then dried *in vacuo* and analysed.

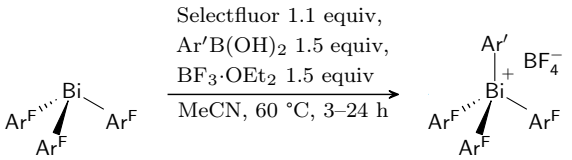

GP-4: tri(4-fluorophenyl)bismuthine **2**, Selectfluor (1.05 equiv) and the boronic acid of choice (1.25 equiv) were loaded in a 10 mL microwave tube and suspended in MeCN (0.1 M). $BF_3{\cdot}OEt_2$ (1.25 equiv) was finally added and this solution stirred, heated, worked-up and purified as per GP-3.

Tetra(4-fluorophenyl)bismuthonium tetrafluoroborate (5a)

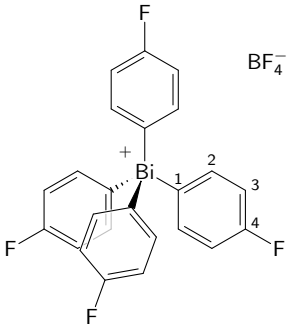

The compound was synthesised according to GP-3, by reacting **2** (4.94 g, 10.0 mmol) with Selectfluor (3.72 g, 10.5 mmol) and 4-fluorophenylboronic acid (1.75 g, 12.5 mmol). Recrystallisation from DCM/CyH yielded the desired pure product (6.56 g, 9.70 mmol, 97%), whose characteristic data were in accordance with the literature.[75] The resulting crystals were suitable for X-ray diffraction analysis: details can be found in Section 6.8. **^{1}H NMR** (500.13 MHz, $CDCl_3$): δ 7.79 ($dd^{II\ ord.}$, J = 8.7, 5.2 Hz, 8H, *2*), 7.38 ($t^{II\ ord.}_{app.}$, J = 8.5 Hz, 8H, *3*). **^{13}C{^{1}H} NMR** (125.76 MHz, $CDCl_3$): δ 165.2 (d, J = 255.6 Hz, *4*), 138.0 (d, J = 8.6 Hz, *2*), 133.2 (d, J = 3.6 Hz, *1*), 120.1 (d, J = 21.9 Hz, *3*). **^{19}F NMR** (470.59 MHz, $CDCl_3$): δ −103.87 (tt, J = 8.4, 5.2 Hz, 4F), −147.63 (s, 4F). **HRMS** (ESI^+, *m/z*) Calcd. for $C_{24}H_{16}BiF_4^+$ (M+): 589.0987. Found: 589.0986. Error: 0.17 ppm. ν_{max} (neat, cm^{-1}): 1589, 1574, 1483, 1392, 1303, 1230, 1160, 1056, 1002, 819, 570, 500, 413. **m.p.** (°C): 241–242.

(4-Cyanophenyl)tri(4-fluorophenyl)bismuthonium tetrafluoroborate (5b)

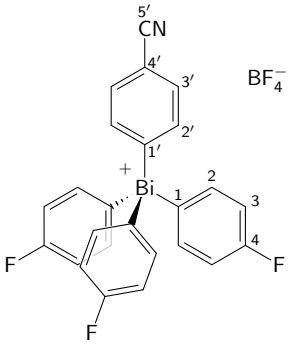

The compound was synthesised according to GP-4, by reacting **2** (103 mg, 0.209 mmol) with Selectfluor (74.4 mg, 0.210 mmol), 4-cyanophenylboronic acid (44.1 mg, 0.250 mmol) and $BF_3{\cdot}Et_2O$ (37 µL, 0.30 mmol). Recrystallisation from DCM/CyH yielded the desired pure product (66.0 mg, 0.965 mmol, 46%). The resulting crystals were suitable for X-ray diffraction analysis: details can be found in Section 6.8. **^{1}H NMR** (500.13 MHz, $(CD_3)_2SO$): δ 8.14 ($dd^{II\ ord.}$, J = 8.5 Hz, 2H, *3′*), 8.08 ($dd^{II\ ord.}$, J = 8.3 Hz, 2H, *2′*), 7.96 ($dd^{II\ ord.}$, J = 8.5, 5.6 Hz, 6H, *2*), 7.58 ($t^{II\ ord.}_{app.}$, J = 9.2 Hz, 6H, *3*). **^{13}C{^{1}H} NMR** (125.76 MHz, $(CD_3)_2SO$): δ 163.7 (d, J = 249.8 Hz, *4*), 151.8 (*1′*), 140.8 (d, J = 3.3 Hz, *1*), 138.1 (d, J = 8.2 Hz, *2*), 136.5 (*2′*), 134.4 (*3′*), 118.7 (d, J = 21.7 Hz, *3*), 117.9 (*5′*), 113.8 (*4′*). **^{19}F NMR** (470.59 MHz, $(CD_3)_2SO$): δ −107.64 (tt, J = 9.2, 5.6 Hz, 3F), −148.28 (s, 4F). **HRMS** (ESI^+, *m/z*) Calcd. for $C_{25}H_{16}BiF_3N^+$ (M+): 596.1033. Found: 596.1037. Error: 0.67 ppm. ν_{max} (neat, cm^{-1}): 2234, 1574, 1484, 1392, 1231, 1161, 1031, 1002, 965, 816, 570, 499. **m.p.** (°C): 271–272.

Tri(4-fluorophenyl)(4-(trifluoromethyl)phenyl)bismuthonium tetrafluoroborate (5c)

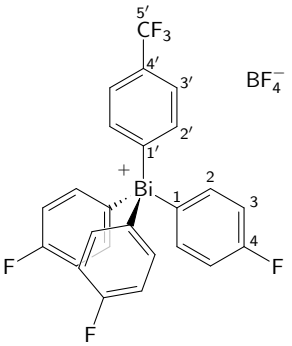

The compound was synthesised according to GP-3, by reacting **2** (103 mg, 0.207 mmol) with Selectfluor (74.4 mg, 0.210 mmol) and 4-(trifluoromethyl)phenylboronic acid (47.5 mg, 0.250 mmol). Recrystallisation from DCM/Et_2O yielded the desired pure product (55.7 mg, 0.0767 mmol, 37%). **^{1}H NMR** (500.13 MHz, $CDCl_3$): δ 7.94 (d, J = 8.2 Hz, 2H, *2′*), 7.89 (d, J = 8.1 Hz, 2H, *3′*), 7.78 (dd, J = 8.4, 5.2 Hz, 6H, *2*), 7.36 (t, J = 8.4 Hz, 6H, *3*). **^{13}C{^{1}H} NMR** (125.76 MHz, $CDCl_3$): δ 165.2 (d, J = 256.1 Hz, *4*), 142.9 (*1′*), 138.1 (d, J = 8.8 Hz, *2*), 136.4 (*2′*), 134.6 (q, J = 33.5 Hz, *4′*), 133.2 (d, J = 3.6 Hz, *1*), 129.0 (q, J = 3.6 Hz, *3′*), 123.2 (q, J = 273.4 Hz, *5′*), 120.1 (d, J = 22.1 Hz, *3*). **^{19}F NMR** (470.59 MHz, $CDCl_3$): δ −63.30 (s, 3F, *5′*), −103.64 (tt, J = 8.4, 5.2 Hz, 3F, *4*), −147.24 (s, 4F). **HRMS** (ESI^+, *m/z*) Calcd. for $C_{25}H_{16}BiF_6^+$ (M+): 639.0955. Found: 639.0954. Error: 0.16 ppm. ν_{max} (neat, cm^{-1}): 1575, 1484, 1394, 1322, 1276, 1261, 1230, 1161, 1116, 1062, 1045, 1001, 819, 764, 750, 502. **m.p.** (°C): 98–100.

(4-Chlorophenyl)tri(4-fluorophenyl)bismuthonium tetrafluoroborate (5d)

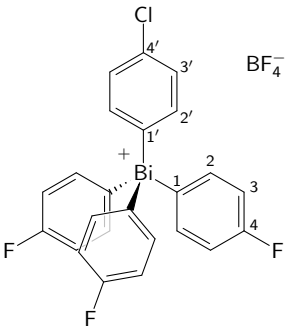

The compound was synthesised according to GP-3, by reacting **2** (103 mg, 0.207 mmol) with Selectfluor (74.4 mg, 0.210 mmol) and 4-chlorophenylboronic acid (39.1 mg, 0.250 mmol). Recrystallisation from DCM/Et_2O yielded the desired pure product (93.3 mg, 0.135 mmol, 65%). The resulting crystals were suitable for X-ray diffraction analysis: details can be found in Section 6.8. **^{1}H NMR** (500.13 MHz, $CDCl_3$): δ 7.82–7.73 (m, 6H, *2*), 7.73–7.68 (m, 2H, *2′*), 7.66–7.58 (m, 2H, *3′*), 7.41–7.30 (m, 6H, *3*). **^{13}C{^{1}H} NMR** (125.76 MHz, $CDCl_3$): δ 165.2 (d, J = 255.3 Hz, *4*), 139.6 (*4′*), 138.0 (d, J = 8.8 Hz, *2*), 137.0 (*2′*), 136.2 (*1′*), 132.9 (d, J = 3.5 Hz, *1*), 132.6 (*3′*), 120.0 (d, J = 21.8 Hz, *3*). **^{19}F NMR** (470.59 MHz, $CDCl_3$): δ −103.91 (tt, J = 8.4, 5.1 Hz, 3F), −147.75 (s, 4F). **HRMS** (ESI^+, *m/z*) Calcd. for $C_{24}H_{16}BiClF_3^+$ (M+): 605.0691. Found: 605.0712. Error: 3.47 ppm. ν_{max} (neat, cm^{-1}): 1572, 1484, 1391, 1220, 1163, 1067, 997, 805, 569, 503, 482. **m.p.** (°C): 211–212.

Tri(4-fluorophenyl)(4-iodo)bismuthonium tetrafluoroborate (5e)

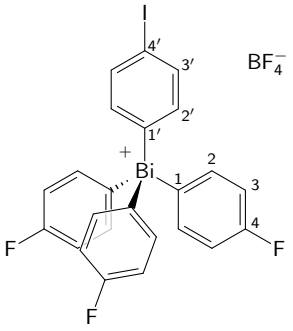

The compound was synthesised according to GP-3, by reacting **2** (103 mg, 0.207 mmol) with Selectfluor (74.4 mg, 0.210 mmol) and 4-iodophenylboronic acid (62.0 mg, 0.250 mmol). Recrystallisation from DCM/Et_2O yielded the desired pure product (70.3 mg, 0.0897 mmol, 43%). ^{1}**H NMR** (500.13 MHz, $CDCl_3$): δ 7.99 ($d^{II ord.}$, J = 8.3 Hz, 2H, *3′*), 7.77 ($dd^{II\ ord.}$, J = 8.6, 5.2 Hz, 6H, *2*), 7.48 ($d^{II ord.}$, J = 8.3 Hz, 2H, *2′*), 7.36 ($t^{II\ ord.}_{app.}$, J = 8.6 Hz, 6H). ^{13}**C{^{1}H} NMR** (125.76 MHz, $CDCl_3$): δ 165.2 (d, J = 255.5 Hz, *4*), 141.4 (*3′*), 138.04 (d, J = 8.3 Hz, *2*), 137.97 (*1′*), 137.0 (*2′*), 133.0 (d, J = 3.5 Hz, *1*), 120.1 (d, J = 21.8 Hz, *3*), 100.4 (*4′*). ^{19}**F NMR** (470.59 MHz, $CDCl_3$): δ −103.82 (tt, J = 8.3, 5.2 Hz, 3F), −147.62 (s, 4F). **HRMS** (ESI^+, *m/z*) Calcd. for $C_{24}H_{16}BiF_3I^+$ (M+): 697.0047. Found: 697.0042. Error: 0.72 ppm. ν_{max} (neat, cm^{-1}): 1573, 1484, 1224, 1162, 1060, 985, 801, 764, 750, 500, 466. **m.p.** (°C): 220–222.

Tri(4-fluorophenyl)(phenyl)bismuthonium tetrafluoroborate (5f)

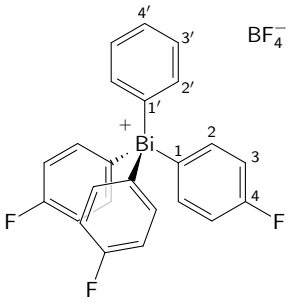

The compound was synthesised according to GP-3, by reacting **2** (99.5 mg, 0.201 mmol) with Selectfluor (74.4 mg, 0.210 mmol) and phenylboronic acid (30.5 mg, 0.250 mmol). Recrystallisation from DCM/Et_2O yielded the desired pure product (78.0 mg, 0.119 mmol, 59%). The resulting crystals were suitable for X-ray diffraction analysis: details can be found in Section 6.8. ^{1}**H NMR** (500.13 MHz, $CDCl_3$): δ 7.80 ($dd^{II\ ord.}$, J = 8.7, 5.3 Hz, 6H, *2*), 7.77–7.73 (m, 2H, *2′*), 7.72–7.66 (m, 2H, *3′*), 7.66–7.61 (m, 1H, *4′*), 7.37 ($t^{II\ ord.}_{app.}$, J = 8.7 Hz, 6H). ^{13}**C{^{1}H} NMR** (125.76 MHz, $CDCl_3$): δ 165.2 (d, J = 254.8 Hz, *4*), 138.3 (*1′*), 138.1 (d, J = 8.7 Hz, *2*), 135.8 (*2′*), 133.1 (d, J = 3.1 Hz, *1*), 132.9 (*4′*), 132.7 (*3′*), 120.0 (d, J = 21.9 Hz, *3*). ^{19}**F NMR** (470.59 MHz, $CDCl_3$): δ −104.15 (tt, J = 8.4, 5.2 Hz, 3F), −148.08 (s, 4F). **HRMS** (ESI^+, *m/z*) Calcd. for $C_{24}H_{17}BiF_3^+$ (M+): 571.1081. Found: 571.1101. Error: 3.50 ppm. ν_{max} (neat, cm^{-1}): 1573, 1483, 1391, 1225, 1161, 1044, 1004, 818, 733, 501. **m.p.** (°C): 180–182.

(4-Biphenyl)tri(4-fluorophenyl)bismuthonium tetrafluoroborate (5g)

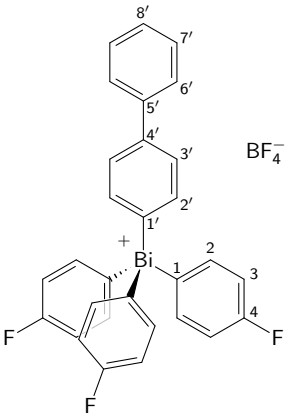

The compound was synthesised according to GP-3, by reacting **2** (103 mg, 0.207 mmol) with Selectfluor (74.4 mg, 0.210 mmol) and 4-biphenylboronic acid (49.5 mg, 0.250 mmol). Recrystallisation from DCM/Et_2O yielded the desired pure product (110 mg, 0.150 mmol, 72%). **^{1}H NMR** (500.13 MHz, $CDCl_3$): δ 7.87 ($d^{IIord.}$, J = 8.5 Hz, 2H, *3′*), 7.85–7.78 (m, 8H, *2 and 2′*), 7.62–7.55 (m, 2H, *6′*), 7.51–7.44 (m, 2H, *7′*), 7.43–7.40 (m, 1H, *8′*), 7.36 ($t^{II\ ord.}_{app.}$, J = 8.6 Hz, 6H, *3*). **^{1}H{^{1}H} NMR** (500.13 MHz, $CDCl_3$): δ 7.87 (*3′*), 7.82 (2′), 7.82 (d, J = 5.1 Hz, *2*), 7.57 (*6′*), 7.47 (*7′*), 7.41 (*8′*), 7.36 (d, J = 8.5 Hz, *3*). **^{13}C{^{1}H} NMR** (125.76 MHz, $CDCl_3$): δ 165.2 (d, J = 255.2 Hz, *4*), 145.9 (*4′*), 139.1 (*5′*), 138.1 (d, J = 8.8 Hz, *2*), 136.3 (*1′*), 136.2 (*2′*), 132.7 (d, J = 3.2 Hz, *1*), 131.0 (*3′*), 129.3 (*7′*), 128.8 (*8′*), 127.5 (*6′*), 120.0 (d, J = 21.9 Hz *3*). **^{19}F NMR** (470.59 MHz, $CDCl_3$): δ −104.09 (tt, J = 8.4, 5.1 Hz, 3F), −148.25 (s, 4F) **HRMS** (ESI^+, *m/z*) Calcd. for $C_{30}H_{21}BiF_3^+$ (M+): 647.1394. Found: 647.1387. Error: 1.08 ppm. ν_{max} (neat, cm^{-1}): 1574, 1484, 1393, 1226, 1163, 1051, 998, 941, 823, 760, 697, 501. **m.p.** (°C): 192–193.

Tri(4-fluorophenyl)(4-(trimethylsilyl)phenyl)bismuthonium tetrafluoroborate (5h)

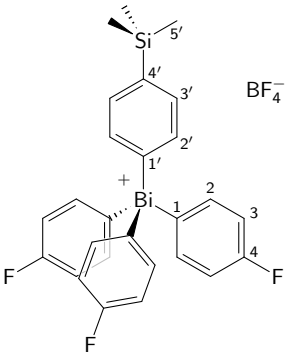

The compound was synthesised according to GP-3, by reacting **2** (103 mg, 0.207 mmol) with Selectfluor (74.4 mg, 0.210 mmol) and 4-(trimethylsilyl)phenylboronic acid (48.5 mg, 0.250 mmol). Recrystallisation from DCM/Et_2O yielded the desired pure product (109 mg, 0.150 mmol, 72%). The resulting crystals were suitable for X-ray diffraction analysis: details can be found in Section 6.8. **^{1}H NMR** (500.13 MHz, $CDCl_3$): δ 7.87–7.75 (m, 8H, *2 and 3′*), 7.72 (d, J = 7.7 Hz, 2H, *2′*), 7.36 ($t^{II\ ord.}_{app.}$, J = 8.6 Hz, 6H, *3*), 0.30 (s, 9H, *5′*). **^{13}C{^{1}H} NMR** (125.76 MHz, $CDCl_3$): δ 165.1 (d, J = 255.2 Hz, *4*), 147.3 (*4′*), 138.7 (*1′*), 138.1 (d, J = 8.3 Hz, *2*), 137.3 (*3′*), 134.9 (*2′*), 133.0 (d, J = 3.6 Hz, *1*), 119.9 (d, J = 21.8 Hz, *3*), −1.3 (*5′*). **^{19}F NMR** (470.59 MHz, $CDCl_3$): δ −104.24 (tt, J = 8.5, 5.2 Hz, 3F), −148.29 (s, 4F). **HRMS** (ESI^+, *m/z*) Calcd. for $C_{27}H_{25}BiF_3Si^+$ (M+): 643.1476. Found: 643.1468. Error: 1.24 ppm. ν_{max} (neat, cm^{-1}): 1575, 1485, 1394, 1228, 1163, 1058, 1000, 844, 821, 802, 760, 502, 482. **m.p.** (°C): 188–189.

Tri(4-fluorophenyl)(*p*-tolyl)bismuthonium tetrafluoroborate (5i)

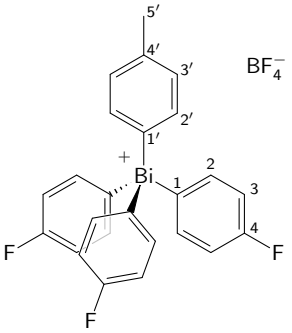

The compound was synthesised according to GP-3, by reacting **2** (103 mg, 0.207 mmol) with Selectfluor (74.4 mg, 0.21 mmol) and *p*-tolylboronic acid (34.0 mg, 0.25 mmol). Recrystallisation from DCM/Et_2O yielded the desired pure product (87.5 mg, 0.130 mmol, 63%). **^{1}H NMR** (500.13 MHz, $CDCl_3$): δ 7.78 ($dd^{II\ ord.}$, J = 8.7, 5.2 Hz, 6H, *2*), 7.62 (d, J = 7.9 Hz, 2H, *2′*), 7.49 (d, J = 7.9 Hz, 2H, *3′*), 7.35 ($t^{II\ ord.}_{app.}$, J = 8.8, 8.4 Hz, 6H, *3*), 2.44 (s, 3H, *5′*). **^{13}C{^{1}H} NMR** (125.76 MHz, $CDCl_3$): δ 165.1 (d, J = 255.1 Hz, *4*), 143.8 (*4′*), 138.1 (d, J = 8.8 Hz, *2*), 135.6 (*2′*), 134.3 (*1′*), 133.4 (*3′*), 132.7 (d, J = 3.4 Hz, *1*), 119.9 (d, J = 21.8 Hz, *3*), 21.7 (*5′*). **^{19}F NMR** (470.59 MHz, $CDCl_3$): δ −104.29 (tt, J = 8.6, 5.2 Hz, 3F), −148.53 (s, 4F). **HRMS** (ESI^+, *m/z*) Calcd. for $C_{25}H_{19}BiF_3^+$ (M+): 585.1237. Found: 585.1242. Error: 0.85 ppm. ν_{max} (neat, cm^{-1}): 1574, 1484, 1392, 1231, 1161, 1032, 1002, 823, 795, 570, 519, 502. **m.p.** (°C): 182–182.

(4-(Methoxy)phenyl)tri(4-fluorophenyl)bismuthonium tetrafluoroborate (5j)

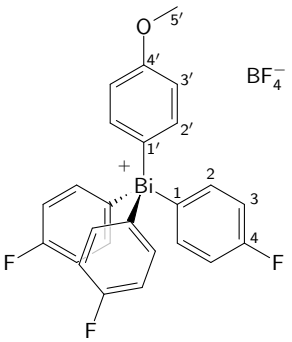

Tri(4-fluorophenyl)bismuthine **2** (100 mg, 0.202 mmol, 1.00 equiv), Selectfluor (72.4 mg, 0.204 mmol, 1.01 equiv) and 4-(methoxy)phenylboronic acid (31.2 mg, 0.205 mmol, 1.01 equiv) were loaded in a 10 mL microwave tube and suspended in MeCN (1.0 M). This suspension was stirred with a cross-shaped stirrer bar at 400 rpm at rt for 1 h. At completion, the solvent was evaporated under reduced pressure and the residues dissolved in DCM and water and transferred in separatory funnel, where the organic phase was extracted three times with water. The resulting organic phase was then dried over $MgSO_4$, filtered over filter paper and evaporated to dryness under vacuum. The crude material was purified by recrystallisation from CyH/DCM and the desired pure compound was isolated by filtration on a Büchner funnel as colourless crystals (86.5 mg, 0.126 mmol, 62%). **^{1}H NMR** (500.13 MHz, $CDCl_3$): δ 7.79 ($dd^{II\ ord.}$, J = 8.4, 5.1 Hz, 6H, *2*), 7.68 ($d^{IIord.}$, J = 8.7 Hz, 2H, *2′*), 7.36 ($t^{II\ ord.}_{app.}$, J = 8.8 Hz, 6H, *3*), 7.18 (d^{IIord}, J = 8.8 Hz, 2H, *3′*), 3.86 (s, 3H, *5′*). **^{13}C{^{1}H} NMR** (125.76 MHz, $CDCl_3$): δ 165.2 (d, J = 255.2 Hz, *4*), 163.0 (*4′*), 138.1 (d, J = 8.9 Hz, *2*), 137.3 (*2′*), 132.9 (d, J = 3.6 Hz, *1*), 127.8 (*1′*), 119.9 (d, J = 21.8 Hz, *3*), 118.3 (*3′*),

55.8 (*5′*). **^{19}F NMR** (470.59 MHz, $CDCl_3$): δ −104.26 (tt, J = 8.4, 5.2 Hz, 3F), −148.31 (s, 4F). **HRMS** (ESI^+, *m/z*) Calcd. for $C_{25}H_{19}BiF_3O^+$ (M+): 601.1186. Found: 601.1183. Error: 0.50 ppm. ν_{max} (neat, cm^{-1}): 2924, 1575, 1486, 1393, 1298, 1257, 1230, 1183, 1163, 1054, 820, 571, 504.

(4-(*N*,*N*-Dimethylamino)phenyl)tri(4-fluorophenyl)bismuthonium tetrafluoroborate (5k)

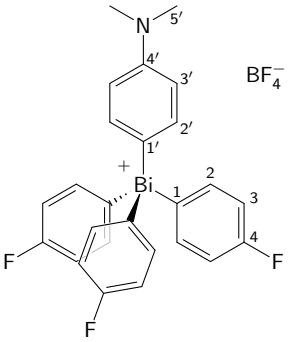

Tri(4-fluorophenyl)bismuthine **2** (103 mg, 0.208 mmol) and Selectfluor (74.9 mg, 0.211 mmol) were loaded in a 10 mL microwave tube and dissolved in MeCN (2 mL, 0.1 M). This solution was stirred with a cross-shaped stirrer bar at 400 rpm at 0 °C for 1 h. At that point (4-(*N*,*N*-Dimethylamino))phenylboronic acid (34.4 mg, 0.208 mmol) was added and this solution stirred for an additional 1 h at 0 °C. The solvent was then evaporated and the crude triturated with hot toluene and then purified by recrystallisation from DCM/Et_2O. The crystals were finally isolated by filtration on a Büchner funnel, washed with Et_2O and dried under vacuum, yielding the desired pure product (23.4 mg, 0.0334 mmol, 16%). **^{1}H NMR** (500.13 MHz, $CDCl_3$): δ 7.79 ($dd^{II\ ord.}$, J = 8.8, 5.3 Hz, 6H, *2*), 7.54 (d, J = 8.8 Hz, 2H, *2′*), 7.35 ($t^{II\ ord.}_{app.}$, J = 8.6 Hz, 6H, *3*), 6.88 (d, J = 9.1 Hz, 2H, *3′*), 3.04 (s, 6H, *5′*). **^{13}C{^{1}H} NMR** (125.76 MHz, $CDCl_3$): δ 165.1 (d, J = 255.1 Hz, *4*), 152.8 (*4′*), 138.1 (d, J = 8.3 Hz, *2*), 136.7 (*2′*), 132.7 (d, J = 3.5 Hz, *1*), 120.8 (*1′*), 119.8 (d, J = 21.8 Hz, *3*), 115.1 (*3′*), 40.1 (*5′*). **^{19}F NMR** (470.59 MHz, $CDCl_3$): δ −104.66 (tt, J = 8.4, 5.2 Hz, 3F), −149.18 (br, 4F). **HRMS** (ESI^+, *m/z*) Calcd. for $C_{26}H_{22}BiF_3N^+$ (M+): 614.1503. Found: 614.1510. Error: 1.14 ppm. ν_{max} (neat, cm^{-1}): 3092, 1573, 1483, 1377, 1222, 1162, 1033, 1000, 794, 502, 414. **m.p.** (°C): 166–167.

(3-Cyanophenyl)tri(4-fluorophenyl)bismuthonium tetrafluoroborate (5l)

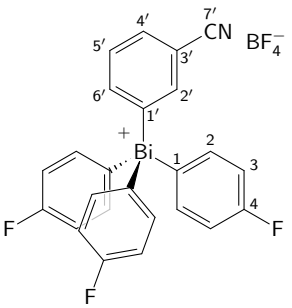

The compound was synthesised according to GP-4, by reacting **2** (98.6 mg, 0.199 mmol) with Selectfluor (83.1 mg, 0.235 mmol), 3-cyanophenylboronic acid (45.7 mg, 0.311 mmol) and $BF_3{\cdot}Et_2O$ (37 µL, 0.30 mmol). Recrystallisation from DCM/CyH yielded the desired pure product (62.1 mg, 0.0909 mmol, 46%). The resulting crystals were suitable for X-ray diffraction analysis: details

can be found in Section 6.8. **^{1}H NMR** (500.13 MHz, $(CD_3)_2O$): δ 8.55 (br, 1H, *2′*), 8.41 (d, J = 7.9 Hz, 1H, *6′*), 8.24–8.17 (m, 6H, *2*), 8.14 (dt, J = 7.8, 1.4 Hz, 1H, *4′*), 7.99 (t, J = 7.9 Hz, 1H, *5′*), 7.60 (t, J = 8.8 Hz, 6H, *3*). **^{13}C{^{1}H} NMR** (125.76 MHz, $(CD_3)_2O$): δ 164.9 (d, J = 251.6 Hz, *4*), 141.5 (*1′*), 140.5 (*6′*), 139.5 (*2′*), 138.7 (d, J = 8.8 Hz, *2*), 135.7 (*4′*), 135.1 (d, J = 2.8 Hz, *1*), 132.4 (*5′*), 119.2 (d, J = 22.2 Hz, *3*), 117.3 (*7′*), 115.6 (*3′*). **^{19}F NMR** (470.59 MHz, $(CD_3)_2O$): δ −107.34 (tt, J = 8.9, 5.3 Hz, 3F), −151.12 (s, 4F). **HRMS** (ESI^+, *m/z*) Calcd. for $C_{25}H_{16}BiF_3N^+$ (M+): 596.1033. Found: 596.1040. Error: 1.17 ppm. ν_{max} (neat, cm^{-1}): 1574, 1484, 1393, 1227, 1162, 1054, 1001, 820, 677, 570, 502, 430, 415. **m.p.** (°C): 192–193.

(3-Fluorophenyl)tri(4-fluorophenyl)bismuthonium tetrafluoroborate (5m)

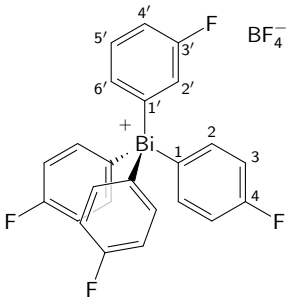

The compound was synthesised according to GP-4, by reacting **2** (99.9 mg, 0.202 mmol) with Selectfluor (74.4 mg, 0.210 mmol), 3-fluorophenylboronic acid (42.0 mg, 0.250 mmol) and $BF_3{\cdot}Et_2O$ (37 µL, 0.30 mmol). Recrystallisation from DCM/Et_2O yielded the desired pure product (87.3 mg, 0.129 mmol, 64%). The resulting crystals were suitable for X-ray diffraction analysis: details can be found in Section 6.8. **^{1}H NMR** (500.13 MHz, $CDCl_3$): δ 7.79 ($dd^{II\ ord.}$, J = 8.6, 5.1 Hz, 6H, *2*), 7.67 (td, J = 8.1, 5.3 Hz, 1H, *5′*), 7.54 (d, J = 7.7 Hz, 1H, *6′*), 7.50–7.43 (m, 1H, *2′*), 7.36 ($t^{II\ ord.}_{app.}$, J = 8.6 Hz, 6H, *2*), 7.30 (td, J = 8.5, 2.5 Hz, 1H, *4′*). **^{1}H{^{1}H} NMR** (500.13 MHz, $CDCl_3$): δ 7.79 (d, J = 5.1 Hz, *2*), 7.67 (d, J = 5.4 Hz, *5′*), 7.54 (*6′*), 7.46 (d, J = 6.9 Hz, *2′*), 7.36 (d, J = 8.4 Hz, *3*), 7.31 (d, J = 8.4 Hz, *4′*). **^{13}C{^{1}H} NMR** (125.76 MHz, $CDCl_3$): δ 165.2 (d, J = 255.5 Hz, *4*), 164.7 (d, J = 257.5 Hz, *3′*), 139.1 (d, J = 5.0 Hz, *1′*), 138.1 (d, J = 8.4 Hz, *2*), 133.8 (d, J = 7.2 Hz, *5′*), 133.1 (d, J = 3.3 Hz, *1*), 131.6 (d, J = 3.7 Hz, *6′*), 122.8 (d, J = 23.1 Hz, *2′*), 120.2 (d, J = 21.2 Hz, *4′*), 120.1 (d, J = 21.9 Hz, *3*). **^{19}F NMR** (470.59 MHz, $CDCl_3$): δ −103.83 (tt, J = 8.9, 5.2 Hz, 3F, *4*), −105.42–−105.56 (m, 1F, *3′*), −147.54 (s, 4F). **HRMS** (ESI^+, *m/z*) Calcd. for $C_{24}H_{16}BiF_4^+$ (M+): 589.0987. Found: 589.0996. Error: 1.53 ppm. ν_{max} (neat, cm^{-1}): 1573, 1484, 1470, 1220, 1163, 1067, 994, 817, 778, 672, 520, 502, 430, 415. **m.p.** (°C): 183–184.

(3-Bromophenyl)tri(4-fluorophenyl)bismuthonium tetrafluoroborate (5n)

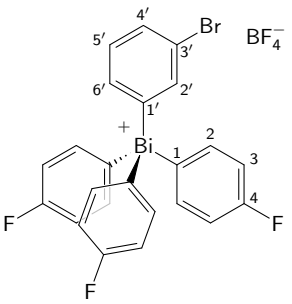

The compound was synthesised according to GP-4, by reacting **2** (106 mg, 0.214 mmol) with Selectfluor (78.9 mg, 0.223 mmol), 3-bromophenylboronic acid (65.5 mg, 0.326 mmol) and $BF_3{\cdot}Et_2O$ (37 µL, 0.30 mmol). Recrystallisation from DCM/CyH yielded the desired pure product (104 mg, 0.141 mmol, 66%). The resulting crystals were suitable for X-ray diffraction analysis: details can be found in Section 6.8. **^{1}H NMR** (400.13 MHz, $(CD_3)_2O$, −50 °C): δ 8.30 (s, 1H, *2′*), 8.21 ($t_{app.}$, J = 6.9 Hz, 6H, *2*), 8.08 (d, J = 7.8 Hz, 1H, *6′*), 7.93 (dd, J = 7.9, 1.9 Hz, 1H, *4′*), 7.75 (t, J = 7.9 Hz, 1H, *5′*), 7.63 (t, J = 8.8 Hz, 6H, *3*). **^{13}C{^{1}H} NMR** (125.76 MHz, $(CD_3)_2O$): δ 165.8 (d, J = 252.0 Hz, *4*), 142.2 (*1′*), 139.6 (br, *2*), 139.0 (br, *2′*), 136.3 (*4′*), 135.7 (d, J = 3.3 Hz, *1*), 135.7 (br, *6′*), 134.5 (br, *5′*), 126.3 (*br*, 3′), 120.1 (d, J = 22.0 Hz, *3′*). **^{19}F NMR** (470.59 MHz, $(CD_3)_2O$): δ −107.63 (dt, J = 8.9, 4.0 Hz, 3F), −150.60 (s, 4F). **HRMS** (ESI^+, *m/z*) Calcd. for $C_{24}H_{16}BiBrF_3^+$ (M+): 649.0186. Found: 649.0209. Error: 3.54 ppm. ν_{max} (neat, cm^{-1}): 1573, 1556, 1484, 1455, 1393, 1222, 1163, 1065, 988, 818, 777, 670, 570, 501, 414. **m.p.** (°C): 190–191.

Tri(4-fluorophenyl)(*m*-tolyl)bismuthonium tetrafluoroborate (5o)

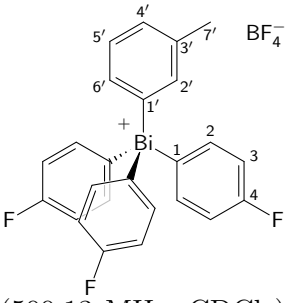

The compound was synthesised according to GP-3, by reacting **2** (98.4 mg, 0.199 mmol) with Selectfluor (78.9 mg, 0.223 mmol) and *m*-tolylboronic acid (42.5 mg, 0.312 mmol). Recrystallisation from DCM/Et_2O yielded the desired pure product (88.9 mg, 0.132 mmol, 66%). The resulting crystals were suitable for X-ray diffraction analysis: details can be found in Section 6.8. **^{1}H NMR** (500.13 MHz, $CDCl_3$): δ 7.80 ($dd^{II\ ord.}$, J = 8.5, 5.3 Hz, 6H, *2*), 7.57 (br, 1H, *2′*), 7.55 ($d_{app.}$, J = 7.6 Hz, 1H, *5′*), 7.50 (d, J = 7.8 Hz, 1H, *6′*), 7.43 (d, J = 7.5 Hz, 1H, *4′*), 7.36 ($t_{app.}^{II\ ord.}$, J = 8.6 Hz, 6H, *3*), 2.42 (s, 3H, *7′*). **^{13}C{^{1}H} NMR** (125.76 MHz, $CDCl_3$): δ 165.2 (d, J = 254.9 Hz, *4*), 143.4 (*3′*), 138.1 (d, J = 8.4 Hz, *2*), 137.5 (*1′*), 136.0 (*2′*), 133.8 (*4′*), 132.7 (d, J = 3.3 Hz, *1*), 132.6 (*6′*), 132.2 (*5′*), 120.0 (d, J = 21.8 Hz, *3*), 21.8 (*7′*). **^{19}F NMR** (470.59 MHz, $CDCl_3$): δ −104.25 (tt, J = 8.5, 5.2 Hz, *4*, 3F), −148.40 (s, 4F). **HRMS** (ESI^+, *m/z*) Calcd. for $C_{25}H_{19}BiF_3^+$ (M+): 585.1237. Found: 585.1243. Error: 1.03 ppm. ν_{max} (neat, cm^{-1}): 1574, 1484, 1392, 1230, 1161, 1054, 998, 824, 775, 679, 570, 502, 413. **m.p.** (°C): 151–152.

Tri(4-fluorophenyl)(3-hydroxy-4-methylphenyl)bismuthonium tetrafluoroborate (5p)

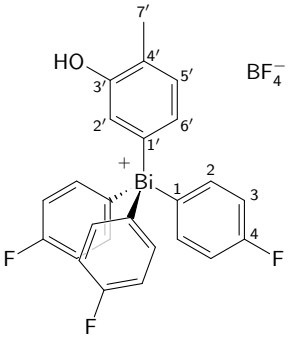

The compound was synthesised according to GP-3, by reacting **2** (97.1 mg, 0.196 mmol) with Selectfluor (76.1 mg, 0.215 mmol) and 3-hydroxy-4-methylphenylboronic acid (47.8 mg, 0.314 mmol). Recrystallisation from DCM/Et_2O yielded the desired pure product (76.4 mg, 0.111 mmol, 57%). ^{1}**H NMR** (500.13 MHz, $CDCl_3$): δ 7.75 (dd$^{\text{II ord.}}$, J = 8.5, 5.2 Hz, 6H, *2*), 7.49 (s, 1H, *OH*), 7.43 (s, 1H, *2′*), 7.36–7.30 (m, 7H, *3 and 5′*), 6.96 (d, J = 7.8 Hz, 1H, *6′*), 2.22 (s, 3H, *7′*). ^{13}**C{^{1}H} NMR** (125.76 MHz, $CDCl_3$): δ 165.3 (d, J = 255.5 Hz, *4*), 158.8 *3′*, 138.03 (d, J = 8.9 Hz, *2*), 134.2 (*5′*), 131.9 (*1′*), 131.5 (*4′*), 130.3 (d, J = 3.5 Hz, *1*), 125.9 (*6′*), 121.6 (*2′*), 120.2 (d, J = 21.9 Hz, *3*), 16.3 (*7′*). ^{19}**F NMR** (470.59 MHz, $CDCl_3$): δ −103.60 (tt, J = 8.5, 5.1 Hz, 3F), −148.70 (s, 4F). **HRMS** (ESI$^+$, *m/z*) Calcd. for $C_{25}H_{19}BiF_3O^+$ (M+): 601.1186. Found: 601.1202. Error: 2.66 ppm. ν_{max} (neat, cm^{-1}): 3425, 1574, 1484, 1392, 1223, 1160, 1001, 813, 765, 750, 498. **m.p.** (°C): 179–180.

(3,5-Dimethylphenyl)tri(4-fluorophenyl)bismuthonium tetrafluoroborate (5q)

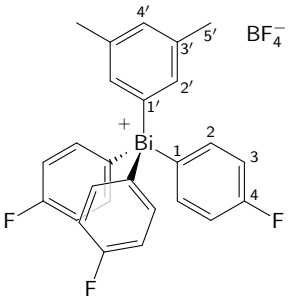

The compound was synthesised according to GP-3, by reacting **2** (103 mg, 0.208 mmol) with Selectfluor (82.5 mg, 0.233 mmol) and 3,5-dimethylphenylboronic acid (45.1 mg, 0.301 mmol). Recrystallisation from DCM/Et_2O yielded the desired pure product (99.1 mg, 0.144 mmol, 69%). The resulting crystals were suitable for X-ray diffraction analysis: details can be found in Section 6.8. ^{1}**H NMR** (500.13 MHz, $CDCl_3$): δ 7.80 (dd$^{\text{II ord.}}$, J = 8.7, 5.3 Hz, 6H, *2*), 7.36 ($t^{\text{II ord.}}_{\text{app.}}$, J = 8.6 Hz, 6H, *3*), 7.32 (s, 2H, *2′*), 7.24 (s, 1H, *4′*), 2.37 (s, 6H, *5′*). ^{13}**C{^{1}H} NMR** (125.76 MHz, $CDCl_3$): δ 165.1 (d, J = 255.2 Hz, *4*), 142.9 (*3′*), 138.2 (d, J = 8.8 Hz, *2*), 137.1 (*1′*), 134.7 (*4′*), 132.8 (*2′*), 132.7 (d, J = 3.3 Hz, *1*), 119.9 (d, J = 21.8 Hz, *3*), 21.7 (*5′*). ^{19}**F NMR** (470.59 MHz, $CDCl_3$): δ −104.32 (tt, J = 8.4, 5.1 Hz, 3F), −148.60 (s, 4F). **HRMS** (ESI$^+$, *m/z*) Calcd. for $C_{26}H_{21}BiF_3^+$ (M+): 599.1396. Found: 599.1394. Error: 0.33 ppm. ν_{max} (neat, cm^{-1}): 1575, 1486, 1393, 1228, 1163, 1051, 1003, 819, 673, 570, 501, 413. **m.p.** (°C): 152–154.

Tri(4-fluorophenyl)(2-(trifluoromethyl)phenyl)bismuthonium tetrafluoroborate (5r)

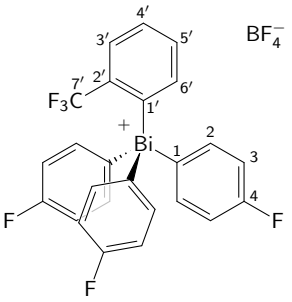

The compound was synthesised according to GP-4, by reacting **2** (104 mg, 0.210 mmol) with Selectfluor (80.6 mg, 0.228 mmol), 2-(trifluoromethyl)phenylboronic acid (59.2 mg, 0.312 mmol) and $BF_3{\cdot}Et_2O$ (37 µL, 0.30 mmol). Recrystallisation from DCM/CyH yielded the desired pure product (87.6 mg, 0.121 mmol, 57%). **^{1}H NMR** (500.13 MHz, $CDCl_3$): δ 8.02 (br, 1H *3′*), 7.84 (br, 1H, *6′*), 7.82–7.70 (m, 8H, *2, 4′ and 5′*), 7.38 (t, J = 8.3 Hz, 6H, *3*). **^{13}C{^{1}H} NMR** (125.76 MHz, $CDCl_3$): δ 165.2 (d, J = 255.5 Hz, *4*), 138.2 (d, J = 8.5 Hz, *2*), 137.0 (*6′*), 136.8 (q, J = 2.8 Hz, *1′*), 135.6 (*5′*), 134.5 (*1*), 133.7 (q, J = 32.0 Hz, *2′*), 132.9 (*4′*), 129.9 (q, J = 3.8 Hz, *3′*), 123.5 (q, J = 273.9 Hz, *7′*), 120.1 (d, J = 21.7 Hz, *3*). **^{19}F NMR** (470.59 MHz, $CDCl_3$): δ −58.71 (s, 3F, *7′*), −104.03 (tt, J = 8.7, 5.2 Hz, 3F, *4*), −148.06 (s, 4F). **HRMS** (ESI$^+$, *m/z*) Calcd. for $C_{25}H_{16}BiF_6^+$ (M+): 639.0955. Found: 639.0945. Error: 1.56 ppm. ν_{max} (neat, cm^{-1}): 1484, 1320, 1228, 1162, 1045, 1000, 817, 772, 500. **m.p.** (°C): 159–160.

(2-Chlorophenyl)tri(4-fluorophenyl)bismuthonium tetrafluoroborate (5s)

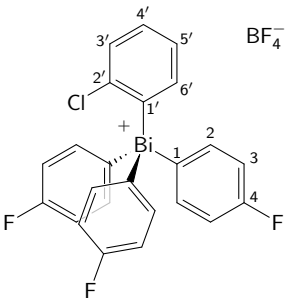

The compound was synthesised according to GP-4, by reacting **2** (100 mg, 0.202 mmol) with Selectfluor (81.4 mg, 0.230 mmol), 2-chlorophenylboronic acid (38.8 mg, 0.248 mmol) and $BF_3{\cdot}Et_2O$ (37 µL, 0.30 mmol). Recrystallisation from DCM/CyH yielded the desired pure product (102 mg, 0.147 mmol, 74%). The resulting crystals were suitable for X-ray diffraction analysis: details can be found in Section 6.8. **^{1}H NMR** (500.13 MHz, $CDCl_3$): δ 7.85 (dd$^{\text{II ord.}}$, J = 8.6, 5.2 Hz, 6H, *2*), 7.694 (d, J = 8.0 Hz, 1H, *3′*), 7.691 (d, J = 8.0 Hz, 1H, *6′*), 7.61 (td, J = 7.7, 1.6 Hz, 1H, *5′*), 7.55 (td, J = 7.6, 1.5 Hz, 1H, *4′*), 7.38 ($t^{\text{II ord.}}_{\text{app.}}$, J = 8.6 Hz, 6H, *3*). **^{13}C{^{1}H} NMR** (125.76 MHz, $CDCl_3$): δ 165.1 (d, J = 255.3 Hz, *4*), 142.0 (*2′*), 138.4 (*1′*), 138.1 (d, J = 8.6 Hz, *2*), 137.5 (*3′*), 134.4 (*5′*), 133.7 (d, J = 3.5 Hz, *1*), 131.3 (*6′*), 130.6 (*4′*), 120.0 (d, J = 21.9 Hz, *3*). **^{19}F NMR** (470.59 MHz, $CDCl_3$): δ −104.12 (tt, J = 8.3, 5.1 Hz, 3F), −148.10 (s, 4F). **HRMS** (ESI$^+$, *m/z*) Calcd. for $C_{24}H_{16}BiClF^+$ (M+): 605.0708. Found: 605.0691. Error: 2.81 ppm. ν_{max} (neat, cm^{-1}): 1573, 1486, 1392, 1229, 1162, 1049, 1028, 998, 827, 761, 570, 503, 410. **m.p.** (°C): 191–192.

(2-Fluorophenyl)tri(4-fluorophenyl)bismuthonium tetrafluoroborate (5t)

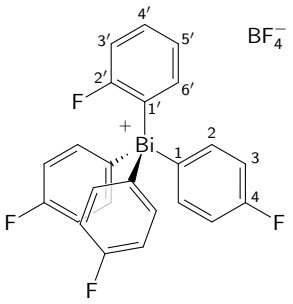

The compound was synthesised according to GP-4, by reacting **2** (99.5 mg, 0.201 mmol) with Selectfluor (78.9 mg, 0.229 mmol), 2-fluorophenylboronic acid (44.9 mg, 0.321 mmol) and $BF_3{\cdot}Et_2O$ (37 µL, 0.30 mmol). Recrystallisation from DCM/CyH yielded the desired pure product (75.0 mg, 0.111 mmol, 55%). The resulting crystals were suitable for X-ray diffraction analysis: details can be found in Section 6.8. **^{1}H NMR** (500.13 MHz, $CDCl_3$): δ 7.84 (dd, J = 8.8, 5.1 Hz, 6H, *2*), 7.70 (ddd, J = 7.6, 4.2, 1.5 Hz, 1H, *6′*), 7.66 (ddd, J = 8.2, 6.2, 1.7 Hz, 1H, *4′*), 7.47 (td, J = 7.6, 1.0 Hz, 1H, *5′*), 7.43 (td, J = 8.2, 7.4, 1.0 Hz, 1H, *3′*), 7.38 (t, J = 8.5 Hz, 6H, *3*). **^{1}H{^{1}H} NMR** (500.13 MHz, $CDCl_3$): δ 7.84 (d, J = 5.1 Hz, *2*), 7.70 (d, J = 4.2 Hz, *6′*), 7.67 (d, J = 6.2 Hz, *4′*), 7.47 (s, *5′*), 7.43 (d, J = 7.4 Hz, *3′*), 7.38 (d, J = 8.5 Hz, 1H, *3*). **^{13}C{^{1}H} NMR** (125.76 MHz, $CDCl_3$): δ 165.2 (d, J = 255.3 Hz, *4*), 163.3 (d, J = 241.7 Hz, *2′*), 138.0 (d, J = 8.5 Hz, *2*), 136.3 (d, J = 6.7 Hz, *6′*), 135.2 (d, J = 8.0 Hz, *4′*), 132.9 (d, J = 3.4 Hz, *1*), 128.3 (d, J = 2.6 Hz, *5′*), 126.0 (d, J = 33.2 Hz, *1′*), 120.0 (d, J = 21.9 Hz, *3*), 117.4 (d, J = 23.6 Hz, *3′*). **^{19}F NMR** (470.59 MHz, $CDCl_3$): δ −93.88 (ddd, J = 7.4, 6.2, 4.2 Hz, 1F, *2′*), −103.98 (tt, J = 8.5, 5.1 Hz, 3F), −147.78 (s, 4F). **HRMS** (ESI^+, *m/z*) Calcd. for $C_{24}H_{16}BiF_4^+$ (M+): 589.0986. Found: 589.0993. Error: 1.19 ppm. ν_{max} (neat, cm^{-1}): 1574, 1484, 1468, 1443, 1393, 1228, 1162, 1004, 816, 570, 501, 434, 414. **m.p.** (°C): 177–178.

(2-Biphenyl)tri(4-fluorophenyl)bismuthonium tetrafluoroborate (5u)

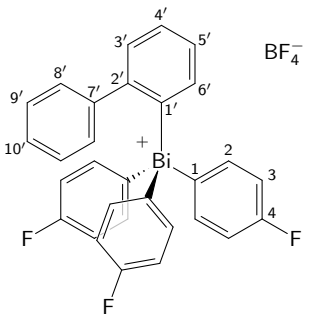

The compound was synthesised according to GP-4, by reacting **2** (99.4 mg, 0.201 mmol) with Selectfluor (78.7 mg, 0.222 mmol), 3-bromophenylboronic acid (62.0 mg, 0.313 mmol) and $BF_3{\cdot}Et_2O$ (37 µL, 0.30 mmol). Recrystallisation from DCM/CyH yielded the desired pure product (122 mg, 0.166 mmol, 83%). The resulting crystals were suitable for X-ray diffraction analysis: details can be found in Section 6.8. **^{1}H NMR** (500.13 MHz, $CDCl_3$): δ 7.79 (d, J = 7.6 Hz, 1H, *6′*), 7.74–7.66 (m, 2H, *3′ and 4′*), 7.67–7.60 (m, 1H, *5′*), 7.50 (dd, J = 8.9, 5.3 Hz, 6H, *2*), 7.32–7.20 (m, 9H, *3, 8′ and 10′*), 7.12 (t, J = 7.7 Hz, 2H, *9′*). **^{1}H{^{1}H} NMR** (500.13 MHz, $CDCl_3$): δ 7.79 (s, *6′*), 7.69 (s, *3′ and 4′*), 7.66 (s, *5′*), 7.49 (d, J = 5.0 Hz, *2*), 7.28 (s, *8′*), 7.26 (d,

J = 8.4 Hz, *3*), 7.24 (s, *10′*), 7.12 (s, *9′*). **^{13}C{^{1}H} NMR** (125.76 MHz, $CDCl_3$): δ 164.8 (d, J = 254.4 Hz, *4*), 147.7 (*2′*), 143.8 (*1′*), 141.6 (*7′*), 137.9 (d, J = 8.2 Hz, *2*), 135.1 (*6′*), 134.7 (d, J = 3.5 Hz, *1*), 133.0 (*3′*), 132.6 (*4′*), 131.0 (*5′*), 129.5 (*8′*), 129.4 (*9′ and 10′*), 119.6 (d, J = 21.7 Hz, *3*). **^{19}F NMR** (470.59 MHz, $CDCl_3$): δ −104.93 (tt, J = 8.4, 5.2 Hz, 3F), −148.33 (s, 4F). **HRMS** (ESI^+, *m/z*) Calcd. for $C_{30}H_{21}BiF_3^+$ (M+): 647.1394. Found: 647.1413. Error: 2.94 ppm. ν_{max} (neat, cm^{-1}): 1576, 1485, 1223, 1162, 1053, 991, 818, 746, 706, 506. **m.p.** (°C): 173–174.

Tri(4-fluorophenyl)(*o*-tolyl)bismuthonium tetrafluoroborate (5v)

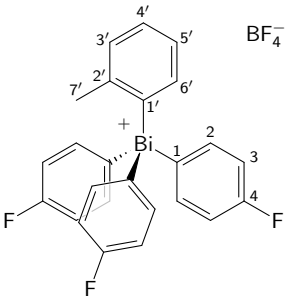

The compound was synthesised according to GP-4, by reacting **2** (994 mg, 2.01 mmol) with Selectfluor (716 mg, 2.02 mmol), *o*-tolyllboronic acid (280 mg, 2.06 mmol) and $BF_3{\cdot}Et_2O$ (370 µL, 3.00 mmol). Recrystallisation from DCM/CyH yielded the desired pure product (1.03 g, 1.54 mmol, 76%). The resulting crystals were suitable for X-ray diffraction analysis: details can be found in Section 6.8. **^{1}H NMR** (500.13 MHz, $CDCl_3$): δ 7.80 ($dd_{app.}$, J = 8.6, 5.2 Hz, 6H, *2*), 7.61–7.54 (m, 1H, *3′*), 7.54–7.48 (m, 2H, *5′ and 6′*), 7.48–7.40 (m, 1H, *4′*), 7.35 ($t^{II\ ord.}_{app.}$, J = 8.6 Hz, 6H, *3*), 2.39 (s, 3H, *7′*). **^{13}C{^{1}H} NMR** (125.76 MHz, $CDCl_3$): δ 165.1 (d, J = 255.2 Hz, *4*), 142.7 (*1′*), 141.1 (*2′*), 138.1 (d, J = 8.4 Hz, *2*), 135.5 (*6′*), 133.5 (*3′*), 133.1 (*5′*), 132.6 (d, J = 3.3 Hz, *1*), 129.8 (*4′*), 120.1 (d, J = 21.8 Hz, *3*), 25.4 (*7′*). **^{19}F NMR** (470.59 MHz, $CDCl_3$): δ −104.28 (tt, J = 8.4, 5.4 Hz, 3F), −149.05 (s, 4F). **HRMS** (ESI^+, *m/z*) Calcd. for $C_{25}H_{19}BiF_3^+$ (M+): 585.1237. Found: 585.1253. Error: 2.73 ppm. ν_{max} (neat, cm^{-1}): 1573, 1485, 1228, 1162, 1034, 1000, 828, 756, 505. **m.p.** (°C): 160–161.

(2-Ethylphenyl)tri(4-fluorophenyl)bismuthonium tetrafluoroborate (5w)

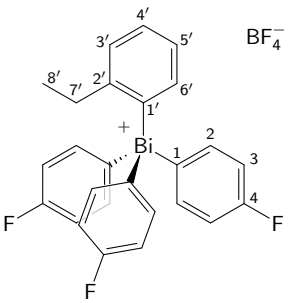

The compound was synthesised according to GP-4, by reacting **2** (95.6 mg, 0.193 mmol) with Selectfluor (72.9 mg, 0.206 mmol), (2-ethylphenyl)boronic acid (36.3 mg, 0.242 mmol) and $BF_3{\cdot}Et_2O$ (370 µL, 3.00 mmol). Recrystallisation from DCM/CyH yielded the desired pure product (101 mg, 0.148 mmol, 76%). **^{1}H NMR** (500.13 MHz, $CDCl_3$): δ 7.81 ($dd^{II\ ord.}$, J = 8.5, 5.2 Hz, 6H, *2*), 7.64 (t, J = 7.3 Hz, 1H, *3′*), 7.61 ($d^{IIord.}$, J = 7.4 Hz, 1H, *4′*), 7.54 ($d^{IIord.}$, J = 7.7 Hz, 1H, *6′*), 7.47 (t, J = 6.9 Hz, 1H, *5′*), 7.37 ($t^{II\ ord.}_{app.}$, J = 8.4 Hz, 6H,

3), 2.66 (q, J = 7.5 Hz, 2H, *7′*), 1.09 (t, J = 7.5 Hz, 3H, *8′*). **^{13}C{^{1}H} NMR** (125.76 MHz, $CDCl_3$): δ 165.1 (d, J = 255.4 Hz, *4*), 148.3 (*2′*), 141.8 (*1′*), 138.1 (d, J = 8.3 Hz, *2*), 135.3 (*6′*), 133.4 (d, J = 3.5 Hz, *1*), 133.2 (*4′*), 131.8 (*3′*), 130.1 (*5′*), 120.0 (d, J = 21.8 Hz, *3*), 33.1 (*7′*), 15.1 (*8′*). **^{19}F NMR** (470.59 MHz, $CDCl_3$): δ −104.36 (tt, J = 8.5, 5.2 Hz, 3F), −148.66 (s, 4F). **HRMS** (ESI^+, *m/z*) Calcd. for $C_{26}H_{22}BiF_3^+$ (M+): 600.1472. Found: 600.1441. Error: 5.17 ppm. ν_{max} (neat, cm^{-1}): 1574, 1484, 1394, 1224, 1161, 1031, 1001, 832, 817, 756, 570. **m.p.** (°C): 120–122.

(2-Formylphenyl)tri(4-fluorophenyl)bismuthonium tetrafluoroborate (5x)

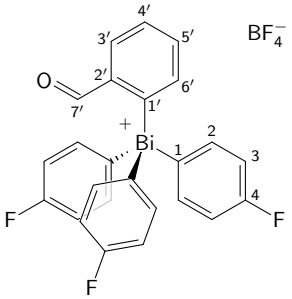

The compound was synthesised according to GP-4, by reacting **2** (125 mg, 0.252 mmol) with Selectfluor (93.5 mg, 0.263 mmol), (2-formylphenyl)boronic acid (41.4 mg, 0.276 mmol) and $BF_3{\cdot}Et_2O$ (370 µL, 3.00 mmol). Recrystallisation from DCM/CyH yielded the desired pure product (129 mg, 0.187 mmol, 75%). The resulting crystals were suitable for X-ray diffraction analysis: details can be found in Section 6.8. **^{1}H NMR** (500.13 MHz, $CDCl_3$): δ 10.12 (d, J = 1.1 Hz, 1H, *7′*), 8.29 (dd, J = 7.3, 1.6 Hz, 1H, *3′*), 7.96 (td, J = 7.5, 1.6 Hz, 1H, *5′*), 7.90 (td, J = 7.4, 1.1 Hz, 1H, *4′*), 7.85 (d, J = 7.6 Hz, 1H, *6′*), 7.75 ($dd^{II\ ord.}$, J = 8.6, 5.3 Hz, 6H, *2*), 7.33 ($t^{II\ ord.}_{app.}$, J = 8.6 Hz, 6H, *3*). **^{13}C{^{1}H} NMR** (125.76 MHz, $CDCl_3$): δ 192.8 (*7′*), 164.9 (d, J = 254.3 Hz, *4*), 139.3 (*5′*), 138.5 (*2′*), 138.3 (*3′*), 138.02 (d, J = 8.3 Hz, *2*), 136.4 (*6′*), 136.0 (*1′*), 135.63 (d, J = 3.1 Hz, *1*), 133.4 (*4′*), 119.7 (d, J = 21.6 Hz, *3*). **^{19}F NMR** (470.59 MHz, $CDCl_3$): δ −105.21 (tt, J = 8.5, 5.3 Hz, 3F), −148.80 (s, 4F). **HRMS** (ESI^+, *m/z*) Calcd. for $C_{25}H_{17}BiF_3O^+$ (M+): 599.1030. Found: 599.1069. Error: 6.51 ppm. ν_{max} (neat, cm^{-1}): 1666, 1573, 1485, 1390, 1227, 1161, 1051, 1036, 1001, 821, 768, 504. **m.p.** (°C): 224–226.

Tri(4-fluorophenyl)(1-naphthyl)bismuthonium tetrafluoroborate (5y)

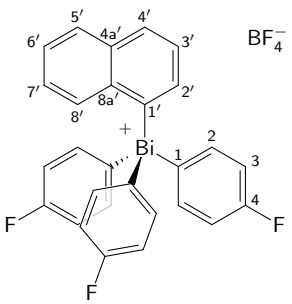

The compound was synthesised according to GP-3, by reacting **2** (98.7 mg, 0.200 mmol) with Selectfluor (78.4 mg, 0.221 mmol) and 21-naphthylboronic acid (56.0 mg, 0.326 mmol). Recrystallisation from DCM/Et_2O yielded the desired pure product (81.8 mg, 0.115 mmol, 58%). The resulting crystals were suitable for X-ray diffraction analysis: details can be found in Section 6.8. **^{1}H NMR**

(500.13 MHz, $CDCl_3$): δ 8.16 (d, J = 8.1 Hz, 1H, *4′*), 8.06 (d, J = 8.2 Hz, 1H, *5′*), 7.90 (d, J = 7.3 Hz, 1H, *2′*), 7.84 ($dd^{II\ ord.}$, J = 8.5, 5.2 Hz, 6H, *2*), 7.68 (dd, J = 8.1, 7.3 Hz, 1H, *3′*), 7.63 (dt, J = 8.2, 4.0 Hz, 1H, *6′*), 7.51 (d, J = 3.8 Hz, 2H, *7′ and 8′*), 7.35 ($t^{II\ ord.}_{app.}$, J = 8.6 Hz, 6H, *3*). **^{13}C{^{1}H} NMR** (125.76 MHz, $CDCl_3$): δ 165.2 (d, J = 255.9 Hz, *4*), 138.4 (*4a′*), 138.3 (d, J = 8.4 Hz, *2*), 136.8 (*2′*), 136.2 (*1′*), 135.4 (*8a′*), 133.6 (*4′*), 132.4 (d, J = 3.0 Hz, *1*), 130.4 (*5′*), 129.1 (*7′*), 128.1 (*3′*), 127.8 (*6′*), 126.9 (*8′*), 120.1 (d, J = 21.9 Hz, *3*). **^{19}F NMR** (470.59 MHz, $CDCl_3$): δ −103.97 (tt, J = 8.4, 5.2 Hz, 3F), −148.86 (s, 4F). **HRMS** (ESI^+, *m/z*) Calcd. for $C_{28}H_{19}BiF_3^+$ (M+): 621.1237. Found: 621.1205. Error: 5.15 ppm. ν_{max} (neat, cm^{-1}): 1576, 1485, 1276, 1260, 1226, 1161, 1024, 816, 790, 750, 500. **m.p.** (°C): 203–204.

Tri(4-fluorophenyl)(2-methoxyphenyl)bismuthonium tetrafluoroborate (5z)

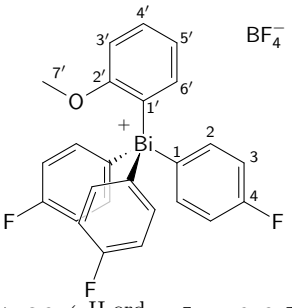

The compound was synthesised according to GP-3, by reacting **2** (104 mg, 0.210 mmol) with Selectfluor (74.9 mg, 0.211 mmol) and 2-methoxyphenylboronic acid (49.4 mg, 0.325 mmol). Recrystallisation from DCM/Et_2O yielded the desired pure product (98.4 mg, 0.143 mmol, 68%).**^{1}H NMR** (500.13 MHz, $CDCl_3$): δ 7.78 ($dd^{II\ ord.}$, J = 8.6, 5.3 Hz, 6H, *2*), 7.68–7.61 (m, 2H, *4′ and 6′*), 7.36 ($t^{II\ ord.}_{app.}$, J = 8.6 Hz, 6H, *3*), 7.31–7.25 (m, 2H, *3′ and 5′*), 3.79 (s, 3H, *7′*). **^{13}C{^{1}H} NMR** (125.76 MHz, $CDCl_3$): δ 165.1 (d, J = 255.1 Hz, *4*), 159.3 (*2′*), 138.0 (d, J = 8.7 Hz, *2*), 135.7 (*6′*), 134.9 (*4′*), 132.4 (d, J = 3.6 Hz, *1*), 128.5 (*1′*), 125.2 (*5′*), 119.8 (d, J = 21.8 Hz, *3*), 113.3 (*3′*), 56.9 (*7′*). **^{19}F NMR** (470.59 MHz, $CDCl_3$): δ −104.58 (tt, J = 8.6, 5.2 Hz, 3F), −149.66 (s, 4F). **HRMS** (ESI^+, *m/z*) Calcd. for $C_{25}H_{19}BiF_3O^+$ (M+): 601.1186. Found: 601.1179. Error: 1.16 ppm. ν_{max} (neat, cm^{-1}): 1590, 1573, 1484, 1435, 1392, 1225, 1162, 1035, 1003, 822, 502. **m.p.** (°C): 172–173.

Tri(4-fluorophenyl)(2-isopropoxyphenyl)bismuthonium tetrafluoroborate (5aa)

The compound was synthesised according to GP-4, by reacting Ar^F_3Bi **2** (99.1 mg, 0.201 mmol) with Selectfluor (74.4 mg, 0.210 mmol), (2-isopropoxyphenyl)boronic acid (40.4 mg, 0.224 mmol) and $BF_3{\cdot}Et_2O$ (37 µL, 0.30 mmol). Recrystallisation from DCM/CyH yielded the desired pure product (116 mg, 0.162 mmol, 81%).

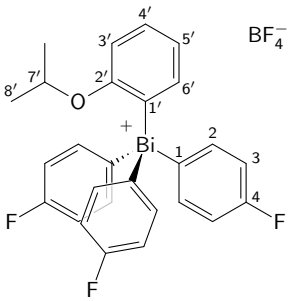

The resulting crystals were suitable for X-ray diffraction analysis: details can be found in Section 6.8. **^{1}H NMR** (500.13 MHz, $CDCl_3$): δ 7.83 (dd$^{\text{II ord.}}$, J = 8.6, 5.2 Hz, 6H, *2*), 7.66 (d, J = 7.7 Hz, 1H, *6′*), 7.62 (ddd, J = 8.6, 7.4, 1.5 Hz, 1H, *4′*), 7.36 ($t^{\text{II ord.}}_{\text{app.}}$, J = 8.6 Hz, 6H, *3*), 7.23 (dd, J = 7.5, 1.1 Hz, 1H, *5′*), 7.21 (d, J = 8.3 Hz, 1H, *3′*), 4.65 (hept, J = 6.1 Hz, 1H, *7′*), 0.98 (d, J = 6.0 Hz, 6H, *8′*). **^{13}C{^{1}H} NMR** (125.76 MHz, $CDCl_3$): δ 165.1 (d, J = 255.1 Hz, *4*), 157.6 (*2′*), 138.0 (d, J = 8.3 Hz, *2*), 136.4 (*6′*), 134.8 (*4′*), 132.7 (d, J = 3.0 Hz, *1*), 128.8 (*1′*), 124.6 (*5′*), 119.7 (d, J = 21.7 Hz, *3*), 113.9 (*3′*), 72.1 (*7′*), 21.5 (*8′*). **^{19}F NMR** (470.59 MHz, $CDCl_3$): δ −104.68 (tt, J = 8.5, 5.2 Hz, 3F), −149.38 (s, 4F). **HRMS** (ESI$^+$, *m/z*) Calcd. for $C_{27}H_{23}BiF_3O^+$ (M+): 629.1499. Found: 629.1452. Error: 7.47 ppm. ν_{max} (neat, cm^{-1}): 1574, 1485, 1466, 1394, 1279, 1221, 1162, 1051, 1000, 941, 819, 761, 504. **m.p.** (°C): 177–178.

Tri(4-fluorophenyl)(2-(trifluoromethoxy)phenyl)bismuthonium tetrafluoroborate (5ab)

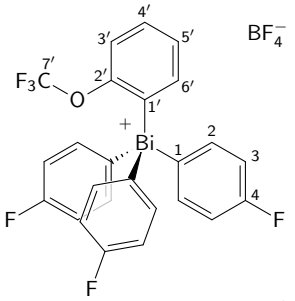

The compound was synthesised according to GP-4, by reacting **2** (95.3 mg, 0.192 mmol) with Selectfluor (72.0 mg, 0.203 mmol), (2-(trifluoromethoxy)phenyl)boronic acid (51.3 mg, 0.249 mmol) and $BF_3{\cdot}Et_2O$ (37 µL, 0.30 mmol). Recrystallisation from DCM/CyH yielded the desired pure product (108 mg, 0.145 mmol, 75%). The resulting crystals were suitable for X-ray diffraction analysis: details can be found in Section 6.8. **^{1}H NMR** (500.13 MHz, $CDCl_3$): δ 7.89–7.75 (m, 7H, *2 and 6′*), 7.71 (ddd, J = 8.8, 7.4, 1.6 Hz, 1H, *4′*), 7.63–7.52 (m, 2H, *3′ and 5′*), 7.38 ($t^{\text{II ord.}}_{\text{app.}}$, J = 8.6 Hz, 6H, *3*). **^{13}C{^{1}H} NMR** (125.76 MHz, $CDCl_3$): δ 165.2 (d, J = 255.3 Hz, *4*), 150.9 (*2′*), 137.9 (d, J = 8.4 Hz, *2*), 137.0 (*6′*), 134.7 (*4′*), 133.1 (d, J = 3.6 Hz, *1*), 131.6 (*1′*), 129.7 (*5′*), 119.99 (d, J = 21.9 Hz, *3*), 119.95 (q, J = 262.9 Hz, *7′*), 119.0 (d, J = 2.8 Hz, *3′*). **^{19}F NMR** (470.59 MHz, $CDCl_3$): δ −56.91 (d, J = 2.0 Hz, 3F, *7′*), −103.97 (tt, J = 8.4, 5.1 Hz, 3F, *4*), −147.76 (s, 4F). **HRMS** (ESI$^+$, *m/z*) Calcd. for $C_{25}H_{16}BiF_6O^+$ (M+): 655.0904. Found: 655.0850. Error: 8.24 ppm. ν_{max} (neat, cm^{-1}): 1576, 1485, 1234, 1186, 1159, 1067, 1001, 987, 818, 572, 502. **m.p.** (°C): 122–124.

(2-Fluoro-6-methoxyphenyl)tri(4-fluorophenyl)bismuthonium tetrafluoroborate (5ac)

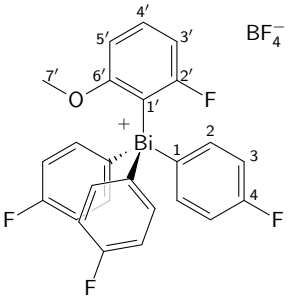

The compound was synthesised according to GP-4, by reacting **2** (97.7 mg, 0.198 mmol) with Selectfluor (74.6 mg, 0.211 mmol), (2-fluoro-6-methoxyphenyl)boronic acid (44.2 mg, 0.260 mmol) and $BF_3{\cdot}Et_2O$ (37 µL, 0.30 mmol). Recrystallisation from DCM/CyH yielded the desired pure product (112 mg, 0.159 mmol, 80%). ^{1}**H NMR** (500.13 MHz, $CDCl_3$): δ 7.83 (dd$^{\text{II ord.}}$, J = 8.5, 5.3 Hz, 6H, *2*), 7.60 (td, J = 8.3, 6.8 Hz, 1H, *4′*), 7.35 (t$^{\text{II ord.}}_{\text{app.}}$, J = 8.6 Hz, 6H, *3*), 7.09–7.00 (m, 2H, *3′ and 5′*), 3.73 (s, 3H, *7′*). ^{13}**C{^{1}H} NMR** (125.76 MHz, $CDCl_3$): δ 165.0 (d, J = 254.5 Hz, *4*), 164.0 (d, J = 246.2 Hz, *2′*), 161.3 (d, J = 10.8 Hz, *6′*), 137.7 (d, J = 8.4 Hz, *2*), 136.4 (d, J = 9.2 Hz, *4′*), 134.2 (d, J = 3.4 Hz, *1*), 119.6 (d, J = 21.9 Hz, *3*), 117.0 (d, J = 33.2 Hz, *1′*), 110.4 (d, J = 23.2 Hz, *3′*), 109.2 (d, J = 2.6 Hz, *5′*), 57.1 (*7′*). ^{19}**F NMR** (470.59 MHz, $CDCl_3$): δ −96.62 (t, J = 7.0 Hz, 1F, *2′*), −104.78 (tt, J = 8.4, 5.2 Hz, 3F, *4*), −149.18 (s, 4F). **HRMS** (ESI$^+$, *m/z*) Calcd. for $C_{25}H_{19}BiF_4O^+$ (M+H): 620.1171. Found: 620.1139. Error: 5.16 ppm. ν_{max} (neat, cm^{-1}): 1595, 1574, 1485, 1470, 1393, 1324, 1163, 1063, 999, 819, 780, 568, 502. **m.p.** (°C): 158–159.

(4-Chloro-2-methylphenyl)tri(4-fluorophenyl)bismuthonium tetrafluoroborate (5ad)

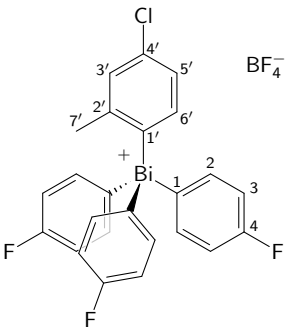

The compound was synthesised according to GP-3, by reacting **2** (124 mg, 0.251 mmol) with Selectfluor (95.0 mg, 0.268 mmol) and 4-chloro-2-methylphenylboronic acid (45.5 mg, 0.267 mmol). Recrystallisation from DCM/CyH yielded the desired pure product (95.4 mg, 0.135 mmol, 54%). ^{1}**H NMR** (500.13 MHz, $CDCl_3$): δ 7.81 (dd$^{\text{II ord.}}$, J = 8.7, 5.2 Hz, 6H, *2*), 7.56 (d, J = 2.3 Hz, 1H, *3′*), 7.50 (d, J = 8.4 Hz, 1H, *6′*), 7.44 (dd, J = 8.4, 2.4 Hz, 1H, *5′*), 7.38 (t$^{\text{II ord.}}_{\text{app.}}$, J = 8.6 Hz, 6H, *3*), 2.39 (s, 3H, *7′*). ^{13}**C{^{1}H} NMR** (125.76 MHz, $CDCl_3$): δ 165.2 (d, J = 255.7 Hz, *4*), 144.2 (*2′*), 140.4 (*1′*), 139.4 (*4′*), 138.1 (d, J = 8.5 Hz, *2*), 136.4 (*6′*), 133.3 (d, J = 3.5 Hz, *1*), 133.2 (*3′*), 129.7 (*5′*), 120.1 (d, J = 21.9 Hz, *3*), 25.2 (*7′*). ^{19}**F NMR** (470.59 MHz, $CDCl_3$): δ −103.96 (tt, J = 8.3, 5.1 Hz, 3F), −147.95 (s, 4F). **HRMS** (ESI$^+$, *m/z*) Calcd. for $C_{25}H_{18}BiClF_3^+$ (M+): 619.0848. Found: 619.0861. Error: 2.10 ppm. ν_{max} (neat, cm^{-1}): 1574, 1483, 1392, 1226, 1162, 1050, 1000, 823, 504. **m.p.** (°C): 210–212.

(4-Fluoro-2-methylphenyl)tri(4-fluorophenyl)bismuthonium tetrafluoroborate (5ae)

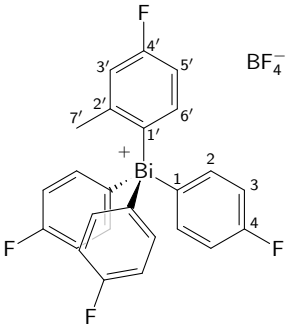

The compound was synthesised according to GP-4, by reacting **2** (1.00 g, 2.03 mmol) with Selectfluor (724 mg, 2.04 mmol), (4-fluoro-2-methylphenyl)boronic acid (318 mg, 0.207 mmol) and $BF_3{\cdot}Et_2O$ (37 µL, 0.30 mmol). Recrystallisation from DCM/CyH yielded the desired pure product (1.16 g, 1.68 mmol, 82%). The resulting crystals were suitable for X-ray diffraction analysis: details can be found in Section 6.8. **^{1}H NMR** (500.13 MHz, $CDCl_3$): δ 7.80 (dd$^{\text{II ord.}}$, J = 8.5, 5.2 Hz, 6H, *2*), 7.55 (dd, J = 8.7, 5.4 Hz, 1H, *6′*), 7.37 (t$^{\text{II ord.}}_{\text{app.}}$, J = 8.5 Hz, 6H, *3*), 7.27 (dd, J = 9.1, 2.7 Hz, 1H, *3′*), 7.16 (td$_{\text{app.}}$, J = 8.3, 2.8 Hz, 1H, *5′*), 2.39 (s, 3H, *7′*). **^{13}C{^{1}H} NMR** (125.76 MHz, $CDCl_3$): δ 165.21 (d, J = 254.9 Hz, *4′*), 165.19 (d, J = 256.0 Hz, *4*), 145.6 (d, J = 8.2 Hz, *2′*), 138.1 (d, J = 8.3 Hz, *2*), 137.5 (d, J = 9.0 Hz, *6′*), 136.6 (d, J = 2.8 Hz, *1′*), 133.0 (d, J = 3.2 Hz, *1*), 120.6 (d, J = 22.0 Hz, *3′*), 120.1 (d, J = 21.8 Hz, *3*), 117.1 (d, J = 21.9 Hz, *5′*), 25.3 (*7′*). **^{19}F NMR** (470.59 MHz, $CDCl_3$): δ −104.02 (tt, J = 8.4, 5.1 Hz, 3F, *4*), −105.27 (ddd, J = 9.2, 8.1, 5.3 Hz, 1F, *4′*), −148.23 (s, 4F). **HRMS** (ESI$^+$, *m/z*) Calcd. for $C_{25}H_{18}BiF_4^+$ (M+): 603.1143. Found: 603.1198. Error: 9.12 ppm. $\boldsymbol{\nu}_{\text{max}}$ (neat, cm^{-1}): 1574, 1486, 1395, 1227, 1163, 1002, 820, 503. **m.p.** (°C): 202–204.

Tri(4-fluorophenyl)(4-methoxy-2-methylphenyl)bismuthonium tetrafluoroborate (5af)

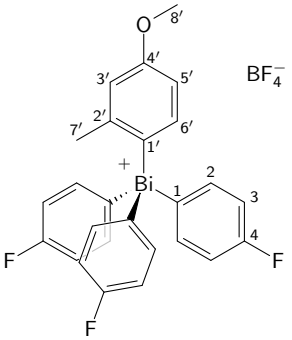

The compound was synthesised according to GP-4, by reacting **2** (125 mg, 0.254 mmol) with Selectfluor (93.3 mg, 0.263 mmol), (4-methoxy-2-methylphenyl)boronic acid (44.3 mg, 0.267 mmol) and $BF_3{\cdot}Et_2O$ (37 µL, 0.30 mmol). Recrystallisation from DCM/CyH yielded the desired pure product (128 mg, 0.182 mmol, 72%). **^{1}H NMR** (500.13 MHz, $CDCl_3$): δ 7.81 (dd, J = 8.7, 5.2 Hz, 6H, *2*), 7.46 (d, J = 8.6 Hz, 1H, *6′*), 7.37 (t, J = 8.6 Hz, 6H, *3*), 7.07 (d, J = 2.8 Hz, 1H, *3′*), 6.97 (dd, J = 8.6, 2.8 Hz, 1H, *5′*), 3.85 (s, 3H, *8′*), 2.35 (s, 3H, *7′*). **^{13}C{^{1}H} NMR** (125.76 MHz, $CDCl_3$): δ 165.2 (d, J = 255.3 Hz, *4*), 163.1 (*4′*), 144.4 (*2′*), 138.1 (d, J = 8.5 Hz, *2*), 137.0 (*6′*), 132.9 (d, J = 3.3 Hz, *1*), 131.6 (*1′*), 120.0 (d, J = 21.8 Hz, *3*), 119.3 (*3′*), 115.0 (*5′*), 55.8 (*8′*), 25.4 (*7′*). **^{19}F NMR** (470.59 MHz, $CDCl_3$): δ −104.37 (td, J = 8.7, 4.4 Hz, 3F), −148.96

(s, 4F). **HRMS** (ESI$^+$, *m/z*) Calcd. for $C_{26}H_{21}BiF_3O^+$ (M+): 615.1343. Found: 615.1415. Error: 11.70 ppm. ν_{max} (neat, cm^{-1}): 1587, 1575, 1562, 1485, 1393, 1300, 1284, 1227, 1162, 1051, 1003, 833, 818, 795, 501. **m.p.** (°C): 193–195.

Tri(4-fluorophenyl)(mesityl)bismuthonium tetrafluoroborate (5ag)

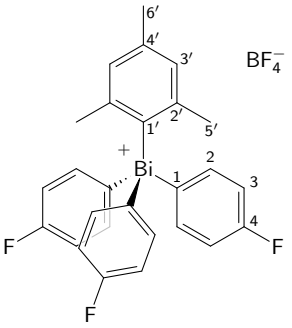

The compound was synthesised according to GP-3, by reacting **2** (99.3 mg, 0.201 mmol) with Selectfluor (78.6 mg, 0.222 mmol) and mesitylboronic acid (52.3 mg, 0.319 mmol). Recrystallisation from DCM/CyH yielded the desired pure product (101 mg, 0.144 mmol, 71%). The resulting crystals were suitable for X-ray diffraction analysis: details can be found in Section 6.8. ^{1}**H NMR** (500.13 MHz, $CDCl_3$): δ 7.84 (dd$^{\text{II ord.}}$, J = 8.7, 5.4 Hz, 6H, *2*), 7.33 (t$^{\text{II ord.}}_{\text{app.}}$, J = 8.6 Hz, 6H, *3*), 7.17 (s, 2H, *3′*), 2.36 (s, 3H, *6′*), 2.31 (s, 6H, *5′*). ^{13}**C{^{1}H} NMR** (125.76 MHz, $CDCl_3$): δ 164.8 (d, J = 254.5 Hz, *4*), 144.3 (*1′*), 143.2 (*4′*), 142.8 (*2′*), 137.7 (d, J = 8.3 Hz, *2*), 136.9 (d, J = 3.5 Hz, *1*), 132.0 (*3′*), 119.8 (d, J = 21.7 Hz, *3*), 26.0 (5′), 21.2 (*6′*). ^{19}**F NMR** (470.59 MHz, $CDCl_3$): δ −105.18 (tt, J = 8.5, 5.2 Hz, 3F), −148.92 (s, 4F). **HRMS** (ESI$^+$, *m/z*) Calcd. for $C_{27}H_{23}BiF_3^+$ (M+): 613.1550. Found: 613.1539. Error: 1.79 ppm. ν_{max} (neat, cm^{-1}): 1575, 1484, 1392, 1233, 1161, 1075, 984, 817, 569, 505, 417. **m.p.** (°C): 187–188.

Tri(4-fluorophenyl)(2,4,6-triisopropylphenyl)bismuthonium tetrafluoroborate (5ah)

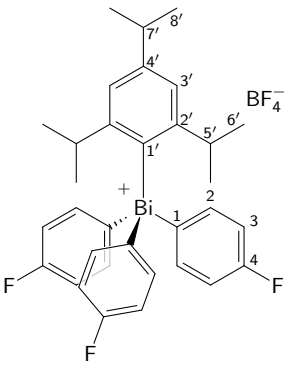

The compound was synthesised according to GP-4, by reacting **2** (203 mg, 0.381 mmol) with Selectfluor (158 mg, 0.446 mmol), (2,4,6-triisopropylphenyl)boronic acid (105 mg, 0.423 mmol) and $BF_3{\cdot}Et_2O$ (55 µL, 0.45 mmol). Recrystallisation from DCM/CyH yielded the desired pure product (123 mg, 0.157 mmol, 41%). The resulting crystals were suitable for X-ray diffraction analysis: details can be found in Section 6.8. ^{1}**H NMR** (500.13 MHz, $CDCl_3$): δ 7.85 (dd$^{\text{II ord.}}$, J = 8.8, 5.2 Hz, 6H, *2*), 7.33 (t$^{\text{II ord.}}_{\text{app.}}$, J = 8.6 Hz, 6H, *3*), 7.30 (s, 3H, *3′*), 2.96 (hept, J = 6.9 Hz, 1H, *7′*), 2.78 (hept, J = 6.6 Hz, 2H, *5′*), 1.29 (d, J = 6.9 Hz, 6H, *8′*), 1.04 (d, J = 6.6 Hz, 12H, *6′*). ^{13}**C{^{1}H} NMR** (125.76 MHz, $CDCl_3$): δ 164.7 (d, J = 254.4 Hz,

4), 154.1 (*4′*), 153.3 (*2′*), 145.7 (*1′*), 138.1 (d, J = 3.4 Hz, *1*), 137.5 (d, J = 8.2 Hz, *2*), 126.1 (*3′*), 119.6 (d, J = 21.7 Hz, *3*), 38.6 (*5′*), 34.3 (*7′*), 24.4 (*6′*), 23.9 (*8′*). **^{19}F NMR** (470.59 MHz, $CDCl_3$): δ −105.31 (tt, J = 8.4, 5.2 Hz, 3F), −148.65 (s, 4F). **HRMS** (ESI^+, *m/z*) Calcd. for $C_{33}H_{35}BiF_3^+$ (M+): 697.2489. Found: 697.2480. Error: 1.29 ppm. ν_{max} (neat, cm^{-1}): 1573, 1483, 1393, 1223, 1161,1058, 1002, 820, 765, 570, 500, 413. **m.p.** (°C): 178–179.

(2,6-Dimethylphenyl)tri(4-fluorophenyl)bismuthonium tetrafluoroborate (5ai)

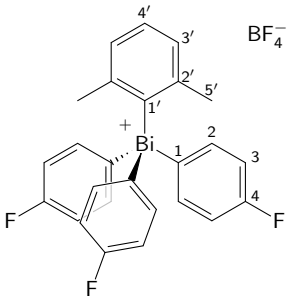

The compound was synthesised according to GP-4, by reacting **2** (202 mg, 0.408 mmol) with Selectfluor (150.0 mg, 0.423 mmol), 2,6-dimethylphenylboronic acid (67.0 mg, 0.447 mmol) and $BF_3{\cdot}Et_2O$ (55 µL, 0.45 mmol). Recrystallisation from DCM/CyH yielded the desired pure product (267 mg, 0.389 mmol, 92%). The resulting crystals were suitable for X-ray diffraction analysis: details can be found in Section 6.8. **^{1}H NMR** (500.13 MHz, $CDCl_3$): δ 7.87 ($dd^{II\ ord.}$, J = 8.5, 5.2 Hz, 6H, *2*), 7.41 (td, J = 7.4, 1.4 Hz, 1H, *4′*), 7.38–7.29 (m, 8H, *3 and 3′*), 2.36 (s, 6H, *5′*). **^{13}C{^{1}H} NMR** (125.76 MHz, $CDCl_3$): δ 164.9 (d, J = 255.0 Hz, *4*), 147.8 (*1′*), 143.2 (*2′*), 137.6 (d, J = 8.2 Hz, *2*), 137.1 (d, J = 3.5 Hz, *1*), 119.8 (d, J = 21.8 Hz, *3*), 26.2 (*5′*). **^{19}F NMR** (470.59 MHz, $CDCl_3$): δ −105.06 (tt, J = 8.5, 5.2 Hz, 3F), −148.84 (s, 4F). **HRMS** (ESI^+, *m/z*) Calcd. for $C_{26}H_{21}BiF_3^+$ (M+): 599.1394. Found: 599.1397. Error: 0.50 ppm. ν_{max} (neat, cm^{-1}): 1576, 1484, 1463, 1392, 1224, 1161, 1096, 1055, 1004, 931, 831, 813, 787, 762, 568, 502, 412. **m.p.** (°C): 230–231.

(2,6-Dimethoxyphenyl)tri(4-fluorophenyl)bismuthonium tetrafluoroborate (5aj)

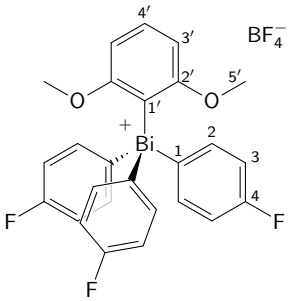

The compound was synthesised according to GP-3, by reacting **2** (133 mg, 0.250 mmol) with Selectfluor (95.0 mg, 0.268 mmol) and 2,6-dimethoxyphenylboronic acid (48.4 mg, 0.266 mmol). Recrystallisation from DCM/CyH yielded the desired pure product (124 mg, 0.173 mmol, 69%). **^{1}H NMR** (500.13 MHz, $CDCl_3$): δ 7.77 ($dd^{II\ ord.}$, J = 8.5, 5.3 Hz, 6H, *2*), 7.55 (t, J = 8.2 Hz, 1H, *4′*), 7.32 ($t_{app.}^{II\ ord.}$, J = 8.7 Hz, 6H, *3*), 6.86 (d, J = 8.3 Hz, 2H, *3′*), 3.68 (s, 6H, *5′*). **^{13}C{^{1}H} NMR** (125.76 MHz, $CDCl_3$): δ 164.8 (d, J = 253.7 Hz, *4*),

161.2 (*2′*), 137.7 (d, J = 8.4 Hz, *2*), 136.1 (*4′*), 135.4 (br, *1*), 119.2 (d, J = 21.7 Hz, *3*), 119.2 (*1′*),[¶] 106.4 (*3′*), 56.6 (*5′*). **^{19}F NMR** (470.59 MHz, $CDCl_3$): δ −105.74 (br, 3F), −150.45 (s, 4F). **HRMS** (ESI^+, *m/z*) Calcd. for $C_{26}H_{21}BiF_3O_2^+$ (M+): 631.1292. Found: 631.1308. Error: 2.54 ppm.

Tri(4-fluorophenyl)(2-furyl)bismuthonium tetrafluoroborate (5ak)

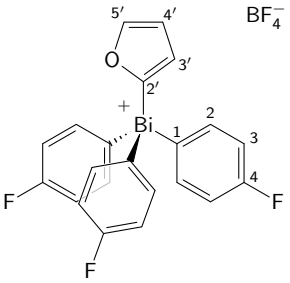

The compound was synthesised according to GP-3, by reacting **2** (98.3 mg, 0.199 mmol) with Selectfluor (71.7 mg, 0.202 mmol) and 2-furylboronic acid (33.9 mg, 0.303 mmol). Recrystallisation from DCM/Et_2O yielded the desired pure product (66.2 mg, 0.102 mmol, 51%). The resulting crystals were suitable for X-ray diffraction analysis: details can be found in Section 6.8. **^{1}H NMR** (500.13 MHz, $CDCl_3$): δ 7.95 ($dd^{II\ ord.}$, J = 8.9, 5.2 Hz, 6H, *2*), 7.92 (d, J = 1.8 Hz, 1H, *5′*), 7.37 ($t^{II\ ord.}_{app.}$, J = 8.6 Hz, 6H, *3*), 6.96 (d, J = 3.4 Hz, 1H, *3′*), 6.74 (dd, J = 3.5, 1.8 Hz, 1H, *4′*). **^{13}C{^{1}H} NMR** (125.76 MHz, $CDCl_3$): δ 165.2 (d, J = 255.2 Hz, *4*), 154.1 (*2′*), 151.3 (*5′*), 137.9 (d, J = 8.4 Hz, *2*), 135.1 (d, J = 3.5 Hz, *1*), 126.7 (*3′*), 119.8 (d, J = 22.0 Hz, *3*), 112.1 (*4*). **^{19}F NMR** (470.59 MHz, $CDCl_3$): δ −103.01–−105.28 (br, 3F), −147.12 (s, 4F). **HRMS** (ESI^+, *m/z*) Calcd. for $C_{22}H_{15}BiF_3O^+$ (M+): 561.0873. Found: 561.0889. Error: 2.85 ppm. ν_{max} (neat, cm^{-1}): 1574, 1482, 1393, 1276, 1261, 1226, 1162, 1056, 1000, 822, 750, 498. **m.p.** (°C): 185–186 (decomp.).

Tri(4-fluorophenyl)(3-furyl)bismuthonium tetrafluoroborate (5al)

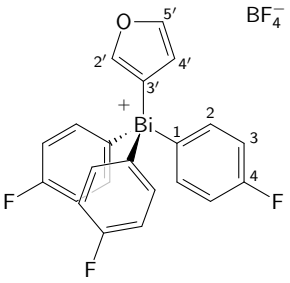

The compound was synthesised according to GP-3, by reacting **2** (95.6 mg, 0.194 mmol) with Selectfluor (74.9 mg, 0.211 mmol) and 3-furylboronic acid (35.4 mg, 0.316 mmol). Recrystallisation from DCM/Et_2O yielded the desired pure product (82.1 mg, 0.127 mmol, 65%). The resulting crystals were suitable for X-ray diffraction analysis: details can be found in Section 6.8. **^{1}H NMR** (500.13 MHz, $CDCl_3$): δ 7.82 ($dd^{II\ ord.}$, J = 9.0, 5.1 Hz, 6H, *2*), 7.82–7.81 (m, 2H, *2′ and 5′*), 7.35 ($t^{II\ ord.}_{app.}$, J = 8.7 Hz, 6H), 6.67 (dd, J = 1.7, 1.2 Hz, 1H, *4′*). **^{13}C{^{1}H} NMR** (125.76 MHz, $CDCl_3$): δ 165.2 (d, J = 255.3 Hz, *4*), 151.8 (*2′*),

[¶]Hidden underneath the previous peak: only detected *via* indirect observation by HMBC

146.2 (*5′*), 137.7 (d, J = 8.3 Hz, *2*), 132.8 (d, J = 3.5 Hz, *1*), 119.8 (d, J = 21.9 Hz, *3*), 115.9 (*3′*), 113.8 (*4′*). **^{19}F NMR** (470.59 MHz, $CDCl_3$): δ −103.96 (tt, J = 8.3, 5.1 Hz, 3F), −147.18 (s, 4F). **HRMS** (ESI^+, *m/z*) Calcd. for $C_{22}H_{15}BiF_3O^+$ (M+): 561.0873. Found: 561.0886. Error: 2.32 ppm. ν_{max} (neat, cm^{-1}): 1574, 1484, 1394, 1276, 1261, 1222, 1163, 764, 750, 598 569 499. **m.p.** (°C): 157–158.

Tri(4-fluorophenyl)(2-thienyl)bismuthonium tetrafluoroborate (5am)

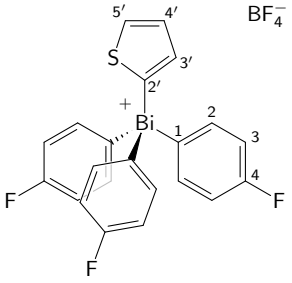

The compound was synthesised according to GP-3, by reacting **2** (101 mg, 0.205 mmol) with Selectfluor (79.4 mg, 0.224 mmol) and 2-thienylboronic acid (42.8 mg, 0.335 mmol). Recrystallisation from DCM/Et_2O yielded the desired pure product (98.1 mg, 0.148 mmol, 72%). The resulting crystals were suitable for X-ray diffraction analysis: details can be found in Section 6.8. **^{1}H NMR** (500.13 MHz, $CDCl_3$): δ 7.94 (dd, J = 4.9, 1.0 Hz, 2H, *5′*), 7.91 ($dd^{II\ ord.}$, J = 8.8, 5.1 Hz, 6H, *2*), 7.48 (dd, J = 3.6, 1.0 Hz, 1H, *3′*), 7.44 (dd, J = 4.9, 3.6 Hz, 1H, *4′*), 7.37 ($t^{II\ ord.}_{app.}$, J = 8.5 Hz, 6H, *3*). **^{13}C{^{1}H} NMR** (125.76 MHz, $CDCl_3$): δ 165.2 (d, J = 255.2 Hz, *4*), 140.0 (*3′*), 137.8 (d, J = 8.9 Hz, *2*), 136.0 (*5′*), 135.0 (d, J = 3.4 Hz, *1*), 132.1 (*2′*), 130.3 (*4′*), 119.8 (d, J = 22.3 Hz, *3*). **^{19}F NMR** (470.59 MHz, $CDCl_3$): δ −103.94 (tt, J = 8.6, 5.1 Hz, 3F), −147.02 (s, 4F). **HRMS** (ESI^+, *m/z*) Calcd. for $C_{22}H_{15}BiF_3S^+$ (M+): 577.0645. Found: 577.0653. Error: 1.39 ppm. ν_{max} (neat, cm^{-1}): 1573, 1483, 1392, 1276, 1261, 1220, 1163, 998, 820, 764, 750.0, 569, 502. **m.p.** (°C): 185–186.

Tri(4-fluorophenyl)(3-thienyl)bismuthonium tetrafluoroborate (5an)

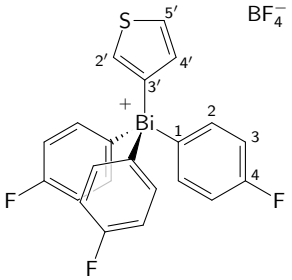

The compound was synthesised according to GP-3, by reacting **2** (97.2 mg, 0.197 mmol) with Selectfluor (81.0 mg, 0.229 mmol) and 3-thienylboronic acid (39.9 mg, 0.312 mmol). Recrystallisation from DCM/Et_2O yielded the desired pure product (81.6 mg, 0.123 mmol, 63%). The resulting crystals were suitable for X-ray diffraction analysis: details can be found in Section 6.8. **^{1}H NMR** (500.13 MHz, $(CD_3)_2SO$): δ 8.25 (dd, J = 2.7, 1.2 Hz, 1H, *2′*), 8.04 (dd, J = 5.0, 2.7 Hz, 1H, *5′*), 7.96 ($dd^{II\ ord.}$, J = 8.5, 5.6 Hz, 6H, *2*), 7.57 ($t^{II\ ord.}_{app.}$, J = 8.9 Hz, 6H, *3*), 7.47 (dd, J = 5.0, 1.2 Hz, 1H, *4′*). **^{13}C{^{1}H} NMR** (125.76 MHz, $(CD_3)_2SO$): δ 163.6 (d, J = 249.7 Hz, *4*), 140.4 (d, J = 3.3 Hz, *1*), 137.8 (d, J = 8.3 Hz, *2*),

136.4 (*2′*), 135.2 (*3′*), 131.8 (*4′*), 129.2 (*5′*), 118.6 (d, J = 21.6 Hz, *3*). **^{19}F NMR** (470.59 MHz, $(CD_3)_2SO$): δ −107.77 (tt, J = 9.1, 5.4 Hz, 3F), −148.27 (s, 4F). **HRMS** (ESI^+, *m/z*) Calcd. for $C_{22}H_{15}BiF_3S^+$ (M+): 577.0645. Found: 577.06449. Error: 0.02 ppm. ν_{max} (neat, cm^{-1}): 1573, 1484, 1393, 1276, 1221, 1163, 1057, 1000, 821, 764, 569, 501. **m.p.** (°C): 177–178.

(2-Acetylthiophen-3-yl)tri(4-fluorophenyl)bismuthonium tetrafluoroborate (5ao)

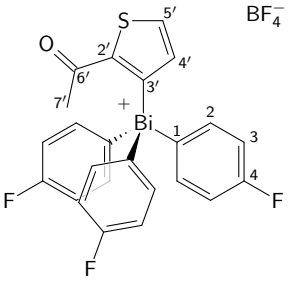

The compound was synthesised according to GP-3, by reacting **2** (98.8 mg, 0.200 mmol) with Selectfluor (76.8 mg, 0.217 mmol) and (2-acetylythiophen-3-yl)boronic acid (55.4 mg, 0.326 mmol). Recrystallisation from DCM/Et_2O yielded the desired product.‖ The resulting crystals were suitable for X-ray diffraction analysis: details can be found in Section 6.8. **^{1}H NMR** (500.13 MHz, $CDCl_3$): δ 8.05 (d, J = 5.0 Hz, 1H, *5′*), 7.79 (dd$^{II\ ord.}$, J = 8.6, 5.4 Hz, 6H, *2*), 7.41 (d, J = 4.9 Hz, 1H, *4′*), 7.34 ($t^{II\ ord.}_{app.}$, J = 8.7 Hz, 6H, *3*), 2.66 (s, 3H, *7′*). **^{13}C{^{1}H} NMR** (125.76 MHz, $CDCl_3$): δ 191.2 (*6′*), 165.0 (d, J = 254.6 Hz, *4*), 145.6 (*2′*), 139.3 (*3′*), 138.1 (*5′*), 137.8 (d, J = 8.3 Hz, *2*), 135.7 (d, J = 3.3 Hz, *1*), 134.0 (*4′*), 119.6 (d, J = 21.7 Hz, *3*), 27.6 (*7′*). **^{19}F NMR** (470.59 MHz, $CDCl_3$): δ −104.99 (tt, J = 8.6, 5.3 Hz, 3F), −149.27 (s, 4F). **HRMS** (ESI^+, *m/z*) Calcd. for $C_{24}H_{17}BiF_3OS^+$ (M+): 619.0751. Found: 619.0773. Error: 3.55 ppm. ν_{max} (neat, cm^{-1}): 1645, 1575, 1483, 1386, 1231, 1160, 1060, 1001, 749, 505.

(3,5-Dimethylisoxazol-4-yl)tri(4-fluorophenyl)bismuthonium tetrafluoroborate (5ap)

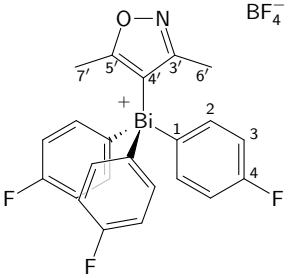

The compound was synthesised according to GP-3, by reacting **2** (103 mg, 0.208 mmol) with Selectfluor (74.9 mg, 0.211 mmol) and 3,5-dimethylisoxazol-4-ylboronic acid (45.5 mg, 0.323 mmol). Recrystallisation from MeCN/Tol yielded the desired pure product (79.2 mg, 0.117 mmol, 56%). The resulting crystals were suitable for X-ray diffraction analysis: details can be found in Section 6.8. **^{1}H NMR** (500.13 MHz, $CDCl_3$):** δ 7.84 (dd$^{II\ ord.}$, J = 8.6, 5.0 Hz, 6H, *2*), 7.40 ($t^{II\ ord.}_{app.}$, J = 8.5 Hz, 6H, *3*), 2.24 (s, 3H, *6′*), 1.99 (s, 3H, *7′*). **^{13}C{^{1}H} NMR**

‖ The compound co-crystalised with 12% of compound **5a**.

** Assignment achieved by comparison with other 3,5-disubstituted isoxazoles in the literature.[452]

(125.76 MHz, $CDCl_3$):** δ 177.6 (*5′*), 165.4 (d, J = 256.2 Hz, *4*), 161.8 (*3′*), 137.8 (d, J = 8.8 Hz, *2*), 131.9 (d, J = 3.4 Hz, *1*), 120.3 (d, J = 22.2 Hz, *3*), 109.7 (*4′*), 13.6 (*6′*), 12.6 (*7′*). **^{19}F NMR** (470.59 MHz, $CDCl_3$): δ −103.08 (tt, J = 8.6, 4.9 Hz, 3F), −147.29 (s, 4F). **HRMS** (ESI^+, *m/z*) Calcd. for $C_{23}H_{18}BiF_3NO^+$ (M+): 590.1139. Found: 590.1161. Error: 3.73 ppm. ν_{max} (neat, cm^{-1}): 1576, 1484, 1395, 1227, 1162, 1114, 1066, 1001, 834, 817, 744, 503. **m.p.** (°C): 190–191.

Tri(4-fluorophenyl)(1*H*-indazol-4-yl)bismuthonium tetrafluoroborate (5aq)

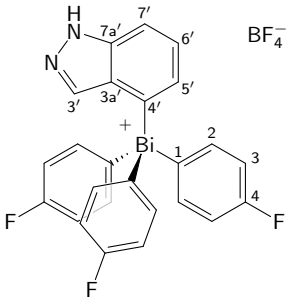

The compound was synthesised according to GP-3, by reacting **2** (102 mg, 0.206 mmol) with Selectfluor (77.0 mg, 0.217 mmol) and 1*H*-indazol-4-ylboronic acid (49.1 mg, 0.303 mmol). Recrystallisation from DCM/Et_2O yielded the desired pure product (80.1 mg, 0.115 mmol, 56%). **^{1}H NMR** (500.13 MHz, $(CD_3)_2O$): δ 12.82 (s, 1H, *NH*), 8.35–8.09 (br, 6H, *2*), 8.04 (d, J = 8.3 Hz, 1H, *7′*), 7.89–7.63 (br, 1H, *5′*), 7.76 (s, 1H, *3′*), 7.71 ($t^{IIord.}$, J = 7.7 Hz, 1H, *6′*), 7.60 (t, J = 8.8 Hz, 7H, *3*). **^{13}C{^{1}H} NMR** (125.76 MHz, $(CD_3)_2O$): δ 165.9 (d, J = 252.2 Hz, *4*), 143.0 (*7a′*), 139.6 (br, *2*), 135.3 (d, J = 3.4 Hz, *1*), 134.2 (*3′*), 131.2 (*4′*), 130.9 (*5′*), 128.8 (*6′*), 127.9 (*3a′*), 120.3 (d, J = 21.5 Hz, *3*), 115.9 (*7′*). **^{19}F NMR** (470.59 MHz, $(CD_3)_2O$): δ −107.23 (tt, J = 9.1, 5.3 Hz, 3F), −151.32 (s, 4F). **HRMS** (ESI^+, *m/z*) Calcd. for $C_{25}H_{17}BiF_3N_2^+$ (M+): 611.1135. Found: 611.1142. Error: 1.15 ppm. ν_{max} (neat, cm^{-1}): 3371, 3092, 1573, 1483, 1393, 1222, 1162, 1056, 1002, 819, 792, 764, 750, 571, 502. **m.p.** (°C): 223-224.

Tri(4-fluorophenyl)(1-methyl-1*H*-indazol-4-yl)bismuthonium tetrafluoroborate (5ar)

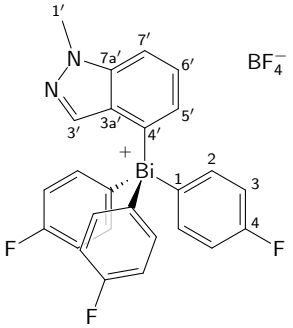

The compound was synthesised according to GP-3, by reacting **2** (97.0 mg, 0.196 mmol) with Selectfluor (69.8 mg, 0.197 mmol) and 1-methyl-1*H*-indazol-4-ylboronic acid (55.4 mg, 0.315 mmol). Recrystallisation from DCM/Et_2O yielded the desired pure product (98.7 mg, 0.139 mmol, 71%). **^{1}H NMR** (500.13 MHz, $CDCl_3$): δ 7.85 ($dd^{II\ ord.}$, J = 8.6, 5.2 Hz, 6H, *2*), 7.71 (dt, J = 8.3, 0.8 Hz, 1H, *7′*), 7.58 (dd, J = 8.3, 7.1 Hz, 1H, *6′*), 7.53 ($d^{IIord.}$, J = 7.1 Hz, 1H, *5′*), 7.43 (d, J = 0.9 Hz, 1H, *3′*), 7.35 ($t^{II\ ord.}_{app.}$, J = 8.6 Hz, 6H, *3*), 4.13 (s, 3H, *1′*). **^{13}C{^{1}H} NMR** (125.76 MHz, $CDCl_3$): δ 165.2 (d, J = 255.4 Hz, *4*), 141.4 (*7a′*), 138.2 (d, J = 8.3 Hz, *2*), 132.7 (d, J = 3.6 Hz, *1*), 131.8 (*3′*),

130.2 (*5′*), 129.6 (*4′*), 128.2 (*6′*), 127.7 (*3a′*), 120.08 (d, J = 21.9 Hz, *3*), 114.0 (*7′*), 36.3 (*1′*). **^{19}F NMR** (470.59 MHz, $CDCl_3$): δ −103.87 (tt, J = 8.4, 5.1 Hz, 3F), −148.04 (s, 4F). **HRMS** (ESI^+, *m/z*) Calcd. for $C_{25}H_{18}BiF_3N_2$ (M+): 625.12987. Found: 625.1299. Error: 0.05 ppm. ν_{max} (neat, cm^{-1}): 1572, 1483, 1393, 1320, 1219, 1162, 1050, 1000, 902, 824, 782, 504. **m.p.** (°C): 208–209.

(4-Fluorophenyl)triphenylbismuthonium tetrafluoroborate (5as)

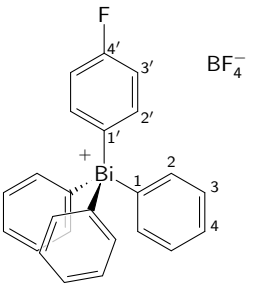

The compound was synthesised according to GP-3, by reacting triphenylbismuthine (88.1 mg, 0.200 mmol) with Selectfluor (74.4 mg, 0.210 mmol) and 4-fluorophenylboronic acid (35.0 mg, 0.250 mmol). Recrystallisation from DCM/Et_2O yielded the desired pure product (77.0 mg, 0.124 mmol, 62%). The resulting crystals were suitable for X-ray diffraction analysis: details can be found in Section 6.8. **^{1}H NMR** (500.13 MHz, $CDCl_3$): δ 7.83 ($dd^{II\ ord.}$, J = 8.4, 5.2 Hz, 2H, *2′*), 7.78 (d, J = 7.6 Hz, 6H, *2*), 7.68 (t, J = 7.5 Hz, 6H, *3*), 7.65–7.58 (m, 3H, *4*), 7.36 ($t_{app.}^{II\ ord.}$, J = 8.6 Hz, 2H, *3′*). **^{13}C{^{1}H} NMR** (125.76 MHz, $CDCl_3$): δ 165.1 (d, J = 254.5 Hz, *4′*), 138.3 (d, J = 8.6 Hz, *2′*), 138.0 (*1*), 136.0 (*2*), 132.8 (d, J = 3.6 Hz, *1′*), 132.7 (*4*), 132.6 (*3*), 119.9 (d, J = 21.8 Hz, *3′*). **^{19}F NMR** (470.59 MHz, $CDCl_3$): δ −104.65 (tt, J = 8.4, 5.2 Hz, 1F), −149.14 (s, 4F). **HRMS** (ESI^+, *m/z*) Calcd. for $C_{24}H_{19}BiF^+$ (M+): 535.1269. Found: 535.1261. Error: 1.49 ppm. ν_{max} (neat, cm^{-1}): 1575, 1563, 1485, 1474, 1436, 1230, 1164, 1048, 989, 822, 728, 683, 504, 434. **m.p.** (°C): 171–172.

6.5 Arylation products

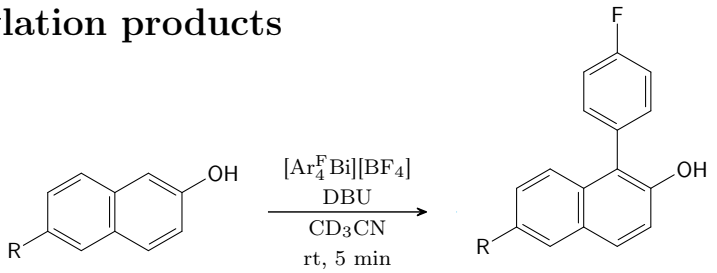

GP-5: tetra(4-fluorophenyl)bismuthonium tetrafluoroborate **5a** (1 equiv) and a naphthol derivative (1 equiv) were added to an NMR tube and dissolved in CD_3CN (0.6 mL). DBU (1.5 equiv) was then added and the reaction was monitored by NMR spectroscopy. At completion it was quenched with a few drops of TFA. The reaction mixture was then transferred into a 10 mL round-bottom flask with some DCM and all the solvents were evaporated under reduced pressure. The resulting crude was diluted with EtOAc (0.5 mL), loaded on a preparative TLC plate with a 100 µL micro-syringe and eluted with 250 mL of the appropriate solvent mixture.

6-Bromo-1-(4-fluorophenyl)naphthalen-2-ol (17a)

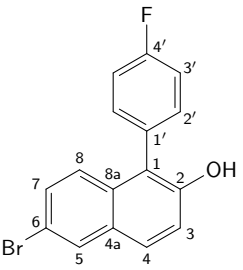

According to GP-5, 6-bromonaphthalen-2-ol (44.6 mg, 0.200 mmol), tetra(4-fluorophenyl)bismuthonium tetrafluoroborate **5a** (135 mg, 0.200 mmol) and DBU (46 µL, 0.30 mmol) were reacted together. The desired product was isolated upon purification by preparative TLC as a colourless oil (57.7 mg, 0.182 mmol, 91%), whose characteristic data are in accordance with the literature.[318] **^{1}H NMR** (500.13 MHz, C_6D_6): δ 7.75 (d, J = 2.1 Hz, 1H, *5*), 7.30 (dd, J = 9.0, 2.1 Hz, 1H, *7*), 7.25 (d, J = 8.9 Hz, 1H, *4*), 7.10 (d, J = 8.9 Hz, 1H, *3*), 7.05 (d, J = 9.0 Hz, 1H, *8*), 6.86–6.70 (m, 4H, *2′ and 3′*), 4.30 (s, 1H, *OH*). **^{1}H{^{1}H} NMR** (500.13 MHz, C_6D_6): δ 7.75 (s, *5*), 7.30 (s, *7*), 7.25 (s, *4*), 7.10 (s, *3*), 7.05 (s, *8*), 6.79 (d, $^4J_{F-H}$ = 5.5 Hz, *2′*), 6.75 (d, $^3J_{F-H}$ = 8.5 Hz, *3′*). **^{13}C{^{1}H} NMR** (125.76 MHz, C_6D_6): δ 163.0 (d, ^1J = 247.1 Hz, *4′*), 151.2 (*2*), 133.0 (d, ^3J = 8.2 Hz, *2′*), 132.5 (*8a*), 130.52 (*5*), 130.49 (*4a*), 130.1 (*7*), 129.8 (d, ^4J = 3.6 Hz, *1′*), 129.2 (*4*), 126.6 (*8*), 120.5 (*1*), 118.8 (*3*), 117.5 (*6*), 116.7 (d, ^2J = 21.6 Hz, *3′*). **^{19}F NMR** (470.59 MHz, C_6D_6): δ −113.01 (tt, J = 8.4, 5.9 Hz). **^{1}H NMR** (500.13 MHz, CD_3CN): δ 8.00 (d, J = 2.1 Hz, 1H, *5*), 7.73 (d, J = 8.9 Hz, 1H, *4*), 7.39 (dd, J = 9.1, 2.2 Hz, 1H, *7*), 7.36–7.31 (m, 2H, *2′*), 7.30–7.23 (m, 4H, *3, 8 and 3′*), 7.09 (br, 1H, *OH*). **^{13}C{^{1}H} NMR** (125.76 MHz, CD_3CN): δ 163.3 (d, J = 244.0 Hz, *4′*), 152.7 (*2*), 133.9 (d, J = 8.0 Hz, *2′*), 133.3 (*8a*), 132.3 (d, J = 3.3 Hz, *1′*), 130.72 (*5*), 130.71

(*4a*), 130.2 (*7*), 129.3 (*4*), 127.3 (*8*), 121.7 (*1*), 120.2 (*3*), 117.1 (*6*), 116.4 (d, J = 21.5 Hz, *3′*). **^{19}F NMR** (470.59 MHz, CD_3CN): δ −116.48 (tt, J = 9.0, 5.6 Hz). **HRMS** (ESI$^-$, *m/z*) Calcd. for $C_{16}H_9BrFO^-$ (M−H): 314.9826. Found: 314.9839. Error: 4.13 ppm. ν_{max} (neat, cm^{-1}): 3521, 1705, 1585, 1500, 1337, 1220, 1166, 1146, 933, 835, 817, 809, 503.

6-Iodo-1-(4-fluorophenyl)naphthalen-2-ol (17b)

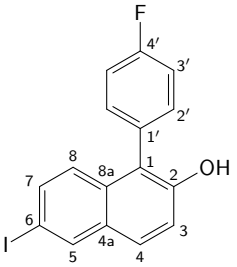

According to GP-5, 6-iodonaphthalen-2-ol (27.0 mg, 0.100 mmol), tetra(4-fluorophenyl)bismuthonium tetrafluoroborate **5a** (67.6 mg, 0.100 mmol) and DBU (23 µL, 0.15 mmol) were reacted together. The desired product was isolated upon purification by preparative TLC as a colourless oil (32.1 mg, 0.0882 mmol, 88%), whose characteristic data are in accordance with the literature.[318] **^{1}H NMR** (500.13 MHz, $CDCl_3$): δ 8.18 (d, J = 1.9 Hz, 1H, *5*), 7.69 (d, J = 8.9 Hz, 1H, *4*), 7.56 (dd, J = 8.9, 1.8 Hz, 1H, *7*), 7.37 (dd$^{\text{II ord.}}$, J = 8.7, 5.4 Hz, 2H, *2′*), 7.29 ($t^{\text{II ord.}}_{\text{app.}}$, J = 8.7 Hz, 2H, *3′*), 7.25 (d, J = 8.9 Hz, 1H, *3*), 7.09 (d, J = 8.9 Hz, 1H, *8*), 5.07 (s, 1H, *OH*). **^{13}C{^{1}H} NMR** (125.76 MHz, $CDCl_3$): δ 163.1 (d, J = 248.6 Hz, *4′*), 150.9 (*2*), 136.8 (*5*), 135.2 (*7*), 133.1 (d, J = 7.9 Hz, *2′*), 132.4 (*8a*), 130.8 (*4a*), 129.4 (d, J = 3.5 Hz, *1′*), 128.8 (*4*), 126.4 (*8*), 120.3 (*1*), 118.4 (*3*), 117.0 (d, J = 21.5 Hz, *3′*), 88.5 (*6*). **^{19}F NMR** (470.59 MHz, $CDCl_3$): δ −112.50 (tt, J = 8.6, 5.5 Hz). **HRMS** (ESI$^-$, *m/z*) Calcd. for $C_{16}H_9FIO^-$ (M−H): 362.9688. Found: 362.9685. Error: 0.83 ppm. ν_{max} (neat, cm^{-1}): 1612, 1579, 1509, 1459, 1379, 1338, 1307, 1272, 1222, 1168, 1149, 947, 881, 837, 818, 670, 547, 527, 500, 436.

6-Deutero-1-(4-fluorophenyl)naphthalen-2-ol (17c)

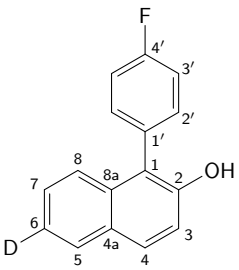

According to GP-5, 6-deuteronaphthalen-2-ol (14.5 mg, 0.100 mmol), tetra(4-fluorophenyl)bismuthonium tetrafluoroborate **5a** (67.6 mg, 0.100 mmol) and DBU (23 µL, 0.15 mmol) were reacted together. The desired product was isolated upon purification by preparative TLC as a colourless oil (21.3 mg, 0.0890 mmol, 89%). The compound was initially characterised by NMR spectroscopy in $CDCl_3$, however, protons *7* and *8* resonated at the same frequency (but the corresponding carbon atoms were easily distinguishable, *i.e.* 124.5 and 126.6 ppm, as determined by HSQC) and a full assignment could not be achieved, so C_6D_6 was employed instead. This solvent

change allowed for the deconvolution of the two aforementioned proton signals and the full assignment of the structure. **^{1}H NMR** (500.13 MHz, $CDCl_3$): δ 7.83 (s, 1H, *5*), 7.82 (d, J = 8.9 Hz, 1H, *4*), 7.41 ($dd^{II\ ord.}$, J = 8.8, 5.3 Hz, 2H, *2′*), 7.36 ($d_{app.}$, J = 1.1 Hz, 2H, *7 and 8*), 7.30 ($t^{II\ ord.}_{app.}$, J = 8.6 Hz, 2H, *3′*), 7.26 (d, J = 8.9 Hz, 1H, *3*), 5.10 (br, 1H, *OH*). **^{13}C{^{1}H} NMR** (125.76 MHz, $CDCl_3$): δ 163.0 (d, J = 248.0 Hz, *4′*), 150.4 (*2*), 133.5 (*8a*), 133.2 (d, J = 8.1 Hz, *2′*), 130.1 (d, J = 3.5 Hz, *1′*), 129.9 (*4*), 129.1 (*4a*), 128.1 (*5*), 126.7 (*7*††), 124.5 (*8*††), 123.28 (t, J = 24.4 Hz, *6*), 120.1 (*1*), 117.5 (*3*), 116.9 (d, J = 21.7 Hz, *3′*). **^{19}F NMR** (470.59 MHz, $CDCl_3$): δ −113.10 (tt, J = 8.6, 5.4 Hz).**^{1}H NMR** (500.13 MHz, C_6D_6): δ 7.61 (s, 1H, *5*), 7.54 (d, J = 8.9 Hz, 1H, *4*), 7.36 (dt, J = 8.5, 0.8 Hz, 1H, *8*), 7.21 (d, J = 8.9 Hz, 1H, *3*), 7.18 (dd, J = 8.3, 1.0 Hz, 1H, *7*), 6.87 ($dd^{II\ ord.}$, J = 8.7, 5.5 Hz, 2H, *2′*), 6.75 ($t^{II\ ord.}_{app.}$, J = 8.7 Hz, 2H, *3′*), 4.78 (s, 1H, *OH*). **^{13}C{^{1}H} NMR** (125.76 MHz, C_6D_6): δ 163.0 (d, J = 247.1 Hz, *4′*), 151.0 (*2*), 134.1 (*8a*), 133.2 (d, J = 8.0 Hz, *2′*), 130.4 (d, J = 3.9 Hz, *1′*), 130.1 (*4*), 129.5 (*4a*), 128.4 (*5*), 126.8 (*7*), 124.8 (*8*), 123.4 (t, J = 23.9 Hz, *6*), 120.4 (*1*), 117.8 (*3*), 116.6 (d, J = 20.9 Hz, *3′*). **^{19}F NMR** (470.59 MHz, C_6D_6): δ −113.48 (tt, J = 8.7, 5.5 Hz). **HRMS** (ESI$^-$, *m/z*) Calcd. for $C_{16}H_9DFO^-$ (M−H): 238.0784. Found: 238.0793. Error: 3.78 ppm. ν_{max} (neat, cm^{-1}): 3538, 1617, 1589, 1506, 1459, 1381, 1211, 1163, 1155, 835, 817, 794, 686, 657, 490.

1-(4-Fluorophenyl)naphthalen-2-ol (17d)

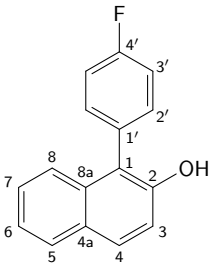

According to GP-5, naphthalen-2-ol (10.8 mg, 0.0750 mmol), tetra(4-fluorophenyl)bismuthonium tetrafluoroborate **5a** (50.7 mg, 0.0750 mmol) and DBU (16 µL, 0.11 mmol) were reacted together. The desired product was isolated upon purification by preparative TLC as a colourless oil (17.1 mg, 0.0720 mmol, 96%), whose characteristic data are in agreement with the literature (^{1}H, ^{19}F NMR in $CDCl_3$ HRMS and IR).[318] The structure was assigned by NMR spectroscopy in C_6D_6. The ^{13}C NMR spectrum of the deuterated analogue **17c** was used to univocally determine the ^{13}C NMR chemical shift of carbon *6*. Without this, the assignment of carbons *6* and *8* would have been ambiguous. The characterisation and assignment in CD_3CN is reported for completeness. The assignment relied on the identification of a crucial correlation between proton *5* and carbon *6* by H2BC, an NMR experiment that was not originally available. **^{1}H NMR** (500.13 MHz, C_6D_6): δ 7.65–7.58 (m, 1H, *5*), 7.54 (d, J = 8.8 Hz, 1H,

††Assignment confirmed by similarity with the unambiguous spectrum in C_6D_6 (*vide infra*).

4), 7.40–7.32 (m, 1H, *8*), 7.20 (d, J = 8.9 Hz, 1H, *3*), 7.22–7.12 (m, 2H[‡‡], *6 and 7*), 6.90–6.83 (m, 2H, *2′*), 6.80–6.72 (m, 2H, *3′*), 4.72 (s, 1H, *OH*). **^{13}C{^{1}H} NMR** (125.76 MHz, C_6D_6): δ 163.0 (d, J = 247.7 Hz, *4′*), 151.0 (*2*), 134.1 (*8a*), 133.2 (d, J = 8.3 Hz, *2′*), 130.4 (d, J = 4.0 Hz, *1′*), 130.1 (*4*), 129.5 (*4a*), 128.5 (*5*), 126.9 (*7*), 124.8 (*8*[§§]), 123.7 (*6*), 120.4 (*1*), 117.8 (*3*), 116.6 (d, J = 21.6 Hz, *3′*). **^{19}F NMR** (470.59 MHz, C_6D_6): δ −113.48 (tt, J = 8.6, 5.5 Hz). **^{1}H NMR** (500.13 MHz, CD_3CN): δ 7.83 (ddd, J = 7.6, 1.4, 1.1 Hz, 1H, *5*), 7.81 (d, J = 9.0 Hz, 1H, *4*), 7.37 (dd$^{\text{II ord.}}$, J = 8.8, 5.7 Hz, 2H, *2′*), 7.35–7.30 (m, 3H, *6, 7 and 8*), 7.28 ($t^{\text{II ord.}}_{\text{app.}}$, J = 8.9 Hz, 2H, *3′*), 7.22 (d, J = 8.9 Hz, 1H, *3*), 6.73 (s, 1H, *OH*). **^{13}C{^{1}H} NMR** (125.76 MHz, CD_3CN): δ 163.3 (d, J = 243.7 Hz, *4′*), 152.2 (*2*), 134.8 (*8a*), 134.1 (d, J = 8.3 Hz, *2′*), 132.9 (d, J = 3.2 Hz, *1′*), 130.3 (*4*), 129.7 (*4a*), 129.0 (*5*), 127.5 (*7*), 125.2 (*8*), 124.1 (*6*), 121.5 (*1*), 119.0 (*3*), 116.4 (d, J = 21.4 Hz, *3′*). **^{19}F NMR** (470.59 MHz, CD_3CN): δ −116.88 (tt, J = 9.1, 5.6 Hz). **HRMS** (ESI$^-$, *m/z*) Calcd. for $C_{16}H_{10}FO^-$ (M−H): 237.0721. Found: 237.0717. Error: 1.69 ppm. ν_{max} (neat, cm^{-1}): 1574, 1479, 1433, 1316, 1289, 1227, 1155, 1131, 1088, 1023, 1008, 909, 825, 763, 740, 713, 587, 564, 498. **m.p.** (°C): 111–112.

6-Methoxy-1-(4-fluorophenyl)naphthalen-2-ol (17e)

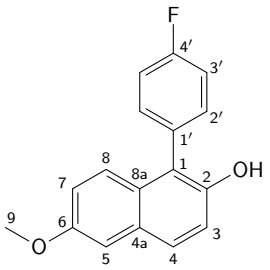

According to GP-5, 6-methoxynaphthalen-2-ol (20.2 mg, 0.116 mmol), tetra(4-fluorophenyl)bismuthonium tetrafluoroborate **5a** (77.9 mg, 0.116 mmol) and DBU (26 µL, 0.17 mmol) were reacted together. The desired product was isolated upon purification by preparative TLC as a colourless oil (29.6 mg, 0.110 mmol, 95%), whose characteristic data are in agreement with the literature.[453] **^{1}H NMR** (500.13 MHz, CD_3CN): δ 7.70 (d, J = 8.8 Hz, 1H, *4*), 7.35 (dd$^{\text{II ord.}}$, J = 8.8, 5.6 Hz, 2H, *2′*), 7.26 ($t^{\text{II ord.}}_{\text{app.}}$, J = 9.0 Hz, 2H, *3′*), 7.27–7.22 (m, 1H, *5 and 8*), 7.18 (d, J = 8.8 Hz, 1H, *3*), 7.00 (dd, J = 9.3, 2.6 Hz, 1H, *7*), 6.55 (s, 1H, *OH*), 3.86 (s, 3H, *9*). **^{13}C{^{1}H} NMR** (125.76 MHz, CD_3CN): δ 163.3 (d, J = 243.8 Hz, *4′*), 156.7 (*6*), 150.6 (*2*), 133.9 (d, J = 8.2 Hz, *2′*), 133.1 (d, J = 3.3 Hz, *1′*), 130.7 (*4a*), 129.9 (*8a*), 128.9 (*4*), 126.7 (*8*), 121.8 (*1*),119.7 (*7*), 119.4 (*3*), 116.4 (d, J = 21.6 Hz, *3′*), 107.5 (*5*), 56.0 (*9*). **^{19}F NMR** (470.59 MHz, CD_3CN): δ −116.91 (tt, J = 9.1, 5.6 Hz). **HRMS** (ESI$^-$, *m/z*) Calcd. for $C_{17}H_{12}FO_2^-$ (M−H): 267.0827. Found: 267.0831. Error: 1.50 ppm.

[‡‡]Signals partly hidden beneath the solvent peak.

[§§]Assigned by comparison with compound **17c** (*i.e.* by matching this signal with the distinctive triplet generated by C–D coupling).

1-(4-Fluorophenyl)-6-(4,4,5,5-tetramethyl-1,3,2-dioxaborolan-2-yl) naphthalen-2-ol (17g)

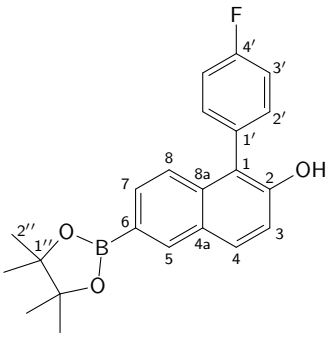

According to GP-5, 6-(4,4,5,5-tetramethyl-1,3,2-dioxaborolan-2-yl)naphthalen-2-ol (27.0 mg, 0.100 mmol), tetra(4-fluorophenyl)bismuthonium tetrafluoroborate **5a** (67.6 mg, 0.100 mmol) and DBU (23 µL, 0.15 mmol) were reacted together. The desired product was isolated upon purification by preparative TLC as a colourless oil (30.0 mg, 0.0822 mmol, 82%), whose characteristic data are in agreement with the literature.[318] **^{1}H NMR** (500.13 MHz, $CDCl_3$): δ 8.33 (d, J = 1.2 Hz, 1H, *5*), 7.85 (d, J = 8.9 Hz, 1H, *4*), 7.70 (dd, J = 8.5, 1.3 Hz, 1H, *7*), 7.39 (dd, J = 8.7, 5.4 Hz, 2H, *2′*), 7.34–7.27 (m, 3H, *8 and 3′*), 7.24 (d, J = 8.9 Hz, 1H, *3*), 5.10 (br, 1H, *OH*), 1.38 (s, 12H, *2″*). **^{11}B NMR** (160.46 MHz, $CDCl_3$): δ 30.7. **^{13}C{^{1}H} NMR** (125.76 MHz, $CDCl_3$): δ 163.0 (d, J = 248.1 Hz, *4′*), 151.5 (*2*), 136.6 (*5*), 135.2 (*8a*), 133.2 (d, J = 8.1 Hz, *2′*), 131.5 (*7*), 130.8 (*4*), 129.9 (d, J = 3.6 Hz, *1′*), 128.5 (*4a*), 123.6 (*8*), 120.0 (*1*), 117.4 (*3*), 116.9 (d, J = 21.5 Hz, *3′*), 84.0 (*1″*), 25.0 (*2″*). Carbon *6* not detected either by direct or indirect observation. **^{19}F NMR** (470.59 MHz, $CDCl_3$): δ −113.01 (tt, J = 8.7, 5.4 Hz). **HRMS** (ESI$^-$, *m/z*) Calcd. for $C_{22}H_{21}BFO_3^-$ (M−H): 363.1573. Found: 363.1590. Error: 4.68 ppm.

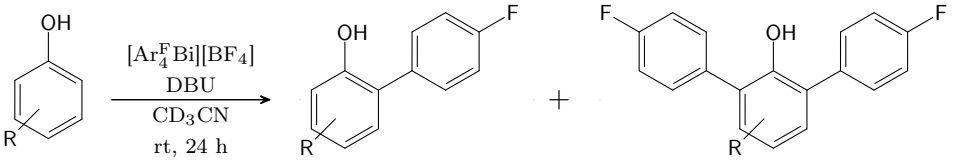

GP-6: tetra(4-fluorophenyl)bismuthonium tetrafluoroborate **5a** (1 equiv) and a phenol of choice (5 equiv) were added to an NMR tube and dissolved in CD_3CN (0.6 mL). DBU (5 equiv) was then added and the solution turned bright orange. The reaction was monitored by NMR spectroscopy at 3 h intervals and at completion was quenched with a few drops of TFA. The reaction mixture was transferred to a 10 mL round-bottom flask with the help of some DCM and all the solvents were evaporated under reduced pressure. The resulting crude was diluted with EtOAc (0.5 mL), loaded on a preparative TLC plate with a 100 µL micro-syringe and eluted with 250 mL of an appropriate solvent mixture.

4′-Fluoro-[1,1′-biphenyl]-2-ol (19a) and 4,4′′-difluoro-[1,1′:3′,1′′-terphenyl]-2′-ol (19b)

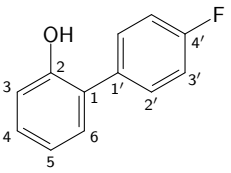

According to GP-6, phenol (49.5 mg, 0.526 mmol), tetra(4-fluorophenyl)bismuthonium tetrafluoroborate **5a** (67.7 mg, 0.100 mmol) and DBU (75 µL, 0.50 mmol) were reacted together for 48 h. The crude mixture was purified by preparatory TLC, which allowed the separation of two bands. The first band ($R_f = 0.2$) contained the mono-arylation product **19a** contaminated with traces of starting material. The latter was fully removed by sublimation affording the pure material as a colourless oil (7.00 mg, 0.0370 mmol, 37%), whose characteristic data are in accordance with the literature.[318] **^{1}H NMR** (500.13 MHz, CD_3CN): δ 7.54 (dd$^{\text{II ord.}}$, J = 8.5, 5.7 Hz, 2H, *2′*), 7.26 (dd, J = 7.6, 1.7 Hz, 1H, *6*), 7.20 (td, J = 7.7, 1.7 Hz, 1H, *4*), 7.16 ($t^{\text{II ord.}}_{\text{app.}}$, J = 8.9 Hz, 2H, *3′*), 6.96 (t, J = 7.5 Hz, 1H, *5*), 6.92 (d, J = 8.2 Hz, 1H, *3*). **^{13}C{^{1}H} NMR** (125.76 MHz, CD_3CN): δ 162.9 (d, J = 243.5 Hz, *4′*), 154.5 (*2*), 135.7 (d, J = 3.2 Hz, *1′*), 132.1 (d, J = 8.1 Hz, *2′*), 131.6 (*6*), 129.8 (*4*), 128.4 (*1*), 121.4 (*5*), 117.0 (*3*), 115.8 (d, J = 21.4 Hz, *3′*). **^{19}F NMR** (470.59 MHz, CD_3CN): δ −117.64 (tt, J = 9.2, 5.5 Hz). **HRMS** (ESI$^-$, *m/z*) Calcd. for $C_{12}H_8FO^-$ (M−H): 187.0565. Found: 187.0569. Error: 2.14 ppm. ν_{max} (neat, cm^{-1}): 3426, 2922, 2851, 1706, 1515, 1483, 1453, 1225, 1159, 834, 754.

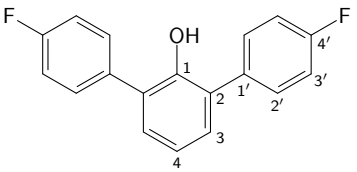

The second band (R_f 0.55) contained the diarylation product **19b**, which was isolated as a colourless oil (2.00 mg, 7.09 µmol, 7%), whose characteristic data are in accordance with the literature.[143] **^{1}H NMR** (500.13 MHz, $CDCl_3$): δ 7.52 (dd$^{\text{II ord.}}$, J = 8.8, 5.4 Hz, 4H, *2′*), 7.24 (d, J = 7.5 Hz, 2H, *3*), 7.17 ($t^{\text{II ord.}}_{\text{app.}}$, J = 8.7 Hz, 4H, *3′*), 7.05 (t, J = 7.6 Hz, 1H, *4*). **^{13}C{^{1}H} NMR** (125.76 MHz, $CDCl_3$): δ 162.6 (d, J = 247.4 Hz, *4′*), 149.4 (*1*), 133.5 (d, J = 3.4 Hz, *1′*), 131.2 (d, J = 8.0 Hz, *2′*), 130.2 (*3*), 128.0 (*2*), 121.0 (*4*), 116.0 (d, J = 21.4 Hz, *3′*). **^{19}F NMR** (470.59 MHz, $CDCl_3$): δ −114.36 (tt, J = 8.7, 5.4 Hz). ν_{max} (neat, cm^{-1}): 3560, 1510, 1450, 1264, 1225, 792, 733, 550.

4,4′′-Difluoro-5′-methoxy-[1,1′:3′,1′′-terphenyl]-2′-ol (20)

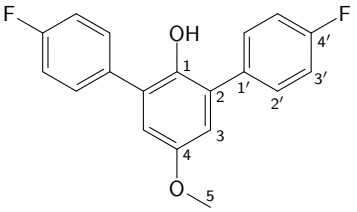

According to GP-6, 4-methoxyphenol (63.6 mg, 0.512 mmol), tetra(4-fluorophenyl)bismuthonium tetrafluoroborate **5a** (67.2 mg, 0.100 mmol) and DBU (75 µL, 0.50 mmol) were reacted together for 6 h. The crude mixture was purified by preparatory TLC,

which allowed the separation of two bands. The first band ($R_f = 0.2$) contained the mono-arylation product and the unreacted starting material. The latter could not be separated satisfactorily from the desired mono-arylation product. The second band ($R_f = 0.35$) contained the di-arylation product **20**, which was isolated as a colourless oil (2.6 mg, 8.3 µmol, 8%) whose characteristic data are reported below: **^{1}H NMR** (500.13 MHz, CD_3CN): δ 7.56 (dd$^{II\ ord.}$, J = 8.8, 5.5 Hz, 4H, *2′*), 7.20 ($t_{app.}^{II\ ord.}$, J = 8.9 Hz, 4H, *3′*), 6.82 (s, 2H, *2*), 3.78 (s, 3H, *5*). **^{13}C{^{1}H} NMR** (125.76 MHz, CD_3CN): δ 163.2 (d, J = 244.3 Hz, *4′*), 154.3 (*4*), 144.8 (*1*), 135.5 (d, J = 3.2 Hz, *1′*), 132.5 (d, J = 8.2 Hz, *3′*), 130.7 (*2*), 116.2 (*3*), 116.1 (d, J = 21.6 Hz, *2′*), 56.4 (*5*). **^{19}F NMR** (470.59 MHz, CD_3CN): δ −116.89 (tt, J = 9.0, 5.5 Hz). **HRMS** (ESI$^-$, *m/z*) Calcd. for $C_{19}H_{13}F_2O_2^-$ (M−H): 311.0889. Found: 311.0891. Error: 0.64 ppm.

4′-Fluoro-4,6-dimethyl-[1,1′-biphenyl]-2-ol (21a) and 4,4′′-difluoro-4′,6′-dimethyl-[1,1′:3′,1′′-terphenyl]-2′-ol (21b)

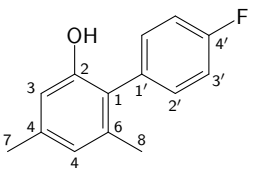

Tetra(4-fluorophenyl)bismuthonium tetrafluoroborate **5a** (67.6 mg, 0.100 mmol, 1 equiv) and 3,5-dimethylphenol (12.2 mg, 0.100 mmol, 1 equiv) were added to an NMR tube and dissolved in CD_3CN (0.6 mL). DBU (22 µL, 0.15 mmol, 1.5 equiv) was then added and the solution turned bright orange. The reaction was monitored by NMR spectroscopy and after 1 h was quenched with a few drops of TFA. The reaction mixture was transferred to a 10 mL round-bottom flask with the help of some DCM and all the solvents were evaporated under reduced pressure. The resulting crude was diluted with EtOAc (0.5 mL), loaded on a preparative TLC plate with a 100 µL micro-syringe and eluted with 250 mL of a 9:1 CyH:EtOAc mixture. Two bands were separated. The first band ($R_f = 0.2$) contained the mono-arylated product **21a**, which was isolated as a colourless oil (2.18 mg, 10.1 µmol, 10%) whose characteristic data are reported below. **^{1}H NMR** (500.13 MHz, $CDCl_3$): δ 7.28 (dd$^{II\ ord.}$, J = 8.7, 5.4 Hz, 2H, *2′*), 7.21 ($t_{app.}^{II\ ord.}$, J = 8.7 Hz, 2H, *3′*), 6.71 (s, 1H, *4*), 6.70 (s, 1H, *3*), 4.64 (s, 1H, *OH*), 2.34 (s, 3H, *7*), 2.05 (s, 3H, *8*). **^{13}C{^{1}H} NMR** (125.76 MHz, $CDCl_3$): δ 162.5 (d, J = 247.0 Hz, *4′*), 152.8 (*2*), 138.8 (*4*), 137.1 (*6*), 132.2 (d, J = 8.1 Hz, *2′*), 131.3 (d, J = 3.6 Hz, *1′*), 124.2 (*1*), 123.0 (*4*), 116.4 (d, J = 21.5 Hz, *3′*), 113.3 (*3*), 21.2 (*7*), 20.3 (*8*). **^{19}F NMR** (470.59 MHz, $CDCl_3$): δ −113.91 (tt, J = 8.6, 5.5 Hz). **HRMS** (ESI$^+$, *m/z*) Calcd. for $C_{14}H_{14}FO^+$ (M+H): 217.1023. Found: 217.1025. Error: 0.92 ppm.

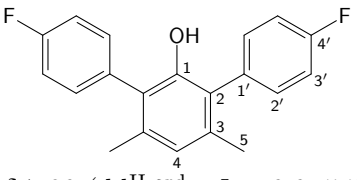

The second band contained the di-arylation product **21b**, which was isolated as a colourless oil (10.3 mg, 33.1 µmol, 33%), whose characteristic data are reported below. ^{1}**H NMR** (500.13 MHz, $CDCl_3$): δ 7.28 (dd$^{\text{II ord.}}$, J = 8.8, 5.5 Hz, 4H, *2′*), 7.16 (t$^{\text{II ord.}}_{\text{app.}}$, J = 8.7 Hz, 4H, *3′*), 6.82 (s, 1H, *4*), 4.61 (s, 1H, *OH*), 2.09 (s, 6H, *5*). ^{13}**C{^{1}H} NMR** (125.76 MHz, $CDCl_3$): δ 162.4 (d, J = 247.0 Hz, *4′*), 150.2 (*1*), 136.7 (*3*), 132.2 (*1′*)[¶¶], 132.1 (d, J = 7.4 Hz, *2′*), 125.1 (*2*), 123.7 (*4*), 116.1 (d, J = 21.1 Hz, *3′*), 20.4 (*5*). ^{19}**F NMR** (470.59 MHz, $CDCl_3$): δ −114.54 (tt, J = 8.8, 5.5 Hz). **HRMS** (ESI$^-$, *m/z*) Calcd. for $C_{20}H_{15}F_2O^-$ (M − H): 309.1096. Found: 309.1099. Error: 0.97 ppm. ν_{max} (neat, cm^{-1}): 3549, 2923, 1601, 1512, 1487, 1450, 1210, 1157, 835, 547, 512.

4′-Fluoro-2,4-dimethyl-[1,1′-biphenyl]-3-ol (22)

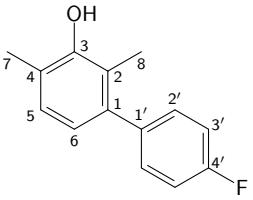

Tetra(4-fluorophenyl)bismuthonium tetrafluoroborate **5a** (82.5 mg, 0.122 mmol, 1.03 equiv) and 2,6-dimethylphenol (14.5 mg, 0.119 mmol, 1.00 equiv) were added to an NMR tube and dissolved in CD_3CN (0.6 mL). DBU (27 µL, 0.18 mmol, 1.5 equiv) was then added and the solution turned bright orange. The reaction was monitored by NMR spectroscopy and after 1 h was quenched with a few drops of TFA. The reaction mixture was transferred to a 10 mL round-bottom flask with the help of some DCM and all the solvents were evaporated under reduced pressure. The resulting crude was diluted with EtOAc (0.5 mL), loaded on a preparative TLC plate with a 100 µL micro-syringe and eluted with 250 mL of a 9:1 CyH:EtOAc mixture. The above-named product **22** was isolated as a colourless oil (17.7 mg, 82.1 µmol, 69%) whose characteristic data are reported below. ^{1}**H NMR** (500.13 MHz, $CDCl_3$): δ 7.36–7.23 (m, 2H, *2′*), 7.11 (t$^{\text{II ord.}}_{\text{app.}}$, J = 8.4 Hz, 2H, *3′*), 7.05 (d, J = 7.6 Hz, 1H, *5*), 6.77 (d, J = 7.6 Hz, 1H, *6*), 4.76 (s, 1H, *OH*), 2.33 (s, 3H, *7*), 2.17 (s, 3H, *8*). ^{1}**H{^{1}H} NMR** (500.13 MHz, $CDCl_3$): δ 7.28 (d, J = 5.5 Hz, *2′*), 7.11 (d, J = 8.9 Hz, *3′*), 7.05 (s, *5*), 6.77 (s, *6*), 4.76 (s, *OH*), 2.33 (s, *7*), 2.17 (s, *8*). ^{13}**C{^{1}H} NMR** (125.76 MHz, $CDCl_3$): δ 162.0 (d, J = 245.4 Hz), 152.5, 140.5, 137.9 (d, J = 3.6 Hz), 131.0 (d, J = 7.8 Hz), 127.9, 122.1, 122.0, 121.0, 115.0 (d, J = 21.6 Hz), 16.1, 13.3. ^{19}**F NMR** (470.59 MHz, $CDCl_3$): δ −116.23 (tt, J = 8.9, 5.5 Hz). **HRMS** (ESI$^-$, *m/z*) Calcd. for $C_{14}H_{12}FO^-$ (M−H): 215.0878. Found: 215.0883. Error: 2.32 ppm. ν_{max} (neat, cm^{-1}): 2923, 2870, 1612, 1513, 1486, 1462, 1219, 1195, 1178, 1157, 1113, 993, 839, 809, 533.

[¶¶]Expected to be a doublet but the second peak of the multiplet is partly hidden beneath the peak at 132.1 ppm

4′-Fluoro-1,3,5-trimethyl-[1,1′-biphenyl]-2(1H)-one (23)

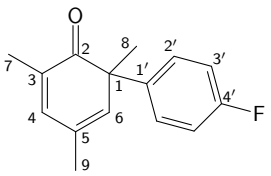

Tetra(4-fluorophenyl)bismuthonium tetrafluoroborate **5a** (70.8 mg, 0.0923 mmol, 1.00 equiv) and mesitol (13.5 mg, 0.0991 mmol, 1.07 equiv) were added to an NMR tube and dissolved in CD_3CN (0.6 mL). DBU (22 µL, 0.14 mmol, 1.5 equiv) was then added and the solution turned bright orange. The reaction was monitored by NMR spectroscopy and after 1 h was quenched with a few drops of AcOH. The reaction mixture was transferred to a 10 mL round-bottom flask with the help of some DCM and all the solvents were evaporated under reduced pressure. The resulting crude was diluted with EtOAc (0.5 mL), loaded on a preparative TLC plate with a 100 µL micro-syringe and eluted with 250 mL of a 9:1 CyH:EtOAc mixture. The above-named product **23** was isolated as a colourless oil (10.3 mg, 44.7 µmol, 48%) whose characteristic data are reported below. **^{1}H NMR** (500.13 MHz, $CDCl_3$): δ 7.25 (dd$^{\text{II ord.}}$, J = 8.9, 5.3 Hz, 2H, *2′*), 6.96 (t, J = 8.7 Hz, 2H, *3′*), 6.76 (dq, J = 2.9, 1.5 Hz, 1H, *4*), 6.01 (dqq, J = 2.9, 1.5, 0.8 Hz, 1H, *6*), 1.99 (d, J = 1.5 Hz, 3H, *9*), 1.88–1.84 (m, 3H, *7*), 1.56 (s, 3H, *8*). **^{13}C{^{1}H} NMR** (125.76 MHz, $CDCl_3$): δ 203.5 (*2*), 162.1 (d, J = 245.3 Hz, *4′*), 142.6 (*4*), 139.4 (*6*), 137.5 (d, J = 3.5 Hz, *1′*), 132.1 (*3*), 128.5 (d, J = 8.1 Hz, *2′*), 127.5 (*5*), 115.4 (d, J = 21.7 Hz, *3′*), 52.9 (*1*), 24.6 (*7*), 21.4 (*8*), 15.7 (*9*). **^{19}F NMR** (470.59 MHz, $CDCl_3$): δ −116.02 (tt, J = 8.7, 5.3 Hz). **HRMS** (ESI$^+$, *m/z*) Calcd. for $C_{15}H_{16}FO^+$ (M+H): 231.1180. Found: 231.1182. Error: 0.87 ppm. ν_{max} (neat, cm^{-1}): 2972, 2921, 2871, 1666, 1649, 1504, 1229, 1162, 830.

6-Hydroxy-2′,4,4-trimethyl-4,5-dihydro-[1,1′-biphenyl]-2(3*H*)-one (24)

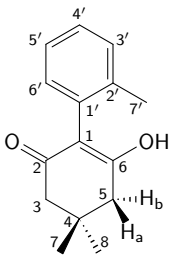

Tri(4-fluorophenyl)(o-tolyl)bismuthonium tetrafluoroborate **5v** (78.5 mg, 0.134 mmol, 1.07 equiv) and dimedone (17.5 mg, 0.125 mmol, 1.00 equiv) were added to an NMR tube and dissolved in THF (0.5 mL). To allow locking of the NMR spectrometer, 0.1 mL of C_6D_6 were added. DBU (24 µL, 0.16 mmol, 1.2 equiv) was then added and the solution turned bright orange. The reaction was monitored by NMR spectroscopy and after 2.5 h was quenched with a few drops of 1 M HCl. The reaction mixture was transferred to a separatory funnel, diluted with Et_2O and extracted with water three times. The organic phase was dried over $MgSO_4$, filtered and concentrated to dryness under reduced pressure. The oily material was dissolved in DCM, acidified with concentrated HCl and extracted three times with DCM to remove Ar^F_3Bi. Drying over $MgSO_4$, filtration and evaporation provided a crude material that was loaded on a preparatory TLC

plate with a 100 µL micro-syringe and eluted with a 3:97 MeOH:DCM mixture. The desired product was isolated from the band with R_f = 0.35–0.55 as a colourless oil (15.0 mg, 0.0651 mmol, 49%), whose characteristic data are in accordance with the literature.[454] **^{1}H NMR** (500.13 MHz, $CDCl_3$): δ 7.38–7.27 (m, 2H, *3′ and 4′*), 7.27–7.15 (m, 1H, *5′*), 7.09–7.00 (m, 1H, *6′*), 5.69 (s, 1H, *OH*), 2.52 (d, J = 17.6 Hz, 1H, *5b*), 2.46 (d, J = 17.6 Hz, 1H, *5a*), 2.38 (s, 2H, *3*), 2.13 (s, 3H, *7′*), 1.19 (s, 3H, *7*), 1.18 (s, 3H, *8*). Correlations between 7′ and 7 and between 7 and 5a determined by NOESY (d8 (mixing time) = 700 ms) **^{13}C{^{1}H} NMR** (125.76 MHz, $CDCl_3$): δ 196.7 (*2*), 169.2 (*6*), 139.0 (*2′*), 131.3 (*6′*), 131.1 (*3′*), 130.0 (*1′*), 129.1 (*4′*), 126.9 (*1′*), 116.7 (*1*), 51.0 (*3*), 41.6 (*5*), 29.0 (*8*), 28.3 (*7*), 18.9 (*7′*). No traces of the diketone tautomer were detected by NMR spectroscopy. **HRMS** (ESI$^+$, *m/z*) Calcd. for $C_{15}H_{19}O_2^+$ (M+H): 231.1380. Found: 231.1385. Error: 2.16 ppm. ν_{max} (neat, cm^{-1}): 2961, 2925, 2854, 1703, 1459, 1410, 1372, 1260, 739.

1-(4-Fluorophenyl)-1*H*-indazole (25a) and 2-(4-fluorophenyl)-1*H*-indazole (25b)

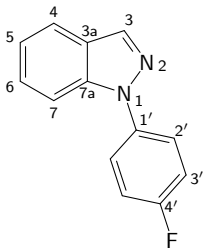

Tetra(4-fluorophenyl)bismuthonium tetrafluoroborate **5a** (71.0 mg, 0.0925 mmol, 1.00 equiv) and indazole (11.7 mg, 0.0987 mmol, 1.07 equiv) were added to an NMR tube and dissolved in CD_3CN (0.6 mL). DBU (22 µL, 0.14 mmol, 1.50 equiv) was then added and the solution turned bright orange. The reaction was monitored by NMR spectroscopy and after 12 h was quenched with a few drops of TFA. The reaction mixture was transferred to a 10 mL round-bottom flask with the help of some DCM and all the solvents were evaporated under reduced pressure. The resulting crude was diluted with EtOAc (0.5 mL), loaded on a preparative TLC plate with a 100 µL micro-syringe and eluted with 250 mL of a 8:2 CyH:EtOAc mixture. Two bands separated. The first band (R_f = 0.30–0.40) contained the 1-arylated product **25a**, which was isolated as a colourless oil (11.3 mg, 53.3 µmol, 58%) and whose characteristic data are in accordance with the literature.[455] **^{1}H NMR** (500.13 MHz, $CDCl_3$): δ 8.20 (d, J = 1.0 Hz, 1H, *3*), 7.81 (dt, J = 8.0, 1.0 Hz, 1H, *4*), 7.72–7.64 (m, 3H, *7 and 2′*), 7.44 (ddd, J = 8.3, 6.9, 1.1 Hz, 1H, *6*), 7.27–7.20 (m, 3H, 5 and 3′). **^{13}C{^{1}H} NMR** (125.76 MHz, $CDCl_3$): δ 161.3 (d, J = 246.6 Hz, *4′*), 139.0 (*7a*), 136.5 (d, J = 3.2 Hz, *1′*), 135.6 (*3*), 127.4 (*6*), 125.4 (*3a*), 124.7 (d, J = 8.2 Hz, *2′*), 121.7 (*5*), 121.5 (*4*), 116.5 (d, J = 23.3 Hz, *3′*), 110.2 (*7*). **^{19}F NMR** (470.59 MHz, $CDCl_3$): δ −115.12 (tt, J = 8.2, 4.7 Hz). **HRMS** (ESI$^+$, *m/z*) Calcd. for $C_{13}H_{10}FN_2^+$ (M+H): 213.0823. Found: 213.0828. Error: 2.35 ppm. ν_{max} (neat, cm^{-1}): 2926, 1513, 1229, 1198, 835.

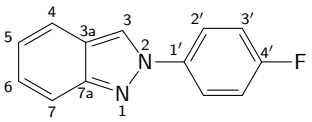

The second band (R_f = 0.50–0.60) contained the 2-arylation product **25b**, which was isolated as a colourless oil (6.0 mg, 28µmol, 31%) and whose characteristic data were in accordance with the literature.[456] ^{1}**H NMR** (500.13 MHz, $CDCl_3$): δ 8.36 (d, J = 1.0 Hz, 1H, *3*), 7.88 (dd, J = 9.0, 4.6 Hz, 2H, *2′*), 7.78 ($dq_{app.}$, J = 8.8, 1.0 Hz, 1H, *7*), 7.71 ($dt_{app.}$, J = 8.5, 1.1 Hz, 1H, *4*), 7.33 (ddd, J = 8.8, 6.6, 1.1 Hz, 1H, *6*), 7.23 (dd, J = 9.1, 8.0 Hz, 2H, *3′*), 7.13 (ddd, J = 8.4, 6.5, 0.8 Hz, 1H, *5*). ^{13}**C{^{1}H} NMR** (125.76 MHz, $CDCl_3$): δ 162.2 (d, J = 248.0 Hz, *4′*), 150.0 (*7a*), 137.0 (d, J = 3.4 Hz, *1′*), 127.1 (*6*), 122.98 (*3a*)***, 122.94 (d, J = 8.9 Hz, *2′*), 122.8 (*5*), 120.6 (*3*), 120.5 (*4*), 118.0 (*7*), 116.6 (d, J = 22.8 Hz, *3′*). ^{19}**F NMR** (470.59 MHz, $CDCl_3$): δ −113.80 (tt, J = 8.1, 4.6 Hz). **HRMS** (ESI^+, m/z) Calcd. for $C_{13}H_{10}FN_2^+$ (M+H): 213.0823. Found: 213.0828. Error: 2.35 ppm.

6.6 Authentic samples of diaryl ethers

Diaryl ethers are sometimes formed as side-products of the bismuth-mediated arylation of certain phenols. In order to correctly assign the corresponding ^{19}F NMR peak when the arylation is performed with $Ar^F_4Bi^+$ these compounds were synthesised independently *via* Ullmann coupling according to the following procedure:

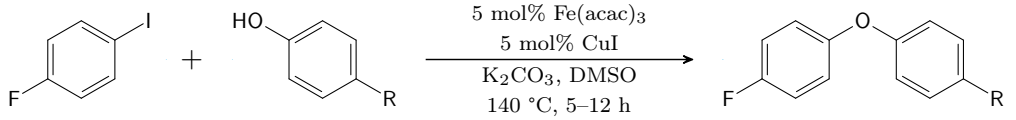

GP-7: the phenol (2.0 mmol, 1.0 equiv), $Fe(acac)_3$, CuI and K_2CO_3 were added to a flame-dried Schlenk tube equipped with a stirrer bar. A series of three cycles of vacuum and dinitrogen was performed, then degassed DMSO (4.0 mL) was added, followed by the aryl iodide (2 mmol, 1.0 equiv). The reactions were heated at 140 °C for 5–12 h, then heating was turned off and the reaction were quenched with 2 M HCl and extracted 3 times with Et_2O. The organic phases were combined, dried over $MgSO_4$ and concentrated under reduced pressure, yielding the desired products without further purification.

***This carbon signal was hidden underneath the peak at 122.94 ppm. Its existence was determined *via* HMBC, however, addition of two drops of C_6D_6 revealed it, as well.

1-Fluoro-4-phenoxybenzene (18a)

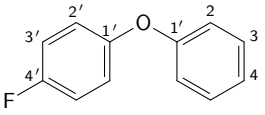

GP-7 was executed for phenol (188 mg, 2.00 mmol), yielding the name compound (356 mg, 1.89 mmol, 95%) as a colourless oil. **^{1}H NMR** (500.13 MHz, CD_3CN): δ 7.42–7.32 (m, 2H, *3*), 7.16–7.07 (m, 3H, *4 and 3′*), 7.02 (dd, J = 9.1, 4.5 Hz, 2H, *2′*), 7.00–6.96 (m, 2H, *2*). **^{13}C{^{1}H} NMR** (125.76 MHz, CD_3CN): δ 158.7 (d, J = 259.7 Hz, *4′*), 157.9 (*1*), 153.1 (d, J = 2.4 Hz, *1′*), 130.0 (*3*), 123.3 (*4*), 120.7 (d, J = 8.4 Hz, *2′*), 118.2, 116.3 (d, J = 23.7 Hz, *3′*). **^{19}F NMR** (470.59 MHz, CD_3CN): δ −121.76 (tt, J = 8.7, 4.6 Hz).

1-Bromo-4-(4-fluorophenoxy)benzene (18b)

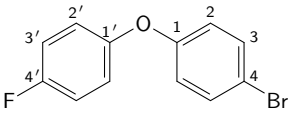

GP-7 was executed for 4-fluorophenol (224 mg, 2.00 mmol), yielding 373 mg of 90% pure product. **^{1}H NMR** (500.13 MHz, CD_3CN): δ 7.51 (d, J = 8.8 Hz, 2H, *3*), 7.16 (t, J = 8.7 Hz, 2H, *3′*), 7.07 (dd, J = 8.9, 4.5 Hz, 2H, *2′*), 6.92 (d, J = 8.7 Hz, 2H, *2*). **^{19}F NMR** (470.59 MHz, CD_3CN): δ −120.98 (tt, J = 8.6, 4.5 Hz).

4,4′-Oxybis(fluorobenzene) (18c)

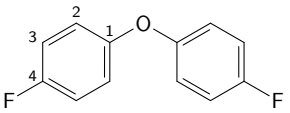

GP-7 was executed for 4-fluorophenol (224 mg, 2.00 mmol), yielding the name compound (374 mg, 1.82 mmol, 91%) as a colourless oil. **^{1}H NMR** (500.13 MHz, CD_3CN): δ 7.11 (t, J = 8.6 Hz, 1H, *3*), 7.00 (dd, J = 9.2, 4.5 Hz, 1H, *2*). **^{13}C{^{1}H} NMR** (125.76 MHz, CD_3CN): δ 159.7 (d, J = 239.3 Hz, *4*), 154.6 (d, J = 2.5 Hz, *1*), 121.1 (d, J = 8.3 Hz, *2*), 117.3 (d, J = 23.6 Hz, *3*). **^{19}F NMR** (470.59 MHz, CD_3CN): δ −121.91 (tt, J = 8.5, 4.6 Hz).

1-Fluoro-4-(*p*-tolyloxy)benzene (18d)

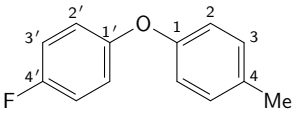

GP-7 was executed for 4-methylphenol (216 mg, 2.00 mmol), yielding the name compound (382 mg, 1.89 mmol, 95%) as a colourless oil. **^{1}H NMR** (500.13 MHz, CD_3CN): δ 7.18 (d, J = 8.5 Hz, 2H, *3*), 7.09 (t, J = 8.6 Hz, 2H, *3′*), 6.98 (dd, J = 9.1, 4.5 Hz, 2H, *2′*), 6.88 (d, J = 8.5 Hz, 2H, *2*), 2.31 (s, 3H, *Me*). **^{13}C{^{1}H} NMR** (125.76 MHz, CD_3CN): δ 159.6 (d, J = 238.9 Hz, *4′*), 156.2 (*1*), 154.6 (d, J = 2.3 Hz, *1′*), 134.1 (*4*), 121.1 (d, J = 8.4 Hz, *2′*), 119.4 (*2*), 117.2 (d, J = 23.6 Hz, *3′*), 20.7 (*Me*). **^{19}F NMR** (470.59 MHz, CD_3CN): δ −122.30 (tt, J = 8.7, 4.5 Hz).

1-(*tert*-Butyl)-4-(4-fluorophenoxy)benzene (18e)

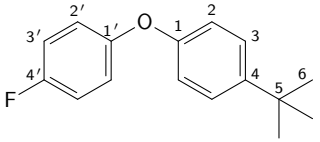

GP-7 was executed for 4-*tert*-butylphenol (300 mg, 2.00 mmol), yielding the name compound (458 mg, 1.88 mmol, 94%) as a colourless oil. **^{1}H NMR** (500.13 MHz, CD_3CN): δ 7.40 (d, J = 8.8 Hz, 2H, *3*), 7.11 (t, J = 9.0 Hz, 2H, *3′*), 6.99 (dd, J = 9.1, 4.5 Hz, 2H, *2′*), 6.90 (d, J = 8.8 Hz, 2H, *2*), 1.30 (s, 9H, *6*). **^{13}C{^{1}H} NMR** (125.76 MHz, CD_3CN): δ 159.7 (d, J = 239.2 Hz, *4′*), 156.3 (*1*), 154.41 (d, J = 2.4 Hz, *1′*), 147.3 (*4*), 127.8 (*3*), 121.4 (d, J = 8.3 Hz, *2′*), 118.8 (*2*), 117.2 (d, J = 23.5 Hz, *2′*), 34.9 (*5*), 31.7 (*6*). **^{19}F NMR** (470.59 MHz, CD_3CN): δ −122.04 (tt, J = 8.7, 4.5 Hz).

1-Fluoro-4-(4-methoxyphenoxy)benzene (18f)

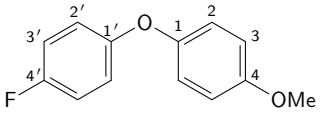

GP-7 was executed for 4-methoxyphenol (248 mg, 2.00 mmol), yielding the name compound (418 mg, 1.92 mmol, 96%) as a colourless oil. **^{1}H NMR** (500.13 MHz, CD_3CN): δ 7.07 (t, J = 8.6 Hz, 2H, *3′*), 7.00–6.88 (m, 6H, *2, 3 and 2′*), 3.77 (s, 3H, *MeO*). **^{13}C{^{1}H} NMR** (125.76 MHz, CD_3CN): δ 159.3 (d, J = 238.4 Hz, *4′*), 157.0 (*4*), 155.5 (d, J = 2.3 Hz, *1′*), 151.5 (*1*), 121.2 (*2*), 120.2 (d, J = 8.4 Hz, *2′*), 117.1 (d, J = 23.6 Hz, *3′*), 115.9 (*3*), 56.3 (*MeO*). **^{19}F NMR** (470.59 MHz, CD_3CN): δ −122.95 (tt, J = 8.7, 4.5 Hz).

6.7 Tridentate ligands and corresponding complexes

1,3-Bis((2-bromobenzyl)oxy)benzene (26)

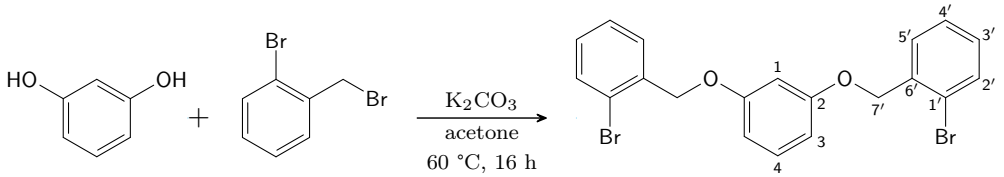

Resorcinol (1.12 g, 10.1 mmol, 1.11 equiv), 2-bromobenzyl bromide (4.54 g, 18.2 mmol, 2.00 equiv) and K_2CO_3 (3.77 g, 27.3 mmol, 3.0 equiv) were loaded into a 100 mL round-bottom flask equipped with a condenser. Acetone was added and the resulting suspension was refluxed at 60 °C for 16 h. Upon complete consumption of the benzyl bromide the reaction was worked up by adding $MgSO_4$ and filtering off the inorganic residues. The crude material was purified by flash chromatography (5% EtOAc/CyH), yielding the desired product (3.77 g, 8.42 mmol, 93%) as a pale yellow

oil. **^{1}H NMR** (500.13 MHz, $CDCl_3$): δ 7.59 (dd, J = 8.0, 1.2 Hz, 2H, *2′*), 7.56 (dd, J = 7.7, 1.7 Hz, 2H, *5′*), 7.34 (td, J = 7.5, 1.2 Hz, 2H, *4′*), 7.23 (t, J = 8.4 Hz, 1H, *4*), 7.19 (td, J = 7.9, 1.6 Hz, 2H, *3′*), 6.68 (t, J = 2.4 Hz, 1H, *1*), 6.64 (dd, J = 8.2, 2.4 Hz, 2H, *3*), 5.14 (s, 4H, *7′*). **^{13}C{^{1}H} NMR** (125.76 MHz, $CDCl_3$): δ 159.9 (*2*), 136.4 (*6′*), 132.8 (*2′*), 130.2 (*4*), 129.4 (*3′*), 129.1 (*5′*), 127.7 (*4′*), 122.5 (*1′*), 107.8 (*3*), 102.5 (*1*), 69.6 (*7′*). **HRMS** (EI^+, *m/z*) Calcd. for $C_{20}H_{17}Br_2O_2$ (M+H): 446.9590. Found: 446.9584. Error: 1.34 ppm. ν_{max} (neat, cm^{-1}): 1591, 1487, 1436, 1256, 1175, 1149, 1067, 1013, 835, 745. **m.p.** (°C): 59–61.

2-Bromo-1,3-bis(bromomethyl)benzene (27) and 2-bromo-1,3-bis(dibromomethyl)benzene (28)

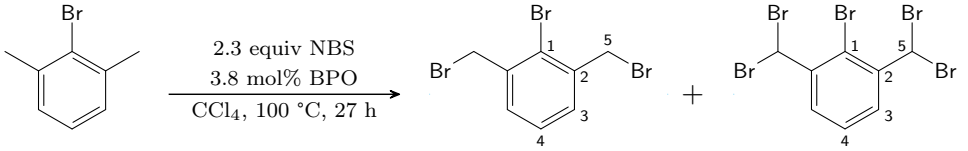

27 **28**

In a 250 mL round-bottom flask equipped with a condenser, 2-bromoxylene (3.80 g, 20.5 mmol, 1.00 equiv), *N*-bromosuccinimide (8.40 g, 47.2 mmol, 2.30 equiv) and benzoyl peroxide (189 mg, 0.78 mmol, 3.8 mol %) were suspended in CCl_4 (125 mL, 0.16 M) and refluxed at 100 °C for 27 h. The solvent was then removed under reduced pressure and the residues dissolved again in $CHCl_3$, filtered, extracted with water (3 × 30 mL). The organic phase was then dried over $MgSO_4$, filtered and concentrated under vacuum. The crude material was purified by flash chromatography (pentane) and crystallised from CyH yielding colourless crystals of the named product (1.51 g, 4.41 mmol, 22%), whose characteristic data are in accordance with the literature.[457] **^{1}H NMR** (500.13 MHz, $CDCl_3$): δ 7.42 (d, J = 7.6 Hz, 2H, *3*), 7.29 (t, J = 7.6 Hz, 1H, *4*), 4.65 (s, 4H, *5*). **^{13}C{^{1}H} NMR** (125.76 MHz, $CDCl_3$): δ 138.6 (*2*), 131.5 (*3*), 128.2 (*4*), 126.8 (*1*), 34.0 (*5*). **HRMS** (EI^+, *m/z*) Calcd. for $C_8H_7Br_3$ (M+): 339.8098. Found: 339.8244. Error: 42.97 ppm. The tetrabrominated species **28** was isolated in a first iteration of the previous procedure, in which 2.1 equiv of NBS were used instead of 2.3 equiv. This caused the partial consumption of 2-bromoxylene, so additional NBS was added, bringing its overall amount to 3.1 equiv and causing the undesired over-bromination. The detail procedure is as follows: in a 250 mL round-bottom flask equipped with a condenser, 2-bromoxylene (3.70 g, 20 mmol, 1.00 equiv), *N*-bromosuccinimide (7.48 g, 42.0 mmol, 2.10 equiv) and benzoyl peroxide (145 mg, 0.600 mmol, 3.8 mol %) were suspended in CCl_4 (125 mL, 0.16 M) and refluxed at 100 °C for 16 h. An aliquot of the reaction mixture was taken and

analysed by NMR spectroscopy: this revealed the presence of a complex mixture of species, including unreacted starting material and mono-brominated product. Notably, all the NBS had been reduced to succinimide. Thus, additional NBS was added (3.56 g, 20.0 mmol, 1.00 equiv) and the reaction was heated at reflux for 5 h more. The solvent was then removed under reduced pressure and the residues dissolved again in $CHCl_3$, filtered, extracted with water (3 × 30 mL). The organic phase was then dried over $MgSO_4$, filtered and concentrated under vacuum. The crude material was purified by flash column chromatography (pentane). Only one pure fraction was isolated (R_f = 0.95, pentane) and was then recrystallised from CyH yielding colourless crystals (1.20 g, 2.40 mmol, 12%) that were identified as the tetrabrominated species **28**. Its spectroscopic data were, in fact, consistent with those reported in the literature.[458] **^{1}H NMR** (500.13 MHz, $CDCl_3$): δ 8.07 (d, J = 7.9 Hz, 2H, *3*), 7.55 (t, J = 7.9 Hz, 1H, *4*), 7.16 (s, 2H, *5*). **^{13}C{^{1}H} NMR** (125.76 MHz, $CDCl_3$): δ 140.7 (*2*), 132.5 (*3*), 129.1 (*4*), 117.1 (*1*), 39.2 (*5*).

2-Bromo-1,3-bis((2-bromobenzyl)oxy)-benzene (29)

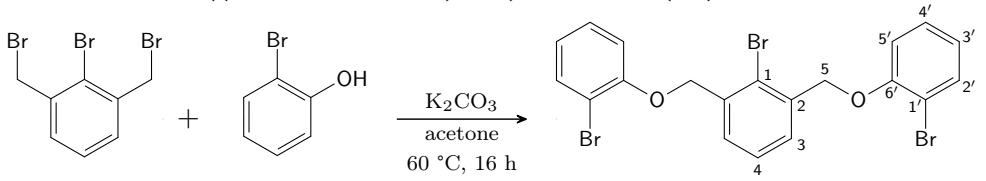

Bromophenol (865 mg, 5.00 mmol, 2.5 equiv), 2-bromo-1,3-bis(bromomethyl)benzene **27** (686 mg, 2.00 mmol, 1.0 equiv) and K_2CO_3 (2.07 g, 15.0 mmol, 7.5 equiv) were loaded into a 50 mL round-bottom flask equipped with a condenser. Acetone (20 mL) was added and the resulting suspension was refluxed at 60 °C for 16 h. Upon complete consumption of the benzyl bromide, as determined by NMR spectroscopy, the reaction mixture was dried over $MgSO_4$, filtered and concentrated under reduced pressure. This also allowed the removal of excess phenol by sublimation and yielded the desired product without further purification as a white solid (717 mg, 1.36 mmol, 68%). The missing mass was lost in the filtration process, presumably due to the relatively low solubility of the product in acetone. **^{1}H NMR** (500.13 MHz, $CDCl_3$): δ 7.70 (d, J = 7.7 Hz, 2H, *3*), 7.59 (dd, J = 7.9, 1.6 Hz, 2H, *2′*), 7.44 (t, J = 7.7 Hz, 1H, *4*), 7.30–7.26 (m, 2H, *4′*), 6.97 (dd, J = 8.2, 1.5 Hz, 2H, *5′*), 6.89 (td, J = 7.7, 1.4 Hz, 2H, *3′*), 5.25 (s, 4H, *5*). **^{13}C{^{1}H} NMR** (125.76 MHz, $CDCl_3$): δ 154.8 (*6′*), 136.3 (*2*), 133.7 (*2′*), 128.7 (*4′*), 128.1 (*4*), 128.0 (*3*), 122.6 (*3′*), 121.0 (*1*), 113.9 (*5′*), 112.6 (*1′*), 70.4 (*5*). **HRMS** (ESI$^+$, *m/z*) Calcd. for $C_{20}H_{19}Br_3NO_2$ (M+ NH_4): 541.8960. Found: 541.8959. Error: 0.18 ppm. ν_{max} (neat, cm^{-1}): 1572, 1479, 1440, 1363, 1279, 1246, 1068, 1028, 739, 647. **m.p.** (°C): 157–158.

1,3-Bis((2-bromobenzyloxy)methyl)-2-bromobenzene (30)

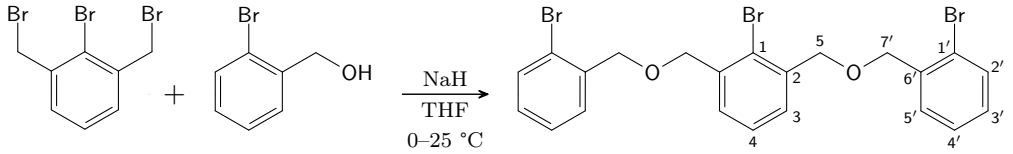

In a 20 mL Schlenk tube, sodium hydride (207 mg of 60% dispersion in mineral oil, 5.18 mmol, 2.73 equiv) was added to a solution of 2-bromobenzyl alcohol (730 mg, 3.90 mmol, 2.05 equiv) in dry THF (5 mL) kept at 0 °C. This suspension was stirred for 30 min, then a solution of 1,3-bis((2-bromobenzyl)oxy)benzene **27** (650 mg, 1.90 mmol, 1.00 equiv) in THF (5 mL) was added drop-wise. The reaction was left to stir overnight, then quenched carefully first with water, then with 1 M HCl, finally extracted with EtOAc (3 × 10 mL). The organic fractions were collected, washed with brine, dried over $MgSO_4$ and concentrated to afford the desired product without further purification (1.04 g, 1.87 mmol, 99%). **^{1}H NMR** (500.13 MHz, $CDCl_3$): δ 7.57 (td, J = 8.2, 1.4 Hz, 4H, *5′*), 7.52 (d, J = 7.5 Hz, 2H, *3*), 7.38 (d, J = 7.6 Hz, 1H, *4*), 7.34 (td, J = 7.7, 1.5 Hz, 2H, *4′*), 7.17 (td, J = 7.7, 1.7 Hz, 2H, *3′*), 4.75 (s, 4H, *5*), 4.73 (s, 4H, *7′*). **^{13}C{^{1}H} NMR** (125.76 MHz, $CDCl_3$): δ 138.0 (*2*), 137.6 (*6′*), 132.7 (*2′*), 129.2 (*5′*), 129.1 (*3′*), 128.3 (*3*), 127.6 (*4′*), 127.5 (*4*), 123.0 (*1*), 122.8 (*1′*), 72.5 (*5*), 72.3 (*7′*). **HRMS** (ESI$^+$, *m/z*) Calcd. for $C_{22}H_{23}Br_3NO_2$ (M+ NH_4): 569.9273. Found: 569.9264. Error: 1.58 ppm. ν_{max} (neat, cm^{-1}): 2922, 2852, 1438, 1392, 1352, 1247, 1122, 1111, 1020, 768, 740, 683. **m.p.** (°C): 121–122.

***N*-(2-Bromobenzyl)propan-2-amine (31)**

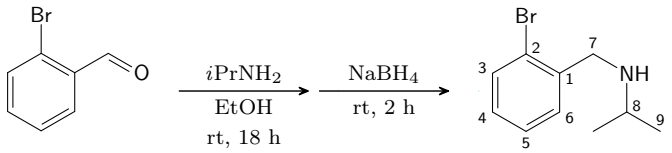

Isopropylamine (4.0 mL, 2.9 g, 49 mmol, 0.98 equiv) was added to a solution of 2-bromobenzaldehyde (5.8 mL, 9.3 g, 50 mmol, 1.0 equiv) in ethanol (100 mL, 0.5 M). The resulting solution was stirred overnight, then, upon confirmation of the complete consumption of the aldehyde, $NaBH_4$ (2.4 g, 63 mmol, 1.25 equiv) was added and this suspension stirred for an additional 2 h. The solvent was then removed under reduced pressure, the solids dissolved in Et_2O (100 mL) and extracted with water (3 × 50 mL). The organic phase was then dried over $MgSO_4$, filtered and concentrated to afford, without further purification, the title compound **31** (10.9 g, 47.8 mmol, 98%) as a pale yellow oil. Characteristic data are in accordance with

the literature.[459] **^{1}H NMR** (500.13 MHz, $CDCl_3$): δ 7.53 (dd, J = 7.9, 1.3 Hz, 1H, *3*), 7.38 (dd, J = 7.5, 1.8 Hz, 1H, *6*), 7.27 (td, J = 7.5, 1.2 Hz, 1H, *5*), 7.10 (td, J = 7.7, 1.7 Hz, 1H, *4*), 3.85 (s, 2H, *7*), 2.83 (hept, J = 6.3 Hz, 1H, *8*), 1.54 (s, 1H, *NH*), 1.11 (d, J = 6.3 Hz, 6H, *9*). **^{13}C{^{1}H} NMR** (125.76 MHz, $CDCl_3$): δ 139.7 (*1*), 132.9 (*3*), 130.5 (*6*), 128.6 (*4*), 127.6 (*5*), 124.1 (*2*), 51.6 (*7*), 48.1 (*8*), 23.0 (*9*). **HRMS** (ESI^+, *m/z*) Calcd. for $C_{10}H_{15}BrN$ (M+H): 228.0382. Found: 228.0380. Error: 0.88 ppm. ν_{max} (neat, cm^{-1}): 2963, 1465, 1439, 1024, 745, 657.

2-Bromo-1,3-bis(bromomethyl)-5-fluorobenzene (32)

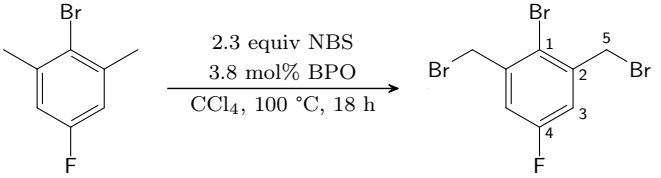

In a 250 mL round-bottom flask equipped with a condenser, 2-bromo-4-fluoro-xylene (5.08 g, 25.0 mmol, 1.00 equiv), *N*-bromosuccinimide (9.57 g, 53.8 mmol, 2.15 equiv) and benzoyl peroxide (391 mg, 1.61 mmol, 3.8 mol%) were suspended in CCl_4 (125 mL, 0.20 M) and refluxed at 100 °C for 18 h. The solvent was then distilled off and the residues dissolved again in $CHCl_3$, filtered, extracted with water (3 × 30 mL). The organic phase was then dried over $MgSO_4$, filtered and concentrated under vacuum. The crude material was purified by flash chromatography (pentane) yielding the named product as a colourless solid (R_f = 0.4, 2.72 g, 7.51 mmol, 30%). **^{1}H NMR** (500.13 MHz, $CDCl_3$): δ 7.18 (d, J = 8.4 Hz, 2H, *3*), 4.59 (s, 4H, *5*). **^{13}C{^{1}H} NMR** (125.76 MHz, $CDCl_3$): δ 161.4 (d, J = 249.0 Hz, *4*), 140.4 (d, J = 7.7 Hz, *2*), 120.8 (d, J = 3.5 Hz, *1*), 118.4 (d, J = 23.2 Hz, *3*), 33.0 (d, J = 1.8 Hz, *5*). **^{19}F NMR** (470.59 MHz, $CDCl_3$): δ −113.27 (t, J = 8.3 Hz). **HRMS** (EI^+, *m/z*) Calcd. for $C_8H_6Br_3F$ (M+): 359.7983. Found: 359.8415. Error: 120.07 ppm. ν_{max} (neat, cm^{-1}): 1583, 1430, 1312, 1209, 1145, 998, 874, 733, 620, 586, 561, 537. **m.p.** (°C): 122–123.

1,3-Bis((2-bromobenzyl(propan-2-amino))methyl)-2-bromo-5-fluorobenzene (33)

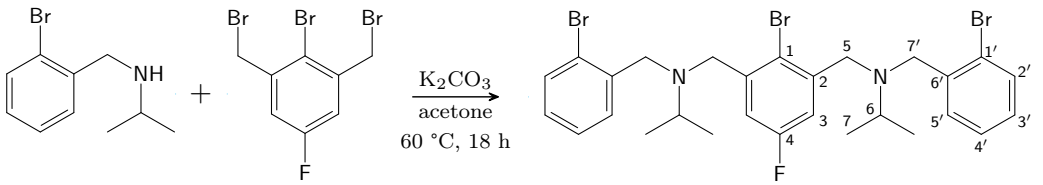

Amine **31** (1.39 g, 6.10 mmol, 2.2 equiv), benzyl bromide **32** (1.00 g, 2.77 mmol, 1.00 equiv) and K_2CO_3 (1.15 g, 8.31 mmol, 3.0 equiv) were loaded into a 100 mL

round-bottom flask equipped with a condenser. Acetone (25 mL) was added and the resulting suspension was refluxed at 60 °C for 18 h. Upon complete consumption of the benzyl bromide, the solvent was evaporated and the residues redissolved in EtOAc (50 mL) and extracted with water (3 × 25 mL). The organic phased was then dried over $MgSO_4$, filtered and concentrated, providing, without further purification, the title compound **33** (1.80 g, 2.74 mmol, 99%) as a colourless solid. **^{1}H NMR** (500.13 MHz, $CDCl_3$): δ 7.55 (dd, J = 7.6, 1.3 Hz, 2H, *5′*), 7.47 (dd, J = 8.0, 1.3 Hz, 2H, *2′*), 7.25 (d, J = 11.0 Hz, 3H, *3*), 7.22 (td, J = 7.5, 1.3 Hz, 1H, *4′*), 7.02 (td, J = 7.6, 1.8 Hz, 2H, *3′*), 3.71 (s, 4H, *7′*), 3.68 (s, 4H, *5*), 2.95 (hept, J = 6.7 Hz, 2H, *6*), 1.13 (d, J = 6.6 Hz, 12H, *7*). **^{13}C{^{1}H} NMR** (125.76 MHz, $CDCl_3$): δ 162.4 (d, J = 243.9 Hz, *4*), 142.2 (d, J = 7.2 Hz, *2*), 139.3 (*6′*), 132.7 (*2′*), 130.3 (*5′*), 128.2 (*3′*), 127.4 (*4′*), 124.3 (*1′*), 118.8 (d, J = 2.6 Hz, *1*), 115.0 (d, J = 24.5 Hz, *3*), 53.8 (*5*), 53.7 (*7′*), 50.5 (*6*), 18.2 (*7*). **^{19}F NMR** (470.59 MHz, $CDCl_3$): δ −115.61 (t, J = 9.5 Hz). **HRMS** (ESI^+, *m/z*) Calcd. for $C_{28}H_{33}Br_3FN_2$ (M+H): 653.0172. Found: 653.0161. Error: 1.68 ppm. ν_{max} (neat, cm^{-1}): 2962, 1580, 1460, 1422, 1386, 1366, 1351, 1164, 1102, 1022, 992, 875, 751, 662, 610. **m.p.** (°C): 120–121.

N-((12-Bromo-3-fluoro-6-isopropyl-5,6,7,12-tetrahydrodibenzo[*c,f*][1,5]azabismocin-1-yl)methyl)-*N*-(2-butylbenzyl)propan-2-amine (34)

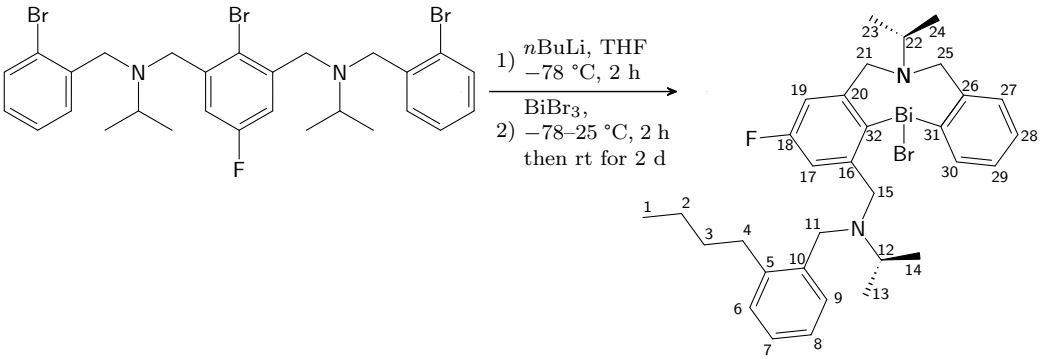

Compound **33** (1.02 g, 1.56 mmol, 1.00 equiv) was loaded into a 20 mL Schlenk tube and dissolved in THF (6 mL). This solution was cooled to −78 °C and *n*BuLi (2.15 mL of a 2.4 M solution in hexanes, 5.14 mmol, 3.30 equiv) was added drop-wise. An aliquot was taken after 2 h, quenched with D_2O, extracted with Et_2O, passed through a $MgSO_4$ plug, concentrated under reduced pressure, dissolved in $CDCl_3$ and analysed by NMR spectroscopy and HRMS. Both methods showed full incorporation of deuterium, so $BiBr_3$ (665 mg, 1.48 mmol, 0.95 equiv) was dissolved in THF (2 mL) and added drop-wise to the reaction mixture, kept at −78 °C throughout the addition process. The temperature was then let to rise to rt over the course of 2 h and maintained for 2 d. The reaction was quenched with

water (10 mL) and extracted with Et_2O (3×10 mL). The combined organic phases were dried over $MgSO_4$ and the solvents were removed under reduced pressure. The resulting crude material was purified by flash column chromatography (4% Et_3N in DCM) and a fraction ($R_f = 0.5$) was isolated as a dark yellow oil (208 mg) and fully characterised. The structure of this pure material was assigned to the name compound **34**, isolated in 18% yield. **^{1}H NMR** (500.13 MHz, $CDCl_3$):[†††] δ 9.13 (d, J = 7.6 Hz, 1H, *30*), 7.58–7.49 (m, 2H, *17 and 29*), 7.51–7.46 (m, 2H, *9 and 27*), 7.39 (td, J = 7.4, 1.3 Hz, 1H, *28*), 7.13–7.05 (m, 3H, *6, 7 and 8*), 6.83 (dd, J = 8.9, 2.6 Hz, 1H, *19*), 4.31 (d, J = 15.5 Hz, 1H, *21*), 4.27 ($d^{IIord.}$, J = 14.5 Hz, 1H, *15*), 4.21 (d, J = 15.5 Hz, 1H, *25*), 4.20 (d, J = 15.5 Hz, 1H, *21′*), 4.10 ($d^{IIord.}$, J = 14.5 Hz, 1H, *15′*), 4.06 (d, J = 15.5 Hz, 1H, *25′*), 3.67 ($d^{IIord.}$, J = 14.0 Hz, 1H, *11*), 3.63 ($d^{IIord.}$, J = 14.0 Hz, 1H, *11′*), 3.21 (p, J = 6.6 Hz, 1H, *22*), 2.97 (p, J = 6.6 Hz, 1H, *12*), 2.72–2.64 (m, 2H, *4*), 1.55–1.46 (m, 2H, *3*), 1.39 (dt, J = 14.9, 7.4 Hz, 2H, *2*), 1.25 (d, J = 6.6 Hz, 4H, *23 or 24*), 1.152 (d, J = 6.6 Hz, 3H, *23 or 24*), 1.148 (d, J = 6.7 Hz, 3H, *13 or 14*), 1.12 (d, J = 6.7 Hz, 3H, *13 or 14*), 0.94 (t, J = 7.3 Hz, 3H, *1*). **^{13}C{^{1}H} NMR** (125.76 MHz, $CDCl_3$): δ 172.9 (br, *32*), 169.1 (br, *31*), 163.0 (d, J = 246.7 Hz, *18*), 155.8 (d, J = 6.7 Hz, *16*), 155.3 (d, J = 6.8 Hz, *20*), 147.4 (*26*), 141.8 (*5*), 140.9 (br, *30*), 137.6 (*10*), 131.9 (*29*), 129.7 (*9*), 129.1 (*6*), 128.41 (*28*), 128.38 (*27*), 126.6 (*7*), 125.6 (*8*), 117.3 (d, J = 21.0 Hz, *17*), 113.5 (d, J = 21.6 Hz, *19*), 60.6 (d, J = 2.6 Hz, *21*), 58.0 (br, *25*), 57.8 (*15*), 53.6 (*22*), 51.7 (*11*), 50.1 (*12*), 33.4 (*3*), 32.3 (*4*), 22.9 (*2*), 21.6 (*23 or 24*), 19.5 (*13 or 14*), 17.7 (*23 or 24*), 17.1 (*13 or 14*), 14.2 (*1*). **^{19}F NMR** (470.59 MHz, $CDCl_3$): δ −113.37 (t, J = 9.9 Hz). **HRMS** (ESI$^-$, *m/z*) Calcd. for $C_{32}H_{41}BiFN_2^+$ (M−Br): 681.3069. Found: 681.3052. Error: 2.50 ppm. ν_{max} (neat, cm^{-1}): 2961, 2929, 1582, 1454, 1365, 1291, 1265, 1159, 1121, 887, 734, 701.

Tri-(2-bromophenyl)phosphine (35) and tri-(2-bromophenyl)-phosphine oxide (36)

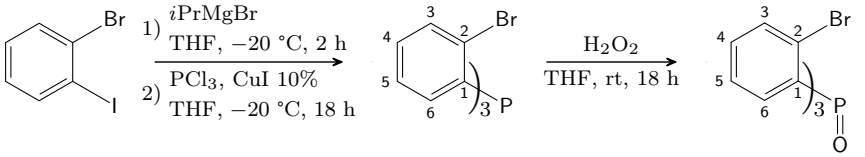

Magnesium turnings (223 mg, 9.19 mmol, 3.68 equiv) and a couple of iodine crystals were loaded in a Schlenk tube, stirred and heated gently under a nitrogen atmosphere until purple vapours developed. THF (11.5 mL) and 2-bromopropane

[†††]Diastereotopic protons are marked with a prime sign.

(860 µL, 1.13 g, 9.19 mmol, 3.68 equiv) were then added. The suspension was stirred at reflux until no more heat developed, then it was let to cool down to room temperature over the course of 30 min. In the meanwhile, in a separate Schlenk tube, 2-bromoiodobenzene (1.12 mL, 2.48 g, 8.75 mmol, 3.5 equiv) was dissolved in THF (8.8 mL) and the solution was thermostated at −20 °C. The freshly prepared *i*PrMgBr was transferred drop-wise with a syringe into this solution, which was then stirred at the same temperature for 2 h. In the meanwhile, 1 mL of PCl_3 was heated at reflux for 30 min in a 10 mL round-bottom flask equipped with an air condenser, to remove traces of HCl. Then the acid-free PCl_3 was transferred into an oven-dried micro-distillation apparatus and distilled under a nitrogen atmosphere to remove trace water. Finally, 220 µL (343 mg, 2.50 mmol, 1.00 equiv) of the purified reagent were measured in a micro-syringe and added drop-wise to the Grignard solution, together with CuI (47.6 mg, 0.250 mmol, 0.100 equiv). Upon completion of the additions, the reaction mixture was allowed to warm up to rt overnight, then was quenched with $NH_4Cl_{sat.aq.}$ (20 mL) and extracted with EtOAc (3×20 mL), dried over $MgSO_4$ and concentrated to dryness under reduced pressure. The crude material was analysed by NMR spectroscopy and showed formation of the desired phosphine **35**, whose NMR data were in accordance with the literature:[460] **^{1}H NMR** (500.13 MHz, $CDCl_3$): δ 7.68–7.60 (m, 3H, *3*), 7.33–7.19 (m, 6H, *4 and 5*), 6.75 (dt, J = 7.7, 2.2 Hz, 3H, *6*). **^{13}C{^{1}H} NMR** (125.76 MHz, $CDCl_3$): δ 136.9 (d, J = 11.8 Hz, *1*), 134.9 (*6*), 133.4 (d, J = 2.7 Hz, *3*), 130.9 (*4*), 130.6 (d, J = 34.1 Hz, *2*), 127.9 (*5*). **^{31}P{^{1}H} NMR** (202.46 MHz, $CDCl_3$): δ −3.40. This material was contaminated with ca. 15% of $Ar_2PH{=}O$, as determined by ^{1}H, ^{31}P NMR spectroscopies (diagnostic coupling constant: $^1J_{P-H}$ = 527 Hz) and HRMS analysis (358.8823 m/z). Moreover, excess 2-bromoiodobenzene was present, too, but the crude material was carried forward as it was and subjected to oxidation: first it was redissolved in THF (50 mL), then 10 mL of H_2O_2 were added (caution: do not concentrate this solution, risk of explosion due to peroxides formation), the solution went moderately hot and, upon cooling, was stirred overnight at rt. The reaction mixture was then diluted with DCM (100 mL) and extracted with aqueous NaOH (2 M, 3×50 mL) to facilitate removal of bis(2-bromophenyl)phosphinic acid formed upon oxidation of bis(2-bromophenyl)phosphine oxide. The organic phases were then combined, dried over $MgSO_4$ and concentrated to dryness under reduced pressure. The resulting crude material was purified by flash column chromatography (50% CyH/EtOAc), finally yielding the desired phosphine oxide **36** as a white solid (R_f = 0.36, 860 mg, 1.67 mmol, 67%), whose characteristic data are reported

here: **^{1}H NMR** (500.13 MHz, $CDCl_3$): δ 7.84–7.74 (m, 3H, *6*), 7.73–7.66 (m, 3H, *3*), 7.45–7.37 (m, 6H, *4 and 5*). **^{13}C{^{1}H} NMR** (125.76 MHz, $CDCl_3$): δ 137.4 (d, J = 10.4 Hz, *6*), 134.9 (d, J = 8.0 Hz, *3*), 133.7 (d, J = 2.6 Hz, *4*), 130.9 (d, J = 112.5 Hz, *1*[461]), 127.2 (d, J = 11.8 Hz, *5*), 126.8 (d, J = 4.5 Hz, *2*). **^{31}P{^{1}H} NMR** (202.46 MHz, $CDCl_3$): δ 31.60. **HRMS** (ESI^+, *m/z*) Calcd. for $C_{18}H_{13}Br_3OP^+$ (M+H): 512.8249. Found: 512.8242. Error: 1.36 ppm. ν_{max} (neat, cm^{-1}): 1575, 1557, 1418, 1251, 1196, 1177, 1131, 1109, 1022, 757, 736, 539. **m.p.** (°C): 235–236.

5,10-[1,2]Benzenodibenzo[*b*,*e*][1,4]phosphabismine 5-oxide (37)

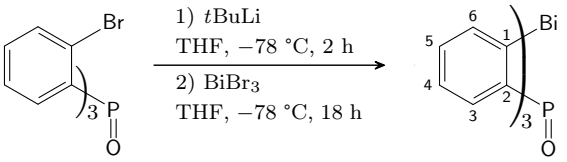

Tri-(2-bromophenyl)-phosphine oxide **36** (772 mg, 1.50 mmol, 1.00 equiv) was dissolved in a Et_2O/THF mixture (15 mL + 3.0 mL). This solution was then cooled down to −78 °C and *t*BuLi (1.7 M solution in pentane, 5.5 mL, 9.2 mmol, 6.2 equiv) was added drop-wise. After 2 h an aliquot was taken, quenched with D_2O, extracted with EtOAc. The organic layer was passed though a $MgSO_4$ plug, then concentrated to dryness and analysed by NMR spectroscopy and HRMS: complete incorporation of deuterium was detected so $BiBr_3$ (673 mg, 1.50 mmol, 1.00 equiv), previously dissolved in THF (3 mL), was added drop-wise to the lithiated species at −78°C. The reaction was allowed to warm to rt overnight then was quenched with water (30 mL) and extracted with EtOAc (3 × 30mL). The organic layers were combined, dried over $MgSO_4$, filtered and concentrated to dryness under reduced pressure. The resulting crude material was recrystallised from CyH/DCM, yielding colourless crystals of the desired bismatriptycene **37** (450 mg, 0.930 mmol, 62%). The resulting crystals were suitable for X-ray diffraction analysis: details can be found in Section 6.8. Characteristic data of this compound were as follows: **^{1}H NMR** (500.13 MHz, $CDCl_3$): δ 8.64 (ddd, J = 10.5, 7.5, 1.4 Hz, 3H, *3*), 8.24 (dd, J = 7.2, 3.2 Hz, 3H, *6*), 7.42 (tdd, J = 7.4, 2.7, 1.2 Hz, 3H, *4*), 7.33 (tt, J = 7.4, 1.4 Hz, 3H, *5*). **^{13}C{^{1}H} NMR** (125.76 MHz, $CDCl_3$): δ 153.0 (*1*), 135.6 (d, J = 11.9 Hz, *6*), 133.0 (d, J = 107.7 Hz, *2*), 132.5 (d, J = 9.7 Hz, *3*), 131.0 (d, J = 2.9 Hz, *5*), 128.9 (d, J = 11.0 Hz, *4*). **^{31}P{^{1}H} NMR** (202.46 MHz, $CDCl_3$): δ 64.60. **HRMS** (ESI^+, *m/z*) Calcd. for $C_{18}H_{13}BiOP^+$ (M+H): 485.0503. Found: 485.0505. Error: 0.41 ppm. ν_{max} (neat, cm^{-1}): 3038, 2957, 2922, 2853, 1731, 1560, 1428, 1281, 1244, 1203, 1130, 1088, 887, 764, 729, 639, 541, 473. **m.p.** (°C): > 300.

Tri(3-fluorophenyl)phosphine oxide (38)

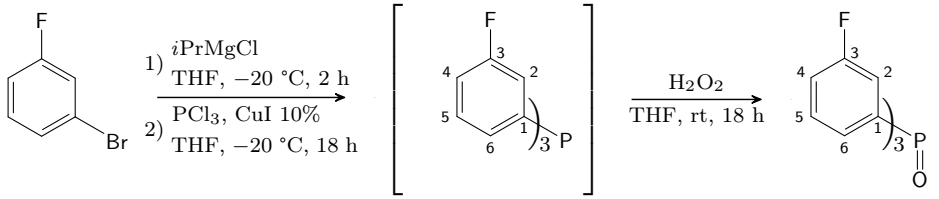

Magnesium turnings (4.00 g, 165 mmol, 3.3 equiv) and a few iodine crystals were loaded in a Schlenk tube, stirred and heated gently under a nitrogen atmosphere until purple vapours developed. THF (150 mL) and 3-bromofluorobenzene (17.3 mL, 27.1 g, 155 mmol, 3.1 equiv) were then added. The suspension was stirred at reflux until no more heat developed, and was allowed to cool down to room temperature over the course of 30 min. In the meanwhile, 6 mL of PCl_3 were heated at reflux for 30 min in a 25 mL round-bottom flask equipped with an air condenser. The acid-free PCl_3 was then transferred into an oven-dried micro-distillation apparatus and distilled under a nitrogen atmosphere. Finally, 4.4 mL (6.9 g, 50 mmol, 1.0 equiv) of the purified reagent was measured in a syringe and added drop-wise to the Grignard solution. Upon completion of the addition, the reaction mixture was allowed to warm up to rt overnight, then was quenched with aqueous $NH_4Cl_{sat.}$ (100 mL) and extracted with Et_2O (3 × 150 mL), dried over $MgSO_4$ and concentrated to dryness under reduced pressure. The resulting sticky yellow material was carried forward as it was and subjected to oxidation: first it was redissolved in THF (200 mL), then 50 mL of H_2O_2 was added, the solution went moderately hot and, upon cooling, was stirred overnight at rt. The reaction mixture was then diluted with DCM (200 mL) and extracted with water (3 × 200 mL). The organic phases were then combined, dried over $MgSO_4$ and concentrated to dryness under reduced pressure. The resulting crude material was recrystallised from CyH/DCM, finally yielding the desired phosphine oxide **38** as colourless crystals (15.4 g, 46.3 mmol, 93%), whose characteristic data are in accordance with the literature.[462] **^{1}H NMR** (500.13 MHz, $CDCl_3$): δ 7.50 (tdd, J = 7.9, 5.1, 3.9 Hz, 3H, *6*), 7.44 (ddt, J = 11.7, 7.6, 1.3 Hz, 3H, *5*), 7.35 (dddd, J = 12.7, 8.3, 2.7, 1.4 Hz, 3H, *2*), 7.29 (dddd, J = 9.3, 8.3, 2.6, 1.1 Hz, 3H, *4*). **^{13}C{^{1}H} NMR** (125.76 MHz, $CDCl_3$): δ 162.6 (dd, J = 251.4, 17.4 Hz, *3*), 133.6 (dd, J = 105.2, 5.6 Hz, *1*), 130.9 (dd, J = 14.4, 7.6 Hz, *6*), 127.8 (dd, J = 9.5, 3.3 Hz, *5*), 119.9 (dd, J = 21.3, 2.7 Hz, *4*), 118.9 (dd, J = 22.6, 11.1 Hz, *2*). **^{19}F NMR** (470.59 MHz, $CDCl_3$): δ −110.08 (tt, J = 8.5, 5.6 Hz). **^{31}P{^{1}H} NMR** (202.46 MHz, $CDCl_3$): δ 27.20. **HRMS** (ESI$^+$, *m/z*) Calcd. for $C_{18}H_{13}F_3OP^+$ (M+H): 333.0651. Found: 333.0656. Error: 1.50 ppm. ν_{max} (neat, cm^{-1}): 3064, 2924, 2849, 1581, 1475, 1423, 1220, 1183, 1102, 895, 879, 790, 605.

Tri(2-(trimethylsilyl)phenyl)phosphine oxide (39a) and phenylbis-(2-(trimethylsilyl)phenyl)phosphine oxide (39b)

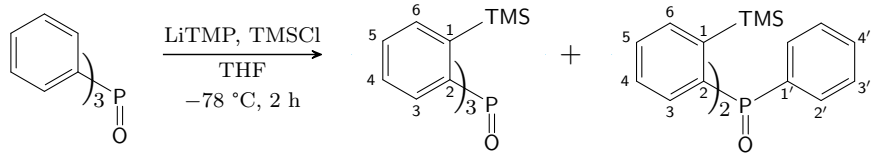

39a **39b**

In a micro-distillation apparatus, 2,2,6,6-tetramethylpiperidine (3 mL) was distilled over CaH_2, then 2.25 mL (1.86 g, 13.2 mmol. 3.30 equiv) were transferred into a 20 mL Schlenk tube and diluted in THF (6.5 mL), then *n*BuLi (2.5 M solution in hexanes, 5.80 mL, 14.5 mmol, 3.63 equiv) was added at −78 °C to this solution, which was then allowed to gradually warm up to room temperature. The solution was stirred at that temperature for 2 h, to allow the excess *n*BuLi to spontaneously decompose.[463] In the meanwhile, TMSCl (3 mL) was distilled to remove trace HCl. In a separate 20 mL Schlenk tube, triphenylphosphine oxide (1.11 g, 4.00 mmol, 1 equiv) was dissolved in THF (6.5 mL) and the solution was cooled down to −78 °C. Then freshly distilled TMSCl (2 mL, 1.74 g, 16.0 mmol, 4.00 equiv) was added, followed by freshly made LiTMP as a THF solution (ca. 2.0 M, 13.2 mmol, 3.3 equiv). The reaction was then stirred cold for 2 h, then allowed to warm up to rt overnight. At that point the reaction was quenched with water (20 mL) and extracted with EtOAc (3 × 20 mL). The organic layers were merged, dried over $MgSO_4$ and concentrated to dryness under vacuum. The resulting crude material was purified by flash column chromatography (30% EtOAc/CyH) allowing the separation of two different fractions. The first (R_f = 0.7) was identified as the desired tri-silylated compound **39a**, isolated as a colourless oil (840 mg, 1.70 mmol, 43%). Its characteristic data are reported below: **^{1}H NMR** (500.13 MHz, $CDCl_3$): δ 7.84 (ddd, J = 7.7, 3.1, 1.3 Hz, 3H, *3*), 7.44 (tdd, J = 7.5, 2.1, 1.3 Hz, 3H, *5*), 7.21 (tdd, J = 7.5, 2.5, 1.3 Hz, 3H, *4*), 6.96 (ddd, J = 13.8, 7.7, 1.4 Hz, 3H, *6*), 0.16 (s, 27H, *TMS*). **^{13}C{^{1}H} NMR** (125.76 MHz, $CDCl_3$): δ 145.6 (d, J = 14.5 Hz, *1*), 141.7 (d, J = 100.6 Hz, *2*), 137.1 (d, J = 14.2 Hz, *3*), 134.0 (d, J = 15.3 Hz, *6*), 130.2 (d, J = 3.2 Hz, *5*), 127.5 (d, J = 13.0 Hz, *4*), 1.3 (*TMS*). **^{31}P{^{1}H} NMR** (202.46 MHz, $CDCl_3$): δ 40.63. **HRMS** (ESI$^+$, *m/z*) Calcd. for $C_{27}H_{40}OPSi_3^+$ (M+H): 495.21191. Found: 495.2119. Error: 0.02 ppm. ν_{max} (neat, cm^{-1}): 2949, 2886, 1421, 1241, 1191, 1118, 1057, 1046, 832, 749, 546, 482. The second fraction (R_f = 0.5) contained the disilylated species **39b**, isolated as a sticky, colourless oil (430 mg, 1.02 mmol, 26%). Its characteristic data are reported here: **^{1}H NMR**

(500.13 MHz, $CDCl_3$): δ 7.86 (ddd, J = 7.7, 3.2, 1.3 Hz, 2H, *6*), 7.54–7.41 (m, 4H, *5, 2′ and 4′*), 7.40 (ddd, J = 8.1, 7.0, 3.0 Hz, 2H, *3′*), 7.23 (tdd, J = 7.5, 2.7, 1.3 Hz, 2H, *4*), 6.94 (ddd, J = 14.1, 7.8, 1.3 Hz, 2H, *3*), 0.22 (s, 18H, *TMS*). **^{31}P{^{1}H} NMR** (202.46 MHz, $CDCl_3$): δ 38.09. **HRMS** (ESI^+, *m/z*) Calcd. for $C_{24}H_{32}OPSi_2^+$ (M+H): 423.1724. Found: 423.1722. Error: 0.47 ppm. ν_{max} (neat, cm^{-1}): 2955, 2898, 1437, 1419, 1239, 1192, 1116, 1051, 834, 772, 749, 543, 473.

Tri(3-fluorophenyl)phosphine oxide, boron trifluoride adduct (40)

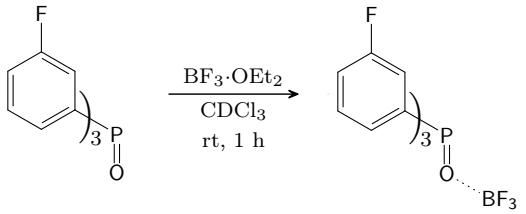

In an NMR tube, phosphine oxide **38** (63 mg, 0.20 mmol, 1.0 equiv) was dissolved in $CDCl_3$ (1.0 mL). Successively, $BF_3{\cdot}OEt_2$ (27 µL, 31 mg, 0.22 mmol, 1.1 equiv) was added and the BF_3 adduct of the phosphine oxide was characterised *in situ* by NMR spectroscopy: **^{1}H NMR** (400.13 MHz, $CDCl_3$): δ 7.62 (tt, J = 7.9, 4.9 Hz, 1H), 7.55–7.37 (m, 3H). **^{13}C{^{1}H} NMR** (100.61 MHz, $CDCl_3$): δ 162.6 (dd, J = 253.3, 19.4 Hz), 131.9 (dd, J = 16.1, 7.7 Hz), 128.9 (dd, J = 11.3, 3.5 Hz), 126.0 (dd, J = 112.6, 6.5 Hz), 122.4 (dd, J = 21.1, 2.8 Hz), 119.8 (dd, J = 23.8, 12.6 Hz). **^{19}F NMR** (376.50 MHz, $CDCl_3$): δ −107.93–−108.23 (m), −143.41 (d, J = 7.6 Hz). **^{31}P{^{1}H} NMR** (161.98 MHz, $CDCl_3$): δ 42.55 – 41.60 (m, J = 7.6 Hz). Crystals suitable for SCXRD analysis were grown by slow evaporation of the solvents over a week. The corresponding report can be found in Section 6.8.

6.8 Crystallographic data

Single crystals were selected, mounted using Fomblin oil on MiTeGen MicroMounts and cooled rapidly to 120(2) K in a stream of cold nitrogen using an Oxford Cryosystems low-temperature device. Data were collected with an Agilent SuperNova diffractometer equipped an Atlas CCD area detector and Cu/Mo microfocus X-ray sources or Agilent SuperNovaII diffractometers equipped either with Atlas S2 or Titan S2 CCD area detectors and copper microfocus X-ray sources. Crystals were kept at 120(2) K during data collection and graphite-monochromated CuKα ($\lambda = 1.54184$ Å) or MoKα ($\lambda = 0.71073$ Å) radiation was used as specified for each case. Absorption corrections were applied using a multiscan method (SADABS). Using Olex2-1.3, crystal structures were solved with the ShelXT[464] structure solution

program using intrinsic phasing and refined with the ShelXL[465] refinement package using least squares minimisation. All non-hydrogen atoms were located using direct methods[466] and difference Fourier syntheses and refined with anisotropic displacement parameters. Hydrogen atoms were constrained in calculated positions and refined with a riding model.

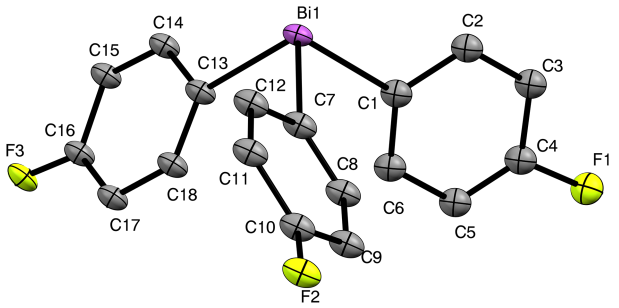

Compound	**2**
Empirical formula	$C_{18}H_{12}F_3Bi$
Formula weight	494.26
Temperature	120(2) K
Crystal system	monoclinic
Space group	$P2_1/c$
a	10.9426(3) Å
b	8.62687(18) Å
c	33.5135(7) Å
α	90°
β	91.704(2)°
γ	90°
Volume	3162.29(12) Å^3
Z	8
ρ_{calc}	2.076 g/cm^3
μ	22.116 mm^{-1}
F(000)	1840.0
Crystal size	0.273 × 0.100 × 0.011 mm^3
Radiation	CuKα ($\lambda = 1.54184$ Å)
2Θ range for data collection	8.084 to 163.000°
Index ranges	$-13 \leq h \leq 13, -11 \leq k \leq 11, -1 \leq l \leq 42$
Reflections collected	6856
Independent reflections	6856 [R_{int} = ?, R_σ = 0.0351]
Data/restraints/parameters	6856/894/398
Goodness-of-fit on F^2	1.044
Final R indexes [$I \geq 2\sigma(I)$]	$R_1 = 0.1897$, $wR_2 = 0.4613$
Final R indexes [all data]	$R_1 = 0.1920$, $wR_2 = 0.4621$
Largest diff. peak/hole	7.87 $e/-11.41$ Å^{-3}

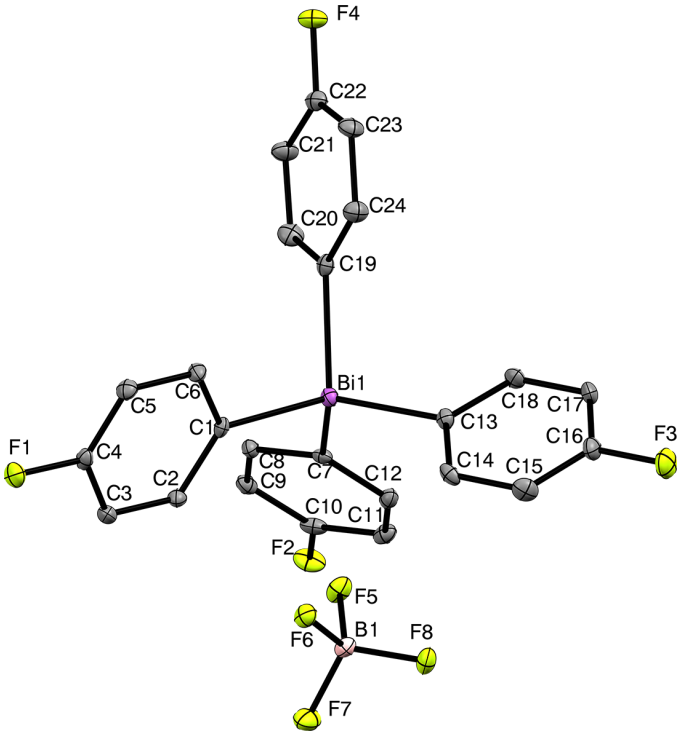

Compound	**5a**
Empirical formula	$C_{24}H_{16}B_3F_8Bi$
Formula weight	676.16
Temperature	120(2) K
Crystal system	orthorhombic
Space group	$P2_12_12_1$
a	10.8168(6) Å
b	14.5260(6) Å
c	14.6217(8) Å
α	90°
β	90°
γ	90°
Volume	2297.4(2) Å^3
Z	4
ρ_{calc}	1.955 g/cm^3
μ	7.749 mm^{-1}
F(000)	1280.0
Crystal size	0.206 × 0.179 × 0.113 mm^3
Radiation	MoKα ($\lambda = 0.71073$ Å)
2Θ range for data collection	6.238 to 61.148°
Index ranges	$-15 \leq h \leq 14, -19 \leq k \leq 20, -19 \leq l \leq 20$
Reflections collected	18652
Independent reflections	6153 [$R_{int} = 0.0382$, $R_\sigma = 0.0474$]
Data/restraints/parameters	6153/0/307
Goodness-of-fit on F^2	1.026
Final R indexes [$I \geq 2\sigma(I)$]	$R_1 = 0.0298$, $wR_2 = 0.0458$
Final R indexes [all data]	$R_1 = 0.0357$, $wR_2 = 0.0476$
Largest diff. peak/hole	0.90 e/ − 1.50 Å^{-3}
Flack parameter	−0.042(4)

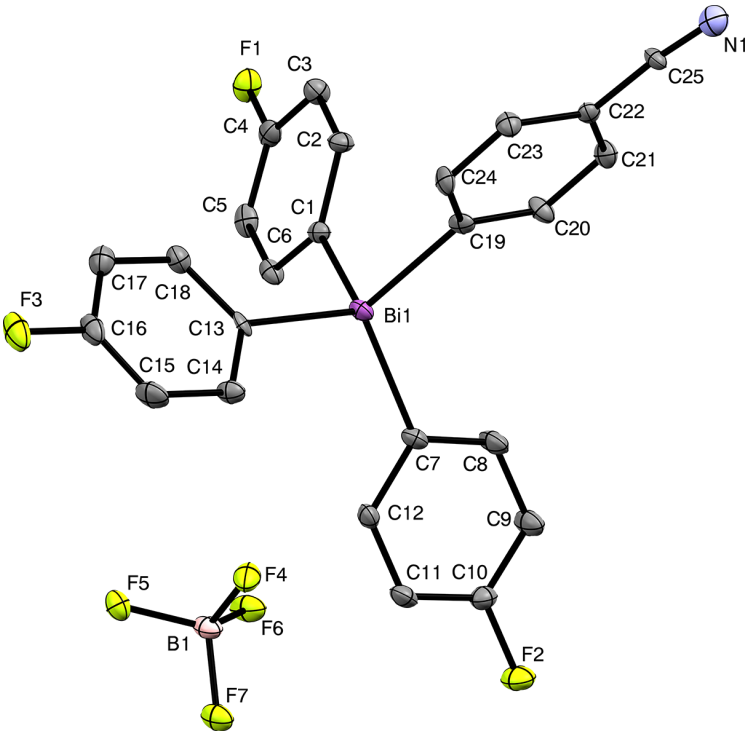

Compound	**5b**
Empirical formula	$C_{25}H_{16}BNF_7Bi$
Formula weight	683.18
Temperature	120(2) K
Crystal system	orthorhombic
Space group	$P2_12_12_1$
a	10.5776(5) Å
b	13.9734(10) Å
c	15.5298(12) Å
α	90°
β	90°
γ	90°
Volume	2295.4(3) Å^3
Z	4
ρ_{calc}	1.977 g/cm^3
µ	7.752 mm^{-1}
F(000)	1296.0
Crystal size	0.378 × 0.089 × 0.040 mm^3
Radiation	MoKα ($\lambda = 0.71073$ Å)
2Θ range for data collection	6.002 to 50.310°
Index ranges	$-12 \leq h \leq 12, -16 \leq k \leq 16, -18 \leq l \leq 18$
Reflections collected	36325
Independent reflections	4114 [$R_{int} = 0.0646$, $R_\sigma = 0.0340$]
Data/restraints/parameters	4114/27/316
Goodness-of-fit on F^2	1.038
Final R indexes [$I \geq 2\sigma(I)$]	$R_1 = 0.0304$, $wR_2 = 0.0598$
Final R indexes [all data]	$R_1 = 0.0331$, $wR_2 = 0.0608$
Largest diff. peak/hole	1.69 e/ − 1.00 Å^{-3}
Flack parameter	−0.036(5)

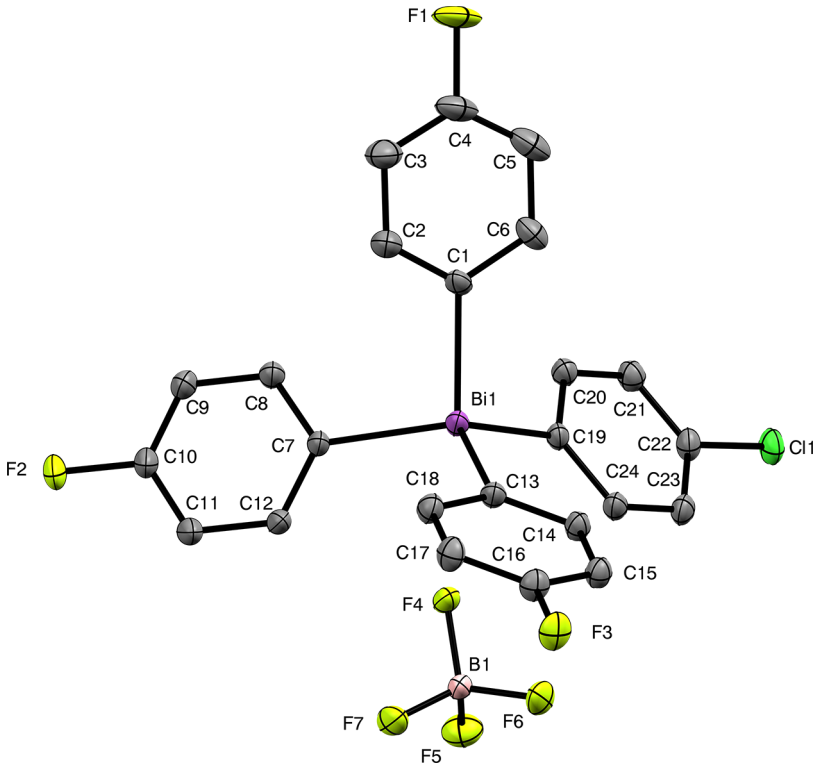

Compound	**5d**
Empirical formula	$C_{24}H_{16}BF_7ClBi$
Formula weight	692.61
Temperature	120(2) K
Crystal system	monoclinic
Space group	$P2_1/n$
a	10.4078(2) Å
b	18.1550(4) Å
c	12.4911(3) Å
α	90°
β	100.627(2)°
γ	90°
Volume	2319.77(9) Å^3
Z	4
ρ_{calc}	1.983 g/cm^3
μ	16.594 mm^{-1}
F(000)	1312.0
Crystal size	0.127 × 0.099 × 0.062 mm^3
Radiation	CuKα (λ = 1.54184 Å)
2Θ range for data collection	8.694 to 147.604°
Index ranges	$-12 \leq h \leq 9, -21 \leq k \leq 22, -11 \leq l \leq 15$
Reflections collected	9995
Independent reflections	4556 [R_{int} = 0.0195, R_σ = 0.0226]
Data/restraints/parameters	4556/919/375
Goodness-of-fit on F^2	1.050
Final R indexes [$I \geq 2\sigma(I)$]	R_1 = 0.0281, wR_2 = 0.0631
Final R indexes [all data]	R_1 = 0.0320, wR_2 = 0.0653
Largest diff. peak/hole	0.74 e/ − 0.97 Å^{-3}

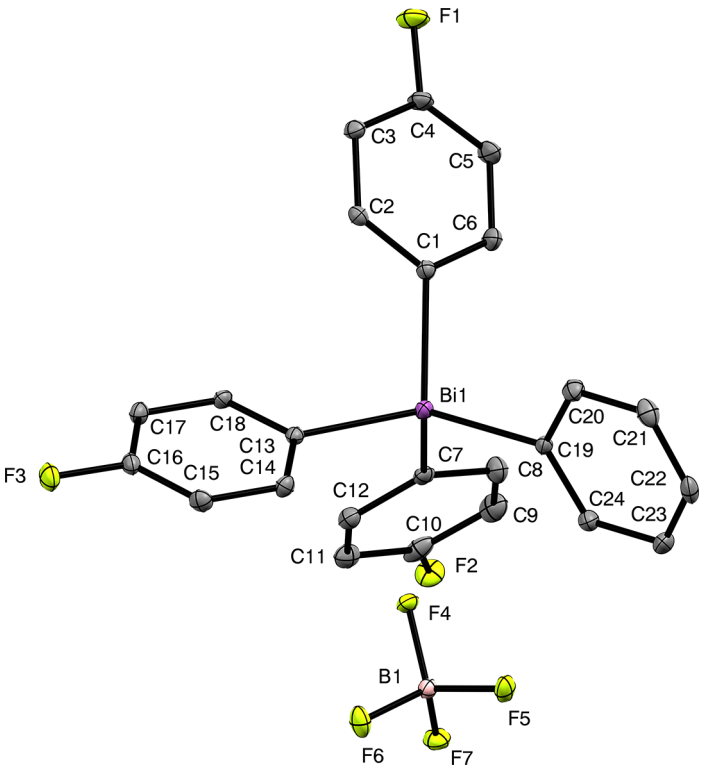

Compound	**5f**
Empirical formula	$C_{24}H_{17}BF_7Bi$
Formula weight	658.16
Temperature	120(2) K
Crystal system	monoclinic
Space group	$P2_1/n$
a	10.4843(3) Å
b	12.6391(4) Å
c	17.6435(5) Å
α	90°
β	104.909(3)°
γ	90°
Volume	2259.27(13) Å^3
Z	4
ρ_{calc}	1.935 g/cm^3
μ	7.870 mm^{-1}
F(000)	1248.0
Crystal size	0.182 × 0.055 × 0.016 mm^3
Radiation	MoKα ($\lambda = 0.71073$ Å)
2Θ range for data collection	5.764 to 61.054°
Index ranges	$-14 \leq h \leq 14, -17 \leq k \leq 17, -25 \leq l \leq 25$
Reflections collected	99791
Independent reflections	6702 [$R_{int} = 0.0686$, $R_\sigma = 0.0394$]
Data/restraints/parameters	6702/1/311
Goodness-of-fit on F^2	1.062
Final R indexes [$I \geq 2\sigma(I)$]	$R_1 = 0.0307$, $wR_2 = 0.0407$
Final R indexes [all data]	$R_1 = 0.0633$, $wR_2 = 0.0487$
Largest diff. peak/hole	1.85 e/ − 1.90 Å^{-3}

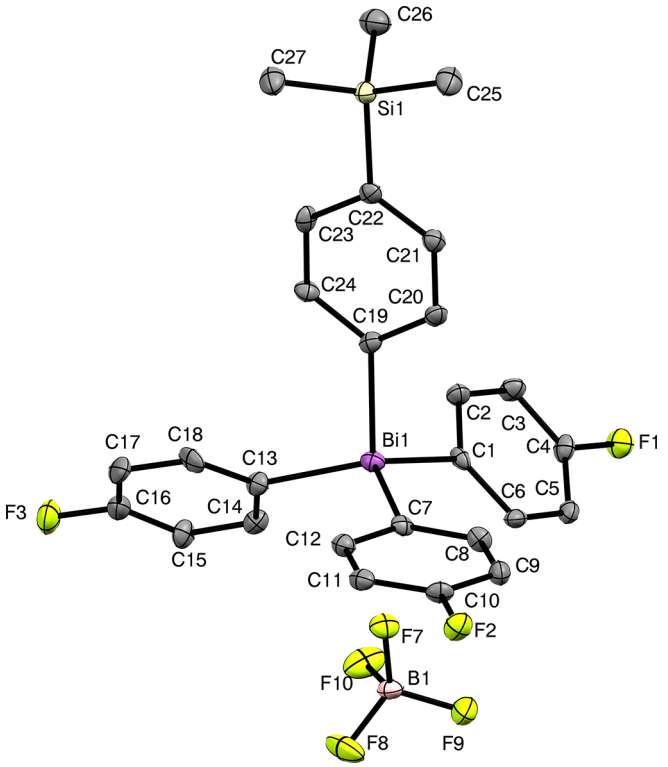

Compound	**5h**
Empirical formula	$C_{27}H_{25}BF_7SiBi$
Formula weight	730.35
Temperature	120(2) K
Crystal system	monoclinic
Space group	$P2_1/c$
a	18.7922(7) Å
b	20.8591(9) Å
c	14.1519(4) Å
α	90°
β	95.614(3)°
γ	90°
Volume	5520.8(4) Å^3
Z	8
ρ_{calc}	1.757 g/cm^3
μ	13.511 mm^{-1}
F(000)	2816.0
Crystal size	0.098 × 0.069 × 0.016 mm^3
Radiation	CuKα ($\lambda = 1.54184$ Å)
2Θ range for data collection	7.574 to 133.202°
Index ranges	$-21 \leq h \leq 22, -19 \leq k \leq 24, -14 \leq l \leq 16$
Reflections collected	31448
Independent reflections	9674 [$R_{int} = 0.1046$, $R_\sigma = 0.1019$]
Data/restraints/parameters	9674/114/704
Goodness-of-fit on F^2	0.981
Final R indexes [$I \geq 2\sigma(I)$]	$R_1 = 0.0571$, $wR_2 = 0.1277$
Final R indexes [all data]	$R_1 = 0.0906$, $wR_2 = 0.1502$
Largest diff. peak/hole	2.09 e/ − 3.30 Å^{-3}

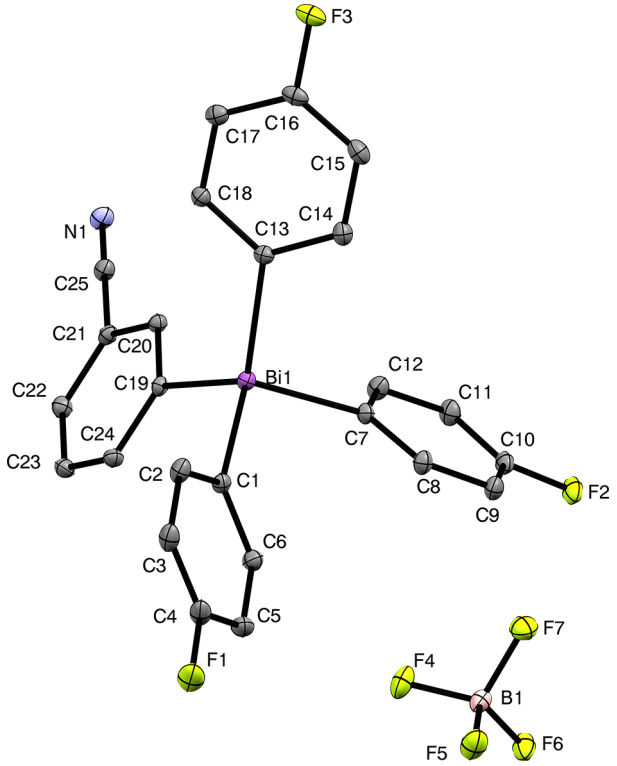

Compound	**5l**
Empirical formula	$C_{25}H_{16}BNF_7Bi$
Formula weight	683.18
Temperature	120(2) K
Crystal system	monoclinic
Space group	P2/c
a	14.3560(4) Å
b	12.4927(2) Å
c	13.1283(2) Å
α	90°
β	97.850(2)°
γ	90°
Volume	2332.43(8) Å^3
Z	4
ρ_{calc}	1.946 g/cm^3
μ	15.479 mm^{-1}
F(000)	1296.0
Crystal size	0.097 × 0.085 × 0.049 mm^3
Radiation	CuKα (λ = 1.54184 Å)
2Θ range for data collection	7.076 to 147.576°
Index ranges	$-17 \leq h \leq 16, -15 \leq k \leq 15, -16 \leq l \leq 16$
Reflections collected	59984
Independent reflections	4730 [R_{int} = 0.0583, R_σ = 0.0195]
Data/restraints/parameters	4730/0/316
Goodness-of-fit on F^2	1.074
Final R indexes [$I \geq 2\sigma(I)$]	R_1 = 0.0228, wR_2 = 0.0605
Final R indexes [all data]	R_1 = 0.0240, wR_2 = 0.0614
Largest diff. peak/hole	0.71 e/ − 1.50 Å^{-3}

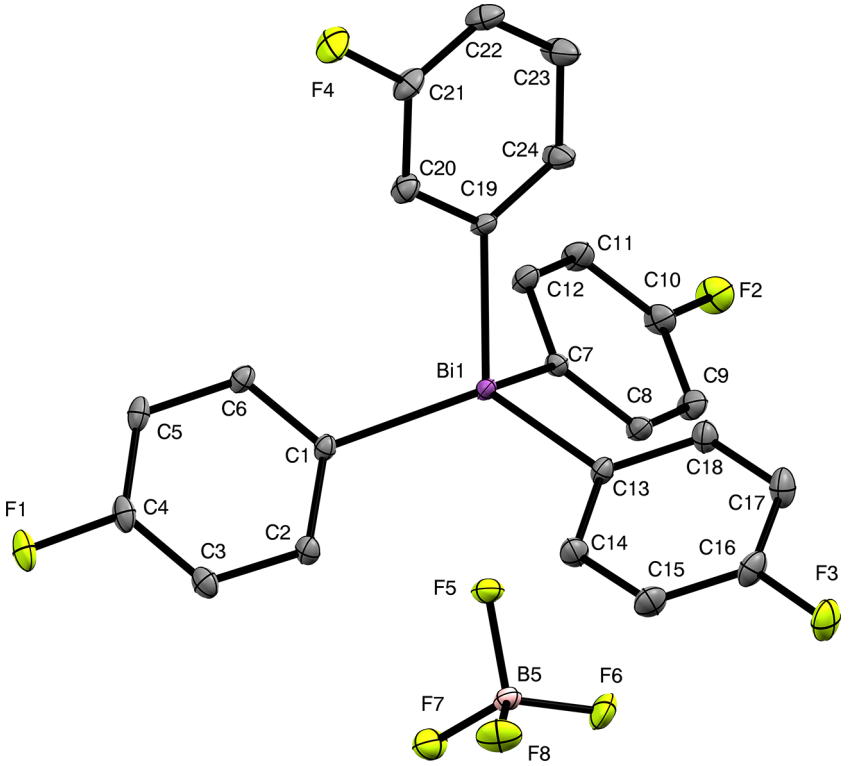

Compound	**5m**
Empirical formula	$C_{24}H_{16}BF_8Bi$
Formula weight	676.16
Temperature	120(2) K
Crystal system	monoclinic
Space group	$P2_1/n$
a	10.30618(15) Å
b	18.0404(2) Å
c	12.14267(18) Å
α	90°
β	99.5208(14)°
γ	90°
Volume	2226.56(5) Å^3
Z	4
ρ_{calc}	2.017 g/cm^3
μ	16.257 mm^{-1}
F(000)	1280.0
Crystal size	0.173 × 0.156 × 0.058 mm^3
Radiation	CuKα ($\lambda = 1.54184$ Å)
2Θ range for data collection	8.864 to 133.148°
Index ranges	$-12 \leq h \leq 11, -21 \leq k \leq 21, -14 \leq l \leq 14$
Reflections collected	29657
Independent reflections	3942 [$R_{int} = 0.0693$, $R_\sigma = 0.0273$]
Data/restraints/parameters	3942/834/375
Goodness-of-fit on F^2	1.030
Final R indexes [$I \geq 2\sigma(I)$]	$R_1 = 0.0302$, $wR_2 = 0.0517$
Final R indexes [all data]	$R_1 = 0.0326$, $wR_2 = 0.0531$
Largest diff. peak/hole	2.15 e/ − 2.07 Å^{-3}

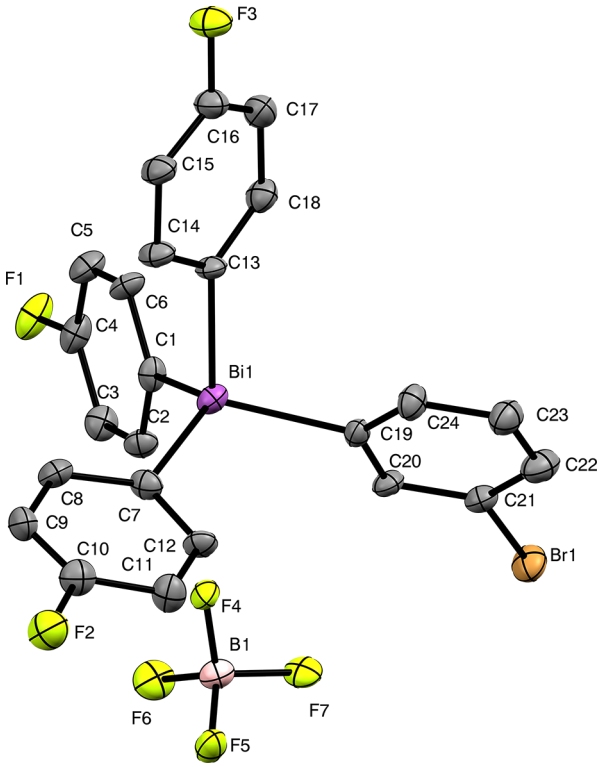

Compound	**5n**
Empirical formula	$C_{24}H_{16}BF_7BrBi$
Formula weight	737.07
Temperature	120(2) K
Crystal system	tetragonal
Space group	$I4_1cd$
a	16.67355(18) Å
b	16.67355(18) Å
c	34.2072(5) Å
α	90°
β	90°
γ	90°
Volume	9509.8(3) Å^3
Z	16
ρ_{calc}	2.059 g/cm^3
μ	17.127 mm^{-1}
F(000)	5536.0
Crystal size	0.122 × 0.095 × 0.057 mm^3
Radiation	CuKα (λ = 1.54184 Å)
2Θ range for data collection	9.11 to 155.75°
Index ranges	$-12 \leq h \leq 20, -21 \leq k \leq 21, -42 \leq l \leq 43$
Reflections collected	30668
Independent reflections	5010 [R_{int} = 0.0787, R_σ = 0.0362]
Data/restraints/parameters	5010/239/344
Goodness-of-fit on F^2	1.134
Final R indexes [$I \geq 2\sigma(I)$]	R_1 = 0.0610, wR_2 = 0.1684
Final R indexes [all data]	R_1 = 0.0645, wR_2 = 0.1729
Largest diff. peak/hole	1.83 e/ − 0.98 Å^{-3}

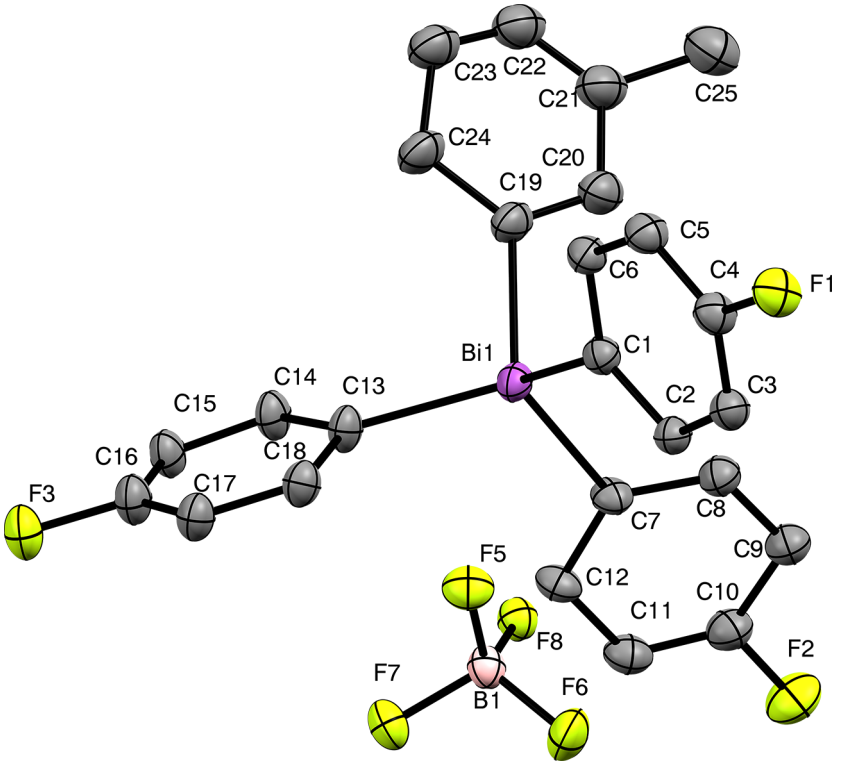

Compound	**5o**
Empirical formula	$C_{25}H_{19}BF_7Bi$
Formula weight	672.19
Temperature	120(2) K
Crystal system	orthorhombic
Space group	$P2_12_12_1$
a	10.7390(4) Å
b	14.6052(5) Å
c	15.2147(7) Å
α	90°
β	90°
γ	90°
Volume	2386.36(16) Å^3
Z	4
ρ_{calc}	1.871 g/cm^3
μ	15.100 mm^{-1}
F(000)	1280.0
Crystal size	0.115 × 0.104 × 0.073 mm^3
Radiation	CuKα (λ = 1.54184 Å)
2Θ range for data collection	8.392 to 148.216°
Index ranges	$-13 \leq h \leq 13, -17 \leq k \leq 17, -18 \leq l \leq 18$
Reflections collected	23689
Independent reflections	4729 [R_{int} = 0.1041, R_σ = 0.0508]
Data/restraints/parameters	4729/589/339
Goodness-of-fit on F^2	1.065
Final R indexes [$I \geq 2\sigma(I)$]	R_1 = 0.0609, wR_2 = 0.1628
Final R indexes [all data]	R_1 = 0.0674, wR_2 = 0.1702
Largest diff. peak/hole	1.19 e/ − 1.66 Å^{-3}

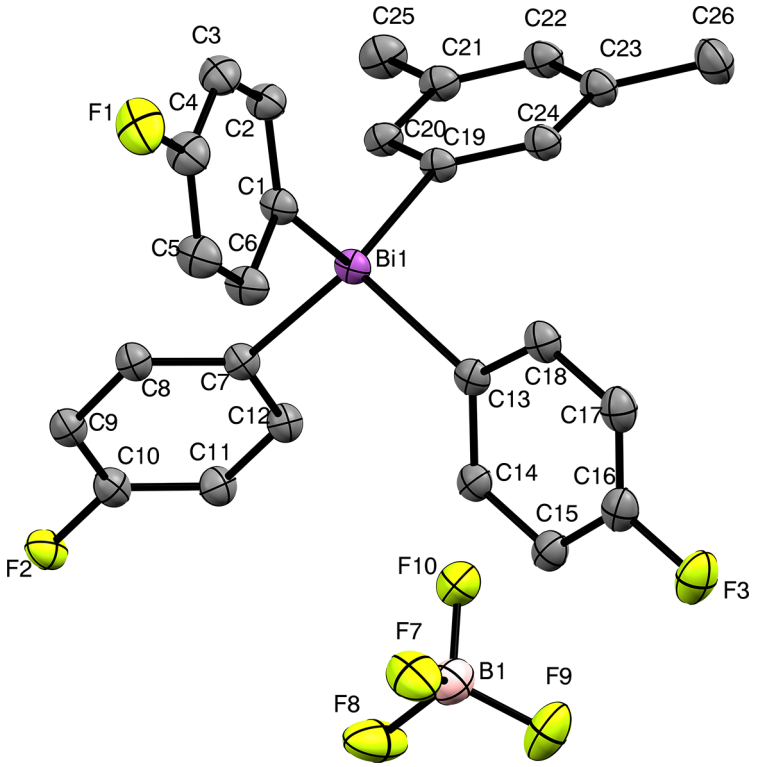

Compound	**5q**
Empirical formula	$C_{26}H_{21}BF_7Bi$
Formula weight	686.22
Temperature	120(2) K
Crystal system	monoclinic
Space group	$P2_1/c$
a	19.4828(5) Å
b	14.5449(3) Å
c	19.8312(5) Å
α	90°
β	118.987(4)°
γ	90°
Volume	4915.7(3) Å^3
Z	8
ρ_{calc}	1.854 g/cm^3
μ	14.676 mm^{-1}
F(000)	2624.0
Crystal size	0.190 × 0.127 × 0.030 mm^3
Radiation	CuKα ($\lambda = 1.54184$ Å)
2Θ range for data collection	7.932 to 133.2°
Index ranges	$-23 \leq h \leq 23, -17 \leq k \leq 17, -23 \leq l \leq 23$
Reflections collected	126192
Independent reflections	8679 [$R_{int} = 0.1379$, $R_\sigma = 0.0367$]
Data/restraints/parameters	8679/1315/692
Goodness-of-fit on F^2	1.065
Final R indexes [$I \geq 2\sigma(I)$]	$R_1 = 0.0896$, $wR_2 = 0.1841$
Final R indexes [all data]	$R_1 = 0.0929$, $wR_2 = 0.1859$
Largest diff. peak/hole	3.03 e/ − 4.48 Å^{-3}

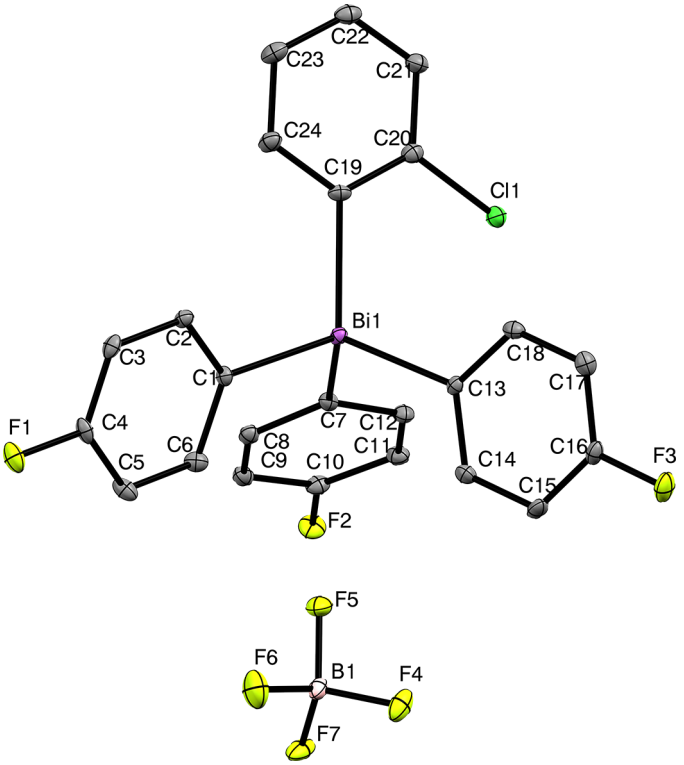

Compound	**5s**
Empirical formula	$C_{24}H_{16}BF_7ClBi$
Formula weight	692.61
Temperature	120(2) K
Crystal system	monoclinic
Space group	$P2_1/n$
a	10.1506(8) Å
b	13.0209(11) Å
c	17.4597(16) Å
α	90°
β	99.507(8)°
γ	90°
Volume	2275.9(3) Å^3
Z	4
ρ_{calc}	2.021 g/cm^3
μ	7.932 mm^{-1}
F(000)	1312.0
Crystal size	0.392 × 0.151 × 0.134 mm^3
Radiation	MoKα ($\lambda = 0.71073$ Å)
2Θ range for data collection	6.258 to 52.738°
Index ranges	$-12 \leq h \leq 12, -16 \leq k \leq 16, -21 \leq l \leq 20$
Reflections collected	14190
Independent reflections	4654 [$R_{int} = 0.0391$, $R_\sigma = 0.0441$]
Data/restraints/parameters	4654/115/316
Goodness-of-fit on F^2	1.050
Final R indexes [$I \geq 2\sigma(I)$]	$R_1 = 0.0321$, $wR_2 = 0.0660$
Final R indexes [all data]	$R_1 = 0.0411$, $wR_2 = 0.0700$
Largest diff. peak/hole	1.46 e/ − 1.98 Å^{-3}

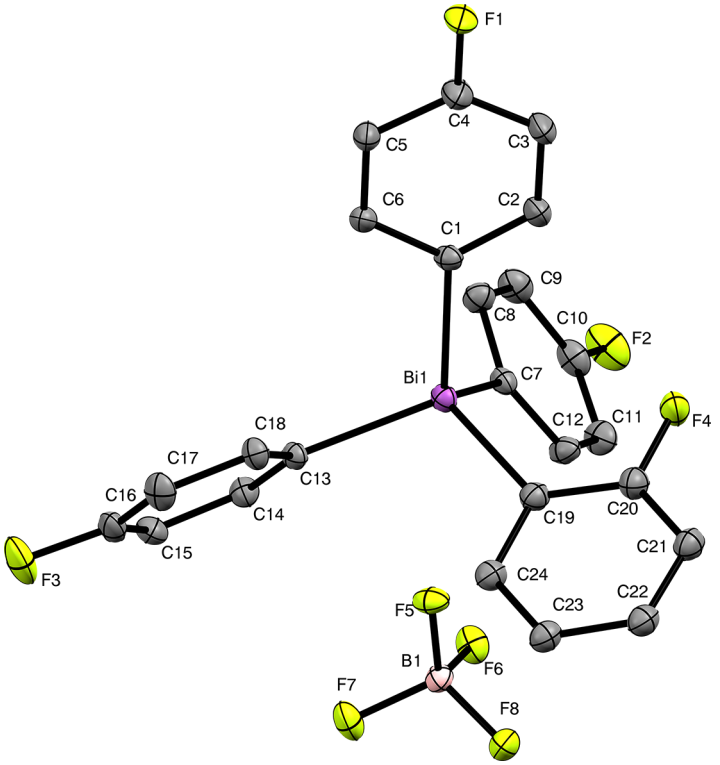

Compound	**5t**
Empirical formula	$C_{24}H_{16}BF_8Bi$
Formula weight	676.16
Temperature	120(2) K
Crystal system	monoclinic
Space group	$P2_1/n$
a	10.5254(3) Å
b	12.7066(4) Å
c	17.7474(5) Å
α	90°
β	104.887(3)°
γ	90°
Volume	2293.92(13) Å^3
Z	4
ρ_{calc}	1.958 g/cm^3
μ	15.780 mm^{-1}
F(000)	1280.0
Crystal size	0.198 × 0.089 × 0.027 mm^3
Radiation	CuKα (λ = 1.54184 Å)
2Θ range for data collection	8.660 to 151.016°
Index ranges	$-13 \leq h \leq 13, -14 \leq k \leq 15, -22 \leq l \leq 22$
Reflections collected	51857
Independent reflections	4699 [R_{int} = 0.1236, R_σ = 0.0406]
Data/restraints/parameters	4699/327/372
Goodness-of-fit on F^2	1.106
Final R indexes [$I \geq 2\sigma(I)$]	R_1 = 0.0498, wR_2 = 0.1373
Final R indexes [all data]	R_1 = 0.0525, wR_2 = 0.1401
Largest diff. peak/hole	4.70 e/ − 3.56 Å^{-3}

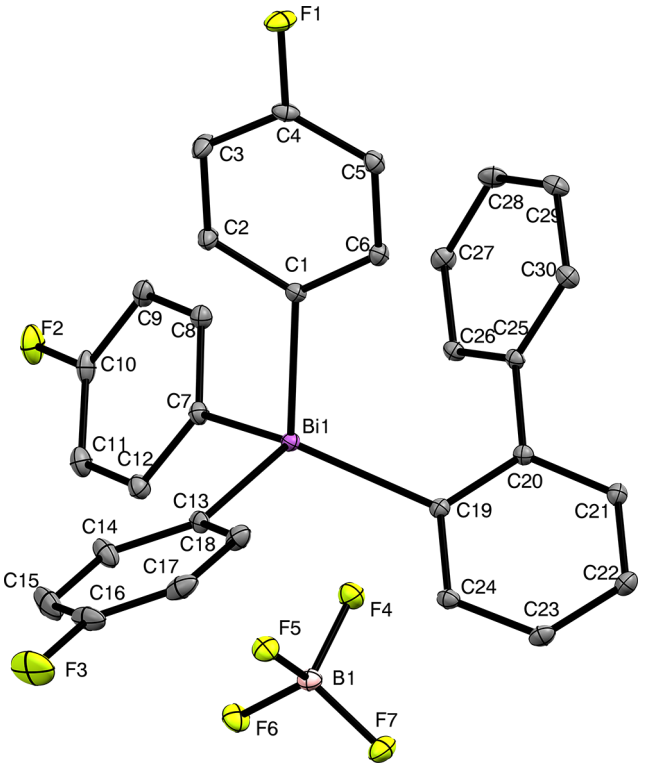

Compound	**5u**
Empirical formula	$C_{30}H_{21}BF_7Bi$
Formula weight	734.26
Temperature	120(2) K
Crystal system	monoclinic
Space group	$P2_1/n$
a	9.30351(16) Å
b	23.2371(4) Å
c	12.5296(2) Å
α	90°
β	100.4488(16)°
γ	90°
Volume	2663.81(8) Å^3
Z	4
ρ_{calc}	1.831 g/cm^3
μ	13.595 mm^{-1}
F(000)	1408.0
Crystal size	0.200 × 0.086 × 0.034 mm^3
Radiation	CuKα ($\lambda = 1.54184$ Å)
2Θ range for data collection	7.610 to 147.468°
Index ranges	$-8 \leq h \leq 11, -25 \leq k \leq 28, -15 \leq l \leq 10$
Reflections collected	10808
Independent reflections	5230 [$R_{int} = 0.0316$, $R_\sigma = 0.0398$]
Data/restraints/parameters	5230/0/352
Goodness-of-fit on F^2	1.047
Final R indexes [$I \geq 2\sigma(I)$]	$R_1 = 0.0277$, $wR_2 = 0.0721$
Final R indexes [all data]	$R_1 = 0.0302$, $wR_2 = 0.0742$
Largest diff. peak/hole	1.09 e/ − 1.58 Å^{-3}

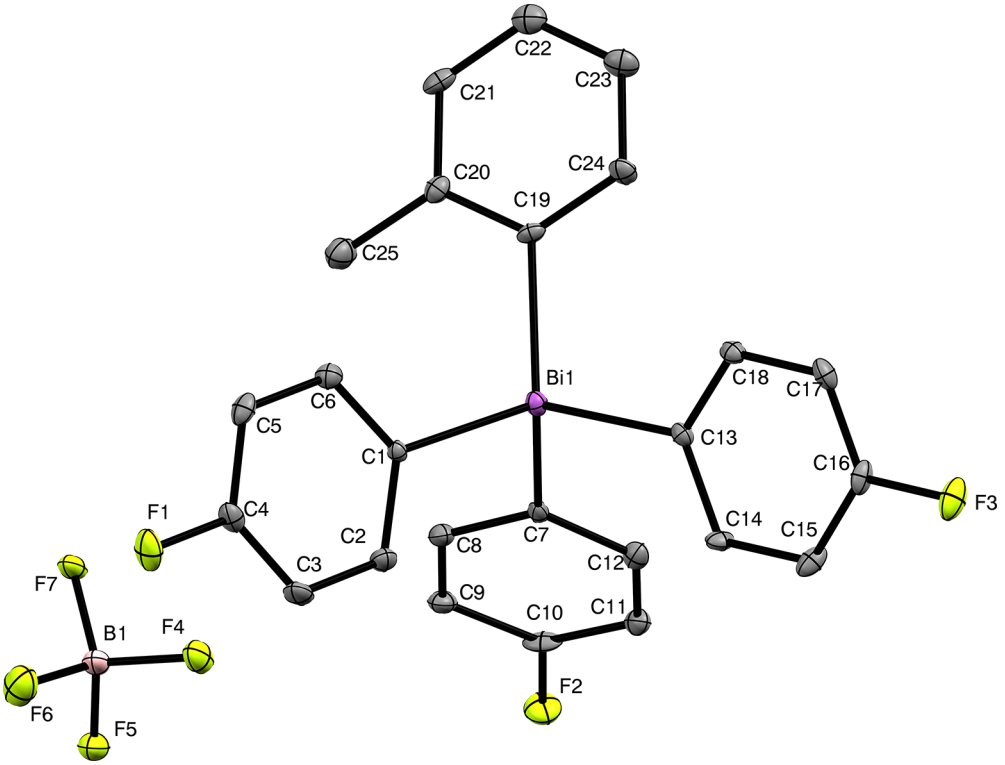

Compound	**5v**
Empirical formula	$C_{25}H_{19}BF_7Bi$
Formula weight	672.19
Temperature	120(2) K
Crystal system	monoclinic
Space group	$P2_1/n$
a	10.1533(7) Å
b	13.1315(10) Å
c	17.3495(12) Å
α	90°
β	98.589(6)°
γ	90°
Volume	2287.2(3) Å^3
Z	4
ρ_{calc}	1.952 g/cm^3
μ	7.776 mm^{-1}
F(000)	1280.0
Crystal size	0.305 × 0.201 × 0.197 mm^3
Radiation	MoKα ($\lambda = 0.71073$ Å)
2Θ range for data collection	6.206 to 50.054°
Index ranges	$-12 \leq h \leq 11, -15 \leq k \leq 15, -18 \leq l \leq 20$
Reflections collected	13148
Independent reflections	4036 [$R_{int} = 0.0345$, $R_\sigma = 0.0334$]
Data/restraints/parameters	4036/236/336
Goodness-of-fit on F^2	1.216
Final R indexes [$I \geq 2\sigma(I)$]	$R_1 = 0.0500$, $wR_2 = 0.1019$
Final R indexes [all data]	$R_1 = 0.0545$, $wR_2 = 0.1035$
Largest diff. peak/hole	3.93 e/ − 3.01 Å^{-3}

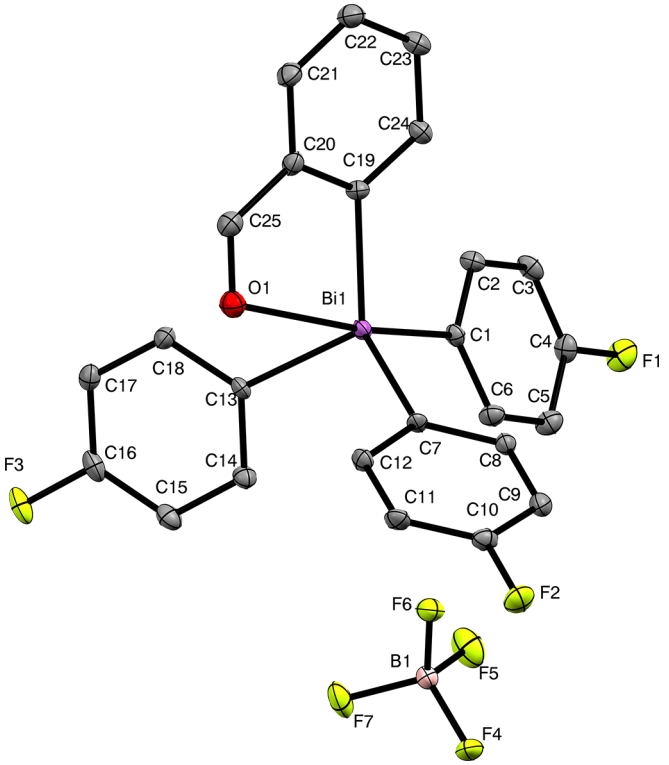

Compound	**5x**
Empirical formula	$C_{25}H_{17}BOF_7Bi$
Formula weight	686.17
Temperature	120(2) K
Crystal system	monoclinic
Space group	$P2_1/n$
a	10.35454(9) Å
b	13.07568(12) Å
c	17.19892(15) Å
α	90°
β	100.5528(9)°
γ	90°
Volume	2289.22(3) Å^3
Z	4
ρ_{calc}	1.991 g/cm^3
μ	15.794 mm^{-1}
F(000)	1304.0
Crystal size	0.139 × 0.074 × 0.021 mm^3
Radiation	CuKα ($\lambda = 1.54184$ Å)
2Θ range for data collection	8.548 to 154.950°
Index ranges	$-7 \leq h \leq 13, -16 \leq k \leq 15, -21 \leq l \leq 21$
Reflections collected	13872
Independent reflections	4719 [$R_{int} = 0.0366$, $R_\sigma = 0.0355$]
Data/restraints/parameters	4719/0/316
Goodness-of-fit on F^2	1.108
Final R indexes [$I \geq 2\sigma(I)$]	$R_1 = 0.0389$, $wR_2 = 0.0984$
Final R indexes [all data]	$R_1 = 0.0411$, $wR_2 = 0.0996$
Largest diff. peak/hole	1.30 e/ − 1.86 Å^{-3}

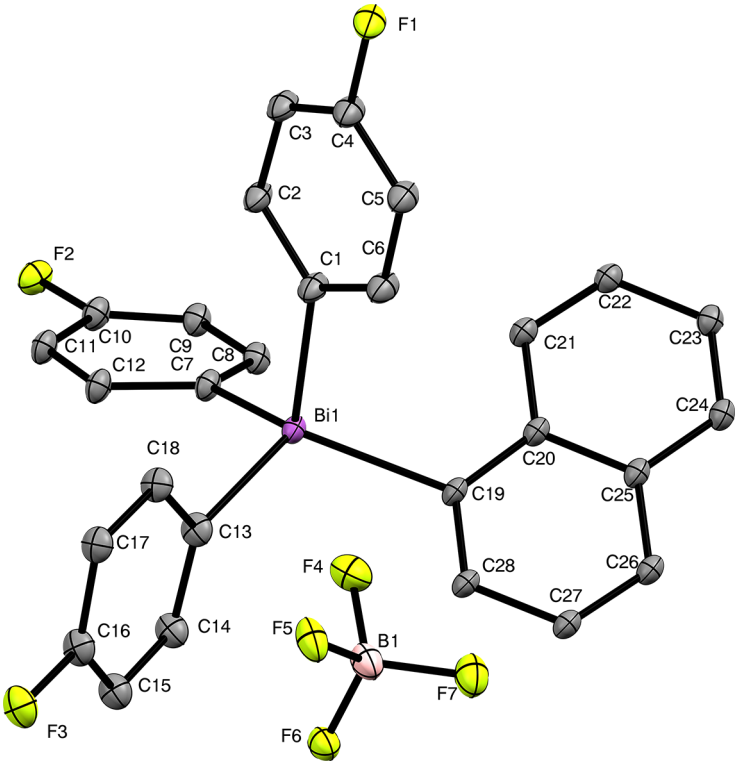

Compound	**5y**
Empirical formula	$C_{28}H_{19}BF_7Bi$
Formula weight	708.22
Temperature	120(2) K
Crystal system	monoclinic
Space group	$P2_1/c$
a	14.48734(18) Å
b	16.8481(2) Å
c	20.5886(3) Å
α	90°
β	94.1077(13)°
γ	90°
Volume	5012.44(12) Å^3
Z	8
ρ_{calc}	1.877 g/cm^3
μ	14.421 mm^{-1}
F(000)	2704.0
Crystal size	0.200 × 0.162 × 0.092 mm^3
Radiation	CuKα (λ = 1.54184 Å)
2Θ range for data collection	6.116 to 149.06°
Index ranges	$-18 \leq h \leq 18, -21 \leq k \leq 21, -2 \leq l \leq 25$
Reflections collected	10093
Independent reflections	10093 [R_{int} = ?, R_σ = 0.0324]
Data/restraints/parameters	10093/999/668
Goodness-of-fit on F^2	1.143
Final R indexes [$I \geq 2\sigma(I)$]	R_1 = 0.1266, wR_2 = 0.3373
Final R indexes [all data]	R_1 = 0.1296, wR_2 = 0.3382
Largest diff. peak/hole	4.70 e/ − 6.47 Å^{-3}

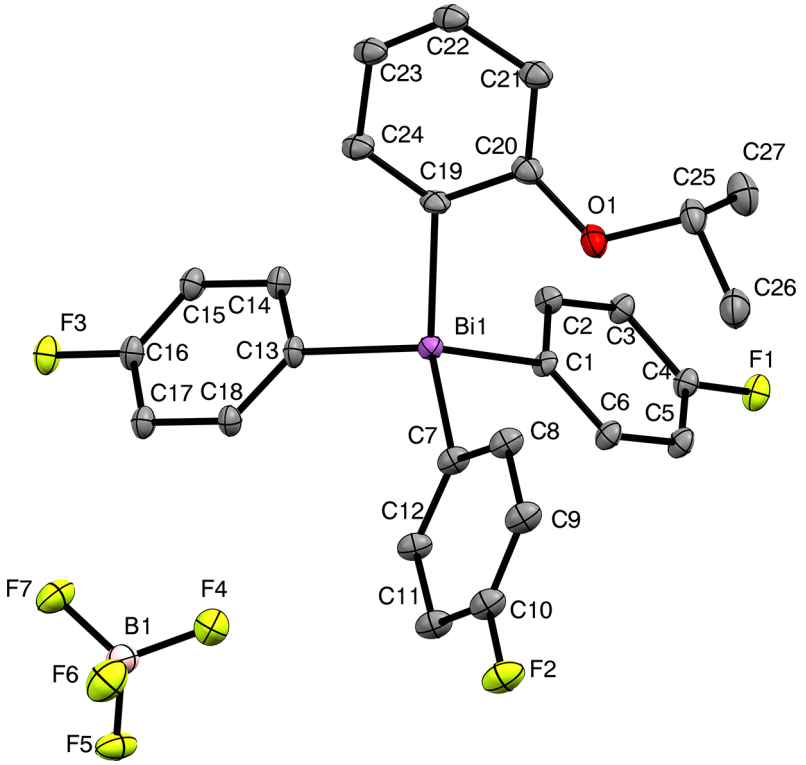

Compound	**5aa**
Empirical formula	$C_{27}H_{23}BOF_7Bi$
Formula weight	716.24
Temperature	120(2) K
Crystal system	orthorhombic
Space group	$P2_12_12_1$
a	9.0853(3) Å
b	10.5162(4) Å
c	27.9908(9) Å
α	90°
β	90°
γ	90°
Volume	2674.32(15) $Å^3$
Z	4
ρ_{calc}	1.779 g/cm^3
μ	13.547 mm^{-1}
F(000)	2624.0
Crystal size	0.229 × 0.182 × 0.024 mm^3
Radiation	CuKα (λ = 1.54184 Å)
2Θ range for data collection	8.982 to 157.82°
Index ranges	$-11 \leq h \leq 11, -11 \leq k \leq 13, -35 \leq l \leq 35$
Reflections collected	18812
Independent reflections	18812 [R_{int} = ?, R_σ = 0.0146]
Data/restraints/parameters	18812/753/339
Goodness-of-fit on F^2	1.740
Final R indexes [$I \geq 2\sigma(I)$]	R_1 = 0.1126, wR_2 = 0.3455
Final R indexes [all data]	R_1 = 0.1141, wR_2 = 0.3488
Largest diff. peak/hole	3.17 $e/-5.73$ $Å^{-3}$

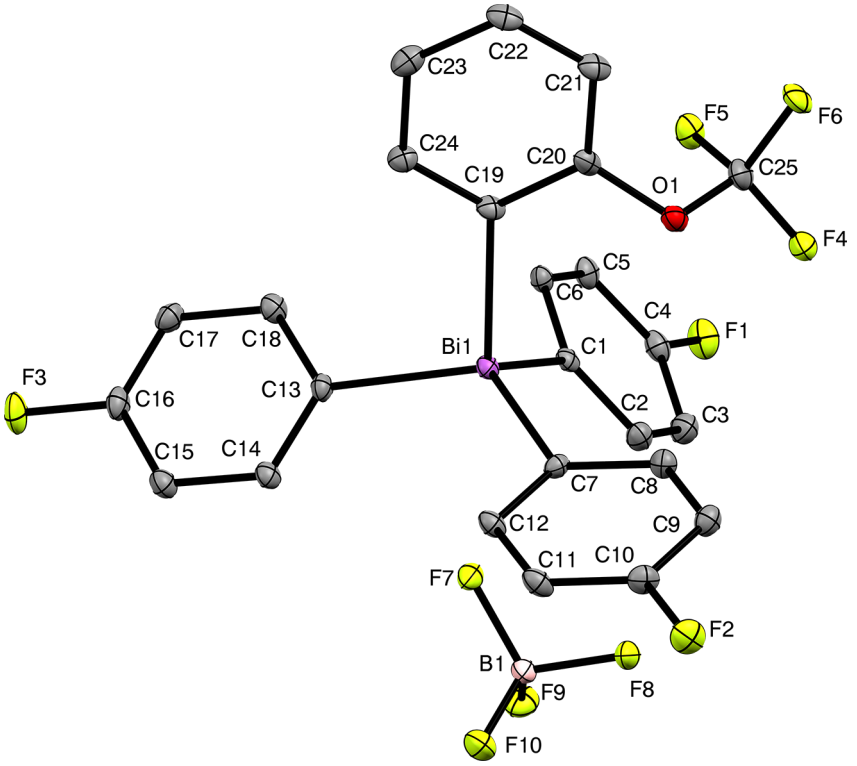

Compound	**5ab**
Empirical formula	$C_{25}H_{16}BOF_{10}Bi$
Formula weight	742.17
Temperature	120(2) K
Crystal system	orthorhombic
Space group	Pbca
a	16.0190(3) Å
b	16.4955(2) Å
c	18.5803(4) Å
α	90°
β	90°
γ	90°
Volume	4909.70(16) Å^3
Z	8
ρ_{calc}	2.008 g/cm^3
μ	14.972 mm^{-1}
F(000)	2816.0
Crystal size	0.434 × 0.094 × 0.023 mm^3
Radiation	CuKα ($\lambda = 1.54184$ Å)
2Θ range for data collection	9.048 to 133.188°
Index ranges	$-18 \leq h \leq 19, -19 \leq k \leq 11, -21 \leq l \leq 22$
Reflections collected	16369
Independent reflections	4321 [$R_{int} = 0.0605$, $R_\sigma = 0.0442$]
Data/restraints/parameters	4321/0/343
Goodness-of-fit on F^2	1.064
Final R indexes [$I \geq 2\sigma(I)$]	$R_1 = 0.0583$, $wR_2 = 0.1653$
Final R indexes [all data]	$R_1 = 0.0634$, $wR_2 = 0.1710$
Largest diff. peak/hole	3.85 e/ − 2.32 Å^{-3}

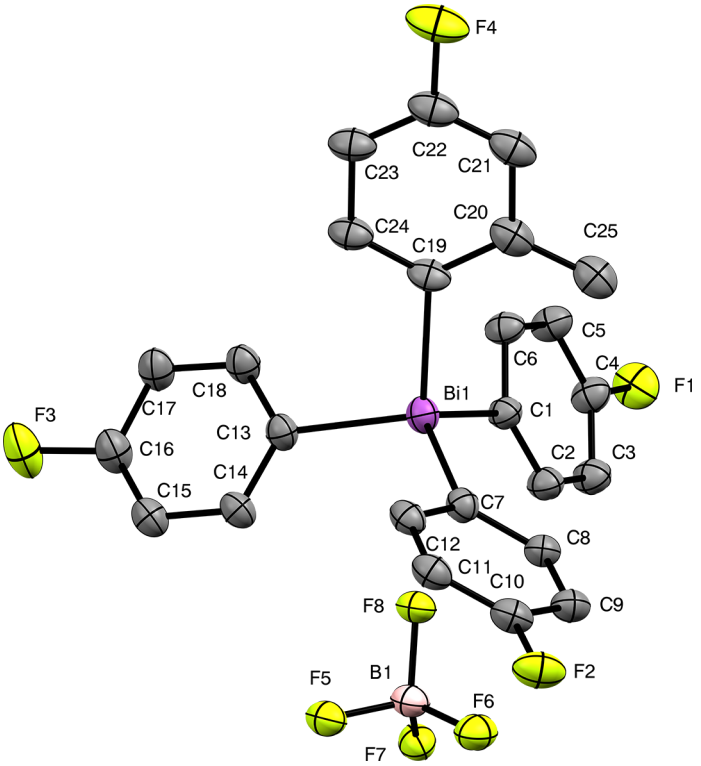

Compound	**5ae**
Empirical formula	$C_{25}H_{18}BF_8Bi$
Formula weight	690.18
Temperature	120(2) K
Crystal system	monoclinic
Space group	$P2_1/c$
a	10.3019(6) Å
b	13.1829(7) Å
c	17.8774(13) Å
α	90°
β	99.583(6)°
γ	90°
Volume	2394.0(3) Å^3
Z	4
ρ_{calc}	1.915 g/cm^3
μ	15.135 mm^{-1}
F(000)	1312.0
Crystal size	0.084 × 0.064 × 0.034 mm^3
Radiation	CuKα (λ = 1.54184 Å)
2Θ range for data collection	8.376 to 157.134°
Index ranges	$-10 \leq h \leq 13, -16 \leq k \leq 16, -22 \leq l \leq 22$
Reflections collected	12915
Independent reflections	4970 [R_{int} = 0.0508, R_σ = 0.0486]
Data/restraints/parameters	4970/474/328
Goodness-of-fit on F^2	1.125
Final R indexes [$I \geq 2\sigma(I)$]	R_1 = 0.0826, wR_2 = 0.2076
Final R indexes [all data]	R_1 = 0.0979, wR_2 = 0.2160
Largest diff. peak/hole	2.38 e/ − 1.32 Å^{-3}

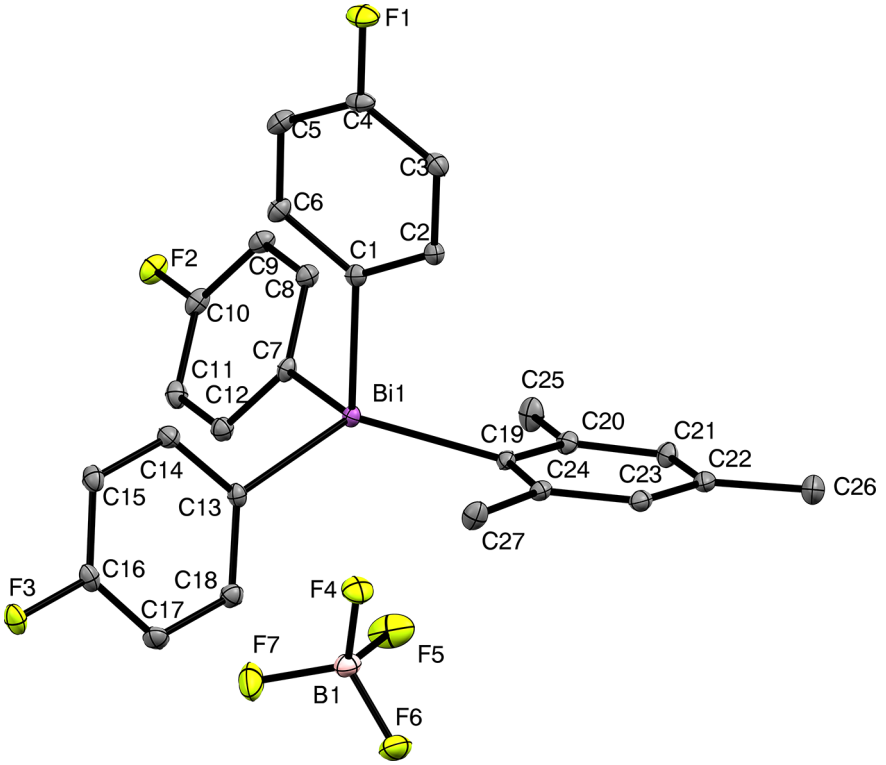

Compound	**5ag**
Empirical formula	$C_{27}H_{23}BF_7Bi$
Formula weight	700.24
Temperature	120(2) K
Crystal system	monoclinic
Space group	$P2_1/n$
a	13.1224(5) Å
b	13.7402(5) Å
c	14.9545(6) Å
α	90°
β	111.267(5)°
γ	90°
Volume	2512.73(18) Å^3
Z	4
ρ_{calc}	1.851 g/cm^3
μ	14.370 mm^{-1}
F(000)	1344.0
Crystal size	0.215 × 0.069 × 0.052 mm^3
Radiation	CuKα (λ = 1.54184 Å)
2Θ range for data collection	7.696 to 148.358°
Index ranges	$-16 \le h \le 16, -17 \le k \le 17, -18 \le l \le 18$
Reflections collected	44415
Independent reflections	5078 [R_{int} = 0.0356, R_σ = 0.0167]
Data/restraints/parameters	5078/171/356
Goodness-of-fit on F^2	1.048
Final R indexes [$I \ge 2\sigma(I)$]	R_1 = 0.0154, wR_2 = 0.0330
Final R indexes [all data]	R_1 = 0.0172, wR_2 = 0.0338
Largest diff. peak/hole	0.55 e/ − 0.51 Å^{-3}

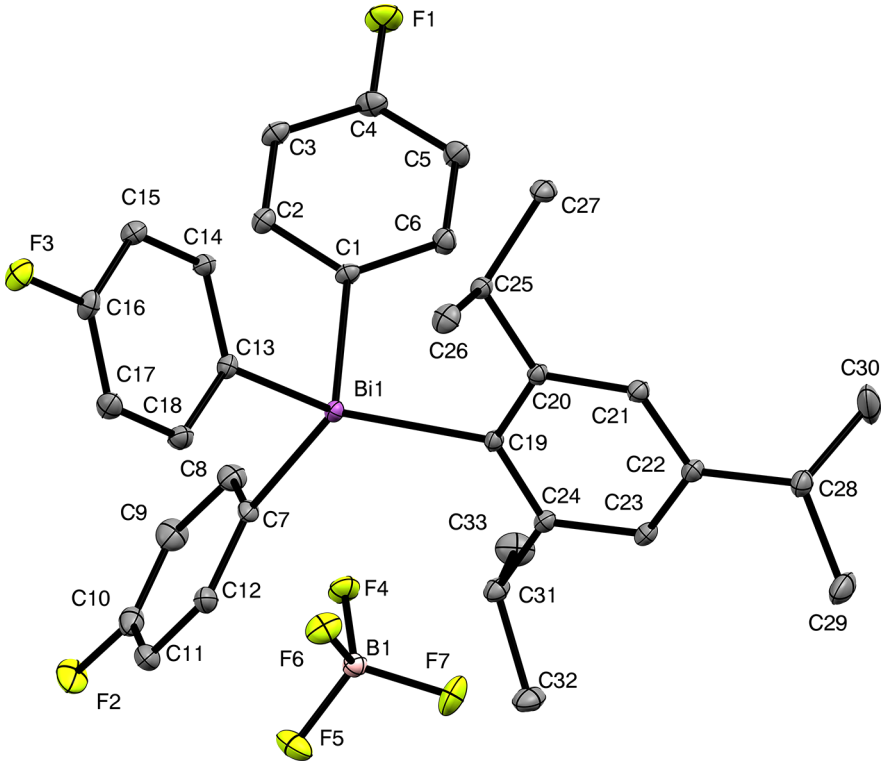

Compound	**5ah**
Empirical formula	$C_{34}H_{36}BF_7Cl_3Bi$
Formula weight	903.77
Temperature	120(2) K
Crystal system	monoclinic
Space group	I2/a
a	19.65030(10) Å
b	12.05730(10) Å
c	31.0618(2) Å
α	90°
β	100.0610(10)°
γ	90°
Volume	7246.29(9) Å^3
Z	8
ρ_{calc}	1.657 g/cm^3
μ	12.103 mm^{-1}
F(000)	3536.0
Crystal size	0.707 × 0.076 × 0.044 mm^3
Radiation	CuKα (λ = 1.54184 Å)
2Θ range for data collection	7.882 to 156.728°
Index ranges	$-24 \leq h \leq 24, -15 \leq k \leq 15, -37 \leq l \leq 38$
Reflections collected	42586
Independent reflections	7608 [R_{int} = 0.0359, R_σ = 0.0194]
Data/restraints/parameters	7608/114/450
Goodness-of-fit on F^2	1.111
Final R indexes [$I \geq 2\sigma(I)$]	R_1 = 0.0236, wR_2 = 0.0658
Final R indexes [all data]	R_1 = 0.0240, wR_2 = 0.0661
Largest diff. peak/hole	0.74 e/ − 0.71 Å^{-3}

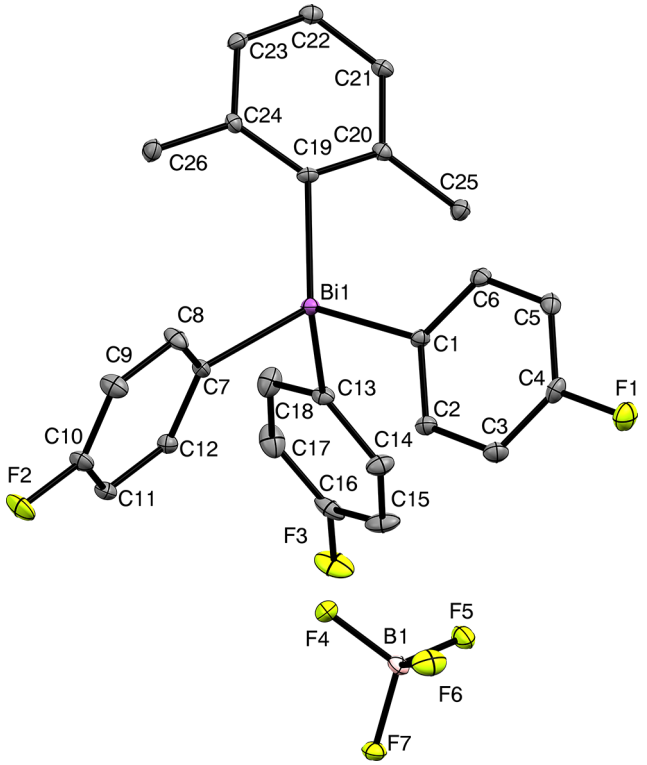

Compound	**5ai**
Empirical formula	$C_{26}H_{21}BF_7Bi$
Formula weight	686.22
Temperature	120(2) K
Crystal system	orthorhombic
Space group	Pbca
a	13.80935(16) Å
b	17.4870(2) Å
c	19.7141(3) Å
α	90°
β	90°
γ	90°
Volume	4760.63(10) Å^3
Z	8
ρ_{calc}	1.915 g/cm^3
μ	15.154 mm^{-1}
F(000)	2624.0
Crystal size	0.138 × 0.097 × 0.052 mm^3
Radiation	CuKα (λ = 1.54184 Å)
2Θ range for data collection	8.972 to 155.978°
Index ranges	$-13 \leq h \leq 17, -20 \leq k \leq 22, -20 \leq l \leq 24$
Reflections collected	15628
Independent reflections	4973 [R_{int} = 0.0225, R_σ = 0.0203]
Data/restraints/parameters	4973/0/318
Goodness-of-fit on F^2	1.119
Final R indexes [$I \geq 2\sigma(I)$]	R_1 = 0.0304, wR_2 = 0.0847
Final R indexes [all data]	R_1 = 0.0322, wR_2 = 0.0859
Largest diff. peak/hole	0.94 e/ − 1.15 Å^{-3}

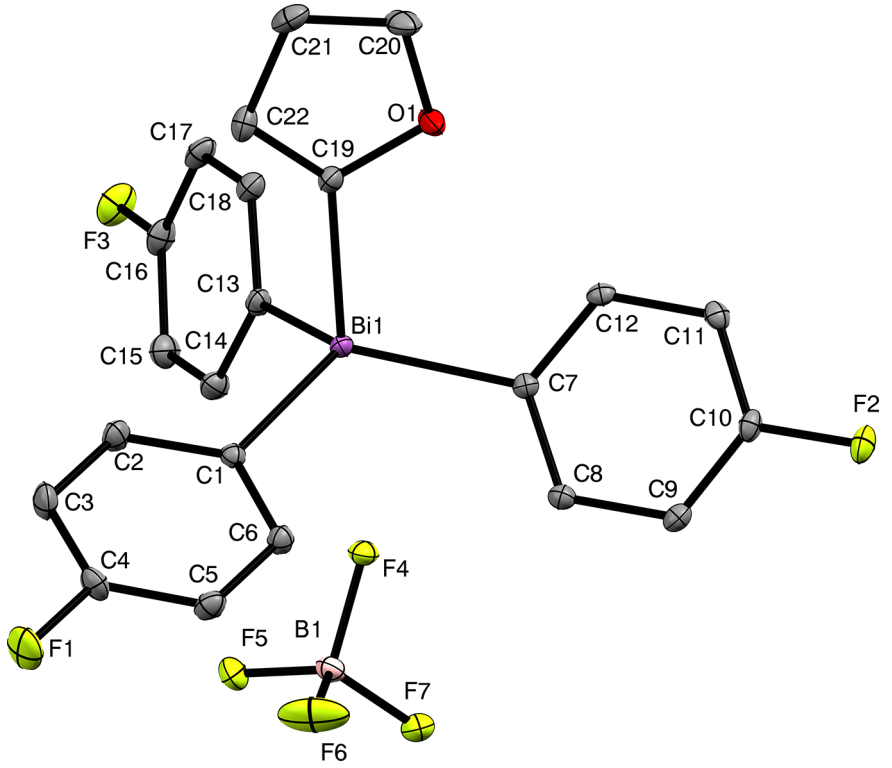

Compound	**5ak**
Empirical formula	$C_{22}H_{15}BOF_7Bi$
Formula weight	648.13
Temperature	120(2) K
Crystal system	monoclinic
Space group	$P2_1/c$
a	9.5084(4) Å
b	15.4720(6) Å
c	15.0628(6) Å
α	90°
β	104.714(4)°
γ	90°
Volume	2143.26(15) Å^3
Z	4
ρ_{calc}	2.009 g/cm^3
μ	8.298 mm^{-1}
F(000)	1224.0
Crystal size	0.262 × 0.038 × 0.032 mm^3
Radiation	MoKα ($\lambda = 0.71073$ Å)
2Θ range for data collection	5.962 to 61.054°
Index ranges	$-13 \leq h \leq 13, -21 \leq k \leq 22, -21 \leq l \leq 21$
Reflections collected	43032
Independent reflections	6077 [$R_{int} = 0.0534$, $R_\sigma = 0.0393$]
Data/restraints/parameters	6077/54/308
Goodness-of-fit on F^2	1.053
Final R indexes [$I \geq 2\sigma(I)$]	$R_1 = 0.0282$, $wR_2 = 0.0468$
Final R indexes [all data]	$R_1 = 0.0469$, $wR_2 = 0.0531$
Largest diff. peak/hole	1.91 e/ − 0.96 Å^{-3}

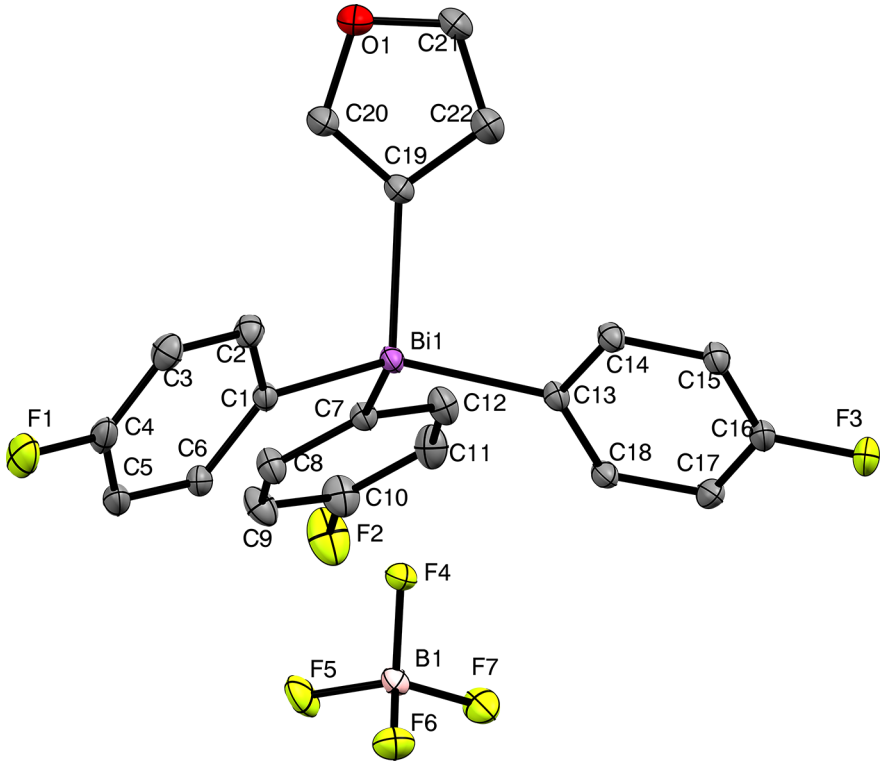

Compound	**5al**
Empirical formula	$C_{22}H_{15}BOF_7Bi$
Formula weight	648.13
Temperature	120(2) K
Crystal system	monoclinic
Space group	$P2_1/n$
a	10.2719(4) Å
b	17.9658(6) Å
c	11.5602(6) Å
α	90°
β	99.168(4)°
γ	90°
Volume	2106.10(15) Å^3
Z	4
ρ_{calc}	2.044 g/cm^3
μ	8.444 mm^{-1}
F(000)	1224.0
Crystal size	0.169 × 0.088 × 0.076 mm^3
Radiation	MoKα ($\lambda = 0.71073$ Å)
2Θ range for data collection	5.772 to 61.042°
Index ranges	$-13 \leq h \leq 14, -25 \leq k \leq 24, -15 \leq l \leq 16$
Reflections collected	47420
Independent reflections	6008 [$R_{int} = 0.0430$, $R_\sigma = 0.0283$]
Data/restraints/parameters	6008/609/374
Goodness-of-fit on F^2	1.070
Final R indexes [$I \geq 2\sigma(I)$]	$R_1 = 0.0329$, $wR_2 = 0.0547$
Final R indexes [all data]	$R_1 = 0.0468$, $wR_2 = 0.0595$
Largest diff. peak/hole	1.99 e/ − 2.20 Å^{-3}

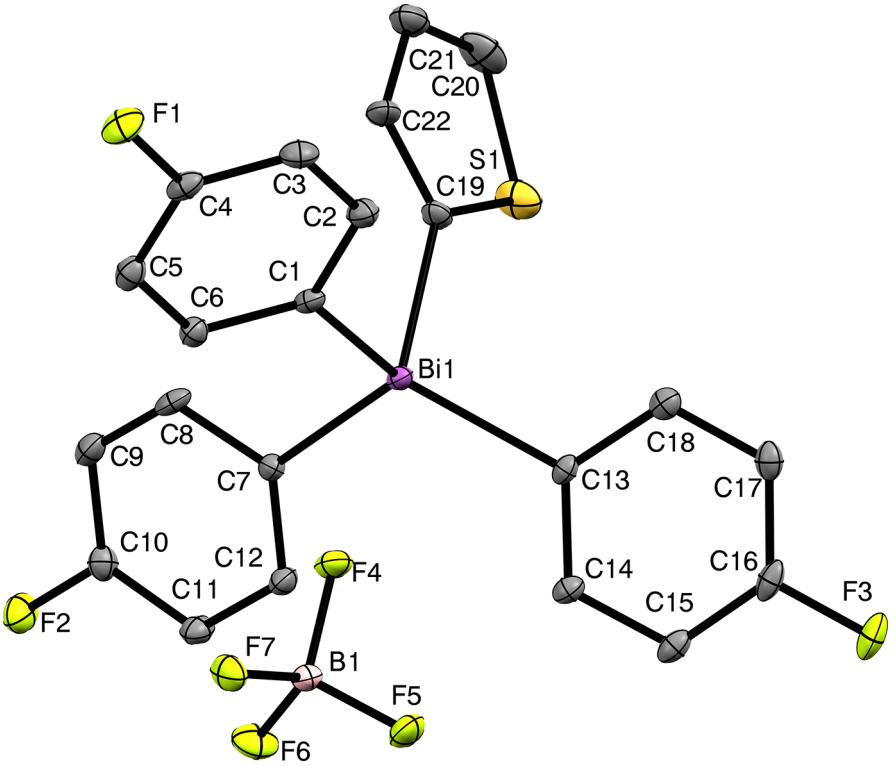

Compound	**5am**
Empirical formula	$C_{22}H_{15}BF_7Bi$
Formula weight	664.19
Temperature	120(2) K
Crystal system	monoclinic
Space group	$P2_1/n$
a	10.3924(4) Å
b	17.5509(6) Å
c	11.8934(4) Å
α	90°
β	97.775(4)°
γ	90°
Volume	2149.36(14) Å^3
Z	4
ρ_{calc}	2.053 g/cm^3
μ	17.640 mm^{-1}
F(000)	1256.0
Crystal size	0.201 × 0.167 × 0.112 mm^3
Radiation	CuKα (λ = 1.54184 Å)
2Θ range for data collection	9.040 to 148.062°
Index ranges	$-12 \leq h \leq 12, -21 \leq k \leq 21, -14 \leq l \leq 14$
Reflections collected	36756
Independent reflections	4333 [R_{int} = 0.0385, R_σ = 0.0171]
Data/restraints/parameters	4333/165/317
Goodness-of-fit on F^2	1.073
Final R indexes [$I \geq 2\sigma(I)$]	R_1 = 0.0201, wR_2 = 0.0490
Final R indexes [all data]	R_1 = 0.0216, wR_2 = 0.0498
Largest diff. peak/hole	1.16 e/ − 1.40 Å^{-3}

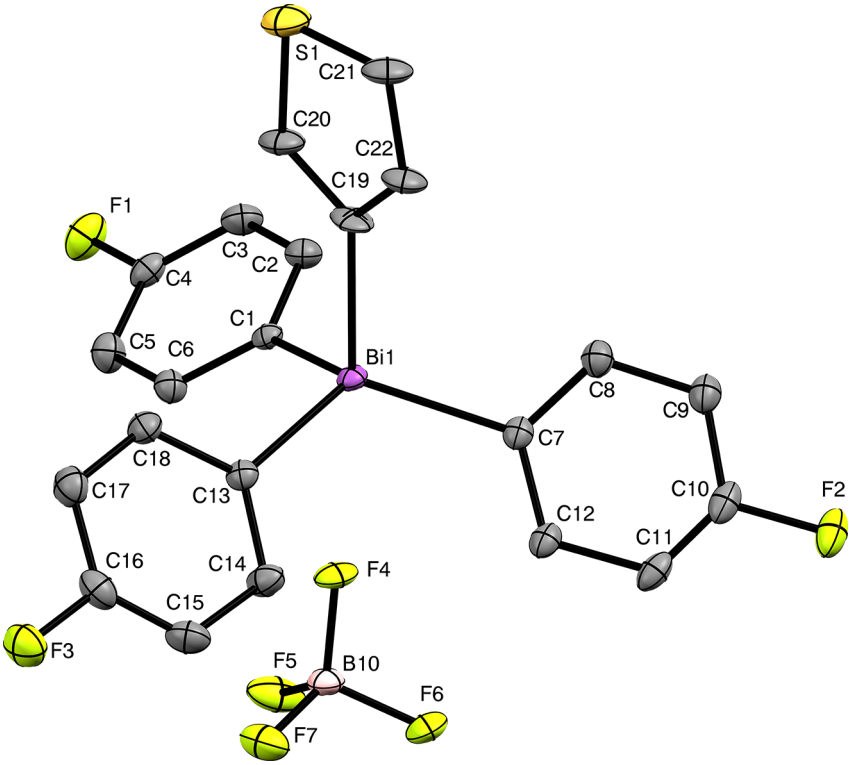

Compound	**5an**
Empirical formula	$C_{22}H_{15}BF_7SBi$
Formula weight	664.19
Temperature	120(2) K
Crystal system	monoclinic
Space group	$P2_1/n$
a	10.3722(3) Å
b	17.6092(4) Å
c	12.0720(3) Å
α	90°
β	97.942(2)°
γ	90°
Volume	2183.74(9) Å^3
Z	4
ρ_{calc}	2.020 g/cm^3
μ	17.362 mm^{-1}
F(000)	1256.0
Crystal size	0.088 × 0.062 × 0.040 mm^3
Radiation	CuKα ($\lambda = 1.54184$ Å)
2Θ range for data collection	8.940 to 148.608°
Index ranges	$-12 \leq h \leq 12, -21 \leq k \leq 21, -14 \leq l \leq 15$
Reflections collected	30657
Independent reflections	4327 [$R_{int} = 0.1005$, $R_\sigma = 0.0446$]
Data/restraints/parameters	4327/766/363
Goodness-of-fit on F^2	1.060
Final R indexes [$I \geq 2\sigma(I)$]	$R_1 = 0.0490$, $wR_2 = 0.1311$
Final R indexes [all data]	$R_1 = 0.0541$, $wR_2 = 0.1369$
Largest diff. peak/hole	1.91 e/ − 2.49 Å^{-3}

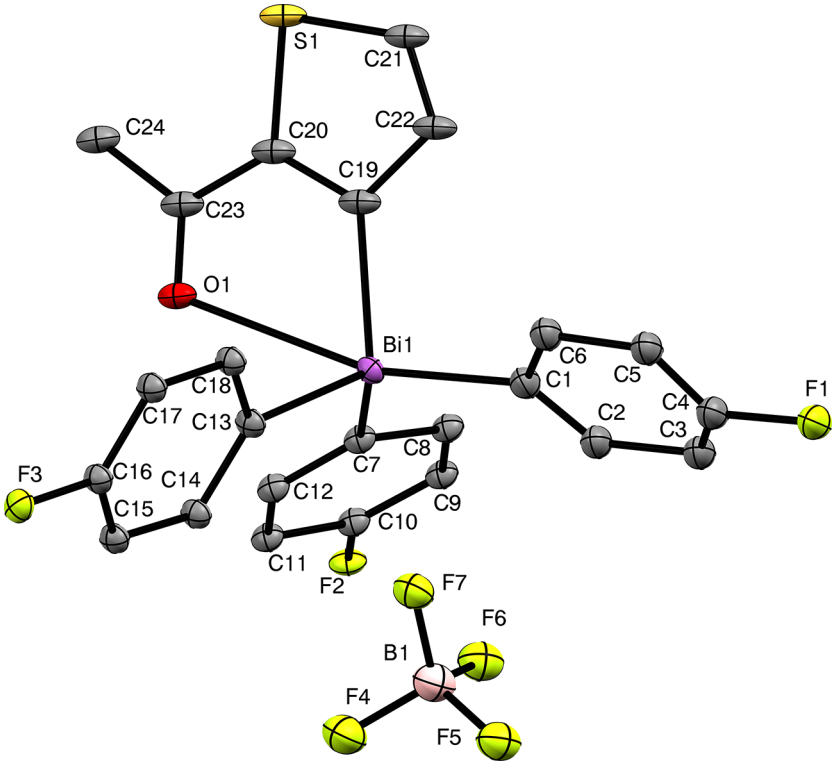

Compound	**5ao**
Empirical formula	$C_{24}H_{17}BOF_7SBi$
Formula weight	706.22
Temperature	120(2) K
Crystal system	monoclinic
Space group	$P2_1/c$
a	9.5668(5) Å
b	22.7564(12) Å
c	11.6025(6) Å
α	90°
β	110.340(5)°
γ	90°
Volume	2368.4(2) $Å^3$
Z	4
ρ_{calc}	1.981 g/cm^3
μ	16.090 mm^{-1}
F(000)	1344.0
Crystal size	0.242 × 0.142 × 0.040 mm^3
Radiation	CuKα ($\lambda = 1.54184$ Å)
2Θ range for data collection	9.01 to 133.202°
Index ranges	$-11 \leq h \leq 11, -27 \leq k \leq 25, -13 \leq l \leq 13$
Reflections collected	38238
Independent reflections	4180 [$R_{int} = 0.0983$, $R_\sigma = 0.0334$]
Data/restraints/parameters	4180/811/317
Goodness-of-fit on F^2	1.260
Final R indexes [$I \geq 2\sigma(I)$]	$R_1 = 0.1257$, $wR_2 = 0.2613$
Final R indexes [all data]	$R_1 = 0.1281$, $wR_2 = 0.2621$
Largest diff. peak/hole	5.62 $e/-3.36$ $Å^{-3}$

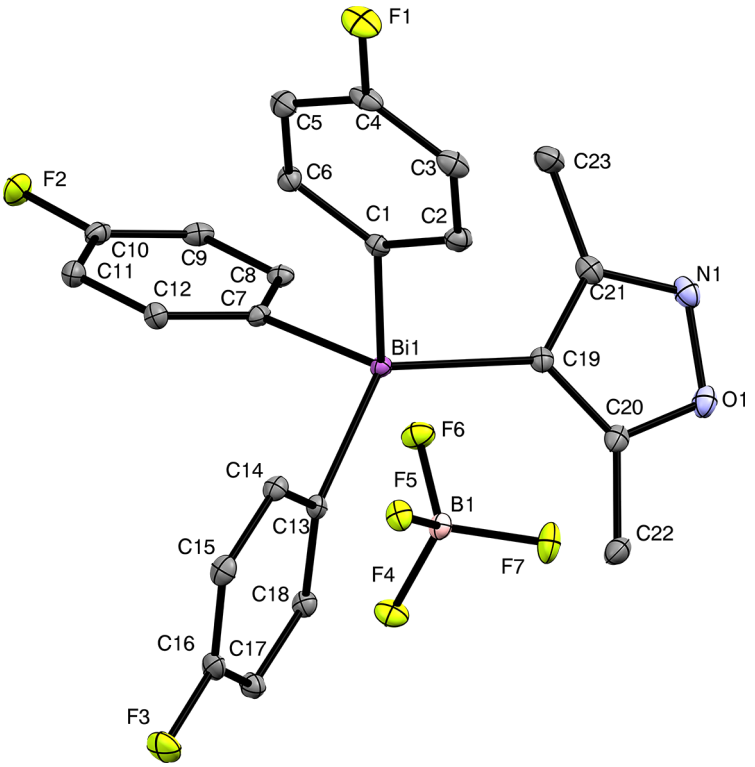

Compound	**5ap**
Empirical formula	$C_{23}H_{18}BNOF_7Bi$
Formula weight	677.17
Temperature	120(2) K
Crystal system	orthorhombic
Space group	Pbca
a	13.4264(3) Å
b	16.7680(4) Å
c	20.0484(5) Å
α	90°
β	90°
γ	90°
Volume	4513.6(2) Å^3
Z	8
ρ_{calc}	1.993 g/cm^3
μ	7.886 mm^{-1}
F(000)	2576.0
Crystal size	0.181 × 0.140 × 0.121 mm^3
Radiation	MoKα ($\lambda = 0.71073$ Å)
2Θ range for data collection	5.624 to 61.176°
Index ranges	$-18 \leq h \leq 19, -23 \leq k \leq 23, -27 \leq l \leq 27$
Reflections collected	101865
Independent reflections	6702 [$R_{int} = 0.0419$, $R_\sigma = 0.0189$]
Data/restraints/parameters	6702/0/310
Goodness-of-fit on F^2	1.019
Final R indexes [$I \geq 2\sigma(I)$]	$R_1 = 0.0203$, $wR_2 = 0.0407$
Final R indexes [all data]	$R_1 = 0.0321$, $wR_2 = 0.0447$
Largest diff. peak/hole	1.72 e/ − 1.19 Å^{-3}

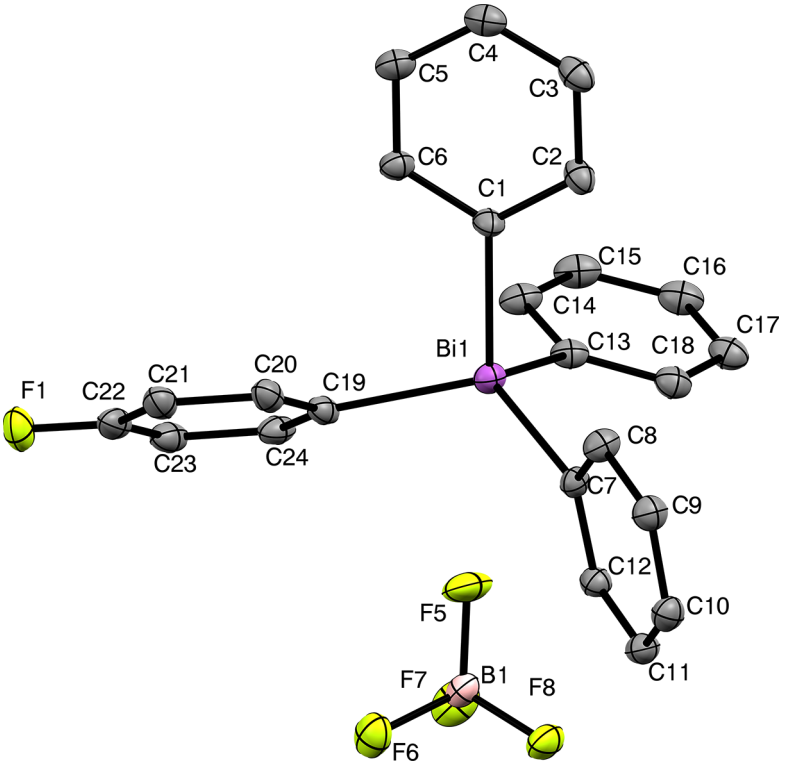

Compound	**5at**
Empirical formula	$C_{24}H_{19}BF_5Bi$
Formula weight	622.18
Temperature	120(2) K
Crystal system	monoclinic
Space group	$P2_1/c$
a	10.2148(5) Å
b	17.9266(7) Å
c	12.6570(6) Å
α	90°
β	111.220(5)°
γ	90°
Volume	2160.56(17) Å^3
Z	4
ρ_{calc}	1.913 g/cm^3
μ	16.478 mm^{-1}
F(000)	1184.0
Crystal size	0.191 × 0.130 × 0.037 mm^3
Radiation	CuKα (λ = 1.54184 Å)
2Θ range for data collection	8.972 to 151.346°
Index ranges	$-12 \leq h \leq 12, -21 \leq k \leq 22, -15 \leq l \leq 15$
Reflections collected	35654
Independent reflections	4404 [R_{int} = 0.0676, R_σ = 0.0273]
Data/restraints/parameters	4404/553/339
Goodness-of-fit on F^2	1.059
Final R indexes [$I \geq 2\sigma(I)$]	R_1 = 0.0419, wR_2 = 0.0956
Final R indexes [all data]	R_1 = 0.0508, wR_2 = 0.1036
Largest diff. peak/hole	1.74 e/ − 1.75 Å^{-3}

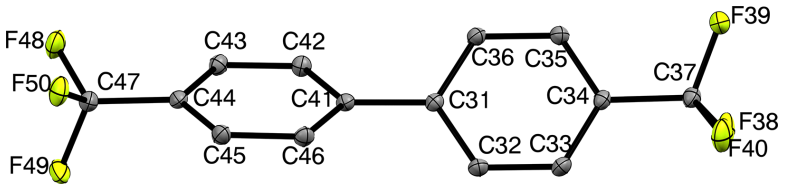

Compound	**9**
Empirical formula	$C_{14}H_8F_6$
Formula weight	290.20
Temperature	120(2) K
Crystal system	orthorombic
Space group	Pbca
a	9.9298(2) Å
b	11.1427(2) Å
c	42.9094(10) Å
α	90°
β	90°
γ	90°
Volume	4747.66(18) Å^3
Z	16
ρ_{calc}	1.624 g/cm^3
μ	0.160 mm^{-1}
F(000)	2336.0
Crystal size	0.1 × 0.05 × 0.05 mm^3
Radiation	MoKα ($\lambda = 0.71073$ Å)
2Θ range for data collection	5.696 to 75.66°
Index ranges	$-16 \leq h \leq 17, -18 \leq k \leq 18, -73 \leq l \leq 65$
Reflections collected	81185
Independent reflections	12326 [$R_{int} = 0.0569$, $R_\sigma = 0.0451$]
Data/restraints/parameters	12326/15/374
Goodness-of-fit on F^2	1.027
Final R indexes [$I \geq 2\sigma(I)$]	$R_1 = 0.0594$, $wR_2 = 0.1411$
Final R indexes [all data]	$R_1 = 0.1161$, $wR_2 = 0.1697$
Largest diff. peak/hole	0.37 e/ − 0.33 Å^{-3}

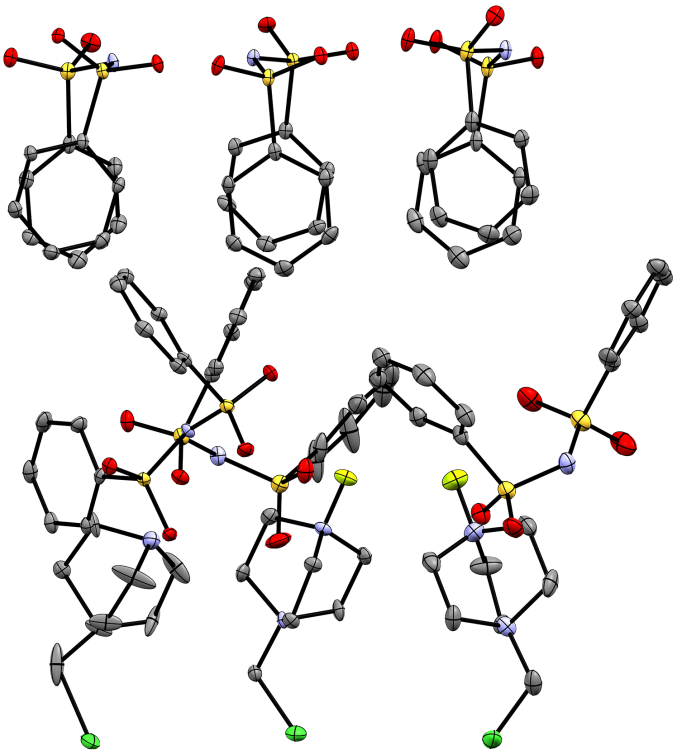

Compound	**13**
Empirical formula	$C_{93}H_{98}Cl_3F_2N_{12}O_{24}S_{12}$
Formula weight	2296.90
Temperature	120(2) K
Crystal system	monoclinic
Space group	$P2_1/c$
a	14.6299(6) Å
b	55.5683(15) Å
c	12.4770(3) Å
α	90°
β	96.172(3)°
γ	90°
Volume	10084.5(6) Å^3
Z	4
ρ_{calc}	1.513 g/cm^3
μ	3.854 mm^{-1}
F(000)	4772.0
Crystal size	0.184 × 0.08 × 0.046 mm^3
Radiation	CuKα ($\lambda = 1.54184$ Å)
2Θ range for data collection	6.860 to 147.828°
Index ranges	$-18 \leq h \leq 17, -68 \leq k \leq 54, -15 \leq l \leq 14$
Reflections collected	43829
Independent reflections	19684 [$R_{int} = 0.0680$, $R_\sigma = 0.0899$]
Data/restraints/parameters	19684/0/1316
Goodness-of-fit on F^2	1.023
Final R indexes [$I \geq 2\sigma(I)$]	$R_1 = 0.1050$, $wR_2 = 0.2591$
Final R indexes [all data]	$R_1 = 0.1416$, $wR_2 = 0.2921$
Largest diff. peak/hole	3.09 e/ − 1.65 Å^{-3}

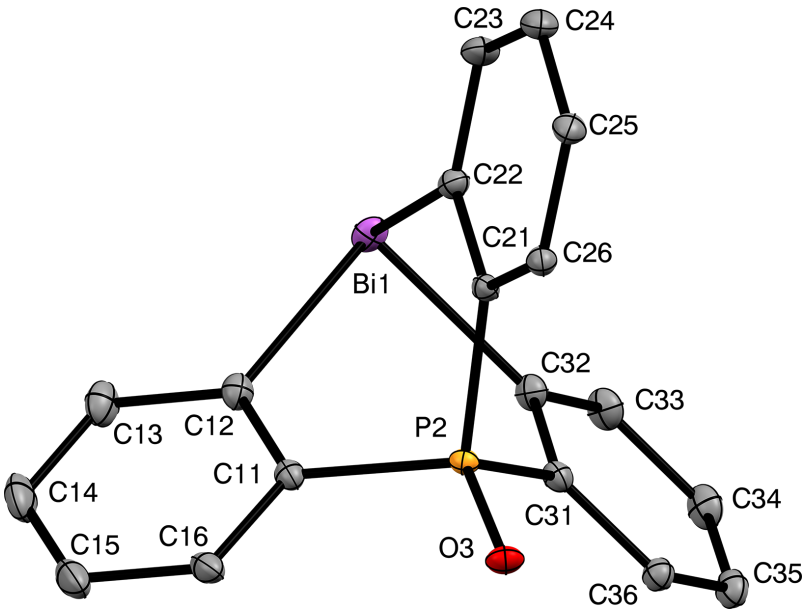

Compound	**37**
Empirical formula	$C_{18}H_{12}BiOP$
Formula weight	484.23
Temperature	120(2) K
Crystal system	monoclinic
Space group	$P2_1/n$
a	8.62100(10) Å
b	8.66760(10) Å
c	20.9128(3) Å
α	90°
β	98.4880(10)°
γ	90°
Volume	1545.56(3) $Å^3$
Z	4
ρ_{calc}	2.081 g/cm^3
μ	11.506 mm^{-1}
F(000)	904.0
Crystal size	0.25 × 0.111 × 0.006 mm^3
Radiation	MoKα ($\lambda = 0.71073$ Å)
2Θ range for data collection	6.132 to 75.614°
Index ranges	$-14 \leq h \leq 14, -14 \leq k \leq 14, -34 \leq l \leq 35$
Reflections collected	57887
Independent reflections	8026 [$R_{int} = 0.0404$, $R_\sigma = 0.0242$]
Data/restraints/parameters	8026/0/190
Goodness-of-fit on F^2	1.064
Final R indexes [$I >= 2\sigma(I)$]	$R_1 = 0.0201$, $wR_2 = 0.0401$
Final R indexes [all data]	$R_1 = 0.0282$, $wR_2 = 0.0425$
Largest diff. peak/hole	0.78 $e/-1.31$ $Å^{-3}$

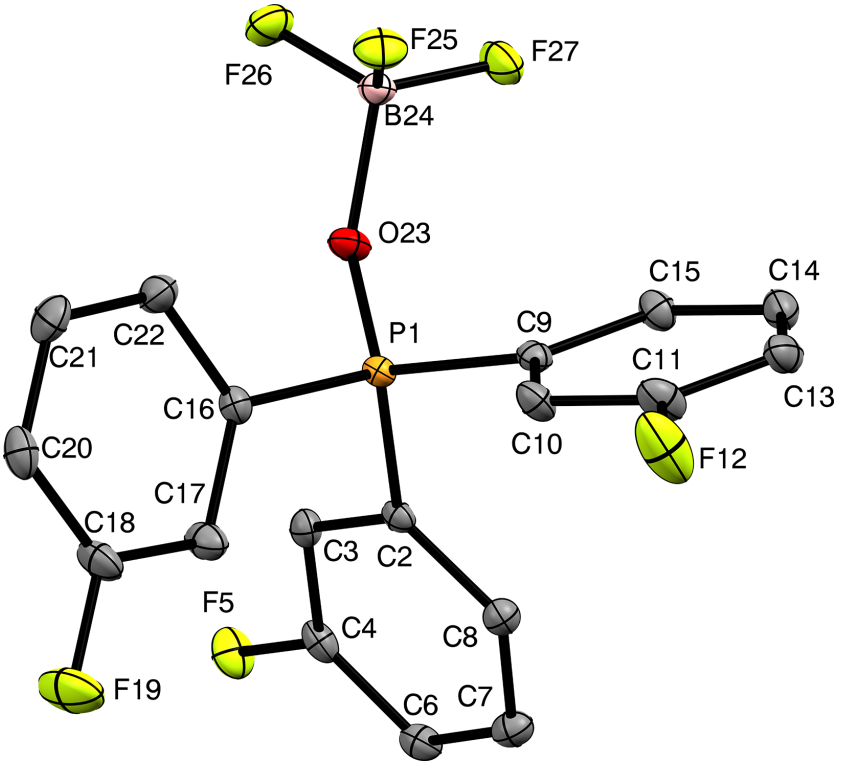

Compound	**40**
Empirical formula	$C_{18}H_{12}BF_6OP$
Formula weight	400.06
Temperature	120(2) K
Crystal system	monoclinic
Space group	$P2_1/n$
a	7.46040(10) Å
b	14.25900(10) Å
c	15.6752(2) Å
α	90°
β	100.1800(10)°
γ	90°
Volume	1641.24(3) $Å^3$
Z	4
ρ_{calc}	1.619 g/cm^3
μ	2.154 mm^{-1}
F(000)	808.0
Crystal size	0.429 × 0.332 × 0.106 mm^3
Radiation	CuKα ($\lambda = 1.54184$ Å)
2Θ range for data collection	8.444 to 144.898°
Index ranges	$-8 \leq h \leq 8, -17 \leq k \leq 17, -19 \leq l \leq 19$
Reflections collected	23186
Independent reflections	3200 [$R_{int} = 0.0285$, $R_\sigma = 0.0151$]
Data/restraints/parameters	3200/0/244
Goodness-of-fit on F^2	1.040
Final R indexes [$I \geq 2\sigma(I)$]	$R_1 = 0.0336$, $wR_2 = 0.0889$
Final R indexes [all data]	$R_1 = 0.0349$, $wR_2 = 0.0899$
Largest diff. peak/hole	0.82 $e/-0.35$ $Å^{-3}$

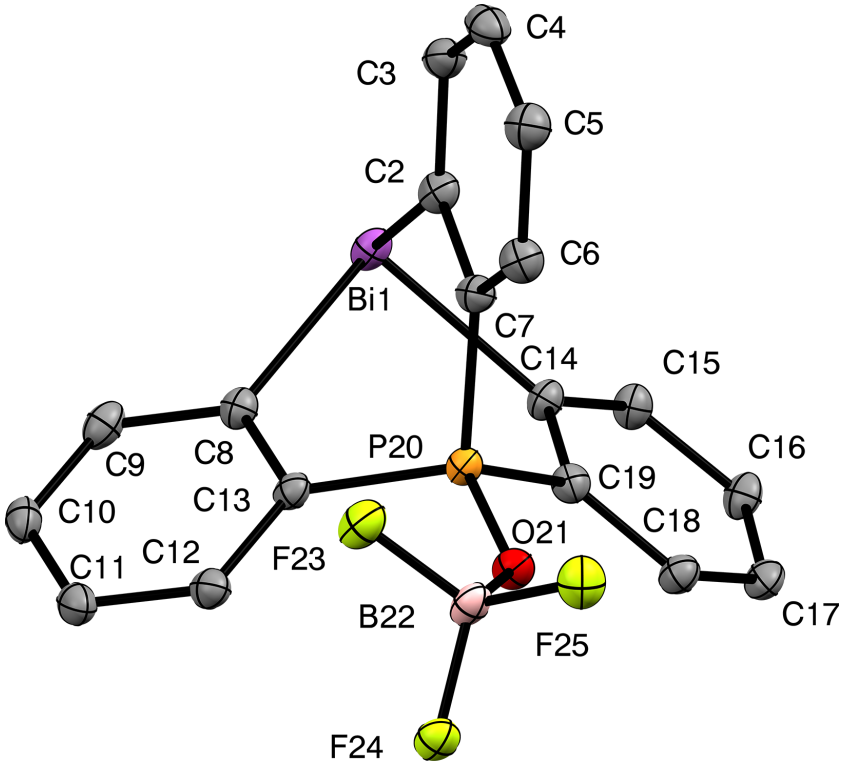

Compound	**41**
Empirical formula	$C_{19}H_{12}BBiCl_3DF_3OP$
Formula weight	672.41
Temperature	120(2) K
Crystal system	monoclinic
Space group	$P2_1/c$
a	8.98348(5) Å
b	14.54847(7) Å
c	32.5221(2) Å
α	90°
β	97.2703(5)°
γ	90°
Volume	4216.33(4) Å^3
Z	8
ρ_{calc}	2.119 g/cm^3
μ	20.958 mm^{-1}
F(000)	2528.0
Crystal size	0.216 × 0.135 × 0.097 mm^3
Radiation	CuKα ($\lambda = 1.54184$ Å)
2Θ range for data collection	6.664 to 151.126°
Index ranges	$-11 \leq h \leq 11, -18 \leq k \leq 18, -40 \leq l \leq 37$
Reflections collected	293461
Independent reflections	8676 [$R_{int} = 0.1260$, $R_\sigma = 0.0257$]
Data/restraints/parameters	8676/0/523
Goodness-of-fit on F^2	1.078
Final R indexes [$I \geq 2\sigma(I)$]	$R_1 = 0.0430$, $wR_2 = 0.1139$
Final R indexes [all data]	$R_1 = 0.0449$, $wR_2 = 0.1152$
Largest diff. peak/hole	2.59 e/ − 1.15 Å^{-3}

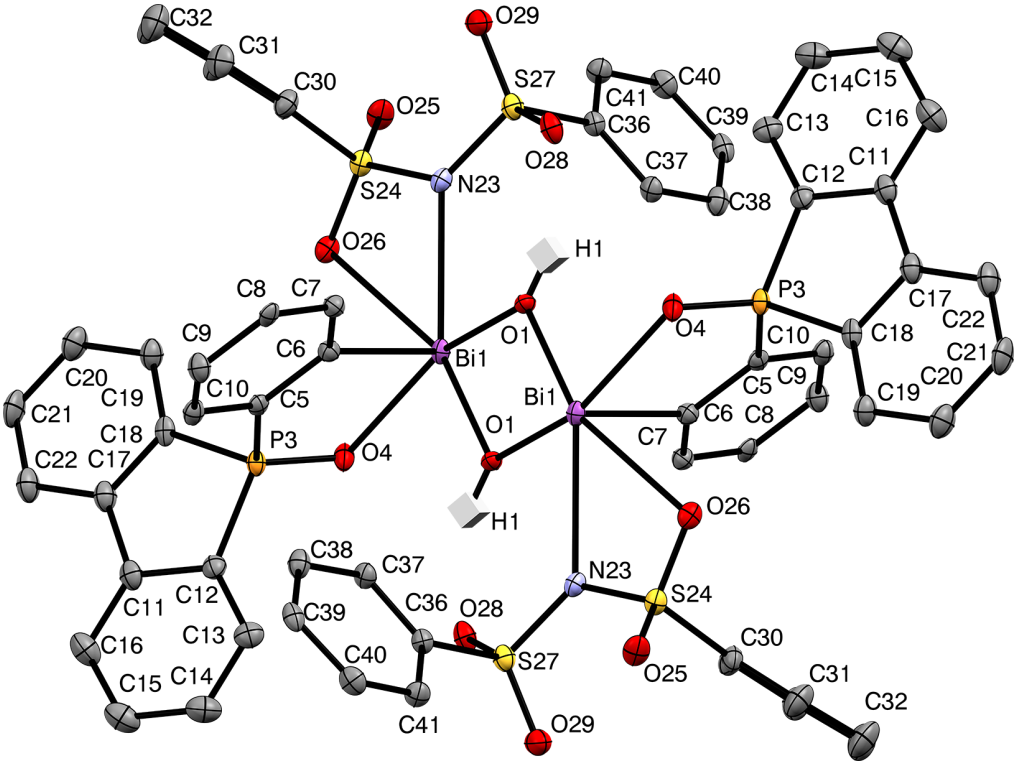

Compound	**42**
Empirical formula	$C_{62}H_{46}Bi_2Cl_6N_2O_{12}P_2S_4$
Formula weight	1850.85
Temperature	120(2) K
Crystal system	triclinic
Space group	P-1
a	8.1415(4) Å
b	14.5171(9) Å
c	14.9136(8) Å
α	105.491(5)°
β	105.835(5)°
γ	95.468(5)°
Volume	1607.05(16) $Å^3$
Z	1
ρ_{calc}	1.912 g/cm^3
μ	15.115 mm^{-1}
F(000)	899.0
Crystal size	0.118 × 0.027 × 0.023 mm^3
Radiation	CuKα ($\lambda = 1.54184$ Å)
2Θ range for data collection	6.424 to 125.308°
Index ranges	$-9 \leq h \leq 8, -16 \leq k \leq 16, -17 \leq l \leq 17$
Reflections collected	5025
Independent reflections	5025 [R_{int} = ?, R_σ = 0.0533]
Data/restraints/parameters	5025/285/411
Goodness-of-fit on F^2	1.180
Final R indexes [$I \geq 2\sigma(I)$]	$R_1 = 0.0700$, $wR_2 = 0.1840$
Final R indexes [all data]	$R_1 = 0.0754$, $wR_2 = 0.1871$
Largest diff. peak/hole	3.13 $e/-3.03$ $Å^{-3}$

6.9 Constants used in Linear Free Energy Relationships

Subst.	σ_m	σ_p	σ_o	$\mathcal{F}$	$\mathcal{R}$	$\mathcal{R}^+$	$\mathcal{R}^-$	wL	wB_1	wB_5
NO_2	0.71	0.78	0.78	0.65	0.13	0.14	0.62	3.95	1.55	2.64
CN	0.56	0.66	1.06	0.51	0.15	0.15	0.49	4.51	1.70	1.70
CF_3	0.42	0.54		0.38	0.16	0.23	0.27	3.96	2.08	2.70
CO_2Et	0.37	0.45		0.34	0.11	0.14	0.41	6.37	1.80	4.17
CO_2Me	0.37	0.45		0.34	0.11	0.15	0.41	5.51	1.68	3.59
CHO	0.35	0.42	0.75	0.33	0.09	0.40	0.70	4.02	1.60	2.55
$CONH_2$	0.28	0.36	0.45	0.26	0.10		0.35	4.62	1.60	3.22
I	0.35	0.18	0.21	0.42	-0.24	-0.28	-0.15	4.51	1.98	1.98
Br	0.39	0.23	0.21	0.45	-0.22	-0.30	-0.20	4.13	1.85	1.85
Cl	0.37	0.23	0.20	0.42	-0.19	-0.31	-0.23	3.81	1.75	1.75
F	0.34	0.06	0.25	0.45	-0.39	-0.52	-0.48	3.13	1.47	1.47
NHMs	0.20	0.03		0.28	-0.25			5.52	1.80	4.31
H	0.00	0.00	0.00	0.03	0.00	0.00	0.00	2.57	1.09	1.09
phenyl	0.06	-0.01		0.12	-0.13	-0.30	-0.10	6.77	1.70	3.27
vinyl	0.06	-0.04		0.13	-0.17			4.72	1.70	3.22
TMS	-0.04	-0.07		0.01	-0.08	0.01		4.98	2.94	3.58
Me	-0.07	-0.17	-0.17	0.01	-0.18	-0.32	-0.18	3.54	1.79	2.12
Et	-0.07	-0.15	-0.17	0.00	-0.15	-0.30	-0.19	4.56	1.70	3.27
***i*Pr**	-0.07	-0.15	-0.23	0.04	-0.19	-0.32	-0.20	4.61	2.02	3.28
***t*Bu**	-0.10	-0.20	-0.52	-0.02	-0.18	-0.17	-0.04	4.58	2.76	3.29
OPh	0.25	-0.03		0.37	-0.40	-0.87	-0.47	6.70	1.58	5.72
OCF_3	0.36	0.33		0.39	-0.04		-0.12	5.23	1.63	3.73
OMe	0.12	-0.27	-0.37	0.29	-0.56	-1.07	-0.55	4.54	1.63	3.18
OEt	0.10	-0.24	-0.08	0.26	-0.50	-1.07	-0.54	4.62	1.62	4.32
O*i*Pr	0.05	-0.45		0.34	-0.79	-1.19		5.52	1.64	4.31
OH	0.12	-0.37	0.04	0.33	-0.70	-0.33		3.31	0.94	1.89
NH_2	-0.16	-0.66	-0.35	0.08	-0.74	-1.38	-0.23	3.37	0.94	1.96
NMe_2	-0.15	-0.83	-0.36	0.15	-0.98	-1.85	-0.27	4.59	1.78	3.24

Table 6.1: Substituents constants employed in LFERs discussed in this Thesis. With the exception of σ_o constants that are from Segala *et al.*,[327] all other descriptors are from Hansch.[313] Weighted Sterimol parameters wL, wB_1 and wB_5 were calculated with wSterimol.[336]

Ar′	wL	wB_1	wB_5	wV_{bur}
***p*-CN**	8.78	1.70	3.25	40.3
***p*-CF_3**	8.28	2.09	3.26	40.3
***p*-$CONH_2$**	9.01	2.04	3.27	40.3
***p*-Cl**	8.15	1.73	3.25	40.4
***p*-I**	8.77	1.97	3.25	40.3
***p*-F**	7.47	1.70	3.26	40.4
H	6.88	1.70	3.25	40.3
***p*-vinyl**	9.12	1.90	3.26	40.3
***p*-Ph**	11.2	2.31	3.32	40.3
***p*-TMS**	9.49	2.90	3.67	39.3
***p*-Me**	7.90	1.87	3.25	40.3
***p*-OMe**	8.78	1.92	3.25	40.3
***p*-NMe_2**	9.05	2.09	3.32	40.3
***m*-CN**	6.88	1.70	4.99	40.3
***m*-F**	6.90	1.70	3.79	40.4
***m*-Br**	6.89	1.74	4.69	40.4
***m*-OMe**	7.01	1.82	5.30	40.4
***m*-CO_2Et**	8.34	1.88	6.81	40.4
***m*-Me**	6.90	1.77	4.39	40.4
3-OH-4-Me	7.81	1.82	4.22	40.3
***m*-OH**	6.89	1.77	4.22	40.4
***m*-NHMs**	6.99	1.90	6.49	40.4
3,5-diMe	6.90	1.94	5.08	40.4
3,5-diCF_3	7.45	2.37	5.08	40.4
***o*-CN**	6.90	1.70	5.07	43.7
***o*-CF_3**	6.88	1.87	5.39	46.1
***o*-Cl**	6.89	1.88	4.45	43.7
***o*-F**	6.90	1.70	3.83	42.0
***o*-OH**	6.89	1.88	4.26	42.5
***o*-Ph**	6.88	2.09	7.06	47.3
***o*-Me**	6.88	1.88	4.45	44.4
***o*-Et**	6.88	1.87	5.39	46.1
***o*-iPr**	6.88	2.12	5.60	45.2
***o*-CHO**	6.89	1.87	4.95	44.5
1-naphthyl	6.95	1.89	5.74	44.0

Ar′	wL	wB_1	wB_5	wV_{bur}
***o*-MeO**	6.88	1.84	5.22	43.9
***o*-EtO**	6.89	1.84	5.87	46.3
***o*-*i*PrO**	6.87	2.02	6.49	46.9
***o*-OCF_3**	6.89	1.93	5.78	44.9
2-Me-5-F	6.90	1.89	4.46	44.4
2-MeO-6-F	6.90	1.81	5.43	44.8
2-Me-4-Cl	8.16	1.89	4.46	44.4
2-Me-4-F	7.48	1.89	4.46	44.4
2-Me-4-MeO	8.78	1.90	4.44	44.2
Mesityl	7.91	2.06	4.47	48.3
TRIP	9.02	3.13	5.67	52.2
2,6-diMe	6.38	1.93	4.48	48.0
2,6-diCF_3	6.90	2.49	5.09	54.9
2,6-diCl	6.91	1.72	4.46	48.0
2,6-diBr	6.90	1.81	4.74	49.3
2,6-diMeO	6.84	2.07	5.39	47.6
2-furyl	6.06	1.83	3.18	38.0
3-furyl	6.05	1.70	3.29	39.1
2-thienyl	6.29	1.73	3.33	40.0
3-thienyl	6.15	1.74	3.29	39.7
3-thienyl-2-acetyl	6.16	1.89	5.55	45.3
***N*-Me-pyrazole**	7.10	1.75	3.68	37.2
3,5-di-Me-isoxazole	5.58	1.92	4.33	44.9
***N*-Boc-MeO-indole**	9.76	2.10	7.14	48.5
6-indole	8.24	1.70	4.20	40.6
1*H*-indazole	6.93	1.71	4.95	42.8
1-Me-4-indazole	7.50	1.78	5.24	42.7
4-dibenzofuryl	7.84	1.70	7.49	42.0
4-aminopyrimidin	7.63	1.83	3.29	40.1

Table 6.2: Steric descriptors used in Chapter 3. These refer to whole Ar′ groups, where Ar′ is the unique ligand in $[Ar_3Ar'Bi][BF_4]$ **5** species, rather than just to their substituents. When only the substitution patter is indicated (*e.g.* *p*-Cl), 'phenyl' is implied. Weighted Sterimol parameters wL, wB_1 and wB_5 were calculated with wSterimol,[336] wV_{bur} was calculated with the script reported in Section 6.10.

6.10 wV_{bur} script

A script was written to calculate wV_{bur} values for all the Ar′ groups in Table 6.2. Requirements: wSterimol (https://github.com/bobbypaton/wSterimol); a locally run version of SambVca 2.1 (https://www.molnac.unisa.it/OMtools/sambvca2.1/). Structure files were generated by drawing every Ar′ group in Reaxys and exporting it as a `.pdb` file. The attachment atom was modelled as a CH_3 unit. The wV_{bur} script was executed on a macOS 10.15.6 system, following this procedure:

1. All files generated in the next steps were placed in the same directory, together with SambVca's source files;
2. Copy and paste the content of the 'PyMol plugin' script reported below into a new file named `export.py`. With PyMol open, open the 'File' tab and select 'Edit pymolrc'. Add the following text to the end of the `pymolrc` file: `run YourPathToTheScript/export.py`. Make sure to replace "YourPathToTheScript" with the actual location of the '`export.py`' file on your computer;
3. Copy and paste the content of the 'PyMol script' into a new file called `export.pml`;
4. Copy and paste the content of the 'Wizard to generate input files for SambVca' script into a file called `prescript.sh`;
5. For every Ar′ group, run wSterimol using the `.pdb` file obtained from Reaxys;
6. Execute the `wBur.sh` from the command line as detailed below. The generation of the files required to run SambVca is generated through an interactive command line tool.

PyMol plugin

The python plugin for PyMol (the command `AddConformers` was copied from the wSterimol software)[336] is as follows:

```
import glob, sys, os
from pymol import cmd

def AddConformers(path = "temp"):
    if os.path.exists(path):
```

```
6           dir_files = [file for file in os.listdir(path) if
            ↪  os.path.isfile(os.path.join(path, file))]  # existing
            ↪  files
7           if len(dir_files) > 0:
8               for file_name in dir_files:
9                   filesplit = file_name.split(".")
10                  if len(filesplit) > 1: # there is an extension
11                      if filesplit[-1] == "pdb": # only pdb is accepted
                        ↪  here
12                          cmd.load(os.path.join(path, file_name)) #load
                            ↪  the structures
13                          BallnStick( filesplit[0] ) # make it look
                            ↪  pretty
14          else: print("Error: No files to load in directory [%s]" %
            ↪  path)
15      else: print("Error: The path doesn't exist [%s]" % path)
16
17  def Export(path = 'temp'):
18      cmd.delete('all')
19      AddConformers(path)
20
21      obj_list = cmd.get_names('all')
22      if os.path.exists(path):
23
24          filelist = [ f for f in os.listdir(path) if
            ↪  f.endswith(".xyz") ]
25          for f in filelist:
26              os.remove(os.path.join(path, f))
27          for obj in range(len(obj_list)):
28              obj_name = 'temp/{}.xyz'.format(obj_list[obj])
29              cmd.save(obj_name, obj_list[obj])
30              print("Saving %s" %  obj_name)
31      else: print("Error: The path doesn't exist [%s]. Have you run
        ↪  wSterimol?" % path)
32
33  cmd.extend("Export", Export)
```

PyMol script

The PyMol `export.pml` script is as follows:

```
os.chdir(sys.argv[1])
Export
```

wSterimol input

wSterimol input file is as follows.[336]

```
SOFTWARE = MOPAC
PROG_EXEC = /opt/mopac/MOPAC2016.exe

SEMI_EMPIRICAL = PM6-D3H4
OPTIMISATION = YES
CHARGE = 0
SPIN = 1
RMSD_CLUSTER_OPT = 0.5
ANGLE_COUNT = 5
ATOMIC_MODEL = bondi
RJCT = 0.5
TEMPERATURE = 298
ENERGYWINDOW_CUTOFF = 1.0 3.0 5.0
PRINT_CUTOFF = 5.0
```

Wizard to generate input files for SambVca

Copy and paste the following text into a file called `prescript.sh`.

```
#!/bin/sh
printf "This wizard will generate the necessary input file for the
↪  SambVca subroutine.\n\n"
read -p "How many atoms to delete. If > 0, one line below to specify
↪  ID of atoms to be deleted: " natomdel
natomdel=${natomdel:-1}
read -p "Id of atoms to be deleted: " idatomdel
idatomdel=${idatomdel:-1000}
printf "How many atoms define the sphere center. If > 1, then middle
↪  point of coordinates: "
```

```
8  read ncentre
9  printf "Id of atoms defining the sphere center: "
10 read idcentre
11 printf "How many atoms define the z-axis. If > 1, then middle point
   ↪  of coordinates: "
12 read nzaxis
13 printf "Id of atoms for z-axis: "
14 read idzaxis
15 printf "How many atoms define the xz-plane. If > 1, then middle point
   ↪  of coordinates: "
16 read nxzplane
17 printf "Id of atoms for xz-plane: "
18 read idxzplane
19 read -p "Sphere radius [default is 3.5]: " rad
20 rad=${rad:-3.5}
21 read -p "Displacement of oriented molecule from sphere center
   ↪  [default is 0]: " displ
22 displ=${displ:-0.0}
23 read -p "Mesh size for numerical integration [default is 0.1]: " mesh
24 mesh=${mesh:-0.10}
25 read -p "Do not remove/remove H atoms from Vbur calculation [0,1
   ↪  default is 0]: "
26 hydro=${hydro:-0}
27 read -p "Is the molecule oriented along negative/positive Z-axis [0,1
   ↪  default is 0]: "
28 orient=${orient:-0}
29 read -p "Do not write/write files for top and bottom surfaces [0,1
   ↪  default is 1]: "
30 surf=${surf:-1}
31
32 printf "$natomdel \t\t ! How many atoms to delete. If > 0, one line
   ↪  below to specify ID of atoms to be deleted
33 $idatomdel \t\t ! Id of atoms to be deleted
34 $ncentre  \t\t ! How many atoms define the sphere center. If > 1,
   ↪  then middle point of coordinates
35 $idcentre  \t\t ! Id of atoms defining the sphere center
```

```
$nzaxis    \t\t ! How many atoms define the z-axis. If > 1, then middle point of coordinates
$idzaxis   \t\t ! Id of atoms for z-axis
$nxzplane  \t\t ! How many atoms define the xz-plane. If > 1, then middle point of coordinates
$idxzplane \t ! Id of atoms for xz-plane
$rad       \t ! Sphere radius
$displ     \t ! Displacement of oriented molecule from sphere center
$mesh      \t ! Mesh size for numerical integration
$hydro     \t\t ! 0/1 = Do not remove/remove H atoms from Vbur calculation
$orient    \t\t ! 0/1 = molecule oriented along negative/positive Z-axis
$surf      \t\t ! 0/1 = Do not write/write files for top and bottom surfaces
103        \t ! number of radii to be read in the following, then radii. All radii are uppercase.
H\t        1.28\nHE\t       1.64\nLI\t       2.13\nBE\t
1.79\nB\t        2.25\nC\t        1.99\nN\t        1.81\nO\t
1.78\nF\t        1.72\nNE\t       1.80\nNA\t       2.66\nMG\t
2.02\nAL\t       2.15\nSI\t       2.46\nP\t        2.11\nS\t
2.11\nCL\t       2.05\nAR\t       2.20\nK\t        3.22\nCA\t
2.70\nSC\t       2.52\nTI\t       2.47\nV\t        2.42\nCR\t
2.41\nMN\t       2.40\nFE\t       2.39\nCO\t       2.34\nNI\t
1.91\nCU\t       1.64\nZN\t       1.63\nGA\t       2.19\nGE\t
2.47\nAS\t       2.16\nSE\t       2.22\nBR\t       2.16\nKR\t
2.36\nRB\t       3.55\nSR\t       2.91\nY\t        2.71\nZR\t
2.61\nNB\t       2.55\nMO\t       2.54\nTC\t       2.53\nRU\t
2.49\nRH\t       2.46\nPD\t       1.91\nAG\t       2.01\nCD\t
1.85\nIN\t       2.26\nSN\t       2.54\nSB\t       2.41\nTE\t
2.41\nI\t        2.32\nXE\t       2.53\nCS\t       4.01\nBA\t
3.14\nLA\t       2.84\nCE\t       2.83\nPR\t       2.81\nND\t
2.80\nPM\t       2.78\nSM\t       2.76\nEU\t       2.75\nGD\t
2.74\nTB\t       2.73\nDY\t       2.70\nHO\t       2.69\nER\t
2.68\nTM\t       2.66\nYB\t       2.64\nLU\t       2.62\nHF\t
2.61\nTA\t       2.60\nW\t        2.55\nRE\t       2.53\nOS\t
```

```
 2.53\nIR\t       2.49\nPT\t       2.01\nAU\t       1.94\nHG\t
    1.81\nTL\t       2.29\nPB\t       2.36\nBI\t       2.42\nPO\t
    2.30\nAT\t       2.36\nRN\t       2.57\nFR\t       4.07\nRA\t
    3.31\nAC\t       2.89\nTH\t       2.87\nPA\t       2.84\nU\t
    2.18\nNP\t       2.80\nPU\t       2.84\nAM\t       2.85\nCM\t
    2.87\nBK\t       2.85\nCF\t       2.87\nES\t       2.87\nFM\t
    2.87\nM\t        2.88\nNO\t       2.88\nLR\t       2.88\n

" > ../$FILE.inp
printf "\nThe input file has been prepared. Starting Vbur
    calculations...\n"
```

wV_{bur} script

The `wVbur.sh` script calculates wV_{bur} for each conformer generated by the wSterimol software. Run as `./wVbur.sh -m /full/path/to/wsterimol/output/`. The `-m` option enables steric maps generation. Below is an example of the required folder nesting: the path to the output file of wSterimol must be a folder (in this example `example_group`) containing the file `weighted.txt` and the subfolder `temp`. The folder `example_group` must be placed in a folder (the name does not matter). The root folder `wVbur` must contain all the files indicated here, including the SambVca applicative.

```
wVbur
├── export.pml
├── export.py
├── groups
│   └── example_group
│       ├── example_group.pdb
│       ├── setup.ini
│       ├── temp
│       └── weighted.txt
├── plot_map.py
├── prescript.sh
├── sambvca21.f
├── sambvca21.x
└── wVbur.sh
```

```
#!/bin/sh
#define option -m to generate steric maps
while getopts m: flag; do
  case "$flag" in
    m) MAP="$OPTARG";;
  esac
done
shift $((OPTIND - 1))
#CDPATH is read in by cd and is not a made up variable name: it allows the use of cd
if [ -n "$MAP" ]; then
  CDPATH="$MAP"
else
CDPATH="$@"
fi

#if path has not been specified:
if [ -z "$CDPATH" ]; then
  echo "\nPlease specify a folder containing the wSterimol output. Stopping...\n"; exit 1
fi

WORK="$CDPATH/temp"
FILE="$(basename  "$CDPATH")"
cd "$WORK"
#if wStermol ran correctly, extract the lines between line number 31 and the *, copies them to a new file and sort them in alphabetical order
if [ ! -f "../weighted.txt" ]; then
    echo "\nweighthed.txt missing: wSterimol didn't run properly. Stopping...\n";
    exit 1
fi
sed -n '31,/*/p' ../weighted.txt >  ../weights.txt && sed -i '' -e '$ d' ../weights.txt
sort -o ../weights.txt  -k1,1 -bd ../weights.txt
```

```
#remove the top empty line
tail -n +2 ../weights.txt > ../weights.tmp && mv ../weights.tmp
    ../weights.txt
awk '{ print $6 }' ../weights.txt > ../onlyweights.txt
awk '{ print $1 }' ../weights.txt > ../conformers.txt
mv ../onlyweights.txt ../weights.txt
#adds the _OPT suffix
sed -n 's/.out/_OPT/p'  ../conformers.txt > ../conformers.tmp && mv
    ../conformers.tmp ../conformers.txt
#generate the input file for sambvca if it doesn't exist
if [ ! -f "../$FILE.inp" ]; then
    printf "\nInput file for sambVca ($FILE.inp) not detected.\n";
    source "../../../prescript.sh"
fi
#add an empty line at the end of the input file
sed -i '' -e '$a\' ../$FILE.inp
#for every entry in conformers.txt create a new input file by copying
    the main one and appending the name of the entry in
    conformers.txt
for i in $(cat ../conformers.txt); do cp ../$FILE.inp "${i}.inp";
    done
#check if xyz files have been exported from PyMol, if not export
    them.
count=$(find ./ -maxdepth 1 -name '*.xyz' | wc -l)
if [ $count -lt 1 ] ; then
    echo "\nConformers have not been exported from PyMol. I'll do it
        for you.\n"
    pymol -Qc ../../../export.pml -- "$CDPATH"
fi
#delete all the conformer xyz files that were not used to calculate
    wSterimol and for which there is no weight associated
sed -e 's/$/.xyz/' ../conformers.txt > ../confxyz.txt
for i in *.xyz; do
    if ! grep -qxFe "$i" ../confxyz.txt; then
        rm -f "$i"
    fi done
```

```
#for every conformer that survived create a sambvca input file
for file in *_OPT.xyz; do FILENAME=${file%%.*}; cat $file >> $FILENAME.inp; done

#run sambvca for every conformer with or without steric map generation
if [ -n "$MAP" ]; then
  for file in *_OPT.xyz; do JOB=${file%%.*}; ../../../sambvca21.x $JOB; ../../../plot_map.py  $JOB-TopSurface.dat 0.2; #../../../plot_map.py  $JOB-BotSurface.dat 0.2;
  done
else
for file in *_OPT.xyz; do JOB=${file%%.*}; ../../../sambvca21.x $JOB;  done
fi

#extract the resulting %Vbur, sort the entries, compare the sorted conformers names before and after SambVca and stop if they don't match to avoid applying a weight to the wrong conformer
grep -r "The %V Bur of the molecule is:     " . > ../Vbur.txt
sort -o ../Vbur.txt  -k1,1 -bd ../Vbur.txt
awk -v OFS='\t' '{ print $1, $9 }' ../Vbur.txt > ../Vbur.tmp && mv ../Vbur.tmp ../Vbur.txt
awk -v OFS='\t' '{ print $1 }' ../Vbur.txt > ../conffinal.txt
sed -e 's/^.\///' -e 's/.out://' ../conffinal.txt > ../conffinal2.txt
if ! cmp -s ../conffinal2.txt ../conformers.txt;
    then
        printf "\nSorting and pairing of conformers went wrong. Stopping...\n\n"; exit 1
fi

#apply the weights, calculate wVbur and print it
paste ../Vbur.txt ../weights.txt | column -s $'\t' -t > ../wVbur.txt
awk '{print $2*$3/100}' ../wVbur.txt  > ../wVbur2.txt
paste ../wVbur.txt ../wVbur2.txt | column -s $'\t' -t > ../wVbur3.txt
mv ../wVbur3.txt ../wVbur.txt && rm ../wVbur?.txt
```

```
sed -i '' -e '$a\' ../wVbur.txt && echo "\nThe calculated wVbur for the group $FILE is:\t\t" >> ../wVbur.txt
result=$(awk '{ sum += $4; } END {printf "%.3g", sum }' "$CDPATH" ../wVbur.txt)
echo "\nThe calculated wVbur for the group $FILE is: "$result"%\n"
sed "$ s/$/$result/" ../wVbur.txt >../wVbur.tmp && mv ../wVbur.tmp ../wVbur.txt

#some tidy up
rm ../Vbur.txt
rm ../weights.txt
rm ../conf*

#remove stale maps, convert new ones to pdf and move them to the maps folder
rm -f *BotSurface*
if [ -n "$MAP" ]; then
    rm -rf maps
    find . -name \*.ps -exec ps2pdf -r1200 {} \;
    mkdir maps
    mv *.pdf maps
    rm -f *.png
    rm -rf *.ps
    for i in maps/*.pdf; do
      mv "$i" "${i%\-TopSurface*}.pdf"
    done
    printf "Steric maps have been generated in the maps subfolder.\n\n"
fi
rm -f *.inp
rm -f *.dat
rm -f *rotated.xyz
```

References

[1] Joachim, K.; Peter, W.; Eberhard, L.; Manfred, L.; Uwe, W. H. 'Bismuth, Bismuth Alloys, and Bismuth Compounds' in *Ullmann's Encyclopedia of Industrial Chemistry*, Wiley: Weinheim, Germany, **2003**.

[2] McCord, C. P.; Baylis, S. J. *J. Occup. Environ. Med.* **1973**, *15* (6), 531–534.

[3] Agricola, G. *De natura fossilium, Libri X;* ; Johann Froben: Basel, Switzerland, **1546**.

[4] Marcillac, P. de; Coron, N.; Dambier, G.; Leblanc, J.; Moalic, J.-P. *Nature* **2003**, *422* (6934), 876–878.

[5] Planck Collaboration *Planck 2018 results. VI. Cosmological parameters;* **2018**.

[6] Mohan, R. *Nat. Chem.* **2010**, *2* (4), 336–336.

[7] Suzuki, H.; Komatsu, N.; Ogawa, T.; Murafuji, T.; Ikegami, T.; Matano, Y. *Organobismuth Chemistry;* Elsevier Science: Amsterdam, **2001**.

[8] Slikkerveer, A.; Wolff, F. A. *Med. Toxicol. Adverse Drug Exp.* **1989**, *4* (5), 303–323.

[9] Collier, W. B. *Manual of therapeutics;* Parke, Davis & Company: Detroit, MI,. **1909**.

[10] Bierer, D. W. *Clin. Infect. Dis.* **1990**, *12* (Suppl. 1), S3–S8.

[11] Maile, F. J.; Pfaff, G.; Reynders, P. *Prog. Org. Coat.* **2005**, *54* (3), 150–163.

[12] Graedel, T. *Resour. Conserv. Recycl.* **2002**, *34* (2), 107–115.

[13] Deb, S.; Abdulghani, S.; Behiri, J. *Biomaterials* **2002**, *23* (16), 3387–3393.

[14] La Fontaine, A.; Keast, V. *Mater. Charact.* **2006**, *57* (4–5), 424–429.

[15] Wittig, G.; Clauß, K. *Justus Liebigs Ann. Chem.* **1952**, *578* (1), 136–146.

[16] Barton, D. H. R.; Finet, J.-P. *Pure Appl. Chem.* **1987**, *59* (8), 937–946.

[17] Nagase, S. 'General and Theoretical Aspects' in *Organic Arsenic, Antimony and Bismuth Compounds*, Patai, S.; ed.; Wiley: Chichester, UK, **1994**, 1–24.

[18] Sanderson, J.; Bayse, C. A. *Tetrahedron* **2008**, *64* (33), 7685–7689.

[19] Pyykkö, P. *Chem. Rev.* **1988**, *88* (3), 563–594.

[20] Onoe, J. *Adv. Quantum Chem.* **2000**, 311–323.

[21] Bagus, P. S.; Lee, Y. S.; Pitzer, K. S. *Chem. Phys. Lett.* **1975**, *33* (3), 408–411.

[22] Desclaux, J. *At. Data Nucl. Data Tables* **1973**, *12* (4), 311–406.

[23] Marquardt, A. *Ber. Dtsch. Chem. Ges.* **1887**, *20* (1), 1516–1523.

[24] De Ketelaere, R.; Delbeke, F.; Van Der Kelen, G. *J. Organomet. Chem.* **1971**, *30* (3), 365–368.

[25] Lemus, A.; Sharma, P.; Cabrera, A.; Rosas, N.; Alvarez, C.; Gomez, E.; Sharma, M.; Cespedes, C.; Hernandez, S. *Main Group Met. Chem.* **2001**, *24* (12), 835–839.

[26] Hébert, M.; Petiot, P.; Benoit, E.; Dansereau, J.; Ahmad, T.; Le Roch, A.; Ottenwaelder, X.; Gagnon, A. *J. Org. Chem.* **2016**, *81* (13), 5401–5416.

[27] Gagnon, A.; Dansereau, J.; Le Roch, A. *Synthesis* **2017**, *49* (8), 1707–1745.

[28] Boymond, L.; Rottländer, M.; Cahiez, G.; Knochel, P. *Angew. Chem., Int. Ed.* **1998**, *37* (12), 1701–1703.

[29] Murafuji, T.; Nishio, K.; Nagasue, M.; Tanabe, A.; Aono, M.; Sugihara, Y. *Synthesis* **2000**, *2000* (9), 1208–1210.

[30] Urgin, K.; Aubé, C.; Pichon, C.; Pipelier, M.; Blot, V.; Thobie-Gautier, C.; Léonel, E.; Dubreuil, D.; Condon, S. *Tetrahedron Lett.* **2012**, *53* (15), 1894–1896.

[31] Urano, M.; Wada, S.; Suzuki, H. *Chem. Commun.* **2003**, 1202–1203.

[32] Stavila, V.; Thurston, J. H.; Prieto-Centurión, D.; Whitmire, K. H. *Organometallics* **2007**, *26* (27), 6864–6866.

[33] Berger, R. J. F.; Rettenwander, D.; Spirk, S.; Wolf, C.; Patzschke, M.; Ertl, M.; Monkowius, U.; Mitzel, N. W. *Phys. Chem. Chem. Phys.* **2012**, *14* (44), 15520–15524.

[34] Jones, P. G.; Blaschette, A.; Henschel, D.; Weitze, A. *Z. Kristallogr.* **1995**, *210* (5), 377–378.

[35] Steele, W. *J. Chem. Thermodyn.* **1979**, *11* (2), 187–192.

[36] Fossheim, R. *Inorg. Chim. Acta* **1999**, *284* (2), 167–174.

[37] Jensen, K. A. *Z. Anorg. Allg. Chem.* **1943**, *250* (3–4), 257–267.

[38] Challenger, F. *J. Chem. Soc. Trans.* **1916**, *109*, 250–251.

[39] Barton, D. H.; Bhatnagar, N. Y.; Finet, J.-P.; Motherwell, W. B. *Tetrahedron* **1986**, *42* (12), 3111–3122.

[40] Ikegami, T.; Suzuki, H. *Organometallics* **1998**, *17* (6), 1013–1017.

[41] Schmuck, A.; Seppelt, K. *Chem. Ber.* **1989**, *122* (5), 803–808.

[42] Combes, S.; Finet, J.-P. *Synth. Commun.* **1996**, *26* (24), 4569–4575.

[43] Robertson, A. P. M.; Burford, N.; McDonald, R.; Ferguson, M. J. *Angew. Chem., Int. Ed.* **2014**, *53* (13), 3480–3483.

[44] Rahman, A. M.; Murafuji, T.; Ishibashi, M.; Miyoshi, Y.; Sugihara, Y. *J. Organomet. Chem.* **2004**, *689* (21), 3395–3401.

[45] Senear, A. E.; Valient, W.; Wirth, J. *J. Org. Chem.* **1960**, *25* (11), 2001–2006.

[46] Suzuki, H.; Ikegami, T.; Matano, Y. *Tetrahedron Lett.* **1994**, *35* (44), 8197–8200.

[47] Matano, Y.; Nomura, H. *Synthesis* **2002**, *2002* (5), 631–634.

[48] Sharutin, V. V.; Sharutina, O. K.; Egorova, I. V.; Ivanenko, T. K.; Bel'skii, V. K. *Russ. J. Gen. Chem.* **2002**, *72* (1), 44–45.

[49] Hawley, D. M.; Ferguson, G.; Harris, G. S. *Chem. Commun. (London)* **1966**, 111–112.

[50] Egorova, I. V.; Zhidkov, V. V.; Grinishak, I. P.; Rezvanova, A. A. *Russ. J. Gen. Chem.* **2014**, *84* (7), 1374–1377.

[51] Akiba, K.-y. *Organo Main Group Chem.* Wiley: Hoboken, NJ,. **2011**.

[52] Matsukawa, S.; Kajiyama, K.; Kojima, S.; Furuta, S.-y.; Yamamoto, Y.; Akiba, K.-y. *Angew. Chem., Int. Ed.* **2002**, *41* (24), 4718–4722.

[53] Murafuji, T.; Azuma, T.; Miyoshi, Y.; Ishibashi, M.; Rahman, A. M.; Migita, K.; Sugihara, Y.; Mikata, Y. *Bioorg. Med. Chem. Lett.* **2006**, *16* (6), 1510–1513.

[54] Green, M. L. H.; Parkin, G. *Dalton Trans.* **2016**, *45* (47), 18784–18795.

[55] Rundle, R. E. *J. Am. Chem. Soc.* **1963**, *85* (1), 112–113.

[56] Nakazawa, H.; Kubo, K.; Miyoshi, K. *Bull. Chem. Soc. Jpn.* **2001**, *74* (12), 2255–2267.

[57] Hoffmann, R.; Howell, J. M.; Muetterties, E. L. *J. Am. Chem. Soc.* **1972**, *94* (9), 3047–3058.

[58] Goodman, J. 'Computational Studies On Metallophosphoranes As Intermediates In Palladium-Phosphine Chemistry'. PhD thesis, Heriot-Watt University, Edinburgh, **2009**.

[59] Berry, R. S. *J. Chem. Phys.* **1960**, *32* (3), 933–938.

[60] Moc, J.; Morokuma, K. *J. Am. Chem. Soc.* **1995**, *117* (47), 11790–11797.

[61] Minkin, V. I. *Pure Appl. Chem.* **1999**, *71* (10), 1919–1981.

[62] Couzijn, E. P. A.; Slootweg, J. C.; Ehlers, A. W.; Lammertsma, K. *J. Am. Chem. Soc.* **2010**, *132* (51), 18127–18140.

[63] Hellwinkel, D.; Bach, M. *J. Organomet. Chem.* **1969**, *17* (3), 389–403.

[64] Schmuck, A.; Buschmann, J.; Fuchs, J.; Seppelt, K. *Angew. Chem., Int. Ed. Engl.* **1987**, *26* (11), 1180–1182.

[65] Schmuck, A.; Seppelt, K.; Pyykkö, P. *Angew. Chem., Int. Ed. Engl.* **1990**, *29* (2), 213–215.

[66] Wittig, G.; Clauß, K. *Justus Liebigs Ann. Chem.* **1952**, *577* (1), 26–39.

[67] Seppelt, K. 'Structure, Color, and Chemistry of Pentaaryl Bismuth Compounds' in *Advances in Organomet. Chem.* Stone, F. G. A.; West, R.; eds.; Academic: Cambridge, MA, **1992**, 207–217.

[68] Doak, G. O.; Long, G. G.; Kakar, S. K.; Freedman, L. D. *J. Am. Chem. Soc.* **1966**, *88* (10), 2342–2343.

[69] Beaumont, R. E.; Goel, R. G. *J. Chem. Soc., Dalton Trans.* **1973**, 1394–1398.

[70] Freedman, L. D.; Doak, G. O. *Chem. Rev.* **1982**, *82* (1), 15–57.

[71] Matano, Y.; Yoshimune, M.; Azuma, N.; Suzuki, H. *J. Chem. Soc., Perkin Trans. 1* **1996**, 1971–1977.

[72] Matano, Y.; Azuma, N.; Suzuki, H. *Tetrahedron Lett.* **1993**, *34* (52), 8457–8460.

[73] Matano, Y.; Azuma, N.; Suzuki, H. *J. Chem. Soc., Perkin Trans. 1* **1994**, 1739–1747.

[74] Matano, Y.; Azuma, N.; Suzuki, H. *J. Chem. Soc., Perkin Trans. 1* **1995**, 2543–2549.

[75] Matano, Y.; Begum, S. A.; Miyamatsu, T.; Suzuki, H. *Organometallics* **1998**, *17* (20), 4332–4334.

[76] Matano, Y.; Begum, S. A.; Miyamatsu, T.; Suzuki, H. *Organometallics* **1999**, *18* (26), 5668–5681.

[77] Barton, D. H. R.; Charpiot, B.; Dau, E. T. H.; Motherwell, W. B.; Pascard, C.; Pichon, C. *Helv. Chim. Acta* **1984**, *67* (2), 586–599.

[78] Ooi, T.; Goto, R.; Maruoka, K. *J. Am. Chem. Soc.* **2003**, *125* (35), 10494–10495.

[79] Suzuki, H.; Ikegami, T.; Azuma, N. *J. Chem. Soc., Perkin Trans. 1* **1997**, 1609–1616.

[80] El-Issa, B. D.; Pyykkö, P.; Zanati, H. M. *Inorg. Chem.* **1991**, *30* (13), 2781–2787.

[81] Denmark, S. E.; Beutner, G. L. *Angew. Chem., Int. Ed.* **2008**, *47* (9), 1560–1638.

[82] Challenger, F.; Richards, O. V. *J. Chem. Soc.* **1934**, 405–411.

[83] Barton, D. H.; Kitchin, J. P.; Lester, D. J.; Motherwell, W. B.; Papoula, M. T. B. *Tetrahedron* **1981**, *37*, 73–79.

[84] Finet, J.-P. *Chem. Rev.* **1989**, *89* (7), 1487–1501.

[85] Barton, D. H. R.; Lester, D. J.; Motherwell, W. B.; Papoula, M. T. B. *J. Chem. Soc., Chem. Commun.* **1979**, 705–707.

[86] Barton, D. H. R.; Lester, D. J.; Motherwell, W. B.; Papoula, M. T. B. *J. Chem. Soc., Chem. Commun.* **1980**, 246–247.

[87] Barton, D. H. R.; Blazejewski, J.-C.; Charpiot, B.; Finet, J.-P.; Motherwell, W. B.; Papoula, M. T. B.; Stanforth, S. P. *J. Chem. Soc., Perkin Trans. 1* **1985**, 2667–2675.

[88] Barton, D. H. R.; Kitchin, J. P.; Motherwell, W. B. *J. Chem. Soc., Chem. Commun.* **1978**, 1099–1100.

[89] Barton, D. H. R.; Blazejewski, J.-C.; Charpiot, B.; Lester, D. J.; Motherwell, W. B.; Papoula, M. T. B. *J. Chem. Soc., Chem. Commun.* **1980**, 827–829.

[90] Razuvaev, G. A.; Osanova, N. A.; Sharutin, V. V. *Dokl. Akad. Nauk SSSR* **1975**, *225* (3), 581–582.

[91] Barton, D. H. R.; Blazejewski, J.-C.; Charpiot, B.; Motherwell, W. B. *J. Chem. Soc., Chem. Commun.* **1981**, 503–504.

[92] Barton, D. H.; Charpiot, B.; Motherwell, W. B. *Tetrahedron Lett.* **1982**, *23* (33), 3365–3368.

[93] Barton, D. H.; Finet, J.-P.; Khamsi, J.; Pichon, C. *Tetrahedron Lett.* **1986**, *27* (31), 3619–3622.

[94] David, S.; Thieffry, A. *Tetrahedron Lett.* **1981**, *22* (50), 5063–5066.

[95] Coles, S. J.; Costello, J. F.; Hursthouse, M. B.; Smith, S. *J. Organomet. Chem.* **2002**, *662* (1–2), 98–104.

[96] Brunner, H.; Obermann, U.; Wimmer, P. *Organometallics* **1989**, *8* (3), 821–826.

[97] Barton, D. H.; Finet, J.-P.; Khamsi, J. *Tetrahedron Lett.* **1986**, *27* (31), 3615–3618.

[98] Barton, D. H. R.; Bhatnagar, N. Y.; Blazejewski, J.-C.; Charpiot, B.; Finet, J.-P.; Lester, D. J.; Motherwell, W. B.; Papoula, M. T. B.; Stanforth, S. P. *J. Chem. Soc., Perkin Trans. 1* **1985**, 2657–2665.

[99] Barton, D. H. R.; Finet, J.-P.; Giannotti, C.; Halley, F. *J. Chem. Soc., Perkin Trans. 1* **1987**, 241–249.

[100] Trost, B.; LaRochelle, R.; Atkins, R. *J. Am. Chem. Soc.* **1969**, *91* (8), 2175–2177.

[101] Trost, B. M.; Arndt, H. C. *J. Am. Chem. Soc.* **1973**, *95* (16), 5288–5298.

[102] Oae, S.; Kawai, T.; Furukawa, N. *Tetrahedron Lett.* **1984**, *25* (1), 69–72.

[103] Oae, S.; Kawai, T.; Furukawa, N.; Iwasaki, F. *J. Chem. Soc., Perkin Trans. 2* **1987**, 405–411.

[104] Grushin, V. V. *Acc. Chem. Res.* **1992**, *25* (11), 529–536.

[105] Ozanne-Beaudenon, A.; Quideau, S. *Angew. Chem., Int. Ed.* **2005**, *44* (43), 7065–7069.

[106] Lancer, K. M.; Wiegand, G. H. *J. Org. Chem.* **1976**, *41* (21), 3360–3364.

[107] Stridfeldt, E.; Lindstedt, E.; Reitti, M.; Blid, J.; Norrby, P.-O.; Olofsson, B. *Chem. Eur. J.* **2017**, *23* (53), 13249–13258.

[108] Barton, D. H. R.; Glover, S. A.; Ley, S. V. *J. Chem. Soc., Chem. Commun.* **1977**, 266–267.

[109] Glover, S. A. *J. Chem. Soc., Perkin Trans. 1* **1980**, 1338–1344.

[110] Tamao, K.; Ishida, N.; Tanaka, T.; Kumada, M. *Organometallics* **1983**, *2* (11), 1694–1696.

[111] Kano, T.; Ohyabu, Y.; Saito, S.; Yamamoto, H. *J. Am. Chem. Soc.* **2002**, *124* (19), 5365–5373.

[112] Uchida, Y.; Onoue, K.; Tada, N.; Nagao, F.; Oae, S. *Tetrahedron Lett.* **1989**, *30* (5), 567–570.

[113] Shen, K.-W.; McEwen, W. E.; Wolf, A. P. *J. Am. Chem. Soc.* **1969**, *91* (6), 1283–1288.

[114] Akiba, K.-y. *Pure Appl. Chem.* **1996**, *68* (4), 837–842.

[115] Finet, J.-P. 'The ligand coupling mechanism' in *Ligand Coupling Reactions with Heteroatomic Compounds*, Elsevier Science: Amsterdam, **1998**, 9–46.

[116] Oae, S.; Uchida, Y. *Acc. Chem. Res.* **1991**, *24* (7), 202–208.

[117] Oae, S.; Takeda, T.; Wakabayashi, S.; Iwasaki, F.; Yamazaki, N.; Katsube, Y. *J. Chem. Soc., Perkin Trans. 2* **1990**, 273–276.

[118] Oae, S.; Takeda, T.; Wakabayashi, S. *Tetrahedron Lett.* **1988**, *29* (35), 4445–4448.

[119] Woodward, R. B.; Hoffmann, R. *Angew. Chem., Int. Ed. Engl.* **1969**, *8* (11), 781–853.

[120] Ugi, I.; Marquarding, D.; Klusacek, H.; Gillespie, P.; Ramirez, F. *Acc. Chem. Res.* **1971**, *4* (8), 288–296.

[121] Schwerdtfeger, P.; Heath, G. A.; Dolg, M.; Bennett, M. A. *J. Am. Chem. Soc.* **1992**, *114* (19), 7518–7527.

[122] Kutzelnigg, W.; Wasilewski, J. *J. Am. Chem. Soc.* **1982**, *104* (4), 953–960.

[123] Bowry, V. W.; Lusztyk, J.; Ingold, K. U. *J. Am. Chem. Soc.* **1991**, *113* (15), 5687–5698.

[124] Morgan, J.; Pinhey, J. T. *J. Chem. Soc., Perkin Trans. 1* **1993**, 1673–1676.

[125] Combes, S.; Finet, J.-P. *Tetrahedron* **1999**, *55* (11), 3377–3386.

[126] Yamamoto, Y.; Akiba, K.-y. 'Ligand-Coupling Reactions of Compounds of Group 15 and Group 16 Elements' in *Chemistry of Hypervalent Compounds*, Akiba, K.-Y.; ed.; Wiley: Chichester, UK, **1999**, 279–294.

[127] Finet, J.-P. 'Ligand coupling involving organobismuth compounds' in *Ligand Coupling Reactions with Heteroatomic Compounds*, Elsevier Science: Amsterdam, **1998**, 159–204.

[128] Sharutin, V. V.; Egorova, I. V.; Sharutina, O. K.; Pakusina, A. P.; Pushilin, M. A. *Russ. J. Coord. Chem.* **2008**, *34* (2), 85–92.

[129] Hoppe, S.; Whitmire, K. H. *Organometallics* **1998**, *17* (7), 1347–1354.

[130] Dewar, M. J. S. *J. Am. Chem. Soc.* **1984**, *106* (1), 209–219.

[131] Hine, J. 'The Principle of Least Nuclear Motion' in *Advances in Physical Organic Chemistry*, Academic: London, **1977**, 1–61.

[132] Morgan, J.; Hambley, T. W.; Pinhey, J. T. *J. Chem. Soc., Perkin Trans. 1* **1996**, 2173–2177.

[133] Crifar, C.; Petiot, P.; Ahmad, T.; Gagnon, A. *Chem. Eur. J.* **2014**, *20* (10), 2755–2760.

[134] Barton, D. H.; Yadav-Bhatnagar, N.; Finet, J.-P.; Khamsi, J.; Motherwell, W. B.; Stanforth, S. P. *Tetrahedron* **1987**, *43* (2), 323–332.

[135] Abramovitch, R. A.; Barton, D. H.; Finet, J.-P. *Tetrahedron* **1988**, *44* (11), 3039–3071.

[136] Lam, P. Y. S. 'Chan-Lam Coupling Reaction: Copper-promoted C-element Bond Oxidative Coupling Reaction with Boronic Acids' in *Synthetic Methods in Drug Discovery*, Blakemore, D. C.; Doyle, P. M.; Fobian, Y. M.; eds.; Royal Society of Chemistry: Cambridge, UK, **2016**, 242–273.

[137] Beletskaya, I. P.; Cheprakov, A. V. *Coord. Chem. Rev.* **2004**, *248* (21–24), 2337–2364.

[138] Ibrahim, S. R.; Mohamed, G. A. *Fitoterapia* **2015**, *106*, 194–225.

[139] Teponno, R. B.; Kusari, S.; Spiteller, M. *Nat. Prod. Rep.* **2016**, *33* (9), 1044–1092.

[140] Quideau, S.; Deffieux, D.; Douat-Casassus, C.; Pouységu, L. *Angew. Chem., Int. Ed.* **2011**, *50* (3), 586–621.

[141] Zhang, H.; Xu, X.; Chen, L.; Chen, J.; Hu, L.; Jiang, H.; Shen, X. ed. by Csermely, P. *PLoS ONE* **2011**, *6* (11), e28253.

[142] Marchais-Oberwinkler, S.; Wetzel, M.; Ziegler, E.; Kruchten, P.; Werth, R.; Henn, C.; Hartmann, R. W.; Frotscher, M. *J. Med. Chem.* **2011**, *54* (2), 534–547.

[143] Bosmans, V.; Poater, J.; Hammink, R.; Tinnemans, P.; Bickelhaupt, F. M.; Mecinović, J. *J. Org. Chem.* **2019**, *84* (6), 3632–3637.

[144] Gross, K. C.; Seybold, P. G. *Int. J. Quantum Chem.* **2001**, *85* (4–5), 569–579.

[145] Hassan, J.; Sévignon, M.; Gozzi, C.; Schulz, E.; Lemaire, M. *Chem. Rev.* **2002**, *102* (5), 1359–1470.

[146] Kranich, R.; Eis, K.; Geis, O.; Mühle, S.; Bats, J. W.; Schmalz, H.-G. *Chem. Eur. J.* **2000**, *6* (15), 2874–2894.

[147] Simonsen, K. B.; Gothelf, K. V.; Jørgensen, K. A. *J. Org. Chem.* **1998**, *63* (21), 7536–7538.

[148] Zembower, D. E.; Zhang, H. *J. Org. Chem.* **1998**, *63* (25), 9300–9305.

[149] Takahata, H.; Ouchi, H.; Kawata, Y.; Ono, M.; Morita, Y.; Yamamoto, Y. *Heterocycles* **2004**, *62* (1), 491–501.

[150] Chopa, A. B.; Silbestri, G. F.; Lockhart, M. T. *J. Organomet. Chem.* **2005**, *690* (17), 3865–3877.

[151] Ishikawa, S.; Manabe, K. *Tetrahedron* **2011**, *67* (52), 10156–10163.

[152] Bolliger, J. L.; Frech, C. M. *Chem. Eur. J.* **2010**, *16* (36), 11072–11081.

[153] Leroux, M.; Vorherr, T.; Lewis, I.; Schaefer, M.; Koch, G.; Karaghiosoff, K.; Knochel, P. *Angew. Chem., Int. Ed.* **2019**, *58* (24), 8231–8234.

[154] Kondo, K.; Suzuki, A.; Akita, M.; Yoshizawa, M. *Angew. Chem., Int. Ed.* **2013**, *52* (8), 2308–2312.

[155] $CDCl_3$Calimsiz, S.; Sayah, M.; Mallik, D.; Organ, M. G. *Angew. Chem., Int. Ed.* **2010**, *49* (11), 2014–2017.

[156] Miyaura, N.; Suzuki, A. *Chem. Rev.* **1995**, *95* (7), 2457–2483.

[157] Lennox, A. J. J.; Lloyd-Jones, G. C. *Chem. Soc. Rev.* **2014**, *43* (1), 412–443.

[158] Cordovilla, C.; Bartolomé, C.; Martínez-Ilarduya, J. M.; Espinet, P. *ACS Catal.* **2015**, *5* (5), 3040–3053.

[159] Casares, J. A.; Espinet, P.; Fuentes, B.; Salas, G. *J. Am. Chem. Soc.* **2007**, *129* (12), 3508–3509.

[160] Abernethy, D. R.; DeStefano, A. J.; Cecil, T. L.; Zaidi, K.; Williams, R. L. *Pharm. Res.* **2010**, *27* (5), 750–755.

[161] Gebel, T.; Lantzsch, H.; Pleßow, K.; Dunkelberg, H. *Mutat. Res. Genet. Toxicol. Environ. Mutagen.* **1997**, *389* (2–3), 183–190.

[162] Schaumlöffel, D. *J. Trace Elem. Med. Biol.* **2012**, *26* (1), 1–6.

[163] Miyamoto, H.; Sakumoto, C.; Takekoshi, E.; Maeda, Y.; Hiramoto, N.; Itoh, T.; Kato, Y. *Org. Process Res. Dev.* **2015**, *19* (8), 1054–1061.

[164] Garrett, C. E.; Prasad, K. *Adv. Synth. Catal.* **2004**, *346* (8), 889–900.

[165] Tang, R.-J.; Milcent, T.; Crousse, B. *J. Org. Chem.* **2018**, *83* (2), 930–938.

[166] Georgiev, D.; Saes, B.; Johnston, H.; Boys, S.; Healy, A.; Hulme, A. *Molecules* **2016**, *21* (1), 88.

[167] Pearson, D. E.; Wysong, R. D.; Breder, C. V. *J. Org. Chem.* **1967**, *32* (7), 2358–2360.

[168] Mori, K.; Itakura, T.; Akiyama, T. *Angew. Chem., Int. Ed.* **2016**, *55* (38), 11642–11646.

[169] Cazorla, C.; De Vries, T. S.; Vedejs, E. *Org. Lett.* **2013**, *15* (5), 984–987.

[170] Calò, V.; Lopez, L.; Pesce, G.; Todesco, P. E. *J. Chem. Soc., Perkin Trans. 2* **1974**, 1192–1195.

[171] Xiong, X.; Yeung, Y.-Y. *ACS Catal.* **2018**, *8* (5), 4033–4043.

[172] Srebnik, M.; Mechoulam, R.; Yona, I. *J. Chem. Soc., Perkin Trans. 1* **1987**, 1423–1427.

[173] Nerdinger, S.; Marchhart, R.; Riebel, P.; Kendall, C.; Johnson, M. R.; Yin, C.-F.; Snieckus, V.; Eltis, L. D. *Chem. Commun.* **1999**, 2259–2260.

[174] Saito, S.; Kano, T.; Hatanaka, K.; Yamamoto, H. *J. Org. Chem.* **1997**, *62* (16), 5651–5656.

[175] Truong, T.; Daugulis, O. *Chem. Sci.* **2013**, *4* (1), 531–535.

[176] Bedford, R. B.; Webster, R. L.; Mitchell, C. J. *Org. Biomol. Chem.* **2009**, *7* (23), 4853–4857.

[177] Dai, H.-X.; Li, G.; Zhang, X.-G.; Stepan, A. F.; Yu, J.-Q. *J. Am. Chem. Soc.* **2013**, *135* (20), 7567–7571.

[178] Long, R.; Yan, X.; Wu, Z.; Li, Z.; Xiang, H.; Zhou, X. *Org. Biomol. Chem.* **2015**, *13* (12), 3571–3574.

[179] Bedford, R. B.; Limmert, M. E. *J. Org. Chem.* **2003**, *68* (22), 8669–8682.

[180] Bedford, R. B.; Betham, M.; Caffyn, A. J. M.; Charmant, J. P. H.; Lewis-Alleyne, L. C.; Long, P. D.; Polo-Cerón, D.; Prashar, S. *Chem. Commun.* **2008**, 990–992.

[181] Bedford, R. B.; Haddow, M. F.; Webster, R. L.; Mitchell, C. J. *Org. Biomol. Chem.* **2009**, *7* (15), 3119–3127.

[182] Denton, R. M.; Scragg, J. T.; Galofré, A. M.; Gui, X.; Lewis, W. *Tetrahedron* **2010**, *66* (40), 8029–8035.

[183] Bedford, R. B.; Coles, S. J.; Hursthouse, M. B.; Limmert, M. E. *Angew. Chem., Int. Ed.* **2003**, *42* (1), 112–114.

[184] Ackermann, L.; Diers, E.; Manvar, A. *Org. Lett.* **2012**, *14* (4), 1154–1157.

[185] Giri, R.; Maugel, N.; Li, J.-J.; Wang, D.-H.; Breazzano, S. P.; Saunders, L. B.; Yu, J.-Q. *J. Am. Chem. Soc.* **2007**, *129* (12), 3510–3511.

[186] Wang, D.-H.; Mei, T.-S.; Yu, J.-Q. *J. Am. Chem. Soc.* **2008**, *130* (52), 17676–17677.

[187] Hennings, D. D.; Iwasa, S.; Rawal, V. H. *J. Org. Chem.* **1997**, *62* (1), 2–3.

[188] Bajracharya, G. B.; Daugulis, O. *Org. Lett.* **2008**, *10* (20), 4625–4628.

[189] Chu, J.-H.; Lin, P.-S.; Wu, M.-J. *Organometallics* **2010**, *29* (18), 4058–4065.

[190] Zhao, X.; Yeung, C. S.; Dong, V. M. *J. Am. Chem. Soc.* **2010**, *132* (16), 5837–5844.

[191] Jeon, W. H.; Lee, T. S.; Kim, E. J.; Moon, B.; Kang, J. *Tetrahedron* **2013**, *69* (25), 5152–5159.

[192] Xiao, B.; Fu, Y.; Xu, J.; Gong, T.-J.; Dai, J.-J.; Yi, J.; Liu, L. *J. Am. Chem. Soc.* **2010**, *132* (2), 468–469.

[193] Whisler, M. C.; MacNeil, S.; Snieckus, V.; Beak, P. *Angew. Chem., Int. Ed.* **2004**, *43* (17), 2206–2225.

[194] Oi, S.; Watanabe, S.-i.; Fukita, S.; Inoue, Y. *Tetrahedron Lett.* **2003**, *44* (48), 8665–8668.

[195] Alder, C. M.; Hayler, J. D.; Henderson, R. K.; Redman, A. M.; Shukla, L.; Shuster, L. E.; Sneddon, H. F. *Green Chem.* **2016**, *18* (13), 3879–3890.

[196] Ochiai, M. 'Reactivities, Properties and Structures' in *Hypervalent Iodine Chemistry*, Wirth, T.; ed.; Springer-Verlag: Berlin, Heidelberg, **2002**, 5–68.

[197] Malmgren, J.; Santoro, S.; Jalalian, N.; Himo, F.; Olofsson, B. *Chem. Eur. J.* **2013**, *19* (31), 10334–10342.

[198] Bielawski, M.; Aili, D.; Olofsson, B. *J. Org. Chem.* **2008**, *73* (12), 4602–4607.

[199] Carreras, V.; Sandtorv, A. H.; Stuart, D. R. *J. Org. Chem.* **2017**, *82* (2), 1279–1284.

[200] Kitamura, T.; Matsuyuki, J.-i.; Taniguchi, H. *Synthesis* **1994**, *1994* (2), 147–148.

[201] Olofsson, B.; Zhu, M.; Jalalian, N. *Synlett* **2008**, *2008* (4), 592–596.

[202] Hossain, M. D.; Kitamura, T. *J. Org. Chem.* **2005**, *70* (17), 6984–6986.

[203] Crowder, J. R.; Glover, E. E.; Grundon, M. F.; Kaempfen, H. X. *J. Chem. Soc.* **1963**, 4578–4585.

[204] Jalalian, N.; Ishikawa, E. E.; Silva, L. F.; Olofsson, B. *Org. Lett.* **2011**, *13* (6), 1552–1555.

[205] Stuart, D. R. *Chem. Eur. J.* **2017**, *23* (63), 15852–15863.

[206] Ciana, C.-L.; Phipps, R. J.; Brandt, J. R.; Meyer, F.-M.; Gaunt, M. J. *Angew. Chem., Int. Ed.* **2010**, *50* (2), 458–462.

[207] Qian, X.; Han, J.; Wang, L. *Tetrahedron Lett.* **2016**, *57* (5), 607–610.

[208] Liu, Q.-S.; Wang, D.-Y.; Yang, J.-F.; Ma, Z.-Y.; Ye, M. *Tetrahedron* **2017**, *73* (26), 3591–3595.

[209] Phipps, R. J.; Gaunt, M. J. *Science* **2009**, *323* (5921), 1593–1597.

[210] Olofsson, B. *Top. Curr. Chem.* **2015**, 135–166.

[211] Bell, H.; May, G.; Pinhey, J.; Sternhell, S. *Tetrahedron Lett.* **1976**, *17* (47), 4303–4306.

[212] Bell, H.; Pinhey, J.; Sternhell, S. *Aust. J. Chem.* **1979**, *32* (7), 1551–1560.

[213] Elliott, G. I.; Konopelski, J. P. *Tetrahedron* **2001**, *57* (27), 5683–5705.

[214] Morgan, J.; Buys, I.; Hambley, T. W.; Pinhey, J. T. *J. Chem. Soc., Perkin Trans. 1* **1993**, 1677–1681.

[215] Pinhey, J. T. *Pure Appl. Chem.* **1996**, *68* (4), 819–824.

[216] Pinhey, J. *Aust. J. Chem.* **1991**, *44* (10), 1353–1382.

[217] Barton, D. H. R.; Donnelly, D. M. X.; Guiry, P. J.; Reibenspies, J. H. *J. Chem. Soc., Chem. Commun.* **1990**, 1110–1111.

[218] Barton, D. H. R.; Donnelly, D. M. X.; Guiry, P. J.; Finet, J.-P. *J. Chem. Soc., Perkin Trans. 1* **1994**, 2921–2926.

[219] Buston, J. E.; Moloney, M. G.; Parry, A. V.; Wood, P. *Tetrahedron Lett.* **2002**, *43* (18), 3407–3409.

[220] Buston, J. E.; Compton, R. G.; Leech, M. A.; Moloney, M. G. *J. Organomet. Chem.* **1999**, *585* (2), 326–330.

[221] Moloney, M. G.; Paul, D. R.; Prottey, S. C.; Thompson, R. M.; Wright, E. *J. Organomet. Chem.* **1997**, *534* (1–2), 195–205.

[222] Moloney, M. G.; Paul, D. R.; Thompson, R. M.; Wright, E. *J. Organomet. Chem.* **1998**, *560* (1–2), 77–88.

[223] Bell, H.; Kalman, J.; Pinhey, J.; Sternhell, S. *Aust. J. Chem.* **1979**, *32* (7), 1521–1530.

[224] Kozyrod, R. P.; Pinhey, J. T. *Tetrahedron Lett.* **1982**, *23* (50), 5365–5366.

[225] Kozyrod, R.; Morgan, J.; Pinhey, J. *Aust. J. Chem.* **1985**, *38* (8), 1147–1153.

[226] Morgan, J.; Pinhey, J. T. *J. Chem. Soc., Perkin Trans. 1* **1990**, 715–720.

[227] McCombie, H.; Saunders, B. C. *Nature* **1947**, *159* (4041), 491–494.

[228] Chang, L. W. *J. Toxicol. Sci.* **1990**, *15* (Suppl. IV), 125–151.

[229] Flora, G.; Gupta, D.; Tiwari, A. *Interdiscip. Toxicol.* **2012**, *5* (2), 47–58.

[230] Matano, Y.; Nomura, H. *J. Am. Chem. Soc.* **2001**, *123* (26), 6443–6444.

[231] Planas, O.; Wang, F.; Leutzsch, M.; Cornella, J. *Science* **2020**, *367* (6475), 313–317.

[232] Planas, O.; Peciukenas, V.; Cornella, J. *J. Am. Chem. Soc.* **2020**, *142* (26), 11382–11387.

[233] Wynn, D. *Talanta* **1984**, *31* (11), 1036–1040.

[234] Kaljurand, I.; Kütt, A.; Sooväli, L.; Rodima, T.; Mäemets, V.; Leito, I.; Koppel, I. A. *J. Org. Chem.* **2005**, *70* (3), 1019–1028.

[235] Coetzee, J. F.; Padmanabhan, G. R. *J. Phys. Chem.* **1965**, *69* (9), 3193–3196.

[236] Kütt, A.; Leito, I.; Kaljurand, I.; Sooväli, L.; Vlasov, V. M.; Yagupolskii, L. M.; Koppel, I. A. *J. Org. Chem.* **2006**, *71* (7), 2829–2838.

[237] Kütt, A. et al. *J. Org. Chem.* **2008**, *73* (7), 2607–2620.

[238] Coetzee, J. F. 'Ionic Reactions in Acetonitrile' in *Progress in Physical Organic Chemistry*, Streitwieser, A. J.; Taft, R. W.; eds.; Wiley: Hoboken, NJ, **1967**, 45–92.

[239] Jurrat, M. 'Bismuth-mediated Arylation'. PhD thesis, University of Nottingham, Nottingham, UK, **2019**.

[240] Klemm, L. H.; Klopfenstein, C. E.; Shabtai, J. *J. Org. Chem.* **1970**, *35* (4), 1069–1075.

[241] Pielhop, T.; Larrazábal, G. O.; Studer, M. H.; Brethauer, S.; Seidel, C.-M.; Rudolf von Rohr, P. *Green Chem.* **2015**, *17* (6), 3521–3532.

[242] Juteau, H.; Gareau, Y.; Lachance, H. *Tetrahedron Lett.* **2005**, *46* (27), 4547–4549.

[243] Kim, H. Y.; Oh, K. *Org. Lett.* **2014**, *16* (22), 5934–5936.

[244] Ravalico, F.; James, S. L.; Vyle, J. S. *Green Chem.* **2011**, *13* (7), 1778–1783.

[245] Barton, D. H. R.; Elliott, J. D.; Géro, S. D. *J. Chem. Soc., Perkin Trans. 1* **1982**, 2085–2090.

[246] Sadamitsu, Y.; Okumura, A.; Saito, K.; Yamada, T. *Chem. Commun.* **2019**, *55* (66), 9837–9840.

[247] Tshepelevitsh, S.; Kütt, A.; Lõkov, M.; Kaljurand, I.; Saame, J.; Heering, A.; Plieger, P. G.; Vianello, R.; Leito, I. *Eur. J. Org. Chem.* **2019**, *2019* (40), 6735–6748.

[248] Coetzee, J. F.; Padmanabhan, G. R. *J. Am. Chem. Soc.* **1965**, *87* (22), 5005–5010.

[249] Hibbert, F. *J. Chem. Soc., Perkin Trans. 2* **1974**, 1862–1866.

[250] Tamres, M.; Searles, S.; Leighly, E. M.; Mohrman, D. W. *J. Am. Chem. Soc.* **1954**, *76* (15), 3983–3985.

[251] Rossini, E.; Netz, R. R.; Knapp, E.-W. *J. Chem. Theory Comput.* **2016**, *12* (7), 3360–3369.

[252] Bandura, A. V.; Lvov, S. N. *J. Phys. Chem. Ref. Data* **2006**, *35* (1), 15–30.

[253] Beitia, J. *Synlett* **2010**, *2011* (1), 139–140.

[254] Pines, E.; Magnes, B.-Z.; Lang, M. J.; Fleming, G. R. *Chem. Phys. Lett.* **1997**, *281* (4–6), 413–420.

[255] Dempsey, J. L.; Winkler, J. R.; Gray, H. B. *J. Am. Chem. Soc.* **2010**, *132* (47), 16774–16776.

[256] Alder, R. W.; Bowman, P. S.; Steele, W. R. S.; Winterman, D. R. *Chem. Commun. (London)* **1968**, 723–724.

[257] Matano, Y. *Organometallics* **2000**, *19* (12), 2258–2263.

[258] Lal, G. S.; Pez, G. P.; Syvret, R. G. *Chem. Rev.* **1996**, *96* (5), 1737–1756.

[259] Xue, X.-S.; Wang, Y.; Li, M.; Cheng, J.-P. *J. Org. Chem.* **2016**, *81* (10), 4280–4289.

[260] Baudoux, J.; Cahard, D. *Org. React.* **2008**, 1–326.

[261] Banks, R. E.; Du Boisson, R. A.; Morton, W. D.; Tsiliopoulos, E. *J. Chem. Soc., Perkin Trans. 1* **1988**, 2805–2811.

[262] Banks, R.; Besheesh, M. *J. Fluorine Chem.* **1995**, *74* (2), 165–166.

[263] Barnette, W. E. *J. Am. Chem. Soc.* **1984**, *106* (2), 452–454.

[264] Umemoto, T.; Tomita, K. *Tetrahedron Lett.* **1986**, *27* (28), 3271–3274.

[265] Umemoto, T.; Harasawa, K.; Tomizawa, G.; Kawada, K.; Tomita, K. *Bull. Chem. Soc. Jpn.* **1991**, *64* (4), 1081–1092.

[266] Gilicinski, A. G.; Pez, G. P.; Syvret, R. G.; Lal, G. *J. Fluorine Chem.* **1992**, *59* (1), 157–162.

[267] Fuchigami, T.; Miyazaki, M. *Electrochim. Acta* **1997**, *42* (13–14), 1979–1984.

[268] Banks, R. E.; Murtagh, V.; An, I.; Maleczka, R. E. '1-(Chloromethyl)-4-fluoro-1,4-diazoniabicyclo[2.2.2]octane Bis(tetrafluoroborate)' in *Encyclopedia of Reagents for Organic Synthesis*, Wiley: Chichester, UK, **2007**.

[269] Zgonnik, V.; Mazières, M.-R.; Plaquevent, J.-C. '1-Fluoro-2,4,6-trimethylpyridinium Tetrafluoroborate' in *Encyclopedia of Reagents for Organic Synthesis*, Wiley: Chichester, UK, **2010**.

[270] Jurić, S.; Portolan, T.; Kronja, O. *Croat. Chem. Acta* **2016**, *89* (1), 65–70.

[271] Differding, E.; Poss, A. J.; Cahard, D.; Shibata, N.; Sikervar, V. '*N*-Fluoro-*N*-(phenylsulfonyl)benzenesulfonamide' in *Encyclopedia of Reagents for Organic Synthesis*, Wiley: Chichester, UK, **2019**.

[272] Rozatian, N.; Ashworth, I. W.; Sandford, G.; Hodgson, D. R. W. *Chem. Sci.* **2018**, *9* (46), 8692–8702.

[273] Zhu, W.; Hu, X.; Wang, F.; Yang, X.; Wu, X. *Chin. J. Chem.* **2014**, *33* (2), 220–224.

[274] Furuya, T.; Ritter, T. *Org. Lett.* **2009**, *11* (13), 2860–2863.

[275] Cazorla, C.; Métay, E.; Andrioletti, B.; Lemaire, M. *Tetrahedron Lett.* **2009**, *50* (27), 3936–3938.

[276] Breen, J. R. 'Selective fluorination strategies'. PhD thesis, Durham University, Durham, UK, **2012**.

[277] Wamser, C. A. *J. Am. Chem. Soc.* **1951**, *73* (1), 409–416.

[278] Cassoux, P.; Kuczkowski, R. L.; Serafini, A. *Inorg. Chem.* **1977**, *16* (12), 3005–3008.

[279] Morris, H. L.; Tamres, M.; Searles, S. *Inorg. Chem.* **1966**, *5* (12), 2156–2160.

[280] Muylle, E.; Kelen, G. van der; Claeys, E. *Spectrochim. Acta, Part A* **1976**, *32* (5), 1149–1154.

[281] Lube, M. S.; Wells, R. L.; White, P. S. *J. Chem. Soc., Dalton Trans.* **1997**, 285–286.

[282] Sreekanth, R.; Prasanthkumar, K. P.; Sunil Paul, M. M.; Aravind, U. K.; Aravindakumar, C. T. *J. Phys. Chem. A* **2013**, *117* (44), 11261–11270.

[283] Banks, R. E.; Besheesh, M. K.; Mohialdin-Khaffaf, S. N.; Sharif, I. *J. Chem. Soc., Perkin Trans. 1* **1996**, 2069–2076.

[284] Heravi, M. R. P. *J. Fluorine Chem.* **2008**, *129* (3), 217–221.

[285] Zaikin, P. A.; Dyan, O. T.; Fadeev, D. S.; Gatilov, Y. V.; Borodkin, G. I. *J. Fluorine Chem.* **2017**, *199*, 20–29.

[286] Zupan, M.; Iskra, J.; Stavber, S. *Bull. Chem. Soc. Jpn.* **1995**, *68* (6), 1655–1660.

[287] Antelo, J. M.; Crugeiras, J.; Leis, J. R.; Ríos, A. *J. Chem. Soc., Perkin Trans. 2* **2000**, 2071–2076.

[288] Roy, A.; Schneller, S. W. *Org. Lett.* **2005**, *7* (18), 3889–3891.

[289] Umemoto, T.; Tomizawa, G. *J. Org. Chem.* **1989**, *54* (7), 1726–1731.

[290] Ying, W.; DesMarteau, D. D.; Gotoh, Y. *Tetrahedron* **1996**, *52* (1), 15–22.

[291] Singh, P.; Khanna, R. *Tetrahedron Lett.* **1982**, *23* (50), 5355–5358.

[292] Lubinkowski, J. J.; Gimenez Arrieche, C.; McEwen, W. E. *J. Org. Chem.* **1980**, *45* (11), 2076–2079.

[293] Lubinkowski, J. J.; Knapczyk, J. W.; Calderon, J. L.; Petit, L. R.; McEwen, W. E. *J. Org. Chem.* **1975**, *40* (21), 3010–3015.

[294] Huynh, M. T.; Anson, C. W.; Cavell, A. C.; Stahl, S. S.; Hammes-Schiffer, S. *J. Am. Chem. Soc.* **2016**, *138* (49), 15903–15910.

[295] Aggarwal, V. K.; Mereu, A. *Chem. Commun.* **1999**, 2311–2312.

[296] Koech, P. K.; Krische, M. J. *J. Am. Chem. Soc.* **2004**, *126* (17), 5350–5351.

[297] Yang, J.-D.; Wang, Y.; Xue, X.-S.; Cheng, J.-P. *J. Org. Chem.* **2017**, *82* (8), 4129–4135.

[298] Christe, K. O.; Dixon, D. A. *J. Am. Chem. Soc.* **1992**, *114* (8), 2978–2985.

[299] Taylor, D. M.; Meier, G. *Tetrahedron Lett.* **2000**, *41* (18), 3291–3294.

[300] Zhang, Y.; Yang, X.-J.; Xie, T.; Chen, G.-L.; Zhu, W.-H.; Zhang, X.-Q.; Yang, X.-Y.; Wu, X.-Y.; He, X.-P.; He, H.-M. *Tetrahedron* **2013**, *69* (24), 4933–4937.

[301] Wang, D.; Wu, L.; Wang, F.; Wan, X.; Chen, P.; Lin, Z.; Liu, G. *J. Am. Chem. Soc.* **2017**, *139* (20), 6811–6814.

[302] Gillespie, R. J.; Hartman, J. S.; Parekh, M. *Can. J. Chem.* **1968**, *46* (10), 1601–1610.

[303] Brown, H. C.; Kanner, B. *J. Am. Chem. Soc.* **1953**, *75* (15), 3865–3865.

[304] Moulis, J. M.; Collomb, J.; Gandini, A.; Cheradame, H. *Polym. Bull.* **1980**, *3* (4), 197–202.

[305] Thompson, C.; Ge, M.; Kahne, D. *J. Am. Chem. Soc.* **1999**, *121* (6), 1237–1244.

[306] Brown, H. J. S.; Wiese, S.; Roberts, J. A. S.; Bullock, R. M.; Helm, M. L. *ACS Catal.* **2015**, *5* (4), 2116–2123.

[307] Alder, R. W. *Chem. Rev.* **1989**, *89* (5), 1215–1223.

[308] Hopkins, H. P.; Jahagirdar, D. V.; Moulik, P. S.; Aue, D. H.; Webb, H. M.; Davidson, W. R.; Pedley, M. D. *J. Am. Chem. Soc.* **1984**, *106* (16), 4341–4348.

[309] Benoit, R. L.; Lefebvre, D.; Fréchette, M. *Can. J. Chem.* **1987**, *65* (5), 996–1001.

[310] Kaljurand, I.; Saame, J.; Rodima, T.; Koppel, I.; Koppel, I. A.; Kögel, J. F.; Sundermeyer, J.; Köhn, U.; Coles, M. P.; Leito, I. *J. Phys. Chem. A* **2016**, *120* (16), 2591–2604.

[311] Solyntjes, S.; Neumann, B.; Stammler, H.-G.; Ignat'ev, N.; Hoge, B. *Eur. J. Inorg. Chem.* **2016**, *2016* (25), 3999–4010.

[312] Piers, W. E.; Chivers, T. *Chem. Soc. Rev.* **1997**, *26* (5), 345–354.

[313] Hansch, C.; Leo, A.; Taft, R. W. *Chem. Rev.* **1991**, *91* (2), 165–195.

[314] Matano, Y.; Miyamatsu, T.; Suzuki, H. *Chem. Lett.* **1998**, *27* (2), 127–128.

[315] Muller, P. *Pure Appl. Chem.* **1994**, *66* (5), 1077–1184.

[316] Jaffe, H. H. *Chem. Rev.* **1953**, *53* (2), 191–261.

[317] Kennedy, J. P.; Feinberg, S. C. *J. Polym. Sci., Polym. Chem. Ed.* **1978**, *16* (9), 2191–2197.

[318] Jurrat, M.; Maggi, L.; Lewis, W.; Ball, L. T. *Nat. Chem.* **2020**, *12* (3), 260–269.

[319] Kumar, A.; Singh, T. V.; Venugopalan, P. *J. Fluorine Chem.* **2013**, *150*, 72–77.

[320] Stavber, S.; Pecan, T. S.; Pape?, M.; Zupan, M. *Chem. Commun.* **1996**, 2247–2248.

[321] Suzuki, H.; Murafuji, T.; Azuma, N. *J. Chem. Soc., Perkin Trans. 1* **1993**, 1169–1175.

[322] Meanwell, N. A. *J. Med. Chem.* **2018**, *61* (14), 5822–5880.

[323] Hammett, L. P. *J. Am. Chem. Soc.* **1937**, *59* (1), 96–103.

[324] Taft, R. W. *J. Am. Chem. Soc.* **1952**, *74* (11), 2729–2732.

[325] Charton, M. *J. Am. Chem. Soc.* **1969**, *91* (3), 615–618.

[326] Takahata, Y.; Chong, D. P. *Int. J. Quantum Chem.* **2005**, *103* (5), 509–515.

[327] Segala, M.; Takahata, Y.; Chong, D. P. *J. Mol. Struct.: THEOCHEM* **2006**, *758* (1), 61–69.

[328] Burns, R. J.; Mati, I. K.; Muchowska, K. B.; Adam, C.; Cockroft, S. L. *Angew. Chem., Int. Ed.* **2020**, *59* (38), 16717–16724.

[329] Milo, A.; Bess, E. N.; Sigman, M. S. *Nature* **2014**, *507* (7491), 210–214.

[330] Ahneman, D. T.; Estrada, J. G.; Lin, S.; Dreher, S. D.; Doyle, A. G. *Science* **2018**, *360* (6385), 186–190.

[331] Verloop, A. 'The Sterimol Approach: Further Development Of The Method And New Applications' in *Pesticide Chemistry: Human Welfare and Environment*, Doyle, P.; Fujita, T.; eds.; Pergamon Press: Oxford, **1983**, 339–344.

[332] Falivene, L.; Cao, Z.; Petta, A.; Serra, L.; Poater, A.; Oliva, R.; Scarano, V.; Cavallo, L. *Nat. Chem.* **2019**, *11* (10), 872–879.

[333] Winstein, S.; Holness, N. J. *J. Am. Chem. Soc.* **1955**, *77* (21), 5562–5578.

[334] Bott, G.; Field, L. D.; Sternhell, S. *J. Am. Chem. Soc.* **1980**, *102* (17), 5618–5626.

[335] Verloop, A.; Hoogenstraaten, W.; Tipker, J. 'Development and Application of New Steric Substituent Parameters in Drug Design' in *Drug Design*, Ariëns, E. J.; ed.; Academic: New York, NY, **1976**, 165–207.

[336] Brethomé, A. V.; Fletcher, S. P.; Paton, R. S. *ACS Catal.* **2019**, *9* (3), 2313–2323.

[337] Piou, T.; Romanov-Michailidis, F.; Romanova-Michaelides, M.; Jackson, K. E.; Semakul, N.; Taggart, T. D.; Newell, B. S.; Rithner, C. D.; Paton, R. S.; Rovis, T. *J. Am. Chem. Soc.* **2017**, *139* (3), 1296–1310.

[338] Iakobson, G.; Du, J.; Slawin, A. M. Z.; Beier, P. *Beilstein J. Org. Chem.* **2015**, *11*, 1494–1502.

[339] Saihara, K.; Shimizu, A.; Abe, H.; Yoshimura, Y. *J. Jpn. Inst. Energy* **2014**, *93* (4), 328–332.

[340] Saihara, K.; Yoshimura, Y.; Fujimoto, H.; Shimizu, A. *J. Mol. Liq.* **2016**, *219*, 493–496.

[341] Bordner, J.; Freedman, L. *Phosphorus Relat. Group V Elem.* **1973**, *3*, 33.

[342] McGary, C. W.; Okamoto, Y.; Brown, H. C. *J. Am. Chem. Soc.* **1955**, *77* (11), 3037–3043.

[343] Brown, H. C.; Okamoto, Y. *J. Am. Chem. Soc.* **1957**, *79* (8), 1913–1917.

[344] Muehlebach, M. et al. 'Discovery and SAR of Pinoxaden: A New Broad Spectrum, Postemergence Cereal Herbicide' in *Pesticide Chemistry: Crop Prot., Public Health, Environmental Safety*, Ohkawa, H.; Miyagawa, H.; Lee, P. W.; eds.; Wiley: Weinheim, Germany, **2007**.

[345] Wittig, G.; Hellwinkel, D. *Chem. Ber.* **1964**, *97* (3), 789–793.

[346] Hellwinkel, D.; Bach, M. *Justus Liebigs Ann. Chem.* **1968**, *720* (1), 198–200.

[347] Ohkata, K.; Takemoto, S.; Ohnishi, M.; Akiba, K.-y. *Tetrahedron Lett.* **1989**, *30* (36), 4841–4844.

[348] Suzuki, H.; Murafuji, T.; Azuma, N. *J. Chem. Soc., Perkin Trans. 1* **1992**, 1593–1600.

[349] Planas, O.; Wang, F.; Leutzsch, M.; Cornella, J. **2019**,

[350] Fedorov, A. Y.; Finet, J.-P. *J. Chem. Soc., Perkin Trans. 1* **2000**, 3775–3778.

[351] Hatakeyama, T.; Nakatsuka, S.; Gotoh, H.; Sasada, Y.; Yanai, M.; Ikuta, T. 'Polycyclic Aromatic Compound'*;* U.S. pat. req. 20180069182. **2018**.

[352] Ashe, A. J.; Diephouse, T. R.; El-Sheikh, M. Y. *J. Am. Chem. Soc.* **1982**, *104* (21), 5693–5699.

[353] Al-Jabar, N.; Massey, A. *J. Organomet. Chem.* **1985**, *287* (1), 57–64.

[354] Uchiyama, Y.; Kuniya, S.; Watanabe, R.; Ohtsuki, T. *Heteroat. Chem.* **2018**, *29* (5–6), e21473.

[355] Tomaschautzky, J.; Neumann, B.; Stammler, H.-G.; Mix, A.; Mitzel, N. W. *Dalton Trans.* **2017**, *46* (5), 1645–1659.

[356] Turner, L. E.; Davidson, M. G.; Jones, M. D.; Ott, H.; Schulz, V. S.; Wilson, P. J. *Inorg. Chem.* **2006**, *45* (16), 6123–6125.

[357] Kindra, D. R.; Peterson, J. K.; Ziller, J. W.; Evans, W. J. *Organometallics* **2014**, *34* (1), 395–397.

[358] Carmalt, C. J.; Cowley, A. H.; Culp, R. D.; Jones, R. A.; Kamepalli, S.; Norman, N. C. *Inorg. Chem.* **1997**, *36* (13), 2770–2776.

[359] Wang, F.; Planas, O.; Cornella, J. *J. Am. Chem. Soc.* **2019**, *141* (10), 4235–4240.

[360] Balazs, L.; Breunig, H. J.; Lork, E.; Soran, A.; Silvestru, C. *Inorg. Chem.* **2006**, *45* (5), 2341–2346.

[361] Soran, A.; Breunig, H. J.; Lippolis, V.; Arca, M.; Silvestru, C. *J. Organomet. Chem.* **2010**, *695* (6), 850–862.

[362] Trubenstein, H. J.; Moaven, S.; Vega, M.; Unruh, D. K.; Cozzolino, A. F. *New J. Chem.* **2019**, *43* (36), 14305–14312.

[363] Hellwinkel, D.; Melan, M. *Chem. Ber.* **1971**, *104* (4), 1001–1016.

[364] Field, J. E.; Venkataraman, D. *Chem. Mater.* **2002**, *14* (3), 962–964.

[365] Zhou, Z.; Wakamiya, A.; Kushida, T.; Yamaguchi, S. *J. Am. Chem. Soc.* **2012**, *134* (10), 4529–4532.

[366] Hellwinkel, D.; Melan, M. *Chem. Ber.* **1974**, *107* (2), 616–626.

[367] Fang, Z.; Zhang, X.; Hing Lai, Y.; Liu, B. *Chem. Commun.* **2009**, 920–922.

[368] Hellwinkel, D.; Wiel, A.; Sattler, G.; Nuber, B. *Angew. Chem., Int. Ed. Engl.* **1990**, *29* (6), 689–692.

[369] Kitamoto, Y.; Suzuki, T.; Miyata, Y.; Kita, H.; Funaki, K.; Oi, S. *Chem. Commun.* **2016**, *52* (44), 7098–7101.

[370] Kuratsu, M.; Kozaki, M.; Okada, K. *Angew. Chem., Int. Ed.* **2005**, *44* (26), 4056–4058.

[371] Krebs, F. C.; Larsen, P. S.; Larsen, J.; Jacobsen, C. S.; Boutton, C.; Thorup, N. *J. Am. Chem. Soc.* **1997**, *119* (6), 1208–1216.

[372] Nakatsuka, S.; Gotoh, H.; Kinoshita, K.; Yasuda, N.; Hatakeyama, T. *Angew. Chem., Int. Ed.* **2017**, *56* (18), 5087–5090.

[373] Yamamura, M.; Nabeshima, T. *Bull. Chem. Soc. Jpn.* **2016**, *89* (1), 42–49.

[374] Yamamura, M.; Hasegawa, T.; Nabeshima, T. *Org. Lett.* **2016**, *18* (4), 816–819.

[375] Hirai, H.; Nakajima, K.; Nakatsuka, S.; Shiren, K.; Ni, J.; Nomura, S.; Ikuta, T.; Hatakeyama, T. *Angew. Chem., Int. Ed.* **2015**, *54* (46), 13581–13585.

[376] Wakamiya, A. et al. *Angew. Chem., Int. Ed.* **2014**, *53* (23), 5800–5804.

[377] Nakatsuka, S.; Gotoh, H.; Kageyama, A.; Sasada, Y.; Ikuta, T.; Hatakeyama, T. *Organometallics* **2017**, *36* (14), 2622–2631.

[378] Hatakeyama, T.; Nakatsuka, S.; Nakajima, K.; Hirai, H.; Ono, Y.; Shiren, K.; Ni, J.; Matsushita, T.; Ikuta, T. 'Polycyclic aromatic compound'*;* 105431439 (China). **2016**.

[379] Kuratsu, M.; Kozaki, M.; Okada, K. *Chem. Lett.* **2004**, *33* (9), 1174–1175.

[380] Deng, N.; Zhang, G. *Org. Lett.* **2019**, *21* (13), 5248–5251.

[381] Okada, K.; Inokawa, H.; Oda, M. *Tetrahedron Lett.* **1991**, *32* (44), 6363–6366.

[382] Okada, K.; Inokawa, H.; Sugawa, T.; Oda, M. *J. Chem. Soc., Chem. Commun.* **1992**, 448–449.

[383] Miller, W. T. *J. Am. Chem. Soc.* **1940**, *62* (10), 2707–2709.

[384] Krespan, C. G. *J. Am. Chem. Soc.* **1961**, *83* (16), 3432–3433.

[385] Ishii, T.; Suzuki, K.; Nakamura, T.; Yamashita, M. *J. Am. Chem. Soc.* **2016**, *138* (39), 12787–12790.

[386] Bartlett, P. D.; Ryan, M. J.; Cohen, S. G. *J. Am. Chem. Soc.* **1942**, *64* (11), 2649–2653.

[387] Ben Saida, A.; Chardon, A.; Osi, A.; Tumanov, N.; Wouters, J.; Adjieufack, A. I.; Champagne, B.; Berionni, G. *Angew. Chem., Int. Ed.* **2019**, *58* (47), 16889–16893.

[388] Wittig, G.; Steinhoff, G. *Angew. Chem., Int. Ed. Engl.* **1963**, *2* (7), 396–396.

[389] Jongsma, C.; Kleijn, J. de; Bickelhaupt, F. *Tetrahedron* **1974**, *30* (18), 3465–3469.

[390] Vermeer, H.; Kevenaar, P. C. J.; Bickelhaupt, F. *Justus Liebigs Ann. Chem.* **1972**, *763* (1), 155–161.

[391] Jongsma, C.; Kok, J. D.; Weustink, R.; Ley, M. V. D.; Bulthuis, J.; Bickelhaupt, F. *Tetrahedron* **1977**, *33* (2), 205–209.

[392] Takahashi, M.; Hatano, K.; Kawada, Y.; Koga, G.; Tokitoh, N.; Okazaki, R. *J. Chem. Soc., Chem. Commun.* **1993**, 1850–1852.

[393] Dechend, F. von; Wichelhaus, H. *Ber. Dtsch. Chem. Ges.* **1875**, *8* (2), 1609–1615.

[394] Weinberg, K. G.; Whipple, E. B. *J. Am. Chem. Soc.* **1971**, *93* (7), 1801–1802.

[395] Weinberg, K. G. *J. Org. Chem.* **1975**, *40* (24), 3586–3589.

[396] McCleland, N. P.; Whitworth, J. B. *J. Chem. Soc.* **1927**, 2753–2757.

[397] Al-Jabar, N.; Massey, A. *J. Organomet. Chem.* **1984**, *276* (3), 331–340.

[398] Humphries, R.; Al-Jabar, N.; Bowen, D.; Massey, A.; Deacon, G. *J. Organomet. Chem.* **1987**, *319* (1), 59–67.

[399] Cullen, W. R.; Wu, A. W. *J. Fluorine Chem.* **1976**, *8* (2), 183–187.

[400] Hellwinkel, D.; Schenk, W. *Angew. Chem., Int. Ed. Engl.* **1969**, *8* (12), 987–988.

[401] Schomburg, D.; Sheldrick, W. S. *Acta Crystallogr., Sect. B: Struct. Crystallogr. Cryst. Chem.* **1976**, *32* (4), 1021–1024.

[402] Earley, R. A.; Gallagher, M. J. *J. Chem. Soc. C* **1970**, 158–163.

[403] Drover, M. W.; Nagata, K.; Peters, J. C. *Chem. Commun.* **2018**, *54* (57), 7916–7919.

[404] Iwai, T.; Konishi, S.; Miyazaki, T.; Kawamorita, S.; Yokokawa, N.; Ohmiya, H.; Sawamura, M. *ACS Catal.* **2015**, *5* (12), 7254–7264.

[405] Uchiyama, Y.; Sugimoto, J.; Shibata, M.; Yamamoto, G.; Mazaki, Y. *Bull. Chem. Soc. Jpn.* **2009**, *82* (7), 819–828.

[406] Rot, N.; de Wijs, W.-J. A.; de Kanter, F. J. J.; Dam, M. A.; Bickelhaupt, F.; Lutz, M.; Spek, A. L. *Main Group Met. Chem.* **1999**, *22* (8), 519–526.

[407] Huisgen, R.; Sauer, J. *Chem. Ber.* **1959**, *92* (1), 192–202.

[408] Kobayashi, J.; Agou, T.; Kawashima, T. *Chem. Lett.* **2003**, *32* (12), 1144–1145.

[409] Hu, L.; Mahaut, D.; Tumanov, N.; Wouters, J.; Robiette, R.; Berionni, G. *J. Org. Chem.* **2019**, *84* (17), 11268–11274.

[410] Agou, T.; Kobayashi, J.; Kawashima, T. *Chem. Lett.* **2004**, *33* (8), 1028–1029.

[411] Massey, A. G. *Adv. Inorg. Chem.* **1989**, *33*, 1–38.

[412] Massey, A.; Al-Jabar, N.; Humphries, R.; Deacon, G. *J. Organomet. Chem.* **1986**, *316* (1–2), 25–39.

[413] Dam, M. A.; Akkerman, O. S.; De Kanter, F. J. J.; Bickelhaupt, F.; Veldman, N.; Spek, A. L. *Chem. Eur. J.* **1996**, *2* (9), 1139–1142.

[414] Al-Jabar, N. A. A.; Jones, J. B.; Brown, D. S.; Colligan, A. H.; Massey, A. G.; Miller, J. M.; Nye, J. W. *Applied Organomet. Chem.* **1989**, *3* (6), 459–468.

[415] Hellwinkel, D.; Blaicher, W.; Krapp, W.; Sheldrick, W. S. *Chem. Ber.* **1980**, *113* (4), 1406–1413.

[416] Uchiyama, Y.; Ohtsuki, T.; Murakami, R.; Shibata, M.; Sugimoto, J. *Eur. J. Org. Chem.* **2016**, *2017* (1), 159–174.

[417] Tsuji, H.; Inoue, T.; Kaneta, Y.; Sase, S.; Kawachi, A.; Tamao, K. *Organometallics* **2006**, *25* (26), 6142–6148.

[418] Chen, L. S.; Chen, G. J.; Tamborski, C. *J. Organomet. Chem.* **1980**, *193* (3), 283–292.

[419] Ishii, A.; Yoshioka, R.; Nakayama, J.; Hoshino, M. *Tetrahedron Lett.* **1993**, *34* (51), 8259–8262.

[420] Ishii, A.; Tsuchiya, T.; Nakayama, J.; Hoshino, M. *Tetrahedron Lett.* **1993**, *34* (14), 2347–2350.

[421] Ishii, A.; Takaki, I.; Nakayama, J.; Hoshino, M. *Tetrahedron Lett.* **1993**, *34* (51), 8255–8258.

[422] Ai-Soudani, A.-R.; Massey, A. G. *Applied Organomet. Chem.* **1988**, *2* (6), 553–556.

[423] Coe, P. L.; Waring, A. J.; Yarwood, T. D. *J. Chem. Soc., Perkin Trans. 1* **1995**, 2729–2737.

[424] Ogawa, T.; Ikegami, T.; Hikasa, T.; Ono, N.; Suzuki, H. *J. Chem. Soc., Perkin Trans. 1* **1994**, 3479–3483.

[425] Shimada, S.; Yamazaki, O.; Tanaka, T.; Suzuki, Y.; Tanaka, M. *J. Organomet. Chem.* **2004**, *689* (19), 3012–3023.

[426] Wing-Wah, S. *Tetrahedron Lett.* **1993**, *34* (39), 6223–6224.

[427] Böckmann, K.; Vögtle, F. *Chem. Ber.* **1981**, *114* (3), 1048–1064.

[428] Sakakura, A.; Ohkubo, T.; Yamashita, R.; Akakura, M.; Ishihara, K. *Org. Lett.* **2011**, *13* (5), 892–895.

[429] Bailey, W. F.; Rathman, T. L. 'The Lithium-Halogen Exchange Reaction in Process Chemistry' in *Process Chemistry in the Pharmaceutical Industry*, Gadamasetti, K.; Braish, T.; eds.; CRC: Boca Raton, FL, **2007**, 205–216.

[430] Merrill, R. E.; Negishi, E. *J. Org. Chem.* **1974**, *39* (23), 3452–3453.

[431] Corey, E. J.; Beames, D. J. *J. Am. Chem. Soc.* **1972**, *94* (20), 7210–7211.

[432] Seebach, D.; Neumann, H. *Chem. Ber.* **1974**, *107* (3), 847–853.

[433] Roschke, F.; Thiele, G.; Dehnen, S.; Mehring, M. *Main Group Met. Chem.* **2019**, *42* (1), 46–50.

[434] List, B.; Monaco, M.; Properzi, R. *Synlett* **2015**, *27* (4), 591–594.

[435] Taguchi, H. 'Iodinating Reagents' in *Iodine Chemistry and Applications*, Kaiho, T.; ed.; Wiley: Hoboken, NJ, **2014**, 249–276.

[436] Bao, R. L.-Y.; Zhao, R.; Shi, L. *Chem. Commun.* **2015**, *51* (32), 6884–6900.

[437] Krasovskiy, A.; Knochel, P. *Angew. Chem., Int. Ed.* **2004**, *43* (25), 3333–3336.

[438] Uchiyama, Y.; Kuniya, S.; Watanabe, R.; Ohtsuki, T. *Phosphorus, Sulfur Silicon Relat. Elem.* **2019**, *194* (4–6), 281–284.

[439] Uchiyama, Y.; Kuniya, S.; Watanabe, R.; Ohtsuki, T. *Phosphorus, Sulfur Silicon Relat. Elem.* **2018**, *194* (4–6), 277–278.

[440] Matano, Y.; Nomura, H.; Hisanaga, T.; Nakano, H.; Shiro, M.; Imahori, H. *Organometallics* **2004**, *23* (23), 5471–5480.

[441] Uchiyama, Y.; Kano, N.; Kawashima, T. *Organometallics* **2001**, *20* (12), 2440–2442.

[442] Harris, R. K.; Becker, E. D.; Menezes, S. M. C. de; Goodfellow, R.; Granger, P. *Pure Appl. Chem.* **2001**, *73* (11), 1795–1818.

[443] Foroozandeh, M.; Adams, R. W.; Meharry, N. J.; Jeannerat, D.; Nilsson, M.; Morris, G. A. *Angew. Chem., Int. Ed.* **2014**, *53* (27), 6990–6992.

[444] Oppermann, H.; Petasch, U. *Z. Naturforsch., B: J. Chem. Sci.* **2003**, *58* (8), 725–740.

[445] Petiot, P.; Gagnon, A. *Eur. J. Org. Chem.* **2013**, *2013* (24), 5282–5289.

[446] Manabe, K.; Ishikawa, S. *Synthesis* **2008**, *2008* (16), 2645–2649.

[447] Cordero-Vargas, A.; Pérez-Martín, I.; Quiclet-Sire, B.; Zard, S. Z. *Org. Biomol. Chem.* **2004**, *2* (20), 3018–3025.

[448] Zhang, Y.-Y.; Lin, J.-D.; Xu, X.-L.; Li, J.-H. *Synth. Commun.* **2010**, *40* (17), 2556–2563.

[449] Buckingham, F.; Calderwood, S.; Checa, B.; Keller, T.; Tredwell, M.; Collier, T. L.; Newington, I. M.; Bhalla, R.; Glaser, M.; Gouverneur, V. *J. Fluorine Chem.* **2015**, *180*, 33–39.

[450] Das, P. J.; Sarmah, B. *Asian J. Chem.* **2015**, *27* (1), 189–191.

[451] Wang, X.; Guram, A.; Ronk, M.; Milne, J. E.; Tedrow, J. S.; Faul, M. M. *Tetrahedron Lett.* **2012**, *53* (1), 7–10.

[452] Baumstark, A. L.; Chrisope, D. R.; Keel, R. A.; Boykin, D. W. *J. Heterocycl. Chem.* **1980**, *17* (8), 1719–1721.

[453] Ghosh, M. K.; Rzymkowski, J.; Kalek, M. *Chem. Eur. J.* **2019**, *25* (41), 9619–9623.

[454] Wheeler, T. N. *J. Org. Chem.* **1979**, *44* (26), 4906–4912.

[455] Shafiee, A.; Esmaeili-Marandi, F.; Saeedi, M.; Mahdavi, M.; Yavari, I.; Foroumadi, A. *Synlett* **2014**, *25* (18), 2605–2608.

[456] Zhang, R.; Liu, Z.; Peng, Q.; Zhou, Y.; Xu, L.; Pan, X. *Org. Biomol. Chem.* **2018**, *16* (11), 1816–1822.

[457] Casitas, A.; Canta, M.; Solà, M.; Costas, M.; Ribas, X. *J. Am. Chem. Soc.* **2011**, *133* (48), 19386–19392.

[458] Bodzioch, A.; Bałczewski, P.; Owsianik, K.; Skalik, J.; Kowalska, E.; Stasiak, A.; Różycka-Sokołowska, E.; Marciniak, B. *Synthesis* **2016**, *48* (20), 3509–3514.

[459] Bhadra, S.; Yamamoto, H. *Angew. Chem., Int. Ed.* **2016**, *55* (42), 13043–13046.

[460] Konishi, S.; Iwai, T.; Sawamura, M. *Organometallics* **2018**, *37* (12), 1876–1883.

[461] Kühl, O. *Phosphorus-31 NMR Spectroscopy;* Springer-Verlag: Heidelberg, Germany, **2008**.

[462] Ketelaere, R. D.; Kelen, G. V. D. *J. Mol. Struct.* **1975**, *27* (1), 25–31.

[463] Stanetty, P.; Mihovilovic, M. D. *J. Org. Chem.* **1997**, *62* (5), 1514–1515.

[464] Sheldrick, G. M. *Acta Crystallogr., Sect. A: Found. Adv.* **2015**, *71* (1), 3–8.

[465] Sheldrick, G. M. *Acta Crystallogr., Sect. C: Struct. Chem.* **2015**, *71* (1), 3–8.

[466] Sheldrick, G. M. *Acta Crystallogr., Sect. A: Found. Crystallogr.* **2007**, *64* (1), 112–122.